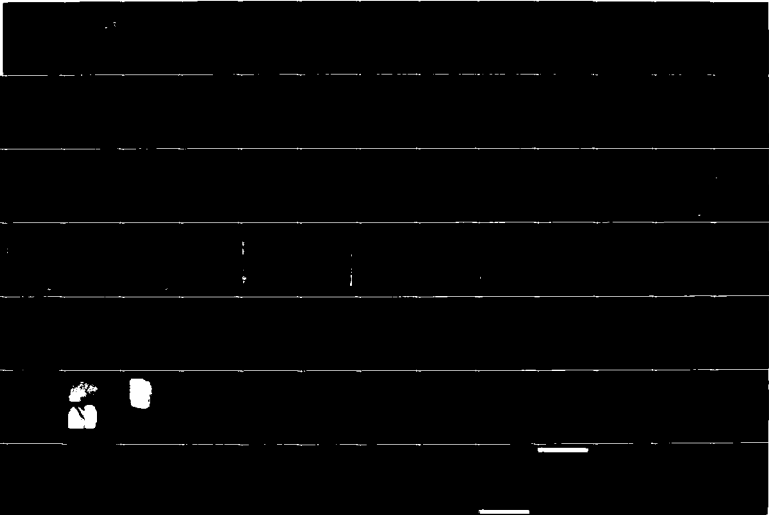


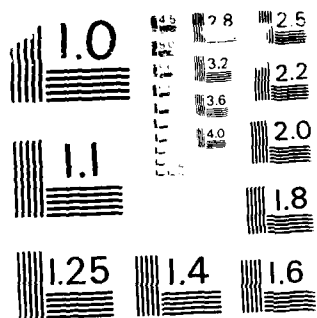
AD-A190 700

HIGH-PERFORMANCE POLYMERIC MATERIALS(U) CINCINNATI UNIV 1/3
OH DEPT OF CHEMISTRY J E MARK 87 DEC 87
AFOSR-TR-87-2011 AFOSR-83-0027

UNCLASSIFIED

F/G 7/6 NE





MICROCOPY RESOLUTION TEST CHART
 NATIONAL BUREAU OF STANDARDS - 1963-A

Unclassified

②

SECURITY

DOCUMENTATION PAGE

1a. REPORT AD-A190 708		1d. RESTRICTIVE MARKINGS Unclassified	
2a. SECURITY CLASSIFICATION Unclassified		3. DISTRIBUTION/AVAILABILITY OF REPORT Approved for public release; Distribution unlimited	
2b. DECLASSIFICATION/DOWNGRADING SCHEDULE		5. MONITORING ORGANIZATION REPORT NUMBER(S) AFOSR-TR. 87-2011	
4. PERFORMING ORGANIZATION REPORT NUMBER(S) AFOSR 83-0027, Final		7a. NAME OF MONITORING ORGANIZATION AFOSR/NC	
6a. NAME OF PERFORMING ORGANIZATION University of Cincinnati	6d. OFFICE SYMBOL (If applicable)	7b. ADDRESS (City, State and ZIP Code) Bldg 410 Bolling AFB DC 20332-6448	
6c. ADDRESS (City, State and ZIP Code) Department of Chemistry University of Cincinnati #172 Cincinnati, Ohio 45221		9. PROCUREMENT INSTRUMENT IDENTIFICATION NUMBER AFOSR-83-0027	
8a. NAME OF FUNDING/SPONSORING ORGANIZATION AFOSR	8b. OFFICE SYMBOL (If applicable) NC	10. SOURCE OF FUNDING NOS.	
8c. ADDRESS (City, State and ZIP Code) Bldg 410 Bolling AFB DC 20332-6448		PROGRAM ELEMENT NO. 61102F	TASK NO. A3
11. TITLE (Include Security Classification) High-Performance Polymeric Materials		PROJECT NO. 2303	WORK UNIT NO.
12. PERSONAL AUTHOR(S) J. E. Mark			
13a. TYPE OF REPORT Final	13b. TIME COVERED FROM 11/1/82 TO 10/31/87	14. DATE OF REPORT (Yr., Mo., Day) 12/7/87	15. PAGE COUNT iv + 232
16. SUPPLEMENTARY NOTATION None			
17. COSATI CODES		18. SUBJECT TERMS (Continue on reverse if necessary and identify by block number)	
FIELD	GROUP	SUB. GR.	
			Rodlike polymers
			Aromatic heterocyclic polymers
			Conformational energies
19. ABSTRACT (Continue on reverse if necessary and identify by block number)			
<p>— A variety of theoretical methods were used to elucidate the structure and properties of rigid rodlike polymer chains which are of interest as high-performance polymeric materials. Semi-empirical molecular mechanics methods were used to calculate the intramolecular and intermolecular energies pertinent to conformational flexibility and chain packing effects. Also, geometry optimized CNDO/2 molecular orbital calculations were carried out to investigate the structure and conformational characteristics of the rodlike polymers, in both the unprotonated and protonated states. Electronic band gap calculations within the extended Hückel approximation were carried out to elucidate the packing and electronic properties of these chains in the crystalline state. Some of these same methods were also used to investigate a variety of molecular species possessing structural</p> <p>(Continued on the back)</p>			
20. DISTRIBUTION/AVAILABILITY OF ABSTRACT UNCLASSIFIED/UNLIMITED <input type="checkbox"/> SAME AS RPT. <input type="checkbox"/> DTIC USERS <input type="checkbox"/>		21. ABSTRACT SECURITY CLASSIFICATION Unclassified	
22a. NAME OF RESPONSIBLE INDIVIDUAL Major Larry P Davis USAF		22c. TELEPHONE NUMBER (Include Area Code) (202) 767-4960	22b. OFFICE SYMBOL NC

**DTIC
SELECTED
JAN 22 1988**

(Subject Terms Continued)

Intermolecular interactions,
Polybenzobisoxazoles
Polybenzobisthiazoles
Chain flexibility

Chain packing,
Electrical conductivity
Ceramic particles
Elastomer reinforcement $\frac{1}{2}$

(Abstract Continued)

features similar to those of the rodlike polymers.

Some random-coil polymers were also studied theoretically and experimentally to provide a test of the theoretical methods developed for the rigid-rod polymers and to provide comparisons with their less flexible counterparts.

In-situ hydrolysis techniques were also developed to precipitate ceramic-type particles into elastomers. The main goal here was to improve mechanical properties and thus provide reinforcement of the elastomeric materials. Since the reactions used are the same as those of the new sol-gel-ceramics technology, considerable insight into both disciplines could be obtained.

DISCLAIMER NOTICE

**THIS DOCUMENT IS BEST QUALITY
PRACTICABLE. THE COPY FURNISHED
TO DTIC CONTAINED A SIGNIFICANT
NUMBER OF PAGES WHICH DO NOT
REPRODUCE LEGIBLY.**

HIGH-PERFORMANCE POLYMERIC MATERIALS

J. E. Mark

Department of Chemistry and the Polymer Research Center
The University of Cincinnati

Final Report, November 1, 1982 - October 31, 1987

Air Force Office of Scientific Research

December 11, 1987

AFOSR-TR-87-2011

AFOSR-TR-87-2011 (AFSO)
This report is unlimited.
This report is reviewed and is
classified in accordance with AFM AFR 190-12.
MATTHEW J. KERPER
Chief, Technical Information Division

23

FOREWORD

This report was prepared at the Department of Chemistry of the University of Cincinnati, under Grant AFOSR 83-0027. The research described herein was administered under the direction of the Air Force Office of Scientific Research, Bolling Air Force Base, Washington, D.C., 20332.

The report covers work carried out between November 1, 1982, and October 31, 1987, and was prepared in December, 1987.

Accession For	
NTIS GRA&I	<input checked="checked" type="checkbox"/>
DTIC TAB	<input type="checkbox"/>
Unannounced	<input type="checkbox"/>
Justification	
By	
Distribution/	
Availability Codes	
Dist	Avail and/or Special
A-1	



A. RESEARCH OBJECTIVES AND ACCOMPLISHMENTS

The first primary objective was to obtain an understanding of the properties of relatively stiff polymer chains, and to provide guidance on how these properties can be exploited to obtain high-performance polymeric materials. More specifically, one goal was to use semi-empirical and quantum-mechanical methods to obtain information on the physical properties of rigid-rod benzobisoxazole (PBO), benzobisthiazole (PBT), and structurally related polymers. These materials are of importance to the Air Force because of their high mechanical strength and excellent thermal stability. Such calculations involve energy calculations on both intramolecular (conformational) effects and interchain interactions for the polymers in both the unprotonated and protonated states. Of particular interest is the extent to which the various ring structures in the chains deviate from coplanarity, and how these deviations affect the ordering of the chains in the crystalline state. A related feature is the protonation of these chains, which occurs in the strongly acidic media used as solvents, and its effect on structure and deviations from coplanarity.

One specific study (21)* involved conformational energy calculations on two polymers (AAPBO and ABPBO) related to PBO. Another (32) addressed chain packing in a ladder polymer (BBL),

*Reference numbers correspond to those in the attached Cumulative List of Publications.

and a less stiff but structurally related polymer (BBB). Good agreement with experimental structural studies was obtained, and the geometry optimization technique was tested on a series of small molecules (16). All of the results obtained on these aspects of the program are summarized in several more general review articles (7,35,43).

Some theoretical and experimental investigations were also carried out on more tractable random-coil polymers in order to evaluate the theoretical methods and to obtain more insight into the properties of the structurally related rigid-rod polymers. These studies specifically involved some polysilanes (6,31,38,47), polygermanes (47), polysiloxanes (9), ethylene-based polyesters (34), and an enzyme inhibitor (DAMP) (2,4).

Electronic band structure calculations were explored with regard to the types of conductivity which may be of interest for electronic applications of the rigid-rod polymers and related materials. Similar calculations were also carried out on relatively small molecules having structural features in common with the PBO and PET polymers. Specific systems studied were PBO (1), two PBO-related polymers (AAPBO and ABPBO) (27), PBT (1,3), two PBT-related polymers (AAPBT and ABPET) (36), substituted polyacetylenes (14), doped trans-polyacetylene (15), two polyynes (17), iridium carbonyl chloride chain (5), and a bis(oxalato)platinate complex (33). Several polymers were found to have relatively small band gaps, and could therefore be of considerable practical importance. Much of this work is summarized in two review articles (42,45).

In collaboration with Professor William J. Welsh (U. Missouri-St. Louis) and Mr. Henry Kurtz (Memphis State U.), theoretical studies of nonlinear optical effects in small molecules and polymers have been initiated. The goals of this project are: 1) to apply existing methodologies to calculate hyperpolarizabilities of small molecules and polymer subunits and 2) to develop new, more accurate methods for the calculation of such hyperpolarizabilities.

Another series of investigations explored the idea of precipitating fillers into elastomers. The goal was to provide reinforcement of these materials. Also, since the hydrolysis reactions used are very similar to those used in the new sol-gel-ceramics technology, advantageous connections between these two disciplines could be obtained.

In one series of studies, silica type fillers were precipitated into unimodal and bimodal siloxane polymers after the curing process (11-13,22,29,37,39,42). It was found that the precipitation could also be carried out during the curing process (18,19), or before it (25). Good reinforcement was observed for these elastomers, and for some thermosets (20) as well. Titania particles (29) and iron oxide particles (40) also gave good reinforcement. In some cases extraction procedures gave even larger increases in mechanical properties and thus even better reinforcement (10).

It may also be possible to introduce deformability into the filler particles by carrying along hydrocarbon groups from the material being hydrolyzed (24,28). Magnetic filler

particles have the advantage that they can be manipulated with an external magnetic field (23).

Particle sizes and particle size distributions have been studied by electron microscopy and small-angle x-ray scattering (8,30). Correlation of this information with hydrolysis conditions and mechanical properties is providing valuable guidance for the exploitation of these materials.

The major results obtained in these reinforcement studies are summarized in a series of review articles (26,31,46).

It is also possible to use compositions and hydrolysis conditions that make the silica the continuous phase, and the polymer the dispersed phase (44). Such polymer-modified ceramics could have extremely attractive properties, for example reduced brittleness.

B. CUMULATIVE LIST OF PUBLICATIONS

1. Calculations of the Electronic Band Structures for Some Rigid Benzobisoxazole and Benzobisthiazole Polymers, D. Bhaumik and J. E. Mark, J. Polym. Sci., Polym. Phys. Ed., **21**, 1111 (1983).
2. CNDO/2 Molecular Orbital Calculations on the Antifolate DAMP and Some of its Analogues, W. J. Welsh, J. E. Mark, V. Cody, and S. F. Zakrzewski, in "Chemistry and Biology of Pteridines: Pteridines and Folic Acid Derivatives", ed. by J. A. Blair, W. de Gruyter Pub. Co., Berlin, 1983.
3. A Theoretical Investigation of Chain Packing and Electronic Band Structure of the Rigid-Rod Polymer Trans-(p-Phenylene Benzobisthiazole) in the Crystalline State, D. Bhaumik and J. E. Mark, J. Polym. Sci., Polym. Phys. Ed., **21**, 2543 (1983).
4. CNDO/2 Molecular Orbital Calculations on the Antifolate DAMP and Some Related Species: Structural Geometries, Ring Distortions, Charge Distributions, and Conformational Characteristics, W. J. Welsh, V. Cody, J. E. Mark, and S. F. Zakrzewski, Cancer Biochem., Biophys., **7**, 27 (1983).
5. Band Structures, Geometry, and Partial Oxidation of Iridium Carbonyl Chloride Chains, D. Bhaumik and J. E. Mark, Synthetic Metals, **6**, 299 (1983).
6. Conformational Analysis and Solid-State ^{29}Si NMR Spectroscopy of Some Polysilanes, W. J. Welsh, J. Ackerman, and J. E. Mark, Polym. Preprints, Div. of Polym. Chem., Inc., ACS, **24(1)**, 131 (1983).

7. Theoretical Investigations on Some Rigid-Rod Polymers Used as High Performance Materials, W. J. Welsh, D. Bhaumik, H. H. Jaffe', and J. E. Mark, Polym. Eng. Sci., **24**, 218 (1984).
8. Particle Sizes of Reinforcing Silica Precipitated Into Elastomeric Networks, Y.-P. Ning, M.-Y. Tang, C.-Y. Jiang, J. E. Mark, and W. C. Roth, J. Appl. Polym. Sci., **29**, 3209 (1984).
9. Dipole Moments of Some Poly(Dimethylsiloxane) Linear Chains and Cyclics, E. Riande and J. E. Mark, Eur. Polym. J., **20**, 517 (1984).
10. Treatment of Filler-Reinforced Silicone Elastomers to Maximize Increases in Ultimate Strength, Y.-P. Ning and J. E. Mark, Polym. Bulletin, **12**, 407 (1984).
11. Effects of Ethylamine Catalyst Concentration in the Precipitation of Reinforcing Silica Filler in an Elastomeric Network, J. E. Mark and Y.-P. Ning, Polym. Bulletin, **12**, 413 (1984).
12. The Effect of Relative Humidity on the Hydrolytic Precipitation of Silica Into an Elastomeric Network, C.-Y. Jiang and J. E. Mark, Colloid Polym. Sci., **262**, 758 (1984).
13. The Effects of Various Catalysts in the In-Situ Precipitation of Reinforcing Silica in Polydimethylsiloxane Networks, C.-Y. Jiang and J. E. Mark, Makromol. Chemie., **185**, 2609 (1984).
14. Theoretical Studies of the Electronic Properties of Substituted Polyacetylenes, K. C. Metzger and W. J. Welsh, Polym. Preprints, Div. of Polym. Chem., Inc., ACS **25(1)**, 195 (1984).

15. A Theoretical Investigation of the Electronic Band Structure in Doped Trans-Polyacetylene, D. Bhaumik and J. E. Mark, Polym. Preprints, Div. of Polym. Chem., Inc., ACS, **25(2)**, 266 (1984).
16. Geometry Optimization Using Symmetry Coordinates, H. Kondo, W. J. Welsh, H. H. Jaffe', and H. Y. Lee, J. Comp. Chem., **5**, 84 (1984).
17. Theoretical Studies in Electrical Conductivity in Polyynes, K. C. Metzger and W. J. Welsh, Polym. Preprints, Div. of Polym. Chem., Inc., ACS, **25(2)**, 270 (1984).
18. Elastomeric Properties of Bimodal Networks Prepared by a Simultaneous Curing-Filling Technique, M.-Y. Tang and J. E. Mark, Polym. Eng. Sci., **25**, 29 (1985).
19. Simultaneous Curing and Filling of Elastomers, J. E. Mark, C.-Y. Jiang, and M.-Y. Tang, Macromolecules, **17**, 2613 (1984).
20. Impact Resistance of Unfilled and Filled Bimodal Thermosets of Poly(dimethylsiloxane), M.-Y. Tang, A. Letton and J. E. Mark, Colloid Polym. Sci., **262**, 990 (1984).
21. Molecular Orbital Conformational Energy Calculations of the Aromatic Heterocyclic Poly(5,5'-Bibenzoxazole-2,2'-Diyl-1,4-Phenylene) and Poly(2,5-Benzoxazole), W. J. Welsh, and J. E. Mark, Polym. Eng. Sci., **25**, 965 (1985).
22. Bimodal Networks and Networks Reinforced by the In-Situ Precipitation of Silica, J. E. Mark, Brit. Polym. J., **17**, 144 (1985).

23. Effects of a Magnetic Field Applied During the Curing of a Polymer Loaded with Magnetic Filler, Z. Rigbi and J. E. Mark, J. Polym. Sci., Polym. Phys. Ed., **23**, 1267 (1985).
24. Hydrolysis of Several Ethylethoxysilanes to Yield Deformable Filler Particles, Y.-P. Ning, Z. Rigbi and J. E. Mark, Polym. Bulletin, **13**, 155 (1985).
25. Precipitation of Reinforcing Filler Into Poly(Dimethylsiloxane) Prior to Its End Linking Into Elastomeric Networks, Y.-P. Ning and J. E. Mark, J. Appl. Polym. Sci., **30**, 3519 (1985).
26. Molecular Aspects of Rubberlike Elasticity, J. E. Mark, Acc. Chem. Res., **18**, 202 (1985).
27. A Theoretical Study of Conformations and Electronic Band Structures for Two Benzoxazole Polymers, K. Nayak and J. E. Mark, Makromol. Chemie, **186**, 2137 (1985).
28. Reinforcing Effects from Silica-Type Fillers Containing Hydrocarbon Groups, J. E. Mark and G. S. Sur, Polym. Bulletin, **14**, 325 (1985).
29. Elastomeric Networks Cross Linked by Silica or Titania Fillers, G. S. Sur and J. E. Mark, Eur. Polym. J., **21**, 1051 (1985).
30. Electron Microscopy of Elastomers Containing In-Situ Precipitated Silica, J. E. Mark, Y.-P. Ning, C.-Y. Jiang, M.-Y. Tang, and W. C. Roth, Polymer, **26**, 2069 (1985).
31. Conformational Analysis of Some Polysilanes and the Precipitation of Reinforcing Silica Into Elastomeric Networks, J. E. Mark, in "Science of Synthetic Chemical

- Processing", ed. by L. L. Hench and D. R. Ulrich, Wiley, New York, 1986.
32. Chain Packing in Two Aromatic Heterocyclic Polymers, One of Which Has a Ladder Structure, K. Nayak and J. E. Mark, Makromol. Chemie, **187**, 1547 (1986).
 33. Band Structure Analysis of a Bis(oxalato)platinate Complex, K. Nayak, D. Bhaumik, and J. E. Mark, Synthetic Metals, **14**, 309 (1986).
 34. Odd-Even Variations in the Melting Points of some Ethylene Polyesters, D. Bhaumik and J. E. Mark, Makromol. Chemie, **187**, 1329 (1986).
 35. Theoretical Studies of Liquid-Crystalline Rodlike Polymers Used as High-Performance Materials, W. J. Welsh and J. E. Mark, Chemical Design Automation News, **1(6)**, 2 (1986).
 36. Conformational and Electronic Band Structure Analysis of a New Type of High Performance Polybenzothiazole Polymers, K. Nayak, J. Mat. Sci., **21**, 2232 (1986).
 37. Comparisons Among Some Tetra-Alkoxysilanes in the Hydrolytic Precipitation of Silica into Elastomeric Networks, G. S. Sur and J. E. Mark, Makromol. Chemie, **187**, 2861 (1986).
 38. Conformational Energies and Unperturbed Chain Dimensions of Polysilane and Polydimethylsilylene, W. J. Welsh, L. DeBolt, and J. E. Mark, Macromolecules, **19**, 2978 (1986).
 39. Ethylamine and Ammonia as Catalysts in the In-Situ Precipitation of Silica in Silicone Networks, Y.-P. Ning and J. E. Mark, Polym. Eng. Sci., **26**, 167 (1986).
 40. Precipitation of Iron Oxide Filler Particles Into an

- Elastomer, S. Liu and J. E. Mark, Polym. Bulletin, **18**, 33 (1987).
41. Theoretical Studies of Electrical Conductivity in Polymers, W. J. Welsh, Chemical Design Automation News, **2**(2), 4 (1987).
42. Reinforcement of a Non-Crystallizable Elastomer by the In-Situ Precipitation of Silica, S. J. Clarson and J. E. Mark, Polym. Comm., **28**, 249 (1987).
43. Conformational Characteristics of Some Liquid-Crystalline Aromatic Heterocyclic Polymers Useable as High-Performance Materials, W. J. Welsh, in "Current Topics in Polymer Science Vol. 1", ed by R. M. Ottenbrite, L. A. Utracki, and S. Inoue, Hanser Publishers, New York, 1987.
44. Polymer-Modified Silica Glasses. I. Control of Hardness, J. E. Mark and C.-C. Sun, Polym. Bulletin, **18**, 5 (1987).
45. Band-Structure Calculations on Polymeric Chains, W. J. Welsh, in "Polymers for High Technology", ed. by M. J. Bowden and S. R. Turner, Am. Chem. Soc., Washington, DC, 1987.
46. In-Situ Generation of Ceramic Particles in Elastomeric Matrices, J. E. Mark, in "Ultrastructure Processing of Ceramics, Glasses, and Composites", ed. by J. Mackenzie and D. R. Ulrich, Wiley, New York, 1988.
47. AM1 and MNDO/2 Molecular Orbital Conformational Energy Calculations on Model Compounds of Simple Polysilanes and Polygermanes, W. D. Johnson and W. J. Welsh, Proceedings of "Silicon-Based Polymer Science Workshop", Polymer Division, ACS, Makaha, Hawaii, November 1987.

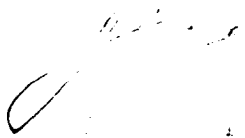
C. PROFESSIONAL PERSONNEL

1. Dr. J. E. Mark, Senior Investigator; Distinguished Research Professor of Chemistry and Director of the Polymer Research Center, The University of Cincinnati.
2. Dr. W. J. Welsh, previously Postdoctoral Fellow and Adjunct Professor, The University of Cincinnati, and Assistant Professor, College of Mount St. Joseph. Presently Associate Professor, University of Missouri at St. Louis.
3. Dr. D. Bhaumik, previously Postdoctoral Fellow, The University of Cincinnati. Presently Computer Scientist, Evans and Sutherland Co.
4. Dr. K. Nayak, previously Graduate Student, The University of Cincinnati. Presently Postdoctoral Fellow, University of Texas at Arlington.
5. Dr. H. H. Jaffé, Professor of Chemistry The University of Cincinnati.
6. Mr. Y.-P. Ning, M.-Y. Tang, C.-Y. Jiang, S. Liu, and C.-C. Sun, Visiting Scholars, the University of Cincinnati.
7. Dr. G. S. Sur, Postdoctoral Fellow, the University of Cincinnati.
8. Mr. K. Metzger, previously Graduate Student, the University of Cincinnati.
9. Dr. A. Letton, previously Graduate Student, the University of Cincinnati. Presently Research Scientist, Dow Chemical Co.
10. Dr. L. DeBolt, previously Graduate Student, the University of Cincinnati. Presently Research Chemist, Sherwin Williams Co.

11. Dr. Z. Rigbi, Visiting Professor, University of Cincinnati.
12. Dr. S. J. Clarson, Postdoctoral Fellow, the University of Cincinnati.
13. Mr. W. D. Johnson, Graduate Student, the University of Missouri at St. Louis

D. INTERACTIONS

Essentially all of this material was presented in talks at National Meetings of the American Chemical Society and American Physical Society, at Gordon Research Conferences, and at various International Conferences. Numerous talks were also given at other universities and at industrial and government research laboratories. All of the work on the rigid polymers has been presented and discussed in detail at various Reviews of the Air Force Ordered Polymers Program, organized by Dr. T. E. Helminiak and held approximately annually at the Wright-Patterson Air Force Base in Ohio.


er 11, 1987

Calculation of Electronic Band Structures for Some Rigid Benzobisoxazole and Benzobisthiazole Polymers

D. BHAUMIK and J. E. MARK, *Department of Chemistry and Polymer Research Center, The University of Cincinnati, Cincinnati, Ohio 45221*

Synopsis

Quantum-mechanical methods were employed to calculate electronic band structures for the polybenzobisoxazole (PBO) and polybenzobisthiazole (PBT) chains originally synthesized and much studied because of their utility as high-performance fibers and films. For *cis*-PBO, *trans*-PBO, and *trans*-PBT chains in their coplanar conformations, the band gaps in the axial direction were found to be 1.72, 1.62, and 1.73 eV, respectively. Since *trans*-PBT is nonplanar, calculations on it were also carried out as a function of the rotation angle ϕ about the C—C bond joining the two ring systems in the repeat unit. The band gap was found to increase markedly with increase in nonplanarity, as would be expected from the decrease in charge delocalization. The calculations suggest the most likely value of ϕ to be ca. 30°, in good agreement with the experimental value 23° obtained by x-ray analysis of a crystalline *trans*-PBT model compound. At this value of ϕ , the calculated value of the band gap is 1.98 eV. All of these values are very close to the corresponding values of 1.4–1.9 eV reported for *trans*-polyacetylene, which should encourage further theoretical and experimental investigations of the electronic properties of these polymers.

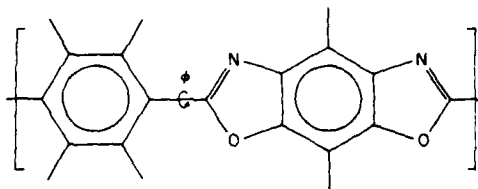
INTRODUCTION

The three polymers of interest in this study are the polybenzobisoxazole (PBO) chain shown in Figure 1, in which the two oxygen atoms of the repeat unit are *cis* to one another, its *trans* modification, and the *trans* modification of the corresponding polybenzobisthiazole (PBT), in which sulfur atoms replace each pair of oxygen atoms. As can be seen from the sketch, these polymers are very rigid and, as a result, they frequently form liquid-crystalline as well as crystalline phases. This has become of considerable interest, since fibers and films from these liquid-crystalline phases can have exceedingly good mechanical properties, even to very high temperatures.¹

Of interest here is the fact that the same structural features that give the desired chain rigidity also give extensive charge delocalization and resonance stabilization. Such characteristics could be conducive to electrical conductivity, a topic of much current interest in polymer science.²⁻¹³ The present goal was therefore to carry out preliminary calculations of electronic band gaps in order to determine whether any of these molecules show promise of being semiconducting, either undoped or as modified by a suitable dopant.

THEORY

For any molecule, including polymers, the LCAO approximation and Bloch's theorem can be used to describe the delocalized crystalline orbitals $\psi_n(\mathbf{k})$ as a periodic combination of functions centered at the atomic nuclei. For a one-

Fig. 1. Repeat unit of the *cis*-PBO chain.

dimensional system in which $N_1 - 1$ cells (repeat units) interact with the reference cell (Fig. 1) and for a basis set of length ω describing the wave function within a given cell, the n th crystal orbital $\psi_n(\mathbf{k})$ is defined as¹⁴⁻¹⁷

$$\psi_n(\mathbf{k}) = \sum_{\mu}^{\omega} C_{n\mu}(\mathbf{k}) \phi_{\mu}(\mathbf{k}) \quad (1)$$

where $\{\phi_{\mu}\}$ is the set of Bloch basis functions

$$\phi_{\mu}(\mathbf{k}) = \frac{1}{N_1^{1/2}} \sum_{j_1=-(N_1-1)/2}^{(N_1-1)/2} \exp(i\mathbf{k} \cdot \mathbf{R}_j) \chi_{\mu}(\mathbf{r} - \mathbf{R}_j) \quad (2)$$

The quantity \mathbf{k} is the wave vector. The position vector \mathbf{R}_j , in the one-dimensional case, is given by

$$\mathbf{R}_j = j_1 \mathbf{a}_1 \quad (3)$$

where \mathbf{a}_1 is the basic vector of the crystal. The crystal orbitals are, therefore,

$$\psi_n(\mathbf{k}) = \frac{1}{N_1^{1/2}} \sum_{j_1=-(N_1-1)/2}^{(N_1-1)/2} \sum_{\mu=1}^{\omega} \exp(i\mathbf{k} \cdot \mathbf{R}_j) C_{n\mu}(\mathbf{k}) \chi_{\mu}(\mathbf{r} - \mathbf{R}_j) \quad (4)$$

where $C_{n\mu}(\mathbf{k})$ is the expansion coefficient of the linear combination. The basis functions χ_{μ} are exponential functions of the Slater form. The present calculations included all the valence atomic orbitals of the H, C, N, and O atoms but for S atoms only s and p orbitals could be considered.

Using the extended Hückel approximation, we obtain the corresponding eigenvalues $E_n(\mathbf{k})$ and coefficients $C_{n\mu}(\mathbf{k})$ from the eigenvalue equation

$$H(\mathbf{k})C_n(\mathbf{k}) = S(\mathbf{k})C_n(\mathbf{k})E_n(\mathbf{k}) \quad (5)$$

TABLE I
Atomic Parameters for the Extended Hückel-Type Calculations

Atom	Orbital χ_{μ}	Slater exponent ζ_{μ}	Valence-state ionization potential $H_{\mu\mu}$ (eV)
H	1s	1.30	-13.6
C	2s	1.625	-21.4
C	2p	1.625	-11.4
N	2s	1.95	-26.0
N	2p	1.95	-13.4
O	2s	2.275	-32.3
O	2p	2.275	-14.8
S	2s	1.817	-20.3
S	2p	1.817	-13.3

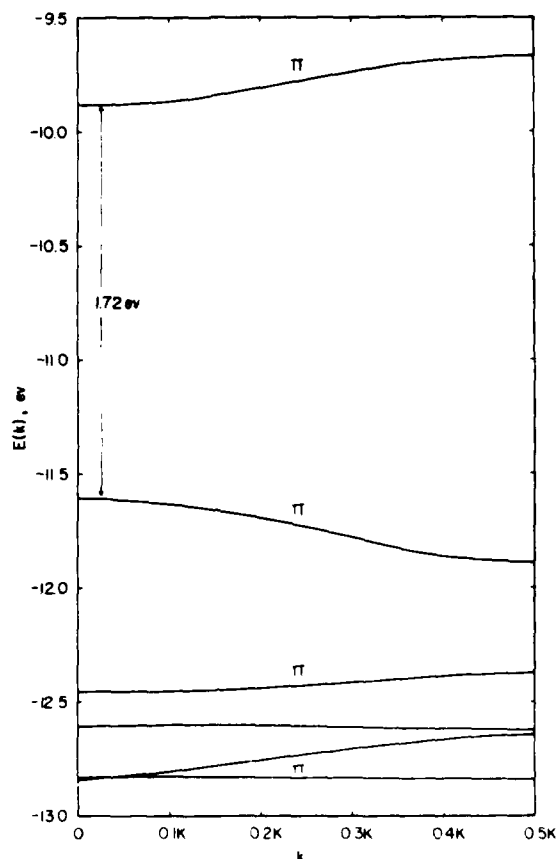


Fig. 2. Calculated band structure for *cis*-PBO in the coplanar conformation.

where $H(\mathbf{k})$ and $S(\mathbf{k})$ are the Hamiltonian and overlap matrices between Bloch orbitals defined as

$$H_{\mu\nu}(\mathbf{k}) = \langle \phi_{\mu}(\mathbf{k}) | H_{\text{eff}} | \phi_{\nu}(\mathbf{k}) \rangle \quad (6)$$

and

$$S_{\mu\nu}(\mathbf{k}) = \langle \phi_{\mu}(\mathbf{k}) | \phi_{\nu}(\mathbf{k}) \rangle \quad (7)$$

The distribution of the $E_n(\mathbf{k})$ values for a given n with respect to \mathbf{k} (usually within the first Brillouin zone: $-0.5\mathbf{K} \leq \mathbf{k} \leq 0.5\mathbf{K}$, where $\mathbf{K} = 2\pi/\mathbf{a}_1$) is the n th energy band. The set of all energy bands describes the band structures of the polymers. The atomic parameters of the extended Hückel calculation used in the present study were obtained from the literature^{16,17} and are detailed in Table I. In the present calculations, lattice sums were carried out to second-nearest neighbors.

The geometrical parameters (bond lengths and bond angles) of the repeat units of PBO and PBT were obtained from the x-ray structural studies conducted on model compounds by Fratini and co-workers.^{18,19} The two PBO polymers have

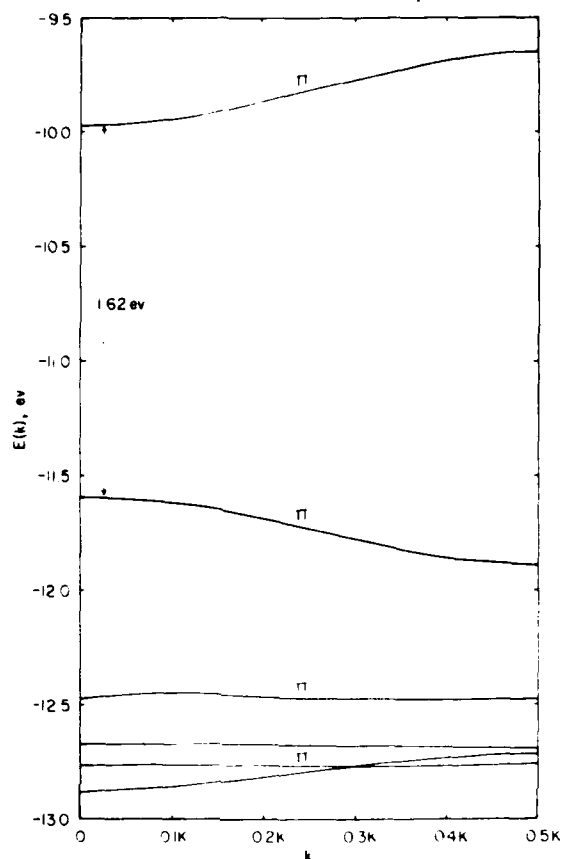


Fig. 3. Calculated band structure for *trans*-PBO in the coplanar conformation.

planar repeat units, but the *trans*-PBT repeat unit has the *p*-phenylene group rotated by 23.2° .^{1,18,19} To determine the most probable configuration of the *trans*-PBT, values of total energy per unit cell $\langle E_t \rangle$ were calculated from their band structures^{16,17} as a function of the dihedral angle ϕ (Fig. 1) in increments of 10° . The equation employed was^{16,20}

$$\langle E_t \rangle = \frac{1}{K} \int_{-K/2}^{K/2} E_t(\mathbf{k}) d\mathbf{k} \quad (8)$$

where $E_t(\mathbf{k})$ is the total energy at \mathbf{k} and, according to the extended Hückel method,

$$E_t(\mathbf{k}) = 2 \sum_n^{\text{occupied}} E_n(\mathbf{k})$$

RESULTS AND DISCUSSION

The repeat units of PBO and PBT contain even numbers of electrons, and therefore there is no partially filled band in their electronic band systems. The

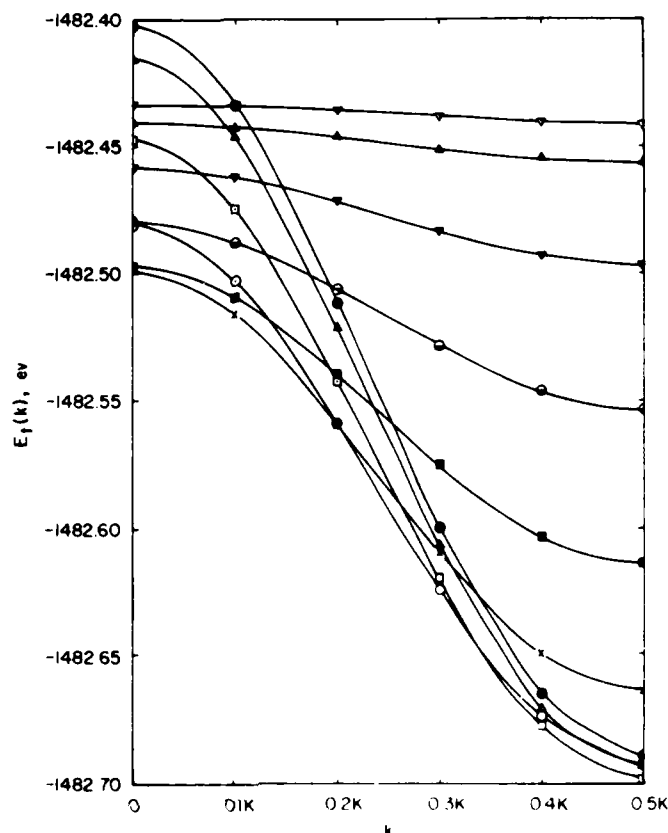


Fig. 4. Dependence of $E_t(\mathbf{k})$ on \mathbf{k} for *trans*-PBT: (●) $\phi = 0^\circ$, (▲) 10° , (◻) 20° , (○) 30° , (×) 40° , (■) 50° , (◐) 60° , (▼) 70° , (▲) 80° , (▼) 90° .

band structures of *cis*- and *trans*-PBO calculated as described above are shown in Figures 2 and 3, respectively. In each of these figures the conduction (i.e., the lowest unoccupied) band and the valence (i.e., the highest occupied) band are shown, along with four other occupied bands immediately below the valence band. The general shapes of the band structures of both polymers are very similar. In each case the valence band and conduction band are both made up of π orbitals. The band gap, which is the difference between the energies of the valence band and the conduction band, is 1.72 eV for *cis*-PBO and 1.62 eV for *trans*-PBO.

For *trans*-PBT, the plots of $E_t(\mathbf{k})$ vs. \mathbf{k} for different values of the dihedral metrical about the zone center of the first Brillouin zone, only one-half ($0 \leq \mathbf{k} \leq 0.5\mathbf{K}$) of each of these curves is shown in the figure. From eq. (8) it is clear that the energy $\langle E_t \rangle$ per repeat unit for a fixed ϕ is equal to the area enclosed by the corresponding $E_t(\mathbf{k})$ vs. \mathbf{k} curve over the range $-0.5\mathbf{K} \leq \mathbf{k} \leq 0.5\mathbf{K}$. The most probable configuration of PBT would correspond to that value of ϕ for which $\langle E_t \rangle$ would be maximum; i.e., when the $E_t(\mathbf{k})$ vs. \mathbf{k} curve encloses minimum area [because the $E_t(\mathbf{k})$ are all negative]. Qualitative estimation shows

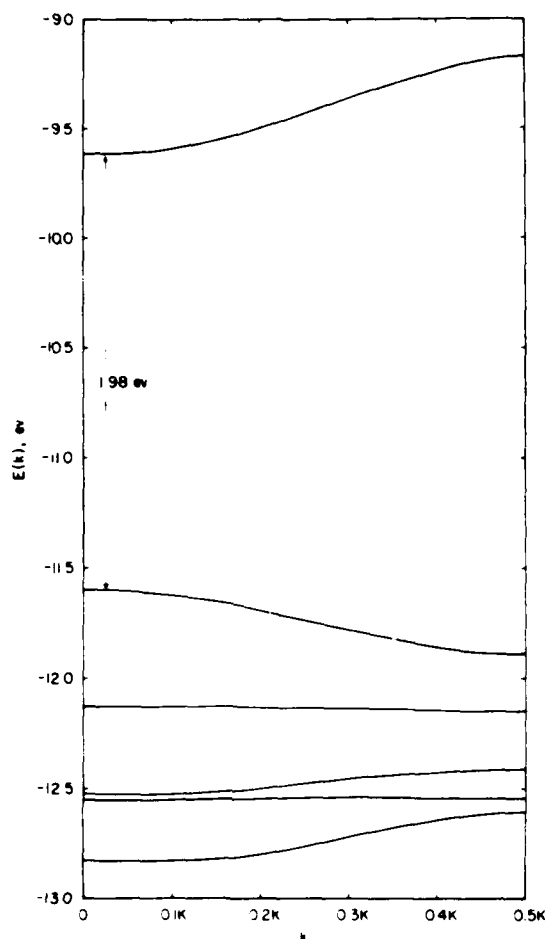


Fig. 5. Calculated band structure for *trans*-PBT in the conformation corresponding to the rotational angle $\phi = 30^\circ$.

that $\phi \approx 30^\circ$ is the prediction for the most stable form of *trans*-PBT. This is in very good agreement with the result obtained from crystal structure analysis of the *trans*-PBT model compound.^{1,18,19} However, both theoretical²¹ and experimental²² investigations indicate that *trans*-PBT polymer occurs in the planar form in the crystalline phase. The present theoretical results are consistent with this preference in that the variation of energy for the range $\phi = 30^\circ - 0^\circ$ is very small compared to that for $\phi = 30^\circ - 90^\circ$ and therefore, if the effect of interchain or interplanar interactions could be considered, the planar form of *trans*-PBT would be the most favorable form, as concluded previously.²¹ The band structure of *trans*-PBT at $\phi = 30^\circ$ is shown in Figure 5. Though the basic form of this band structure is very close to those of *cis*- and *trans*-PBO, the valence and conduction bands of PBT are no longer made up of π orbitals, but are now mixture of σ and π orbitals. The band gap 1.98 eV determined for *trans*-PBT is slightly higher than those of the PBO chains. This is because the overlap be-

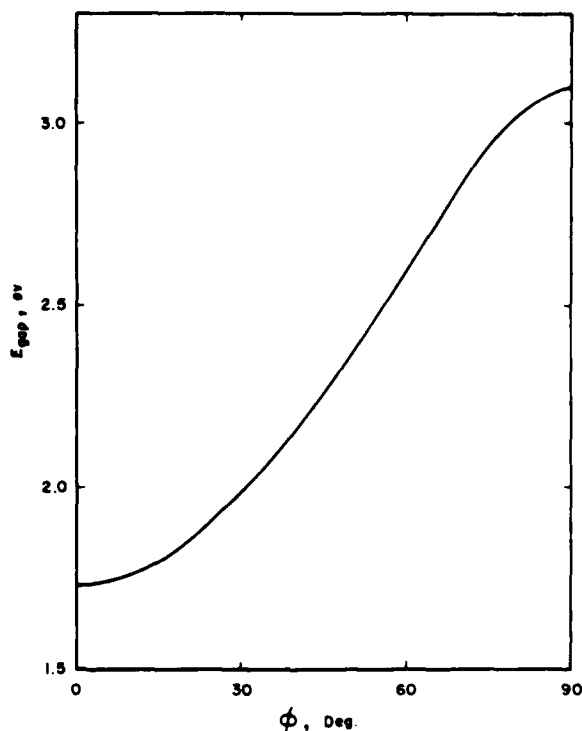


Fig. 6. Dependence of the *trans*-PBT band gap on the rotational angle ϕ .

tween the phenylene orbitals and the bisthiazole orbitals is less in the case of *trans*-PBT, because of its nonplanar structure. This overlap is maximum when the molecule is planar (as in the PBO chains). The variation of band gap with dihedral angle in *trans*-PBT is shown in Figure 6. As the dihedral angle decreases (i.e., the overlap between the phenylene and bisthiazole orbitals increases) the band gap decreases, and finally in the planar form (its favored configuration in the crystalline phase^{21,22}) the band gap becomes 1.73 eV. This value is very close to that of the PBO chains. No pertinent experimental results are available at the present time for comparisons. The only reported experimental value²³ of a band gap for *trans*-PBT is that (0.76 eV) obtained from measurements that may have involved ionic rather than electronic conductivity.

The calculated band gaps in PBO and PBT are similar to those determined experimentally in *trans*-polyacetylene (1.4–1.9 eV),²⁴ a polymer showing considerable promise as a semiconductor.^{4–13} This should encourage further theoretical and experimental investigations of the electronic properties of both PBO and PBT systems.

It is a pleasure to acknowledge financial support from the Air Force Office of Scientific Research (Chemical Structures Program, Division of Chemical Sciences), and Professors R. Hoffmann and M.-H. Whangbo for providing some of their computational programs and some very helpful advice.

References

1. A number of papers on these PBO and PBT polymers may be found in *Macromolecules*, **14**, (4) (1981).
2. W. L. McCubbin, *J. Polym. Sci. Part C*, **30**, 181 (1970).
3. A. F. Garito and A. J. Heeger, *Acct. Chem. Res.*, **7**, 232 (1974).
4. E. P. Goodings, *Chem. Soc. Rev.*, **5**, 95 (1976).
5. A. J. Epstein and J. S. Miller, *Sci. Am.*, **241**, 52 (1979).
6. P. Calvert, *Nature*, **284**, 213 (1980).
7. J. Mort, *Science*, **208**, 819 (1980).
8. H. Kiess and W. Rehwald, *Colloid Polym. Sci.*, **281**, 241 (1980).
9. G. Wegner, *Angew. Chem. Int. Ed. Engl.*, **20**, 361 (1981).
10. G. B. Street and T. C. Clarke, *IBM J. Res. Dev.*, **25**, 51 (1981).
11. D. Bloor, *New Scientist*, **4**, 577 (1982).
12. Papers, Symposium on Conducting Polymers, *Polym. Prepr. Am. Chem. Soc. Div. Polym. Chem.*, **23**, (1) (1982).
13. R. H. Baughman, J. L. Brédas, R. R. Chance, R. L. Elsenbaumer, and L. W. Shacklette, *Chem. Rev.*, **82**, 209 (1982).
14. J.-M. André, in *The Electronic Structure of Polymers and Molecular Crystals*, J.-M. André and J. Ladik, Eds., Plenum, New York, 1974.
15. R. Hoffmann, *J. Chem. Phys.*, **39**, 1397 (1963).
16. M.-H. Whangbo and R. Hoffmann, *J. Am. Chem. Soc.*, **100**, 6093 (1978).
17. M.-H. Whangbo, R. Hoffmann, and R. B. Woodward, *Proc. R. Soc. London Ser. A*, **A366**, 23 (1979).
18. M. W. Wellman, W. W. Adams, D. R. Wiff, and A. V. Fratini, Air Force Technical Report AFML-TR-79-4184, Part I; private communications.
19. M. W. Wellman, W. W. Adams, R. A. Wolff, R. A. Dudis, D. R. Wiff, and A. V. Fratini, *Macromolecules*, **14**, 935 (1981).
20. A. Imamura, *J. Chem. Phys.*, **52**, 3168 (1970).
21. W. J. Welsh, D. Bhaumik, and J. E. Mark, *Macromolecules*, **14**, 947 (1981).
22. J. A. Odell, A. Keller, E. D. T. Atkins, and M. J. Miles, *J. Mater. Sci.*, **16**, 3309 (1981).
23. R. E. Barker, Jr., and K. R. Lawless, Air Force Report No. UVA/525630/M582/102.
24. C. K. Chiang, A. J. Heeger, and A. G. MacDiarmid, *Ber. Bunsenges. Phys. Chem.*, **83**, 407 (1979), and references cited therein.

Received September 30, 1982

Accepted January 13, 1983

CNDO/2 MOLECULAR ORBITAL CALCULATIONS ON THE ANTIFOLATE DAMP
AND SOME OF ITS ANALOGUES: CONFORMATIONAL CHARACTERISTICS

William J. Welsh, James E. Mark

Department of Chemistry and Polymer Research Center, University of Cincinnati,
Cincinnati, OH 45221 (USA)

Vivian Cody

Medical Foundation of Buffalo, Inc., Buffalo, NY 14203 (USA)

and Sigmund F. Zakrzewski

Roswell Park Memorial Institute, Buffalo, NY 14263 (USA)

Introduction

DAMP-ES [2,4-diamino-5-(1-adamantyl)-6-methylpyrimidine ethylsulfonate salt] (Fig. 1) is a potent inhibitor of mammalian dihydrofolate reductase (DHFR) and inhibits growth of cultured cells as effectively as methotrexate (1).

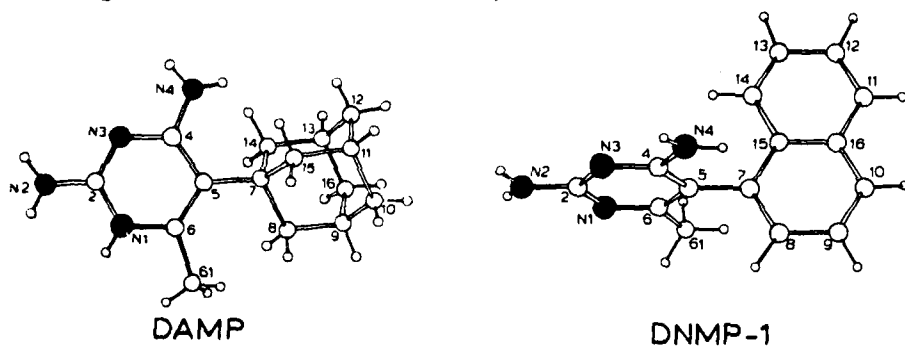


Fig. 1. Illustration of DAMP (protonated) and DNMP-1.

It has been shown (1-4) that the inhibitory activity toward DHFR by antagonists of the diaminopyrimidine class increases with the increased hydrophobicity of lipophilic straight or branched chain hydrocarbon groups substituted in the 5-position. However, the inhibitory activity of 5-(1-adamantyl), and to a lesser degree 5-(1-cyclohexyl)-diaminopyrimidines, is much greater than that predicted by hydrophobicity alone. In contrast, there is almost a complete loss of inhibitory activity

with 5-(1-naphthyl) substitution (DNMP-1) (Fig. 1.) but not with 5-(2-naphthyl) substitution (DNMP-2).

Crystallographic data (5) show that DAMP-ES has a severely distorted, N1 protonated pyrimidine ring and has steric crowding of the 6-methyl and adamantyl hydrogens whereas DNMP-1 (as a methanol complex) has a planar, non-protonated pyrimidine ring that is nearly perpendicular to the naphthalene ring. In the present study CNDO/2 molecular orbital calculations with direct geometry optimization were carried out on DAMP, its N1-protonated form DAMPH^+ , DNMP-1, DNMPH^+-1 , and DNMP-2. The calculated geometries largely reproduce those observed in the crystalline state. In particular, the calculated results corroborate the observed torsional distortions within the pyrimidine ring of DAMP-ES. The electronic charge distributions of DAMP, DNMP-1, and DNMP-2 are nearly identical for equivalent atoms, hence differences in biological activity apparently are not electrostatic in nature. Conformational energies were calculated as a function of rotation about the C5-C7 bond. The results indicate large barriers to rotation for DAMPH^+ , with no conformation being successful in relieving the ring distortions caused by severe steric conflicts. For DNMP-1 and DNMP-2 the C5-C7 bond is more flexible but large barriers are encountered for the coplanar conformations.

Methodology

The general technique is comprised of the semi-empirical CNDO/2 molecular orbital theory (6) nested in an iterative scheme for achieving direct geometry optimization (7,8). This method has already proved successful in characterizing the geometry, electronic structure, and conformational properties of species similar in structure to those studied here (9,10). In the conformational energy calculations, values of the CNDO/2 total energy were calculated as a function of the rotational angle ϕ about the C5-C7 bond varied in increments of 20-30°. The energy associated with a given conformation was taken as the difference in total energy between that conformation and the conformation obtained upon optimization of the structure observed in the crystalline state (5).

Results and Discussion

The observed and calculated geometries of DAMPH^+ and of DNMP-1 are illustrated in Figs. 2 and 3, respectively.

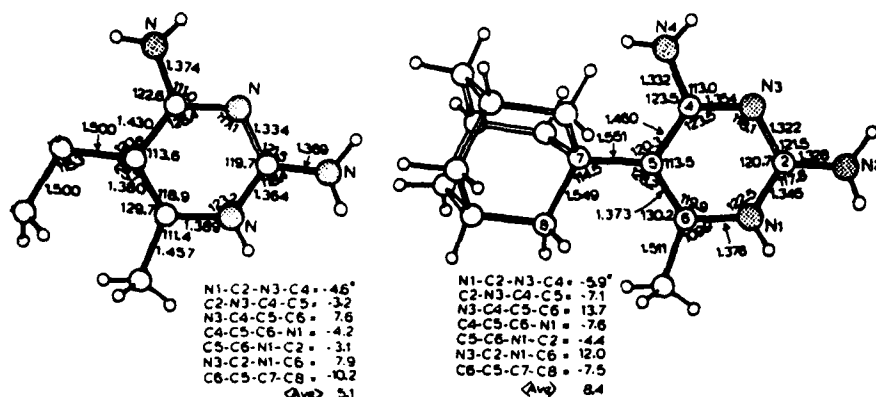


Fig. 2. Calculated (left) and observed geometry of DAMP (protonated).

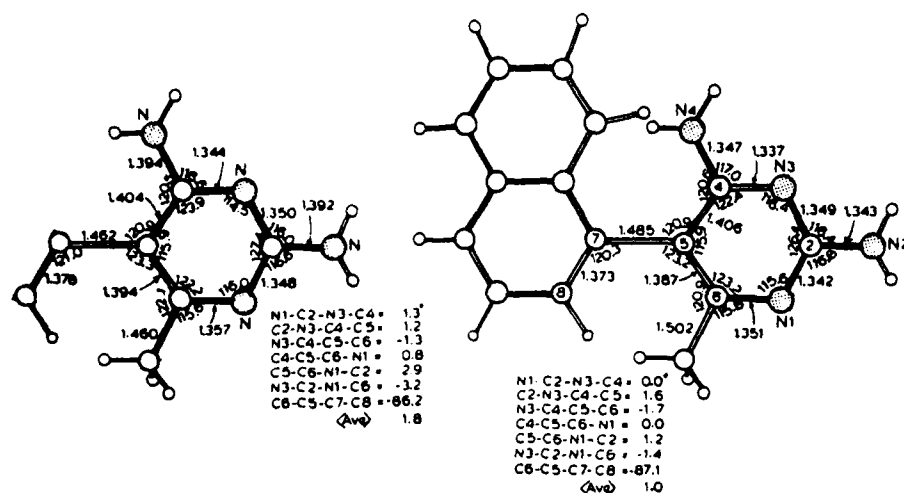


Fig. 3. Calculated (left) and observed geometry of DNMP-1.

Calculated and observed bond angles and bond lengths are nearly identical, and the ring distortions observed in DAMPH⁺ (i.e., protonated DAMP-ES) are also reproduced but with lower values. Likewise, both calculated and observed results for DNMP-1 give a nearly flat pyrimidine ring. Further calculations on DAMP and on DNMPH⁺-1 show the effect on ring protonation on structure. Specifically, with protonation at N1 the bonds about it shorten while the bond angles C6-N1-C2 open

and N1-C2-N3 close by about 6° , with minor adjustments elsewhere. Protonation also increases the extent of ring distortions. The results for DNMP-2 are similar to those for DNMP-1.

The partial atomic charges for selected atoms in DAMP and in DNMP-1 are listed in Table 1.

Table 1. Fractional Charges^a of Selected Atoms in DAMP and DNMP

Atom	DAMP	DNMP
N1	-0.351	-0.353
N3	-0.361	-0.361
N2	-0.308	-0.306
N4	-0.312	-0.314

^aIn units of fraction of the electron's charge.

Their charge distributions are nearly identical, indicating that the observed differences in biological activity are not explicable in terms of electrostatic arguments. Based on comparisons of partial charges, protonation would appear to be preferred at N1 or N3 rather than at N2 or N4.

The conformational energies with respect to rotation ϕ about the C5-C7 bond in DAMPH⁺ and DNMP-1 are illustrated in Fig. 4.

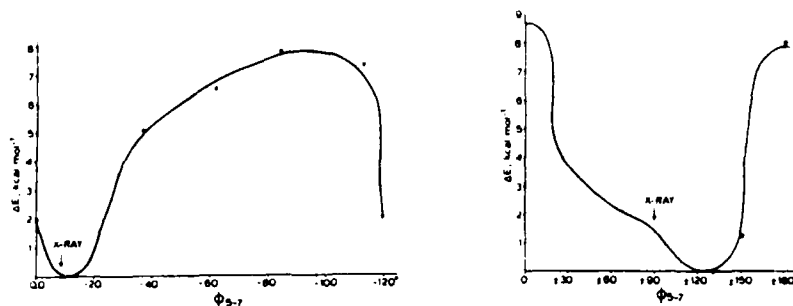


Fig. 4. Calculated conformation energy ΔE versus ϕ_{5-7} for DAMPH⁺ (left) and DNMP-1.

For DAMPH⁺ the conformation of minimum energy corresponds nearly to that found in the crystalline state. The barrier to rotation away from the preferred conformation is very steep and has a broad maximum located in the region 30-110° (within the 0-120° total configuration space) and is about 8.0 kcal mol⁻¹ above the minimum. No value of ϕ was successful in relieving the severe steric conflicts between the adamantyl group and 4- and 6-substituent groups on the pyrimidine ring. The barrier effectively locks the C5-C7 bond and precludes relief of the steric conflicts responsible for the distortions, which are further aggravated by protonation.

The C5-C7 bond in DNMP-1 is overall more flexible than that in DAMPH⁺ in terms of more accessible regions of configuration space. The calculated energy minimum is located at $\phi = 0^\circ$ (corresponding to the coplanar conformation with the naphthyl group nearest the C4-amino group) with a barrier of ca. 1.5 kcal mol⁻¹ to $\phi = 90^\circ$ observed in the crystalline state. Within ca. 30° of either coplanar conformation the energy rises sharply to ca. 8.0-8.5 kcal mol⁻¹. The results in this regard for DNMP-2 are very similar to those obtained for DNMP-1. The calculated preferred conformation of DNMP-1 is hence different from that (perpendicular) observed in the crystalline state and exhibits negligible ring distortions. The geometry and charge distribution are only slightly affected by rotation.

Conclusions

The present results indicate that the methodology is applicable to DAMP and related species. Calculated bond lengths and bond angles are in quantitative agreement with those observed, and the calculated torsional angles can be used in a semi-quantitative fashion for comparisons. It is the intent of the authors to extend these calculations to other, related species to explore further the structural and conformational aspects of DHFR-drug specificity.

Acknowledgments

It is a pleasure to acknowledge the financial support provided by the Air Force Office of Scientific Research (Grant AFOSR 78-3683, Chemical Structures Program, Division of Chemical Sciences).

References

1. Ho, Y. K., Hakala, M. T. and Zakrzewski, S. F., *Cancer Research* 32, 1023-1028 (1972).
2. Kawai, I., Mead, L. H., Drobnik, J. and Zakrzewski, S. F. *J. Med. Chem.* 18, 272 (1975).
3. Ho, Y.K., Zakrzewski, S. F. and Mead, L. H., *Biochemistry* 12, 1003 (1973).
4. Zakrzewski, S. F., *J. Biol. Chem.* 238, 1485, 4002 (1963).
5. Cody, V. and Zakrzewski, S. F., *J. Med. Chem.* 25, 427-430 (1982).
6. Pople, J. A. and Beveridge, D. L., "Approximate Molecular Orbital Theory", McGraw-Hill, New York, N.Y., 1970.
7. Kondo, N., Ph.D. Dissertation, University of Cincinnati (1978).
8. Jaffe', H. H., Program 315, Quantum Chemistry Program Exchange, Indiana University.
9. Welsh, W. J., Jaffe', H. H., Mark, J. E., and Kondo, N., *Die Makromolekulare Chemie* 183, 801 (1982).
10. Welsh, W. J. and Mark, J. E., *Polym. Prepr., American Chemical Society, Div. Polym. Chem.*, 23(2), 193 (1982), and references cited therein.

A Theoretical Investigation of Chain Packing and Electronic Band Structure of the Rigid-Rod Polymer *Trans*-Poly(*p*-Phenylene Benzobisthiazole) in the Crystalline State

D. BHAUMIK and J. E. MARK, *Department of Chemistry and the Polymer Research Center, The University of Cincinnati, Cincinnati, Ohio 45221*

Synopsis

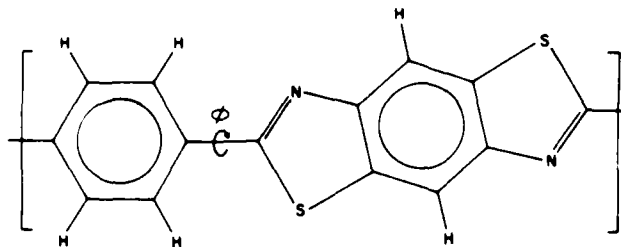
The extended Hückel method was employed to calculate electronic band structures in *trans*-poly(*p*-phenylene benzobisthiazole) (*trans*-PBT) in an attempt to elucidate the packing and electronic properties of these chains in the crystalline state. The unit-cell energies thus calculated indicate that the most stable arrangement for *trans*-PBT corresponds to the chains in planar configurations, at an interplanar spacing of 3.5 Å, and shifted axially by 3.0 Å relative to one another. These calculated results are in good agreement with experimental results obtained on the polymer and on relevant model compounds. No discernible dispersion of the energy bands perpendicular to the planes is observed, indicating that the neighboring chains are electronically noninteractive, as was found earlier for *trans*-polyacetylene and polyethylene. Similarly, the band gap of 1.69 eV in the axial direction for one of a pair of chains was nearly the same as that, 1.73 eV, calculated previously for an isolated *trans*-PBT chain. These values are in the range 1.4–1.9 eV reported for *trans*-polyacetylene, which has been extensively studied because of its promise as a semiconductor.

INTRODUCTION

The rigid-rod polymer *trans*-poly(*p*-phenylene benzobisthiazole) (*trans*-PBT),¹ shown schematically in Figure 1, has been studied with regard to its electronic band structure in a preliminary way.² This first attempt² at characterizing the electrical properties of this interesting class of polymers was very useful, but focused exclusively on the axial direction of the chains. Since the molecules form highly ordered fibers,¹ however, it is possible to carry out experimental measurements perpendicular as well as parallel to the chain direction, and it thus becomes important to calculate the effect of interchain interactions on electronic properties. Obtaining such information on *trans*-PBT in the crystalline state was the goal of the present investigation. Specific aspects of particular interest were the use of band structures to elucidate chain packing arrangements, calculating the energy band gap perpendicular to the chains, and estimating the effect of interchain interactions on the band gap in the axial direction.

THEORY

The band structure calculations used the tight-binding scheme based upon the extended Hückel approximation, all of which is well documented in the lit-

Fig. 1. Repeat unit of the *trans*-PBT chain.

erature.²⁻⁶ In this method the delocalized crystalline orbitals $\psi_n(\mathbf{k})$ are formed from the set of basis atomic orbitals $\{\chi_\mu\}$, in the one-dimensional case, as

$$\psi_n(\mathbf{k}) = \frac{1}{N_1^{1/2}} \sum_{j_1=-(N_1-1)/2}^{(N_1-1)/2} \sum_{\mu=1}^{\infty} \exp(i\mathbf{k} \cdot \mathbf{R}_j) C_{n\mu}(\mathbf{k}) \chi_\mu(\mathbf{r} - \mathbf{R}_j) \quad (1)$$

in which $N_1 - 1$ cells are interacting with the central reference cell, ω is the length of basis set, \mathbf{k} is the wave vector, and \mathbf{R}_j (the position vector) is given by $\mathbf{R}_j = j\mathbf{a}$ (with \mathbf{a} being the basic vector of the crystal). Using the extended Hückel approximation, we obtain the corresponding eigenvalues $E_n(\mathbf{k})$ and coefficients $C_{n\mu}(\mathbf{k})$ from the eigenvalue equation

$$H(\mathbf{k})C_n(\mathbf{k}) = S(\mathbf{k})C_n(\mathbf{k})E_n(\mathbf{k}) \quad (2)$$

where $H(\mathbf{k})$ and $S(\mathbf{k})$ have the usual meaning, as Hamiltonian and overlap matrices, respectively. The distribution of the $E_n(\mathbf{k})$ values for a given n with respect to \mathbf{k} (usually within the first Brillouin zone, $-0.5\mathbf{K} \leq \mathbf{k} \leq 0.5\mathbf{K}$, where $\mathbf{K} = 2\pi/\mathbf{a}$) is the n th energy band. The set of all energy bands describes the band structures of the polymers. The present calculations include all the valence atomic orbitals of the H, C, N, and O atoms but for S atoms only s and p orbitals could be considered because of space limitations in the computer program. The atomic parameters required in the present study were obtained from the literature.^{5,6}

In the present study the crystal lattice was assumed to be one-dimensional, and separate calculations were performed to determine the band structures along the axial and perpendicular (packing) directions. From x-ray crystal structure analysis^{7,8} of the model PBT compound the relative axial shift between two chains was found to be approximately 4.5 Å. Both x-ray and electron diffraction studies,⁹ and molecular mechanics calculations¹⁰ indicate that the polymer is planar in the crystalline state. In the case of the spacing between the two chains, theoretical¹¹ and experimental^{7,8} studies predicted it to be 3.5 Å. As is shown in Figure 2, the unit cell contains two PBT repeat units (A and B) stacked one above the other and separated by 3.5 Å. To predict the relative axial shift between two chains, one chain (e.g., B) is gradually shifted along the axis, in steps of 0.5 Å, to a maximum displacement of 5.0 Å. In doing so a portion [the dotted part in Fig. 2(b)] of the repeat unit B falls outside the unit-cell boundary, and thus the corresponding part (the dashed part in the figure) of the repeat unit is introduced from the opposite side, within the unit-cell boundary, thus always keeping constant the number of atoms of each type within the cell. The chain

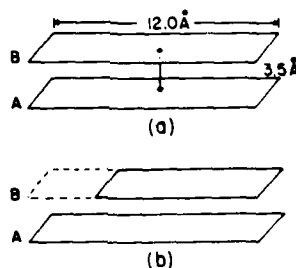


Fig. 2. Sketches showing (a) the stacking of the *trans*-PBT repeat units, and (b) the reconstitution of the upper repeat unit as it is slid relative to the lower one.

B is shifted relative to chain A to a maximum value of only 5.0 Å of the total repeat unit length of ca. 12.0 Å, because of the symmetry of the chains. In each step of the shift the dihedral angle ϕ (Fig. 1) around the C—C bond between the phenylene ring and thiazole part of the *trans*-PBT chains is varied in increments of 10°, from 0° to 90°, to locate the probable configuration of the individual chains in the crystalline state. For each configuration and arrangement the total energy per unit cell $\langle E_t \rangle$ is calculated from its band structure.^{5,6} This is done as a function of the relative axial shift Δx and of the dihedral angle ϕ , respectively, using the equation^{5,12}

$$\langle E_t \rangle = \frac{1}{K} \int_{-K/2}^{K/2} E_t(\mathbf{k}) d\mathbf{k} \quad (3)$$

where $E_t(\mathbf{k})$ is the total energy at \mathbf{k} and, according to the extended Hückel method,

$$E_t(\mathbf{k}) = 2 \sum_n^{\text{occupied}} E_n(\mathbf{k}) \quad (4)$$

The unit-cell structure that corresponds to the minimum total energy is identified as the most stable packing arrangement.

In the present calculations lattice sums were carried out to second-nearest neighbors. The geometrical parameters (bond lengths and bond angles)^{7,9} of the repeat unit of *trans*-PBT were obtained from the x-ray structural studies conducted on model compounds by Fratini and co-workers.^{7,8}

RESULTS AND DISCUSSION

The band structures of the *trans*-PBT unit cell along the perpendicular (packing) direction are computed for different values of relative axial shift Δx and dihedral angle ϕ and the curves of $E_t(\mathbf{k})$ against \mathbf{k} in each case are plotted. From eq. (3) it is clear that the energy $\langle E_t \rangle$ per unit cell will be minimum when the corresponding $E_t(\mathbf{k})$ vs. \mathbf{k} curve encloses maximum area [because the $E_t(\mathbf{k})$ are all negative]. Two representative plots are shown in Figures 3 and 4. Since the curves of $E_t(\mathbf{k})$ against \mathbf{k} are symmetrical about the center of the first Brillouin zone, only one-half ($0 \leq \mathbf{k} \leq 0.5\mathbf{K}$) of each of these curves is shown in the figures. It has been found that whatever the relative shift between the chains, the minimum energy of the unit cell always corresponds to the $\phi = 0^\circ$ configu-

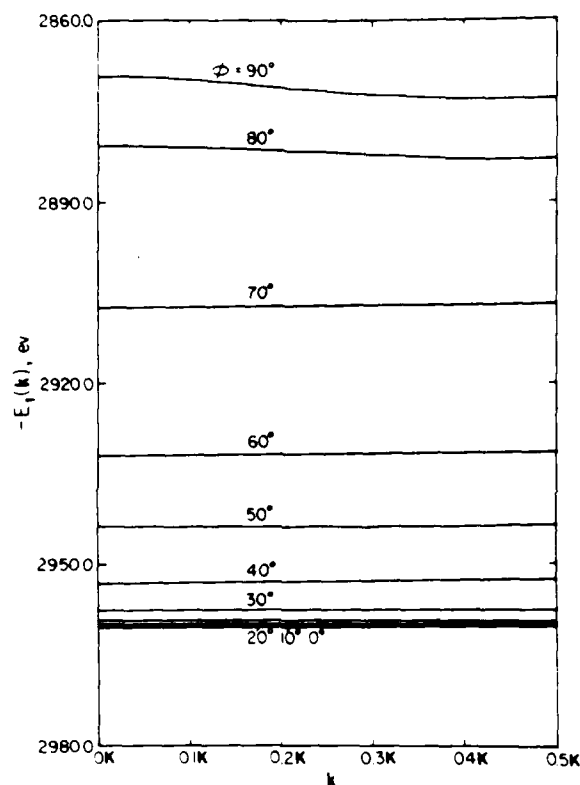


Fig. 3. Dependence of $E_t(\mathbf{k})$ on \mathbf{k} in the packing direction calculated as a function of the dihedral angle ϕ .

ration of the individual chains. Thus the chains are predicted to favor the planar form in the crystalline phase, which is in agreement with experiment⁹ and with the results of molecular mechanics calculations.¹⁰

Figure 3 shows the variation of $E_t(\mathbf{k})$ with \mathbf{k} for different values of the dihedral angle ϕ , for a typical relative shift $\Delta x \approx 3.0 \text{ \AA}$. In the earlier theoretical investigation,² in which interchain interactions were not included, it was found that although $\phi = 30^\circ$ corresponded to the lowest-energy form of *trans*-PBT, the variation of energy in the range $\phi = 30^\circ$ – 0° was very small compared to that for $\phi = 30^\circ$ – 90° . Therefore it was concluded that if the effect of interchain or interplanar interactions could be considered, the planar form of *trans*-PBT would probably be the most favorable. This has been confirmed in the present study. Specifically, it has been found that the inclusion of interchain interactions moves the minimum to $\phi = 0^\circ$, and that the variation of unit-cell energy from 0° to 30° is indeed very small (Fig. 3) as was concluded from molecular mechanics calculations.¹⁰

The plots of $E_t(\mathbf{k})$ against \mathbf{k} for different values of the relative shift at $\phi = 0^\circ$ are shown in Figure 4. It is clear from this figure that a relative shift of $\Delta x \approx 3.0 \text{ \AA}$ will be the most favorable arrangement of the chains. This value is somewhat smaller than the experimental^{7,8} value 4.5 \AA obtained for a PBT model compound, but it is worth mentioning that using molecular mechanics¹¹ a relative

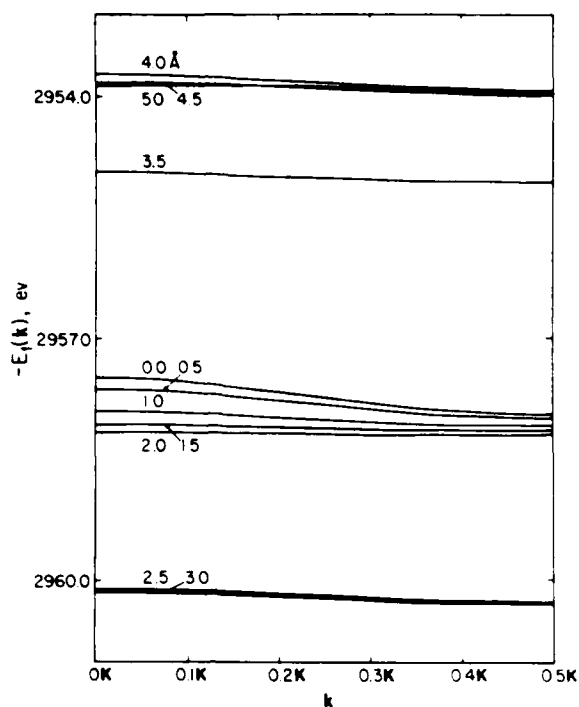


Fig. 4. Dependence of $E_c(k)$ on k in the packing direction calculated as a function of the axial shift Δx between chains.

shift of 3.0 Å was computed for poly(*p*-phenylene benzobisoxazole) (PBO) where the sulfur atoms are replaced by oxygen atoms and the chain is known to be planar. The agreement between theoretical and experimental values of Δx for PBT could, of course, be considerably better for the polymeric chains, which have not yet been studied experimentally in this regard.

Figure 5 represents the arrangement of the two chains at $\Delta x = 3.0$ Å and $\phi = 0^\circ$. The band structures of *trans*-PBT along the perpendicular (packing) direction are shown for this case in Figure 6, where the conduction (lowest unoccupied) band and the valence (highest occupied) band along with four other occupied bands immediately below the valence band are depicted. No discernible dispersion of energy bands along this direction is detected, which indi-

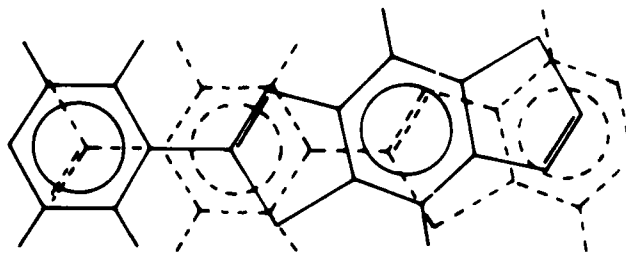


Fig. 5. Sketch of two planar *trans*-PBT repeat units at an axial shift $\Delta x = 3.0$ Å.

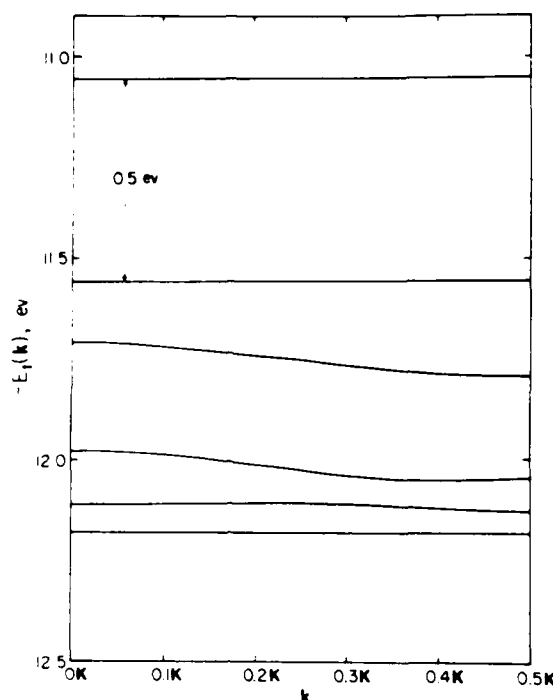


Fig. 6. Band structure in the packing direction for dihedral angle $\phi = 0^\circ$ and axial shift $\Delta x = 3.0$ Å.

cates that neighboring chains are noninteractive. The same conclusion was reached in calculations¹³ of the band structures of polyacetylene and polyethylene. This weakness in chain-chain interaction is expected at the large interchain separation (3.5 Å) of *trans*-PBT chains. Although the sulfur d orbitals could not be included because of the size limitation of the computer program presently available and the large number of atoms in a repeat unit of PBT, the possibility of improvement in dispersion by the inclusion of d orbitals does not appear promising at this large interchain separation. The weak chain-chain interactions could also be anticipated from the weakly dispersed $E_t(k)$ vs. k curves in Figures 3 and 4.

The band structure of the *trans*-PBT unit cell along the axial direction with $\Delta x = 3.0$ Å and $\phi = 0^\circ$ is shown in Figure 7. The computed band gap along this direction is 1.69 eV, which is almost equal to the band gap calculated² in the absence of the interchain interactions for a planar configuration of the chain. This shows that neighboring chains have little effect on the band gap. Most important, however, is the fact that this band gap value is in the range 1.4–1.9 eV reported for *trans*-polyacetylene,¹⁴ which has been extensively studied because of its promise as a semiconductor.

It is a pleasure to acknowledge financial support from the Air Force Office of Scientific Research (Chemical Structures Program, Division of Chemical Sciences), and to thank Professors R. Hoffmann and M.-H. Whangbo for providing some of their computational programs and some very helpful advice.

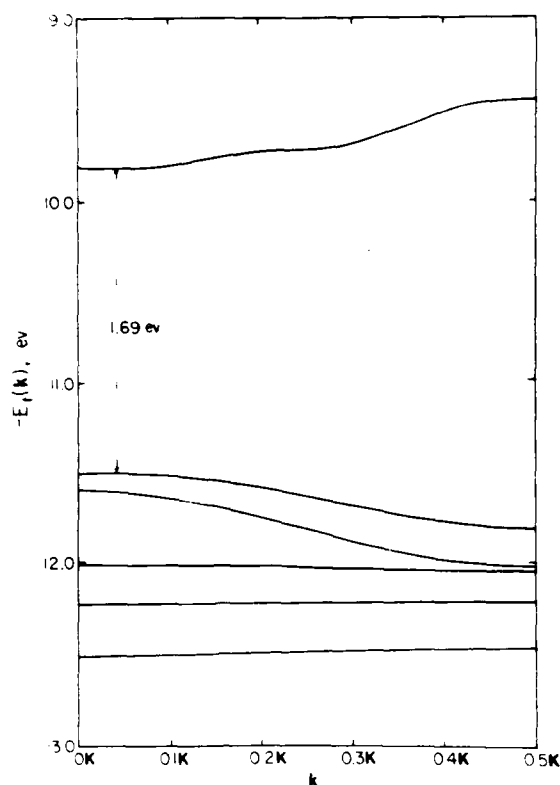


Fig. 7. Band structure in the axial direction for $\phi = 0^\circ$ and $\Delta x = 3.0 \text{ \AA}$. All the bands arise from π orbitals.

References

1. A number of papers on *trans*-PBT polymers may be found in *Macromolecules*, **14** (4) (1981).
2. D. Bhaumik and J. E. Mark, *J. Polym. Sci. Polym. Phys. Ed.*, **21**, 1111 (1983).
3. J.-M. André, in *The Electronic Structure of Polymers and Molecular Crystals*, J.-M. André and J. Ladik, Ed., Plenum, New York, 1974.
4. R. Hoffmann, *J. Chem. Phys.*, **39**, 1397 (1963).
5. M.-H. Whangbo and R. Hoffmann, *J. Am. Chem. Soc.*, **100**, 6093 (1978).
6. M.-H. Whangbo, R. Hoffmann, and R. B. Woodward, *Proc. R. Soc. London Ser. A*, **366**, 23 (1979).
7. M. W. Wellman, W. W. Adams, D. R. Wiff, and A. V. Fratini, Air Force Technical Report AFML-TR-79-4184, part I; private communications.
8. M. W. Wellman, W. W. Adams, R. A. Wolff, R. A. Dudis, D. R. Wiff, and A. V. Fratini, *Macromolecules*, **14**, 935 (1981).
9. J. A. Odell, A. Keller, E. D. T. Atkins, and M. J. Miles, *J. Mater. Sci.*, **16**, 3309 (1981).
10. W. J. Welsh, D. Bhaumik, and J. E. Mark, *Macromolecules*, **14**, 947 (1981).
11. D. Bhaumik, W. J. Welsh, H. H. Jaffé, and J. E. Mark, *Macromolecules*, **14**, 951 (1981).
12. A. Imamura, *J. Chem. Phys.*, **52**, 3168 (1970).
13. R. V. Kasowski, W. Y. Hsu, and E. B. Caruthers, *J. Chem. Phys.*, **72**, 4896 (1980).
14. C. K. Chiang, A. J. Heeger, and A. G. MacDiarmid, *Ber. Bunsenges Phys. Chem.*, **83**, 407 (1979), and references cited therein.

Received June 6, 1983

Accepted July 26, 1983

CNDO/2 MOLECULAR ORBITAL CALCULATIONS ON THE ANTIFOLATE DAMP AND SOME RELATED SPECIES: STRUCTURAL GEOMETRIES, RING DISTORTIONS, CHARGE DISTRIBUTIONS AND CONFORMATIONAL CHARACTERISTICS

W. J. WELSH,[†] V. CODY,[‡] J. E. MARK[†] and S. F. ZAKRZEWSKI[¶]

[†]Department of Chemistry and Polymer Research Center, University of Cincinnati,
Cincinnati, OH 45221, USA; [‡]College of Mt. St. Joseph,
Mount St. Joseph, OH 45051, USA; [§]Medical Foundation of Buffalo, Inc.,
Buffalo, NY 14203, USA; [¶]Roswell Park Memorial Institute,
Buffalo, NY 14263, USA

Geometry-optimized CNDO/2 molecular orbital calculations were carried out on 2, 4-diamino-5-(1-adamantyl)-6-methylpyrimidine (DAMP), a potent inhibitor of mammalian dihydrofolate reductase which is now in clinical trials, and on its inactive 5-(1-naphthyl) analogue (DNMP-1). Crystallographic data show that DAMP (as the ethylsulfonate salt), has a severely distorted, N1 protonated, pyrimidine ring and has steric crowding of the 6-methyl and adamantyl hydrogens whereas DNMP-2 (as a methanol complex) has a planar, nonprotonated pyrimidine ring that is nearly perpendicular to the naphthalene ring. The CNDO/2 results largely reproduce the crystal structure geometry and show that the ring distortions in DAMP are initiated by steric conflicts between the adamantyl group and the 4- and 6-substituents on the ring. In DNMP-1, the non-interfering naphthyl ring induces little strain within the pyrimidine ring and the effect of protonation is negligible. Rotation about the bond joining the two ring groups is restricted in DAMP by a broad barrier of ca. 8.0 kcal mol⁻¹, and no conformation was successful in relieving steric conflicts and hence reducing the ring distortions. In DNMP-1, rotation is less hindered overall with a broad region of accessible conformational space and a maximum barrier of ca. 7.2 kcal mol⁻¹ for the coplanar conformation. The electronic charge distributions of DAMP and DNMP-1 are almost identical and protonation is preferred at N1 rather than at N3 by ca. 3.7 kcal mol⁻¹ for both DAMP and DNMP-1. The calculations establish that the present method of calculation is a predictive tool with regard to the structure and conformational characteristics of these and related species.

INTRODUCTION

DAMP [2, 4-diamino-5-(1-adamantyl)-6-methylpyrimidine] is a potent inhibitor of mammalian dihydrofolate reductase (DHFR) and inhibits growth of cultured cells as effectively as the drug methotrexate (Ho *et al.*, 1972). As a result, DAMP is undergoing Phase I clinical trials as an anti-tumor agent.

It has been shown (Ho, Haskin and Zakrzewski, 1972; Kawai *et al.*, 1975; Zakrzewski, 1963) that the inhibitory activity toward DHFR by antagonists of the diaminopyrimidine class increases with the increased hydrophobicity of lipophilic straight or branched chain hydrocarbon groups substituted in the 5-position. However, the inhibitory activity of 5-(1-adamantyl) and, to a lesser degree, 5-(1-cyclohexyl)-diaminopyrimidines, is much greater than that predicted by hydrophobicity alone, suggesting that other, more subtle features regarding these species play a role in determining activity. In contrast, there is almost a complete loss

of inhibitory activity with 5-(1-naphthyl) substitution (DNMP-1) but not with 5-(2-naphthyl) substitution (DNMP-2) (Kavar *et al.*, 1975; Ho *et al.*, 1973).

The x-ray crystal structure determinations (Cody and Zakrzewski, 1982) of DAMP and DNMP-1 (Figure 1) have been carried out. The data for DAMP, as the ethane-sulfonate salt, show that the pyrimidine ring, protonated at N1, is severely distorted from coplanarity with regard to its 4, 5, 6-substituents as a result of the steric interference of the 6-methyl hydrogens with those of the adamantyl ring. In addition to the twist of these substituents above and below the pyrimidine plane, the angles involving these groups are expanded. The orientation of the adamantyl ring with respect to the pyrimidine ring [C6C5-C7C8] is -7.5° . All of the amino hydrogens are involved in hydrogen bonds. None of these distortions is evident in the structure of DNMP-1 methanol complex. The naphthalene ring is nearly perpendicular [C6C5-C7C8 = -87.1°] to the pyrimidine ring which is itself coplanar with the 4,5,6-substituents. N1 is unprotonated in this structure and all of the amino hydrogens but one are involved in hydrogen bonding. Insertion of DAMP and DNMP-1 into the DHFR binding site, using computer-graphics models based on these data, indicates that their disparity in bioactivity is largely due to severe steric interference encountered by the latter (Cody and Zakrzewski, 1982).

The primary aim of the present study was to conduct a more detailed analysis of the structural, conformational and electronic features of DAMP and its analogues in order to provide a basis for its exceptional bioactivity. The relatively inactive DNMP-1 was also studied because its virtually planar pyrimidine ring provided a clear contrast to the torsionally distorted DAMP.

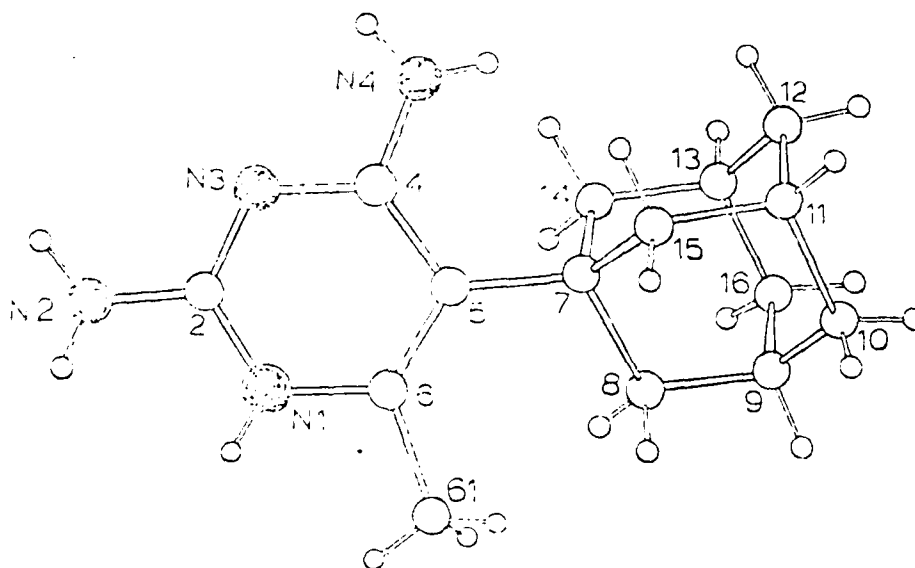


FIGURE 1a

FIGURE 1. Illustration of the pyrimidine ring systems existing in the crystal. (a) DAMP is an ethylsulphonate salt, (b) DNMP-1 is a methanol complex. The corresponding generated molecular volumes of DAMP and DNMP-1. In (a) and (b), nitrogen atoms are represented by circles numbered with respectively, and N, S and O prefix and carbon atoms are represented by circles with numbers alone.

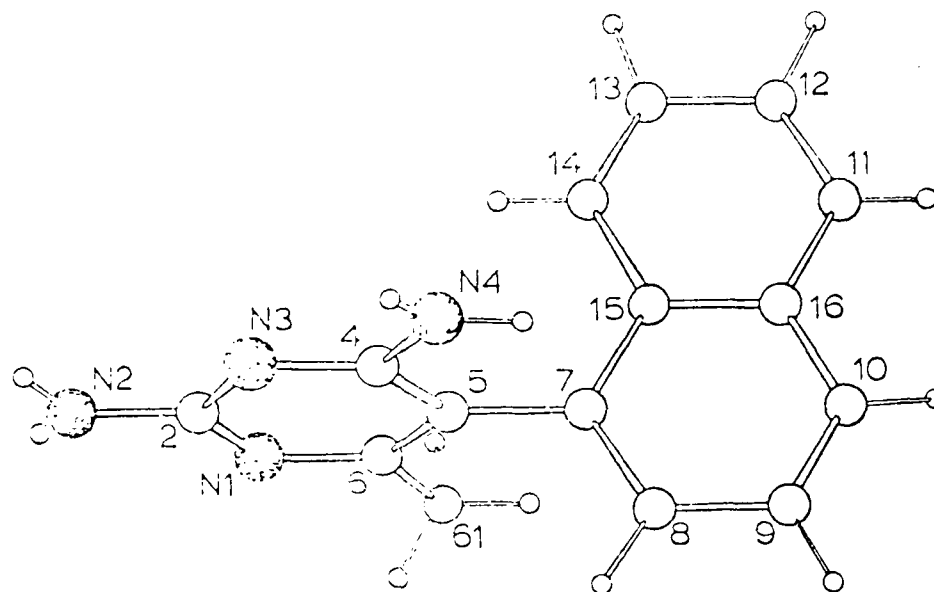


FIGURE 16

Therefore, in order to investigate further the conformational aspects of DIHR-drug specificity of binding and to identify more subtle structural differences in these compounds, calculations based on the CNDO/2 (Complete Neglect of Differential Overlap) method (Pople and Beveridge, 1970) with inclusion of direct geometry optimization (Kondo, 1978; Jaffe, 1970; Welsh *et al.*, 1982) were carried out on DAMP, DAMPH, DNMP-1, DNMPH and other related species. Of particular interest were to 1) determine whether the CNDO/2 technique can successfully predict the crystallographic results, in particular the out-of-plane distortions of the pyrimidine ring as found in DAMP-ES, 2) isolate the individual influence of the 2, 4, 5, 6-substituents and N1 protonation on the out-of-plane distortions, 3) estimate conformational-energy profiles with respect to rotation about the C5-C7 bond, and 4) identify the preferred sites of protonation and compare the energies of protonation of DAMP and DNMP-1.

The present results show that the CNDO/2 technique employed here can successfully predict the structures of DAMP and related species as they exist in the crystalline state. Hence, the present methods can be used as a valuable tool in further studies of this nature. The good agreement obtained between the observed and calculated structures suggests that overall the influence of intermolecular forces in determining the conformational characteristics of these species in the crystal is minimal. Of paramount significance is the ability of CNDO/2 to successfully predict the differences among the species studied with regard to the torsional distortions within the pyrimidine ring. Furthermore, charge distributions obtained by the present methods indicate that the disparity between DAMP and DNMP-1 in biological activity is not electrostatic in nature. For both species protonation is preferred at N1 rather

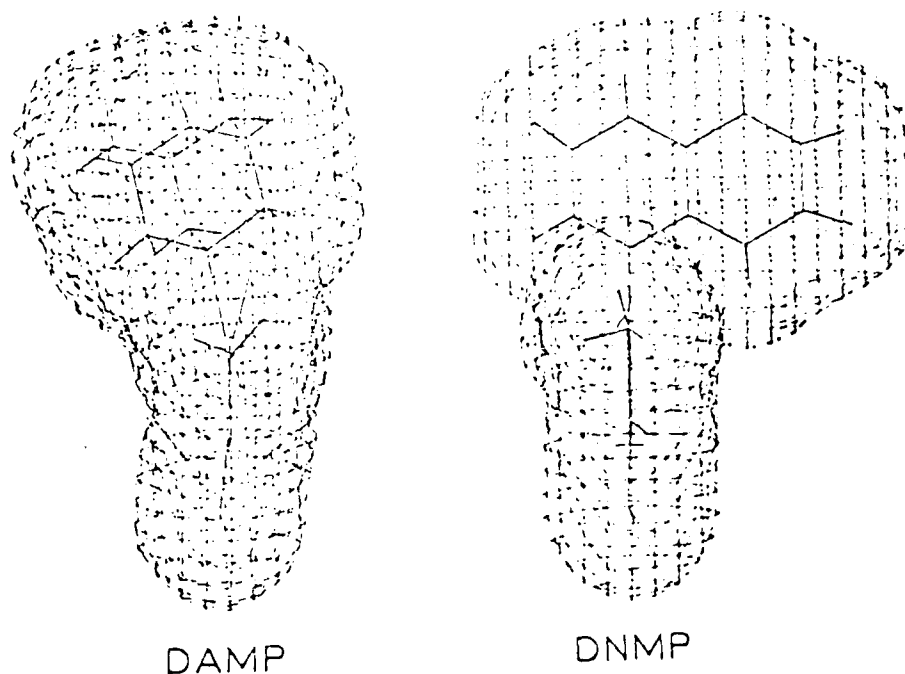


FIGURE 1c

than at N3 or at either the N2 or N4 amino-nitrogens. Also, values of the energy of protonation at N1 for DAMP and DNMP are nearly identical, hence the ring distortions within DAMP do not appear to facilitate protonation associated with tight binding to the enzyme.

METHODOLOGY

The general technique employs the semiempirical CNDO/2 molecular orbital theory (Pople and Beveridge, 1970) nested in an iterative scheme for achieving direct geometry optimization (Kondo, 1978; Jaffe, 1970). This method has already proved successful in characterizing the geometry, electronic structure and conformational properties of species similar in structure to those studied here (Welsh *et al.*, 1982; Welsh and Mark, 1982). The geometry optimization scheme is based upon the gradient of the potential energy function, the computation of which is made more efficient in terms of computer time by exploiting symmetry aspects of the molecule.

Differentiation of the CNDO/2 total energy expression with respect to each of the totally symmetric symmetry coordinates leads to the analytically defined elements of the gradient of the potential energy function. A convergence criterion of 0.1 eV/Å for the absolute value of each gradient element was found to be acceptable (Kondo, 1978).

The CNDO/2 electronic energy is sensitive to changes in the nuclear coordinates of the molecule. Consequently, for the SCF-electronic-energy iteration the convergence criterion, taken as self-consistency between two successive calculations, was set to a

TABLE I
Selected observed^a and calculated^b bond lengths^c, bond angles^d and torsional angles^e for DAMP^f, DNMP^g and related species

Calculated

Observed

TABLE I
Selected observed^a and calculated^b bond lengths, bond angles^c and torsional angles^d for DAMP, DNMP, and related systems

	Observed			Calculated					
	DAMP ^e	DNMP ^e	DAMP ^e	DAMP	DAMP-2H	DAMP-UN	DNMP-1	DNMP ^f	DNMP ^f
Bond lengths									
N1-C2	1.348	1.347	1.346	1.346	1.335	1.334	1.338	1.340	1.340
C2-N3	1.322	1.319	1.317	1.317	1.317	1.310	1.310	1.310	1.310
N3-C4	1.334	1.337	1.336	1.336	1.333	1.332	1.331	1.331	1.331
C4-C5	1.400	1.406	1.409	1.409	1.408	1.404	1.404	1.404	1.417
C5-C6	1.333	1.337	1.335	1.335	1.360	1.345	1.337	1.337	1.337
C6-N1	1.376	1.374	1.370	1.370	—	—	1.367	1.365	1.365
C2-N1	1.338	1.333	1.330	1.330	—	—	1.302	1.302	1.302
C4-N3	1.332	1.337	1.334	1.334	1.400	1.394	1.394	1.394	1.394
C6-C61	1.311	1.312	1.310	1.310	1.462	1.453	1.369	1.362	1.362
C5-C7	1.381	1.381	1.380	1.380	1.490	1.483	1.362	1.362	1.362
C7-C8	1.319	1.319	1.310	1.310	1.500	1.497	1.378	1.378	1.377
RMSD ^g	0.003	0.003	0.003	0.003	0.003	0.003	0.021	0.021	0.021
Bond angles									
N1-C2-N3	120.7	126.4	125.5	125.5	127.2	128.0	127.4	127.4	122.1
C2-N3-C4	118.1	116.4	114.8	114.8	114.5	113.2	114.5	114.5	116.2
N3-C4-C5	113.5	112.4	126.0	126.0	125.3	127.2	125.9	124.9	124.9
C4-C5-C6	119.9	115.9	115.6	115.6	115.3	111.1	115.9	115.9	116.8
C5-C6-N1	125.5	123.2	123.6	123.6	123.3	126.4	123.2	123.2	117.8
C6-N1-C2	117.8	116.8	117.1	117.1	116.3	113.9	116.0	123.6	123.6
N1-C2-N2	121.5	116.7	117.3	117.3	—	—	116.6	117.7	117.7
N3-C4-N4	113.0	117.0	111.6	111.6	—	—	116.0	120.0	120.0
C5-C4-N4	123.5	120.6	122.3	122.3	123.1	—	116.0	115.0	115.0
C5-C6-C61	130.2	130.9	126.8	126.8	126.8	—	120.5	120.1	120.1
N1-C6-C61	109.9	115.8	109.1	109.1	109.9	—	115.6	116.9	116.9
C4-C5-C7	120.1	120.9	120.8	120.8	120.5	122.4	120.9	120.7	120.7
C6-C5-C7	126.2	123.2	126.6	126.6	126.2	126.4	123.3	122.5	122.5
C5-C7-C8	114.5	120.3	115.9	115.9	115.8	115.6	121.0	120.6	120.6
RMSD ^g	1.2	1.2	0.8	0.8	0.8	0.8	0.8	0.8	0.8
Torsional angles									
N1-C2-N3-C4	-5.9	0.0	-4.5	-4.5	-3.1	-1.6	1.3	1.1	1.1
C2-N3-C4-C5	-7.1	1.60	-1.1	-1.1	-0.52	-1.0	1.2	1.1	1.1
N3-C4-C5-C6	13.7	-1.7	5.4	5.4	3.9	2.6	-1.3	-0.87	-0.87
C4-C5-C6-N1	-7.6	0.00	-4.9	-4.9	-4.4	-1.9	0.84	1.4	1.4
C5-C6-N1-C2	-4.4	1.20	-0.46	-0.46	-1.4	-0.13	2.9	3.5	3.5
N3-C2-N1-C6	12.0	-1.4	4.8	4.8	2.5	2.2	-3.2	-3.5	-3.5
C6-C5-C7-C8	-7.5	-87.1	-12.0	-12.0	-11.4	-12.2	-86.2	-86.5	-86.5
AVG ^h	8.4	1.0	3.5	3.5	2.6	1.6	1.8	1.9	1.9
RMSD ^g (°) angles	3.7	3.7	1.2	1.2	1.2	1.2	1.2	1.2	1.2

^aX-ray crystallographic values (Ho, Zakrzewski and Mead, 1973). ^bCNDO/2 method with geometry optimization. ^cIn units of Angstroms.

^dIn units of degrees. ^eNumbering of atoms in accordance with Figure 1. ^fRoot mean square difference between observed and calculated values. ^gAverage of the absolute values of the intra-ring torsional angles.

small value (10^{-2} eV) relative to that typically used (10^{-5} eV) in nonoptimized CNDO/2 calculations (Kondo, 1978). In the conformational energy calculations, values of the CNDO/2 total energy were calculated as a function of the rotational angle ϕ about the C5-C7 bond varied in increments of 20–30°. The energy associated with a given conformation was taken as the difference in total energy between that conformation and the conformation obtained upon optimization of the crystalline-state structure.

RESULTS AND DISCUSSION

In most cases, geometry optimization was obtained both starting from the structural geometry given by x-ray crystallographic analysis (Cody and Zakrzewski, 1982) and after assuming a nearly flat pyrimidine ring. Calculations were carried out on several related species. These include DAMPH⁺, DAMP, DAMP-2H (a species corresponding to DAMP with its 2-NH₂ group replaced by a H atom), and DAMP-UN (a species corresponding to DAMP unsubstituted at the C2, C4, and C6 positions). Also studied were DNMP-1 and its N1-protonated form DNMPH⁺. Pertinent values of the observed and calculated bond lengths, bond angles, and torsional angles for some of these species are listed in Table I.

DAMPH⁺: Comparisons of X-ray and Calculated Structures

The observed and calculated geometries of DAMPH⁺ are listed in columns 2 and 4 of Table I, respectively. Overall agreement between the calculated and observed structures is very good. Specifically, for those values listed in Table I (which include those calculated and observed values with the largest deviations) the root-mean-square difference (RMSD) is 0.063 Å for bond lengths and 1.2° for bond angles.

In general, the CNDO/2 calculated carbon-carbon bond lengths are shorter and carbon-nitrogen longer than those observed crystallographically. This is particularly apparent in the case of the substituent bonds C2-N2, C4-N4, C6-C61, and C5-C7. Although not listed, calculated values of the carbon-carbon bond lengths within the adamantyl group are uniformly smaller than the corresponding observed ones by ca. 3%. These systematic discrepancies appear to be an artifact of the CNDO/2 method since similar trends have been noted in other studies (Tajiri, 1973; Combs, 1975).

The calculated torsional angle about the rotatable bond C5-C7, taken as the angle between planes C6-C5-C7 and C5-C7-C8, is ca. -12.0°. This compares well with the observed values of -7.5° in the crystalline state. Of particular importance are the torsional angles within the pyrimidine ring. It is seen in Table I that the calculated structure also indicates nonplanarity of the pyrimidine ring, although in each case the calculated torsional angle is somewhat less (RMSD=3.7°) than that of the observed structure. Identical results were obtained for optimizations carried out after initially assuming a nearly flat pyrimidine ring.

Species Related to DAMPH⁺

Calculations on various structurally modified forms of DAMPH⁺ were carried out particularly to determine the effects of the N1-protonation and of the substituents on the structure and the ring distortions. Deprotonation of DAMPH⁺ yields DAMP, the calculated geometry of which is summarized in column 5 of Table I.

ized
trons,
ational
associated
that con-
state

structural
(982) and
in several
respon-
(a species
so studied
es. of the
or some of

2 and 4 of
ved struc-
ade those
in square

order and
rticularly
d C5-C7
within the
by or
2 method
(1975)
the angle
with
are the
calculated
cause the
observed
initially

at par-
ts on the
AMP, the

The effect of ring deprotonation on the bond lengths is to slightly lengthen the bonds about N1, with subsequent adjustment of other intra-ring bonds with little or no effect on the lengths of the extra-ring bonds. In terms of bond angles, deprotonation results in a closing of the C6-N1-C2 angle and an opening of the N1-C2-N3 angle, each by about 6.0°, with minor adjustments elsewhere in the ring. Comparison of the calculated intra-ring torsional angles for DAMP and DAMPH⁺ indicates an overall decrease in the magnitude of the ring distortions upon deprotonation, however, still not to the essentially planar state.

Subsequent replacement of the C2-amino group in DAMP by a H atom has a slight effect on the bond lengths (viz., N1-C2 and C2-N3) but negligible effect on the bond angles. Calculated values are listed in column 6 of Table I. However, there is a reduction in the torsional angles within the pyrimidine ring as indicated by comparing the averages of the absolute values of the torsional angles, given in Table I, for DAMPH⁺ (5.1°), DAMP (3.5°) and DAMP-2H (2.6°). Further replacement of the C4-amino and C6-methyl groups by a H atom (with the adamantyl group now as the only substituent on the ring) yields DAMP-CN, the geometry of which is summarized in column 7 of Table I, having nearly a planar ring; subsequent protonation of this species had a negligible effect on the ring distortions. While it is predictable that the ring distortions are instigated by the strong steric repulsions between the adamantyl group and C4- and C6-substituents on the ring, these results indicate that both protonation and C2-amino group further enhance these distortions in DAMP.

DNMP-1; Comparisons of X-ray and Calculated Structures and Effects of Protonation

Again in the case of DNMP-1, good agreement is found between the observed and calculated structural geometries, listed in columns 3 and 8 in Table I, respectively, with the RMSD being 0.021 Å for bond lengths and 0.8° for bond angles. The calculated torsional angle about C5-C7 is -86.2° and is virtually identical to the experimental value of -87.1° (Cody and Zakrewski, 1982). The calculated torsional angles are small and in satisfactory agreement (RMSD=1.2°) with those observed. The CNDO/2 technique employed is successful in correctly predicting a significantly greater degree of torsional distortions in DAMPH⁺ than in DNMP-1.

Similar calculations were carried out on the protonated form of DNMP-1 (DNMPH⁺) to assess the effect of protonation on structure, particularly with regard to

TABLE II
Fractional charges^a of selected atoms in DAMP and DNMP-1

Atom ^b	DAMP	DNMP-1
N1	-0.351	-0.353
C2	0.400	0.403
N3	-0.361	-0.361
C4	0.313	0.319
C5	-0.148	-0.146
C6	0.216	0.223
N2	-0.308	-0.306
N4	-0.312	-0.314

^aIn units of fraction of an electron's charge.

^bNumbering of atoms in accordance with Figure 1.

the planarity of the pyrimidine ring. The calculated geometry is summarized in column 9 of Table I. The effect of protonation on the bond lengths and bond angles within the pyrimidine ring is similar to that already indicated in DAMP, i.e., a slight lengthening of the bonds attached to N1, and an increase, again by about 6°, in the intra-ring bond angle about N1 with a subsequent decrease in bond angle N1-C2-N3 by about 5°. Other effects of protonation on the bond lengths and bond angles are small.

The effect of protonation of DNMP-1 on the torsional angles within the pyrimidine ring is negligible. This small influence of protonation on the distortions in DNMP is in contrast to the significant one found in DAMP. The adamantyl group in DAMPH⁺ appears to potentiate the effect of protonation and ring substitution on the distortions, whereas in DNMP-1 the naphthalene ring, assuming a nearly perpendicular orientation with respect to the pyrimidine ring, produces little or no distortions on its own and the effects of protonation of the ring on the distortions are negligible.

Charge Distributions in DAMP and DNMP-1

Fractional charges for selected atoms in DAMP and DNMP-1 are listed in Table II. It is seen that the charge distribution for the atoms listed is virtually identical for the two species, indicating that the differences in biological activity between DAMP and DNMP-1 are not explicable in terms of electrostatic arguments. Of particular interest here are the four nitrogen atoms N1, N2, N3, and N4 since these atoms are likely points of attachment of the antifolate inhibitor to the enzyme and are also potential sites of protonation. For both species, N1 and N3 are appreciably more negative than N2 and N4. In addition, the charges on N1 and N3 are nearly identical, as they are on N2 and N4. Hence, the charge distribution suggests that protonation should be preferred at N1 or N3. Similar analysis of the calculated DAMPH⁺ structure reveals that upon protonation the fractional charge of N1 drops to -0.223 but that of N3 remains nearly the same at -0.332. (The fractional charge of the bonded proton in DAMPH⁺ is only 0.200, indicating appreciable charge delocalization.)

Sites and Energies of Protonation

The preferred site of protonation of DAMP and DNMP-1 was obtained by comparing the total energies of each species protonated at N1, N2, N3 or N4 (see Figure 1). For both species protonation is preferred at N1 over N3 by *ca.* 0.16 eV or 3.7 kcal mol⁻¹ and over N2 or N4 by *ca.* 1.6 eV or 37.0 kcal mol⁻¹. The preference for protonation of an intra-ring nitrogen rather than an extra-ring nitrogen agrees with the results of an *ab initio* calculation on the protonation of aminopyridine (Fossey, 1981) and is consistent with the more negative charge of the intra-ring nitrogens. The preference for N1 over N3 appears much more subtle in nature. The bonded proton in DAMPH⁺ carries a charge of -0.22e⁻ in both cases, the N-H⁺ bond lengths are identical at 1.068 Å and only slight differences in charge exist for equivalent atoms in the two protonated forms; hence, this preference does not appear largely due to differences in charge delocalization effects. Conformational changes, particularly those involving the ring torsional angles, do result from protonation, and small differences are noted for protonation at N1 as compared with N3. The preference for N1 over N3 therefore appears to be largely steric (conformational) rather than electronic in character.

Energies of protonation at N1 of DAMP and DNMP-1 were compared as a means of assessing the effect of the torsional ring distortions in DAMP on ease of protonation. The results indicate a slight preference for protonation of DNMP-1 over DAMP by *ca.*

0.008 eV or 0.18 kcal mol⁻¹. It is known that methotrexate is N1-protonated while the natural substrate is unprotonated when bound to DHFR, and this difference is purported to account for the enzyme's enhanced affinity for the drug (Matthews *et al.*, 1977). However, it appears that the torsional distortions in DAMP do not facilitate its protonation relative to that for a planar ring structure as found in DNMP-1. The exceptional bioactivity of DAMP, above that expected on the basis of lipophilicity alone, is not the result of improved ease of protonation as a result of the distorted ring structure. Another structural feature in DAMP which may play a role in its enhanced bioactivity, however, is the slight "warping" or elbow observed in the molecule (Figure 1c), as a result of C7 being 0.37 Å above the pyrimidine plane (Cody and Zakrzewski, 1982). This could allow a better accommodation within the DHFR binding pocket relative to the alternative colinear form. Such a possibility is currently under investigation by the present authors but will involve a detailed study of various conformational forms of DAMP within the binding pocket of DHFR.

Conformational-Energy Calculations

The present methods were used to determine the conformational energies associated with rotation about C5-C7 in both DAMP and DNMP-1. For DAMP the conformation of minimum energy corresponds nearly to that found in the crystalline state (Figure 2a). The barrier to rotation away from the preferred conformation is very steep and has a broad maximum located in the region 30-90° (within the 0-120° total configuration space) and is about 8.0 kcal mol⁻¹ above the minimum. High rotational barriers associated with adamantyl groups have been observed by others (Lomas and

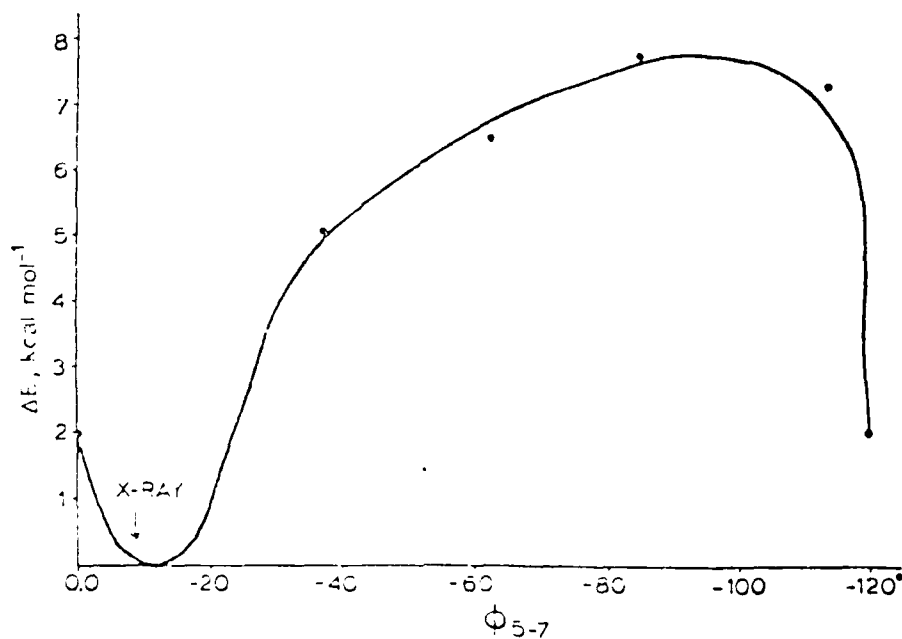


FIGURE 2a

FIGURE 2 CNDO/2 calculated conformational energies ΔE vs. ϕ_{5-7} for (a) DAMPH⁺, (b) DNMP-1 and (c) DNMP-2.

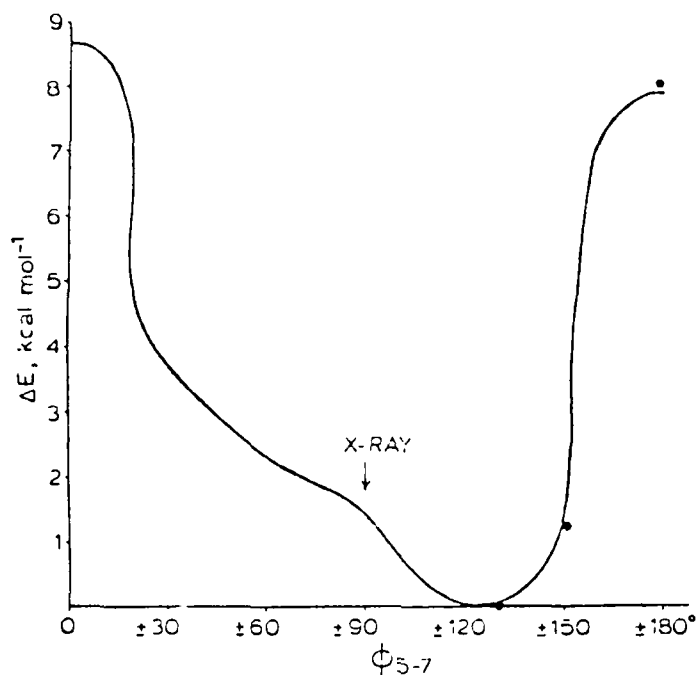


FIGURE 2b

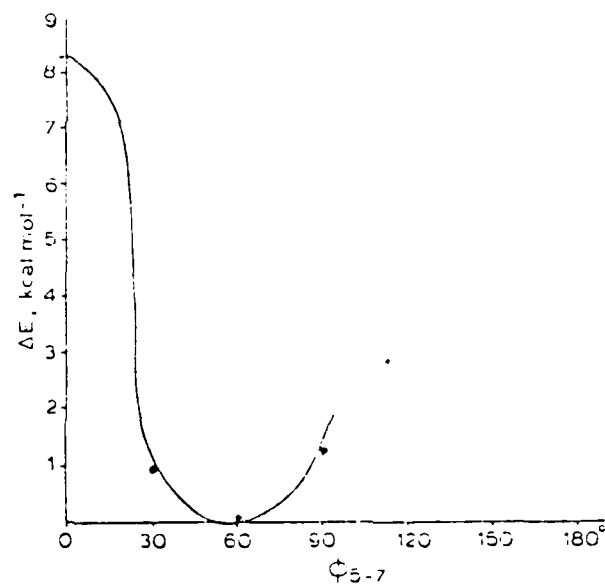


FIGURE 2c

Due to the
between
The
resp
and b
The
more
confo
2.0 kcal
mol⁻¹
associ
 $\phi=0^\circ$
mol⁻¹
confor
crystal
charge
regard

CONC

The p
DAN
tive
thes
con
spe
spe
sign
incr
pres
tion:

ACK

It is
Res
Am

REF

Cod
Com
Foss
Ho, Y
Ho, Y
Jaffe, I
Kavai
Kondo
Lomas,

Dubois, 1981). No value of ϕ was successful in relieving the severe steric conflicts between the adamantyl group and 4- and 6-substituent groups on the pyrimidine ring. The barrier effectively locks the C5-C7 bond and precludes relief of the steric conflicts responsible for the distortions. The distortions are further aggravated by protonation and by the presence of the C2-amino group.

The C5-C7 bond in DNMP-1 is overall more flexible than that in DAMP in terms of more accessible regions of conformational space (Figure 2a). Using the perpendicular conformation as reference ($\phi=0^\circ$, $E=0.0$ kcal mol⁻¹), the energy rises slowly to ca. 2.0 kcal mol⁻¹ at $\phi=-60^\circ$ (toward the 4-amino group) then rises sharply to ca. 7.2 kcal mol⁻¹ at $\phi=-90^\circ$ (a coplanar conformation). These high energy conformations are associated with corresponding increases in the ring distortion. Rotation away from $\phi=0^\circ$ toward the 6-methyl group shows a gradual decrease in energy, to ca. -1.5 kcal mol⁻¹ at $\phi=60^\circ$, followed by another maximum at $\phi=90^\circ$. The calculated preferred conformation of DNMP-1 is hence different from that (perpendicular) observed in the crystalline state and exhibits a complete absence of ring distortions. The geometry and charge distribution are only slightly affected by rotation. Preliminary results in this regard for DNMP-2 (Figure 2c) exhibit a profile similar to that for DNMP-1.

CONCLUSIONS

The present results indicate that the methodology used can be applied successfully to DAMP and related species. Calculated bond lengths and bond angles are in quantitative agreement with those observed, and the calculated torsional angles, while less than those observed, can be used in a semiquantitative or qualitative fashion for comparisons. It is the intent of the authors to extend these calculations to other related species to explore further the structural and conformational aspects of DHFR-drug specificity. Particular attention, for example, is being focused on the observed significant variation in biological activity with alteration of the C6-substituent, i.e., increasing for the sequence -H, -methyl and -ethyl, then decreasing for n-propyl. The present methods should prove useful for establishing the structural and conformational basis of this variation.

ACKNOWLEDGMENTS

It is a pleasure to acknowledge the financial support (W.W. J.M.) provided by the Air Force Office of Scientific Research (Grant AFOSR 78-2683, Chemical Structures Program, Division of Chemical Sciences) and the American Cancer Society grant CA-2161 (V.C.S.Z.).

REFERENCES

- Coates, V. and S. F. Zlotrowski (1982), *J. Med. Chem.* 25, 427.
- Combs, L. L. and M. H. L. (1978), *J. Med. Chem.* 21, 512.
- Fossey, J. A., Loupy, and H. Strydom (1981), *Tetrahedron* 37, 1935.
- Ho, Y. K., M. F. H. and S. F. Zlotrowski (1972), *Cancer Res.* 32, 1023.
- Ho, Y. K., S. F. Zlotrowski and L. H. Mead (1973), *Biochemistry* 12, 1003.
- Jaffe, H. H. (1979), Program 315, Quantum Chemistry Program Exchange, Indiana University.
- Kay, L. L., H. Mead, L. Drobniak and S. F. Zlotrowski (1975), *J. Med. Chem.* 18, 272.
- Kondo, N. (1978), Ph.D. Dissertation, University of Cincinnati.
- Lomas, J. S. and J. E. Dubois (1981), *Tetrahedron* 37, 2273.

- Mann, C. D. W., R. A. Yocum, J. E. Jones, J. E. Latta, A. E. Ham, N. N. Yang, J. K. Stille, M. Lee, M. Williams, and K. H. Ogilvie, (1977), *Synthetic* 1977, 452.
- Pople, J. A. and D. L. Pritchard, (1973), *Approximate Molecular Orbital Theory*, McGraw-Hill, New York.
- Tajiri, A., S. Takeda, and H. Hatanaka (1973), *Bull. Chem. Soc. Japan* 46, 1836.
- Welsh, W. J., H. H. Jaffe, J. E. Mark, and S. Kowalski (1972), *The Macromolecular Chemistry* 181, 501.
- Welsh, W. J. and J. E. Mark, (1982), *Polym. Prepr., Am. Chem. Soc., Div. Polym. Chem.* 23(1), 192, 303, 305.
- Zakrzewski, S. L. (1963), *J. Am. Chem.* 235, 1388, 3002.

BAND STRUCTURES, GEOMETRY, AND PARTIAL OXIDATION IN IRIDIUM CARBONYL CHLORIDE CHAINS

D. BHAKMIK and J. E. MARK

Department of Chemistry and the Polymer Research Center, The University of Cincinnati, Cincinnati, OH 45221 (U.S.A.)

(Received June 6, 1983)

Summary

The extended Hückel method was employed to calculate electronic band structures in iridium carbonyl chloride chains in an attempt to elucidate their equilibrium geometry and partial oxidation. The unit cell energies thus calculated indicate that alternate $\text{Ir}(\text{CO})_3\text{Cl}$ units are staggered relative to one another, with 50% positional disorder in the crystalline phase. Bound states are not possible in the $\text{Ir}(\text{CO})_3\text{Cl}$ chain without partial oxidation of Ir, indicating that the repeat unit must be nonstoichiometric. A small amount of partial oxidation of Ir gives a bound state of the chain when the Ir-Ir separation is set equal to 2.844 Å, in agreement with experimental observations.

Introduction

The Krogmann salts [1, 2] such as those of Pt and Ir are square-planar complexes of d^8 transition-metal ions stacked in columns in the crystalline phase, with the metal atoms aligned along the columnar axis. These continuous chains are often referred to as 'one-dimensional conductors' [3 - 5] because of their metal-like conductivities along the stacking direction. A major family of these compounds is nonstoichiometric [3 - 5], giving a partially filled conduction band for high electrical conductivity. However, controversy has arisen concerning the iridium carbonyl chloride chain, a segment of which is shown in Fig. 1. It was originally characterized as $\text{Ir}(\text{CO})_3\text{Cl}$ [3, 6, 7], but later reported to be nonstoichiometric $\text{Ir}(\text{CO})_{2.93}\text{Cl}_{1.07}$ [8] (Ir oxidation 1.07) or $\text{Ir}(\text{CO})_3\text{Cl}_{1.1}$ [9] (Ir oxidation 1.1). The observed Ir-Ir distance of 2.844 Å [8] requires an oxidation state of $\text{Ir}^{1.3}$ for good agreement with the empirical correlation [3] obtained from Pauling's bond distance-bond number relationship [10]. Also, the measured high conductivity ($0.2 \Omega^{-1} \text{ cm}^{-1}$) [11] and low activation energy (0.064 eV) are in support of the partial oxidation of iridium; unoxidized chain complexes have much smaller conductivities and higher activation energies.

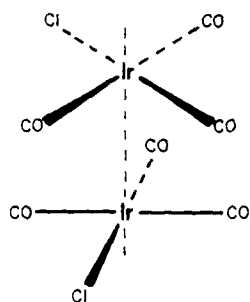


Fig. 1. A segment of the iridium carbonyl chloride chain.

In the present work, attempts are made to explain the geometrical structure of the $\text{Ir}(\text{CO})_3\text{Cl}$ chain and to determine the oxidation state of iridium from the band structure analysis.

Theory

For any molecule, including polymeric chains, the LCAO approximation and Bloch's Theorem can be used to develop the crystal orbitals $\psi_n(k)$. For a one-dimensional system in which $N - 1$ cells are interacting with the reference cell and for a basis set of length ω describing the wave function within a given cell, the n th crystal orbital $\psi_n(k)$ is defined as [12 - 16]

$$\psi_n(k) = \frac{1}{N^{1/2}} \sum_{j=-(N-1)/2}^{(N-1)/2} \sum_{\mu=1}^{\omega} \exp(ik \cdot R_j) C_{n\mu}(k) \chi_{\mu}(r - R_j) \quad (1)$$

where the quantity k is the wave vector and R_j is the one-dimensional position vector given by $R_j = ja$ with a the basic vector of the crystal. $C_{n\mu}$ is the expansion coefficient of the linear combination and $\{\chi_{\mu}\}$ is the set of basis functions of Slater form. Calculations included all the valence atomic orbitals of the Ir, C and O atoms, but for Cl atoms only s and p orbitals were considered. The unit cell contains two $\text{Ir}(\text{CO})_3\text{Cl}$ units and, in the present calculations, lattice sums were carried out to second-nearest neighbors.

Using the extended Hückel approximation, the corresponding eigenvalues $E_n(k)$ are obtained from the eigenvalue equation

$$H(k)C_n(k) = S(k)C_n(k)E_n(k) \quad (2)$$

where $H(k)$ and $S(k)$ are the usual Hamiltonian and overlap matrices.

The distribution of the $E_n(k)$ values for a given n with respect to k (usually within the first Brillouin zone, $-0.5K \leq k \leq 0.5K$, where $K = 2\pi/a$) is the n th energy band. Since the variation of $E_n(k)$ with k would be symmetrical about the center of the first Brillouin zone, computations were performed to determine only one half ($0 \leq k \leq 0.5K$) of the energy band. The set of all energy bands describes the band structures of the compound.

TABLE 1
Atomic parameters for the extended Hückel-type calculations

Atom	Orbital χ_μ	Slater exponent ^a		Valence state ionization potential $H_{\mu\mu}$ (eV)
		ζ_1	ζ_2	
C	2s	1.625	—	—21.4
	2p	1.625	—	—11.4
O	2s	2.275	—	—32.3
	2p	2.275	—	—14.8
Cl	3s	2.356	—	—24.2
	3p	2.039	—	—15.0
Ir	6s	2.504	—	—8.09
	6p	2.484	—	—4.57
	5d	5.796 (0.6698)	2.557 (0.5860)	—12.5

^aTwo Slater exponents for the 5d function, with double zeta expansion coefficients in parentheses.

The extended Hückel parameters for C, O and Cl were obtained from the literature [17, 18]. Following Summerville and Hoffmann [17], the valence state ionization potentials $H_{\mu\mu}$ for Ir were assumed the same as those for Rh [17], which is directly above Ir in the group VIII elements in the periodic table and whose electronic configuration is similar to that of Ir. Its orbital exponents ζ_μ were taken from the work of Basch and Gray [19]. All these parameters are summarized in Table 1. The geometrical parameters (bond lengths and bond angles) of $\text{Ir}(\text{CO})_3\text{Cl}$ were obtained from X-ray results [3, 8].

To determine the most stable geometrical configuration of the chain, the distance $r_{\text{Ir-Ir}}$ between the two Ir atoms was varied from 2.5 Å to 4.0 Å in steps of 0.1 Å. For each $r_{\text{Ir-Ir}}$ value, the dihedral angle ϕ between the two Cl atoms in the unit cell was also varied ($\phi = 0^\circ$ for chlorine-chlorine *cis*), keeping the other geometrical parameters fixed. For each arrangement of $\text{Ir}(\text{CO})_3\text{Cl}$ units, the total energy per unit cell $\langle E_t \rangle$ was calculated from its band structure as a function of both $r_{\text{Ir-Ir}}$ and ϕ . The equation employed was [14, 16]

$$\langle E_t \rangle = \frac{1}{K} \int_{-K/2}^{K/2} E_t(k) dk \quad (3)$$

where $E_t(k)$ is the total energy at k and, according to the extended Hückel method,

$$E_t(k) = 2 \sum_n^{\text{occupied}} E_n(k)$$

The unit cell structure which corresponds to the minimum total energy is identified as the most stable packing arrangement.

To calculate $\langle E_t \rangle$ for the partially oxidized states the energy loss per unit cell due to the electron removal from the valence band had to be determined. For that, the Fermi level E_f or the Fermi momentum k_f was calculated from the integrated density of states $n(E)$ for the valence band. The expression for $n(E)$, which is the number of electrons per unit cell when the energy levels are occupied up to E , is given by [14]

$$n(E) = \int_{E_b}^E g(E) dE \quad (4)$$

where E_b is the bottom of the valence band. The quantity $g(E)$, the density of states, is given by

$$g(E) = \frac{1}{\pi} \frac{dk}{dE}$$

for one-dimensional systems. For each increment of partial oxidation δ of Ir ($\text{Ir}^{1+\delta}$; $\delta = 0.05, 0.1, 0.2, 0.3, 0.4, 0.5, 0.6, 0.7$), the energy loss per unit cell caused by electron removal was calculated from the Fermi momentum k_f .

Results and discussion

The variation of $\langle E_t \rangle$ with ϕ was analyzed for different $r_{\text{Ir-Ir}}$. Equation (3) indicates that for a fixed value of $r_{\text{Ir-Ir}}$ (a constant), the total energy per unit cell $\langle E_t \rangle$ is directly proportional to the area enclosed by the curve of $E_t(k)$ against k . Figure 2 shows one such typical $E_t(k)$ versus k plot (for $r_{\text{Ir-Ir}} = 2.844 \text{ \AA}$) for various values of ϕ . It is seen from this Figure that the curve for $\phi = 135^\circ$ encloses the maximum area. Because the $E_t(k)$ are all negative, the total energy $\langle E_t \rangle$ would be minimum at this value of ϕ . This has also been observed for other values of $r_{\text{Ir-Ir}}$. Therefore, $\phi = 135^\circ$ (the Ir-Cl bond of one $\text{Ir}(\text{CO})_3\text{Cl}$ unit bisecting the angle between Ir-CO bonds of another unit in the unit cell) corresponds to the minimum energy configuration of the $\text{Ir}(\text{CO})_3\text{Cl}$ chain. Since there are two equivalent configurations ($\phi = 135^\circ, 225^\circ$) of this arrangement, it is expected that there would be 50% positional disorder in the $\text{Ir}(\text{CO})_3\text{Cl}$ crystal structure. This conclusion is in agreement with X-ray structure analysis [3]. On this basis, the rest of the results presented here correspond to this staggered arrangement ($\phi = 135^\circ$) of alternate $\text{Ir}(\text{CO})_3\text{Cl}$ units.

To determine the most stable separation between the $\text{Ir}(\text{CO})_3\text{Cl}$ units, again the curves for the variation of $E_t(k)$ against k for different values of $r_{\text{Ir-Ir}}$ were drawn. The results are shown in Fig. 3. Since, in this case $r_{\text{Ir-Ir}}$ is varying (a is not constant), the direct proportionality of $\langle E_t \rangle$ with the enclosed area is no longer valid. Equation (3) was then evaluated analytically for each value of $r_{\text{Ir-Ir}}$, obtaining an analytical expression for $E_t(k)$ by polynomial fit. The results are summarized in Fig. 4, which shows that total

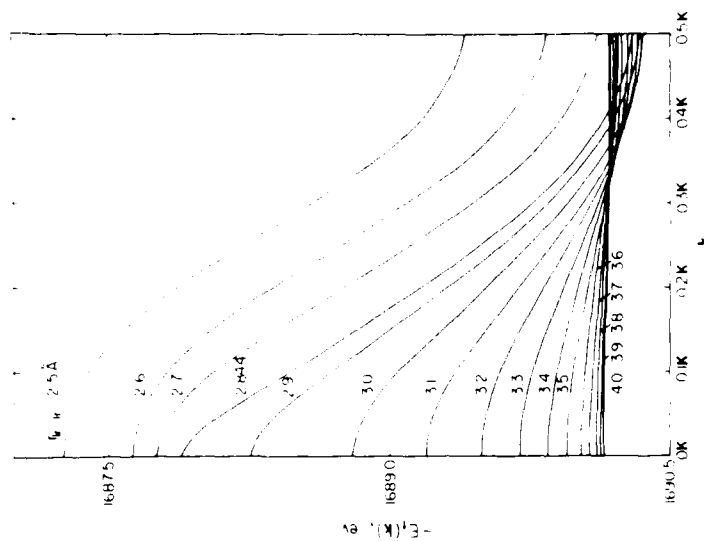


Fig. 2. The dependence of $E_i(k)$ on k for various values of ϕ , at $r_{1r} = 2.844 \text{ \AA}$.

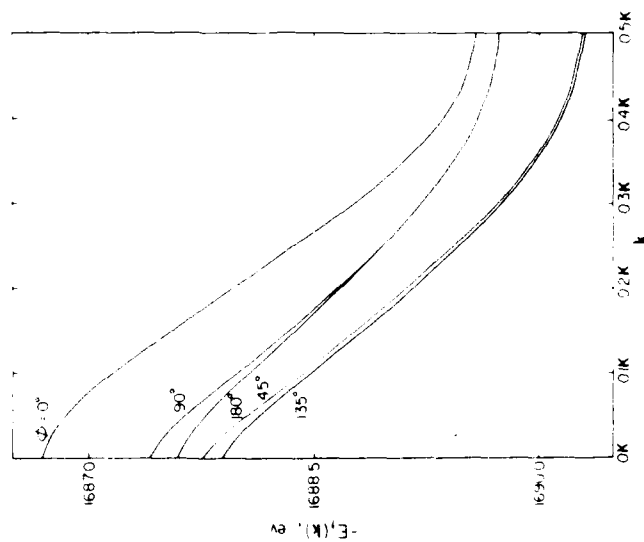


Fig. 3. The dependence of $E_i(k)$ on k for various values of r_{1r} .

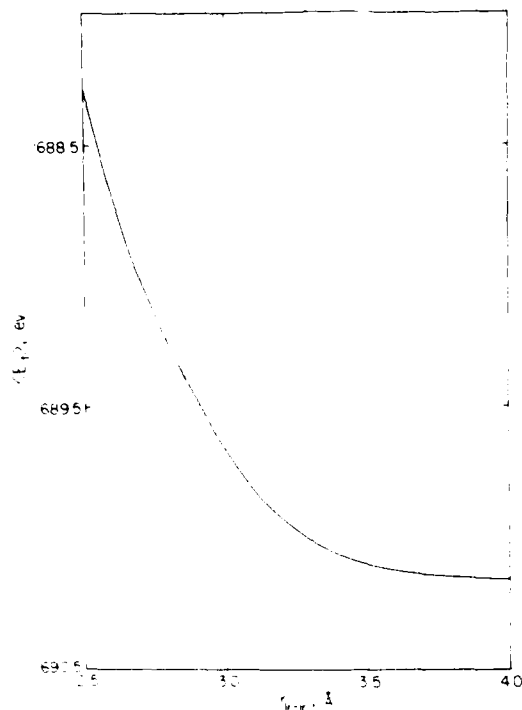


Fig. 4. The total energy per unit cell for the unoxidized $\text{Ir}(\text{CO})_3\text{Cl}$ chain as a function of $r_{\text{Ir-Ir}}$.

energy per unit cell $\langle E_t \rangle$ decreases monotonically with increase in $r_{\text{Ir-Ir}}$. This indicates that the $\text{Ir}(\text{CO})_3\text{Cl}$ chain would not be in a bound state. At $r_{\text{Ir-Ir}} = 2.844$ Å, the experimentally measured [8] distance, the chain is less stable than the isolated $\text{Ir}(\text{CO})_3\text{Cl}$ units by 0.83 eV (19.2 kcal mol $^{-1}$). Therefore to get a bound state of the chain, the Ir would apparently have to be partially oxidized.

The band structure of the $\text{Ir}(\text{CO})_3\text{Cl}$ chain at a typical value of $r_{\text{Ir-Ir}} = 2.844$ Å is shown in Fig. 5, where the uppermost p_z band is the lowest vacant band and the highest occupied band has d_{z^2} antibonding character. For the partial oxidation, electrons have to be removed from this band. An analytical expression for $E(k)$ for the d_{z^2} band was determined by a polynomial fit and eqn. (4) was evaluated analytically for different values of E . The results of this analysis are shown in Fig. 6 for $r_{\text{Ir-Ir}} = 2.844$ Å, where $n(E)$ is normalized so that $n(E)$ becomes two electrons at the top of the d_{z^2} band. Since a unit cell contains two $\text{Ir}(\text{CO})_3\text{Cl}$ subunits, the partial oxidation state $\text{Ir}^{1+\delta}$ corresponds to an electron removal of 2δ per unit cell. From examination of Fig. 6 it is apparent that for $\delta = 0.05, 0.1, 0.2, 0.3, 0.4, 0.5, 0.6$ and 0.7 , the Fermi momenta k_f turn out to be nearly $0.025K, 0.05K, 0.10K, 0.15K, 0.20K, 0.25K, 0.30K$, and $0.35K$, respectively. The analysis

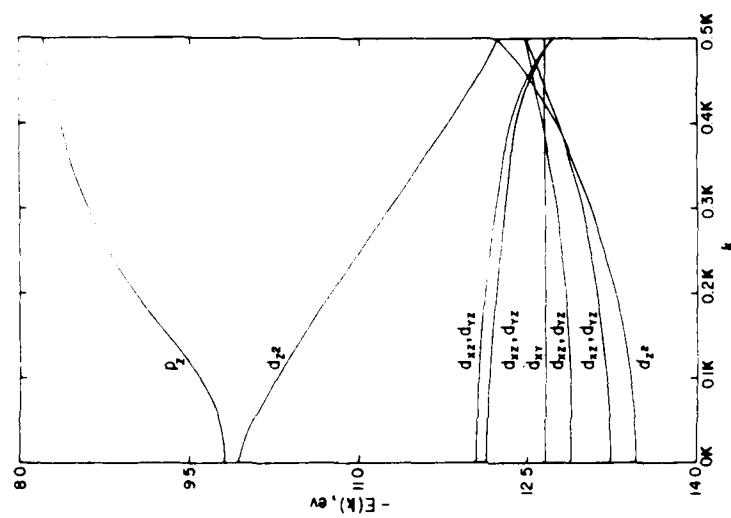


Fig. 5. The band structure of the $\text{Ir}(\text{CO})_3\text{Cl}$ chain at $r_{\text{Ir-Cl}} = 2.844 \text{ \AA}$.

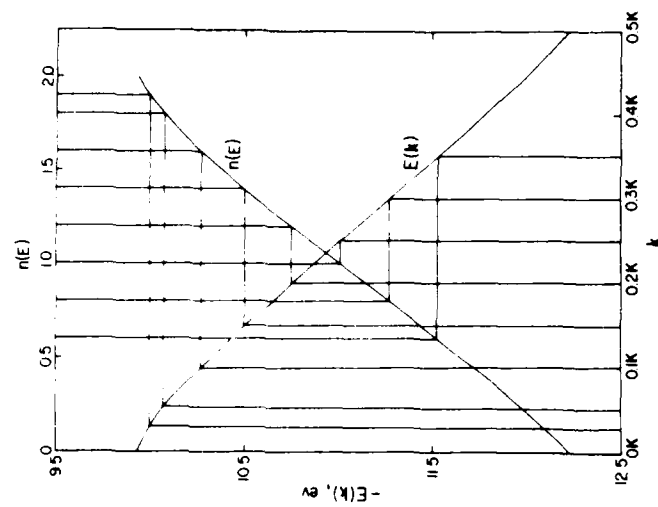


Fig. 6. The d_{z^2} band and its integrated density of states for $r_{\text{Ir-Cl}} = 2.844 \text{ \AA}$. The lines show the correlation between δ and k_{F} .

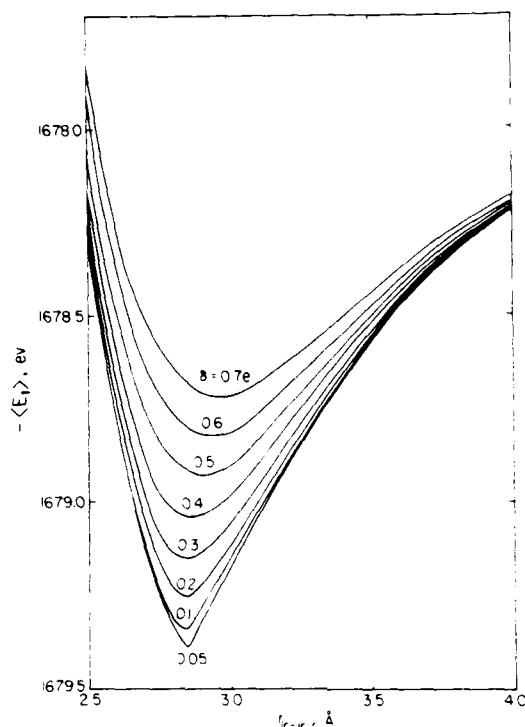


Fig. 7. The total energy per unit cell for the partially oxidized $\text{Ir}(\text{CO})_3\text{Cl}$ chain as a function of $r_{\text{Ir-Ir}}$ for various values of δ

of $n(E)$ at other values of $r_{\text{Ir-Ir}}$ reveals the same correlation between k_f and δ as the above. Although relevant experimental data on $\text{Ir}(\text{CO})_3\text{Cl}$ are lacking, the calculated results are in agreement with experimental findings on Pt complexes [20].

From knowledge of the Fermi momentum k_f for various amounts of partial oxidation, the modified total energy per unit cell $\langle E_t \rangle$ for different values of $r_{\text{Ir-Ir}}$ was calculated. The results are shown in Fig. 7. From the analysis of such curves it is found that the equilibrium value of $r_{\text{Ir-Ir}}$ becomes 2.844 Å for $\delta = 0.05$ to 0.3 and then it increases with increase in partial oxidation. Also, the depth of the potential well decreases with increase of partial oxidation. This behavior of the $\text{Ir}(\text{CO})_3\text{Cl}$ chain is the opposite of that shown by Pt complexes [3, 5], where $r_{\text{Pt-Pt}}$ decreases (to a minimum value of ~ 2.8 Å) with increasing partial oxidation. This is because in the case of $\text{Ir}(\text{CO})_3\text{Cl}$ the conduction d_z band width is larger for smaller values of $r_{\text{Ir-Ir}}$. This leads to a smaller energy loss for the lower state of oxidation giving smaller values of the equilibrium distance. But as the amount of partial oxidation increases, the variation of the loss of energy with $r_{\text{Ir-Ir}}$ decreases, creating the energy minima at higher values of $r_{\text{Ir-Ir}}$. The present calculated results are in agreement with the experimental observation [8] that the

iridium-iridium distance is 2.844 Å for a small amount of partial oxidation ($\delta = 0.07 - 0.10$) of iridium.

Acknowledgements

It is a pleasure to acknowledge financial support from the Air Force Office of Scientific Research (Chemical Structures Program, Division of Chemical Sciences), and to thank Professors R. Hoffmann and M.-H. Whangbo for providing computational programs and some very helpful advice.

References

- 1 K. Krogmann, *Angew. Chem. Int. Ed.*, **8** (1969) 35.
- 2 M. J. Minot and J. H. Perlstein, *Phys. Rev. Lett.*, **26** (1971) 371.
- 3 A. H. Reis, Jr. and S. W. Peterson, *Ann. N.Y. Acad. Sci.*, **313** (1978) 560.
- 4 E. P. Goodings, *Chem. Soc. Rev.*, **5** (1976) 95.
- 5 A. E. Underhill and D. M. Watkins, *Chem. Soc. Rev.*, **9** (1980) 429.
- 6 W. Heiber, H. Lagailly and H. Mayar, *Z. Anorg. Allg. Chem.*, **246** (1941) 138.
- 7 E. O. Fischer and K. S. Brenner, *Z. Naturforsch., Teil B*, **17** (1962) 774.
- 8 K. Krogmann, W. Binder and H. D. Hausen, *Angew. Chem. Int. Ed.*, **7** (1968) 812.
- 9 A. P. Ginsberg, R. L. Cohen, F. J. DiSalvo and K. W. West, *J. Chem. Phys.*, **60** (1974) 2657.
- 10 L. Pauling, *J. Am. Chem. Soc.*, **69** (1947) 1019; *Nature (London)*, **161** (1948) 1019.
- 11 F. N. LeCrone, M. J. Minot and J. H. Perlstein, *Inorg. Nucl. Chem. Lett.*, **8** (1972) 173.
- 12 J.-M. André, in J.-M. André and J. Ladik (eds.), *The Electronic Structure of Polymers and Molecular Crystals*, Plenum, New York, 1974.
- 13 R. Hoffmann, *J. Chem. Phys.*, **39** (1963) 1397.
- 14 M.-H. Whangbo and R. Hoffmann, *J. Am. Chem. Soc.*, **100** (1978) 6093.
- 15 M.-H. Whangbo, R. Hoffmann and R. B. Woodward, *Proc. R. Soc. London, Ser. A*, **366** (1979) 23.
- 16 D. Bhaumik and J. E. Mark, *J. Polym. Sci., Polym. Phys. Ed.*, **21** (1983) 1111.
- 17 R. H. Summerville and R. Hoffmann, *J. Am. Chem. Soc.*, **98** (1976) 7240; **101** (1979) 3821.
- 18 M.-H. Whangbo and M. J. Foshee, *Inorg. Chem.*, **20** (1981) 113.
- 19 H. Basch and H. B. Gray, *Theor. Chim. Acta*, **4** (1966) 367.
- 20 J. Bernasconi, P. Brüesch, D. Kuse and H. R. Zeller, *J. Phys. Chem. Solids*, **35** (1974) 145.

CONFORMATIONAL ANALYSIS AND SOLID-STATE ^{29}Si NMR SPECTROSCOPY OF SOME POLYSILANES

by

W. J. Welsh, K. Beshah, J. L. Ackerman, and J. E. Mark

Department of Chemistry and the Polymer Research Center
The University of Cincinnati, Cincinnati, Ohio 45221

L. D. David and R. West

Department of Chemistry
The University of Wisconsin, Madison, Wisconsin 53706

Introduction

The configuration-dependent properties of a polymer chain, such as random-coil dipole moments and dimensions, will depend on the relative energies of the conformational states accessible to the skeletal bonds of the chain (1). Likewise, it has been anticipated and recently demonstrated from band gap calculations (2) that the electrical conductivity of a polymer chain will in general vary as a function of the degree of overlap of the orbitals responsible for the conduction of electrons, and this in turn will be conformation dependent. This latter point is pertinent to the polysilanes since recent experimental studies indicate that at least one of these, the phenylmethylsilane polymer (more commonly known as "polysilastyrene"), appears to become semiconducting upon addition of chemical dopants (3). Thus this polymer, and possibly other polysilanes, should be added to the list of conducting and semiconducting polymers, including polyacetylene (4), poly(p-phenylene) (5), poly(p-phenylene sulfide) (6), and polypyrrole (7).

Investigations are underway to measure some of the configuration-dependent properties of a series of substituted polysilanes (8). Results of these experimental studies will be compared with those obtained by theoretical methods based on the rotational isomeric state approximation using conformational energies computed from empirical potential energy functions (1). Electronic band gap calculations are also being carried out on these polymers, particularly as a function of structure and chain configuration, in order to assess their potential as electrical conductors or semiconductors. The present study focuses on calculations of conformational energies of the simplest of these polymers, polysilane itself, $[\text{SiH}_2-]_n$. The results will of course be directly applicable to the prediction and interpretation of configuration-dependent properties and to the analysis of the relation between electrical conductivity and conformation.

High-resolution ^{29}Si NMR measurements were also carried out on a phenylmethylsilane homopolymer and copolymer in the solid state. The mechanical and electrical properties of polysilanes are inherently those of the bulk solid systems. Thus, studies of the molecular origins of these properties require a spectroscopic technique that is feasible for solid systems, and one which can discriminate on the basis of chemical environment. Solid-state high resolution NMR is obviously one such technique.

Molecular Mechanics Calculations

Conformational energies E , calculated using parameterized empirical potential energy functions summing contributions from steric (nonbonded) and torsional terms,

were obtained for the chain segment $-\text{Si}-\text{SiH}_2^a-\text{SiH}_2^b-\text{SiH}_2^c-\text{SiH}_2^d-\text{Si}-$ as a function of the rotational angles ϕ_b and ϕ_c with bonds a and d held in the *trans* ($\phi = 0^\circ$) conformation. Pertinent structural parameters are 2.34 and 1.48 Å, respectively, for the Si-Si and Si-H bond lengths and 109.5° and 110.3°, respectively, for the Si-Si-Si and Si-Si-H bond angles (9). Thus the corresponding C-C (1.53 Å) and C-H (1.10 Å) bond lengths in the structurally analogous *n*-alkanes (1,10) are substantially smaller, and the additional 0.81 Å length of the Si-Si bond relative to C-C would be expected to greatly reduce the severity of repulsive interactions in the polysilanes. At the same time, however, the additional length of 0.38 Å for the Si-H bond over the C-H bond could act to offset this (9). The corresponding C-C-C and C-C-H bond angles are 112° and 109° (1,10), respectively, and these are nearly identical to the corresponding angles for the polysilanes.

The nonbonded interactions were described by the Buckingham potential function (1). As a result of the larger size and greater polarizability of Si relative to C, the potential energy minimum for $\text{Si}\cdots\text{Si}$ is roughly 4 times as deep and located 0.5 Å more distant than that for the $\text{C}\cdots\text{C}$ interaction. Likewise, the potential energy minimum for the $\text{Si}\cdots\text{H}$ interaction is about twice as deep and 0.25 Å more distant than that for $\text{C}\cdots\text{H}$. In the torsional terms, the intrinsic torsional barrier height $E_0 = 0.4 \text{ kcal mol}^{-1}$ for the Si-Si bond is considerably smaller than the corresponding value (2.8 kcal mol^{-1}) for the C-C bond in the *n*-alkanes (1,10,11). This feature will tend to flatten the potential energy surface. Hence, it is seen that the polysilane and the *n*-alkanes actually differ markedly in terms of their geometric (bond lengths) and energy parameters. These differences manifest themselves in the potential energy surfaces calculated for the two types of chains.

Results of the Conformational Analysis

The results are given in terms of a potential energy surface as a function of the rotational angles ϕ_b and ϕ_c . Values of E for the *tt*(0°, 0°), g^+g^+ ($\pm 120^\circ$, $\pm 120^\circ$), and g^-g^- states, which are particularly pertinent to calculations of configuration-dependent properties utilizing the rotational isomeric-state theory (1), are -1.17, -1.88, and 9.08 kcal mol^{-1} , respectively. Hence, g^+g^+ states are preferred over the alternative *tt* states by ca. 0.7 kcal mol^{-1} , while the g^-g^- states are prohibitively repulsive as is typically the case (1). By comparison, in the analogous *n*-alkanes the *tt* state is preferred over the g^-g^- states by ca. 1.0 kcal mol^{-1} (1,10). On the assumption that intermolecular energies generally have only a small effect on conformation (1), the crystalline state conformation could thus be similar to the polyoxymethylene $[\text{CH}_2-\text{O}-]_n$ helix, rather than to the polyethylene $[\text{CH}_2-\text{CH}_2-]_n$ planar zig-zag conformation.

Nearly all regions of the conformational-energy space are within 2.0 kcal mol^{-1} of the energy minima; this is in sharp contrast to the relatively high barriers ($> 6 \text{ kcal mol}^{-1}$) and large regions of prohibitively large energy found for the *n*-alkanes (10). Investigations are underway to determine the influence of both the preference for *gauche* states over *trans* states and the relatively high degree of conformational flexibility on the configuration-dependent properties and electrical conductivity of the polysilanes.

^{29}Si NMR Spectroscopy

This type of solid-state spectroscopy is being used to characterize polysilanes in terms of chemical environment of the silicons in the backbone, relaxation of backbone silicons, (which can elucidate molecular motion of the nucleus under observation) and the quantity and

type of crosslinks. A typical spectrum is shown in Figure 1. Of greatest interest is the study of doped systems,

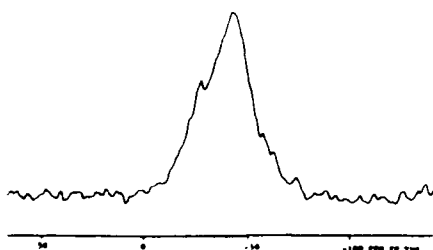


Fig. 1. ^{29}Si spectrum (17.88 MHz) of a poly-(41% phenylmethylsilane, 59% dimethylsilane) block copolymer at $T = 150\text{K}$. The silicon chemical shift anisotropy, about 35 ppm total width, appears to exhibit an asymmetry parameter near unity. Experimental conditions: cross polarization, matching RF fields 42kHz, decoupling RF field about 60kHz, mix time 4 msec, recycle 2 sec, 540 transients.

and the relationship of network structure to the semiconductive properties of polysilane chains. For instance, previous ^{13}C work on undoped polyacetylene (13) indicated that the nominally cis- and trans- materials were structurally pure (i.e., no cis-trans mixtures occurred). The presence of a small concentration of sp^3 hybridized carbon, ascribable to chain ends, crosslinks, or hydrogenated regions, was also indicated. The chemical shifts were "normal", in that the values did not reflect the occurrence of metallic conduction.

Parallel studies on pure and on doped polysilanes are also being carried out in order to understand how the addition of electron acceptors such as AsF_5 influences the chemistry and structure in giving rise to semiconducting properties (3).

Acknowledgement

It is a pleasure to acknowledge financial support from the Air Force Office of Scientific Research.

References

1. P. J. Flory, "Statistical Mechanics of Chain Molecules", Interscience, New York, N.Y., 1969.
2. D. Bhaumik and J. E. Mark, *Polymer Preprints, Div. of Polymer Chemistry, ACS*, 23, 105 (1982); work in progress.
3. R. West, L. D. David, P. I. Djurovich, K. L. Stearley, K. S. V. Srinivasan, and H. Yu, *J. Am. Chem. Soc.*, 103, 7352 (1981).
4. C. K. Chiang, M. A. Drey, S. C. Gau, A. J. Heeger, A. G. MacDiarmid, Y. W. Park, and H. Shirakawa, *J. Am. Chem. Soc.*, 100, 1013 (1978); C. K. Chiang, Y. W. Park, A. J. Heeger, H. Shirakawa, E. J. Louis, and A. G. MacDiarmid, *J. Chem. Phys.*, 69, 5098 (1978).
5. D. M. Ivory, G. G. Miller, J. M. Sowa, L. W. Shacklette, R. R. Chance, R. H. Baughman, *J. Chem. Phys.*, 71, 1506 (1979).
6. J. F. Rabolt, T. C. Clarke, K. K. Kanazawa, J. R. Reynolds, and G. B. Street, *J.C.S. Chem. Comm.*, 347 (1980).
7. K. K. Kanazawa, A. F. Diaz, R. H. Geiss, W. D. Gill, J. F. Kwak, J. A. Logan, J. F. Rabolt, and G. B. Street, *J.C.S. Chem. Comm.*, 854 (1979).
8. Research in progress.
9. J. P. Hummel, J. Stackhouse, and K. Mislow, *Tetrahedron*, 33, 1925 (1977); M. T. Tribble and N. L. Allinger, *ibid.*, 28, 2147 (1972).
10. A. Abe, R. L. Jernigan, and P. J. Flory, *J. Am. Chem. Soc.*, 88, 631 (1966).
11. W. J. Welsh, J. E. Mark, and E. Riande, *Polym. J.*, 12, 467 (1980).
12. K. S. Pitzer, *Adv. Chem. Phys.*, 2, 59 (1959).
13. M. M. Maricq, J. C. Waugh, A. G. MacDiarmid, H. Shirakawa and A. J. Heeger, *J. Am. Chem. Soc.*, 100, 7729 (1978).

Theoretical Investigations on Some Rigid-Rod Polymers Used as High-Performance Materials

WILLIAM J. WELSH^{1,2}, DHARMAJYOTI BHAUMIK¹,
HANS H. JAFFE¹, and JAMES E. MARK¹

¹Department of Chemistry and the Polymer Research Center
University of Cincinnati
Cincinnati, Ohio 45221

²Department of Chemistry
College of Mount St. Joseph
Mount St. Joseph, Ohio 45051

This review focuses on a new type of *para*-catenated aromatic polymer being used in the preparation of high-performance films and fibers of exceptional strength, thermal stability, and environmental resistance, including inertness to essentially all common solvents. Polymers of this type include *cis* and *trans*-poly(*p*-phenylene benzobisoxazole) (PBO), and the *cis* and *trans* forms of the corresponding poly(*p*-phenylene benzobisthiazole) (PBT). The purpose of this paper is to summarize the authors' theoretical work on the structures, conformational energies, intermolecular interactions, and electronic properties of PBO and PBT chains, including the protonated forms known to exist in strong acids. The emphasis is on how such studies provide a molecular understanding of the unusual properties and processing characteristics of this new class of materials.

INTRODUCTION

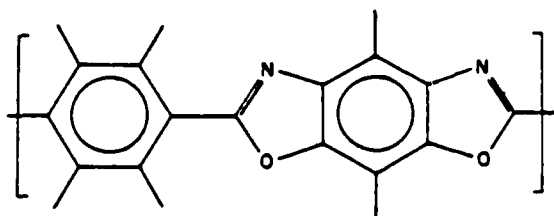
Synthetic polymers now pervade all industrialized societies, with new applications appearing on an almost daily basis (1). One example of a case in which specially synthesized polymers have been particularly impressive in their replacement of non-synthetic or non-polymeric substances is the area of "high-performance" materials. Materials in this category are so designated because of their ability to maintain desirable properties over a wide range in temperature, and frequently despite exposure to very hostile environments. Some specific examples of the superiority of man-made polymers are packaging films that are tougher than the cellulose-based materials they replace, and textile fibers such as Dacron, which are much more durable than most naturally occurring fibers. A more exotic example is the class of aromatic polyamides having high melting points and exhibiting strengths (on a weight basis) well above that of steel (1).

The present review focuses on a new type of *para*-catenated aromatic polymer being used in the preparation of high-performance films and fibers of exceptional strength, thermal stability, and environmental resistance, including inertness to essentially all common solvents. A polymer of this type, a poly(*p*-phenylene benzobisoxazole) (PBO), is illustrated in Fig. 1 (2). The isomer shown here is designated the *cis* form on the basis of the relative locations of the two oxygen atoms in the repeat unit. Other related polymers of interest are the *trans*-PBO and the *cis* and *trans* forms of the cor-

responding poly(*p*-phenylene benzobisthiazole) (PBT), in which the two oxygen atoms are replaced by sulfur atoms.

As can be seen from the sketch, these chains are extremely stiff, approaching the limit of a rigid-rod molecule. Because of their rigidity, they readily form liquid-crystalline phases (3-9), specifically nematic phases in which the chains are aligned axially but are out of register in a random manner. The spinning of films from a liquid-crystalline dope of such a polymer has great advantages (1, 10). The required flow of the system is facilitated, and the chains already have a great deal of the ordering they need in the crystalline fibrous state to exhibit the desired mechanical properties. Not surprisingly, PBO and PBT chains are the focus of the US Air Force's "Ordered Polymers" Program (10), which has been established to develop high-performance materials for aerospace applications. They are being used not only as fibers and films, but also as reinforcing fibrous fillers in amorphous matrices to give "molecular composites" (10-12), where they serve the same purpose as the macroscopic glass or graphite fibers widely used in multi-phase polymer systems.

The purpose of this account is to summarize the authors' theoretical work on the structures, conformational energies, intermolecular interactions, and electronic properties of PBO and PBT chains, including the protonated forms known to exist in strong acids. The emphasis is on how such studies provide a molecular understanding of the unusual

Fig. 1. The *cis*-PBO repeat unit (2).

properties and processing characteristics of this new class of materials.

METHODOLOGY

Both empirical molecular mechanics methods (13) and semiempirical CNDO/2 (Complete Neglect of Differential Overlap) molecular orbital methods (14) were used for the (intramolecular) conformational energy calculations. Only the former, however, has been used to date for the intermolecular interactions. The latter, quantum mechanical technique was modified to include geometry optimization (15, 16), except in the case of molecules containing sulfur (because of the increased number of electrons). In the molecular mechanics calculations the interaction energy E was considered to be the sum of the steric or van der Waals energy, the Coulombic energy, and the bond torsional energy. The van der Waals energies were calculated from Buckingham potential functions, generally with standard values of the function parameters (2). Coulombic interaction energies were obtained using partial charges obtained from the CNDO method; the values of the dielectric constant employed were the order of unity for calculations on the chains alone, and the other of one hundred for the chains dispersed in a strong acid. The torsional contributions for the rotatable *p*-phenylene bonds were taken to be two-fold symmetric, with minimum energy in the coplanar conformations and values of the barrier heights as suggested from pertinent spectroscopic data.

Polarizabilities were calculated using three methods, specifically, second-order perturbation theory combined with the formalism of CNDO/S CI (Configuration Interactions) (17, 18), an empirical scheme based on the additivity of atomic hybrid components (19), and the standard bond polarizability method (20). Electronic band structures, relevant to electrical conductivity, were calculated using the tight-binding scheme based on the extended Hückel theory (21, 22).

The required structural information, in particular bond lengths and bond angles, were generally obtained from X-ray structural studies carried out on model compounds (3).

CONFORMATIONAL ENERGIES AND INTERMOLECULAR INTERACTIONS FOR THE UNPROTONATED CHAINS

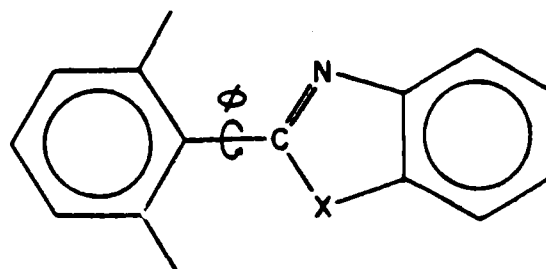
Deviations from Coplanarity

In spite of the rigidity of the PBO and PBT chains, there is some conformational flexibility in that ro-

tations should be permitted (at least to some extent) about the *p*-phenylene groups in each repeat unit. Such rotations ϕ are illustrated in the chain segment shown in Fig. 2 (2). The preparation of high-strength materials consisting of rodlike polymers such as these requires a high degree of alignment of the rods. The extent of intramolecular rotational flexibility and thus deviations from planarity are important in this regard, particularly in terms of chain-packing effects and the solubility characteristics of the polymers.

The molecular mechanics calculations (2) on the segment shown indicated that the lowest energy conformation of *cis*- and *trans*-PBO should correspond to $\phi = 0$ degrees; this is in agreement with the planarity found for the corresponding model compound in the crystalline state (23). Significant nonplanarity is predicted for *trans*-PBT with ϕ estimated to be approximately 55 degrees (2). The nonplanarity predicted for the PBT, but not for the PBO polymers, is due to the fact that the S atom has a much larger van der Waals radius than the O atom (~1.85 versus 1.40 Å) (24). The pertinent experimental value of ϕ , obtained from a crystalline *trans*-PBT model compound, is 23.2 degrees (25). The lack of quantitative agreement between theoretical and experimental results is less significant than the numerical differences in ϕ might suggest. First, the energy changes only gradually with ϕ near the minimum; specifically, the entire range $\phi = 25$ to 90 degrees gives energies within 0.25 kilojoules per mole (kJ mol^{-1}) of the minimum value, and this indicates considerable uncertainty in locating the preferred value of ϕ . Second, the discrepancy between theory and experiment could be due to intermolecular forces, which could strongly favor a more nearly planar conformation for more efficient chain packing. The effect of including intermolecular interactions by minimizing the total (intramolecular and intermolecular) energy of a pair of *trans*-PBT sequences (2) does shift the predicted conformation to the range 0 to 25 degrees, in much better agreement with experiment. The vibrational and electronic absorption spectra of model compounds in the crystalline state and in solution (26) are consistent with this interpretation. The situation is thus very similar to that of biphenyl, for which the dihedral angle is ~42 degrees in the vapor phase, ~23 degrees in the melt, and ~0 degrees in the crystalline state (27).

Another problem with the intramolecular molec-

Fig. 2. Rotatable segment in PBO ($X = O$) and in PBT ($X = S$) (2).

ular mechanics calculations is the fact that the torsional barrier chosen in these calculations may underestimate the true barrier to rotation. In the rigid-rod polymer, the coplanar conformation may be favored by long-range conjugation effects, which are absent in benzaldehyde, the model compound used for the estimate of the barrier. Some evidence in support of this possibility exists in that the length of this bridging bond in the polymers of interest is smaller than the lengths of corresponding bonds in analogous low-molecular-weight species, which suggests some partial double-bond character in these C-C bonds (2). This suggested recourse to CNDO calculations, the results of which are summarized in Fig. 3 (27). In the case of *cis*- and *trans*-PBO, very similar conformational energy profiles were obtained. In both cases, the preferred conformation corresponds to $\phi = 0$ degrees (coplanarity); this result is thus in excellent agreement with the molecular mechanics results and with experiment. The substantial barriers to rotation away from coplanarity imply that conjugation effects between the aromatic moieties (favoring coplanarity) dominate the steric repulsions (disfavoring coplanarity) between the orthohydrogen atoms on the phenylene group and nearby atoms within the heterocyclic group. The CNDO/2 conformational-energy profile of the *trans*-PBT model compound is quite different. The preferred angle is $\phi = 20$ degrees, in good agreement with experiment, but the energy barrier to coplanarity is only about 2.1 kJ mol⁻¹. Beyond $\phi = 20$ degrees, the barrier rises sharply and monotonically, yielding a maximum barrier of ~25.0 kJ mol⁻¹ at $\phi = 90$ degrees. The barrier to rotation is relatively large and should be considered an upper estimate because geometry optimization was not available for sulfur-containing molecules such as PBT. The *cis*-PBT chain is also predicted to be significantly nonplanar, but the experimental results (25) indicate a deviation of only 2.8 to 5.8 degrees from planarity. Molecules of this type are much more complicated than the three others in that they have considerable "bowing" within the repeat unit, a subject (27) dealt with separately in a later section of this review.

In the case of the two PBO polymers, geometry optimization gave bond lengths and bond angles in excellent overall agreement with those observed for the model compounds in the crystalline state (23).

Chain Packing and Intermolecular Interactions

The specific goals in these calculations (28) were elucidation of the nature of the chain packing, and estimation of the corresponding densities, magnitudes of the total interaction energies, and the relative importance of van der Waals and Coulombic contributions.

Because of the complexity of these systems, the calculations were of necessity very approximate, being based on only a pair of the chains of a given type in their planar or nonplanar conformations. The first chain was one repeat unit long, with the

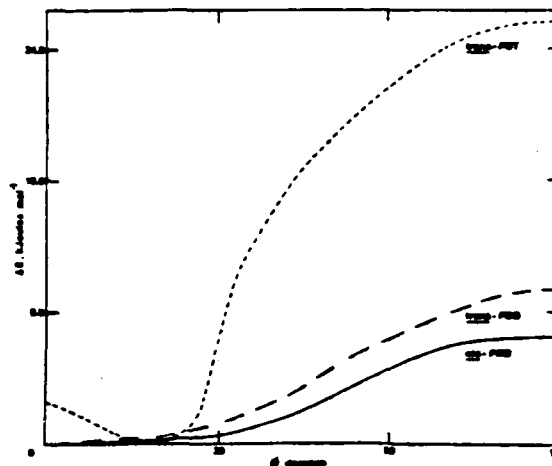


Fig. 3. Dependence of the CNDO conformational energy ΔE on the torsional angle ϕ for the *cis*-PBO, *trans*-PBO and *trans*-PBT model compounds (27). For a given compound, values of ΔE were taken as the difference in total energy E between a given conformation ϕ and the conformation corresponding to the lowest calculated energy.

second being assigned a series of lengths in an attempt to make the interaction energies (per repeat unit) as realistic as possible without making the calculations impracticable. In the initial series of calculations the chains were first placed in parallel arrangements, one above the other, and then one chain was rotated about its axes. The rotations invariably increased the energy, and such arrangements were therefore not considered further. Thus, the calculations to determine minimum-energy arrangements were based primarily on two parallel chains shifted relative to one another. In the case of the density estimates, there are two specific sets of calculations which are relevant, one for a pair of chains above one another $\begin{smallmatrix} \text{H} \\ | \\ \text{H} \end{smallmatrix}$ and the other for a pair alongside one another $\begin{smallmatrix} \text{H} & \text{H} \\ | & | \\ \text{H} & \text{H} \end{smallmatrix}$.

The results (28) show that for pairs of chains above one another the chains are out of register by 3.0 Å in the case of the two PBO polymers (which would place a phenylene group of the upper chain over the bond bridging the two ring systems of the repeat unit of the lower chain) and by 1.5 Å in the case of the *trans*-PBT. These are rather approximate results, in part because of the large number of energy minima occurring as the chains are slid by one another. The latter displacement was predicted to be smaller than the former because of the large size of a sulfur atom relative to oxygen and the much more irregular cross section of the nonplanar PBT molecule. These results are in at least qualitative agreement with the results of X-ray structural studies. The experimental values of these axial shifts were found to be approximately 4.5 Å in the case of model compounds for all three types of molecules (23, 25). The agreement between theoretical and experimental values could, of course, be considerably better for the polymeric chains, which have not yet been studied experimentally in this regard. In the case of the vertical spacings, the theoretical results are in excellent agreement with the experi-

mental value of ~ 3.5 Å for all three types of model compounds (23, 25). For the pairs of chains alongside one another, the spacing is predicted to be approximately 6.1 Å. Although there are no experimental values of this quantity available for comparison, it is important for density estimates which are discussed below.

The interaction energies were found to be rather large, with contributions from only a few repeat units adding up to values approaching typical bond dissociation energies. This suggests that the failure mechanism in such materials might generally be bond breakage rather than chain slippage. The attractions are somewhat larger for the *trans*-PBT chain because S atoms give rise to larger van der Waals attractions than do O atoms because of their much higher polarizability. The Coulombic contributions to the total interaction energy were found to be very small, which suggests that the dielectric constant of a potential solvent for these (unprotonated) polymers should be of no importance, and thus in agreement with experiment (29).

The above information also permits estimation of the densities of the PBO and PBT polymers in the crystalline state. The two polymers were represented as having elliptical cross sections with six such ellipses closely packed around a central ellipse. The densities thus estimated were found to be in good agreement with the experimentally obtained densities of the model compounds (23, 25), particularly in the way they vary with changes in the structure of the repeat unit. The results indicate that the higher density for the PBT polymer is due to the higher atomic weight of S relative to O, rather than to more efficient chain packing.

"Bowing" in the *Cis*-PBT Chains

Model compounds of the *cis*-PBT polymer chain, as illustrated in Fig. 4 (27), have been shown to assume a slightly bowed configuration in the crystalline state (25). The bowing is a result of the planar thiazole rings being inclined in the same direction from the best plane through the atoms of the fused benzene ring by an average of 2.6 degrees. The bowing corresponds to an average inclination of 4.7 degrees between the bonds connecting the end phenylene to the benzobisthiazole and the best plane through the benzobisthiazole group. If present in polymeric *cis*-PBT, this bowing would be expected to interfere with alignment of chains and hence have a deleterious effect on desirable properties.

Of primary interest here is a rough estimate of the strain energy responsible for inducing this molecule to "bow" out of the planar conformation, as exists in the *trans*-PBT and *cis*- and *trans*-PBO model compounds. To this purpose, the CNDO/2 total energy of the *cis*-PBT model compound was calculated (27) and compared to that of a fictitious planar *cis*-PBT model molecule possessing essentially the same structural geometry (in terms of bond angles and bond lengths) as the actual "bowed" molecule. Values of equivalent bond angles and bond lengths in *trans*-PBT and *cis*-PBT

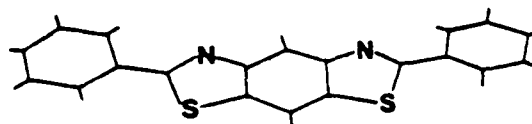


Fig. 4. The *cis*-PBT model compound with the bowing illustrated in two dimensions (27).

model compounds are observed to be nearly identical in the crystalline state (25). The planar *cis*-PBT studied here for comparison can therefore be considered the direct analogue of *trans*-PBT, apart from the fact that the "cis" form apparently does experience considerable strain.

The results gave an energy of -5368 eV and -5308 eV, respectively, for the "bowed" and "flat" forms. This yields an energy difference of ~ 60 eV per molecule (~ 5800 kJ mol $^{-1}$) in favor of the "bowed" form. These numbers should be taken as highly approximate upper limits since geometry optimization could not be implemented and CNDO/2 energies involving second-row atoms like sulfur are typically less reliable. Nevertheless, these results do indicate that rather large energy decreases are obtained by the bowing process. Apparently, after bowing, the molecule's bond angles and lengths "relax" to values experimentally indistinguishable from those of *trans*-PBT (27).

Chains Containing Molecular Swivels

Because of their stiffness, the PBO and PBT chains are very nearly intractable, being insoluble in all but the strongest acids [even when pendant groups are attached to the chains (10)] and very difficult to process into usable films and fibers (3, 10). These materials may be made more tractable, however, by the insertion of a limited number of atoms or groups chosen so as to impart a controlled amount of additional flexibility to the chains. The insertion of even a small number of flexible molecular fragments or "swivels" into such chains will increase their flexibility and tractability by allowing mutual rotation of adjacent chain elements about the swivels' rotatable bonds. (Such swivels also have the advantage of facilitating the polymerization). It is obviously of considerable importance to investigate the effect of the structure, number, and spacing of such swivels along the chain. For example, two closely spaced swivels would decrease the rigidity of the chains but still permit occurrences of nearly parallel conformations conducive to the formation of the desired molecular alignment or organization, as illustrated in Fig. 5 (30).

In swivels of the type Ph-X-Ph-X-Ph, where Ph is phenylene and X is the single atom O, S, Se, or Te, the pairs of rotatable angles should be independent to good approximation and the problem therefore treated in terms of two single swivels. The energy maps obtained for these swivels from molecular mechanics (30) reveal that the sulfur swivel has the advantage both in equilibrium flexibility (more low-energy and thus accessible regions in configuration space) and in dynamic flexibility (lower barriers between energy minima). Also, the Ph-S-Ph swivel

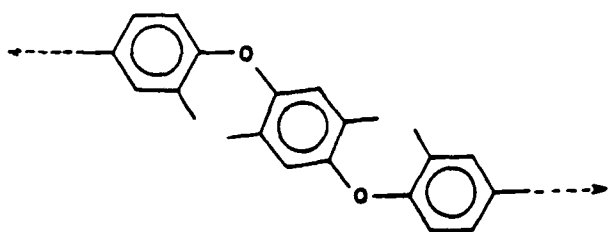


Fig. 5. Two adjacent oxygen para-phenylene swivels (30).

has a larger fraction of the conformational energy map that is energetically accessible. In the case of the double swivels it is of course important to consider which isomeric linkages (o,m,p) have conformations which give nearly colinear continuation of the chain, or at least parallel continuation. The oxygen double swivels have three isomers that provide colinearity (mpm, pop, and mmp), and seven that permit parallel continuation. The sulfur double swivels have no isomers giving colinearity and again seven giving parallelism (30). In the S case, the absence of colinear isomers is related to the values of the various bond angles within the segment. Specifically, the similarity between the bond angles (120 degrees) within the aromatic ring and the COC bond angle (123 degrees) in the oxygen swivel increases the number of nearly colinear arrangements. This simplifying circumstance does not occur in the case of the sulfur swivels since the CSC bond angle is 109 degrees.

A number of somewhat more complicated swivels were also investigated, viz., $-\text{CO}-$, $-\text{SO}_2-$, $-\text{CH}_2-$, and $-\text{C}(\text{CF}_3)_2-$. On the basis of both thermal stability (31) and conformational flexibility, it seems that the most promising swivels from this expanded group are $-\text{O}-$, $-\text{S}-$, $-\text{C}(\text{CF}_3)_2-$, and $-\text{CO}-$ (30).

As is evident from Fig. 5 (30), H atoms on C atoms which are α to the swivel linkage can force the swivel out of the desired coplanar conformation. A simple way to reduce these offending $\text{H}\cdots\text{H}$ repulsions would be to eliminate the responsible atoms altogether. As an example, one or both of the phenylenes in the swivel could be replaced with a pyridylene (Pyr) group in which the nitrogen in the ring replaces the offending CH group. It is found that when even only one of the phenylenes is thus replaced, as in Pyr-O-Ph and Pyr-S-Ph, the repulsions in the coplanar arrangement are greatly reduced and, in general, the flexibility of the swivel increased. As expected, replacement of both of the Ph groups increases both effects.

Wholly aromatic swivels, such as diphenylene and 2,2-dipyridylene, should have the greatest thermal stability. They can maintain parallel continuation of the chain if bonded to it either o,o or m,m; although the p,p isomer provides colinearity, it does not of course give the "kink" needed for additional flexibility. Replacement of one or both of the phenylenes by the 2-pyridylene group would be expected to relieve much of the inter-ring congestion, as already described, and molecular mechanics calculations give results in agreement with this expectation.

Geometry-optimized CNDO/2 calculations were also carried out on a number of the wholly aromatic swivels, viz., biphenyl, 2,2'-bipyridyl, 2-phenylpyridine, 2,2'-bipyrimidyl, and 2-phenylpyrimidine (32). In agreement with the molecular mechanics calculations and with intuition, increase in the number of nitrogen substitutions generally decreases the energy of the coplanar conformation and increases the overall flexibility of the swivel (32).

EFFECTS OF PROTONATION

Polymer Chains

Protonation of the rodlike PBO and PBT chains and their model compounds in acidic media will have significant effects on their solubility, solution behavior, geometry, and conformational characteristics. In fact, only very strong acids such as methane sulfonic acid and polyphosphoric acid are solvents for these materials (29). Recent interest has therefore focused on the extent, nature, and effects of protonation in the polymers in order to gain insights into their solubility behavior and solution properties.

Freezing point depression measurements (33) on PBO and PBT model compounds have indicated that, depending on the acidity of the medium, the PBO model compound can exist as a 2H^+ ion, presumably with one proton on each (highly basic) nitrogen atom, or as a 4H^+ ion, presumably with the other two protons on the oxygen atoms. The PBT model compounds appear to have a greater preference for the smaller number of protons owing to the lower basicity of sulfur atoms relative to oxygen atoms. The CNDO method was used to get charge distributions for such protonated PBO and PBT chains, and molecular mechanics was then used to estimate the magnitudes of the inter-chain Coulombic repulsions (28). It is difficult to relate such results quantitatively to the polymer-solvent dissolution process, which is, of course, controlled by changes in free energy. They are nonetheless of considerable interest in that they indicate that protonation of the chains should greatly decrease the intermolecular attractions, even at the very high dielectric constants characteristics of strong, undiluted acids. This conclusion is consistent with the fact that only extraordinarily strong acids are solvents for these types of polymers (29).

Geometry-optimized CNDO calculations were carried out to characterize the effects of protonation on the conformations of the PBO chain (34). For all three forms, the unprotonated chain and the 2H^+ and 4H^+ ions of the *cis*-PBO model compound, the preferred conformation corresponds to rotation angle $\phi = 0$ degrees, the coplanar form. As ϕ increases, the energy barrier increases monotonically; the maximum barrier is located at $\phi = 90$ degrees with an energy ΔE of ~ 8.4 , 33.6 , and 84.0 kJ mol^{-1} above that of the coplanar form for the unprotonated form, the 2H^+ ion, and the 4H^+ ion, respectively. These results are somewhat surprising in that steric arguments would suggest that repul-

sions between the orthohydrogens on the phenyls and the acidic protons on the benzoxazole ring should render the coplanar conformations *less* preferred than other orientations, and certainly less preferred than the coplanar form for the unprotonated case. Inspection of the geometry-optimized structures of the three species in the coplanar form shows that the rotatable bond is seen to decrease in length with increased protonation. Specifically, the bond lengths are ~ 1.45 , 1.42 , and 1.38 Å for the unprotonated form and the 2H^+ and 4H^+ ions, respectively. Such contractions are typically indicative of strengthening of the bond, in this case the result of enhanced conjugation (favoring coplanarity) between the phenylene rings and the aromatic heterocyclic group. This increased stabilization of the coplanar forms appears to more than offset the repulsive effects of steric interferences.

These conclusions are corroborated by construction of resonance structures for the three species, which indicate significant contributions from resonance structures wherein the rotatable bond assumes a double bond in the case of the protonated forms (34). Additional evidence for the contributions of resonance structures upon protonation is noted in the slight shortening (and thus strengthening) of phenylene C-C bonds parallel to the backbone and the lengthening (and weakening) of those bonds more nearly perpendicular to it. Finally, changes in the UV-visible and Raman spectra upon protonation (35) are consistent with this described increase in conjugation.

Additional geometry-optimized CNDO/2 calculations (36) were carried out to predict the order of protonation within the *cis*-PBO model compound. The results indicate that protonation occurs in the order N, N, O, O, which is consistent with the greater basicity of nitrogen relative to oxygen. Thus, repulsive Coulombic effects between the acidic protons have only a negligible influence on the precise sequence of protonation.

Molecular Swivels

It is likely, and indeed desirable in order to promote solubility, that the nitrogen-containing swivels be protonated in the strong acids in which the PBO and PBT chains are soluble. CNDO calculations (32), for example, on 2,2'-bipyridyl showed that mono- and di-protonation had large effects on its conformational characteristics. While the parent molecule and the diprotonated species both prefer *trans*- over the *cis*-coplanar conformation, just the opposite is true for the mono-protonated case. Hence, the coplanar conformation preferred by the species will be a function of the acidity of the medium, with *trans* preferred in neutral media followed by a preference for *cis* (mono-protonated) and then back to *trans* (di-protonated) with increasing acidity. The results suggest the presence of hydrogen bonding for the mono-protonated bipyridyl in the *cis*-coplanar conformation, as evidenced by the strong preference for this conformation and by the bending of the exo-ring angles about the swivel atom in order to shorten the interatomic

distances to reasonable values for the $\text{N}\cdots\text{H}^+\cdots\text{N}$ hydrogen bond. The species 2,2'-bipyridyl- H_3O^+ and 2,2'-bipyrimidyl- $2\text{H}_2\text{O}$ were also studied in this manner, each in two initial configurations, one with an O-H bond pointing to each N atom and the other with an O-H bond normal to the swivel bond. For each species, the former configuration is the preferred one.

POLARIZABILITIES

The polarizabilities of the PBO and PBT chains are of considerable importance since they are needed for the interpretation of solution property studies such as flow birefringence measurements (37, 38). Experimental studies of this type were carried out to obtain rheological time constants and orientation parameters relevant to the processing of these materials.

The perturbation-CNDO method gave values of the average polarizability that were unrealistically small (39, 40), but the atomic additivity (19) and bond additivity (20) schemes gave more realistic results, in good agreement with each other. The PBT chain is predicted to have a larger value of the average polarizability than the PBO chain, since the C-S bond is much more polarizable than the C-O one. The calculated results were used to estimate values of the anisotropic ratio δ directly applicable to the interpretation of flow birefringence data.

ELECTRICAL CONDUCTIVITY

Of interest here is the fact that the same structural features that give the desired rigidity in PBO and PBT chains also give extensive charge delocalization and resonance stabilization. Such characteristics could be conducive to electrical conductivity, a topic of much current interest in polymer science (41). The present goal was therefore to carry out preliminary calculations of electronic band gaps in order to determine whether any of these molecules show promise of being semi-conducting either undoped or as modified by a suitable dopant.

For *cis*-PBO, *trans*-PBO, and *trans*-PBT chains in their coplanar conformations, the band gaps in the axial direction were found to be 1.72, 1.62, and 1.73 eV, respectively (42). Since *trans*-PBT is nonplanar, calculations on it were also carried out as a function of its rotation angle ϕ , the results being given in Fig. 6. The band gap was found to increase markedly with increase in nonplanarity, as would be expected from the decrease in charge delocalization. The calculations suggest the most likely value of ϕ to be ~ 30 degrees, in good agreement with the experimental value of 23 degrees obtained by X-ray analysis of a crystalline *trans*-PBT model compound (25). At this value of ϕ , the calculated value of the band gap is 1.98 eV. No discernible dispersion of the energy bands perpendicular to the chains is observed (43), indicating that the neighboring chains are electronically non-interactive, as was found earlier for *trans*-polyacetylene and polyethylene (44). All of these values of the axial band gaps in PBO and PBT are very close to the corre-

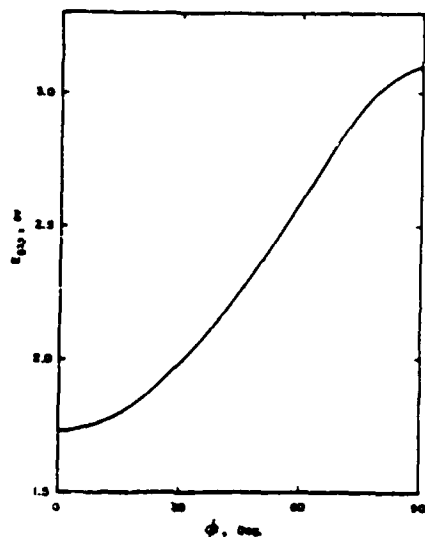


Fig. 6. The dependence of the trans-PBT electronic band gap on the rotational angle ϕ .

sponding values of 1.4 to 1.8 eV reported for trans-polyacetylene (41), a much studied polymer with regard to electrical applications; this should encourage further theoretical and experimental investigations of their electronic properties.

SOME STUDIES ON STRUCTURALLY RELATED MOLECULES

Since the PBO and PBT polymers are so intractable, some theoretical and experimental investigations were also carried out on more tractable random-coil polymers, such as the polyformals (45, 46) $[\text{CH}_2\text{O}(\text{CH}_2)_n\text{O}]$ and polysulfides (47-51) $[(\text{CH}_2)_n\text{S}]$ in order to obtain more insight into the properties of the structurally related rigid-rod polymers. Also, similar calculations were frequently carried out on relatively small molecules having structural features in common with the PBO and PBT polymers, specifically 2-(4-morpholino)benzothiazole (52), and several antifolate enzyme inhibitors (53, 54).

ACKNOWLEDGMENT

It is a pleasure to acknowledge the financial support provided by the Air Force Office of Scientific Research (Grant 78-3683, Chemical Structures Program, Division of Chemical Sciences).

REFERENCES

1. "Polymer Science and Engineering: Challenges, Needs, and Opportunities," ed. by C. G. Overberger and R. Pariser, National Academy Press, National Research Council, Washington, (1981).
2. W. J. Welsh, D. Bhaumik, and J. E. Mark, *Macromolecules*, **14**, 947 (1981).
3. A number of articles on PBO and PBT polymers are in the July/August special issue of *Macromolecules*.
4. P. J. Flory, *Proc. Royal Soc., Part A*, **234**, 60, 73 (1956).
5. M. Warner and P. J. Flory, *J. Chem. Phys.*, **73**, 6327 (1980), and pertinent references cited therein.
6. T. E. Helminiak and G. C. Berry, *Prepr. Am. Chem. Soc. Div. Polym. Chem.*, **18**, 152 (1977).
7. G. C. Berry, in "Contemporary Topics in Polymer Science," Vol. 2, E. M. Pearce and J. R. Schaefgen, Eds., Plenum Press, New York, (1977).
8. C.-P. Wong, H. Ohnuma, and G. C. Berry, *J. Polym. Sci., Polym. Symp.*, **65**, 173 (1978), and other papers in the same issue.
9. A number of relevant articles are in the Dec. 1980 and March 1981 special issues of *Brit. Polym. J.*
10. T. E. Helminiak, *Prepr. Am. Chem. Soc. Div. Org. Coatings Plast. Chem.*, **40**, 475 (1979).
11. G. Hussman, T. E. Helminiak, and W. Adams, *Prepr. Am. Chem. Soc. Div. Org. Coatings Plast. Chem.*, **40**, 797 (1979).
12. M. Wellman, G. Hussman, A. K. Kulshreshtha, and T. E. Helminiak, *Prepr. Am. Chem. Soc. Div. Org. Coatings Plast. Chem.*, **43**, 783 (1980).
13. P. J. Flory, "Statistical Mechanics of Chain Molecules," New York, Wiley-Interscience, (1969).
14. J. A. Pople and D. L. Beveridge, "Approximate Molecular Orbital Theory," McGraw-Hill, New York, N.Y., (1970).
15. N. Kondo, Ph.D. Dissertation, University of Cincinnati (1978).
16. H. H. Jaffe, CNDO/S and CNDO/2 (FORTRAN IV) QCPE 315 (1977).
17. F. T. Marchese and H. H. Jaffe, *Theor. Chim. Acta.*, **45**, 241 (1977).
18. J. Del Bene and H. H. Jaffe, *J. Chem. Phys.*, **48**, 1807 (1968).
19. K. J. Miller and J. A. Savchik, *J. Am. Chem. Soc.*, **101**, 7206 (1979).
20. K. G. Denbigh, *Trans. Faraday Soc.*, **36**, 936 (1940).
21. M.-H. Whangbo, R. Hoffman, and R. B. Woodward, *Proc. R. Soc. Lond., Ser. A*, **366** (1979).
22. J.-M. André, "The Electronic Structure of Polymers and Molecular Crystals," J.-M. André and J. Ladik, Eds., Plenum, New York, (1974).
23. M. W. Wellman, W. W. Adams, D. R. Wiff, and A. V. Fratini, Air Technical Report AFML-TR-79-4184, Part I: priv. commun.
24. A. Bondi, *J. Phys. Chem.*, **68**, 441 (1964).
25. M. W. Wellman, W. W. Adams, R. A. Wolff, D. R. Wiff, and A. V. Fratini, *Macromolecules*, **14**, 935 (1981).
26. G. M. Venkatesh, D. Y. Shen, and S. C. Hsu, *J. Polym. Sci., Polym. Phys. Ed.*, **19**, 1475 (1981).
27. W. J. Welsh and J. E. Mark, *J. Mater. Sci.*, **18**, 1119 (1983).
28. D. Bhaumik, W. J. Welsh, H. H. Jaffe, and J. E. Mark, *Macromolecules*, **14**, 951 (1981).
29. J. C. Holste, C. J. Glover, D. T. Magnuson, K. C. B. Dangayach, T. A. Powell, D. W. Ching, and D. R. Person, Air Force Technical Report AFML-TR-79-4107.
30. W. J. Welsh, D. Bhaumik, and J. E. Mark, *J. Macromol. Sci.-Phys.*, **B20**, 59 (1981).
31. C. Arnold, Jr., *Macromol. Rev.*, **14**, 265 (1979).
32. W. J. Welsh, H. H. Jaffe, N. Kondo, and J. E. Mark, *Makromol. Chemie.*, **183**, 801 (1982).
33. G. C. Berry, Y. Einaga, R. Furukawa, and C. C. Lee, Air Force Technical Report AFWAL-TR-81-4092.
34. W. J. Welsh and J. E. Mark, *Polym. Eng. Sci.*, **23**, 140 (1983).
35. D. Y. Shen, G. M. Venkatesh, D. J. Burchell, P. H. C. Shu, and S. L. Hsu, *J. Polym. Sci., Polym. Phys. Ed.*, **20**, 509 (1982).
36. W. J. Welsh and J. E. Mark, *Polym. Bulletin*, **8**, 21 (1982).
37. G. C. Berry, C.-P. Wong, S. Venkatraman, and S.-G. Chu, Air Force Technical Report AFML-TR-79-4115.
38. S.-G. Chu, S. Venkatraman, G. C. Berry, and Y. Einaga, *Macromolecules*, **14**, 939 (1981).
39. D. Bhaumik, H. H. Jaffe, and J. E. Mark, *Macromolecules*, **14**, 1125 (1981).
40. D. Bhaumik, H. H. Jaffe, and J. E. Mark, *J. Mol. Structure, THEOCHEM*, **87**, 81 (1982).
41. "Symposium on Conducting Polymers" papers, *Prepr. Am. Chem. Soc. Div. Polym. Chem.*, **23**(1) (1982).
42. D. Bhaumik and J. E. Mark, ms. submitted to *J. Polym. Sci., Polym. Phys. Ed.*
43. D. Bhaumik and J. E. Mark, unpublished results.
44. R. V. Kasowski, W. Y. Hsu and E. B. Caruthers, *J. Chem. Phys.*, **72**, 4896 (1980).
45. E. Riande, E. Saiz, and J. E. Mark, *Macromolecules*, **13**, 448 (1980).

46. E. Riande, M. Garcia, and J. E. Mark, *J. Polym. Sci., Polym. Phys. Ed.*, 19, 1739 (1981).
47. W. J. Welsh, J. E. Mark, and E. Riande, *Polymer J.*, 12, 467 (1980).
48. D. Bhaumik and J. E. Mark, *Macromolecules*, 14, 162 (1981).
49. E. Riande, J. Guzman, W. J. Welsh, and J. E. Mark, *Makromol. Chemie.*, 183, 2555 (1982).
50. W. J. Welsh, J. E. Mark, J. Guzman, and E. Riande, *Makromol. Chemie.*, 183, 2565 (1982).
51. J. Guzman, E. Riande, W. J. Welsh, and J. E. Mark, *Makromol. Chemie.*, 183, 2573 (1982).
52. D. Bhaumik and J. E. Mark, unpublished results.
53. W. J. Welsh, V. Cody, J. E. Mark, and S. F. Zakrzewski, *Cancer Biochem. Biophys.*, 0, 111 (1983).
54. W. J. Welsh, J. E. Mark, V. Cody, and S. F. Zakrzewski, "Proceedings of the Seventh International Symposium on Pteridines and Folic Acid Derivatives," ed. by J. A. Blair, W. de Gruyter Pub. Co., Berlin, (1983).

Particle Sizes of Reinforcing Silica Precipitated into Elastomeric Networks

Inherently weak elastomers are generally reinforced by blending particulate fillers into the elastomeric polymer prior to its being cured into a network structure.¹⁻¹¹ A specific, and very important, example is the mixing of high-surface silica (SiO_2) of a few hundred Å diameter into polydimethylsiloxane (PDMS [$-\text{Si}(\text{CH}_3)_2\text{O}-$]).^{1-5,8,11} One disadvantage of this standard approach, however, is the invariable coalescence of the filler particles into large aggregates in an essentially uncontrolled and poorly understood manner.¹¹ The nature and extent of such aggregation obviously would have a large effect on the mechanical properties of the elastomer thus reinforced.

It has recently been demonstrated¹² that it is possible to prepare very tough elastomers by swelling PDMS networks with tetraethyl orthosilicate (TEOS) [$(\text{C}_2\text{H}_5\text{O})_4\text{Si}$], which is then hydrolyzed *in situ*. It was proposed¹² that the hydrolysis of the TEOS gives silica particles which provide the desired reinforcement. The present investigation tests these ideas by means of transmission electron micrographs obtained on thin slices of PDMS elastomers thus prepared. The main goals are to find evidence for such filler particles and, if present, to estimate their sizes and size distribution. Since any such particles would be formed within a polymer matrix which should impede their coalescence into undesired aggregates, the degree of dispersion of the filler particles is also of considerable interest.

EXPERIMENTAL

The network was prepared from vinyl-terminated PDMS chains having number-average molecular weights corresponding to $10^5 M_n = 13.0 \text{ g} \cdot \text{mol}^{-1}$. They were tetrafunctionally end-linked with $\text{Si}[\text{OSi}(\text{CH}_3)_2\text{H}]_4$ in the usual manner,¹³ and the resulting network was extracted with tetrahydrofuran and then toluene for several days to remove soluble material (found to be present to the extent of a few percent). Strips cut from the network sheet were then dried, and one was set aside as a reference material (0 wt % silica).

The other network strips were swelled with TEOS to the maximum extent attainable, which corresponded to a volume fraction of polymer of approximately 0.26. Several strips were placed into an aqueous solution containing 2% by weight of ethylamine, and the hydrolysis of the TEOS was permitted to occur at room temperature for 1.5 h. The weight of the dried strips indicated that 34.4% by weight of filler had been incorporated in this manner.

Thin films having a thickness the order of 10^4 Å were microtomed from both the filled and unfilled samples using the following technique. A piece of network approximately $1 \times 1 \times 4$ mm was inserted into the water-filled cylindrical opening in a copper mount, and was then frozen into place. The entire assembly was cooled to approximately -126°C with vapor from a container of liquid nitrogen, and was then inserted into a similarly cooled Porter-Blum MT-2 Ultramicrotome equipped with a diamond knife. Thin slices obtained in this way were collected on copper grids, and examined in transmission using an RCA 3-G Electron Microscope with double condensor and high magnification pole piece.

RESULTS AND DISCUSSION

The electron micrographs obtained for the filled PDMS network at magnifications of 52,800 \times and 118,800 \times are shown in Figures 1 and 2, respectively. For purposes of comparison, the corresponding (essentially featureless) micrograph for the unfilled network at 118,800 \times is shown in Figure 3. The existence of filler particles in the first network, originally hypothesized on the basis of mechanical properties, is clearly confirmed. The particles have average diameters of approximately 250 Å, which is in the range of particle sizes of fillers¹⁴ typically

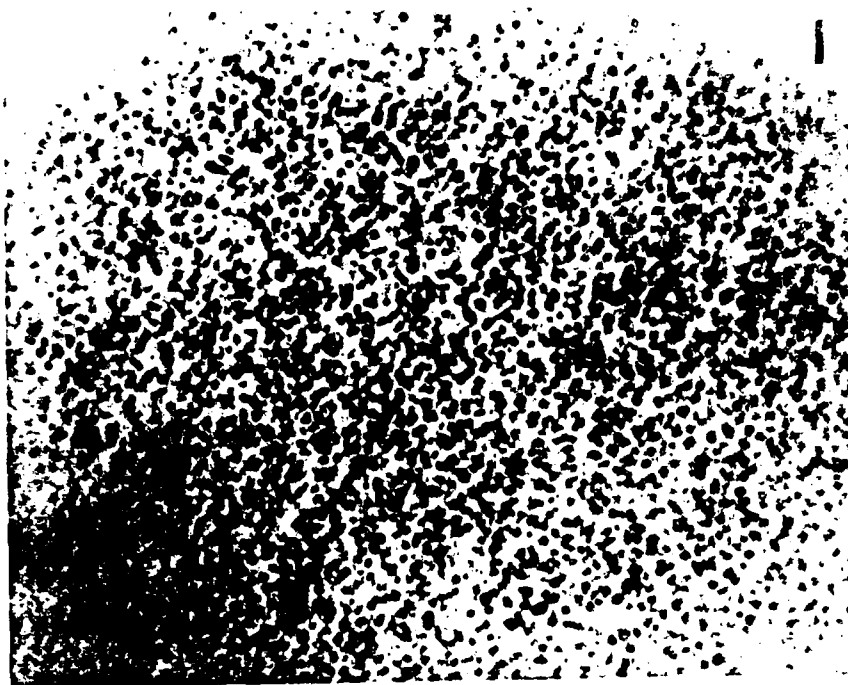


Figure 2



Figure 1



Fig. 3. Micrograph for the unfilled PDMS network at 59,400 \times .

introduced into polymers in the usual blending techniques. The distribution of sizes is relatively narrow, with most values of the diameter falling in the range 200–300 Å.

Most strikingly, there is virtually none of the aggregation of particles essentially invariably present in the usual types of filled elastomers. These materials should therefore be extremely useful in characterizing the effects of aggregation, and could be of considerable practical importance as well.

It is a pleasure to acknowledge the financial support provided by the National Science Foundation through Grant DMR 79-18903-03 (Polymers Program, Division of Materials Research) and by the Air Force of Scientific Research through Grant AFOSR 83-0027 (Chemical Structures Program, Division of Chemical Sciences). M.-Y. T. and C.-Y. J. also wish to thank the Dow Corning Corp. for the Research Fellowships they received.

Fig. 1. Transmission electron micrograph at a magnification of 26,400 \times for the PDMS network containing 34.4 wt % filler. The length of the bar in each figure corresponds to 1000 Å.

Fig. 2. Micrograph for the same filled network at 59,400 \times .

References

- 1 W. J. Botear, in *Rubber Technology*, M. Morton, Ed., Van Nostrand Reinhold, New York, 1973.
- 2 B. B. Boonstra, see Ref. 1.
- 3 K. E. Polmanteer and C. W. Lentz, *Rubber Chem. Technol.*, **48**, 795 (1975).
- 4 E. M. Dannenberg, *Rubber Chem. Technol.*, **48**, 410 (1975).
- 5 M. P. Wagner, *Rubber Chem. Technol.*, **49**, 703 (1976).
- 6 G. Kraus, *Rubber Chem. Technol.*, **51**, 297 (1978).
- 7 G. Kraus, in *Science and Technology of Rubber*, F. R. Eirich, Ed., Academic, New York, 1978.
- 8 E. L. Warrick, O. R. Pierce, K. E. Polmanteer, and J. C. Saam, *Rubber Chem. Technol.*, **52**, 437 (1979).
- 9 B. B. Boonstra, *Polymer*, **20**, 691 (1979).
- 10 Z. Rigbi, *Adv. Polym. Sci.*, **36**, 21 (1980).
- 11 R. K. Iler, *The Chemistry of Silica*, Wiley, New York, 1979.
- 12 J. F. Mark and S.-J. Pan, *Makromol. Chem., Rapid Commun.*, **3**, 681 (1982).
- 13 M. A. Llorente and J. E. Mark, *Macromolecules*, **13**, 681 (1980).

Y.-P. NING
M.-Y. TANG
C.-Y. JIANG
J. E. MARK

Department of Chemistry and the Polymer Research Center
The University of Cincinnati
Cincinnati, Ohio 45221

W. C. ROTH

Analytical Research Department
Dow Corning Corporation
Midland, Michigan 48640

Received January 31, 1984
Accepted February 28, 1984

DIPOLE MOMENTS OF SOME POLY(DIMETHYLSILOXANE) LINEAR CHAINS AND CYCLICS

E. RIANDE* and J. E. MARK†

*Instituto de Plástico Y Caucho, Madrid-6, Spain and †Department of Chemistry and the Polymer Research Center, The University of Cincinnati, Cincinnati, OH 45221, U.S.A.

(Received 26 April 1983)

Abstract—Dielectric constant measurements were carried out on poly(dimethylsiloxane) (PDMS) linear chains $\text{CH}_3\text{-(Si(CH}_3)_2\text{O)}_x\text{-Si(CH}_3)_3$ and cyclics $\text{[Si(CH}_3)_2\text{O]}_n$ for $x \approx 10, 15$ and 70 , in cyclohexane and in benzene at 30°C . Mean-square dipole moments $\langle \mu^2 \rangle$ were calculated from these data, using the method of Debye. The values thus obtained for the linear chains are consistent with results previously reported for short, linear PDMS chains in the undiluted state. Discernible differences among the values in the two solvents and undiluted state are manifestations of the "specific solvent effect" known to be important in longer linear chains the networks of PDMS. The cyclics were found to have dipole moments very similar to those of the corresponding linear chains. The cyclics also showed a specific solvent effect, in the same direction as shown by the linear molecules.

INTRODUCTION

The chain molecules which have been most extensively studied with regard to conformation-dependent properties are those of poly(dimethylsiloxane) (PDMS). Experimental investigations have focused on their random-coil dimensions [1], dipole moments [2-4], network thermoelasticity [1, 5], stress-optical coefficients [6, 7], and ring-chain cyclization constants [8, 9]. Theoretical studies carried out to interpret, and even predict, such properties are based on the well-known rotational isomeric state theory [1], and have been notably successful in this regard. Unusual features of these chain molecules which make them attractive to both experimentalists and theorists are their tractability and high-temperature stability [10, 11], semi-inorganic nature [12], marked polarity [1, 2-4], unusual equation of state parameters [13], abnormal entropies of dilution and excess volumes [14], extraordinary flexibility and permeability [10, 11, 15], and (because of unequal skeletal bond angles) a low-energy conformation that approximates a closed polygon [1, 2]. Another interesting feature is the existence of cyclics $\text{[Si(CH}_3)_2\text{O]}_n$ covering a wide range in degree of polymerization x [8, 9, 16], as well as the unusual linear chains $\text{CH}_3\text{-(Si(CH}_3)_2\text{O)}_x\text{-Si(CH}_3)_3$.

The present investigation is concerned with the determination of experimental values of the mean-square dipole moment $\langle \mu^2 \rangle$ of PDMS linear chains

and cyclics having $x \approx 10, 15$ and 70 . The required dielectric constant measurements are carried out in solution, in both cyclohexane and benzene. Comparisons with previous results [2, 3] obtained on short, linear PDMS chains in the undiluted state are used to document the dependence of $\langle \mu^2 \rangle$ on solvent medium. Also of interest are possible differences in $\langle \mu^2 \rangle$ between linear chains and cyclics having essentially the same degree of polymerization [16].

EXPERIMENTAL

Three PDMS linear polymers (L1, L2, L3) and three cyclics (C1, C2, C3) were generously provided by Professor J. A. Semiyen. The (number-average) number n of Si—O and O—Si skeletal bonds and polydispersity indices are given in the second and third columns of Table I.

At least four solutions of each of the samples were prepared in both cyclohexane and benzene, with the weight fraction w of polymer ranging from 0.0035 to 0.036. Specific volumes v of the solutions were then determined by dilatometry, indices of refraction \bar{n} by differential refractometry, and dielectric constants ϵ with the usual capacitance bridge and a miniature three-terminal cell [17]. All measurements pertain to 30°C .

RESULTS AND DISCUSSION

Values of the concentration dependence of the quantities of interest were expressed as $d\epsilon/dw$, $d\Delta\epsilon/dw$, and $d\Delta\bar{n}/dw$, where $\Delta\epsilon = (\epsilon - \epsilon_1)$ is the

Table I. Experimental data and results for the PDMS linear chains and cyclics in cyclohexane at 30°C .

Polymer	n	M_w/M_n	$-dv/dw$	$d\Delta\epsilon/dw$	$-d\Delta\bar{n}/dw$	$\langle \mu^2 \rangle / \text{nm}^2$
L1	20.1	1.01	0.215	0.433	0.016	0.178
L2	31.6	1.01	0.255	0.473	0.006	0.190
L3	141.1	1.07	0.250	0.502	0.004	0.213
C1	19.7	1.13	0.220	0.542	-0.002	0.182
C2	29.6	1.05	0.252	0.524	0.006	0.209
C3	139.2	1.06	0.260	0.491	0.008	0.203

Table 1. Experimental data and results for the PDMS linear chains and cycles in benzene at 30°C

Exptl.	d/d_0	dM/d_0	dM/d_0	$n \cdot nm^2$
L1	0.052	0.354	0.098	0.266
L2	0.058	0.408	0.078	0.289
L3	0.078	0.502	0.078	0.298
C1	0.112	0.491	0.086	0.209
C2	0.112	0.463	0.084	0.282
C3	0.113	0.488	0.082	0.329

difference between the dielectric constants of the solution and solvent, and $\Delta\tilde{n}$ serves the same purpose for the index of refraction. The results for the solutions in cyclohexane are given in columns four to six of Table 1, and for the solutions in benzene in columns two to four of Table 2. Mean-square dipole moments were calculated from the Debye equation

$$\langle \mu^2 \rangle = (9kT/4\pi N)(P_\infty) \quad (1)$$

where k is the Boltzmann constant, $T = 303.2\text{K}$ is the absolute temperature, N is Avogadro's number, and (P_∞) is the molar orientation polarization at infinite dilution. The latter is given by

$$(P_\infty) = P_\infty^s - R_\infty^s - P_A \quad (2)$$

where P_∞^s is the total molar polarization of the solute and R_∞^s is its molar refraction, both at infinite dilution. The values of P_∞^s and R_∞^s were obtained from [18]

$$P_\infty^s = [(n^2 - 1)(n^2 + 2)] [M(d\epsilon/dw + \epsilon_0)] \\ + [3Mr_s [(n^2 - 2)^2] (d\epsilon/dw) \quad (3)$$

$$R_\infty^s = [(n^2 - 1)(n^2 + 2)] [M(d\epsilon/dw + \epsilon_0)] \\ + [6Mr_s [(n^2 - 2)^2] (d\epsilon/dw) \quad (4)$$

when M is the molecular weight of the solute. The atomic polarization P_A was calculated from [3]

$$P_A = 7.81 + 5.66v \quad (5)$$

For symmetric chains such as PDMS at any length [4, 19], the mean-square dipole moment $\langle \mu^2 \rangle$ is identical to the value $\langle \mu^2 \rangle_0$ for the chain when unperturbed by excluded volume interactions [1, 20]. Its ratio to the number n of (polar) skeletal bonds and the square of the Si—O bond moment m is thus equal to the much-used *dipole moment ratio* $n^{-1} \cdot nm^2$ [4]. Values of the ratio calculated using the known result $m = 0.60\text{D}$ [2, 3] are given in the final columns of Tables 1 and 2. We estimate the uncertainty in these values to be approx. 10%.

For linear PDMS chains having $n \geq 20$, the experimental value of the dipole moment ratio, the undiluted state as obtained from the Onsager method is approx. 0.34 [3], the theoretical, rotational isomeric state value is 0.27 [3]. At $n \geq 140$, only the theoretical value, ~ 0.24 [3], is available. The present results are thus seen to be consistent with previous experimental and theoretical results on short, linear PDMS chains. The differences between the results in cyclohexane, in benzene, and in the undiluted state are most likely a manifestation of a "specific solvent effect", i.e., segment solvent interactions which presumably change conformational sequences along the chain backbone. Such an effect of the medium on

conformation-dependent properties of PDMS has previously been demonstrated for dimensions [1] and dipole moments [19] of long linear chains, and elongation moduli of elastomeric networks [21].

The results obtained on the cycles indicate that they have values of the dipole moment ratio very similar to those of the corresponding linear chains. At least for the range of n investigated, the dipole moment thus seems less generally useful than other properties [16] which have been used to characterize differences between PDMS linear chains and cycles. Finally, it is interesting to note that the cycles also showed a specific solvent effect, in the same direction as that shown by the linear chains.

A recent study [22] covering a wider range in n has concluded that for $n \geq 10$, the dipole moments of cyclic and linear PDMS chains are identical within experimental error, and that both cycles and linear chains exhibit a specific solvent effect. This study thus confirms the two major conclusions reached in the present investigation.

Acknowledgements—It is a pleasure to thank Professor J. A. Semlyen for the PDMS samples, and to acknowledge the financial support provided J. E. M. by the Air Force Office of Scientific Research through Grant AFOSR-83-0027 (Chemical Structures Program, Division of Chemical Sciences).

REFERENCES

1. P. J. Flory, *Statistical Mechanics of Chain Molecules*, Interscience, New York (1969).
2. J. E. Mark, *J. Chem. Phys.*, **49**, 1398 (1968).
3. C. Salton and J. E. Mark, *J. Chem. Phys.*, **54**, 801 (1971).
4. J. E. Mark, *Acc. Chem. Res.*, **7**, 218 (1974).
5. J. E. Mark, *Makromol. Chem.*, **11**, 138 (1976).
6. M. H. Liberman, Y. Abe and P. J. Flory, *Macromolecules*, **5**, 550 (1972).
7. B. Ermiar and P. J. Flory, *Macromolecules*, **16**, 1607 (1983).
8. J. A. Semlyen and P. V. Wright, *Polymer*, **10**, 848 (1969).
9. J. A. Semlyen, *Pure Appl. Chem.*, **53**, 1797 (1981) and pertinent references cited therein.
10. W. J. Boschee, *Rubber Technology*, (Edited by M. Morton), Van Nostrand Reinhold, New York (1973).
11. E. I. Warrick, O. R. Pierce, K. F. Pomanteer and J. C. Salam, *Rubber Chem. Tech.*, **52**, 437 (1979).
12. J. E. Mark, *Macromolecules*, **11**, 627 (1978).
13. H. Shih and P. J. Flory, *Macromolecules*, **5**, 758 (1972).
14. P. J. Flory and H. Shih, *Macromolecules*, **5**, 761 (1972).
15. J. Brandrup and E. H. Immergut, *Polymer Handbook*, Wiley-Interscience, New York (1975).
16. C. J. C. Edwards, S. Battie, W. Barchard, R. E. L. Stepto and J. A. Semlyen, *Polymer*, **23**, 875 (1982) and relevant references cited therein.
17. I. Riandi, *J. Polym. Sci., Polym. Phys. Ed.*, **14**, 2231 (1976).
18. G. Hedestrand, *Z. phys. Chem.*, **4**, 428 (1929); I. E. Haverstadt and W. D. Kumler, *J. Am. Chem. Soc.*, **64**, 2988 (1942).
19. S. C. Liao and J. E. Mark, *J. Chem. Phys.*, **59**, 3828 (1973), and pertinent references cited therein.
20. P. J. Flory, *Principles of Polymer Chemistry*, Cornell University Press, Ithaca (1953).
21. C. U. Yu and J. E. Mark, *Macromolecules*, **7**, 229 (1974).
22. M. S. Beevers, S. J. Mumby, S. J. Clarson and J. A. Semlyen, *Polymer*, **24**, 1868 (1983).

Elastomers

Treatment of Filler-Reinforced Silicone Elastomers to Maximize Increases in Ultimate Strength

Y.-P. Ning and J. E. Mark

Department of Chemistry and the Polymer Research Center, The University of Cincinnati,
Cincinnati, Ohio 45221, USA

Summary

Model elastomers prepared by end linking poly(dimethylsiloxane) chains were filled in situ by the ethylamine-catalyzed hydrolysis of tetraethylorthosilicate. The increases in modulus and ultimate strength obtained from the presence of filler were enhanced by a swelling-extraction treatment of the elastomers with tetrahydrofuran. The effect may be due to hydrolytic formation of additional particle surface silanol groups or removal of adsorbed small molecules, thereby increasing the number of sites for particle-polymer bonding.

Introduction

It has recently been demonstrated that it is possible to reinforce already cross-linked elastomers by the in-situ precipitation of silica particles generated in the hydrolysis of tetraethylorthosilicate (TEOS) $[\text{Si}(\text{OC}_2\text{H}_5)_4]$ (1-10). The reactions are typically carried out with a thus swollen network of poly(dimethylsiloxane) (PDMS) and yield essentially unagglomerated particles with diameters of 150-250 Å (1). The reinforcing effects of these fillers have been demonstrated by measurements of ultimate properties in elongation (1-5,8-10) and in impact tests (6).

The efficacy of any filler depends on the strength of the particle-elastomer interactions, which in turn depend on the number and types of groups on the particle surface. Silanol groups are thought to be particularly effective in this regard. Thus, it is of interest to try to hydrolyze any surface ethoxy groups occurring because of only partial hydrolysis of some of the TEOS. Similarly, it would be important to try to extract any adsorbed small molecules such as water, or the hydrolysis catalyst and byproduct, ethylamine and ethanol. The present investigation was carried out to ascertain whether it is in fact possible to obtain increased reinforcement in in-situ filled PDMS networks by means of an extended swelling extraction technique.

Some Experimental Details

The PDMS network employed was prepared by tetrafunctionally end linking (11) vinyl terminated chains which had a number-average molecular

sample of Figure 1, $K = 1.5$, and $\alpha = 0.2$. Again, Figure 1 is a plot of initial elongation. Strips were cut from the network about a rectangular area, sealed in liquid, the network reformed, and the strips were cut from the volume fraction of polymer of approximately 0.56. The swollen strips were then placed into a 20% solution of ethylene glycol (20% EG), and the hydrolysis permitted the loss of crosslinking. Values of the initial elongation f_0 obtained from the rupture of the dried strips are given in the first column of Table I. The elongation of each strip were

TABLE I

Ultimate elongation of dry strips

at 2 filler	Elongation treatment	f_0 mm	$f_{0.2}$ mm	$f_{0.4}$ mm
0.0	F	1.0	0.60	0.40
Al ₂ O ₃	F	1.0	0.60	0.40
62.0	F	1.0	0.60	0.40
63.0	F	1.0	0.60	0.40

^a 21 specimens treated with 10% EG at temperature of 100°C.

^b Elongation at rupture.

Ultimate strength, as determined by the initial stress at rupture, decayed rapidly for rupture.

Temperature rupture decayed of a 10% EG at 100°C.

then sealed at room temperature for 24 hours in a rectangular area, then chosen because it is a 20% EG solution. The strips were then dried under vacuum for 24 hours. The strips have lost only 0.8–1.0% by weight.

Both untreated and 10% EG treated strips were used in all experiments to obtain the stress-strain curves at 20% EG (Fig. 1). The unfilled and unfilled samples were used for the purpose of comparing the elastomeric properties of polymer network with the network stress $f = f_0/A$ (where f is the equilibrium stress, f_0 is K , and A is the initial cross-sectional area), and the initial stress or modulus f_0/A (where f_0 is the initial stress, f_0 is the elongation or relative length of the strip). All stress-strain curves were plotted for rupture behavior with the measurements f_0 and $f_{0.2}$ as the capture points of the samples.

Results and Discussion

The stress-strain curves for the unfilled and filled networks are presented in Figure 1. The typical curves are shown in the inset of Figure 1.

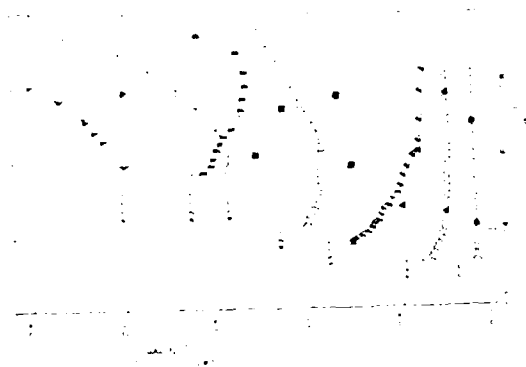


Figure 1. The reduced stress-strain curves for the unfilled and filled networks at 20% EG. The network corresponds to the at 2 filler in the network, and the dotted line is specific treatment with 10% EG. The dashed line is the results obtained out of rupture at 20% EG, the recoverability, and the vertical dotted line is the rupture points.

the dependence of the reduced stress on reciprocal elongation. As is frequently the case for filled elastomers, some of the specimens did not exhibit complete recoverability, with repeat determinations giving values of the modulus lying below the previous values. Figure 1 shows the data of Figure 1 plotted in such a way that the area under each stress-strain curve corresponds to the energy f_0 of rupture (Fig. 1), which is the initial recovery of elastomer toughness. Its values, along with values of the extreme extensibility $f_{0.2}$ and ultimate strength $f_{0.4}$ are given in the first three columns of the Table.

The in situ filled and unfilled networks are shown in Figure 1. The f_0 for the unfilled network with regard to value of f_0 is 1.0, and $f_{0.2}$ and ultimate strength $f_{0.4}$. This is the case for the unfilled



Fig. 2. Dependence of the function $f(x)$ on x for different values of the parameter α . The curves are labeled with numbers 1 through 6, corresponding to the values $\alpha = 0.1, 0.2, 0.3, 0.4, 0.5, 0.6$ respectively.

considered in [1, 2]. It is shown that the function $f(x)$ is a solution of the boundary value problem for the Poisson equation in the unit square $0 \leq x \leq 1, 0 \leq y \leq 1$ with the boundary conditions $f(0, y) = f(1, y) = 0$ and $f(x, 0) = f(x, 1) = 1$. The function $f(x)$ is also a solution of the boundary value problem for the Poisson equation in the unit square $0 \leq x \leq 1, 0 \leq y \leq 1$ with the boundary conditions $f(0, y) = f(1, y) = 1$ and $f(x, 0) = f(x, 1) = 0$. The function $f(x)$ is also a solution of the boundary value problem for the Poisson equation in the unit square $0 \leq x \leq 1, 0 \leq y \leq 1$ with the boundary conditions $f(0, y) = f(1, y) = 0$ and $f(x, 0) = f(x, 1) = 0$.

Acknowledgments

The author wishes to thank the members of the Department of Mathematics of the University of Illinois at Chicago for their hospitality and for the use of the facilities of the Department of Mathematics of the University of Illinois at Chicago during the period of his stay there.

References

1. L. E. Eidelman and A. P. Poritskiy, *Math. Notes*, **19**, No. 4, 611 (1975).
2. G. V. Vainikko and L. E. Eidelman, *Math. Notes*, **19**, No. 4, 611 (1975).
3. L. E. Eidelman and L. E. Eidelman, *Math. Notes*, **19**, No. 4, 611 (1975).
4. L. E. Eidelman and A. P. Poritskiy, *Math. Notes*, **19**, No. 4, 611 (1975).

5. L. E. Eidelman and A. P. Poritskiy, *Math. Notes*, **19**, No. 4, 611 (1975).
6. L. E. Eidelman, A. P. Poritskiy, and L. E. Eidelman, *Math. Notes*, **19**, No. 4, 611 (1975).
7. L. E. Eidelman, A. P. Poritskiy, and L. E. Eidelman, *Math. Notes*, **19**, No. 4, 611 (1975).
8. L. E. Eidelman and L. E. Eidelman, *Math. Notes*, **19**, No. 4, 611 (1975).
9. L. E. Eidelman and L. E. Eidelman, *Math. Notes*, **19**, No. 4, 611 (1975).
10. L. E. Eidelman and L. E. Eidelman, *Math. Notes*, **19**, No. 4, 611 (1975).
11. L. E. Eidelman and L. E. Eidelman, *Math. Notes*, **19**, No. 4, 611 (1975).
12. L. E. Eidelman and L. E. Eidelman, *Math. Notes*, **19**, No. 4, 611 (1975).
13. L. E. Eidelman and L. E. Eidelman, *Math. Notes*, **19**, No. 4, 611 (1975).
14. L. E. Eidelman and L. E. Eidelman, *Math. Notes*, **19**, No. 4, 611 (1975).
15. L. E. Eidelman and L. E. Eidelman, *Math. Notes*, **19**, No. 4, 611 (1975).
16. L. E. Eidelman and L. E. Eidelman, *Math. Notes*, **19**, No. 4, 611 (1975).
17. L. E. Eidelman and L. E. Eidelman, *Math. Notes*, **19**, No. 4, 611 (1975).
18. L. E. Eidelman and L. E. Eidelman, *Math. Notes*, **19**, No. 4, 611 (1975).
19. L. E. Eidelman and L. E. Eidelman, *Math. Notes*, **19**, No. 4, 611 (1975).
20. L. E. Eidelman and L. E. Eidelman, *Math. Notes*, **19**, No. 4, 611 (1975).

Received by the Editor July 1, 1975

Effects of Ethylamine Catalyst Concentration in the Precipitation of Reinforcing Silica Filler in an Elastomeric Network

J. E. Mark and Y.-P. Ning

Department of Chemistry and the Polymer Research Center, The University of Cincinnati,
Cincinnati, Ohio 45221, USA

SUMMARY

Ethylamine is found to be an effective catalyst for the hydrolysis of tetraethyloxosilicate in the in-situ filling of a polymer network. The silica filler thus precipitated strongly reinforces the elastomer, increasing its modulus, ultimate strength, and rupture energy. Increase in ethylamine concentration increases the rate of filler precipitation, and also increases the ultimate properties at constant weight % filler.

Introduction

In a recent study (1), a variety of inorganic and organic acids, bases, and salts were evaluated as catalysts for the hydrolysis of tetraethyloxosilicate (TEOS) when the reaction



is carried out within an elastomeric network, the filler thus precipitated "in-situ" provides considerable reinforcement (2).

One of the most promising of the catalysts identified in this survey (1) was ethylamine, which was therefore chosen for the present more detailed investigation. The primary purpose was to determine the effects of the ethylamine catalyst concentration on both the rate of filler precipitation, and the ultimate properties of the resulting filled elastomers in elongation.

EXPERIMENTAL DETAILS

The networks were prepared from vinyl-terminated polydimethylsiloxane (PDMS) chains obtained from the McGraw-Hull Corporation; they had a number-average molecular weight corresponding to $M_n = 100,000$ g/mol. The chains were tetrafunctional and linked with Si(OH) groups in the usual manner (3), and the resulting network, extracted with tetrahydrofuran and then toluene for several days to remove soluble material, found to be present to the extent of a few percent. Strips cut from the network sheet were then dried, and one was set aside as a reference material (0 wt % filler).

The other network strips were sectioned with the maximum extent stretchable, which corresponded to a volume fraction of approximately 0.56. Several strips were placed side by side. Pieces of two aqueous solutions containing 1.0 and 3.5 g/l by weight of ethylamine, respectively. The hydrolysis of the film was permitted to occur at room temperature for the periods of time specified in the second column of Table I. Values of the weight W filler incorporated in the second column of Table I.

TABLE I
Reaction Conditions, Amount of Filler Per Strip, and
Ultimate Properties of the Filled Elastomer

Reaction Conditions			Ultimate Properties			
Wt % EA ^a	Time, hrs	Wt % Filler	σ_b lb/in ²	ϵ_b in/in	σ_b lb/in ²	ϵ_b in/in
2.0	0.0	0.0	1.02	0.533	0.122	
	1.5	11.6	1.03	0.505	0.479	
	3.0	31.0	2.33	0.949	0.806	
	5.7	62.0	2.33	2.15	1.41	
	8.0	63.0	2.01	2.16	1.51	
	19.0	50.5	2.15	2.02	3.13	
35.0	0.0	0.0	1.02	0.533	1.15	
	1.0	20.0	2.25	1.00	0.125	
	1.5	50.3	2.15	2.92	2.02	
	2.0	69.8	2.12	3.55	2.50	
	4.0	50.2	2.55	2.21	2.04	

^a Ethylamine, in aqueous solution.

^b Elongation at rupture.

Ultimate strength, in approximately 0.5 mmol stress at rupture.

Energy required for rupture.

Weights of the dried strips, are given in the third column of the table. Portions of each of the networks were used in elongation experiments to obtain the stress-strain isotherms at 25°C. in 10% increments. The elongation at rupture of the primary network was the initial strain ϵ_0 (Table I) in the equilibrium elastic force and $\Delta\epsilon$ the additional elongation at rupture. The initial strain ϵ_0 was the initial strain ϵ_0 in the elongation at rupture ϵ_b of the strip. All stress-strain measurements were carried out in the rupture portion of the samples, and were generally repeated at least two times for reproducibility.

Results and Discussion

As can be seen from Table I, the rate of precipitation of ethylamine greatly increases the rate of precipitation of the filler. For example, after 1.5 hrs of reaction time, the 35.0% ethylamine solution has precipitated over four times as much filler as the 2.0% solution. Also, at the higher concentration, the maximum weight precipitated is reached in less than one tenth of the time.

Typical stress-strain isotherms obtained as described at 25°C. are presented in Figure 1. The data are shown in the usual way (σ/ϵ) but are

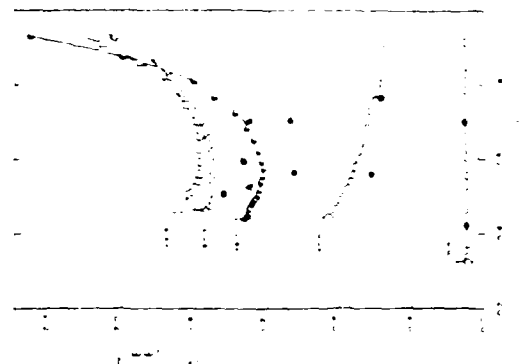


Figure 1. The reduced stress shown as a function of reciprocal elongation for the second series of filled-plastic networks at 25°C. Filled symbols are for results obtained out of sequence for test for reusability, and each curve is labelled with the weight % filler present in the network. The vertical dashed lines locate the rupture points.

the dependence of the reduced stress on reciprocal elongation. As frequently the case for filled elastomers (15,18), some of the networks did not exhibit complete reusability. In any case, the precision and efficiency of the filler are demonstrated by the marked similarity in modulus, with marked upturn at the higher elongations.

Figure 2 shows the data of Figure 1 plotted in a way that the area under each stress-strain curve corresponds to the energy E_p of

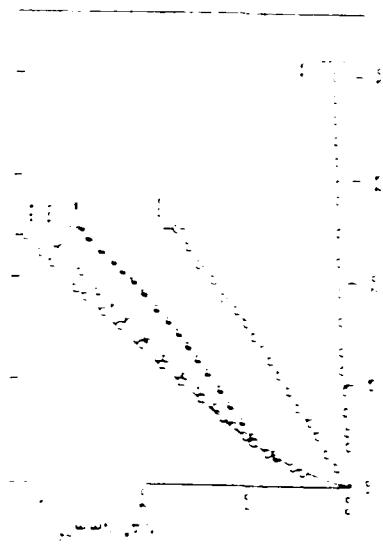


Figure 2. The minimal stress σ_{\min} as a function of elongation λ for the same networks characterized in Figure 1.

rupture (9), which is the standard measure of elastomer toughness. Its values, along with values of the maximum extensibility λ_m and ultimate strength f_u are given in the last three columns of the table. Increases in λ filler decrease σ_{\min} but increase f_u . The latter effect predominates and f_u increases accordingly.

Of considerable interest is the observation that even at constant weight λ filler, the elastomers prepared from the more concentrated ethylene solution had better ultimate properties. This must be due to differences in the nature of the filler particles, in particular their average size, size distribution, or degree of agglomeration (19). Such differences can, of course, be studied using transmission electron microscopy (19) and light scattering instrumentation (20).

Acknowledgements

It is a pleasure to acknowledge the financial support provided by the National Science Foundation through Grant DMR 79-10301-01 (Polymers Program, Division of Materials Research) and by the Air Force Office of Scientific Research through Grant AFOSR 83-0027 (Chemical Structures Program, Division of Chemical Sciences).

References

1. C. Y. Ning and J. F. Mark, *Macromol. Chem.*, **185**, 609 (1984).
2. J. F. Mark and C. Y. Ning, *Makromol. Chem., Rapid Commun.*, **3**, 481 (1982).
3. C. Y. Ning and J. F. Mark, *Polym. Eng. Sci.*, **24**, 600 (1984).
4. J. F. Mark, C. Y. Ning, and M. F. Tseng, *Macromolecules*, **17**, 600 (1984).
5. C. Y. Ning and J. F. Mark, *Colloid Polym. Sci.*, **262**, 600 (1984).
6. C. Y. Ning, A. Jortson, and J. F. Mark, *Colloid Polym. Sci.*, **262**, 600 (1984).
7. M. A. Florjanczyk and J. F. Mark, *Macromolecules*, **13**, 601 (1980).
8. J. F. Mark and L. L. Sullivan, *J. Chem. Phys.*, **65**, 1006 (1977).
9. M. A. Florjanczyk, A. J. Antkowiak, and J. F. Mark, *J. Polym. Sci., Polym. Phys. Ed.*, **19**, 671 (1981).
10. M. A. Florjanczyk, A. J. Antkowiak, and J. F. Mark, *J. Polym. Sci., Polym. Phys. Ed.*, **18**, 2263 (1980).
11. J. F. Mark, *Adv. Polym. Sci.*, **44**, 1 (1982).
12. J. F. Mark and F. J. Flory, *J. Appl. Phys.*, **37**, 6615 (1966).
13. L. R. G. Treloar, "The Physics of Rubber Elasticity", Clarendon Press, Oxford (1975).
14. J. F. Mark, *Rubber Chem. Technol.*, **48**, 695 (1975).
15. Z. Ripski, *Adv. Polym. Sci.*, **36**, 71 (1980).
16. J. F. Colmanster and C. M. Toner, *Rubber Chem. Technol.*, **48**, 235 (1975).
17. R. R. Rounstra, *Polymer*, **20**, 691 (1979).
18. C. Y. Ning and J. F. Mark, ms. submitted to *Macromolecules*.
19. C. Y. Ning, M. F. Tseng, C. Y. Ning, J. F. Mark, and M. C. Gentry, *J. Appl. Polym. Sci.*, **29**, 600 (1984).
20. D. M. Scharfer and J. F. Mark, unpublished results.

Accepted September 21, 1984

SHORT COMMUNICATION

The effect of relative humidity on the hydrolytic precipitation of silica into an elastomeric network

C. N. Jiang and J. E. Mark

Department of Chemistry and the Polymer Research Center, The University of Cincinnati, Cincinnati, Ohio, USA

Key words: Filled elastomers, silica filler, insitu reinforcement, poly(dimethylsiloxane).

It has been shown [1,2] that it is possible to fill already cured networks of poly(dimethylsiloxane) (PDMS $[-Si(CH_3)_2O-]$ by swelling them with tetraethyorthosilicate (TEOS $[Si(OC_2H_5)_4]$), which is then hydrolyzed in an aqueous solution of acid, base, or salt as catalyst. The silica precipitated insitu in this way consists of particles approximately 200 Å in diameter, according to electron microscopy measurements [2], and gives a substantial improvement in the ultimate properties and toughness of the elastomeric networks thus treated [1,3-5]. The present investigation focuses on the simplification of this technique by carrying it out with TEOS-swollen PDMS networks simply exposed to air at various values of the relative humidity.

Experimental details

The PDMS sample employed consisted of hydroxyl-terminated chains having a number-average molecular weight of 8.0×10^5 g mol⁻¹, and was generously provided by the Dow Corning Corporation. The chains were tetrafunctional and linked with TEOS in the undiluted state, in the usual manner [6]. The resulting network sheets, which were approximately 1 mm thick, were extracted at room temperature using tetrahydrofuran for three days followed by toluene for three days. Sol fractions amounted to a few wt %. Test strips cut from the sheets were approximately 3 mm wide and 30 mm long.

The extracted test strips were weighed and then placed into TEOS until swollen to equilibrium (which corresponded to a volume fraction of polymer of approximately 0.26). Each strip was then placed on a porous support and inserted into one of four containers in which the relative humidity was maintained at values of 21% (ambient conditions), 53%, 75%, or 100%. The TEOS was permitted to react with the moisture thus provided for the intervals

Table 1. Reaction conditions and the properties of the insitu filled networks

Relative humidity, %	Reaction time, hr	ζ , 1/cm ³	Weight Swell From Dry	From ζ	α	$(\sigma/A^*)_{\infty}$, N/mm ²	$10^3 E_{\infty}$, /mm ⁻¹
21	0	—	2.3	—	—	—	—
	1	—	2.4	—	—	—	—
	2	—	2.5	—	—	—	—
53	0	0.962	2.0	0.0	2.59	0.48	0.44
	1	1.04	17.2 ± 1.4	18.6	2.24	1.14	0.66
	2	1.18	12.0 ± 0.6	29.3	2.19	1.89	0.96
	3	1.25	—	30.0	2.12	3.16	1.68
75	0	—	17.1 ± 2.7	—	—	—	—
	1	—	30.1 ± 1.2	—	—	—	—
	2	—	52.5 ± 1.7	—	—	—	—
100	0	—	19.8 ± 3.3	—	—	—	—
	1	—	32.7 ± 1.3	—	—	—	—
	2	—	47.1 ± 1.6	—	—	—	—

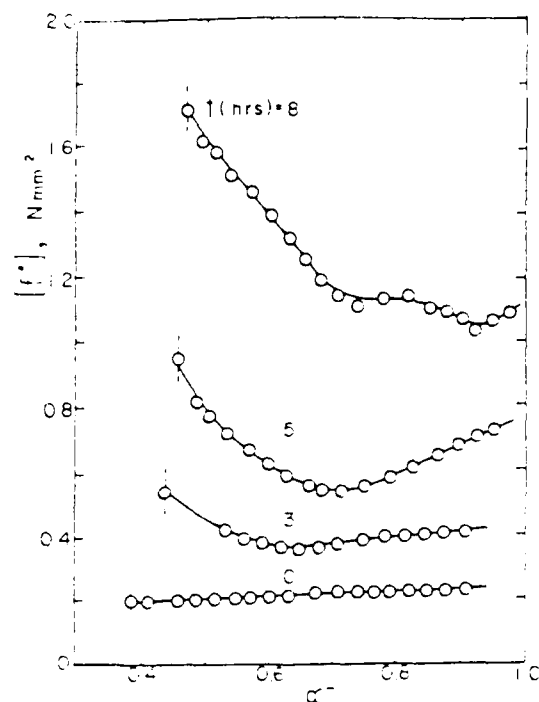


Fig. 1. The reduced stress shown as a function of reciprocal elongation for typical networks treated at 55% relative humidity. The results pertain to 25°C, and each curve is labelled with the reaction time in hrs. The vertical dashed lines locate the rupture points of the networks.

of time specified in column two of table 1. The samples were then dried under vacuum, and reweighed to constant weight to determine the wt % silica introduced. Duplicate or triplicate determinations were made in most cases.

Values of the density ρ of one series of networks were measured by pycnometry; the results are given in column three of the table. Stress-strain data in elongation were then obtained for these same samples at 25°C, in the usual manner [6-8]. The nominal stress to be obtained was given by $f^* \equiv f/A^*$ where f is the equilibrium elastic force and A^* the undeformed cross-sectional area, and the reduced stress or modulus [6-12] by $f^{**} \equiv f^*/a = f^*/l$, where $a = L/L_0$ is the elongation or relative length of the sample.

Results and discussion

Values of the wt % silica which were obtained from the changes Δw in weight of the samples are given in column four of the table. The present, simplified precipitation method is seen to be successful in that filler is introduced in amounts comparable to those introduced when the TEOS is in direct contact with liquid water and acid catalysts. As expected, relative humidity at low ambient conditions increase the rate

of TEOS hydrolysis. It is important to note that only very small amounts of silica are precipitated under ambient conditions, even with these very large excesses of TEOS. This indicates that the amounts of silica which may be unintentionally formed [4] from the TEOS widely used in PDMS end-linking cures must be negligibly small. It is also possible to use the densities of the filled networks, unfilled network, and silica ($\sim 2.6 \text{ g cm}^{-3}$) [11] to estimate the wt % silica introduced. These values are given in column 5 of the table. There is reasonably good agreement, but as observed elsewhere [4], such values of the wt % silica can be significantly less than those obtained directly from the changes in network weight, indicating that not all of the hydrolyzed TEOS is converted all the way to pure silica.

The stress-strain results obtained were first represented in terms of the dependence of the modulus on reciprocal elongation [10,12]. The isotherms thus obtained are shown in figure 1. The insitu filled networks are seen to have elongation moduli which are much larger than that of the unfilled network. In addition, the upturns in $[f^*]$ observed at higher elongations clearly demonstrate [13] the desired reinforcing effect. Increase in filler content would be expected to decrease the elongation a_r at rupture, and this is confirmed by the results shown in column six of the table.

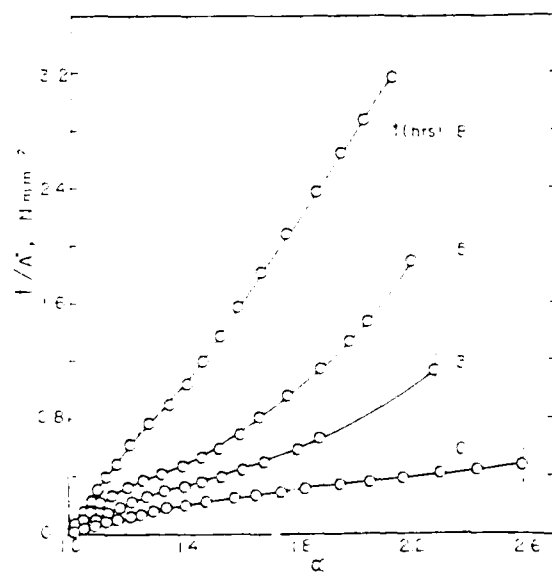


Fig. 2. The nominal stress shown as a function of elongation for the same networks characterized in figure 1. In this representation, the area under each curve represents the energy E_r required for network rupture.

Figure 2 shows the data of figure 1 plotted in such a way that the area under each stress-strain curve corresponds to the energy E_r of rupture [1, 8], which is the standard measure of elastomer toughness. Increase in filler content is seen to give significant increases in both E_r and in the ultimate strength, as represented by the value (f/A^*) , of the nominal stress at rupture. Values of both quantities are given in the last two columns of the table. This insitu precipitation technique, in spite of its simplicity, is obviously extremely effective in improving the mechanical properties of PDMS elastomers.

Acknowledgements

It is a pleasure to acknowledge the financial support provided by the National Science Foundation through Grant DMR 79-18923-03 (Polymers Program, Division of Materials Research) and by the Air Force Office of Scientific Research through Grant AFOSR 83-0027 (Chemical Structures Program, Division of Chemical Sciences). C.-Y.J. also wishes to thank the Dow Corning Corporation for the Research Fellowship he received.

References

1. Mark JE, Fan S-J (1982) *Makromol Chem Rapid Comm* 3:681
2. Ning Y-P, Tang M-Y, Jiang C-Y, Mark JE, Koth WC (1984) *J Appl Polym Sci* 29:200
3. Jiang C-Y, Mark JE (1984) *Makromol Chem* 185:200
4. Mark JE, Jiang C-Y, ms submitted to *Macromolecules*
5. Tang M-Y, Mark JE (1984) *Polym Eng Sci* 24:200
6. Mark JE, Sullivan JL (1977) *J Chem Phys* 66:1006
7. Liorente MA, Andrad AL, Mark JE (1980) *J Polym Sci, Polym Phys Ed* 18:2263
8. Liorente MA, Andrad AL, Mark JE (1981) *J Polym Sci Polym Phys Ed* 19:621
9. Mark JE, Fiori PJ (1966) *J Appl Phys* 37:4635
10. Treloar LRG (1975) *The Physics of Rubber Elasticity*, 3rd Ed., Clarendon Press, Oxford
11. Weast RC (1982) *CRC Handbook of Chemistry and Physics*, 63rd Ed. CRC Press, Cleveland
12. Mark JE (1975) *Rubber Chem Technol* 48:495
13. Mark JE (1979) *Polym Eng Sci* 19:409

Received February 20, 1984;
accepted April 25, 1984

Authors' address:

Dr. J. E. Mark
Department of Chemistry
Mail Location 172
Polymer Research Center
University of Cincinnati
Cincinnati, OH 45221-0172

The effects of various catalysts in the in-situ precipitation of reinforcing silica in polydimethylsiloxane networks

C. Y. Huang^a, J. I. Mark*

Department of Chemistry and the Polymer Research Center, The University of Cincinnati, Cincinnati, Ohio 45221, USA

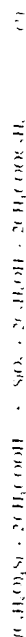
(Date of receipt: February 3, 1984)

SUMMARY

A variety of inorganic and organic acids, bases, and salts were studied as catalysts for the hydrolysis of tetraethyl orthosilicate, the reaction previously employed for the precipitation of silica within already cured elastomeric networks of polydimethylsiloxane. These systems were compared with regard to the amount of silica precipitated at room temperature, and the extent of reinforcement as judged by the upturns in the stress-strain isotherms at high strains. On this basis, the acids were the least effective and the salts the most effective.

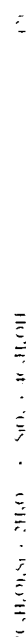
Introduction

A recent investigation¹ demonstrated that it is possible to reinforce already cured elastomers of polydimethylsiloxane (PDMS), $\text{[Si(CH}_3\text{)}_2\text{O]}_n$, by the "in situ" precipitation of silica (SiO_2). The reaction employed for this purpose was



where a small amount of water is required for the hydrolysis. It required several half-hour periods at 120°C, even as facilitated by a phase transfer agent.² The reinforcement thus obtained is particularly important in the case of PDMS elastomers, which are inherently weak in the unfilled state.³ Also, the method employed is of considerable interest for a number of reasons,⁴ including avoidance of "structuring" (primary gelation) of the system before it can be conveniently processed^{5,6}. The in situ formation of silica proceeds without significant hydrolysis and subsequent reorganization of the silicone network.⁷

The present investigation was carried out to find more convenient conditions for the efficient precipitation of SiO_2 at room temperature^{1-3,8}, using the simplified reaction



A variety of acids, bases and salts were employed, and the resulting networks compared with regard to their filler content and degree of improvement of their ultimate properties.

* Visiting scholar from the Changchun Institute of Chemical Industry, S. China, China

Experimental part

Preparation of elastomers. Hydroxyl-terminated PDMS chains having a number-average molecular weight of 8000 g./mol.¹ were endcapped with triethoxysilane (HOSi), in the undiluted state, in the usual manner.¹² The resulting network sheets, which were approximately 1 mm thick, were extracted using tetrahydrofuran and then toluene. Test strips cut from the sheets were approximately 3 mm wide and 30 mm long.

Preparation of catalyst solutions. The thirty-seven reagents employed and their formulas are given in the first two columns of Tab. 1. They were dissolved in water to the concentrations given in column three, and the resulting values of the pH (as determined from a standard pH meter) are given in the following columns.

Precipitation of silica. The extracted PDMS strips were weighed and then placed into H₂O₂ until swollen to equilibrium (which corresponded to a volume fraction of polymer of 0.76). Each swollen strip was then immersed in one of the aqueous solutions for 0.5–5.0 h, at 25°C. The strips, which generally turned very cloudy because of the precipitated SiO₂, were dried first in air for 24 h and then under vacuum to constant weight. The increase in dry weight gave the amount of SiO₂ precipitated within the sample in the allotted time. Each sample thus prepared is identified by the codes given in column six. Large increases in density, consistent with the formation of filler particles, were observed. Electron microscopy and light scattering also showed the presence of filler particles.^{13a}

Stress-strain measurements. Equilibrium stress-strain data were obtained in elongation in the usual manner^{12,13b} on the miswollen samples at 25°C. The nominal stress was given by $f^* = f/A^*$, where f is the elastic force and A^* the undeformed cross-sectional area, and the reduced stress or modulus^{12,13b} by $[f^*] = f^*/(a - a^*)$, where $a - a^*$ is the elongation or relative length of the sample.

Results and discussion

Most of the substances studied showed a significant capacity to catalyze the precipitation reaction given in Eq. (2). They did vary considerably in their efficiency, however, as can be seen from the amounts of precipitated SiO₂ (given in the seventh column of Tab. 1). The substances which were most efficient in this regard were the amines, amides, and salts.

The stress-strain isotherms obtained on the filled networks were first represented as plots of the modulus against reciprocal elongation, as suggested by the Mooney-Rivlin equation^{16,17a}

$$[f^*] = 2C_1 + 2C_2/a^2 \quad (3)$$

Typical isotherms, for networks chosen from the various classes of catalysts, are shown in Fig. 1. In situ filled networks are seen to have values of the modulus which are much higher than those of the corresponding unfilled network (curve D). Furthermore, the upturns in $[f^*]$ observed at higher elongations clearly demonstrate the desired reinforcing effects^{16,18}. The values of the ultimate properties, specifically the ultimate strength and maximum extensibility, are given in the last two columns of Tab. 1. With regard to ultimate strength, the best networks resulted from the use of amines and salts.

The effect of various catalysts on

2611

Tab. 1. Silica precipitation conditions and results, and ultimate properties of the filled networks (f^* : nominal stress at rupture; a : elongation at rupture)

Substance	Formula	Precipitation conditions			Precipitation results			Ultimate properties	
		conc. in wt.-% (in H ₂ O)	pH	reaction time in h	SiO ₂ content in wt.-%	designa- tion	f^* , N/mm ²	a , mm	
Reference materials	H ₂ O	—	—	—	1	—	0.0	0.48	2.6
Water	—	—	—	—	—	—	—	—	—
Inorganic acids	HCl	1.0	1.6	1	3.1	3.1	23.1	—	—
Hydrochloric	—	—	—	—	—	—	—	—	—
Sulfuric	H ₂ SO ₄	1.0	1.7	1	4.1	4.1	22.7	—	—
Formic	HCOOH	5.0	2.4	1	5.1	5.1	26.7	—	—
Organic acids	—	—	—	—	—	—	—	—	—
Acetic	CH ₃ COOH	88.0	0.24	0.5	5.4	5.4	9.9	0.39	0.4
Amines	—	—	—	—	—	—	—	—	—
Ammonia	—	—	—	—	—	—	—	—	—
Amides	—	—	—	—	—	—	—	—	—
Salts	—	—	—	—	—	—	—	—	—
Ammonium chloride	—	—	—	—	—	—	—	—	—
Sodium chloride	—	—	—	—	—	—	—	—	—
Potassium chloride	—	—	—	—	—	—	—	—	—
Calcium chloride	—	—	—	—	—	—	—	—	—
Sodium acetate	—	—	—	—	—	—	—	—	—
Potassium acetate	—	—	—	—	—	—	—	—	—
Calcium acetate	—	—	—	—	—	—	—	—	—
Sodium oxalate	—	—	—	—	—	—	—	—	—
Potassium oxalate	—	—	—	—	—	—	—	—	—
Calcium oxalate	—	—	—	—	—	—	—	—	—
Sodium citrate	—	—	—	—	—	—	—	—	—
Potassium citrate	—	—	—	—	—	—	—	—	—
Calcium citrate	—	—	—	—	—	—	—	—	—
Sodium tartrate	—	—	—	—	—	—	—	—	—
Potassium tartrate	—	—	—	—	—	—	—	—	—
Calcium tartrate	—	—	—	—	—	—	—	—	—
Sodium succinate	—	—	—	—	—	—	—	—	—
Potassium succinate	—	—	—	—	—	—	—	—	—
Calcium succinate	—	—	—	—	—	—	—	—	—
Sodium malonate	—	—	—	—	—	—	—	—	—
Potassium malonate	—	—	—	—	—	—	—	—	—
Calcium malonate	—	—	—	—	—	—	—	—	—
Sodium fumarate	—	—	—	—	—	—	—	—	—
Potassium fumarate	—	—	—	—	—	—	—	—	—
Calcium fumarate	—	—	—	—	—	—	—	—	—
Sodium maleate	—	—	—	—	—	—	—	—	—
Potassium maleate	—	—	—	—	—	—	—	—	—
Calcium maleate	—	—	—	—	—	—	—	—	—
Sodium itaconate	—	—	—	—	—	—	—	—	—
Potassium itaconate	—	—	—	—	—	—	—	—	—
Calcium itaconate	—	—	—	—	—	—	—	—	—
Sodium crotonate	—	—	—	—	—	—	—	—	—
Potassium crotonate	—	—	—	—	—	—	—	—	—
Calcium crotonate	—	—	—	—	—	—	—	—	—
Sodium acrylate	—	—	—	—	—	—	—	—	—
Potassium acrylate	—	—	—	—	—	—	—	—	—
Calcium acrylate	—	—	—	—	—	—	—	—	—
Sodium methacrylate	—	—	—	—	—	—	—	—	—
Potassium methacrylate	—	—	—	—	—	—	—	—	—
Calcium methacrylate	—	—	—	—	—	—	—	—	—
Sodium vinylcarbazole	—	—	—	—	—	—	—	—	—
Potassium vinylcarbazole	—	—	—	—	—	—	—	—	—
Calcium vinylcarbazole	—	—	—	—	—	—	—	—	—
Sodium styrene sulfonate	—	—	—	—	—	—	—	—	—
Potassium styrene sulfonate	—	—	—	—	—	—	—	—	—
Calcium styrene sulfonate	—	—	—	—	—	—	—	—	—
Sodium dodecyl sulfate	—	—	—	—	—	—	—	—	—
Potassium dodecyl sulfate	—	—	—	—	—	—	—	—	—
Calcium dodecyl sulfate	—	—	—	—	—	—	—	—	—
Sodium lauryl sulfate	—	—	—	—	—	—	—	—	—
Potassium lauryl sulfate	—	—	—	—	—	—	—	—	—
Calcium lauryl sulfate	—	—	—	—	—	—	—	—	—
Sodium myristate	—	—	—	—	—	—	—	—	—
Potassium myristate	—	—	—	—	—	—	—	—	—
Calcium myristate	—	—	—	—	—	—	—	—	—
Sodium palmitate	—	—	—	—	—	—	—	—	—
Potassium palmitate	—	—	—	—	—	—	—	—	—
Calcium palmitate	—	—	—	—	—	—	—	—	—
Sodium stearate	—	—	—	—	—	—	—	—	—
Potassium stearate	—	—	—	—	—	—	—	—	—
Calcium stearate	—	—	—	—	—	—	—	—	—
Sodium oleate	—	—	—	—	—	—	—	—	—
Potassium oleate	—	—	—	—	—	—	—	—	—
Calcium oleate	—	—	—	—	—	—	—	—	—
Sodium linoleate	—	—	—	—	—	—	—	—	—
Potassium linoleate	—	—	—	—	—	—	—	—	—
Calcium linoleate	—	—	—	—	—	—	—	—	—
Sodium myristoleate	—	—	—	—	—	—	—	—	—
Potassium myristoleate	—	—	—	—	—	—	—	—	—
Calcium myristoleate	—	—	—	—	—	—	—	—	—
Sodium elaeostearate	—	—	—	—	—	—	—	—	—
Potassium elaeostearate	—	—	—	—	—	—	—	—	—
Calcium elaeostearate	—	—	—	—	—	—	—	—	—
Sodium arachidate	—	—	—	—	—	—	—	—	—
Potassium arachidate	—	—	—	—	—	—	—	—	—
Calcium arachidate	—	—	—	—	—	—	—	—	—
Sodium behenate	—	—	—	—	—	—	—	—	—
Potassium behenate	—	—	—	—	—	—	—	—	—
Calcium behenate	—	—	—	—	—	—	—	—	—
Sodium erucate	—	—	—	—	—	—	—	—	—
Potassium erucate	—	—	—	—	—	—	—	—	—
Calcium erucate	—	—	—	—	—	—	—	—	—
Sodium ricinoleate	—	—	—	—	—	—	—	—	—
Potassium ricinoleate	—	—	—	—	—	—	—	—	—
Calcium ricinoleate	—	—	—	—	—	—	—	—	—
Sodium castor oil	—	—	—	—	—	—	—	—	—
Potassium castor oil	—	—	—	—	—	—	—	—	—
Calcium castor oil	—	—	—	—	—	—	—	—	—
Sodium stearic acid	—	—	—	—	—	—	—	—	—
Potassium stearic acid	—	—	—	—	—	—	—	—	—
Calcium stearic acid	—	—	—	—	—	—	—	—	—
Sodium myristic acid	—	—	—	—	—	—	—	—	—
Potassium myristic acid	—	—	—	—	—	—	—	—	—
Calcium myristic acid	—	—	—	—	—	—	—	—	—
Sodium palmitic acid	—	—	—	—	—	—	—	—	—
Potassium palmitic acid	—	—	—	—	—	—	—	—	—
Calcium palmitic acid	—	—	—	—	—	—	—	—	—
Sodium stearic acid	—	—	—	—	—	—	—	—	—
Potassium stearic acid	—	—	—	—	—	—	—	—	—
Calcium stearic acid	—	—	—	—	—	—	—	—	—
Sodium myristic acid	—	—	—	—	—	—	—	—	—
Potassium myristic acid	—	—	—	—	—	—	—	—	—
Calcium myristic acid	—	—	—	—	—	—	—	—	—
Sodium palmitic acid	—	—	—	—	—	—	—	—	—
Potassium palmitic acid	—	—	—	—	—	—	—	—	—
Calcium palmitic acid	—	—	—	—	—	—	—	—	—
Sodium stearic acid	—	—	—	—	—	—	—	—	—
Potassium stearic acid	—	—	—	—	—	—	—	—	—
Calcium stearic acid	—	—	—	—	—	—	—	—	—
Sodium myristic acid	—	—	—	—	—	—	—	—	—
Potassium myristic acid	—	—	—	—	—	—	—	—	—
Calcium myristic acid	—	—	—	—	—	—	—	—	—
Sodium palmitic acid	—	—	—	—	—	—	—	—	—
Potassium palmitic acid	—	—	—	—	—	—	—	—	—
Calcium palmitic acid	—	—	—	—	—	—	—	—	—
Sodium stearic acid	—	—	—	—	—	—	—	—	—
Potassium stearic acid	—	—	—	—	—	—	—	—	—
Calcium stearic acid	—	—	—	—	—	—	—	—	—
Sodium myristic acid	—	—	—	—	—	—	—	—	—
Potassium myristic acid	—	—	—	—	—	—	—	—	—
Calcium myristic acid	—	—	—	—	—	—	—	—	—
Sodium palmitic acid	—	—	—	—	—	—	—	—	—
Potassium palmitic acid	—	—	—	—	—	—	—	—	—
Calcium palmitic acid	—	—	—	—	—	—	—	—	—
Sodium stearic acid	—	—	—	—	—	—	—	—	—
Potassium stearic acid	—	—	—	—	—	—	—	—	—
Calcium stearic acid	—	—	—	—	—	—	—	—	—
Sodium myristic acid	—	—	—	—	—	—	—	—	—
Potassium myristic acid	—	—	—	—	—	—	—	—	—
Calcium myristic acid	—	—	—	—	—	—	—	—	—
Sodium palmitic acid	—	—	—	—	—	—	—	—	—
Potassium palmitic acid	—	—	—	—	—	—	—	—	—
Calcium palmitic acid	—	—	—	—	—	—	—	—	—
Sodium stearic acid	—	—	—	—	—	—	—	—	—
Potassium stearic acid	—	—	—	—	—	—	—	—	—
Calcium stearic acid	—	—	—	—	—	—	—	—	—
Sodium myristic acid	—	—	—	—	—	—	—	—	—
Potassium myristic acid	—	—	—	—	—	—	—	—	—
Calcium myristic acid	—	—	—	—	—	—	—	—	—
Sodium palmitic acid	—	—	—	—	—	—	—	—	—
Potassium palmitic acid	—	—	—	—	—	—	—	—	—
Calcium palmitic acid	—	—	—	—	—	—	—	—	—
Sodium stearic acid	—	—	—	—	—	—	—	—	—
Potassium stearic acid	—	—	—	—	—	—	—	—	—
Calcium stearic acid	—	—	—	—	—	—	—	—	—
Sodium myristic acid	—	—	—	—	—	—	—	—	—
Potassium myristic acid	—	—	—	—	—	—	—	—	—
Calcium myristic acid	—	—	—	—	—	—	—	—	—
Sodium palmitic acid	—	—	—	—	—	—	—	—	—
Potassium palmitic acid	—	—	—	—	—	—	—	—	—
Calcium palmitic acid	—	—	—	—	—	—	—	—	—
Sodium stearic acid	—	—	—	—	—	—	—	—	—
Potassium stearic acid	—	—	—	—	—	—	—	—	—
Calcium stearic acid	—	—	—	—	—	—	—	—	—
Sodium myristic acid	—	—	—	—	—	—	—	—	—
Potassium myristic acid	—	—	—	—	—	—	—	—	—
Calcium myristic acid	—	—	—	—	—	—	—	—	—
Sodium palmitic acid	—	—	—	—	—	—	—	—	—
Potassium palmitic acid	—	—	—	—	—	—	—	—	—
Calcium palmitic acid	—	—	—	—	—	—	—	—	—
Sodium stearic acid	—	—	—	—	—	—	—	—	—
Potassium stearic acid	—	—	—	—	—	—	—	—	—
Calcium stearic acid	—	—	—	—	—	—	—	—	—
Sodium myristic acid	—	—	—	—	—	—	—	—	—
Potassium myristic acid	—	—	—	—	—	—	—	—	—
Calcium myristic acid	—	—	—	—	—	—	—	—	—
Sodium palmitic acid	—	—	—	—					

Tab. 1. Continued

Precipitation conditions				Precipitation results			Ultimate properties	
Substance	Formula	conc. in wt.-% (in H ₂ O)	pH	reaction time min	elasto- mer designa- tion	SiO ₂ content in wt.-%	η^* N-cm ² /g	α
N,N-Dimethylformamide	HCON(CH ₃) ₂	4.9	4.6	1	24.1	34.2	—	—
				2	24.2	32.7	—	—
				3	24.3	34.7	0.92	2.1
Acetamide	CH ₃ CONH ₂	5.0	4.9	1	25.1	25.5	—	—
				2	25.2	33.7	—	—
				3	25.3	43.9	0.85	1.7
N,N-Diethyl-m-toluidamide	CH ₃ -C ₆ H ₄ CON(C ₂ H ₅) ₂	5.2	5.1	1	26.1	5.1	—	—
				2	26.2	8.9	—	—
				3	26.3	13.5	0.30	1.7
Urea	OC(NH ₂) ₂	5.0	6.2	1	27.1	39.0	—	—
				2	27.2	46.5	—	—
				3	27.3	55.2	2.15	1.6
Silicon-nitrogen compounds								
1,1,1,3,3,3-Hexamethyldisilazane	(CH ₃) ₆ Si ₂ NHSi(CH ₃) ₃	5.0	10.3	1	28.1	1.8	—	—
				2	28.2	1.8	—	—
				3	28.3	1.7	0.40	2.3
3-Aminopropyltriethoxysilane	H ₂ N(CH ₂) ₃ Si(OC ₂ H ₅) ₃	5.0	10.4	1	29.1	5.0	—	—
				2	29.2	6.2	—	—
				3	29.3	8.4	0.53	2.0
Salts								
Sodium silicate	Na ₂ SiO ₃	4.3	12.4	1	30.1	26.3	—	—
				2	30.2	28.3	—	—
				3	30.3	26.9	1.23	2.0
The effects of various salts on								
Potassium dihydrogenphosphate	KH ₂ PO ₄	5.0	4.0	1	31.1	38.7	—	—
				2	31.2	49.5	—	—
				3	31.3	57.3	3.10	1.9
Cupric chloride	CuCl ₂	4.0	3.2	1	32.1	33.3	—	—
				2	32.2	44.0	—	—
				3	32.3	51.2	2.30	1.8
Sodium chloride	NaCl	5.0	5.2	1	33.1	32.5	—	—
				2	33.2	41.1	—	—
				3	33.3	49.5	2.29	1.9
Ammonium chloride	NH ₄ Cl	5.0	4.4	1	34.1	35.1	—	—
				2	34.2	46.3	—	—
				3	34.3	55.0	3.04	1.8
Magnesium acetate	Mg(OOCCH ₃) ₂	3.3	7.0	1	35.1	36.0	—	—
				2	35.2	47.3	—	—
				3	35.3	56.5	2.78	1.9
Lead acetate	Pb(OOCCH ₃) ₂	4.3	5.2	1	36.1	35.2	—	—
				2	36.2	47.7	—	—
				3	36.3	55.5	2.83	1.9
Zinc acetate	Zn(OOCCH ₃) ₂	5.0	5.4	1	37.1	37.8	—	—
				2	37.2	48.7	—	—
				3	37.3	54.6	2.78	1.8
Stannous 2-ethylhexanoate	Sn(OOCCH(C ₂ H ₅)(CH ₂) ₄ CH ₃) ₂	sat.	3.2	1	38.1	53.3	—	—
				2	38.2	40.3	—	—
				3	38.3	40.8	0.58	1.3
Trisodium salt of ethylene-diaminetetraacetic acid	NaOOCCH ₂ -N(CH ₂ CH ₂ N)-CH ₂ COONa NaOOCCH ₂ -N(CH ₂ CH ₂ N)-CH ₂ COOH	5.0	9.2	1	39.1	19.0	—	—
				2	39.2	40.8	—	—
				3	39.3	76.3	3.70	1.8

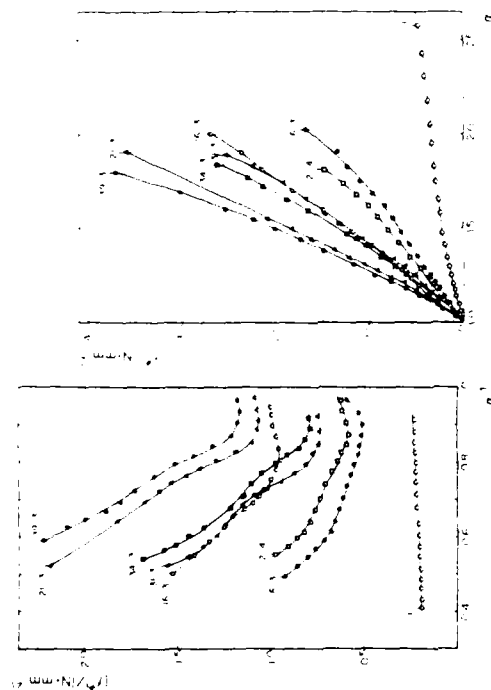


Fig. 1

Fig. 1. The reduced stress $[\sigma']$ shown as a function of reciprocal elongation α^{-1} for typical SdO-filled PDMS networks at 25°C. Each curve is identified by the code given in column six of Table I, and the vertical dashed lines locate the rupture points.

Fig. 2. The nominal stress F^* shown as a function of elongation α for the same networks characterized in Fig. 1. In this representation, the area under each curve corresponds to the energy required for network rupture.

Fig. 2

Overall, the acids seemed to be the least useful and the salts the most useful. For example, networks prepared using formic acid were quite weak and those prepared using hydrochloric, trifluoroacetic, or oxalic acid were brittle. On the other hand, networks prepared using potassium phosphate or ammonium chloride were very strong, and those prepared using diethylamine or the trisodium salt of ethylenediaminetetraacetic acid were unusually tough.

Fig. 2 shows the data of Fig. 1 plotted in such a way that the area under each stress-strain curve corresponds to the energy F_r of rupture¹⁰, which is the standard measure of elastomer toughness. The values of $10^5 F_r$ for the curves shown range from 0.44 J mm^{-1} (curve 1) to 1.53 J mm^{-1} (curve 21-3). Thus, the in situ reinforcement technique can easily bring about a nearly four-fold increase in toughness in an elastomer in a relatively rapid, simple manner. It could therefore be of considerable commercial importance.

The Effects of Various Catalysts on

It is a pleasure to acknowledge the financial support provided by the National Science Foundation through Grant DMR 79-186-03 (Polymers Program), Division of Materials Research, and by the Air Force Office of Scientific Research through Grant AFOSR 83-0027 (Polymers Program), Division of Chemical Sciences, C. Y. Hong wishes to thank the Air Force Office of Scientific Research for the Research Fellowship he received.

1. J. F. Mark, S. T. Pan, Makromol. Chem., Rapid Commun. **3**, 681 (1982).
2. C. M. Stark, C. J. Jotta, "Phase Transfer Catalysis: Principle and Techniques", Academic Press, N.Y., 1978.
3. K. F. Wattick, G. R. Pierré, K. F. Pothmann, J. C. Salam, Rubber Chem. Technol. **48**, 798 (1975).
4. W. Stöber, A. Funk, F. Böhm, J. Colloid Interface Sci. **26**, 67 (1968).
5. H. Hachbar, W. Stöber, J. Colloid Interface Sci. **30**, 568 (1969).
6. V. S. A. 634,558 (1972), inv. W. Stöber.
7. R. K. Iler, J. Phys. Chem. **56**, 673 (1952).
8. R. K. Iler, J. Am. Chem. Soc. **74**, 2929 (1952).
9. F. S. 2,383,633 (1945), inv. J. S. Kirk.
10. G. 2,131,941 (1970), inv. A. S. Patel, D. G. Wirth, Jr., J. Z. Yeager.
11. K. Unger, B. Sharf, J. Colloid Interface Sci. **55**, 372 (1976).
12. J. F. Mark, J. L. Sullivan, J. Chem. Phys. **66**, 1006 (1977).
13. Y. P. Ning, M. Y. Tang, C. Y. Hong, J. F. Mark, W. C. Poeh, J. Appl. Polym. Sci. **29** (1984), D. W. Schaefer, J. F. Mark, unpublished results.
14. M. A. Florentie, A. I. Andrad, J. F. Mark, J. Polym. Sci., Polym. Phys. Ed. **18**, 2263 (1980).
15. P. J. Flory, "Principles of Polymer Chemistry", Cornell University Press, Ithaca, N.Y., 1953.
16. J. F. Mark, P. J. Flory, J. Appl. Phys. **37**, 4635 (1966).
17. I. R. G. Treloar, "The Physics of Rubber Elasticity", Clarendon Press, Oxford, 1976.
18. J. F. Mark, Rubber Chem. Technol. **48**, 495 (1975).
19. J. F. Mark, Polym. Eng. Sci. **19**, 253, 409 (1979).
20. M. A. Florentie, A. I. Andrad, J. F. Mark, J. Polym. Sci., Polym. Phys. Ed. **19**, 621 (1981).

THEORETICAL STUDIES OF THE ELECTRONIC PROPERTIES OF SUBSTITUTED POLYACETYLENES

Kenneth C. Metzger¹ and William J. Welch^{1,2}

¹Department of Chemistry and Polymer Research Center,

University of Cincinnati, Cincinnati, OH 45221.

²Department of Chemistry, College of Mount St. Joseph,
Mount St. Joseph, OH 45051.

INTRODUCTION

Polyacetylene, $(CH)_x$, the simplest organic polymer with a fully conjugated backbone, has generated considerable interest due to its unusual electronic properties. Specifically, through selective doping the polymer's electrical conductivity can be made to vary many orders of magnitude, from insulator to semiconductor (1). The structure of the polymer chain appears to be one of the key determinants for the electronic properties of the polymer/dopant systems (1). Recent structural evidence and theoretical calculations (1-3) suggest a planar backbone structure for *cis* and *trans* forms of $(CH)_x$. However, many aspects of the structure and characteristics of $(CH)_x$ are not well-defined due to its intractability and its insolubility in most solvents. Many other polymeric systems have been proposed or actually investigated with regard to their potential as conductors or semiconductors (1), among these the halogen-substituted polyacetylenes (4).

It appears that electrical conductivity is sensitive to the degree of conjugation along the chain backbone, and this in turn varies directly with the extent of chain planarity (5). In the case of substituted polyacetylenes in particular, it is crucial for effective conductivity that the substituent's bulk not cause appreciable deviations from planarity in an attempt to reduce steric conflicts. Among the halogen-substituted polyacetylenes, the fluorine atom is just small enough ($r_{vdw} = 1.30$ Å) to render attractive F...F interactions even for the planar chain in which case the four-bond F...F interatomic distance is closest (2.60 Å). However, with substitution of chlorine ($r_{vdw} = 1.80$ Å) steric conflicts between pendant chlorine atoms will render the planar conformation highly repulsive, and this effect would become more severe for Br and I substitution. In this study, quantum mechanical theoretical methods are used to calculate the electronic band gaps and band widths of the $(CF)_x$ chain and compared with those similarly calculated for $(CH)_x$ itself. Calculations have been carried out as a function of rotation about the single bonds along the backbone in order to assess the dependence of conductivity on chain planarity. Likewise, the sensitivity of the calculated band gaps to small changes in structure (bond angles, bond lengths) has been investigated.

THEORY

In all calculations presented here, the chains assumed the *trans* geometry about the C=C double bonds, and rotations ϕ about the intervening single C-C bonds were carried out in increments of 30° with $\phi = 0^\circ$ corresponding to the planar, zig-zag ("*trans*") conformation (6). The delocalized crystalline molecular orbitals needed in the quantum mechanical approach employed were obtained using the tight-binding scheme based on the extended huckel approximation (6,7). The calculations included all of the valence atomic orbitals of the C, F, and H atoms comprising the chains. In the present calculations, lattice sums were carried out to second nearest neighbors.

STRUCTURAL INFORMATION

In Table 1, the structural parameters used for the

Table 1. Structural parameters used for the present calculations for perfluoropolyacetylene $(CF)_x$ and polyacetylene $(CH)_x$.

	$(CF)_x$	$(CH)_x$
bond lengths ^a		
C=C	1.352	1.342
C-C	1.440	1.436
C-H	--	1.121
C-F	1.336	--
bond angles ^b		
C=C-C	126.6	127.0
C=C-H	--	118.0
C=C-F	117.3	--

^ain units of Angstroms.

^bin units of degrees.

present calculations are summarized. These values were selected, in the case of $(CH)_x$, from available experimental structural data (2,8) on the polymer and from results of extensive *ab initio* and CNDO/2 (Complete Neglect of Differential Overlap) molecular orbital calculations. In the case of $(CF)_x$, the CNDO/2-calculated values used were found to be in close agreement with experimental values given for small-molecule analogues (9).

RESULTS AND DISCUSSION

Calculated values of the band gaps E_g and band widths BW for both $(CF)_x$ and $(CH)_x$ as a function of the rotational angle ϕ are presented in Table II. Interestingly, $(CH)_x$ and $(CF)_x$ give nearly identical values of both E_g and BW at every value of ϕ considered. Within this level of approximation at least, it appears that substituting F for H in polyacetylene has a negligible effect on the polymer's intrinsic electrical conductivity. For both polymers, values of E_g with a minimum ($E_g = 0.4-0.7$ eV) at the planar conformations ($\phi = 0^\circ$ and 180°) and a maximum ($E_g = 4.3$ eV) when the planes of the chain on either side of the rotated bond are mutually perpendicular ($\phi = 90^\circ$). These results are consistent with the expectation of a direct relationship between conductivity and degree of conjugation (5), both of which should be largest at $\phi = 0^\circ$ and 180° and smallest at $\phi = 90^\circ$. The experimentally determined value of E_g for $(CH)_x$ is 1.4-1.8 eV (9). Inasmuch as these experimental values fall between that given by these calculations for $\phi = 0^\circ$ and 180° ($E_g = 0.7$ eV) and that for $\phi = 90^\circ$ ($E_g = 4.3$ eV), the present results may suggest considerable deviations from planarity along the backbone.

The bandwidth BW of the highest occupied molecular orbital may be related to some extent to the degree of delocalization of the π system along the chain backbone and to the charge carrier mobility in the band (1). For both polymers, values of the BW were a maximum (2.6 eV) for the planar conformations and a minimum (4.1-4.4 eV)

at $\phi = 90^\circ$, with a large BW value indicating a high degree of π delocalization and of carrier mobility.

Calculations were also carried out to assess the sensitivity of E_g and BW values to small changes in structural geometry. The most spectacular effect in $(CF)_x$ was obtained by increasing the backbone C-C bond lengths and decreasing the C-C bond lengths both by 0.02 Å. At $\phi = 0^\circ$, this small change reduced the calculated value of E_g from 0.72 eV to 0.40 eV. Such a structural modification would be indicative of increased conjugation along the chain backbone, hence the result suggests a very strong relationship between high conductivity and a high degree of conjugation. In the other direction, decreasing the C-C bond lengths and increasing the C-C bond lengths by 0.02 Å from their original values resulted in an increase in E_g from 0.72 eV to 1.04 eV. These results also point out that, by the present methods, calculated band gaps are extremely sensitive to the structural geometry chosen for the backbone. Calculated values of E_g and BW were virtually insensitive to small changes in bond angles along the backbone, with increasing or decreasing the C-C-C bond angle by 2.0° producing no effect. Likewise, shortening or lengthening the C-H bonds in $(CH)_x$ or the C-F bonds in $(CF)_x$ by 0.02 Å had a negligible effect on the calculated E_g and BW values. It appears

Table II. Calculated values of the band gap^a (E_g) and band width^b (BW) for $(CH)_x$ and $(CF)_x$ as a function of rotational angle ϕ .

ϕ^b	$(CH)_x$		$(CF)_x$	
	E_g^a	BW ^a	E_g^a	BW ^a
0	0.75	6.9	0.72	6.9
30	1.6	5.3	1.7	5.3
60	3.5	3.8	3.6	3.7
90	4.4	3.5	4.2	3.5
120	2.7	4.6	2.5	4.7
150	1.2	6.0	1.1	6.1
180	0.6	6.8	0.6	6.8

^aIn units of electron-volts.

^bIn units of degrees.

then that conductivity is directly and strongly dependent on the degree of conjugation along the backbone, and the other structural modifications are of minor or negligible consequence.

ACKNOWLEDGEMENTS

The authors wish to acknowledge the support provided for their research by the Plastics Institute of America and by the Air Force Office of Scientific Research (Grant AFOSR 83-0027, to Professor J. E. Mark (Chemical Structures Program, Division of Chemical Sciences)). We also wish to acknowledge several very helpful conversations with Dr. John Ziegler of the Sandia National Laboratories.

REFERENCES

1. R. H. Baughman, J. L. Bredas, K. C. Chance, K. Eisenbaumer, and L. W. Shacklette, *Chem. Rev.*, **82**, 209 (1982).
2. R. H. Baughman, S. L. Hau, G. P. Fez, and A. J. Signorelli, *J. Chem. Phys.*, **68**, 5405 (1978).
3. B. J. Orchard, S. K. Tripathy, and A. J. Hopfinger, *J. Appl. Phys.*, **52**, 5952 (1981).
4. J. Ziegler, Sandia National Laboratories, has recently prepared a poly(fluoroacetylene), $(CH=CF)_x$, having some structural imperfections in the main chain.
5. K. C. Wheeland, *J. Am. Chem. Soc.*, **98**, 3926 (1976).
6. D. Bhaumik and J. E. Mark, *J. Polym. Sci., Polym. Phys. Ed.*, **21**, 000 (1983).
7. M. H. Whangbo and R. Hoffman, *J. Am. Chem. Soc.*, **100**, 6093 (1978).
8. C. H. Chang, A. L. Andreasen, and S. H. Bauer, *J. Org. Chem.*, **36**, 922 (1971).
9. J. L. Bredas, R. R. Chance, and R. H. Baughman, *J. Chem. Phys.*, **76** (7), 3673 (1982).

A THEORETICAL INVESTIGATION OF THE ELECTRONIC BAND STRUCTURE IN DOPED *trans*-POLYACETYLENE

S. Bhattacharya and J. E. Mark, Department of Chemistry and the Polymer Research Center, The University of Cincinnati, Cincinnati, OH 45221

Introduction

It has recently been discovered that doping can increase the electric conductivity of *trans*-polyacetylene (t-CH), shown in Figure 1, by about twelve orders of

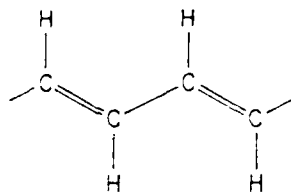


Figure 1. The *trans*-polyacetylene chain.

magnitude.¹⁻³ The dopants AsF_5 and I_2 have been most widely used but other halides and metal ions are also effective. Experimental investigations demonstrate the existence of I_3^- species in iodine-doped polyacetylene, Br_3^- in the bromine-doped polymer, and Cl_3^- in the chlorine-doped polymer. However, the lack of complete structural information for these polymers has hindered progress towards an understanding of their electronic properties. In the present work preliminary attempts are made to understand the axial electronic band structures of acceptor-doped polyacetylenes. The dopants studied were I_3^- and Br_3^- anions.

Method of Calculation

The electronic band structures were calculated using the tight-binding scheme based on the extended Hückel approximation.⁴ The parameters required for C , H , I and Br atoms were obtained from the literature.^{5,10} In the present calculations lattice sums were carried out to second-nearest neighbors.

Geometry optimization by means of the *ab-initio* STO-3G quantum mechanical method¹¹ was used to calculate bond lengths and bond angles for the t-CH. The calculated values for C-C, C=C and C-H bond lengths are 1.483, 1.323 and 1.084 Å, respectively. The C-C-C bond angle is 123.98° and C-C-H angle is 119.93°. The corresponding parameters for I_3^- and Br_3^- anions were obtained from the literature.¹² Both the molecules are linear with iodine-iodine and bromine-bromine bond lengths of 3.1 Å and 2.7 Å, respectively.

The unit cell has been modeled to consist of the species $\text{C}_{18}\text{H}_{18}(\text{A})_2$, (where A is I or Br), which represents a doping level of 33 wt %. The reasons for this choice of concentration are that (a) it is close to the highest observed dopant level for iodine-doped polyacetylene ($\text{C}_{18}\text{H}_{18}\text{I}_{10}$);¹³ (b) the size of the unit cell is within the dimensional limitations of the computer program available; (c) the system thus defined gives a closed shell problem. The same concentration was used for iodine- and bromine-doped polyacetylene for a comparative study of the calculated and experimental results at fixed concentration.

In these preliminary calculations the I_3^- or Br_3^- anions were placed symmetrically over the polyacetylene chain at a distance equal to the sum of van der Waals radii of C and I or Br atoms. For I and Br the separations are 3.5 Å and 3.0 Å, respectively. In this arrangement the separations between the iodine anions and bromine anions become 4.7 Å (in agreement with experiment¹⁴) and 5.5 Å, respectively.

Results and Discussion

To test the utility of the theoretical method, the band structure of the undoped t-CH₂ was calculated. This is shown in Figure 2. Because of the large unit

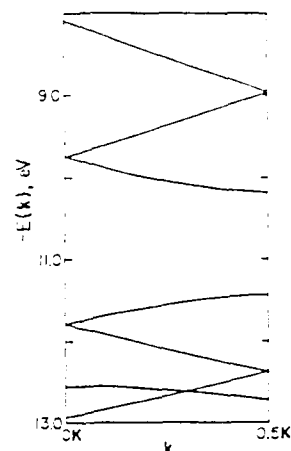


Figure 2. The band structure of undoped *trans*-polyacetylene.

cell, the Brillouin zone is one-ninth as long as the primitive unit cell, and there are nine bands each for the π and π^* states. Among these, the three lowest π and the three highest π^* and one σ states are shown in the figure. The calculated band gap 1.3 eV is in good agreement with the experimental estimates of 1.4 - 1.9 eV.⁴ The band-gap minimum is at the zone edge of the primitive unit cell. This agrees with the picture of a band gap arising from alternating single and double-bond lengths driven by a Peierls distortion.^{15,16} The present model, therefore, clearly agrees with the experimental observations.

Figures 3 and 4 show the effects of doping *trans*-polyacetylene with iodine and bromine, respectively. The broken-line bands are for the iodine or bromine dopants. In both cases the highest occupied valence band of undoped polyacetylene becomes the lowest unoccupied conduction band, and this conduction band almost overlaps the valence band at the zone center. (The band gaps for iodine- and bromine-doped polyacetylene are 0.018 and 0.033 eV, respectively). These almost degenerate bands will result in a partially fixed band at the zone center of these doped polymers, thus giving them metallic characteristics. The dispersion of the valence and conduction bands of iodine- and bromine-doped t-CH are 0.56 and 0.35 eV and 0.50 and 0.33 eV, respectively. This slight increase in band gap and decrease in valence and conduction band dispersion in going from iodine-doped polyacetylene to bromine-doped polyacetylene explain the observed decrease in conductivity at constant doping concentration (assuming other relevant factors remain constant). Finally, the bands due to the dopants are flat since the interionic distances are more than the sum

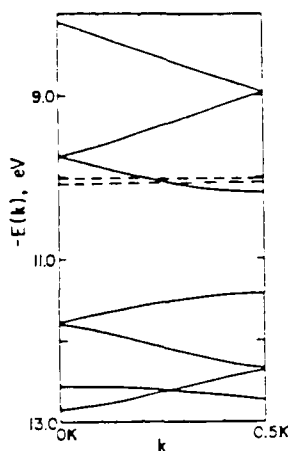


Figure 3. The band structure for iodine-doped trans-polyacetylene.

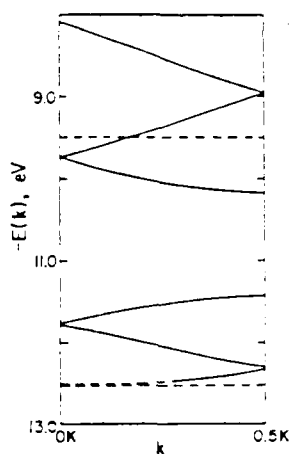


Figure 4. The band structure for bromine-doped trans-polyacetylene.

of the van der Waals radii of the corresponding ions. (For iodine the sum of van der Waals radii is 4.32 Å, but the minimum separation is 4.7 Å; the corresponding quantities for bromine are 3.4 and 5.5 Å respectively. Additional calculations in progress include interchain interactions and variation of the relative orientations of the anions with respect to the polyacetylene chain. The results should yield a clearer understanding of the variations in the band gap and changes in the nature of the valence and conduction bands.

It is a pleasure to acknowledge the financial support provided by the Air Force Office of Scientific Research (Chemical Structures Program, Division of Chemical Sciences).

References

- (1) C. K. Chiang, A. J. Heeger and A. G. MacDiarmid, Ber. Bunsenges. Phys. Chem., **83**, 407 (1979), and references cited therein.
- (2) Y. W. Park, M. A. Druy, C. K. Chiang, A. J. Heeger, A. G. MacDiarmid, H. Snirakawa and S. Ikeda, Polym. Lett., **17**, 195 (1979).
- (3) A. G. MacDiarmid and A. J. Heeger, "Molecular Metals", W. E. Hatfield (Ed.), Plenum Press, New York, 161 (1979).
- (4) R. H. Baughman, N. S. Murthy, G. G. Miller and L. W. Shacklette, J. Chem. Phys., **79**, 1065 (1983).
- (5) R. V. Kasowski, E. Caruthers and W. Y. Hsu, Phys. Rev. Lett., **44**, 676 (1980).
- (6) D. Bhaumik and J. E. Mark, J. Polym. Sci., Polym. Phys. Ed., **21**, 1111 (1983).
- (7) D. Bhaumik and J. E. Mark, J. Polym. Sci., Polym. Phys. Ed., **21**, 2543 (1983).
- (8) M.-H. Whangbo and R. Hoffmann, J. Am. Chem. Soc., **100**, 6093 (1978).
- (9) R. H. Summerville and R. Hoffmann, J. Am. Chem. Soc., **98**, 7240 (1976).
- (10) M.-H. Whangbo and M. J. Foshee, Inorg. Chem., **20**, 113 (1981).
- (11) Gaussian 80, Program No. 437, Quantum Chemistry Program Exchange, Indiana University, Bloomington, Indiana.
- (12) F. A. Cotton and G. Wilkinson, "Advanced Inorganic Chemistry", 3rd Ed., Wiley-Interscience, New York (1972).
- (13) S.-C. Gau, J. Milliken, A. Pron, A. G. MacDiarmid, and A. J. Heeger, J. Chem. Soc. Chem. Comm., **66** (1979).
- (14) R. E. Peierls, "Quantum Theory of Solids", 1st Ed., Oxford Univ. Press, Oxford, England, (1955), p. 10b; M. J. Rice and S. Strassler, Solid State Commun., **13**, 125 (1973).
- (15) F. M. Grant and I. P. Batra, Solid State Commun., **29**, 225 (1979).

Geometry Optimization Using Symmetry Coordinates

H. Kondo, H. H. Jaffe,* H. Y. Lee, and William J. Welsh

Department of Chemistry, University of Cincinnati, Cincinnati, Ohio 45221

Received 25 April 1983; accepted 26 August 1983

The use of symmetry coordinates (SC) in geometry optimization is discussed. A computer program, incorporating the use of SC, together with analytical calculation of the gradient and quadratic acceleration, is described. Also reported are careful test results on a series of small molecules and typical results with a long series of molecules up to quite large size (40–60 atoms).

INTRODUCTION

For the last several years we have been interested in the use of molecular symmetry in molecular orbital calculations.¹ The program we have developed, CNDO/S,² makes extensive use of point-group symmetry throughout.

In this article we would like to report on the simplifications afforded by the use of symmetry in the process of geometry optimization. The Hamiltonian operator, and consequently the gradient of the potential energy, transform of necessity in the totally symmetric irreducible representations (irrep) of the applicable point group (PG). As a result, any derivatives of the gradient with respect to coordinates that are not totally symmetric (or do not contain a totally symmetric component) vanish identically. Therefore when the energy is expressed in terms of symmetry coordinates (SC), derivatives (gradient elements) are required only with respect to those coordinates that transform in the totally symmetric irrep.

A molecule consisting of N atoms has $3N - 6$ ($3N - 5$ if it is linear) internal degrees of freedom (DF); without use of symmetry, all the internal DF must be optimized. Moreover, while it is generally easy to separate out the 3 translational DF, separation of the 3 (or 2) rotational ones is not trivial. On the other hand, even molecules with only relatively low symmetry have significantly fewer than $3N$ totally symmetric DF. Thus in formaldehyde, H_2CO , transforming in the PG C_{2v} , there are 6 internal DF, but only 4 totally symmetric SC. In acetone, also C_{2v} , there are 24

internal coordinates, but only 9 totally symmetric SC. The larger the molecule and the higher its symmetry, the greater the simplification achieved by the use of the SC.

Optimization using SC of any molecule requires an initial test structure which transforms in some PG, say G . The converged structure will transform in the same group, or possibly in a PG to which G is a subgroup; however, the final structure cannot be of lower symmetry than the test structure. Special provisions have to be made in case the test structure is too symmetric (cf. below).

The model used in this work is the semi-empirical CNDO/2 method,³ which has permitted relatively simple analytic expressions for the gradient elements.⁴ The program we have developed is fully automatic, using an initial test structure to get started, and proceeds via a steepest descent method with a quadratic acceleration.^{5,6}

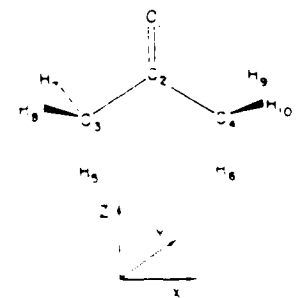
SYMMETRY COORDINATES

We have chosen the most naive method of defining the SC, ξ . Different definitions were required for asymmetric and symmetric top molecules, i.e. molecules having no axis, proper or improper, of order greater than two, and molecules having just one such axis, respectively. Spherical tops having several noncoincident axes of order greater than two are treated in a subgroup of lower symmetry.

For the asymmetric tops, the ξ are simply linear combinations of the Cartesian displacement coordinates of sets of symmetrically equivalent atoms. Projection of the x , y , and z

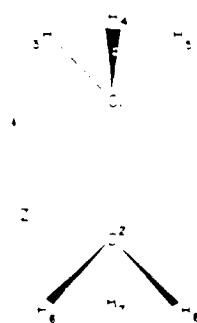
*To whom all correspondence should be addressed.

Table I. The totally symmetric symmetry coordinate for acetone.

	
$\rho_1 = r_1$	$\rho_2 = r_2$
$\rho_3 = r_3$	$\rho_4 = r_4$
$\rho_5 = r_5$	$\rho_6 = r_6$
$\rho_7 = r_7$	$\rho_8 = r_8$
$\rho_9 = r_9$	$\rho_{10} = r_{10}$
$\rho_{11} = r_{11}$	$\rho_{12} = r_{12}$
$\rho_{13} = r_{13}$	$\rho_{14} = r_{14}$
$\rho_{15} = r_{15}$	$\rho_{16} = r_{16}$
$\rho_{17} = r_{17}$	$\rho_{18} = r_{18}$
$\rho_{19} = r_{19}$	$\rho_{20} = r_{20}$
$\rho_{21} = r_{21}$	$\rho_{22} = r_{22}$
$\rho_{23} = r_{23}$	$\rho_{24} = r_{24}$
$\rho_{25} = r_{25}$	$\rho_{26} = r_{26}$
$\rho_{27} = r_{27}$	$\rho_{28} = r_{28}$
$\rho_{29} = r_{29}$	$\rho_{30} = r_{30}$
$\rho_{31} = r_{31}$	$\rho_{32} = r_{32}$
$\rho_{33} = r_{33}$	$\rho_{34} = r_{34}$
$\rho_{35} = r_{35}$	$\rho_{36} = r_{36}$
$\rho_{37} = r_{37}$	$\rho_{38} = r_{38}$
$\rho_{39} = r_{39}$	$\rho_{40} = r_{40}$
$\rho_{41} = r_{41}$	$\rho_{42} = r_{42}$
$\rho_{43} = r_{43}$	$\rho_{44} = r_{44}$
$\rho_{45} = r_{45}$	$\rho_{46} = r_{46}$
$\rho_{47} = r_{47}$	$\rho_{48} = r_{48}$
$\rho_{49} = r_{49}$	$\rho_{50} = r_{50}$
$\rho_{51} = r_{51}$	$\rho_{52} = r_{52}$
$\rho_{53} = r_{53}$	$\rho_{54} = r_{54}$
$\rho_{55} = r_{55}$	$\rho_{56} = r_{56}$
$\rho_{57} = r_{57}$	$\rho_{58} = r_{58}$
$\rho_{59} = r_{59}$	$\rho_{60} = r_{60}$
$\rho_{61} = r_{61}$	$\rho_{62} = r_{62}$
$\rho_{63} = r_{63}$	$\rho_{64} = r_{64}$
$\rho_{65} = r_{65}$	$\rho_{66} = r_{66}$
$\rho_{67} = r_{67}$	$\rho_{68} = r_{68}$
$\rho_{69} = r_{69}$	$\rho_{70} = r_{70}$
$\rho_{71} = r_{71}$	$\rho_{72} = r_{72}$
$\rho_{73} = r_{73}$	$\rho_{74} = r_{74}$
$\rho_{75} = r_{75}$	$\rho_{76} = r_{76}$
$\rho_{77} = r_{77}$	$\rho_{78} = r_{78}$
$\rho_{79} = r_{79}$	$\rho_{80} = r_{80}$
$\rho_{81} = r_{81}$	$\rho_{82} = r_{82}$
$\rho_{83} = r_{83}$	$\rho_{84} = r_{84}$
$\rho_{85} = r_{85}$	$\rho_{86} = r_{86}$
$\rho_{87} = r_{87}$	$\rho_{88} = r_{88}$
$\rho_{89} = r_{89}$	$\rho_{90} = r_{90}$
$\rho_{91} = r_{91}$	$\rho_{92} = r_{92}$
$\rho_{93} = r_{93}$	$\rho_{94} = r_{94}$
$\rho_{95} = r_{95}$	$\rho_{96} = r_{96}$
$\rho_{97} = r_{97}$	$\rho_{98} = r_{98}$
$\rho_{99} = r_{99}$	$\rho_{100} = r_{100}$

coordinates of one atom in each set by a projection operator in the totally symmetric irrep generates all the needed SC for that set; at most one totally symmetric SC is generated from each Cartesian coordinate of any atom. Table I shows the SC thus generated for acetone.

For symmetric top molecules, the Cartesian coordinates are first transformed into cylindrical polar coordinates. The SCs are then the appropriate linear combinations of the latter. Thus, for ethane, $\tilde{S}_1 = z_1 = z_2$, $\tilde{S}_2 = z_3 = z_4 = z_5 = z_6$, $\tilde{S}_3 = z_7 = z_8$.



and $\tilde{S}_4 = \rho_1 = \rho_2 = \rho_3 = \rho_4 = \rho_5 = \rho_6$. Note that with 18 internal coordinates for D_{3h} or D_{3d} , only 6 are totally symmetric.

Provisions have been made within the program to freeze certain SC or to allow optimization of only selected SC.

The use of the totally symmetric SC automatically generates the remaining SC for the molecule. For example, if the totally symmetric SC for acetone are used, the remaining SC for acetone are generated by the program.

symmetry. Actually, in our experience carrying along one or more redundant coordinates has not slowed convergence.

GRADIENT ALGORITHM

The total electronic energy of a molecule can be broken up into two parts: a part containing terms each of which depends only on a single atom, and another part which depends on pairs (and larger groups) of atoms. Within the CNDO-2 and CNDO-3 approximation:

$$E = \sum_A E_A + \sum_{A \neq B} E_{AB} \quad (1)$$

where A and B refer to atoms. The first set of terms in eq. (1) is geometry independent, and hence need not concern us further. The second set of terms, E_{AB} , in the CNDO methods can be broken up into three parts:

$$E_{AB}(R_{AB}, S_{\rho\sigma}, \gamma_{AB}) = E'_{AB}(S_{\rho\sigma}) + E''_{AB}(\gamma_{AB}) - E'''_{AB}(R_{AB})$$

Here, R_{AB} is the interatomic distance, $S_{\rho\sigma}$ is the overlap integral between atomic orbitals ρ on A and σ on B , and γ_{AB} is the semi-empirically averaged electron repulsion integral of CNDO. $S_{\rho\sigma}$ and γ_{AB} , of course, themselves are functions of R_{AB} . With these definitions, the gradient elements become

$$\begin{aligned} g_i &= \frac{\partial E}{\partial \tilde{S}_i} = \sum_{A \neq B} \frac{\partial E_{AB}}{\partial \tilde{S}_i} \\ &= \sum_{A \neq B} \left[\sum_{\rho} \sum_{\sigma} \frac{\partial E'_{AB}}{\partial S_{\rho\sigma}} \frac{\partial S_{\rho\sigma}}{\partial R_{AB}} \right. \\ &\quad \left. + \frac{\partial E''_{AB}}{\partial \gamma_{AB}} \frac{\partial \gamma_{AB}}{\partial R_{AB}} - \frac{\partial E'''_{AB}}{\partial R_{AB}} \right] \\ &\quad \times \sum_{m,n} \frac{\partial R_{AB}}{\partial q_{mn}} \frac{\partial q_{mn}}{\partial \tilde{S}_i} \end{aligned} \quad (2)$$

Here the q_{mn} are the three coordinates of the two atoms A and B . All partial derivatives in eq. (2) can be readily evaluated analytically.

STEEPEST DESCENT AND QUADRATIC ACCELERATION

The gradient is a vector pointing in the direction of the steepest increase of the energy. Thus in the n th iteration a new structure is de-

obtained by moving in the negative direction of the gradient by an arbitrarily chosen step a' :

$$|s^{n+1}\rangle = |s^n\rangle - a'|g^n\rangle$$

where $|g^n\rangle$ is the gradient.

Whenever an optimization is carried out by a steepest descent method on a function that is quadratic or nearly quadratic in each of the independent variables, quadratic acceleration methods improve the rate of convergence. We have chosen the method of Fletcher and Powell¹⁷ to accelerate convergence. The improved coordinates q^{n+1} at the $(n+1)$ th step are generated by the recursion relation:

$$|s^{n+1}\rangle = |s^n\rangle - a^n|H^n g^n\rangle$$

where at the n th iteration the Hessian matrix H^n is an approximation to the inverse of the matrix G of the 2nd-order partial derivatives

$$G_{ij} = \frac{\partial^2 E}{\partial s_i \partial s_j}$$

The initial matrix H^1 is taken as the unit matrix, and successive approximations are generated by the recursion relation

$$H^{n+1} = H^n - \frac{c^n \cdot c^n}{c^n \cdot s^n} + \frac{H^n s^n \cdot s^n H^n}{s^n \cdot H^n s^n}$$

with $c^n = -a^n H^n |g^n\rangle$ and $s^n = |s^{n+1}\rangle - |s^n\rangle$.

The use of the quadratic acceleration method assumes the potential energy function to be quadratic in each of the SC's. One frequently finds in the literature statements that this method insures convergence in a calculable number of iterations. However, the assumption of quadratic dependence of the energy on geometry variables is, at best, an approximation, and hence no statement about the rate of convergence can be made in general. Furthermore, we have encountered a number of cases in which the approximation to the Hessian matrix is inadequate. Such behavior has been particularly frequent when torsional angles were involved. In such cases optimization sometimes converged more rapidly by a steepest descent without quadratic acceleration. Occasionally, the Hessian becomes non-(positive definite); in that case, quadratic acceleration is restarted from a unit matrix for H .

Table II. The treatment of step size.

Iteration	$ g_{\max} $	$ g_{\min} $
1 ^a	0.000000	0.000000
2-5	0.000000	0.000000
6-10	0.000000	0.000000
11-15	0.000000	0.000000

^aThe iteration n is rejected.

^bExcept in the first iteration after an α reduction.

CONVERGENCE

A crucial, but unfortunately difficult, parameter in obtaining good convergence is the step size, a^n . The initial step size a^1 must be held quite small, otherwise problems in the self-consistent-field (SCF) convergence are frequently encountered. However, convergence of the optimization is greatly accelerated by continually increasing the step size. Although no truly optimal pattern could be found, we have chosen the pattern shown in Table II.

It may appear natural and desirable to use the magnitude of the change in the SC between successive iterations as the criterion when convergence has been achieved. However, there is no guarantee that at a given precision of calculation a preset degree of precision of SC can be achieved. Therefore, we have chosen the absolute magnitude of the maximum gradient element g_{\max} as the convergence criterion. Although this magnitude is an adjustable parameter, we have used 0.0000001 for most calculations.

REDUCED SYMMETRY

As indicated above, optimization using SC cannot reduce the symmetry below that of the initial test structure. This must be true because any SC that distorts a structure to one of lower symmetry is necessarily nontotally symmetric, and hence the corresponding gradient element vanishes. This is illustrated in Figure 1.

In order to cope with this problem, we have included a special program step which permits distortion of the converged structure in any desired manner by a small but finite amount. Such distortions must be made according to chemical insight into likely structures of the molecule. Distortion in the direction of each nontotally symmetric SC is insufficient, at least in

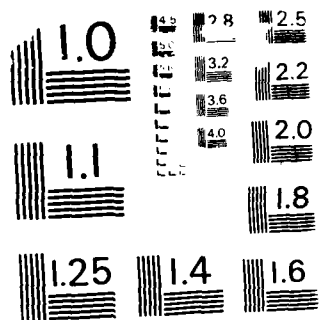
AD-A198 788

HIGH-PERFORMANCE POLYMERIC MATERIALS(U) CINCINNATI UNIV 2/3
ON DEPT OF CHEMISTRY J E MARR 87 DEC 87
AFOSR-IR-87-2811 AFOSR-83-8827

UNCLASSIFIED

F/G 7/6

NL



MICROCOPY RESOLUTION TEST CHART
NATIONAL BUREAU OF STANDARDS - 1963-A

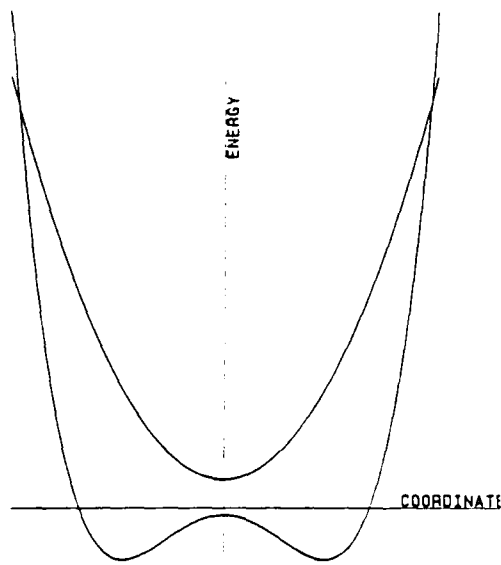


Figure 1. Saddle point and minimum.

the absence of *normal* coordinates. If the energy is decreased by such a distortion, indicating that the geometry obtained is a saddle point rather than a (local) minimum, the optimal geometry has lower symmetry, and optimization is reinitiated automatically in the distorted symmetry.

RESULTS

The program has been tested on a large variety of molecules. It is found that the final converged geometry is independent of the initial test structure. With a convergence criterion of 0.1 eV/Å, in a series of 6 molecules containing 4 to 10 atoms, bond lengths never deviated from the average by more than 0.001 Å, and bond angles had an average variation of $\pm 0.15^\circ$. In some 45 runs, convergence required an average of 12.7 iterations reducing the energy and 1–2 iterations which were rejected because the energy increased. The number of iterations appears to be, because of the quadratic acceleration and the dynamic variation of step size, nearly independent of starting geometry. Typical data are shown in the Appendix.⁸ The total energy of the converged structures also was independent of starting geometry, in each case agreeing to better than 0.001 eV.

Final structures of the test molecules transformed in various pg, including C_1 , C_{2v} , C_{2h} , and D_{2h} . In some cases, optimization was initiated

from a structure transforming in a subgroup of the pg of the final structure. In all such cases, the final structure was the same as when optimization was initiated in the proper pg. Even the number of iterations required for convergence was not significantly affected in this way, although, of course, the computing time was increased because of the larger number of SC required.

In the test molecules, converged geometries agreed with experimental values within an average of ± 0.04 Å for bond lengths and $\pm 3^\circ$ for bond angles. This level of agreement, of course, depends only on the model (CNDO/2) chosen, not on the optimization method.

Further, less extensive tests have been made on a large number of molecules in symmetries as low as C_1 and as high as D_{6h} .⁹ Convergence in cyclic molecules tends to be somewhat slower, but the final geometries also are independent of starting ones, and energy constancy was observed whenever tests were made.

For large molecules, 40–60 atoms, at times convergence is slow, particularly where, in the potential surface, narrow troughs exist. Sometimes as many as 50–100 iterations are required for convergence in these cases.¹⁰ A practical measure that seems to improve efficiency is to alternate between using and not using quadratic acceleration every so many (5–10) iterations. This device reduces the extent of oscillation within the potential energy trough and so speeds up convergence.

One of the many useful features that our CNDO/2 program incorporates is an option allowing for rotation of groups of atoms about designated bonds prior to geometry optimization. This has proved particularly useful in the conformational analysis of several large molecules where CNDO/2 energies have been calculated as a function of some rotational angle, $E(\phi)$ vs. ϕ . Here the number of iterations needed for optimization can be reduced significantly for each successive rotational angle by a judicious choice of initial geometry. Specifically, since in general geometrical parameters (bond lengths and bond angles) vary smoothly with changing rotational angle, it is advantageous to use the previously converged (optimized) structural geometry corresponding to a nearby angle as the initial geometry for a successive calculation at a new ϕ value, rather than to repeatedly reinitialize the geometry at some arbitrary starting point. In this way, needless computational redundancy is obviated.

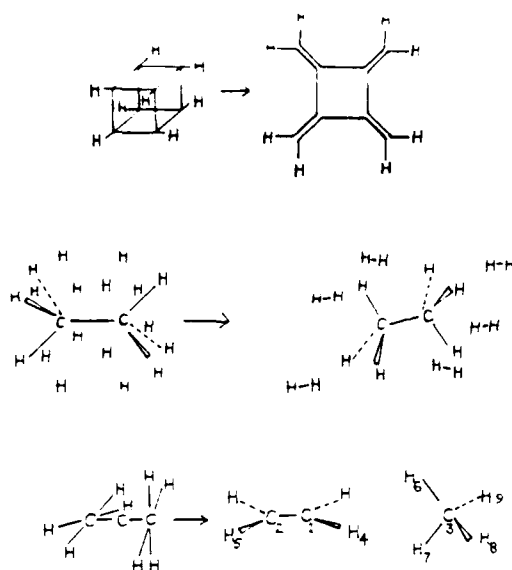


Figure 2. Some irrational structures and the corresponding converged geometries.

The power of the method is also indicated by experiences with the optimization of some irrational structures which had been generated exclusively to test certain symmetry routines. In each case, the optimization converged on a chemically reasonable structure, even if it was necessary to break up the array of atoms into two or more molecules. Figure 2 illustrates some rather astounding examples of such cases. The most amazing finding, perhaps, is the fact that an SCF calculation with a single Slater determinant converges, both for the ridiculous test structures and for the converged structures involving several separated molecules in the same determinant.

The improvement of energy in the first iteration in such cases sometimes exceeded 1000 eV.

The CNDO/2 method has frequently been criticized for giving poor optimized structures.¹¹ Our program, which uses this method, obviously cannot provide results better than the model. However, in our hands the method has produced excellent results with a great economy in computing time.

References

1. H. H. Jaffe' and R. L. Ellis, *J. Comput. Phys.*, **16**, 20 (1971).
2. J. Del Bene and H. H. Jaffe', *J. Chem. Phys.*, **43**, 1807 (1968).
3. J. A. Pople, D. P. Santry, and G. A. Segal, *J. Chem. Phys.*, **43**, 5129 (1965); J. A. Pople and G. A. Segal, *J. Chem. Phys.*, **43**, 5136 (1965).
4. Cf., e.g., P. Pulay and F. Török, *Mol. Phys.*, **25**, 1153 (1973).
5. F. S. Acton, *Numerical Methods that Work*, Harper & Row, New York, 1970, Chap. 17.
6. Cf. also J. W. McIver and A. Komornicki, *Chem. Phys. Lett.*, **10**, 303 (1971).
7. R. Fletcher and M. J. D. Powell, *Comput. J.*, **6**, 163 (1963).
8. Copies of the appendix are available from H. H. J. upon request.
9. In view of the relative scarcity of molecules transforming as spherical tops, and of the special problems involved with the absence of preferred direction, the program can deal with spherical tops only in symmetric or asymmetric top subgroups.
10. W. J. Welsh, H. H. Jaffe', J. E. Mark, and N. Kondo, *Makromol. Chem.*, **183**, 801 (1982); W. J. Welsh and J. E. Mark, *J. Mater. Sci.*, in press; W. J. Welsh and J. E. Mark, *Polym. Bull.*, **8**, 21 (1982); W. J. Welsh, V. Cody, J. E. Mark, and S. F. Zakrzewski, *Cancer Biochem. Biophys.*, in press.
11. D. Perahia and A. Pullman, *Chem. Phys. Lett.*, **19**, 173 (1973).

THEORETICAL STUDIES OF ELECTRICAL CONDUCTIVITY
IN POLYNYNESKenneth C. Metzger¹ and William J. Welch^{1,2}¹Department of Chemistry and Polymer Research Center,
University of Cincinnati, Cincinnati, OH 45221.²Department of Chemistry, College of Mt. St. Joseph,
Mt. St. Joseph, OH 45051.

INTRODUCTION

Quantum mechanical calculations have been used in extending the understanding of the theoretical basis for electrical conductivity in certain organic polymers (1-5). Recent structural evidence and theoretical calculations for polyacetylene (CH)_x indicate that the structure of the polymer chain is a key determinant in the resulting conductivity of the various polymer/dopant systems (6-8). Conductivity in such systems appears to be sensitive to the degree of conjugation along the chain backbone, which in turn is directly related to the degree of chain planarity (6,8,9). These calculations have also been useful in designing polymer chains or linkages that may have potential as conductors or semi-conductors (8,10). Other conjugated polymeric systems have been suggested (6), including various polynyne (-CEC-X-CEC-) where X may be a group IV, V or VI element (11). Undoped organosilicon polynyne have been shown to possess resistivities that classify them as organic semiconductors (12). In the present calculations, the band structure of (-CEC-S-CEC-) has been investigated. Due to the stiffness of the chain and the absence of substituents on any of the atoms in the chain backbone, there should be a minimum of steric conflicts for any conformation. Also, deviations from planarity can only occur by rotations about the C-S single bonds.

For comparison, calculations have also been carried out on the band structure of carbyne (-CEC-) to assess the added effect of the sulfur atom on the conjugated system. The calculations have also been extended to explore the sensitivity of calculated band gaps to small changes in the structural geometry of the unit cell.

THEORY

The band structures of (-CEC-S-CEC-) and (-CEC-) were calculated using the tight binding approximation of the extended Hückel method to obtain the delocalized crystalline molecular orbitals (1,3). The present calculations included all of the valence atomic orbitals of C, but only the s and p orbitals for S atoms could be considered. Lattice sums were carried out to second nearest neighbors. From the calculated band structures, the band gap E_g and the band width BW were used to characterize the potential conductivity of the polymer with reference to similarly calculated values for trans (CH)_x (8). The structural parameters used for the present calculations on (-CEC-S-CEC-) and (-CEC-) are given in Table I. The values for the CEC triple and C-C single bond lengths were selected from extensive *ab initio* calculations on carbyne (-CEC-) (13). Values for the C-S bond length and the C-S-C bond angle were selected from experimental structural data for small molecule analogs (14). In the present calculations, the (-CECSC-CEC-) chains were assumed fixed in a planar zig-zag conformation with respect to the sequence of rigid (-SC-CEC-) segments.

RESULTS AND DISCUSSION

The calculated band gaps E_g and band widths BW for both (-CECSC-CEC-) and (-CEC-) are presented in Table II. Comparing these values with those calculated for trans (CH)_x (E_g = 0.75 eV, BW = 6.9 eV) (8) suggests that

Table I. Structural Parameters used for the present calculations.

	(-CEC-S-CEC-) _x	(-CEC-) _x
Bond Lengths ^a		
CEC	1.116	1.116
C-C	1.339	1.339
C-S	1.685	--
Bond Angle ^b		
C-S-C	100.0°	--

^aIn units of Angstroms.^bIn units of degrees.Table II. Calculated values of the band gap E_g and band width BW.

	(-CEC-S-CEC-) _x	(-CEC-) _x
E _g ^a	3.2	1.5
BW ^a	0.2	2.3

^aIn units of electron-volts.

neither of these polymers would approach the electrical conductivity of trans (CH)_x. This is particularly the case with (-CECSC-CEC-) in that the value of BW is very small, indicating virtually no dispersion of the highest occupied valence band. Therefore, it is predicted that this polymer chain would behave as an insulator even in the doped state, particularly given that the band structure was calculated for the planar conformation which would possess maximum π overlap. Carbyne (-CEC-) _x, however, is a fully conjugated linear chain, and its lower E_g value would appear to render it better suited as a potential electrical conductor or semiconductor. However, it may be surprising that, compared with the analogous (CH)_x, (-CEC-) _x gives a considerably higher E_g value and lower BW value. Preliminary studies suggest an explanation based on the nature of the bonds within the chains. Specifically, in calculations on (CH)_x (8) the alternating single and double bonds were assigned lengths of 1.435 Å and 1.342 Å, respectively. Correspondingly, the lengths given for the single and triple bonds in (-CEC-) _x are 1.339 Å and 1.116 Å. Hence, the disparity in lengths between the two types of bonds is much smaller in (CH)_x [0.09 Å] than in (-CEC-) _x [0.223 Å], and our studies on model systems such as (C₆₀)_x, having complete uniformity in bond lengths, indicate a correspondence between bond length uniformity along the backbone and favorable values of E_g and BW (15). Of course, the degree of bond-length uniformity and the degree of conjugation within these chains are essentially equivalent concepts, hence these results again point to a correlation between conjugation along the chain backbone and conductivity.

Comparison of the calculated BW values for (-CEC-) and (-CECSC-CEC-) suggests that the addition of the S atom greatly affects the conjugation along the chain, and this agrees with the observation that the more homogeneous the structure of the chain, the greater the probability of conductive behavior (6). Certainly, insertion of the S

atom in the otherwise fully conjugated chain disrupts both homogeneity and the rodlike character. These results on (-CECSCC-) are disappointing, however, when compared with the well known conductivity of poly(p-phenylene sulfide) (16). In this connection, the band structures of other polyynes are under current investigation in order to assess the effect of other heteroatoms within the chain backbone on conductivity.

The choice of structural parameters (i.e., bond lengths and bond angles) is of necessity somewhat arbitrary, hence it is essential to assess the sensitivity of our calculated E_g and BW values to changes in the structural geometry of the unit cell. The reference polymeric system, trans (CH)_n, and its perfluorinated analog trans (CF)_n were used for this purpose. The most spectacular effect was obtained by simultaneously increasing the lengths of the C=C bonds and decreasing those of the C-C bonds. For (CF)_n in the trans conformation, such a modification of only 0.02 Å reduced the value of E_g from 0.72 eV to 0.40 eV. This result is reasonable since such a modification is tantamount to increasing the extent of conjugation along the chain, and this should translate to lower E_g values. In the other direction, decreasing the C=C bonds and increasing the C-C bonds by 0.02 Å resulted in an increase in E_g from 0.72 eV to 1.04 eV. In contrast, calculated E_g values were nearly insensitive to small ($\pm 2.0^\circ$) changes in backbone bond angles. Thus, these analyses suggest that conductivity is directly and strongly dependent on the degree of conjugation along the chain backbone, and other small modifications in structure are of relatively minor significance.

REFERENCES

1. M. H. Whangbo and R. Hoffman, J. Am. Chem. Soc., **100**, 6093 (1978).
2. S. K. Tripathy, D. Kitchen, and M. A. Gruy, Macromolecules, **16**, 190 (1983).
3. D. Binaumik and J. E. Mark, J. Polym. Sci., Polym. Phys. Ed., **21**, 1111 (1983).
4. J. L. Bredas, R. Silbey, D. S. Boudreaux, and R. H. Chance, J. Am. Chem. Soc., **105**, 6555 (1983).
5. J. L. Bredas, R. R. Chance, R. H. Baughman, and R. Silbey, J. Chem. Phys., **76**, 3673 (1982).
6. R. H. Baughman, J. L. Bredas, R. R. Chance, K. L. Eisenbaumer, and L. W. Shacklette, Chem. Rev., **82**, 209 (1982).
7. R. H. Baughman, N. S. Murthy, and G. G. Miller, J. Chem. Phys., **79**, 515 (1983).
8. K. C. Metzger and W. J. Welsh, Polymer Preprints, American Chemical Society, Division of Polymer Chemistry, **25**, 195 (1984).
9. R. C. Wheland, J. Am. Chem. Soc., **98**, 3926 (1976).
10. J. L. Bredas and R. H. Baughman, J. Polym. Sci., Polymer Letters Edition, **21**, 475 (1983).
11. J. Zeigler, Sandia National Laboratories, private communication.
12. O. A. Novikova, Ukrainski Khimicheski Zhurnal, **39**, 1270 (1973).
13. H. Teramae and T. Yamabe, Theoret. Chim. Acta, **64**, 1 (1983).
14. D. Den Engelsen, J. Mol. Spectrosc., **30**, 483 (1969).
15. J. C. W. Chien, F. E. Karasz, Makromol. Chem., **3**, 655 (1982).
16. R. R. Chance, L. W. Shacklette, G. G. Miller, D. M. Ivory, J. M. Sowa, and R. H. Baughman, J. Chem. Soc. Commun., 347 (1980); J. F. Rabolt, T. C. Clarke, K. K. Kanazawa, J. R. Reynolds, and G. B. Street, J. Chem. Soc. Chem. Commun., 348 (1980); T. C. Clarke, K. K. Kanazawa, V. Y. Lee, J. F. Rabolt, J. R. Reynolds, and G. B. Street, J. Polym. Sci., Polym. Phys. Ed., **20**, 117 (1982).

ACKNOWLEDGEMENTS

The authors wish to acknowledge the support provided for their research by the Plastic Institute of America and by the Air Force Office of Scientific Research (Grant AFOSR 83-0027, to Professor J. E. Mark (Chemical Structures Program, Division of Chemical Sciences)). We also wish to acknowledge several very helpful conversations with Dr. John Zeigler of the Sandia National Laboratories.

Elastomeric Properties of Bimodal Networks Prepared by a Simultaneous Curing-Filling Technique

M.-Y. TANG* and J. E. Mark

Department of Chemistry and the Polymer Research Center
The University of Cincinnati
Cincinnati, Ohio 45221

If the tetraethylorthosilicate (TEOS) used to end link hydroxyl-terminated poly(dimethylsiloxane) chains is present in excess, there are two effects on the resulting network structure. First, some of the excess TEOS hydrolyzes to give *in situ* precipitation of reinforcing silica particles. In addition, some can cause extension of the polymer chains, particularly of the shorter chains in the case of a bimodal network. In the present investigation, the ultimate strength and toughness of such bimodal networks was found to go through a maximum with increase in the amount of excess TEOS used in the curing-filling procedure.

INTRODUCTION

When an elastomeric network is prepared by end linking polymer chains, it is possible to achieve any desired distribution of network chain lengths simply by proper choice of the polymer chains employed. This technique, for example, has been used for the preparation of bimodal networks (1) of very short and relatively long chains of poly(dimethylsiloxane) (PDMS) $[-Si(CH_3)_2O-]$, the end-linking agent being tetraethylorthosilicate (TEOS) $[Si(OC_2H_5)_4]$. Such (unfilled) networks were found to be unusually tough elastomers (1, 2). Another, much more common, way of obtaining toughness is to employ a reinforcing filler, typically silica (SiO_2) in the case of PDMS networks (3, 4). Of interest here is the fact that a technique has now been developed for the simultaneous curing and filling of PDMS elastomers (5), the desired *in situ* filling being accomplished by the hydrolysis of TEOS present in excess of that required for the end-linking process.

The present investigation explores one possible route for preparing PDMS elastomers which are both bimodal and filled, specifically by the simultaneous curing and *in situ* filling of a bimodal mixture of PDMS chains. Of particular interest are the ultimate strength and toughness of the resulting elastomers.

EXPERIMENTAL DETAILS

The two hydroxyl-terminated PDMS samples employed were generously provided by the Dow Corning Corporation, and had number-average mo-

lecular weights corresponding to 660 and 21.3×10^4 g mol⁻¹. They were mixed to give two batches in which the short chains were present to the extent of 94 and 97 mole percent, respectively. Portions from both of these batches were mixed with TEOS in amounts characterized by the molar composition ratio $r = [OC_2H_5]/[OH]$, where the $-OC_2H_5$ groups are on the TEOS and the $-OH$ groups appear as chain ends on the PDMS. Specific values of this ratio are given in the second column of Table 1. The catalyst employed, stannous-2-ethyl-hexanoate, was present to the extent of 1.0 weight percent of the PDMS. Both series of mixtures of these components appeared to be perfectly homogeneous. They were poured into molds to a depth of 1.0 to 1.5 mm, and the reaction was allowed to proceed at room temperature for three days. The water required for the hydrolysis of the TEOS was simply absorbed from the humidity in the air.

The resulting networks were extracted in tetrahydrofuran and toluene in the usual manner (6, 7); the sol fractions thus obtained were generally small, as can be seen from the values given in column three of Table 1. The densities ρ of these extracted materials were determined by pycnometry. Swelling equilibrium measurements were also carried out on portions of the extracted samples. Unswollen portions cut from each network sheet were used in the elongation experiments carried out to obtain the stress-strain isotherms at 25°C (2, 6, 7). The nominal stress was given by $f^* = f/A^*$, where f is the equilibrium elastic force and A^* the undeformed cross-sectional area, and the reduced stress or modulus (6-8) by $[f^*] = f^*/(\alpha - \alpha^{-2})$, where $\alpha = L/L_1$ is the elongation or relative length of the sample.

* Visiting scholar from the Chengguang Institute of Chemical Industry, Sichuan, China.

Table 1. Network Characteristics and Elastomeric Properties.

Composition		Weight percent SiO ₂								
Mole percent short chains ^a	<i>r</i> ^b	Sol fraction, percent	<i>v</i> _{2m} ^c	<i>ρ</i> , g cm ⁻³	From Δ <i>w</i>	From <i>ρ</i>	<i>α</i> _u ^d	<i>α</i> _r ^e	(<i>f</i> / <i>A</i> [*]) _{r,f} ^f <i>N</i> mm ⁻²	10 ³ <i>E</i> _r ^g <i>J</i> mm ⁻²
94	0.52	5.4	—	0.954	—	—	1.39	2.25	0.653	0.418
	0.80	4.5	—	0.957	—	—	1.21	2.39	2.03	0.964
	1.02	4.3	0.289	0.959	0.00	0.00	1.29	2.22	2.03	0.800
	1.29	4.7	0.299	0.966	1.97	1.11	1.26	2.10	2.51	0.851
	1.49	4.8	0.303	0.968	2.70	1.62	1.23	2.06	2.14	0.773
	1.84	4.8	0.304	0.973	3.33	2.30	1.24	2.07	2.93	0.888
	2.14	4.4	—	0.976	—	2.72	1.22	1.96	3.07	0.906
	2.49	5.1	0.304	0.980	4.59	3.37	1.23	2.05	3.75	1.07
	2.86	4.9	0.307	0.981	5.76	3.62	1.19	2.04	4.01	1.14
	3.28	4.7	—	0.988	—	4.64	1.21	2.00	4.44	1.06
	3.56	4.6	0.307	0.996	6.05	5.90	1.18	1.86	3.82	0.780
	3.76	4.2	—	0.998	—	6.21	1.18	1.80	3.56	0.770
	4.03	4.4	0.316	1.005	8.13	7.32	1.15	1.86	3.50	0.913
	5.00	4.5	0.321	1.011	9.94	8.17	1.13	1.75	2.65	0.604
97	0.68	6.4	—	0.964	—	—	1.21	1.64	0.735	0.176
	1.00	6.3	0.321	0.967	0.00	0.00	1.21	1.62	0.934	0.275
	1.40	7.3	0.327	0.979	2.50	1.83	1.19	1.89	2.76	0.833
	1.74	7.2	0.327	0.989	3.20	3.44	1.16	1.94	4.16	1.21
	2.08	7.4	0.335	0.989	4.40	3.50	1.16	1.87	3.73	1.04
	2.59	8.2	0.339	0.993	5.99	4.10	1.12	1.63	1.91	0.483
	3.05	8.8	0.339	1.003	7.08	5.55	1.11	1.60	2.27	0.505

^a Of molecular weight 880 g mol⁻¹, in mixtures with long chains having 21.3 × 10⁴ g mol⁻¹.^b Molar composition ratio of —OC₂H₅ TEOS groups to —OH chain ends.^c Volume fraction of polymer present at swelling equilibrium in benzene at room temperature.^d Elongation at upturn in modulus.^e Elongation at rupture.^f Ultimate strength as represented by the nominal stress at rupture.^g Energy required for rupture.

RESULTS AND DISCUSSION

The swelling equilibrium results indicated strong reinforcing effects from the precipitated silica. Specifically, the degree of swelling decreased as the composition ratio r increased: this is shown in column four of Table 1, by the increasing values of the volume fraction v_{2m} of polymer at swelling equilibrium. Also, the densities (given in column five) increased with increase in r , because of the high density of silica (~ 2.6 g cm⁻³) (16) relative to PDMS (~ 0.96 g cm⁻³).

The amounts of SiO₂ precipitated were estimated in two ways. Values obtained from the increase Δw in weight of polymer are given in column six of Table 1, and those from the densities of filled network, polymer, and silica are given in the following column. The latter values are approximately 20 percent smaller than the former, which indicates that not all of the TEOS hydrolyzed is converted all the way to pure silica. In any case, in both series of networks, the weight of filler does show the expected increase with increase in r .

Some typical stress-strain isotherms, selected from those obtained from the networks having 94 mole percent short chains, are shown in Fig. 1. This representation is based on the equation (8, 9)

$$[f^*] = 2C_1 + 2C_2\alpha^{-1} \quad (1)$$

where $2C_1$ and $2C_2$ are constants, and thus the reduced stress is plotted against reciprocal elongation. Increase in the composition ratio r decreases

the value of α_u of the elongation at which the upturn in $[f^*]$ becomes discernible, as can be seen from both the figure and from column eight of Table 1. Increase in r thus gives the expected increase in amount of precipitated filler, with the associated upturn in $[f^*]$ occurring at smaller deformations. This increase in filler content should also cause a decrease in the elongation α_r at rupture. As shown by the values of α_r given in column nine, this is confirmed by most of the data. The data on the networks containing 97 mole percent short chains scatter too badly to be definitive in this regard.

Figure 2 shows the data of Fig. 1 plotted in such a way that the area under each stress-strain curve corresponds to the energy E_r of rupture (2, 10), which is the standard measure of elastomer toughness. Increase in filler content is seen to give significant increases in both E_r and in the ultimate strength, as represented by the value $(f/A^*)_{r,f}$ of the nominal stress at rupture. Values of both quantities for all of the samples are given in the last two columns of Table 1. The most extensive set of results, those for the networks having 94 mole percent of short chains, are also presented as a function of the composition ratio r in Fig. 3. Both $(f/A^*)_{r,f}$ and E_r go through a maximum with increase in excess TEOS. This could be due to the weight percent of silica becoming so large as to make the networks relatively brittle. Alternatively, or in addition, some of the excess TEOS could cause chain extension, which would be particularly serious in the case of the very short chains, because of their

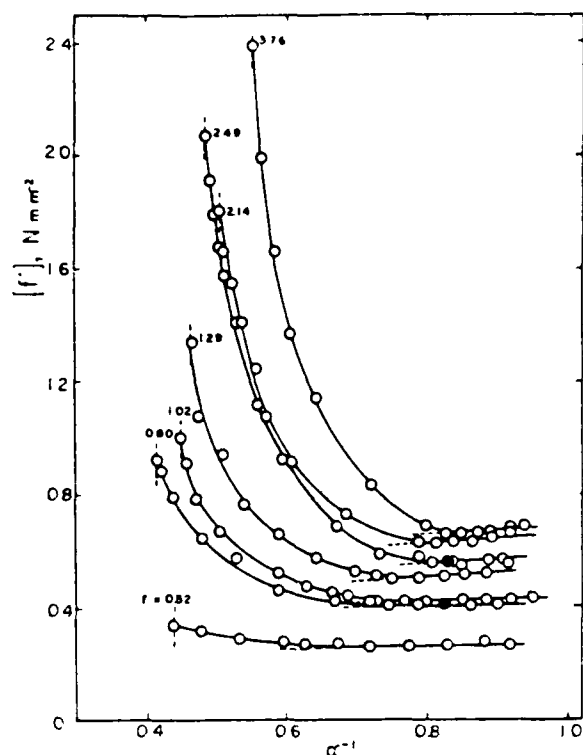


Fig. 1 The reduced stress shown in a function of reciprocal elongation for typical networks having 94 mole percent short chains. The results pertain to 25°C, and each curve is labelled with its value of the molar composition ratio $r = [-OC_2H_5]/[-OH]$. The open circles locate results gotten using a series of increasing values of the elongation and the filled circles results obtained out of sequence to test for reversibility. The short extensions of the linear portions of the curves, which were located by least-squares analysis, help locate the values α_u of the elongation at which the upturns in $[f^*]$ just become discernible. The vertical dashed lines locate the rupture points of the samples.

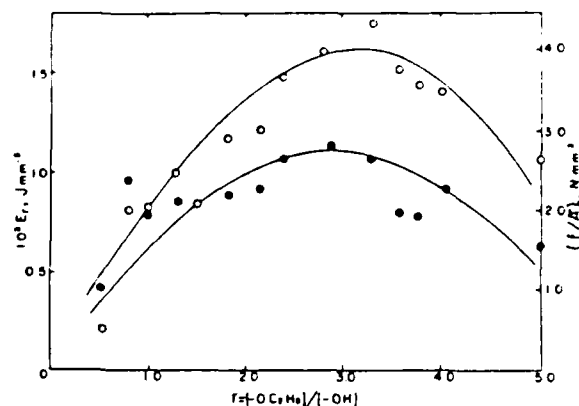
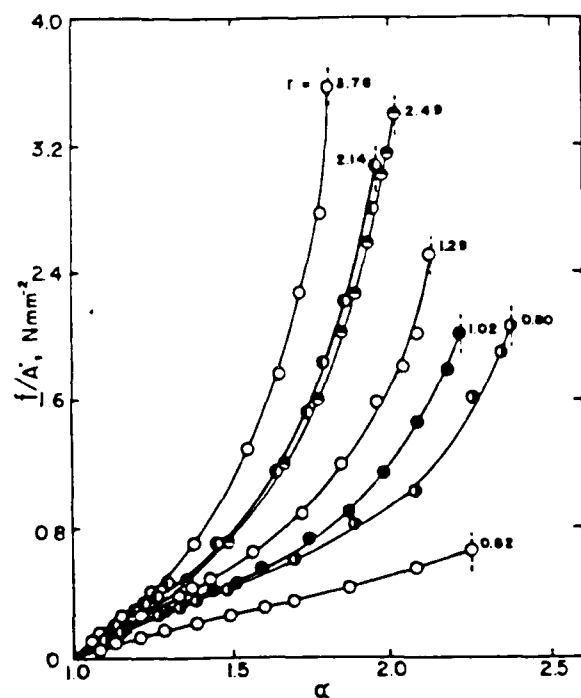


Fig. 3. The effect of the composition ratio on the ultimate strength and energy for rupture of all of the networks having 94 mole percent short chains.

very high number density of end groups. Thus, excess TEOS can be used to improve the properties of bimodal PDMS networks by the *in situ* precipitation of silica but complications, such as the effects of chain extension, must also be taken into account.

ACKNOWLEDGMENTS

It is a pleasure to acknowledge the financial support provided by the National Science Foundation through Grant DMR 79-18903-03 (Polymers Program, Division of Materials Research) and by the Air Force Office of Scientific Research through Grant AFOSR 83-0027 (Chemical Structures Program, Division of Chemical Sciences). M.-Y.T. also wishes to thank the Dow Corning Corporation for the Research Fellowship he received.

REFERENCES

1. J. E. Mark, *Adv. Polym. Sci.*, **44**, 1 (1982).
2. M. A. Llorente, A. L. Andrad, and J. E. Mark, *J. Polym. Sci., Polym. Phys. Ed.*, **19**, 621 (1981).
3. M. P. Wagner, *Rubber Chem. Technol.*, **49**, 703 (1976).
4. E. L. Warrick, O. R. Pierce, K. E. Polmanteer, and J. C. Saam, *Rubber Chem. Technol.*, **52**, 437 (1979).
5. J. E. Mark, C.-Y. Jiang, and M.-Y. Tang, ms. submitted to *Macromolecules*.
6. J. E. Mark and J. L. Sullivan, *J. Chem. Phys.*, **66**, 1006 (1977).
7. M. A. Llorente, A. L. Andrad, and J. E. Mark, *J. Polym. Sci., Polym. Phys. Ed.*, **18**, 2263 (1980).
8. L. R. G. Treloar, "The Physics of Rubber Elasticity," Clarendon Press, Oxford (1975).
9. J. E. Mark, *Rubber Chem. Technol.*, **48**, 495 (1975).
10. J. E. Mark and S.-J. Pan, *Macromol. Chem., Rapid Commun.*, **3**, 681 (1982).

Fig. 2 The nominal stress shown as a function of elongation for the same networks characterized in Fig. 1. In this representation, the area under each curve represents the energy E_r required for network rupture.

Reprinted from *Macromolecules*, 1984, 17, 2613
 Copyright © 1984 by the American Chemical Society and reprinted by permission of the copyright owner.

Simultaneous Curing and Filling of Elastomers

James E. Mark,* Cheng-Yong Jiang,[†] and Ming-Yang Tang[†]

Department of Chemistry and the Polymer Research Center, The University of Cincinnati, Cincinnati, Ohio 45221. Received February 15, 1984

ABSTRACT: A method previously developed for the precipitation of reinforcing silica filler within an already cured elastomer is extended so as to permit simultaneous curing and filling. Specifically, tetraethyl orthosilicate is used to end-link hydroxyl-terminated chains of poly(dimethylsiloxane), with the excess present being hydrolyzed to finely divided SiO_2 . Increase in the amount of filler thus formed decreases the elongation required for the desired upturns in modulus and increases the maximum extensibility, ultimate strength, and energy required for rupture of the network.

Introduction

Elastomers which cannot readily undergo strain-induced crystallization are very weak in the unfilled state.¹⁻³ Networks of poly(dimethylsiloxane) (PDMS) $[-\text{Si}(\text{CH}_3)_2-\text{O}-]$ are in this category, primarily because of the very low melting point (-40°C)⁴ of this polymer. As a result, PDMS elastomers used in most applications are invariably filled with a "high-structure" particulate silica (SiO_2) in order to improve their mechanical properties.⁵⁻⁶ The incorporation of such fillers in PDMS or any high-viscosity polymer, however, is a difficult, time-consuming, and energy-intensive process.⁵⁻⁶ It can also cause premature gelation ("structuring" or "crepe hardening").⁹ For these and other reasons,¹⁰ it would be advantageous to be able either to precipitate reinforcing SiO_2 into an already cured network or to generate it during the curing process. The first goal was achieved in two earlier studies^{10,11} in which tetraethyl orthosilicate (TEOS) $[\text{Si}(\text{OC}_2\text{H}_5)_4]$ was hydrolyzed to precipitate the desired SiO_2 filler into a cross-linked PDMS network. The present investigation extends this work so as to permit the simultaneous curing and filling of an elastomer material.

Experimental Details

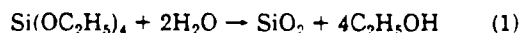
The polymers employed, two hydroxyl-terminated PDMS samples having number-average molecular weights corresponding to $10^{-3}M_n = 21.3$ and 8.00, respectively, were generously provided by Dow Corning Corp. Portions of them were mixed with TEOS in amounts characterized by the molar feed ratio $r = [\text{OC}_2\text{H}_5]/[\text{OH}]$, where the OC_2H_5 groups are on the TEOS and

the OH groups appear as chain ends on the PDMS. Specific values of this ratio, which range upward from 1.0 (stoichiometric balance), are given in the third column of Table I. The catalysts employed, dibutyltin diacetate and stannous 2-ethyl hexanoate, were present to 0.8–1.0 and 1.7 wt %, respectively, of the PDMS. Both series of mixtures of these three components appeared to be perfectly homogeneous. They were poured into molds to a depth of 1.0–1.5 mm, and the reaction was allowed to proceed at room temperature for 3 days. The water required for the hydrolysis of the TEOS was generally simply absorbed from the humidity in the air,¹² but in a few test cases, additional liquid water was added to the reaction media.

The resulting networks were extracted in tetrahydrofuran and toluene in the usual manner;^{13,14} the sol fractions thus obtained are small, as can be seen from the values given in column four of Table I. The densities ρ of these extracted materials were determined by pycnometry. Swelling measurements in benzene at room temperature were also carried out on portions of the extracted samples. Similarly, other unswollen portions were used in the elongation experiments carried out to obtain the stress-strain isotherms at 25°C .^{13,14} The nominal stress was given by $f^* \equiv f/A^*$, where f is the elastic force and A^* the undeformed cross-sectional area, and the reduced stress or modulus¹³⁻¹⁵ by $[f^*] \equiv f^*/(\alpha - \alpha^{-2})$, where $\alpha = L/L_i$ is the elongation or relative length of the sample.

Results and Discussion

The simplest equation for the hydrolysis of TEOS is



but the reaction in the presence of the hydroxyl-terminated PDMS is probably much more complicated, with some chains bonded to incompletely hydrolyzed products. In any case, electron microscopy results¹⁶ indicate the particles to be unagglomerated, with an average diameter of

* Visiting scholar from the Chenguang Institute of Chemical Industry, Sichuan, China.

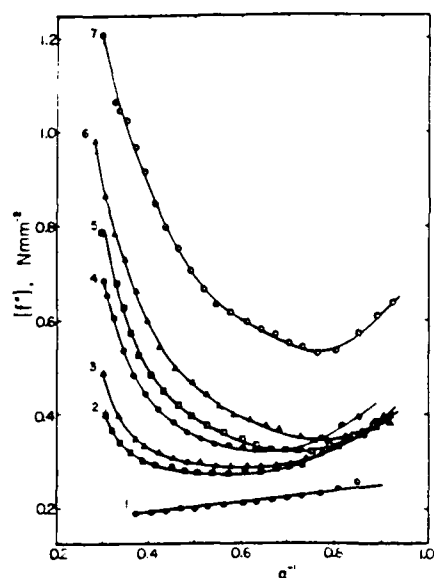


Figure 1. Reduced stress shown as a function of reciprocal elongation for the first series of SiO_2 -filled PDMS networks at 25 °C. Each curve is identified by the designation given in column one of Table I, and the vertical dashed lines locate the rupture points. The results shown in the remaining figures also pertain to this series of networks.

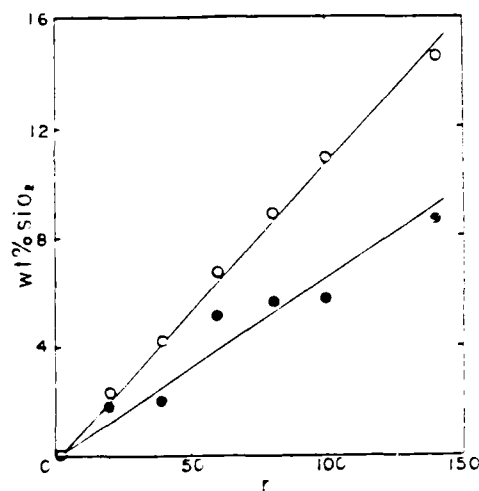


Figure 2. Weight percent silica precipitated within the PDMS networks shown as a function of the feed ratio $r = [\text{OC}_2\text{H}_5]/[\text{OH}]$, where the OC_2H_5 groups are on the tetraethyl orthosilicate and the OH groups are at the ends of the polymer. The open circles show the results obtained from the change in weight of the polymer and the filled circles from the density of the filled network.

200 Å. There was also ample evidence for very strong reinforcing effects from the precipitated silica. Specifically, the degree of swelling decreased as the feed ratio r increased; this is shown in column five of Table I by the increasing values of the volume fraction v_{2m} of polymer at swelling equilibrium. Also, the densities (given in column six) increased with increase in r , because of the high density of silica ($\sim 2.6 \text{ g cm}^{-3}$)¹⁷ relative to PDMS ($\sim 0.95 \text{ g cm}^{-3}$). Finally, the networks prepared with an excess of TEOS ($r \gg 1$) have values of the modulus which are much higher than those of the network prepared using $r = 1.0$ (curve 1). Typical results, for the first series of networks, are shown in Figure 1. Furthermore, the upturns in $[f^*]$

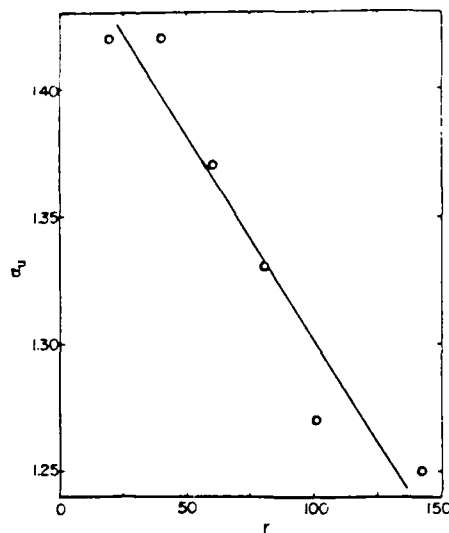


Figure 3. Effect of the feed ratio on the elongation at the initial upturn in modulus.

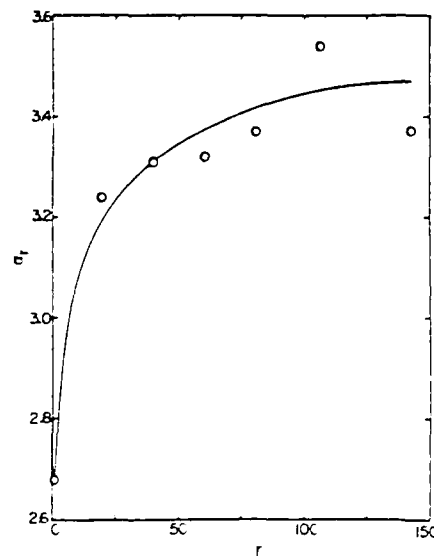


Figure 4. Dependence of the maximum extensibility on the feed ratio.

observed at high elongations clearly demonstrate the desired reinforcing effects.^{1,10,11,16}

The amounts of SiO_2 precipitated were estimated in two ways. Values obtained from the increase Δw in weight of polymer are given in column seven of Table I, and those from the densities of filled network, polymer, and silica are given in the following column. The latter values are approximately 30% smaller than the former, which is consistent with the expectation, already mentioned, that the filler is not entirely pure SiO_2 . Larger amounts of silica were precipitated in the case of the shorter chain network ($10^{-3}M_r = 8.00$), presumably because these networks contained larger amounts of TEOS. The amounts are represented relative to the stoichiometrically balanced amount, and this reference amount is larger for the end-linking of shorter chains. In both series of networks, the weight of filler does show the expected increase with increase in r , as in shown in Figure 2.

The values of the elongation α_u at which the modulus increases because of the reinforcing effects are given in column nine of Table I. They show the expected decrease

Table I
Preparation and Properties of the Silica-Filled Networks

network	$10^{-3}M_r$	r^a	sol fraction	ν_{2m}^b	$\rho, g\ cm^{-3}$	wt % SiO_2		a_u^c	a_r	$(f/A^*)_r^d$ $N\ mm^{-2}$	$10^3 E_r^e$ $J\ mm^{-3}$
						from Δu	from ρ				
1	21.3	1.0	0.043	0.293	0.955	0.00	0.00		2.68	0.481	0.489
2	21.3	19.5	0.034	0.319	0.966	2.28	1.80	1.42	3.24	1.25	1.18
3	21.3	39.9	0.033	0.326	0.967	4.56	1.96	1.42	3.31	1.58	1.49
4	21.3	60.4	0.032	0.328	0.987	6.75	5.12	1.37	3.32	2.21	1.93
5	21.3	80.8	0.031	0.334	0.990	8.83	5.59	1.33	3.37	2.59	2.03
6	21.3	101.3	0.030	0.338	0.993	10.83	5.74	1.27	3.54	3.39	2.93
7	21.3	142.2	0.029	0.373	1.010	14.56	8.61	1.25	3.37	3.99	3.73
8	8.00	1.0	0.046	0.324	0.954	0.00	0.00		1.59	0.310	0.120
9	8.00	5.2	0.047	0.363	0.962	1.29	1.16	1.68	1.87	0.507	0.240
10	8.00	10.0	0.047	0.384	0.983	5.02	4.44	1.47	2.05	0.730	0.417
11	8.00	20.4	0.050	0.409	1.002	8.31	7.50	1.24	2.49	2.11	1.21

^aFeed ratio of OC_2H_5 TEOS groups to OH chain ends. ^bVolume fraction of polymer present at swelling equilibrium in benzene at room temperature. ^cElongation at initial upturn in modulus. ^dUltimate strength as represented by the nominal stress at rupture. ^eEnergy required for rupture.

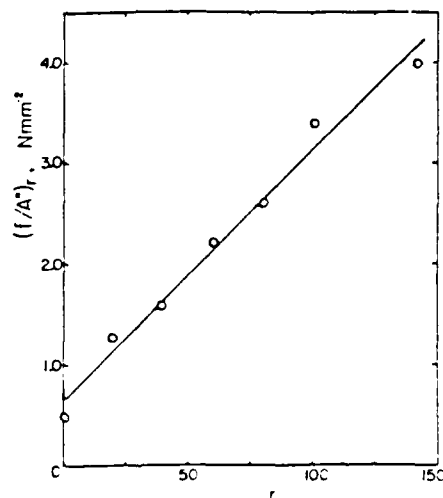


Figure 5. Effect of the feed ratio on the ultimate strength as characterized by the nominal stress at rupture.

with increase in the amount of silica generated, as is shown by the typical results presented in Figure 3. Values of the maximum extensibility or elongation a_r at rupture are given in the following column. Their increase with r , as shown in Figure 4, clearly demonstrates the reinforcement-induced improvement in this ultimate property. Much more striking increases are observed for the ultimate strength, as represented by the nominal stress at rupture. These results are shown in part in Figure 5 and are tabulated in their entirety in column 11 of Table I. Networks prepared in contact with excess water were not as strong as those described in Table I. The fact that these samples were cloudy indicates the presence of unusually large silica particles, which would be less effective as reinforcing agents.

Figure 6 shows the data of Figure 1 plotted in such a way that the area under each stress-strain curve corresponds to the energy E_r of rupture,^{1b} which is the standard measure of elastomer toughness. The values of $10^3 E_r$ for the two series of networks range from 0.49 and 0.12 $J\ mm^{-3}$ ($r = 1.0$) to 3.73 and 1.21 $J\ mm^{-3}$ ($r \gg 1$), respectively. The specific values are given in the last column of Table I, and typical results are shown as a function of r in Figure 7. Thus, this reinforcement technique can easily bring about a tenfold increase in toughness. Furthermore it is achieved in a manner that avoids the complications of the elaborate milling techniques usually used to blend an already formed

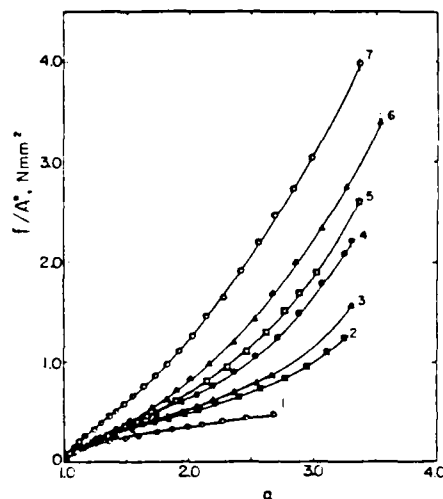


Figure 6. Nominal stress shown as a function of elongation for the same networks characterized in Figure 1. In this representation, the area under each curve corresponds to the energy required for network rupture.

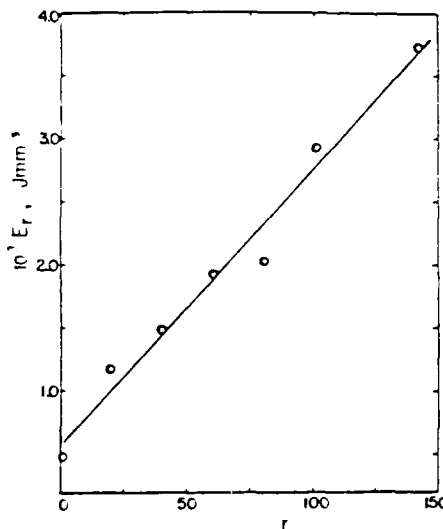


Figure 7. Effect of the feed ratio on the energy required for network rupture.

filler into a high molecular weight polymer.

Acknowledgment. It is a pleasure to acknowledge the

financial support provided by the National Science Foundation through Grant DMR 79-18903-03 (Polymers Program, Division of Materials Research) and by the Air Force Office of Scientific Research through Grant AFOSR 83-0027 (Chemical Structures Program, Division of Chemical Sciences). C.-Y.J. and M.-Y.T. also wish to thank Dow Corning Corp. for the Research Fellowships they received.

References and Notes

- (1) Flory, P. J. "Principles of Polymer Chemistry"; Cornell University Press: Ithaca, NY, 1953.
- (2) Mark, J. E.; Kato, M.; Ko, J. *J. Polym. Sci., Part C* **1976**, *54*, 217.
- (3) Smith, T. L. *Polym. Eng. Sci.* **1977**, *17*, 129.
- (4) Brandrup, J.; Immergut, E. "Polymer Handbook", 2nd ed.; Wiley-Interscience: New York, 1975.
- (5) Polmanteer, K. E.; Lentz, C. W. *Rubber Chem. Technol.* **1975**, *48*, 795.
- (6) Dannenberg, E. M. *Rubber Chem. Technol.* **1975**, *48*, 410.
- (7) Wagner, M. P. *Rubber Chem. Technol.* **1976**, *49*, 703.
- (8) Warrick, E. L.; Pierce, O. R.; Polmanteer, K. E.; Saam, J. C. *Rubber Chem. Technol.* **1979**, *52*, 437.
- (9) Hamilton, J. R. "Silicone Technology"; Interscience: New York, 1970.
- (10) Mark, J. E.; Pan, S.-J. *Makromol. Chem., Rapid Commun.* **1982**, *3*, 681.
- (11) Jiang, C.-Y.; Mark, J. E., manuscript in preparation.
- (12) The observed ease of hydrolysis of TEOS suggests that preparing model PDMS elastomers by the use of TEOS could inadvertently introduce some SiO₂ into the networks.
- (13) Mark, J. E.; Sullivan, J. L. *J. Chem. Phys.* **1977**, *66*, 1006.
- (14) Liorente, M. A.; Andrady, A. L.; Mark, J. E. *J. Polym. Sci., Polym. Phys. Ed.* **1980**, *18*, 2263.
- (15) Mark, J. E.; Flory, P. J. *J. Appl. Phys.* **1966**, *37*, 4635.
- (16) Ning, Y.-P.; Tang, M.-Y.; Jiang, C.-Y.; Mark, J. E.; Roth, W. C. *J. Appl. Polym. Sci.* **1984**, *29*, 3209.
- (17) Weast, R. C. "CRC Handbook of Chemistry and Physics", 63rd ed.; CRC Press, Inc.: Cleveland, 1982.
- (18) Mark, J. E. *Polym. Eng. Sci.* **1979**, *19*, 254, 409.
- (19) Liorente, M. A.; Andrady, A. L.; Mark, J. E. *J. Polym. Sci., Polym. Phys. Ed.* **1981**, *19*, 621.

SHORT COMMUNICATION

Impact resistance of unfilled and filled bimodal thermosets of poly(dimethylsiloxane)

M.-Y. Tang*, A. Letton**, and J. E. Mark*

Departments of Chemistry* and Chemical Engineering** and the Polymer Research Center, The University of Cincinnati, Cincinnati, Ohio USA

Key words: Bimodal networks, thermosets, poly(dimethylsiloxane), impact strength, filled elastomers, rupture energies.

Introduction

Incorporating very short (non-elastomeric) chains in an elastomeric network, thereby giving a bimodal distribution of chain lengths, is known to have a significant toughening effect [1-3]. (In such networks, the short chains are thought to increase the ultimate strength because of their limited extensibility, and the long chains to retard the spread of rupture nuclei). The present investigation considers the related possibility of incorporating very long (elastomeric) chains in a relatively brittle thermoset in an attempt to improve its impact resistance. Bimodal networks of poly(dimethylsiloxane) (PDMS) are employed, both in the unfilled state and after filling by the in-situ precipitation (4) of reinforcing silica particles.

Experimental Details

The two polymers employed were hydroxyl-terminated polydimethylsiloxane chains (PDMS) having number-average molecular weights M_n of 660 g mol⁻¹ and 21.5×10^3 g mol⁻¹, respectively. They were generously provided by the Dow Corning Corporation of Midland, MI. After careful drying, these two components were mixed to give the compositions listed in columns one and two of table 1. They were tetrafunctional end linked using tetraethoxyorthosilicate (TEOS) [Si(OC₂H₅)₄], at room temperature, in the usual manner [2, 5]. In brief, the end linking is a condensation reaction catalyzed by stannous-2-ethyl-hexanoate, and was allowed to proceed at room temperature for a total of 2 days. TEOS present in excess of the amount required for reaction with the PDMS end groups is hydrolyzed to reinforcing silica from the moisture present in the air. Electron microscopy results reported elsewhere (7) showed such filler particles to have an average diameter of 250 Å, with almost all the particles in the range 200-300 Å. The amounts of TEOS employed were characterized by the molar com-

position ratio $r = [\text{OC}_2\text{H}_5]/[\text{OH}]$, where the -OC₂H₅ groups are on the TEOS and the -OH groups appear as chain ends on the PDMS. Specific values of this ratio are given in the third column of table 1. The catalyst employed was present to the extent of 1.6 wt % of the PDMS.

The resulting networks were extracted in tetrahydrofuran and toluene as described elsewhere [2, 5, 6, 8]. In the case of the unfilled networks, the changes in weight represent the sol fraction, which was found to correspond to approximately 5 wt %. One series of

Table 1. Network characteristics, and stress-strain and impact test results

Short Chains ^{a)}		r^b	Wt % Filler	(f/A) ^{c)} N mm ⁻²	10 ³ E ^{d)} J mm ⁻¹	IS ^{e)} J mm ⁻¹
Mol %	Wt %					
100.0	100.0	1.0	0.0	0.568	0.039	0.0212
99.4	83.3	1.0	0.0	0.695	0.068	0.0313
		1.5	4.4	0.835	0.102	0.0376
98.5	66.7	1.0	0.0	0.774	0.133	0.0356
		1.5	3.4	1.01	0.166	0.0757
97.0	50.0	1.0	0.0	1.45	0.397	0.147
		1.7	3.2	4.15	1.21	0.461
94.2	33.3	1.0	0.0	2.45	0.963	0.386
		2.5	4.6	3.75	1.07	0.306
90.8	23.3	1.0	0.0	1.64	0.769	0.221
		2.5	2.5	3.19	1.09	0.394

^{a)} Having a number-average molecular weight $M_n = 660$ g mol⁻¹, in mixtures with long chains having $M_n = 21.5 \times 10^3$ g mol⁻¹.

^{b)} Molar composition ratio of -OC₂H₅ TEOS groups to -OH chain ends.

^{c)} Ultimate strength, as represented by the nominal stress at rupture.

^{d)} Energy for rupture.

^{e)} Impact strength.

unswollen sheets, which were approximately 1 mm thick, were cut into strips (3 mm wide and 30 mm long); another series, approximately 2.5 mm thick, were cut into circular discs (35 mm diameter). The strips were used in elongation measurements carried out to obtain the stress-strain isotherms at 25 °C [2, 5, 6, 8]. The discs were studied in a small-scale instrumented dart impact tester with an impact duration time of approximately 4 msec [9] in order to obtain relative values of their impact strength.

Results and Discussion

In the case of the filled networks, the amount of silica precipitated from the excess TEOS was obtained from the increase in weight of the networks. The stress-strain data were analyzed in terms of the nominal stress $f^* \equiv f/A^*$ where f is the equilibrium elastic force and A^* the undeformed cross-sectional area, and the reduced stress or modulus [2, 10] $[f^*] \equiv f^*/(\alpha - \alpha^{-2})$, where $\alpha = L/L_0$ is the elongation or relative length of the sample.

The first representation of the data was in terms of the Mooney-Rivlin relationship, in which the reduced stress is expected to vary linearly with reciprocal elongation for relatively small deformations [2, 11, 12]. The results are shown in figure 1. In the case of the unfilled (U) networks, the large increases in $[f^*]$ at high elongations are caused by the limited extensibility of the short chains [2, 6]; in the filled (F) networks, the upturns are seen to be enhanced by the reinforcing effect of the silica particles [4]. It is also useful to plot the nominal stress f/A^* directly against elongation since the area under such a curve corresponds to the energy E_r of rupture, the standard measure of toughness [2, 4, 6]. Values of f/A^* at rupture and E_r are given in columns five and six of the table.

Results from the dart impact tests gave values of the impact strength (IS) in units of energy per unit thickness ($J\ mm^{-1}$). Specific values are given in the final column of the table, and both E_r and IS are shown as a function of composition in figure 2. There is seen to be a good correlation between E_r and IS as measures of impact resistance, with both exhibiting a maximum [3] as the mol % of short chains is decreased. Incorporation of 6–7 mol % of long chains is seen to greatly increase E_r and IS and thus the impact resistance of the 100% short-chain network, which is very nearly a brittle thermoset. It is important to note that it is essential that the long chains be *linked* into the network structure. Only approximately 0.08 mol % of the long chains could be introduced by swelling, because of the very high crosslink density of the 100% short-chain network. Similarly, although it would be possible to have inert long chains present during the end linking

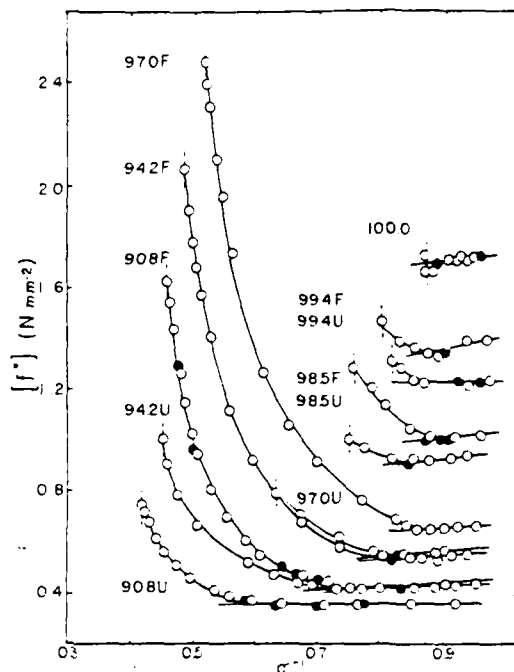


Fig. 1. The reduced stress shown as a function of reciprocal elongation at 25 °C. Each curve is labelled with the mol % of short chains present in the network, and U and F specify unfilled and filled, respectively. The open circles locate the results obtained using a series of increasing values of the elongation α , and filled circles the results obtained out of sequence to test for reversibility. The vertical dashed lines locate the rupture points, and the short extensions of the linear portions of the isotherms help locate the values of α at which the upturn in $[f^*]$ first becomes discernible.

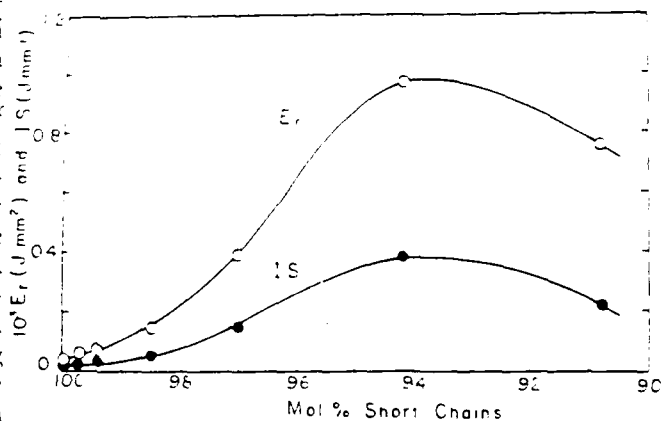


Fig. 2. The energy for rupture and the impact strength shown as a function of composition for the unfilled networks.

procedure, syneresis [13] would almost certainly occur, with the long chains being exuded from the network structure.

Thus, it has been clearly demonstrated that linking long chains into a thermoset network can greatly improve its impact resistance.

Acknowledgements

It is a pleasure to acknowledge the financial support provided by the National Science Foundation through Grant DMR 79-18903-03 (Polymers Program, Division of Materials Research) and by the Air Force Office of Scientific Research through Grant AFOSR 83-0027 (Chemical Structures Program, Division of Chemical Sciences). M.-Y.T. also wishes to thank the Dow Corning Corporation for the Research Fellowship he received.

References

1. Mark JE (1982) (eds) Mark JE, Lal J, *Elastomers and Rubber Elasticity*, American Chemical Society, Washington, DC
2. Mark JE (1982) *Adv Polym Sci* 44:1
3. Tang MY, Mark JE, ms submitted to *Macromolecules*
4. Mark JE, Pan SJ (1982) *Makromol Chem, Rapid Commun* 3:681
5. Mark JE, Sullivan JL (1977) *J Chem Phys* 66:1006
6. Liorente MA, Andrady AL, Mark JE (1981) *J Polym Sci, Polym Phys Ed* 19:621
7. Ning YP, Tang MY, Jiang CY, Mark JE, Koth WC (1984) *J Appl Polym Sci* 29:000
8. Liorente MA, Andrady AL, Mark JE (1980) *J Polym Sci, Polym Phys Ed* 18:2263
9. Steger JR, Monsanto Company, private communication
10. Mark JE, Flory PJ (1966) *J Appl Phys* 37:4635
11. Treloar LRG (1975) *The Physics of Rubber Elasticity*, 3. Ed., Clarendon Press, Oxford
12. Mark JE (1975) *Rubber Chem Technol* 48:495
13. Mark JE (1970) *J Am Chem Soc* 92:7252

Received March 14, 1984;
accepted April 27, 1984

Authors' addresses:

M.-Y. Tang
Chenguang Institute of Chemical Industry
Sichuan, China

A. Letton
Department of Chemical Engineering
The University of Cincinnati
Cincinnati, OH 45221, USA

J. E. Mark
Department of Chemistry
The University of Cincinnati
Cincinnati, OH 45221, USA

Molecular Orbital Conformational Energy Calculations of the Aromatic Heterocyclic Poly(5,5'-Bibenzoxazole-2,2'-Diyl-1,4-Phenylene) and Poly(2,5-Benzoxazole)

W. J. WELSH

*Department of Chemistry and Polymer Research Center
University of Cincinnati
Cincinnati, Ohio 45221*

and

*Department of Chemistry
College of Mount St. Joseph
Mount St. Joseph, Ohio 45051*

and

J. E. MARK

*Department of Chemistry and Polymer Research Center
University of Cincinnati
Cincinnati, Ohio 45221*

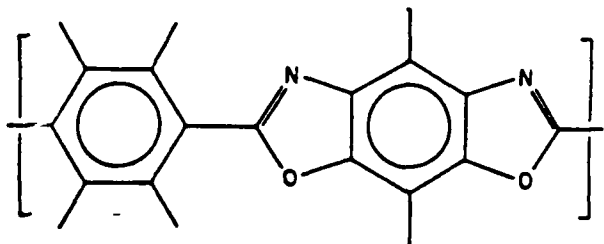
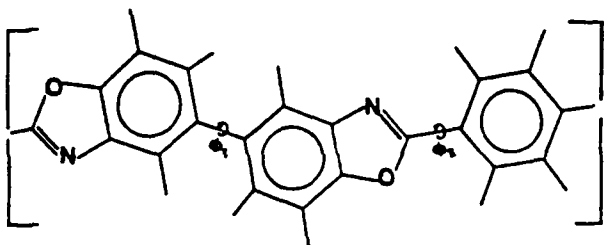
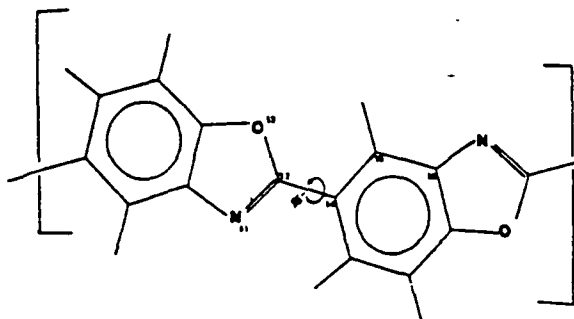
Interest in potential high-performance polymers, leading to characterization and development of the rodlike poly(*p*-phenylene benzobisoxazoles) (PBO) and poly(*p*-phenylene benzobisthiazoles) (PBT), has recently been extended to a related group of polymers referred to as AAPBO, ABPBO, AAPBT, and ABPBT. In this study, geometry-optimized CNDO/2 molecular orbital calculations have been carried out on AAPBO and ABPBO model compounds to determine conformational energies as a function of rotation about each type of rotatable bond within the repeat units. For AAPBO, which contains two types of rotatable bonds per repeat unit, the bond between the benzoxazole group and *p*-phenylene group prefers the coplanar conformation with a barrier to free rotation of 2.1 kcal mol⁻¹, while the bond between the benzoxazole groups prefers a conformation approximately 60 degrees away from coplanarity with a barrier to coplanarity and to free rotation of 3.6 kcal mol⁻¹. For ABPBO, which contains only the former type of rotatable bond per repeat unit, the coplanar conformations were preferred with a barrier to free rotation of 1.6 kcal mol⁻¹. These results are in excellent agreement with the results of both theoretical and experimental studies on the structurally analogous PBO. They are also consistent with the liquid crystalline behavior found for ABPBO but not for AAPBO.

INTRODUCTION

The rigid rodlike polymers poly(*p*-phenylene benzobisoxazole) (PBO) (Fig. 1) and poly(*p*-phenylene benzobisthiazole) (PBT) belong to a class of materials known as high-performance polymers since films and fibers processed from them exhibit exceptional strength and modulus, thermo-oxidative stability, and resistance to most common solvents (1). In fact, PBO and PBT have been the focus

of the U.S. Air Force's "Ordered Polymers" Program aimed at exploiting these characteristics for aerospace applications (1 to 3). More recently, interest has extended to a related group of polymers, poly(5,5'-bibenzoxazole-2,2'-diyl-1,4-phenylene) (AAPBO) and poly(2,5-benzoxazole) (2,5-ABPBO) and to analogues of each containing a sulfur in place of the oxygen atom (4). The repeat units are illustrated in Figs. 2 and 3, respectively.

Chains such as these should possess at least some

Fig. 1. Illustration of the *cis*-PBO repeat unit.Fig. 2. Illustration of the AAPBO chain segment indicating the rotations ϕ_1 and ϕ_2 about the two rotatable bonds.Fig. 3. Illustration of the 2,5-ABPBO chain segment indicating the rotation ϕ' about the one rotatable bond. Numeration of selected atoms is also indicated.

flexibility perpendicular to the axial direction as a result of rotations (indicated by ϕ_1 , ϕ_2 , and ϕ' in the sketches) about the single bonds joining the aromatic moieties. In the present study, geometry-optimized CNDO/2 (Complete Neglect of Differential Overlap) molecular orbital calculations (2, 3, 5 to 7) were carried out on AAPBO and 2,5-ABPBO chain segments to obtain conformational energies with respect to the rotations indicated in the sketches. Of particular interest was to determine the preferred conformations and to assess the extent of rotational flexibility about these bonds. The results can be compared with those obtained in similar studies of the PBO polymers (2, 3, 5).

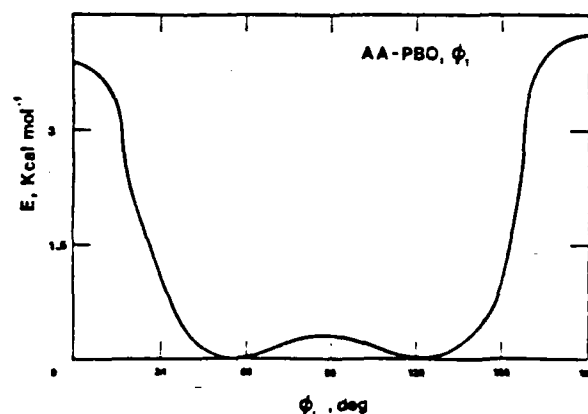
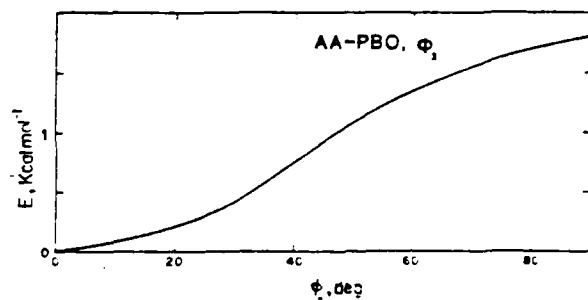
METHODOLOGY

The theory and methodology of the present calculations are discussed in detail elsewhere (2, 3, 5). Briefly, the technique involves an iterative scheme for achieving direct geometry optimization, wherein the total energy of the species is calculated using the CNDO/2 method (6, 7). In all cases, geometry optimization was obtained after assuming an initial structural geometry taken from the x-ray crystallographic studies of Fratini, et al., for the PBO model

compound (8) and setting the torsional angle ϕ between the planes of the two ring groups (with $\phi = 0^\circ$ taken as the coplanar form) at a specified, desired value. Calculations were usually carried out with ϕ varied in intervals of 20 degrees. Because of symmetry, scans were necessary only for the ranges $\phi = 0$ to 180 degrees, and 0 to 90 degrees. The conformational energy E associated with a given angle ϕ was taken as the difference in the CNDO/2 total energy between that conformation and the conformation of lowest energy.

RESULTS AND DISCUSSION

Conformational energies E as a function of ϕ_1 and ϕ_2 in AAPBO are plotted in Figs. 4 and 5, respectively. A broad energy minimum was found in the region $60^\circ < \phi_1 < 120^\circ$ (within the 0 to 180 degree conformational energy space). On either side of this minimum the energy rose sharply and continuously, giving two similar energy maxima of $E \approx 3.6$ kcal mol $^{-1}$ at 0 and 180 degrees. Thus the conformational energy profile obtained is nearly identical to that calculated for biphenyl in a similar analysis (5). This is reasonable since the two species are structurally similar in the vicinity of the rotatable bond. The highly repulsive energy associated with the coplanar conformations can be ascribed primarily to steric repulsions between *ortho*-hydrogens on adjacent ring systems. Specifically, at $\phi_1 = 0$ and 180 degrees these $H \cdots H$ interaction distances are 1.8 to 1.9 Å, which are considerably smaller than

Fig. 4. Plot of the conformational energy E as a function of rotation angle ϕ_1 in AAPBO.Fig. 5. Plot of the conformational energy E as a function of rotation angle ϕ_2 in AAPBO.

the sum (2.60 Å) of their van der Waals radii. As discussed elsewhere (3, 5), the preferences for non-coplanar conformations calculated for these moieties are consistent with the experimental findings for biphenyl in the gaseous state ($\phi_{\min} = 42$ degrees) (9) and in the liquid state ($\phi_{\min} = 23$ degrees) (10). The structural geometry of AAPBO in the vicinity of the other rotatable bond is nearly identical to that found in PBO model compounds, and the results of both the present calculations and of earlier calculations on PBO (3, 11) indicate a preference for the coplanar conformations with a maximum of $E = 2.1$ kcal mol⁻¹ at $\phi_2 = 90$ degrees. These results also agree with the coplanar conformations observed by x-ray crystallographic analysis for PBO model compounds in the crystalline state (8).

Values of E versus ϕ' in 2,5-ABPBO are plotted in Fig. 6. Conformational energy minima were found at $\phi = 0$ and 180 degrees (the coplanar forms) with a maximum energy $E = 1.6$ kcal mol⁻¹, located at $\phi' = 90$ degrees (the perpendicular form). Calculations carried out on the analogous 2,6-ABPBO gave nearly identical results. It should be noted that the absence of exact symmetry in energy profile about $\phi = 90$ degrees, most conspicuous in Fig. 6, is due to the lack of complete conformational symmetry for these species about $\phi = 90$ degrees, as inspection of Fig. 3 will confirm. Again, these results are in agreement with those obtained from theoretical studies of the structurally analogous PBO polymer model compounds (3). They are also consistent with the coplanarity or near-coplanarity observed for the PBO model compounds in the crystalline state (8).

As discussed in detail elsewhere (11), both the preference for the coplanar conformations and the shortness of the C—C rotatable bond (1.45 to 1.47 Å) (8, 11) in these species relative to that (1.53 Å) for a typical C—C single bond suggest a considerable degree of conjugation between adjacent ring systems in these chains. The variation in selected bond lengths and atomic partial charges with ϕ' found for 2,5-AAPBO, as indicated in Table I, corroborates this conclusion. Specifically, with rotation

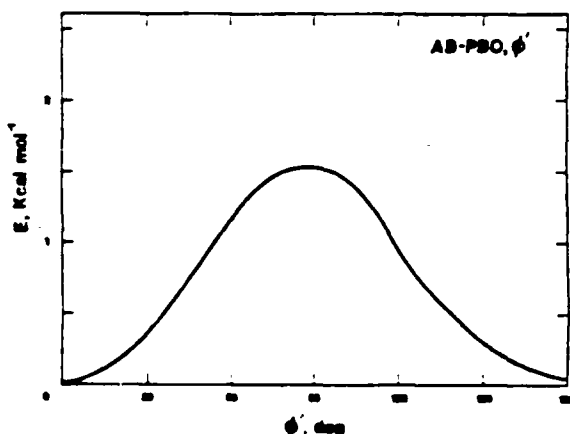


Fig. 6 Plot of the conformational energy E as a function of rotation angle ϕ in 2,5-ABPBO

Table I. Variation of Selected Bond Lengths^a and Partial Charges^b with Rotation ϕ' in 2,5-ABPBO. Numeration of Atoms is as Indicated in Fig. 3.

	0°	45°	90°
Bond Lengths^a			
C12-C14	1.4464	1.4485	1.4510
C15-C16	1.3843	1.3857	1.3868
N11-C12	1.3225	1.3212	1.3194
C12-O13	1.3727	1.3715	1.3706
Partial Charges^b			
N11	-0.309	-0.312	-0.317
O13	-0.293	-0.291	-0.289
C12	+0.342	+0.349	+0.358
C14	-0.027	-0.021	-0.013

^a In units of Angstroms.

^b In units of fraction of an electron's charge.

away from the coplanar conformation ($\phi' = 0$ degrees) the lengths of bonds C12-C14 and C15-C16 increase while those of bonds N11-C12 and C12-O13 decrease. These changes are exactly as would be predicted based on the reasonable assumption that conjugation between adjacent ring systems should be a maximum near $\phi' = 0$ degrees and a minimum near $\phi' = 90$ degrees. This loss in conjugation concomitant with rotation is further evidenced by the noted changes in the atomic partial charges, these changes the result of a shift in electron density from C12 and C14 (i.e., from the rotatable bond) to N11 within the ring system.

In summary, the present calculations indicate preferences for non-planar conformations in AAPBO and for planar conformations in 2,5-ABPBO. These conclusions are consistent with the liquid crystalline behavior observed for 2,5-ABPBO but not for AAPBO (4).

ACKNOWLEDGMENT

It is a pleasure to acknowledge the financial support provided by the Air Force Office of Scientific Research (Grant 83-0027, Chemical Structures Program, Division of Chemical Sciences).

REFERENCES

1. T. E. Helminiak, *Preprints of ACS Division of Organic Coatings and Plastics Chemistry*, 40, 475 (1979), a number of articles on PBO and PBT polymers are in the July/August, 1981, issue of *Macromolecules*.
2. W. J. Welsh and J. E. Mark, *Polym. Eng. Sci.*, 23, 37 (1983).
3. W. J. Welsh, D. Bhaumik, H. H. Jaffe, and J. E. Mark, *Polym. Eng. Sci.*, 24, 218 (1984).
4. J. F. Wolfe, private communications.
5. W. J. Welsh, H. H. Jaffe, J. E. Mark, and N. Kondo, *Die Makromolekulare Chemie*, 183, 801 (1982).
6. J. A. Pople and D. L. Beveridge, "Approximate Molecular Orbital Theory," McGraw-Hill, New York, New York (1970).
7. N. Kondo, Ph.D. Dissertation, University of Cincinnati (1978); H. H. Jaffe, CNDO/S and CNDO/2 (FORTRAN IV) QCPE 315 (1977).
8. M. W. Wellman, W. W. Adams, D. R. Wiff, and A. V. Fratini, Air Force Tech. Report AFML-TR-79-4184, Part I.
9. A. A. Menningen, O. Bastiansen, *Skr. K. Nor. Vidensk. Selsk.* No. 4 (1958).
10. H. Suzuki, *Bull. Chem. Soc., Jpn.*, 32, 1340 (1959).
11. W. J. Welsh and J. E. Mark, *J. Mater. Sci.*, 16, 1119 (1983).

Bimodal Networks and Networks Reinforced by the *in situ* Precipitation of Silica

-22-

James E. Mark

Department of Chemistry and the Polymer Research Center, The University of Cincinnati, Cincinnati, Ohio 45221, U.S.A.

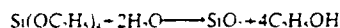
The goal of primary interest in these investigations was the development of novel methods for preparing elastomeric networks having unusually good ultimate properties. The first technique employed involves endlinking mixtures of very short and relatively long functionality-terminated chains to give bimodal networks. Such (unfilled) elastomers show very large increases in reduced stress or modulus at high elongations because of the very limited extensibility of the short chains present in the networks. The second technique employs the *in situ* precipitation of reinforcing silica either after, during, or before network formation. The reaction involves hydrolysis of tetraethyorthosilicate, using a variety of catalysts and precipitation conditions, and the effectiveness of the technique is gauged by stress-strain measurements carried out to yield values of the maximum extensibility, ultimate strength, and energy of rupture of the filled networks. Information on the filler particles thus introduced is obtained from density determinations, light scattering measurements, and electron microscopy.

Keywords
model network;
bimodal networks;
ultimate properties;
network reinforcement;
precipitated silica;
filler particle sizes

1 INTRODUCTION

Preparing an elastomer by endlinking polymer chains permits control of the network structure,^{1,2} in particular the network chain length distribution. One important result of this new synthetic versatility is the ability to form bimodal networks which consist of mixtures of very short and relatively long chains.³⁻¹⁰ Such bimodal elastomers have been prepared from polydimethylsiloxane (PDMS) [$-\text{Si}(\text{CH}_3)_2\text{O}-$] and found to have unusually good ultimate properties, even in the unfilled state, as is documented in the present review. A variety of experimental studies show that this improvement in properties is primarily due to the very limited extensibility of the short chains present in the networks.¹ This limited extensibility and its effects on elastomeric properties are being investigated using a non-Gaussian theory of rubber-like elasticity based on network distribution functions generated from Monte Carlo simulations utilising rotational isomeric state information on the chains of interest.¹¹⁻¹³

Silica may be prepared by the hydrolysis



of tetraethyorthosilicate (TEOS), in the presence of any of a variety of catalysts. There are three techniques by which silica thus precipitated can be used to reinforce an elastomeric material. First, an already-cured network, for example prepared from PDMS, may be swollen in TEOS and the TEOS hydrolysed *in situ*.¹⁴⁻¹⁵ Alternatively, hydroxyl-terminated PDMS may be mixed with TEOS, which then serves simultaneously to tetrafunctionally endlink the PDMS into a network structure and to act as a source of SiO_2 upon hydrolysis.¹⁶⁻²¹ Finally, TEOS mixed with vinyl-terminated PDMS can be hydrolysed to give a SiO_2 -filled polymer capable of subsequent endlinking by means of a multifunctional silane.²² Some mechanical properties of typical PDMS elastomers reinforced in these ways are described, as are results on the average size, size distribution, and extent of agglomeration of the filler particles.¹⁵

2 BIMODAL NETWORKS

2.1 Typical experimental results

In elongation measurements, the elastomeric quantity of prim-

ary interest is the reduced stress or modulus^{3,23}

$$[f^*] = f^*/(a - a^{-2}) \quad (1)$$

where $f^* = f/A^*$ is the nominal stress, f the equilibrium elastic force, A^* the undeformed cross-sectional area of the sample, and $a = L/L_0$ the relative length or elongation. It is generally plotted as a function of reciprocal elongation as suggested by the semi-empirical equation of Mooney and Rivlin:^{24,25}

$$[f^*] = 2C_1 + 2C_2 a^{-1} \quad (2)$$

where $2C_1$ and $2C_2$ are constants independent of elongation.

Some typical isotherms obtained for bimodal PDMS networks are shown in Fig. 1. Of particular interest here are the large, reversible increases in modulus observed at high elongations.

2.2 Origin of improvement in properties

The observed increases in modulus represent an important improvement in the ultimate strength of an elastomer, and their origin is therefore of considerable interest. A variety of experimental studies^{4,5,9,11} are relevant in this regard. The effect of temperature on the stress-strain isotherms is of particular importance with regard to the possibility of strain-induced crystallisation in the network. Temperatures were found to have little effect on the elongation at which the upturn in $[f^*]$ becomes discernible, the elongation at rupture, and the magnitude of the increase in $[f^*]$. These results thus indicate that the anomalous behaviour is not due to strain-induced crystallisation.

Also relevant here are force-temperature ('thermoelastic') results⁴ obtained at elongations sufficiently large to give large increases in $[f^*]$ in the stress-strain isotherm. Such curves show no deviations from linearity which could be attributed to strain-induced crystallisation. Similarly, birefringence-temperature measurements show no non-linearity that could be attributed to crystallisation, or to other intermolecular orderings of the network chains.

The most striking evidence involves the effect of swelling on the isotherms. Results on unfilled PDMS networks as is illustrated in Figs 2 and 3,⁹ show that swelling does not diminish the upturns in modulus and, in fact, frequently enhances them.

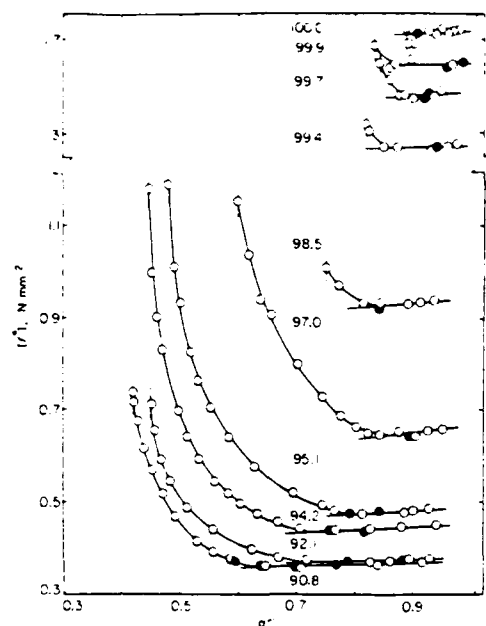


Fig. 1. Stress-strain isotherms (25°C) in the Mooney-Rivlin representation for (unfilled) PDMS bimodal networks in which the short chains have a number-average molecular weight of 660 g mol⁻¹, and the long chains 21.3 × 10⁴ g mol⁻¹. Each curve is labelled with the mol % of short chains present in the network. The open circles locate the results obtained using a series of increasing values of the elongation α , and filled circles the results obtained out of sequence to test for reversibility. The short extensions of the linear portions of the isotherms help locate the values of α at which the upturn in $[f']$ first becomes discernible. The linear portions of the isotherms were located by least-squares analysis. (Reprinted from ref. 6 by courtesy of John Wiley & Sons, Inc.)

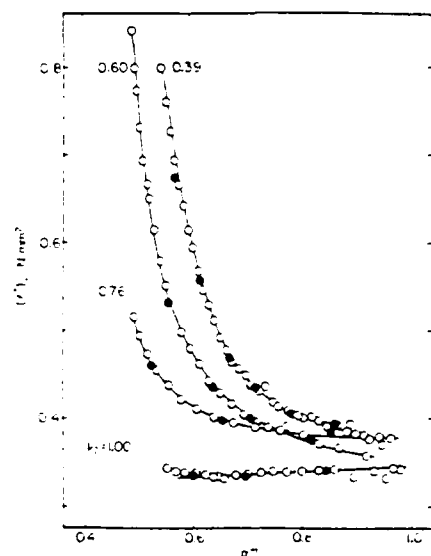


Fig. 2. The effect of swelling on isotherms (25°C) for unswollen and swollen (unfilled) PDMS bimodal networks (220, 18.5 × 10⁴ g mol⁻¹) containing 85 mol % of the short chains. Each curve is labelled with the volume fraction v_2 of polymer present in the network; the diluent was a linear DMS oligomer having 8-11 repeat units. (Reprinted from ref. 9 by courtesy of the American Chemical Society.)

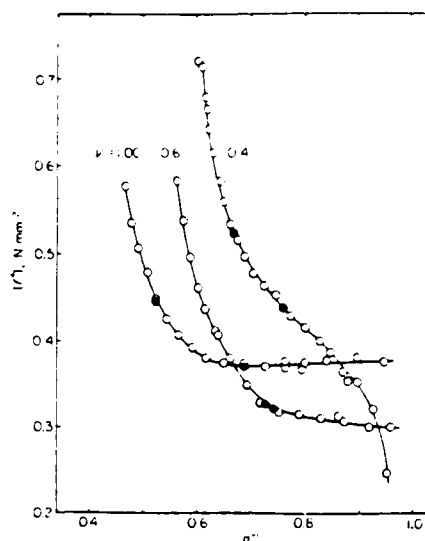


Fig. 3. The effect of swelling on isotherms for (unfilled) PDMS bimodal networks containing 90 mol % of the short chains; see legend to Fig. 2. (Reprinted from ref. 9 by courtesy of the American Chemical Society.)

Similar results are obtained for filled PDMS networks, as is shown by the results presented in Fig. 4.¹⁰

All of the above experimental results indicate that the increases in $[f']$ are due to an intramolecular effect, specifically to the limited extensibility of the very short network chains.^{3, 11-13, 20}

2.3 Theoretical interpretation

Since the above results demonstrate that the upturns in modulus are due to limited chain extensibility, it becomes

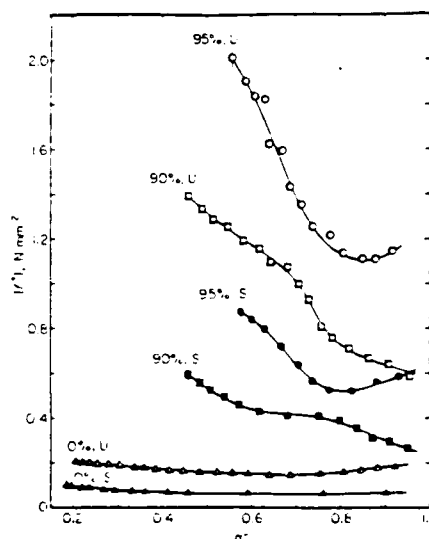


Fig. 4. The effect of swelling on isotherms for fume silica-filled bimodal networks of PDMS (860, 21.3 × 10⁴ g mol⁻¹) in the unswollen (U) state and swollen (S) with *n*-hexadecane to $v_2 = 0.3$. The numbers specify the mol % of short chains present in the network. Fume(d) silica refers to a commercial grade precipitated from the vapour phase. (Reprinted from ref. 10 by courtesy of John Wiley & Sons, Inc.)

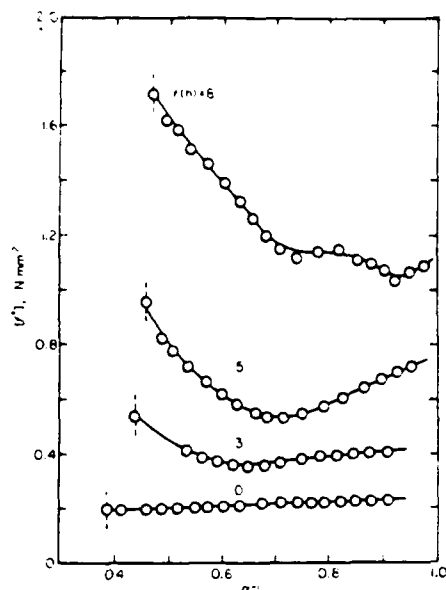


Fig. 5 Isotherms for a (unimodal unswollen) PDMS elastomer (8.6×10^3 g mol $^{-1}$) which was silica-reinforced by hydrolysis of tetraethylorthosilicate (TEOS) present as diluent in the network.¹⁷ The reaction was carried out at 53% relative humidity, and each curve is labelled with the reaction time. (Reprinted from ref. 17 by courtesy of Dr. Dietrich Steinkopff Verlag.)

important to interpret them in terms of a non-Gaussian theory of rubber-like elasticity. A recent novel approach¹¹⁻¹³ to this problem utilises the wealth of information which rotational isomeric state theory²² provides on the spatial configurations of chain molecules. Specifically, Monte Carlo calculations based on the rotational isomeric state approximation are used to simulate spatial configurations, and thus distribution functions for the end-to-end separation of the chains.²³ These distribution functions are used in place of the Gaussian function in the standard three-chain network model¹⁴ in the affine limit to give a molecular theory of rubber-like elasticity which is very useful for the interpretation of elastomeric properties at high elongations.

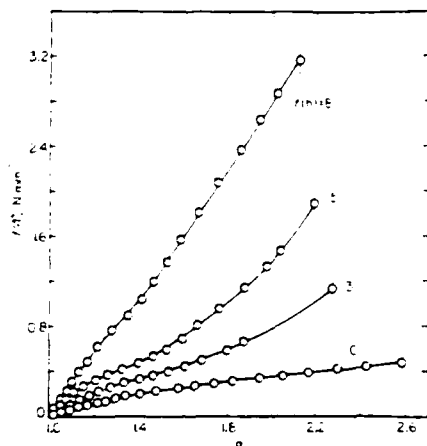


Fig. 6 The nominal stress shown as a function of elongation for the same networks characterised in Fig. 5.¹⁷ In this representation, the area under each curve represents the energy E_r required for network rupture. (Reprinted from ref. 17 by courtesy of Dr. Dietrich Steinkopff Verlag.)

3 NETWORKS REINFORCED BY *IN SITU* PRECIPITATION OF SILICA

3.1 After crosslinking

Figures 5 and 6 show typical elongation isotherms obtained for PDMS networks reinforced by swelling with TEOS, which was subsequently hydrolysed *in situ* to give silica filler particles.¹⁷ Increase in reaction time is seen to increase the amount of filler precipitated, as evidenced by increases in moduli, in upturns in moduli, and in toughness.

3.2 During crosslinking

It would of course be advantageous if the *in situ* precipitation could be carried out simultaneously with the curing reaction. Filled PDMS networks have in fact been prepared in this way, using hydroxyl-terminated chains and sufficient TEOS for both the endlinking process and the hydrolysis reaction to form the filler. Isotherms obtained for some of these networks are shown in Fig. 7.²⁰ Again, very good reinforcement is seen to occur.

In the experiments cited,²⁰ the ratio r of TEOS ethoxy groups to PDMS hydroxyl end groups, a measure of the excess TEOS available for hydrolysis, ranged from 1.0 to 15.0. The effect of this variable on the weight % filler precipitated is shown in Fig. 8.²⁰ Estimates obtained from the densities of polymer, silica, and filled network are seen to be smaller than those obtained directly from the increase in weight of the network. This indicates that either the filler particles have not been completely converted to silica or the particles contain a significant number

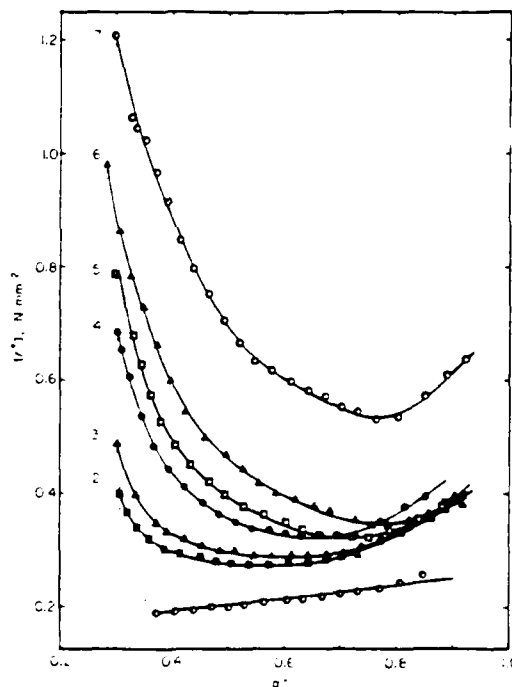


Fig. 7 Isotherms for PDMS networks prepared using TEOS to simultaneously endlink hydroxyl-terminated chains (21.3×10^3 g mol $^{-1}$) and to provide filler upon its hydrolysis.²⁰ For samples 1-6, the filler thus incorporated amounted to 0.0, 2.28, 4.56, 6.75, 8.83, 10.8 and 14.6 wt %, respectively. Additional information on these samples is given in Figs 8 and 9. (Reprinted from ref. 20 by courtesy of the American Chemical Society.)

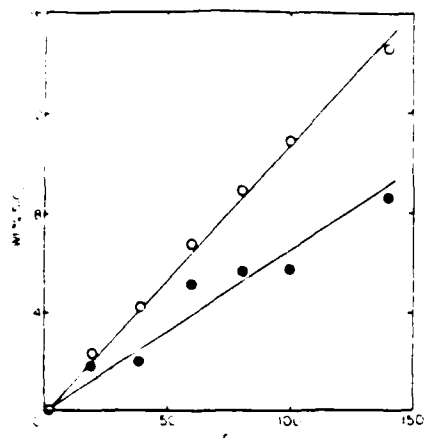


Fig. 8. The wt % filler precipitated within the PDMS networks shown as a function of the feed ratio $r = [\text{OC}_2\text{H}_5] / [\text{OH}]$, where the $-\text{OC}_2\text{H}_5$ groups are on the TEOS and the $-\text{OH}$ groups are on the ends of the polymer.²⁰ The open circles show the results obtained from the change in weight of the polymer and the filled circles from the density of the filled network. See legend to Fig. 7. (Reprinted from ref. 20 by courtesy of the American Chemical Society.)

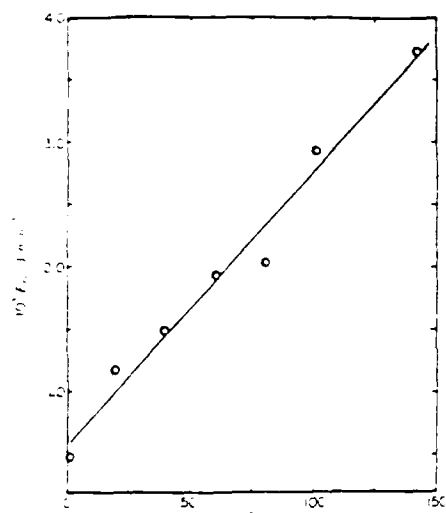


Fig. 9. The effect of the feed ratio on the energy required for network rupture.²⁰ See legend to Fig. 7. (Reprinted from ref. 20 by courtesy of the American Chemical Society.)

of voids.²⁰ In any case, increase in r increases the amount of filler introduced and, as shown in Fig. 9,²⁰ increases elastomer toughness (as measured by the energy E_r required for rupture).

3.3 Before crosslinking

In the above 'in situ' techniques, removal of the byproduct $\text{C}_2\text{H}_5\text{OH}$ and unreacted TEOS causes a significant decrease in volume, which could be disadvantageous in some applications. For this reason a technique was developed for the precipitation of the silica into samples of PDMS to give stable polymer-filler suspensions which remained capable of being endlinked, subsequently, with no substantial changes in volume.

In brief, TEOS was added to vinyl-terminated PDMS and then hydrolysed to give polymer-filler suspensions which showed no signs of particle agglomeration or settling. After drying, the viscous liquids could be endlinked with a multifunctional silane to give filled elastomers with very good mechanical properties.

3.4 Characterisation of the filler particles

Transmission electron microscopy¹¹ and light scattering measurements¹² are being used to study the filler particles. As illustration, an electron micrograph for a PDMS elastomer in which TEOS had been hydrolysed is shown in Fig. 10.¹¹ The existence of filler particles in the network, originally hypothesised on the basis of mechanical properties,¹³ is clearly confirmed. The particles have average diameters of approximately 250 Å, which is in the range of particle sizes of fillers typically introduced into polymers in the usual blending techniques. The distribution of sizes is relatively narrow, with most values of the diameter falling in the range 200–300 Å.¹¹



Fig. 10. Transmission electron micrograph at a magnification of 118800 \times for an *in situ* filled PDMS network containing 34.4 wt % filler.¹¹ The length of the bar corresponds to 1000 Å. (Reprinted from ref. 22 by courtesy of John Wiley & Sons, Inc.)

Most strikingly, there is virtually none of the aggregation of particles essentially invariably present in the usual types of filled elastomers. Therefore, these materials should be extremely useful in characterising the effects of aggregation, and could be of considerable practical importance as well.¹¹

4 ACKNOWLEDGEMENTS

It is a pleasure to acknowledge the financial support provided by the National Science Foundation through Grant DMR 74-18403-03 (Polymers Program, Division of Materials Research) and by the Air Force Office of Scientific Research through Grant AFOSR 83-0027 (Chemical Structures Program, Division of Chemical Sciences).

References

1. Mark, J. E., *Makromol. Chem.* 1979, Suppl. 2, 87.
2. Mark, J. E., *Rubber Chem. Technol.*, 1981, 54, 809.
3. Mark, J. E., *Adv. Polym. Sci.*, 1982, 44, 1.
4. Mark, J. E., in *Elastomers and Rubber: Elasticity*, Eds. Mark, J. E. & Lal, J., 1982, Washington: American Chemical Society.
5. Zhang, Z.-M. & Mark, J. E., *J. Polym. Sci., Polym. Phys. Ed.* 1982, 20, 473.
6. Mark, J. E. & Tang, M.-Y., *J. Polym. Sci., Polym. Phys. Ed.* 1984, 22, 1849.

7. Tang, M.-Y. & Mark, J.E. *Macromolecules*, 1984, 17, 2616.
8. Tang, M.-Y., Garrido, L. & Mark, J.E. *Polymer*, 1984, 25, 347.
9. Mark, J.E. *Macromolecules*, 1984, 17, 2924.
10. Jiang, C.-Y., Mark, J.E. & Stebilton, L. *J. Appl. Polym. Sci.*, 1984, 29, 4411.
11. Mark, J.E. & Curcio, J.G. *J. Chem. Phys.*, 1983, 79, 5705.
12. Curcio, J.G. & Mark, J.E. *J. Chem. Phys.*, 1984, 80, 4521.
13. Mark, J.E. & Curcio, J.G. *J. Chem. Phys.*, 1984, 80, 5262.
14. Mark, J.E. & Pan, S.-J. *Makromol. Chem. Rapid Comm.*, 1982, 3, 681.
15. Ning, Y.-P., Tang, M.-Y., Jiang, C.-Y., Mark, J.E. & Roth, W.C., *J. Appl. Polym. Sci.*, 1984, 29, 3209.
16. Jiang, C.-Y. & Mark, J.E. *Makromol. Chem.*, 1984, 185, 2609.
17. Jiang, C.-Y. & Mark, J.E. *Colloid Polym. Sci.*, 1984, 262, 758.
18. Ning, Y.-P. & Mark, J.E. *Polym. Eng. Sci.*, in press.
19. Tang, M.-Y. & Mark, J.E. *Polym. Eng. Sci.*, 1985, 25, 29.
20. Mark, J.E., Jiang, C.-Y. & Tang, M.-Y. *Macromolecules*, 1984, 17, 2613.
21. Tang, M.-Y., Letton, A. & Mark, J.E. *Colloid Polym. Sci.*, 1984, 262, 990.
22. Ning, Y.-P. & Mark, J.E. *J. Appl. Polym. Sci.*, in press.
23. Mark, J.E. & Flory, P.J. *J. Appl. Phys.*, 1969, 37, 4635.
24. Treloar, L.R.G. *The Physics of Rubber Elasticity*, 1975. Oxford: Clarendon Press.
25. Mark, J.E. *Rubber Chem. Technol.*, 1975, 48, 495.
26. Mark, J.E. *Polym. J.*, 1985, 17, 265.
27. Flory, P.J. *Statistical Mechanics of Chain Molecules*, 1969. New York: Interscience.
28. Conrad, J.C. & Flory, P.J. *Macromolecules*, 1976, 9, 41.
29. Right, Z., private communication.
30. Schaefer, D.W., Ning, Y.-P. & Mark, J.E., unpublished results.

Effects of a Magnetic Field Applied during the Curing of a Polymer Loaded with Magnetic Filler

INTRODUCTION

The effects of finely divided fillers on the properties of a crosslinked elastomer have been studied *in extenso* from many points of view. Of particular interest, of course, is the marked improvement in mechanical properties frequently provided by certain fillers. In such filled systems, anisotropy of mechanical properties can arise if the filler particles or their agglomerates are asymmetric, since they are then oriented as a result of the flow of the uncrosslinked mix during the mechanical operations of forming (calendering, extrusion, drawing, or molding). In fact, fibrous fillers are often used for the express purpose of introducing mechanical anisotropy.

Rigbi and Jilken¹ studied the effects of a magnetic field on the behavior of rubber filled with a ferrite powder and cured in the field-free state. Since the ferrite was randomly distributed within the matrix, no directional effects were observed, nor were they expected. Goldberg, Hansford, and van Heerden² observed linear polarization of transmitted light by an aqueous ferrofluid* between two microscope slides, and showed that the particles of ferrite in the ferrofluid (frozen while in a magnetic field) were aligned in necklacelike formations, as predicted by de Gennes and Pincus.³

This preliminary report describes a first attempt at obtaining alignment of essentially spherical filler particles, to give anisotropy of mechanical properties similar to that obtained in the case of fibrous fillers.

EXPERIMENTAL

The filler employed was an extremely fine commercial magnetic powder (MG-410 Magnaglo, probably a magnesium ferrite with very little residual magnetism, produced by the Magnaflux Corp., Chicago). The particles are very nearly spherical, with an average diameter of approximately 10 μm . In a preliminary experiment, this magnetic filler was mixed into a low-viscosity polydimethylsiloxane (PDMS) having a number-average molecular weight of $10^{-3}M_n = 13.0 \text{ g mol}^{-1}$, and the mixture was poured into an aluminum mold placed between the poles of a permanent Alnico magnet having a field strength of about 580 G. The particles readily migrated toward the poles of the magnet. This demonstrated that the field would be capable of orienting the particles in a higher-molecular-weight polymer of sufficiently high viscosity to restrict migration of the particles during the crosslinking procedure. Such a polymer, having a molecular weight of $10^{-3}M_n = 266 \text{ g mol}^{-1}$, was generously provided by Dr. C. L. Lee of the Dow-Corning Corporation. A solution of the polymer in ethyl acetate was prepared, and the MG-410 powder was well mixed into it with a suitable amount (1.3 wt %) of benzoyl peroxide. The solution was poured into shallow trays, allowed to dry in air, and then finally subjected to vacuum for 4 h to eliminate any traces of solvent. The mastic obtained was cured in an aluminum mold in a press at 140°C for 20 min, and then at 180°C for another hour, all the time in the magnetic field supplied by the permanent magnet described. No postcuring treatment was given. The final product contained about 31.5% by weight of magnetic filler, calculated on the basis of the solid components of the solutions. This corresponds to roughly 6% by volume. The cured sheet was allowed to rest for 7 days, after which rectangular strips were cut out parallel and perpendicular to the vector of the magnetic field. Some of these were used in equilibrium swelling studies, and others in elongation measurements.

In the swelling test,⁴ benzene was used as the solvent, at room temperature, and the increases in sample length as well as in weight were recorded.

* Stable suspension of magnetic powder in a liquid carrier. Such materials are produced, for example, by Ferrofluidics Corp., Nashua, NH.

TABLE I
Swelling Equilibrium and Stress-Strain Results

Strip length relative to magnetic field	Swelling equilibrium ^a		Elongation moduli ^b (N mm ⁻²)	
	W/W _i	L/L _i	[f] ($\alpha = 1.1$)	[f] _{max}
Parallel	2.58	1.35	0.61	0.98
Perpendicular	2.44	1.25	0.15	0.28

^a Relative increases in weight and length of strips.

^b Values of the reduced stress at an elongation of 10% and at the maximum.

Stress-strain curves were obtained at 26°C using techniques described elsewhere.⁴⁻⁶ The strips had a cross-sectional area A^* of about 8 mm² and a gauge length of about 14 mm, with about 22 mm between the grips. Samples were held in the grips between two thin rubber sheets to minimize slippage. Preliminary investigation showed that considerable relaxation was to be expected under tension. It was therefore decided to extend the strips in steps, each within 15 s of the previous step, and to read the force two minutes later. In this way, the data obtained for the two specimens would be directly comparable.

RESULTS AND DISCUSSION

The results of the swelling tests are presented in columns 2 and 3 of Table I. The overall degree of swelling is given by the relative increase in weight W/W_i . Within experimental error, it is the same for the two samples, as would be expected. The relative increase in length

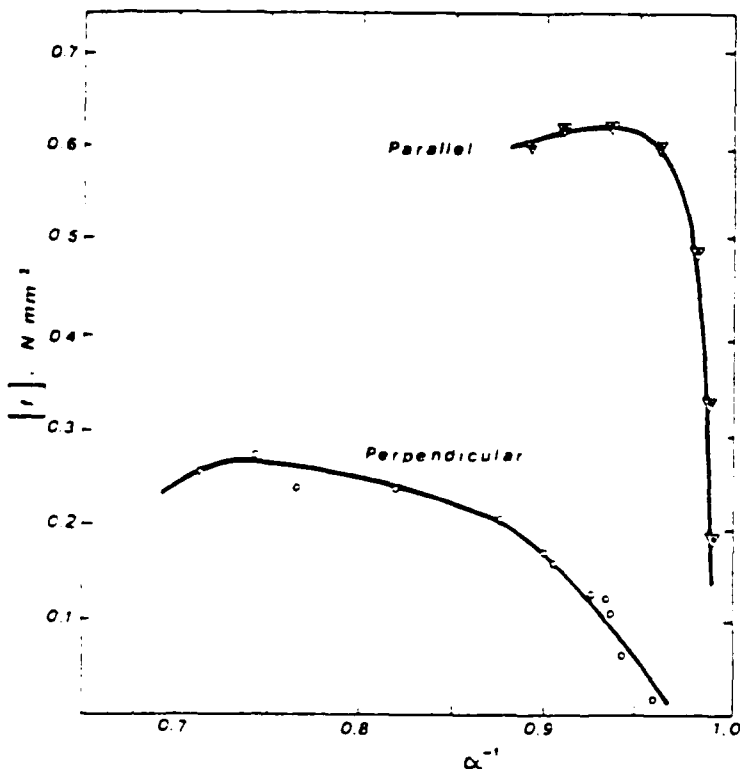


Fig. 1. Reduced stress shown as a function of reciprocal elongation for filled elastomeric strips cut parallel and perpendicular to the magnetic field imposed during curing.

L/L_i seems to be small, presumably case, if it is real, the smaller projection in that direction.

The stress-strain where f is the relative length of 1. The isotherms invariably have a results obtained the usual behavior and its maximum. They show the magnetic field. F exceeds the corre-

The results an elastomeric material interesting because

It is a pleasure National Science of Materials Research AFOSR 83-0027

1. Z. Rigbi and
2. P. Goldberg
3. P. G. de Ge
4. J. E. Mark
5. M. A. Llorer
6. M. A. Llorer
- (1980).
7. B. B. Boonst
8. J. E. Mark
9. L. R. G. Tre
10. J. E. Mark

Department of Ch
The University of
Cincinnati, Ohio

Received June 26
Accepted January

* On leave from

L/L_0 seems to be larger for the strip cut parallel to the magnetic field, but the difference is small, presumably because of solvent-induced debonding at the filler/matrix interface.⁷ In any case, if it is real, the larger increase in length for the parallel-cut strip could be explained by the smaller projected area of the filler particles in relation to the projected area of matrix in that direction.

The stress-strain data were treated in terms of the reduced stress⁸ $[f] \equiv f/A^*(\alpha - \alpha^{-2})$, where f is the elastic force, A^* is the undeformed cross-sectional area, and $\alpha = L/L_0$ is the relative length or elongation. Values are shown as a function of reciprocal elongation in Figure 1. The isotherms are seen to be very different from those usually obtained, which almost invariably have a constant, positive slope in the region of low to moderate elongation.^{9,10} The results obtained from the present samples thus represent very interesting departures from the usual behavior of elastomers, filled or unfilled.¹⁰ Values of the reduced stress at $\alpha = 1.10$ and its maximum value for the two samples are given in the last two columns of Table I. They show the highly anisotropic nature of the reinforcement obtained in the presence of the magnetic field. For example, the maximum value of $[f]$ for the strip cut parallel to the field exceeds the corresponding value for the perpendicular strip by a factor of more than 2!

The results achieved show that even spherical filler particles can be aligned within an elastomeric material, with reinforcement that is important because of its magnitude and interesting because of its anisotropy.

It is a pleasure to acknowledge the financial support provided to one of us (J. E. M.) by the National Science Foundation through Grant No. DMR 79-18903-03 (Polymer Program, Division of Materials Research), and by the Air Force Office of Scientific Research through Grant No. AFOSR 83-0027 (Chemical Structures Program, Division of Chemical Sciences).

References

1. Z. Rigbi and L. Jilken, *J. Magn. Magn. Mater.*, **37**, 267 (1983).
2. P. Goldberg, J. Hansford, and P. J. van Heerden, *J. Appl. Phys.*, **42**, 3874 (1971).
3. P. G. de Gennes and P. A. Pincus, *Phys. Kondens. Mater.*, **11**, 189 (1970).
4. J. E. Mark and J. L. Sullivan, *J. Chem. Phys.*, **66**, 1006 (1977).
5. M. A. Llorente and J. E. Mark, *J. Chem. Phys.*, **71**, 682 (1979).
6. M. A. Llorente, A. L. Andraday, and J. E. Mark, *J. Polym. Sci. Polym. Phys. Ed.*, **18**, 2263 (1980).
7. B. B. Boonstra and G. L. Taylor, *Rubber Chem. Technol.*, **38**, 799 (1952).
8. J. E. Mark and P. J. Flory, *J. Appl. Phys.*, **37**, 4635 (1966).
9. L. R. G. Treloar, *The Physics of Rubber Elasticity*, 3rd ed., Clarendon, Oxford, 1975.
10. J. E. Mark, *Rubber Chem. Technol.*, **48**, 495 (1975).

Z. RIGBI*
J. E. MARK

Department of Chemistry and the Polymer Research Center
The University of Cincinnati
Cincinnati, Ohio 45221

Received June 26, 1984
Accepted January 14, 1985

* On leave from the Technion-Israel Institute of Technology, Haifa, Israel.

Reinforcing Fillers

Hydrolysis of Several Ethylethoxysilanes to Yield Deformable Filler Particles

Y.-P. Ning, Z. Rigbi*, and J.E. Mark

Department of Chemistry and the Polymer Research Center, The University of Cincinnati, Cincinnati, Ohio 45221, USA

Summary

A technique is devised for incorporating organic groups in filler particles, thus giving them some deformability. Hoped-for increases in toughness were not obtained, presumably because of replacement of some surface silanol groups by less reactive organic groups, thus decreasing filler-matrix bonding and elastomer reinforcement.

Introduction

A series of recent experimental investigations (1-9) has focused on the hydrolysis of tetraethoxysilane (TEOS) $[\text{Si}(\text{OC}_2\text{H}_5)_4]$ to give filler particles capable of reinforcing elastomeric networks. The reactions are typically carried out within a TEOS-swollen network of poly(dimethylsiloxane) (PDMS) and yield essentially unagglomerated particles with diameters of 150-250 Å (7). The reinforcing effects of these fillers have been clearly demonstrated by measurements of stress-strain isotherms in elongation (1-5,8,9), and by falling-dart impact tests (6).

It is conceivable that the reinforcing effect could be enhanced if the filler particles could be given some degree of deformability or toughness. This could be accomplished by the retention of organic groups in the particles, for example by including some silanes of the type $(\text{C}_2\text{H}_5)_x\text{Si}(\text{OC}_2\text{H}_5)_{4-x}$ in the hydrolysis reaction. Of primary interest would be hydrolysis of mixtures of TEOS with silanes of lower functionality ($x = 3$ and 2). It would be hoped that the effects of the particle deformability thus obtained would predominate over the effects of the diminished filler-PDMS bonding caused by the decreased number of silanol groups on the particle surfaces.

The present study addresses these questions, using the hydrolysis of TEOS, $\text{C}_2\text{H}_5\text{Si}(\text{OC}_2\text{H}_5)_3$, $(\text{C}_2\text{H}_5)_2\text{Si}(\text{OC}_2\text{H}_5)_2$, and mixtures thereof. Measurements of the elongation moduli and ultimate properties of the PDMS networks filled in this way are used to evaluate the effectiveness of the reinforcement obtained.

Some Experimental Details

The network was prepared from vinyl-terminated poly(dimethylsiloxane) (PDMS) chains obtained from the McGhan NuSil Corporation; they had a

* On leave from the Technion-Israel Institute of Technology

number-average molecular weight corresponding to $10^{-4} M = 13.0 \text{ g mol}^{-1}$. The chains were tetrafunctionally end linked with $\text{Si}(\text{OC}_2\text{H}_5)_4$ in the usual manner (10), and the resulting network extracted with tetrahydrofuran and then toluene for a total of six days to remove soluble material (found to be present to the extent of 5.2 wt %). Strips cut from the network sheet were then dried, and one was set aside as a reference material (0 wt % filler).

The three ethoxysilanes investigated were obtained from the Fisher Scientific Company. They are listed in the first two columns of Table I.

Table I
Reaction Conditions and Amount of Filler Precipitated

Reaction Conditions				
Silane A	Silane B	Wt A/Wt B	Reaction time, hrs.	Wt % filler
--	--	--	0.0	0.0
$\text{Si}(\text{OC}_2\text{H}_5)_4$	--	100/0	0.6 1.0 4.9	7.7 11.6 36.4 53.0
$\text{C}_2\text{H}_5\text{Si}(\text{OC}_2\text{H}_5)_3$	--	100/0	8.0 17.0	2.5 4.8
$(\text{C}_2\text{H}_5)_2\text{Si}(\text{OC}_2\text{H}_5)_2$	--	100/0	5.0 8.0 17.0	2.7 5.2 8.6
$\text{Si}(\text{OC}_2\text{H}_5)_4$	$\text{C}_2\text{H}_5\text{Si}(\text{OC}_2\text{H}_5)_3$	90/10	1.5 5.0 8.0 7.0 22.5	15.3 43.7 46.6 38.1
$\text{Si}(\text{OC}_2\text{H}_5)_4$	$(\text{C}_2\text{H}_5)_2\text{Si}(\text{OC}_2\text{H}_5)_2$	70/30	1.5 5.0 7.0 22.5	10.5 35.4 39.3 29.3
$\text{Si}(\text{OC}_2\text{H}_5)_4$	$(\text{C}_2\text{H}_5)_2\text{Si}(\text{OC}_2\text{H}_5)_2$	90/10	1.5 5.0 7.0 22.5	14.8 48.4 48.0 37.0
$\text{Si}(\text{OC}_2\text{H}_5)_4$	$(\text{C}_2\text{H}_5)_2\text{Si}(\text{OC}_2\text{H}_5)_2$	70/30	1.5 5.0 7.0 22.5	10.3 37.2 41.1 30.5

and the compositions employed are given in the following column. The network strips to be filled were swollen with the specified ethoxysilane to the maximum extent attainable, which corresponded to a volume fraction of polymer of 0.21 - 0.23. The swollen strips were then placed into a 2.0 wt % aqueous solution of ethylamine. The hydrolysis of the ethoxysilane was permitted to occur at room temperature for the periods of time specified in the fourth column of Table I. Values of the wt % filler incorporated, obtained from the weights of the dried strips, are given in the final column.

Portions of each of the networks were used in elongation experiments to obtain the stress-strain isotherms at 25°C (11-14). The elastomeric properties of primary interest were the nominal stress $f \equiv F/A^*$ (where f is the equilibrium elastic force and A^* the undeformed cross-sectional area), and the reduced stress or modulus $(f') \equiv f'/(\alpha - \alpha^2)$ (where $\alpha = l/l_1$ is the elongation or relative length of the strips). All stress-strain measurements were carried out to the rupture points of the samples, and were generally repeated in pairs to test for reproducibility.

Results and Discussion

Figure 1 shows the amount of filler precipitated as a function of

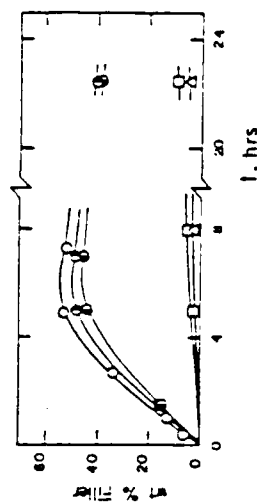


Figure 1. Time dependence of the wt % filler precipitated by the hydrolysis of $\text{Si}(\text{OC}_2\text{H}_5)_4$ (Δ), $\text{C}_2\text{H}_5\text{Si}(\text{OC}_2\text{H}_5)_3$ (\circ), $\text{Si}(\text{OC}_2\text{H}_5)_4/\text{C}_2\text{H}_5\text{Si}(\text{OC}_2\text{H}_5)_3$ (■), weight ratio 90/10 of $\text{Si}(\text{OC}_2\text{H}_5)_4/\text{C}_2\text{H}_5\text{Si}(\text{OC}_2\text{H}_5)_3$ (\square), and weight ratio 90/10 of $\text{Si}(\text{OC}_2\text{H}_5)_4/(\text{C}_2\text{H}_5)_2\text{Si}(\text{OC}_2\text{H}_5)_2$ (\square).

time for the five systems investigated. The rate of hydrolysis is seen to be largest for the TEOS. The curves for both the TEOS and its mixtures go through a maximum, the origin of which is probably loss of colloidal silica. The rates of hydrolysis of the pure $\text{C}_2\text{H}_5\text{Si}(\text{OC}_2\text{H}_5)_3$ and $(\text{C}_2\text{H}_5)_2\text{Si}(\text{OC}_2\text{H}_5)_2$ are seen to be very small.

This was confirmed in separate tests in which the hydrolysis of the pure silanes was observed using acetone as a solvent in the silanes

and the ethylamine solution. Whereas the product of hydrolysis of the TEOS was a particulate silica, the hydrolysis of $C_2H_5Si(OC_2H_5)_3$ resulted in a mixture of a viscous liquid and a waxy solid.²⁵ The product of the hydrolysis of $(C_2H_5)_2Si(OC_2H_5)_2$ was a liquid. These cannot, of course, be considered to be particulate fillers in themselves, and their primary role is to add deformability when used in mixtures with TEOS.

Some typical stress-strain isotherms obtained as described above are presented in Figure 2. The data are shown in the usual way (15-17), as the dependence of the reduced stress on reciprocal elongation. As is frequently the case for filled elastomers (18-20), some of the isotherms did not exhibit complete reversibility. Figure 3 shows the data of Figure 2 plotted in such a way that the area under each stress-strain curve corresponds to the energy E_r of rupture (12), which is the standard measure of elastomer toughness. Its values, along with values of the

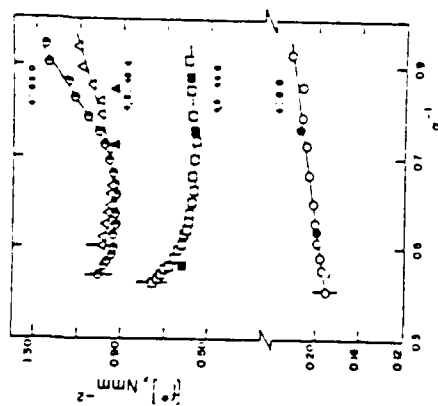


Figure 2. The reduced stress as a function of reciprocal elongation for several filled PDMS networks at 25°C. Each curve is labelled with the number of ethoxy groups in the silane or silane mixture being hydrolyzed, followed by the wt % filler thereby precipitated into the PDMS network. Filled symbols are for results obtained out of sequence to test for reversibility, and the vertical dashed lines locate the rupture points.

maximum extensibility α_r and ultimate strength f^* are given in the last three columns of Table II. Reference to the values of the extensibility

Table II

Ultimate Properties of the Filled Networks

Filler Characteristics			Ultimate Properties		
Silane A	Silane B	Wt A/Wt B	$\frac{f^*}{f_r}$	$\frac{b}{10^3}$	$\frac{E}{10^3}$
--	--	--	2.48	0.422	0.394
$Si(OC_2H_5)_4$	--	100/0	--	--	--
$C_2H_5Si(OC_2H_5)_3$	--	100/0	--	--	--
$(C_2H_5)_2Si(OC_2H_5)_2$	--	100/0	2.37	2.09	1.55
$Si(OC_2H_5)_4$	$C_2H_5Si(OC_2H_5)_3$	90/10	1.89	0.565	0.288
$Si(OC_2H_5)_4$	$(C_2H_5)_2Si(OC_2H_5)_2$	70/30	1.87	0.525	0.258
$Si(OC_2H_5)_4$	$(C_2H_5)_2Si(OC_2H_5)_2$	90/10	2.26	0.831	0.571
$Si(OC_2H_5)_4$	$(C_2H_5)_2Si(OC_2H_5)_2$	70/30	2.37	0.776	0.539
$Si(OC_2H_5)_4$	$(C_2H_5)_2Si(OC_2H_5)_2$	90/10	1.85	1.16	0.541
$Si(OC_2H_5)_4$	$(C_2H_5)_2Si(OC_2H_5)_2$	70/30	1.85	1.16	0.541

^a Elongation at rupture.

^b Ultimate strength, as represented by the nominal stress at rupture.

^c Energy required for rupture.

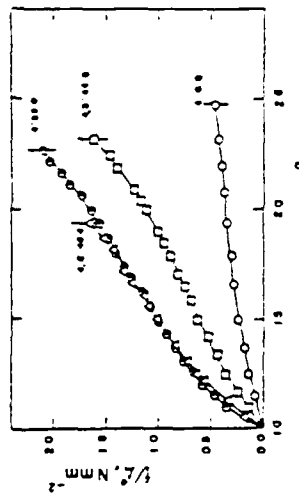


Figure 3. The nominal stress as a function of elongation for the same networks characterized in Figure 2. The area under the curves corresponds to the energy required for network rupture.

indicates that the products of the hydrolysis of the pure lower allenes act more as plasticizers for the network polymer than as reinforcing fillers.

The TEOS hydrolysis is seen to give the strongest reinforcement, with the other two pure ethoxysilanes being essentially ineffective in this regard. In the case of the particles formed from the silane mixtures, the loss of silanol groups on the filler surfaces is presumably the origin of the decreased reinforcement. The concept of creating deformable filler particles giving improved reinforcement, however, does seem to have merit and other approaches to achieve this goal will be attempted.

Acknowledgements

It is a pleasure to acknowledge the financial support provided by the National Science Foundation through Grant DMR 79-18903-03 (Polymers Program, Division of Materials Research) and by the Air Force Office of Scientific Research through Grant AFOSR 83-0027 (Chemical Structures Program, Division of Chemical Sciences).

References

1. J. E. Mark and S.-J. Pan, Makromol. Chem., Rapid Commun., **3**, 681 (1982).
2. C.-Y. Jiang and J. E. Mark, Makromol. Chem., **185**, 000 (1984).
3. M.-Y. Tang and J. E. Mark, Polym. Eng. Sci., **24**, 000 (1984).
4. J. E. Mark, C.-Y. Jiang, and M.-Y. Tang, Macromolecules, **17**, 000 (1984).

5. C.-Y. Jiang and J. E. Mark, Colloid Polym. Sci., **262**, 758 (1984).
6. M.-Y. Tang, A. Letton, and J. E. Mark, Colloid Polym. Sci., **262**, 000 (1984).
7. Y.-P. Ning, M.-Y. Tang, C.-Y. Jiang, J. E. Mark, and W. C. Roth, J. Appl. Polym. Sci., **29**, 3209 (1984).
8. Y.-P. Ning and J. E. Mark, *ms. submitted to J. Appl. Polym. Sci.*
9. J. E. Mark and Y.-P. Ning, Polym. Bulletin, **12**, 413 (1984).
10. M. A. Llorente and J. E. Mark, Macromolecules, **13**, 681 (1980).
11. J. E. Mark and J. L. Sullivan, J. Chem. Phys., **66**, 1006 (1977).
12. M. A. Llorente, A. L. Andrad, and J. E. Mark, J. Polym. Sci., Polym. Phys. Ed., **19**, 621 (1981).
13. M. A. Llorente, A. L. Andrad, and J. E. Mark, J. Polym. Sci., Polym. Phys. Ed., **18**, 2263 (1980).
14. J. E. Mark, Adv. Polym. Sci., **44**, 1 (1982).
15. J. E. Mark and P. J. Flory, J. Appl. Phys., **37**, 4635 (1966).
16. L. R. G. Treloar, "The Physics of Rubber Elasticity", Clarendon Press, Oxford (1975).
17. J. E. Mark, Rubber Chem. Technol., **48**, 495 (1975).
18. Z. Riggbi, Adv. Polym. Sci., **36**, 21 (1980).
19. K. E. Polesniak and C. W. Lentz, Rubber Chem. Technol., **48**, 795 (1975).
20. B. B. Bonnatra, Polymers, **20**, 691 (1979).

Accepted February 1, 1986

Precipitation of Reinforcing Filler Into Polydimethylsiloxane Prior to Its End Linking Into Elastomeric Networks

INTRODUCTION

Particulate fillers having high surface area are much used for the reinforcement of elastomers, a classic example being the addition of carbon black to natural rubber.¹ Another equally important example is the addition of silica (SiO_2) to polydimethylsiloxane (PDMS) [$-\text{Si}(\text{CH}_3)_2\text{O}-$],^{2,3} which would otherwise yield elastomers much too weak for most applications.^{4,5}

Such fillers are generally blended into the (uncrosslinked) polymers, which are invariably of sufficiently high molecular weight (and viscosity) to greatly complicate the mixing process. For this and other reasons,⁶ methods were recently developed for either precipitating silica into already-formed networks, or precipitating it simultaneously with the curing process.⁶⁻⁹ The reaction is the simple, catalyzed hydrolysis of tetraethylorthosilicate (TEOS)



In this *in situ* technique, however, removal of the byproduct $\text{C}_2\text{H}_5\text{OH}$ and unreacted TEOS causes a significant decrease in volume, which could be disadvantageous in some applications.

The present investigation was undertaken to determine a practical way to avoid this difficulty. The specific goal was the precipitation of the silica into samples of PDMS to give stable polymer-filler suspensions which remained capable of being end linked, subsequently, with no substantial changes in volume.

EXPERIMENTAL

Although both hydroxyl-terminated and vinyl-terminated PDMS have been end-linked into highly elastomeric networks, only the latter could be used in this study since the former reacts with TEOS.¹⁰ The two vinyl-terminated polymers chosen had number-average molecular weights of 5.5×10^4 and $13.0 \times 10^4 \text{ g mol}^{-1}$, and were provided by the McGhan NuSil Corp. The catalysts⁶ tested were sodium hydroxide, acetic acid, zinc acetate, ethylamine, triethylamine, and EDTA (ethylene diamine tetraacetic acid trisodium salt monohydrate). The TEOS to be hydrolyzed to filler was obtained from the Fisher Co., and all reactions were run at room temperature.

Preliminary studies conducted in aqueous solutions were unsuccessful, and those carried out using the water vapor present in the air were only partially successful. The best results were obtained as follows. Weighed amounts of the PDMS and TEOS, a small amount of the catalyst stannous-2-ethyl hexanoate, and a magnetic stirring bar were placed into a small beaker which was then placed (uncovered) into a larger covered jar containing a 2-5 wt % aqueous solution of ethylamine. In the case of the second polymer, a protective atmosphere of nitrogen was also employed. The stirred PDMS-TEOS mixtures were thus continuously exposed to water-ethylamine vapor. Sufficient filler was precipitated by this technique for the mixture to become cloudy after only 15 min. The reaction was allowed to proceed for 2 days at room temperature.

The polymer-filler suspensions prepared in this way were dried under vacuum for several days; they showed no signs of particle agglomeration or settling. The resulting viscous liquids were weighed and then end-linked¹¹ with $\text{Si}[\text{OSi}(\text{CH}_3)_2\text{H}]_4$, using chloroplatinic acid as catalyst

Figure 1b. A sample of each of the unfilled polymers was included for purposes of comparison. These reactions were also run at room temperature, for a period of 2-3 days.

Portions of each of the networks were used in elongation experiments to obtain the stress-strain isotherms at 25°C.^{12,13} The elastomeric properties of primary interest were the nominal stress $f^* \equiv f/A^*$ (where f is the equilibrium elastic force and A^* the undeformed cross-sectional area) and the reduced stress or modulus¹²⁻¹⁴ $[f^*] \equiv f^*/(a - a^{-2})$ (where $a = L/L_0$ is the elongation or relative length of the strips). All stress-strain measurements were carried out to the rupture points of the samples, and were generally repeated in part to test for reproducibility.

RESULTS AND DISCUSSION

The amounts of filler precipitated into the two polymers were obtained directly from the measured increases in weight. For the two samples of the lower molecular weight polymer the amounts were 3.3 and 10.2 wt %, and for the other 29.7 and 62.0 wt %. These values were actually somewhat larger than expected from complete hydrolysis of the TEOS, indicating that some OC_2H_5 groups may remain in the filler or water molecules may be absorbed onto the filler surfaces.

The stress-strain isotherms obtained are presented in Figure 1. The data are shown in the usual way,¹⁵ as the dependence of the reduced stress on reciprocal elongation. As is frequently the case for filled elastomers,^{1,2} some of the isotherms did not exhibit complete reversibility. In any case, the presence and efficacy of the filler are demonstrated by the marked increases in modulus. In the case of the higher molecular weight polymer, the increases are larger, with marked upturns at the higher elongations. This is due to the larger amounts of filler these samples contain, and possibly also to more reactive particle surfaces (since these precipitations were carried out under nitrogen).

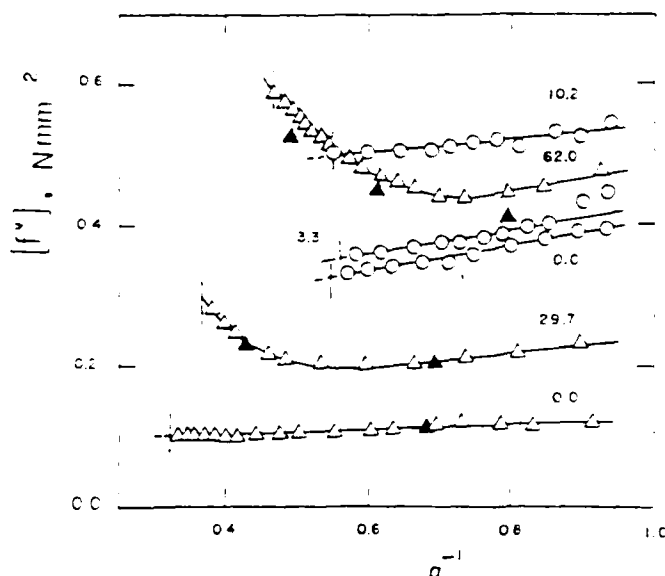


Fig. 1. The reduced stress shown as a function of reciprocal elongation for the two series of filled PDMS networks at 25°C. The circles locate results obtained using polymer having a molecular weight of $5.5 \times 10^3 \text{ g mol}^{-1}$, and the triangles a molecular weight of 13.0×10^3 . Filled symbols are for results obtained out of sequence to test for reversibility, and each curve is labeled with the wt % of filler present in the network. The vertical dashed lines locate the rupture points.

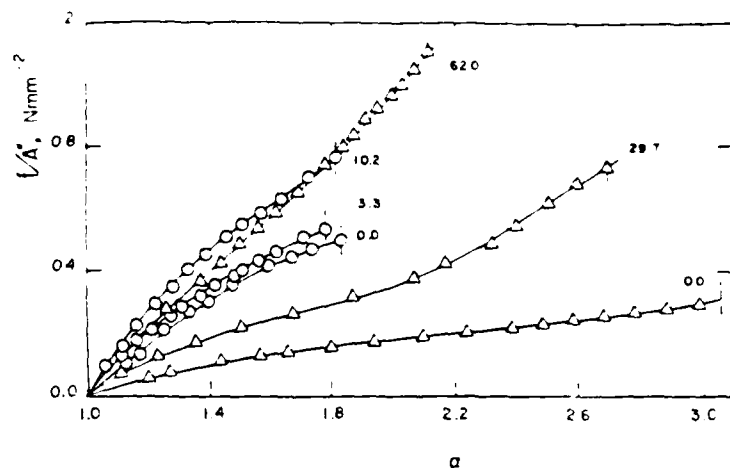


Fig. 2. The nominal stress shown as a function of elongation for the same networks characterized in Figure 1. In this representation, the area under each curve corresponds to the energy required for network rupture.

Figure 2 shows the data of Figure 1 plotted in such a way that the area under each stress-strain curve corresponds to the energy E_r of rupture,^{1b} which is the standard measure of elastomer toughness. It is seen that this simple technique can easily increase the toughness of an elastomer by a factor of 2 and could therefore be of considerable practical importance.

CONCLUSIONS

Previous methods developed to precipitate reinforcing silica either into already-formed elastomeric networks or during the curing process are extended to permit precipitation into a polymer prior to its crosslinking. This modification avoids significant changes in volume during or after curing which could be disadvantageous in some applications.

It is a pleasure to acknowledge the financial support provided by the National Science Foundation through Grant DMR 79-18903-03 (Polymers Program, Division of Materials Research) and by the Air Force Office of Scientific Research through Grant AFOSR 83-0027 (Chemical Structures Program, Division of Chemical Sciences).

References

1. Z. Rigbi, *Adv. Polym. Sci.*, **36**, 21 (1980).
2. K. E. Poimanteer and C. W. Lentz, *Rubber Chem. Technol.*, **48**, 795 (1975).
3. B. B. Boonstra, *Polymer*, **20**, 691 (1979).
4. T. L. Smith, *Polym. Eng. Sci.*, **17**, 129 (1977).
5. J. E. Mark, *Polym. Eng. Sci.*, **19**, 409 (1979).
6. J. E. Mark and S.-J. Pan, *Makromol. Chem. Rapid Comm.*, **3**, 681 (1982).
7. C.-Y. Jiang and J. E. Mark, *Colloid Polym. Sci.*, **262**, 758 (1984).
8. J. E. Mark, C.-Y. Jiang, and M.-Y. Tang, *Macromolecules*, **17**, 2613 (1984).
9. C.-Y. Jiang and J. E. Mark, *Makromol. Chem.*, **185**, 2609 (1984).
10. J. E. Mark, *Adv. Polym. Sci.*, **44**, 1 (1982).
11. M. A. Liorente and J. E. Mark, *Macromolecules*, **13**, 681 (1980).
12. J. E. Mark and J. L. Sullivan, *J. Chem. Phys.*, **66**, 1006 (1977).
13. M. A. Liorente, A. L. Andrády, and J. E. Mark, *J. Polym. Sci., Polym. Phys. Ed.*, **18**, 2263 (1980).

- 14 J. E. Mark and P. J. Flory, *J. Appl. Phys.*, **37**, 4635 (1966).
15 M. A. Llorente, A. L. Andrad, and J. E. Mark, *J. Polym. Sci., Polym. Phys. Ed.*, **19**, 621 (1981).

Y.-P. NING*
J. E. MARK

Department of Chemistry and the
Polymer Research Center

The University of Cincinnati
Cincinnati, Ohio 45221

Received October 30, 1984
Accepted January 28, 1985

* Present address: Shandong Institute of Chemical Engineering, Qingdao City, People's Republic of China.

Reprinted from *Accounts of Chemical Research*, 1985 18, 202.
Copyright © 1985 by the American Chemical Society and reprinted by permission of the copyright owner.

Molecular Aspects of Rubberlike Elasticity

JAMES E. MARK

Department of Chemistry and Polymer Research Center, University of Cincinnati, Cincinnati, Ohio 45221

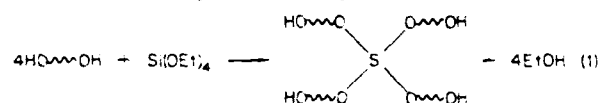
Received April 12, 1985

The elasticity associated with rubberlike materials is very different from that exhibited by atomic or low molecular weight substances such as metals, crystals, and glasses.¹⁻⁵ In particular, the extensibility of "elastomers" is much higher, frequently amounting to well over 1000%. Most strikingly, such high deformations are generally completely recoverable. The way this recoverability is achieved, however, is the main source of the problems encountered in characterizing rubberlike materials and in developing useful structure-property relationships.^{3,4}

Specifically, elastomers consist of polymer chains and the extraordinarily large numbers of spatial arrangements such molecules can exhibit is the origin of their very high extensibility.¹⁻³ Achieving recoverability requires preventing the chains from irreversibly sliding by one another, and this is accomplished by joining different chains with "cross-links", as is illustrated in Figure 1.³ Relatively few are required, with a typical degree of cross-linking involving only one skeletal atom out of approximately 200. The techniques generally used to introduce cross-links are peroxide thermolysis, high-energy irradiation, and sulfur addition to skeletal or side-chain unsaturation.¹ All are statistical processes, and the number of cross-links thus introduced and their placements along the chains are uncontrolled and essentially unknown. Furthermore, their introduction into the material makes it intractable in that it is no longer soluble in any solvent. The numerous standard characterization techniques based on measurements on isolated chains in solution¹ are therefore categorically

inapplicable. Thus, the very process of forming the required network structure thwarts its characterization. It is the lack of reliable structural information that is the problem in obtaining structure-property relationships in the area of rubberlike elasticity.

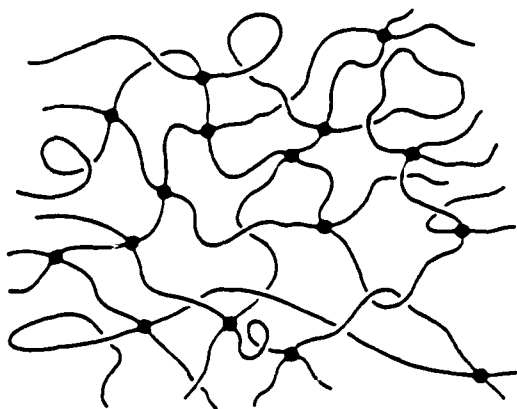
Now, however, it is possible to prepare "model" elastomeric networks,⁴⁻¹⁵ which are materials prepared in a way that provides independent information on their structures. An important example is reaction 1 in which



OH~OH represents a hydroxyl-terminated chain of poly(dimethylsiloxane) (PDMS) $[-\text{Si}(\text{CH}_3)_2\text{O}-]$.¹¹ In this approach, some solution characterization technique such as gel permeation chromatography is first used to obtain the number-average molecular weight M_n of the uncross-linked chains and the distribution about this average. Then carrying out the above reaction so as to

- (1) Flory, P. J. *"Principles of Polymer Chemistry"*; Cornell University Press: Ithaca, NY, 1953.
- (2) Treloar, L. R. G. *"The Physics of Rubber Elasticity"*, 3rd ed.; Clarendon Press: Oxford, 1975.
- (3) Mark, J. E. *J. Chem. Educ.* 1981, 58, 898.
- (4) Mark, J. E. *Makromol. Chem. Suppl.* 1979, 2, 87.
- (5) Mark, J. E. *Pure Appl. Chem.* 1981, 53, 1495.
- (6) Mark, J. E. *Rubber Chem. Technol.* 1981, 54, 809.
- (7) Mark, J. E. *Adv. Polym. Sci.* 1982, 44, 1.
- (8) Mark, J. E. In *"Elastomers and Rubber Elasticity"*; Mark, J. E., Lal, J., Eds.; American Chemical Society: Washington, DC, 1982.
- (9) Mark, J. E. *Polym. J. (Tokyo)* 1985, 17, 265.
- (10) Mark, J. E. *Br. Polym. J.* 1985, 17, 144.
- (11) Mark, J. E.; Sullivan, J. L. *J. Chem. Phys.* 1977, 66, 1006.
- (12) Llorente, M. A.; Mark, J. E. *Macromolecules* 1980, 13, 681.
- (13) Jiang, C.-Y.; Mark, J. E.; Chang, V. S. C.; Kennedy, J. P. *Polym. Bull.* 1984, 11, 319.
- (14) Brotzman, R. W.; Flory, P. J., manuscript in preparation.
- (15) Ning, Y.-P.; Mark, J. E.; Iwamoto, N.; Eichinger, B. E. *Macromolecules* 1985, 18, 55.

A biographical sketch of the author was published earlier. In *Acc. Chem. Res.* 1974, 7, 218, and 1979, 12, 49. He is spending the 1985-1986 academic year at the IBM Research Laboratory in San Jose, CA.



(2)

$$2 \begin{array}{c} \text{~~~~~} \\ \text{acac} \end{array} \rightarrow 2 \text{Pd}^{2+} \rightarrow \begin{array}{cc} \text{~~~~~} & \text{~~~~~} \\ \text{acac} & \text{acac} \\ \text{Pd}^{2+} & \text{Pd}^{2+} \\ \text{acac} & \text{acac} \\ \text{~~~~~} & \text{~~~~~} \end{array} \quad (3)$$

(28) Mark, J. E. *Rubber Chem. Technol.* 1975, 48, 495.

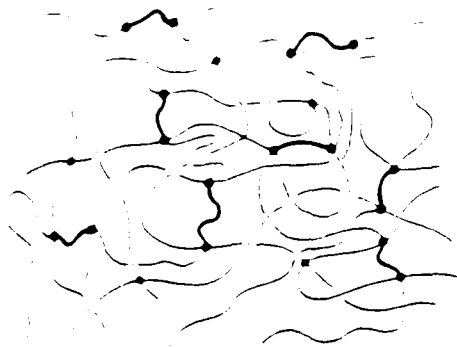


Figure 2. A network having a bimodal distribution of network chain lengths.⁴ The very short polymer chains are arbitrarily represented by heavy lines and the relatively long chains by thinner lines.

lower right-hand corner of Figure 1 do not contribute significantly at elastic equilibrium. There are disagreements²⁹⁻³¹ in this area, however, and this issue has not yet been resolved to everyone's satisfaction.

Bimodal Networks

End linking a mixture of very short and relatively long chains gives a bimodal network, as is shown schematically in Figure 2.⁴ The first application of such networks was in the testing of the "weakest link" theory, in which it is assumed that rupture of an elastomer is initiated by the shortest network chains (because of their very limited extensibility).^{3,4} Bimodal networks containing a relatively small but significant number of very short chains, however, did not show any decreases in ultimate properties. The strain is apparently reapportioned (nonaffinely) within the network so as to ignore as long as possible the difficultly deformable short chains. It is thus the (implicit) assumption of an affine deformation that is the error in the weakest link concept.

An important bonus is obtained if very large numbers (~95 mol %) of short chains are incorporated in a bimodal network. Specifically, the networks are found to have both high ultimate strength and high extensibility, which means they are unusually tough.⁷⁻¹⁰ Apparently the short chains give high values of the modulus and ultimate strength because of their very limited extensibility, and the long chains somehow delay the growth of the rupture nuclei required for catastrophic failure of the sample.

It is also possible to prepare bimodal networks which are spatially as well as compositionally heterogeneous, as is illustrated in Figure 3.⁴ This is done by pre-reacting the short chains to form heavily cross-linked clusters which are then joined to the long chains in the second step of the process.³² Such networks could serve as models for elastomers cured with peroxides which are not totally miscible with the elastomeric matrix.

Non-Gaussian Theory

Since it was concluded that the increases in modulus and ultimate strength are due to limited chain exten-



Figure 3. A bimodal network which is spatially as well as compositionally heterogeneous with respect to chain length.⁴

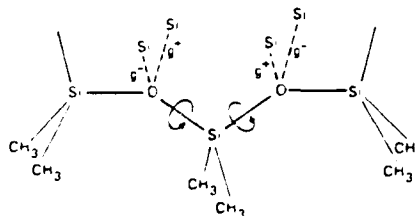


Figure 4. The poly(dimethylsiloxane) chain, illustrating how typical conformations have different energies and frequencies of occurrence because of the different interactions they engender (after ref 33).

sibility, it became important to try to interpret these results in terms of a non-Gaussian theory of rubberlike elasticity. The novel approach taken utilized the wealth of information which rotational isomeric state (RIS) theory³⁵ provides on the spatial configurations of chain molecules. Comparisons between theoretical and experimental values of properties dependent on the spatial configurations of the chains give the energies for the permitted conformations, some of which are shown for the PDMS chain in Figure 4. Specifically, Monte Carlo calculations based on the RIS approximation were used to simulate spatial configurations, and thus distribution functions for the end-to-end separation r of the chains.³⁴ These distribution functions are used in place of the Gaussian function in the standard three-chain network model² in the affine limit to give a molecular theory of rubberlike elasticity which is unique to the particular polymer of interest.³⁵⁻³⁷ Most important, it is applicable to the regions of very large deformation where limited chain extensibility gives rise to elastomeric properties significantly different from those in the Gaussian limit. One important result is an improved understanding of the increases in modulus observed in short-chain networks at very high elongations.

Interpenetrating Networks

If two types of chains differ in their end groups, it is possible simultaneously to end link them into two networks that interpenetrate^{38,39} one another. Such a network could, for example, be made by reacting hy-

(33) Flory, P. J. "Statistical Mechanics of Chain Molecules"; Wiley-Interscience: New York, 1969.

(34) Conrad, J. C.; Flory, P. J. *Macromolecules* 1976, 9, 41.

(35) Mark, J. E.; Curro, J. G. *J. Chem. Phys.* 1983, 79, 5705.

(36) Curro, J. G.; Mark, J. E. *J. Chem. Phys.* 1984, 80, 4521.

(37) Mark, J. E.; Curro, J. G. *J. Chem. Phys.* 1984, 80, 5262.

(38) Sperling, L. H. "Interpenetrating Polymer Networks and Related Materials"; Plenum Press: New York, 1981.

(39) Frisch, K. C.; Kiemper, D.; Frisch, H. L. *Polym. Eng. Sci.* 1982, 22, 1143.

(29) Valles, E. M.; Macosko, C. W. *Macromolecules* 1979, 12, 673.

(30) Pearson, D. S.; Graessley, W. W. *Macromolecules* 1980, 13, 1001.

(31) Meyers, K. O.; Bye, M. L.; Merrill, E. W. *Macromolecules* 1980, 13, 1045.

(32) Mark, J. E.; Andrad, A. L. *Rubber Chem. Technol.* 1981, 54, 366.

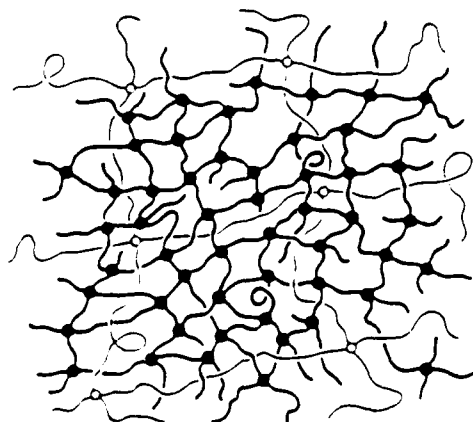
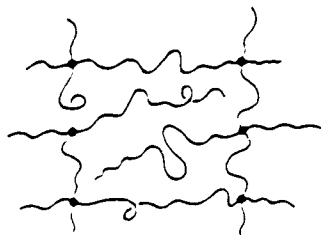


Figure 5. A bimodal interpenetrating network, in which the short-chain cross-links are represented by filled circles and the long-chain ones by open circles.

(a) Excess difunctional chains



(b) Monofunctional chains

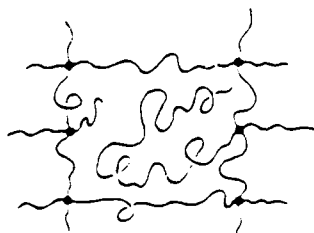


Figure 6. Two methods for preparing networks having dangling chains of known length, present in known concentration.

dioxyl-terminated PDMS chains with tetraethylorthosilicate while reacting vinyl-terminated PDMS chains with a multifunctional silane.⁴⁰ A bimodal network of this type is shown in Figure 5. Interpenetrating networks in general can be very unusual with regard to both equilibrium and dynamic mechanical properties.^{38,39}

Dangling-Chain Networks

Mechanical properties can be adversely affected by network irregularities such as dangling ends (chains attached to the network at only one end).^{41,42} and it is therefore very important to characterize their effects. Model networks containing dangling chains of known lengths and concentrations can be prepared in several ways, two of which are shown in Figure 6. If, during

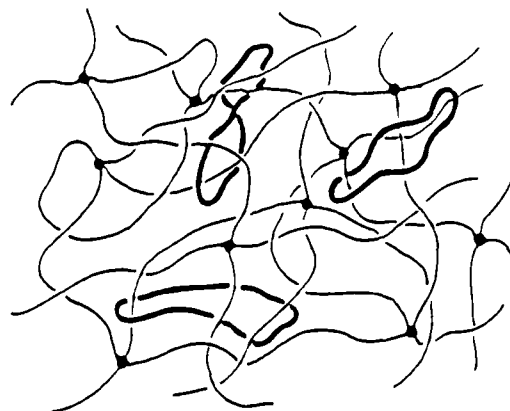


Figure 7. Cyclics trapped by linear chains which passed through them prior to being end linked into a tetrafunctional network.⁴⁶

the end-linking process, more difunctional chains are present than is required to react with all the functional groups on the end-linking molecules, then the known excess number of chain ends is equal to the number of dangling ends. In this method, the dangling chains must of course have the same average length as the elastically effective chains. The second method overcomes this limitation by the inclusion of monofunctional chains of any desired length. In this way the dangling chains can be either much shorter or much longer than the elastically effective chains. A mixture of dangling chain lengths can also be introduced as is, in fact, shown in the lower portion of Figure 6.

Studies^{41,42} of the mechanical properties of such networks show that dangling-chain irregularities do significantly decrease ultimate properties, as should be expected.

Sorption and Extraction of Diluents

End-linking functionally terminated chains in the presence of chains with inert ends yields networks through which the unattached chains "reptate".^{43,44} Networks of this type have been used to determine the efficiency with which unattached chains can be extracted from an elastomer, as a function of their lengths and the degree of cross-linking of the network. The efficiency was found to decrease with increase in molecular weight of the diluent and with increase in degree of cross-linking,^{43,44} as expected. It was also found to be more difficult to extract diluent present during the cross-linking than to extract the same diluents absorbed into the networks after cross-linking. Such comparisons can provide valuable information on the arrangements and transport of chains within complex network structures.

It was also found that if relatively large PDMS cyclics are present when linear PDMS chains are end linked, approximately one quarter are permanently trapped by one or more network chains threading through them, as is shown in Figure 7.⁴⁵ It should be possible to correlate the fraction of a cyclic trapped with its effective "hole" size, as estimated from Monte Carlo sim-

(40) Mark, J. E.; Ning, Y.-P. *Polym. Eng. Sci.* 1985, 25, 000.

(41) Andrad, A. L.; Liorente, M. A.; Snaral, M. A.; Rahalkar, R. R.; Mark, J. E.; Sullivan, J. L.; Yu, C. U.; Falender, J. R. *J. Appl. Polym. Sci.* 1981, 26, 1829.

(42) Jiang, C.-Y.; Mark, J. E. *Prepr., Div. Polym. Chem., Inc.* 1983, 24 (2), 97.

(43) Mark, J. E.; Zhang, Z.-M. *J. Polym. Sci., Polym. Phys. Ed.* 1983, 21, 1971.

(44) Garrido, L.; Mark, J. E. *J. Polym. Sci., Polym. Phys. Ed.* 1985, 23, 000.

(45) Garrido, L.; Mark, J. E.; Carlson, S. J.; Semlyen, J. A. *Polym. Commun.* 1985, 26, 53.

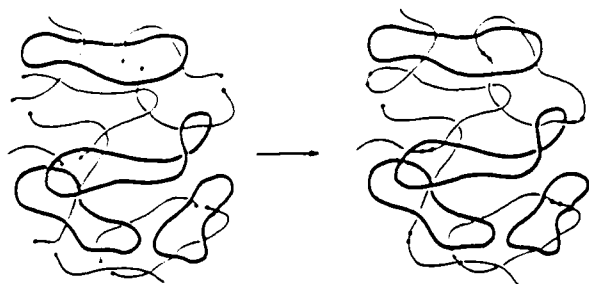


Figure 8. Preparation of a "chain mail" network, not having any cross-links at all. Linear chains passing through the cyclics are difunctionally end linked to form series of interpenetrating cyclics, which would be a gel.⁴⁵

ulations³⁵ of its spatial configurations.

It may also be possible to use this technique to form a network having no cross-links whatsoever. Mixing linear chains with large amounts of cyclic and then difunctionally end linking them could give sufficient cyclic interlinking to yield an "Olympic" or "chain mail" network, as is illustrated in Figure 8. Such materials could have highly unusual equilibrium and dynamic mechanical properties. Attempts to prepare some are in progress.

Elastomers Filled in Situ

There are three techniques by which silica can be precipitated into an elastomeric material. First, an already-cured network, for example, prepared from PDMS, may be swollen in TEOS and the TEOS hydrolyzed in situ.^{18,19,46} Alternatively, hydroxyl-terminated PDMS may be mixed with TEOS, which then serves simultaneously to tetrafunctionally end link the PDMS into a network structure and to act as a source of SiO_2 upon hydrolysis.^{20,46} Finally, TEOS mixed with vinyl-terminated PDMS can be hydrolyzed to give a SiO_2 -filled polymer capable of subsequent end linking by means of a multifunctional silane.^{21,46}

Stress-strain isotherms obtained on in situ filled PDMS show the presence and efficacy of the filler: this is demonstrated by the large increases in modulus, with marked upturns at the higher elongations.^{18,20,21} There are also large increases in the energy E_r of rupture, which is the standard measure of elastomer toughness. Increase in percent filler generally decreases the maximum extensibility α , but increases the ultimate strength. The latter effect predominates and E_r increases accordingly. In some cases, extremely large levels of reinforcement are obtained. Such networks behave nearly as thermosets, with some brittleness (small α_r), but with extraordinarily large values of the modulus [f^*].⁴⁰

Transmission electron microscopy⁴⁷ and light scattering and neutron scattering measurements⁴⁸ are being used to study the filler particles. As illustration, an electron micrograph for a PDMS elastomer in which TEOS has been hydrolyzed is shown in Figure 9.⁴⁷ The

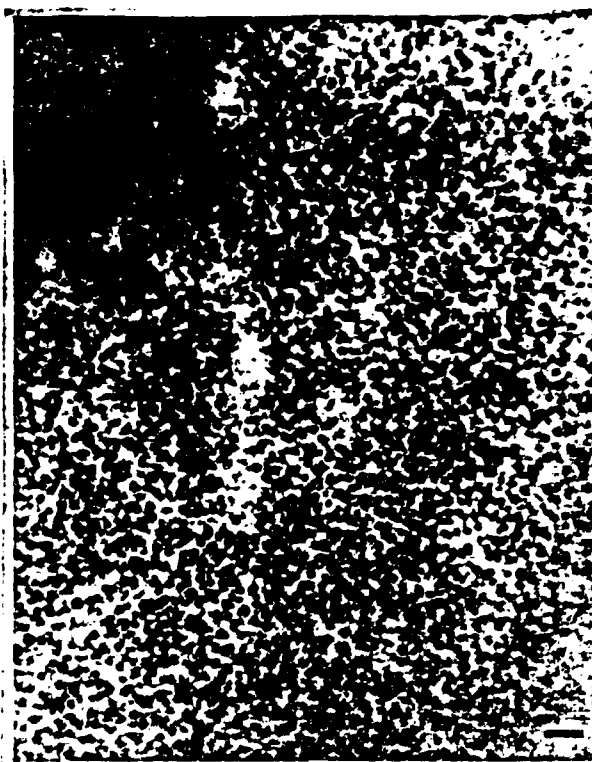


Figure 9. Transmission electron micrograph for a poly(dimethylsiloxane) network containing 34.4 wt % SiO_2 filler introduced by the in situ hydrolysis of tetraethyl orthosilicate.⁴⁷ The length of the bar in the figure corresponds to 1000 Å.

existence of filler particles in the network, originally hypothesized on the basis of mechanical properties,¹⁸ is clearly confirmed. The particles have average diameters of approximately 250 Å, which is in the range of particle sizes of fillers typically introduced into polymers in the usual blending techniques.^{16,17} The distribution of sizes is relatively narrow, with most values of the diameter falling in the range 200–300 Å.⁴⁷

Most strikingly, there is virtually none of the aggregation of particles essentially invariably present in the usual types of filled elastomers. These materials should therefore be extremely useful in characterizing the effects of aggregation and could be of considerable practical importance as well.⁴⁷

Concluding Remarks

Preparing and studying "model" elastomers having controlled and known network structures is seen to provide a great deal of valuable molecular information on rubberlike elasticity. Additional advantages include the preparation of unusually tough elastomers and materials of possibly unique equilibrium and dynamic mechanical properties. Analogous techniques for obtaining model filled systems could well be equally rewarding.

I wish to thank my collaborators for their fine work in the various projects described in this review. It is also a pleasure to acknowledge the financial support provided by the National Science Foundation through grant DMR 84-15082 (Polymers Program, Division of Materials Research) and by the Air Force Office of Scientific Research through grant AFOSR 83-0027 (Chemical Structures Program, Division of Chemical Sciences).

(46) Mark, J. E. In "Proceedings of the Second International Conference on Ultrastructure Processing of Ceramics, Glasses, and Composites", Hench, L. L., Ulrich, D. R., Eds.; Wiley: New York, 1986.

(47) Ning, Y.-P.; Tang, M.-Y.; Jiang, C.-Y.; Mark, J. E.; Roth, W. C. *J. Appl. Polym. Sci.* 1984, 29, 3209.

(48) Schaefer, D. W.; Ning, Y.-P.; Sur, G. S.; Mark, J. E., unpublished results.

A theoretical study of conformations and electronic band structures for two benzoxazole polymers

Kesunath Narasimhan, James E. Mark*

Department of Chemistry and the Polymer Research Center, The University of Cincinnati, Cincinnati, OH 45221, USA

(Date of receipt: February 13, 1985)

SUMMARY

The extended Hückel method within the tight binding approximation was applied to two benzoxazole polymers of a type much studied because of their excellent mechanical properties. Specifically, band structure calculations were carried out in part to identify the most stable conformation of the polymers in the crystalline state. In the preferred conformation of one polymer the rotational angle between the benzoxazole groups is 20° , and that between the benzoxazole group and the *p* phenylene group is 0° . The other polymer consists simply of benzoxazole groups, and these are predicted to be coplanar. The above conformational predictions are in excellent agreement with the results of both experimental and theoretical studies on relevant model compounds. In addition, the band gaps in the axial direction were found to be 1.86 and 2.31 eV, respectively, and these values are close to the corresponding experimental values 1.4 to 1.8 eV reported for *trans* polyacetylene. In both benzoxazole polymers the band gap was found to increase with increase in nonplanarity due to the concomitant reduction in charge delocalization.

Introduction

There is currently a great deal of interest in the synthesis, characterization, and applications of aromatic heterocyclic polymers such as the polybenzimidazoles (PBI's), polybenzothiazoles (PBT's), and the polybenzoxazoles (PBO's)¹⁻⁹. Techniques for their preparation have now been delineated, and their very high mechanical strength and thermal stability has been documented. Their potential applications are numerous and include their use as high performance fibers and films, and fillers in "molecular composites".

Two polymers of the PBO type have recently been synthesized and experiments to characterize them are underway^{1,9}. They are poly(5,5'-bibenzoxazole-2,2'-diyl-1,4-phenylene) (AAPBO) and poly(2,5-benzoxazole) (ABPBO), and their structures are shown in Figs. 1 and 2, respectively. The present investigation focuses on calculations of electronic band structures^{1,2,9}, which are used both to predict the low-energy (preferred) conformations and the energy band gaps relevant to the possible use of these materials as semiconductors. In the case of the AAPBO the sequence chosen for the present calculations consists of two chemical repeating units in which the second unit is rotated 180° with respect to the first unit about the bond joining the two units. In a similar manner, the ABPBO sequence consists of four chemical repeating units in which the second two units are rotated 180° with respect to the first two units about

0025-116X/85/00100

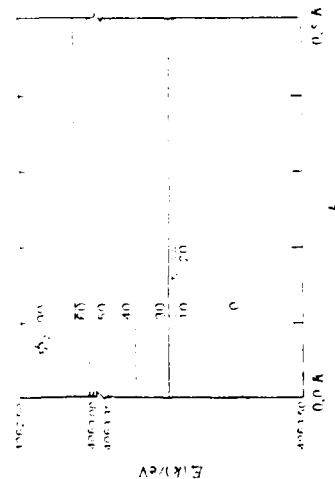


Fig. 4. Dependence of $E_1(k)$ on k and ϕ_1 at $\phi_2 = 20^\circ$ for AAPBO.

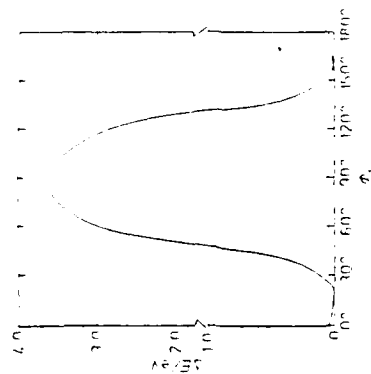


Fig. 5. The conformational energy ΔF shown as a function of the rotational angle ϕ_1 for AAPBO.

180° , $0^\circ \leq \phi_1 \leq 90^\circ$) using increments of 10° for the AAPBO chain. The results are shown in Figs. 3 and 4. For different torsional rotations, the total energy per unit cell (E_1) was calculated, using a polynomial fit for $E_1(k)$ in Eq. (2). For AAPBO the preferred (minimum energy) conformation corresponded to $\phi_1 = 20^\circ$ and $\phi_2 = 0^\circ$. The energy ΔF relative to that of the preferred conformation is shown as a function of ϕ_1 in Fig. 5. Minima occur both at 20° and 160° (with very small energy differences in the range 0° , 20° and 160° , 180°), and a maximum occurs at 90° . The non planarity would tend to reduce the repulsions between ortho hydrogen atoms located on neighboring benzoxazole rings. The preferred angle of 20° for its supplement (160°) is very close to the angle 23° (157°) observed for biphenyl in the liquid state¹⁰. It is also in at least semi quantitative agreement with calculated and experimental results

on this polymer and on other structurally related polymers and model compounds^{4,19}. The other prediction, that $\phi_2 = 0^\circ$, is also in good agreement with theory and experiment^{4,19,20}.

Typical results obtained for AAPBO are shown in Fig. 6. The predictions of coplanarity ($\phi' = 0^\circ$) is also in good agreement with previous results^{4,19,20}.

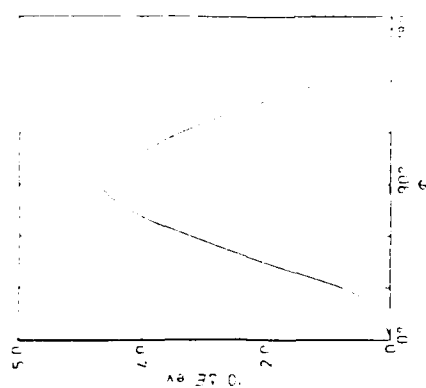


Fig. 6. The conformational energy ΔF shown as a function of the rotational angle ϕ for AAPBO.

The axial band structures calculated at these preferred conformations for AAPBO and AAPBO are shown in Figs. 7 and 8. The band gap E_g , which is the difference in the energy between the uppermost filled valence band and lowest unoccupied conduc-

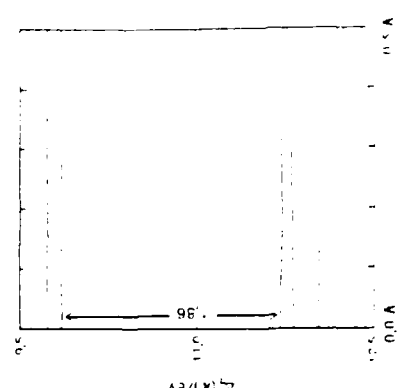


Fig. 7. Band structure for the preferred conformation ($\phi_1 = 20^\circ$ or 160° and $\phi_2 = 0^\circ$) of AAPBO.

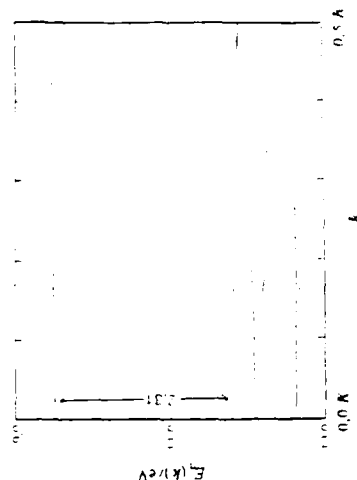


Fig. 8. Band structure for the preferred conformation ($\phi = 0^\circ$) of AAPBO.

tion band, was calculated to be 1.86 eV for AAPBO and 2.31 eV for ABPBO. Both the conduction and valence bands are found to be composed of π orbitals, as was found for *cis*- and *trans*-PBO polymers⁹. The band gaps determined for the AAPBO and ABPBO chains are slightly higher than those for PBO. Such differences could be attributed to the loss of conjugation due to the non planar conformation obtained in the case of AAPBO and to the lack of phenylene moieties in the case of the ABPBO. The absence of phenylene groups presumably reduces the conjugation between the π orbitals and interrupts charge delocalization. In any case, AAPBO seems to be a better candidate than ABPBO as a semiconducting material because of its smaller band gap. However, the band gaps obtained for AAPBO and ABPBO polymers are lower than those of poly(*p*-phenylene) and poly(*m*-phenylene) which range from 3.2 to 4.9 eV¹⁰. This suggests that these aromatic heterocyclic polymers could be advantageous with regard their electronic behavior.

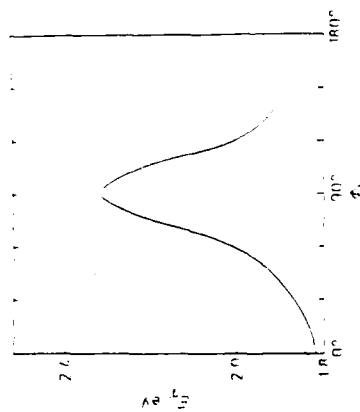


Fig. 9. Dependence of the band gap E_g on the rotational angle ϕ_1 at $\phi_2 = 0^\circ$ for AAPBO.

Unfortunately there are no experimental results presently available for comparison with these theoretical predictions. However, the calculated values of E_g are close to the value of 1.4 to 1.8 eV experimentally observed for *trans*-polyacetylene¹¹, a polymer much studied because of its promise as a semiconductor. The disordered, amorphous narrow width of the uppermost filled valence band could possibly be due to the large size of the unit cell considered and the inherent one electron approximation of the present methodology. In any case, rotations away from coplanarity increase E_g for both AAPBO and ABPBO, because of decreased charge delocalization, as was concluded previously^{9,10}. Results for the AAPBO chain are illustrated in Fig. 9.

The present results are encouraging and should prompt additional theoretical and experimental investigations on this interesting class of chain molecules.

It is a pleasure to acknowledge financial support provided by the Air Force Office of Scientific Research (Chemical Structures Program, Division of Chemical Sciences), and several very helpful discussions with Dr. D. Bhaumik of the University of Cincinnati.

- 11 J. F. Helminiak, Preprints of ACS Division of Organic Coating and Plastics Chemistry 40, 455 (1979). A number of articles on PBO and PBI polymers, for example, appear in the July/August 1981 issue of *Macromolecules*.
- 12 W. J. Welch, J. E. Mark, *J. Polym. Sci. Polym. Phys. Ed.* **21**, 1111, 2543 (1983).
- 13 D. Bhaumik, J. E. Mark, *J. Polym. Sci. Polym. Phys. Ed.* **21**, 1111, 2543 (1983).
- 14 W. J. Welch, D. Bhaumik, H. H. Jaffe, J. E. Mark, *Polym. Eng. Sci.* **24**, 218 (1984).
- 15 S. J. Bai, W. F. Huang, D. R. Wiff, G. Price, M. Hunsaker, S. J. Krause, T. Haddock, W. W. Adams, and J. I. O'Brien, W. W. Adams, F. G. Imbert, A. V. Fratini, Abstracts, Am. Phys. Soc. Meeting, Detroit 1984.
- 16 J. E. Wolfe, SRI, private communications.
- 17 D. Bhaumik, J. E. Mark, *Synth. Metals* **6**, 209 (1983).
- 18 K. Nayak, J. E. Mark, submitted to *J. Appl. Phys.*
- 19 R. Hoffman, *J. Chem. Phys.* **39**, 1397 (1963).
- 20 M. H. Whangbo, R. Hoffman, *J. Am. Chem. Soc.* **100**, 6693 (1978).
- 21 M. W. Wellmann, W. W. Adams, R. A. Wolff, D. S. Dudas, D. R. Wiff, A. V. Fratini, *Macromolecules* **14**, 935 (1981).
- 22 F. Grolh, *Acta. Chem. Scand.* **27**, 945 (1973).
- 23 A. V. Fratini, F. M. Cross, J. E. O'Brien, W. W. Adams, submitted to *J. Macromol. Sci., Phys.*
- 24 H. Suzuki, *Bull. Chem. Soc. Jpn.* **32**, 1340 (1959).
- 25 W. J. Welch, J. E. Mark, *Polym. Eng. Sci.* **25**, (1985).
- 26 M. W. Wellmann, W. W. Adams, D. R. Wiff, A. V. Fratini, *Air Force Tech. Report AFJL-TR-79-4184*, Part I.
- 27 W. J. Welch, D. Bhaumik, J. E. Mark, *Macromolecules* **14**, 947 (1981).
- 28 D. Bhaumik, W. J. Welch, H. Jaffe, J. E. Mark, *Macromolecules* **14**, 951 (1981).
- 29 J. L. Redas, R. R. Chance, R. H. Baughman, S. R. Silbey, *J. Chem. Phys.* **76**, 3673 (1982).
- 30 C. K. Chiang, A. J. Heeger, A. G. MacDiarmid, *Ber. Bunsenges. Phys. Chem.* **83**, 407 (1979).

Reinforcing Effects from Silica-Type Fillers Containing Hydrocarbon Groups

J. E. Mark* and G. S. Sur**

Department of Chemistry and the Polymer Research Center, University of Cincinnati,
Cincinnati, OH 45221 USA

Summary

Curing hydroxyl-terminated chains of poly(dimethylsiloxane) is achieved by reacting them with tetraethoxysilane, vinyltriethoxysilane, methyltriethoxysilane, and phenyltriethoxysilane, with excess amounts of the silanes hydrolyzed in-situ to filler particles. When triethoxysilanes are used, the vinyl, methyl, and phenyl groups must be part of the filler particles and, in at least some cases, the resulting reinforcement is better than that given by the silica particles obtained from the (unsubstituted) tetraethoxysilane.

Introduction

In an earlier study (1), an attempt was made to obtain deformable filler particles by hydrolysis of mixtures of tetraethoxysilane (TEOS) with ethyltriethoxysilane and diethyldiethoxysilane. A sequential process was used, with vinyl-terminated chains of poly(dimethylsiloxane) (PDMS) first being end linked into a network structure, followed by its swelling in the silane mixture, and the hydrolysis of the silanes to give filler particles (1-14). The technique was not very successful in that the resulting filled networks did not have unusually good ultimate properties.

This approach is modified in the present investigation. Specifically, the silanes employed are TEOS, vinyltriethoxysilane (VTEOS), methyltriethoxysilane (MTEOS), and phenyltriethoxysilane (PTEOS), and the curing and in-situ precipitation are carried out simultaneously in an attempt to improve the bonding between the filler particles and the elastomeric matrix.

Experimental Details

The polymers employed, two hydroxyl-terminated PDMS samples having number-average molecular weights corresponding to $10^{-3}M_n = 18.0$ and 26.0 g mol⁻¹, respectively, were provided by Petrarch Systems Inc. Portions were mixed with TEOS, VTEOS, MTEOS, and PTEOS in amounts characterized by the molar feed ratio $r = [OC_2H_5]/[OH]$, where the $-OC_2H_5$ groups are on the silanes and the $-OH$ groups appear as chain ends on the PDMS. Specific values of this ratio, which range upward from 1.0 (stoichiometric

* Presently at IBM Research Laboratory, San Jose, CA 95193 USA

** On leave from Yeungnam University, Daegu 660 Korea

balance), are given in the third column of Table I. The catalyst

Table I
Preparative Details and Properties of the Filled Networks

$10^{-3} \rho_p, \frac{\text{g}}{\text{cm}^3}$	Silane	Network Designation	Sol Fraction	$\rho, \frac{\text{g}}{\text{cm}^3}$	McT Filler	$\alpha, \frac{\text{cm}^3}{\text{g}}$	$(f/A^*)_{\text{r}}, \frac{\text{g}}{\text{cm}^2}$	$10^3 L_{\text{r}}, \frac{1}{\text{cm}}$
18.0	TEOS	1 T-1	0.058	0.955	0.00	3.48	0.19	0.28
		5C T-5C	0.047	0.976	4.42	2.20	0.45	0.61
		10C T-10C	0.040	0.990	6.18	2.32	0.55	0.93
	PTEOS	5C V-5C	0.036	0.973	4.23	2.81	0.55	1.1
		10C V-10C	0.021	1.12	8.15	1.96	0.40	0.39
	MTEOS	5C M-5C	0.032	0.961	3.45	2.71	0.79	1.46
		10C M-10C	0.045	0.985	5.94	2.42	0.96	1.37
	PTEOS	5C P-5C	0.030	0.962	3.54	1.89	0.71	0.69
		10C P-10C	0.031	1.34	17.3	1.50	0.59	0.33
26.0	TEOS	1 T-1	0.082	0.955	0.00	3.60	0.17	0.31
		5C T-5C	0.075	1.04	6.24	2.34	0.94	1.16
		10C T-10C	0.070	1.29	13.8	2.90	1.23	1.94
	PTEOS	5C V-5C	0.052	0.984	5.97	2.86	1.03	1.64
		10C V-10C	0.046	1.12	7.93	2.86	1.20	2.07
	MTEOS	5C M-5C	0.051	1.16	10.3	2.38	0.44	0.57
		10C M-10C	0.051	1.23	12.9	2.17	0.45	0.81
	PTEOS	5C P-5C	0.078	1.04	6.35	2.37	1.26	1.82
		10C P-10C	0.071	1.23	12.7	2.46	3.07	2.51

M_n : molecular weight of the network chains.

ρ : mass ratio of OC_2H_5 groups on the silane to OH groups on the polymer.

L_{r} : length at room temperature.

L_{r} : elongation at rupture.

f^* : nominal stress at rupture.

E_{r} : energy required for rupture.

employed, stannous-2-ethylhexanoate, was present in an amount corresponding to 1.0 wt % of the PDMS. Both series of mixtures of these components appeared to be perfectly homogeneous. They were poured into molds to a depth of 1 mm, and the reaction was allowed to proceed at room temperature for two days. The water required for the hydrolysis was simply absorbed from the humidity in the air.

The resulting networks were extracted in tetrahydrofuran in the usual manner (15,16); the sol fractions thus obtained are small, as can be seen from the values given in column five of the table. The densities ρ of the extracted materials, determined by pycnometry, are reported in column six, and values of the wt % filler, determined from the increases in weight, are given in column seven.

Unswollen portions were used in the elongation experiments carried out to obtain the stress-strain isotherms at 25°C (15-17). The nominal stress was given by $f^* \equiv f/A^*$, where f is the elastic force and A^* the undeformed cross-sectional area, and the reduced stress or modulus by $[f^*] \equiv f^*/(\alpha - \alpha^{-2})$, where $\alpha = L/L_i$ is the elongation or relative length of the sample.

Results and Discussion

Typical stress-strain isotherms obtained for the networks having $M_n = 16.0 \times 10^3 \text{ g mol}^{-1}$ are shown in Figure 1, and some for $M_n = 26.0 \times 10^3 \text{ g mol}^{-1}$ in Figure 2. Values of the maximum extensibility or elongation

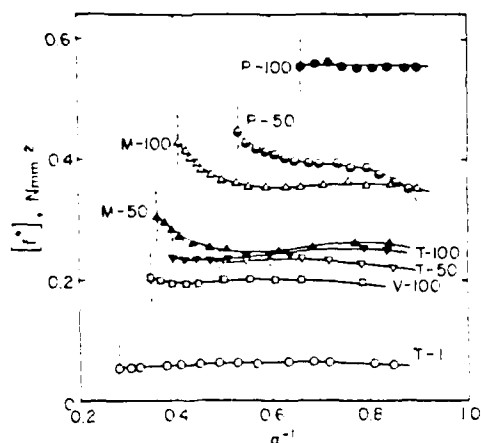


Figure 1. The reduced stress shown as a function of reciprocal elongation at 25°C for typical filled PDMS networks having $M_n = 16.0 \times 10^3 \text{ g mol}^{-1}$. Each curve is identified by the designation given in column four of the Table, and the vertical dashed lines locate the rupture points.

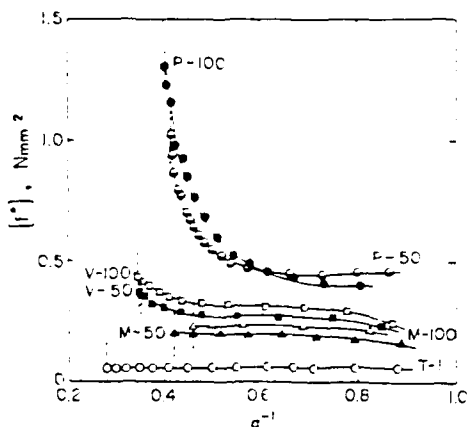


Figure 2. The reduced stress shown as a function of reciprocal elongation for the networks having $M_n = 26.0 \times 10^3 \text{ g mol}^{-1}$.

at rupture obtained from all the curves of this type are given in column eight of the table. Similarly obtained values of the ultimate strength, as represented by the nominal stress at rupture, are given in the following column.

Figure 3 shows some of the data plotted in such a way that the area under each curve corresponds to the energy E_r required for rupture. Values are listed in the final column of the table.

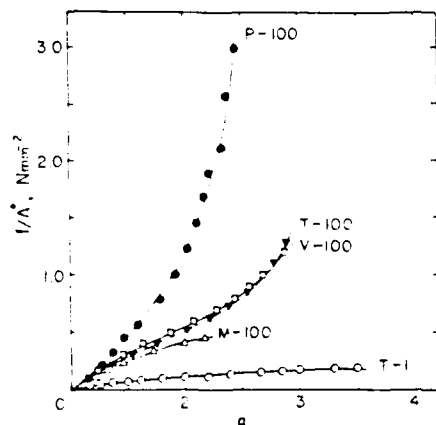


Figure 3. The nominal stress shown as a function of elongation for selected networks having $M_n = 26.0 \times 10^3 \text{ g mol}^{-1}$.

There are seen to be large increases in modulus in general, and some large upturns in modulus at high elongations as well. The desired reinforcing effects (18) are thus clearly in evidence.

Of considerable interest is the observation that, at comparable wt % filler, the fillers containing vinyl, methyl, or phenyl groups frequently give better reinforcement than that given by the silica particles obtained from the TEOS. The PTEOS system seems particularly interesting in this regard. The improvements could be due to deformability of some of the filler particles. A definite conclusion, however, would require examination of stretched and quenched samples by electron microscopy, a very difficult but conceivably achievable goal.

Acknowledgements

It is a pleasure to acknowledge financial support provided by the National Science Foundation through Grant DMR 84-15082 (Polymers Program, Division of Materials Research) and by the Air Force Office of Scientific Research through Grant AFOSR 85-0027 (Chemical Structures Program, Division of Chemical Sciences). G. S. S. also wishes to thank the Educational Ministry of Korea for the Research Fellowship he received.

References

1. Y.-P. Ning, Z. Rigbi, and J. E. Mark, Polym. Bulletin, **13**, 155 (1985).
2. J. E. Mark and S.-J. Pan, Makromol. Chem., Rapid Commun., **3**, 681 (1982).
3. C.-Y. Jiang and J. E. Mark, Makromol. Chemie, **185**, 2609 (1984).
4. M.-Y. Tang and J. E. Mark, Polym. Eng. Sci., **25**, 29 (1984).
5. J. E. Mark, C.-Y. Jiang, and M.-Y. Tang, Macromolecules, **17**, 2613 (1984).
6. C.-Y. Jiang and J. E. Mark, Colloid Polym. Sci., **262**, 758 (1984).
7. M.-Y. Tang, A. Letton, and J. E. Mark, Colloid Polym. Sci., **262**, 990 (1984).
8. Y.-P. Ning, M.-Y. Tang, C.-Y. Jiang, J. E. Mark, and W. C. Roth, J. Appl. Polym. Sci., **29**, 3209 (1984).
9. J. E. Mark and Y.-P. Ning, Polym. Bulletin, **12**, 413 (1984).
10. Y.-P. Ning and J. E. Mark, J. Appl. Polym. Sci., **30**, 000 (1985).
11. Y.-P. Ning and J. E. Mark, Polym. Eng. Sci., **25**, 000 (1985).
12. J. E. Mark, Brit. Polym. J., **17**, 000 (1985).
13. G. S. Sur and J. E. Mark, Eur. Polym. J., **21**, 000 (1985).
14. G. S. Sur and J. E. Mark, ms. submitted to Makromol. Chemie.
15. J. E. Mark and J. L. Sullivan, J. Chem. Phys., **66**, 1006 (1977).
16. M. A. Llorente, A. L. Andrad, and J. E. Mark, J. Polym. Sci., Polym. Phys. Ed., **19**, 621 (1981).
17. J. E. Mark and P. J. Flory, J. Appl. Phys., **37**, 4635 (1966).
18. J. E. Mark, Polym. Eng. Sci., **19**, 254, 409 (1979).

Accepted September 16, 1986

ELASTOMERIC NETWORKS CROSS-LINKED BY SILICA OR TITANIA FILLERS

G. S. SUR and J. E. MARK

Department of Chemistry and the Polymer Research Center, The University of Cincinnati,
 Cincinnati, OH 45221, U.S.A.

(Received 8 May 1985)

Abstract—Triethoxysilyl-terminated poly(dimethylsiloxane) (PDMS) was prepared by reacting triethoxysilane with vinyl-terminated PDMS having a number-average molecular weight of $11.3 \times 10^3 \text{ g mol}^{-1}$. Particles of silica and titania generated *in situ* by the hydrolysis of tetraethoxysilane and titanium *n*-propoxide, respectively, were found to end-link this polymer. The presence of a stable elastomeric network structure was confirmed by stress-strain measurements in elongation.

INTRODUCTION

Chemical modification is now a common way of extending the utility of polymeric materials [1-4]. A particularly important example is the placement of reactive groups at the ends of a polymer chain so that it can be end-linked into an elastomeric structure [5,6]. Typically, hydroxyl groups are placed on chains of poly(dimethylsiloxane) (PDMS) $[-\text{Si}(\text{CH}_3)_2\text{O}-]$, which are then joined by a multi-functional reactant such as tetraethoxysilane (TEOS). It would be very interesting if such ethoxy groups could be placed on the chain-ends, since they could then be reacted with the hydroxyl groups present on the surface of many reinforcing filler particles [7-9]. In this way curing and filling could be accomplished in a one-step process.

The present investigation was carried out for this purpose. Specifically, triethoxysilyl groups are placed on the ends of PDMS chains into which fume silica (SiO_2) is mixed, or into which silica or titania (TiO_2) are precipitated by hydrolysis of appropriate silicon and titanium compounds. The stability of the networks thus formed is gauged by stress-strain measurements carried out to rupture.

EXPERIMENTAL

Vinyl-terminated PDMS having a number-average molecular weight of $11.3 \times 10^3 \text{ g mol}^{-1}$ and a commercial fume silica were generously provided by the Dow Corning Corporation. TEOS (Fisher) and titanium *n*-propoxide (Aldrich) were used without further purification.

Triethoxysilyl-terminated PDMS was prepared by reaction of the vinyl-terminated PDMS with a small excess of triethoxysilane, using chloroplatinic acid as catalyst, in sealed flasks at 70° for a period of 1 day. The hydrogen attached to the silicon atom in the silane simply adds to the vinyl double bond. Removal of the unreacted triethoxysilane under reduced pressure resulted in a colourless viscous liquid. A small portion of the product was characterized by standard chemical titration.

In the first experiments, attempts were made to react the triethoxysilane-terminated PDMS with the commercial silica. The ingredients were well mixed and 1 wt % of stannous-2-ethylhexanoate was added as catalyst. The mixtures were poured into moulds to a depth of 1 mm, and the

reaction was allowed to proceed at room temperature for 3 days.

In a second set of experiments, attempts to obtain cross-linked networks were based on reaction of the triethoxysilane-terminated PDMS with silica obtained by the "*in situ*" hydrolysis of TEOS [10-21]. In brief, the PDMS, TEOS and catalyst were thoroughly mixed. They were then poured into moulds to a depth of approx. 1 mm, allowed to stand for 24 hr at room temperature, after which they were placed under vacuum (500 mm Hg). The water required for the hydrolysis was obtained simply from the humidity in the air. In the final experiments, titanium *n*-propoxide was used instead of TEOS, thereby providing titania particles. The conditions were the same as those used for the TEOS.

The resulting networks were extracted in tetrahydrofuran for 4 days, deswelled in tetrahydrofuran-methanol mixtures, and then dried.

The stress-strain isotherms were obtained on strips cut from the dried (unswollen) networks, at 25° , in the usual manner [5,6]. Stress-strain measurements were made using a sequence of increasing values of the elongation or relative length of the sample $\alpha = L/L_0$, with frequent inclusions of values out of sequence to test for reversibility. Entire stress-strain isotherms were frequently repeated two or three times. The nominal stress was given by $f^* \equiv f/A^*$ where f is the elastic force and A^* the undeformed cross-sectional area, and the reduced stress or modulus [5,6,22,23] by $[f^*] \equiv f^*(\alpha - \alpha^{-1})$.

RESULTS AND DISCUSSION

The amounts of filler incorporated in the PDMS networks are given in the third column of Table 1. In the case of the fume silica blended into the polymer, some gel was formed. As shown in column five of Table 1, however, the sol fraction was very high, and the networks were too weak for reliable stress-strain measurements. Apparently the surface concentration of reactive silanol groups on this filler was too small to give a high degree of chain-end linking.

The results were considerably better for the networks in which SiO_2 to TiO_2 was precipitated *in situ*. The sol fractions were smaller and reversible stress-strain isotherms were obtained. The results are shown in Figs 1 and 2. The moduli approached 0.2 N mm^{-2} , which is indicative of relatively efficient

Table I. Structure and ultimate properties of the networks

Formula	Filler		Network		Ultimate properties		
	Origin	Wt %	Designation	Sol fraction	α_r^*	f_r^{**} (N mm ⁻²)	$10^3 E_r^\ddagger$ (J mm ⁻¹)
SiO ₂	Fume	0.46	—	0.40	—	—	—
		1.96	—	0.42	—	—	—
SiO ₂	In-situ	0.88	SiO ₂ -1	0.20	1.8	0.19	0.08
	Ppt	1.60	SiO ₂ -2	0.31	1.6	0.16	0.05
TiO ₂	In-situ	0.92	TiO ₂ -1	0.20	2.3	0.38	0.26
	Ppt	1.47	TiO ₂ -2	0.31	1.6	0.19	0.07

*Elongation at rupture †Ultimate strength as measured by the nominal stress at rupture
‡Energy required for rupture

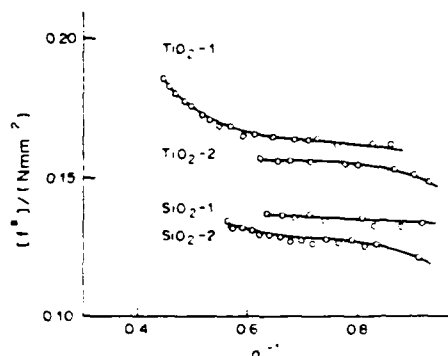


Fig. 1. The reduced stress or modulus shown as a function of reciprocal elongation at 25° for the stable PDMS networks. Each curve is identified by the code given in column four of the Table.

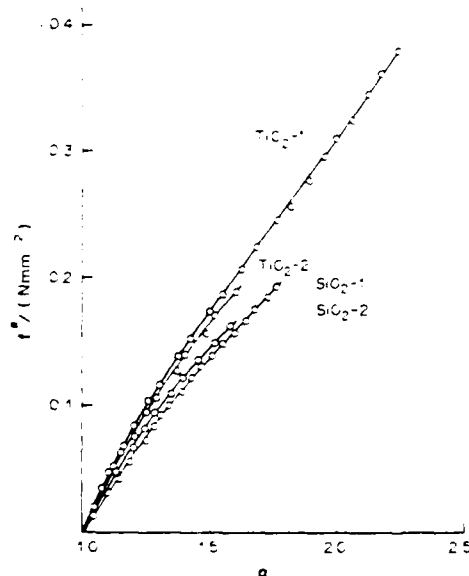


Fig. 2. The nominal stress shown as a function of elongation for the same networks characterized in Fig. 1. In this representation, the area under each curve corresponds to the energy E_r required for rupture [24].

end-linking. Values of the maximum extensibility, ultimate strength, and energy to rupture, given in the last three columns of the Table, are also consistent with a stable, elastomeric network structure.

Additional studies could show this new technique to have practical as well as fundamental importance.

Acknowledgements—It is a pleasure to acknowledge the financial support provided (J.E.M.) by the National Science Foundation through Grant DMR 84-15082 (Polymers Program, Division of Materials Research), and by the Air Force Office of Scientific Research through Grant AFOSR 83-0027 (Chemical Structures Program, Division of Chemical Sciences). G.S.S. also thanks the Educational Ministry of Korea for a Research Fellowship.

REFERENCES

1. J. A. Moore (Ed.), *Reactions on Polymers*, D. Reidel, Boston, Mass. (1973).
2. E. M. Fettes (Ed.), *Chemical Reactions of Polymers*, Wiley-Interscience, New York (1964).
3. L. D. Loan and F. H. Winslow, Reactions of macromolecules. In *Macromolecules: An Introduction to Polymer Science* (Edited by F. A. Bovey and F. H. Winslow), Chap. 7, Academic Press, New York (1979).
4. R. J. Ceresa, The chemical modification of polymers. In *Science and Technology of Rubber* (Edited by F. R. Eirich), Academic Press, New York (1978).
5. J. E. Mark and J. L. Sullivan, *J. chem. Phys.* **66**, 1006 (1977).
6. M. A. Llorente, A. L. Andraday, and J. E. Mark, *J. Polym. Sci., Polym. Phys. Ed.* **18**, 2263 (1980).
7. D. Leyden and W. Collins, *Silylated Surfaces*, Gordon & Breach, New York (1980).
8. B. Arkies, *Chemtech.* **7**, 766 (1977).
9. E. P. Plueddemann, *Silane Coupling Agents*, Plenum Press, New York (1982).
10. J. E. Mark and S.-J. Pan, *Makromolekul. Chem., Rapid Commun.* **3**, 681 (1982).
11. C.-Y. Jiang and J. E. Mark, *Makromolekul. Chem.* **185**, 2609 (1984).
12. M.-Y. Tang and J. E. Mark, *Polym. Engng Sci.* **25**, 29 (1985).
13. J. E. Mark, C.-Y. Jiang and M.-Y. Tang, *Macromolecules* **17**, 2613 (1984).
14. C.-Y. Jiang and J. E. Mark, *Colloid Polym. Sci.* **262**, 758 (1984).
15. M.-Y. Tang, A. Letton and J. E. Mark, *Colloid Polym. Sci.* **262**, 990 (1984).
16. Y.-P. Ning, M.-Y. Tang, C.-Y. Jiang, J. E. Mark and W. C. Roth, *J. appl. Polym. Sci.* **29**, 3209 (1984).
17. Y.-P. Ning and J. E. Mark, *J. appl. Polym. Sci.* **30** (1985).
18. J. E. Mark and Y.-P. Ning, *Polym. Bull.* **12**, 413 (1984).
19. Y.-P. Ning, Z. Rigbi and J. E. Mark, *Polym. Bull.* **13**, 155 (1985).
20. Y.-P. Ning and J. E. Mark, *Polym. Engng Sci.* **25** (1985).
21. J. E. Mark, *Br. Polym. J.* **17**, 144 (1985).
22. P. J. Flory, *Principles of Polymer Chemistry*, Cornell University Press, Ithaca, New York (1953).
23. J. E. Mark and P. J. Flory, *J. appl. Phys.* **37**, 4635 (1966).
24. M. A. Llorente, A. L. Andraday and J. E. Mark, *J. Polym. Sci., Polym. Phys. Ed.* **19**, 621 (1981).

Electron microscopy of elastomers containing *in-situ* precipitated silica

J. E. Mark*, Y.-P. Ning, C.-Y. Jiang and M.-Y. Tang

Department of Chemistry and the Polymer Research Center, University of Cincinnati, Cincinnati, Ohio 45221, USA

and W. C. Roth

Analytical Research Department, Dow Corning Corporation, Midland, Michigan 48640, USA

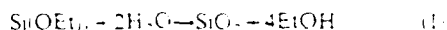
(Received 6 May 1985)

Transmission electron microscopy is used to characterize reinforcing silica particle precipitated as filler into networks of polydimethylsiloxane by the hydrolysis of tetraethylorthosilicate. Particle diameters were typically 200 Å, with relatively narrow distributions. Aggregation is generally very low but, as expected, becomes more pronounced with increase in amount of filler. Acidic catalysts give less well defined particles than basic ones, and large catalyst concentrations give unusually small particle diameters. Permitting the particles to digest in contact with water and catalyst seems to make them better defined, more uniform in size, and less aggregated.

(Keywords: electron microscopy; elastomers; silica; polydimethylsiloxane)

INTRODUCTION

If a network of polydimethylsiloxane (PDMS, $[-Si(CH_3)_2O-]$) is swelled with tetraethylorthosilicate (TEOS) and the TEOS hydrolysed, silica particles are deposited within the network structure¹⁻⁴. The reaction is



and is catalysed by a variety of substances⁵, in the vicinity of room temperature. The presence of filler particles was shown indirectly by the reinforcement observed in stress-strain measurements on the dried networks¹⁻⁴, and directly from two electron micrographs⁶.

The present investigation was carried out to provide additional information on the silica generated by this *in-situ* precipitation technique. Electron microscopy is used to determine average particle diameters and their distributions, the smoothness of the particles, and the extent of their aggregation. Of primary interest is the dependence of these quantities on temperature, reaction time, the nature of the catalyst, catalyst concentration, and ageing.

EXPERIMENTAL

Preparation of networks

The networks were prepared from PDMS chains that had either vinyl groups or hydroxyl groups at both ends. All samples were tetrafunctionally end linked in the usual manner, the former type with $Si[OSi(CH_3)_2H]_4$ ⁷ and the latter with TEOS⁸. Their values of the number-average molecular weight, which becomes the molecular weight M_c between crosslinks, are given in the second column of

Table 1. Each network was extracted for several days to remove soluble material, which was found to be present to the extent of only a few per cent.

Precipitation of silica

Strips cut from the network sheets were weighed and then swelled with TEOS to the maximum extent attainable. The extent varied with M_c , but in all cases corresponded to a volume fraction of polymer of 0.2–0.3, which means there is a large excess of TEOS available for hydrolysis. The degree of crosslinking of the samples studied should therefore be unimportant (as should also be the nature of the functional groups originally present on the chain ends).

Each swollen strip was placed in one of several aqueous catalyst solutions, and the hydrolysis of the TEOS permitted to occur at the desired temperature for the desired period of time⁹. Details are given in columns 3–6 of Table 1. The final sample in the series was permitted to 'age' in contact with its catalyst solution for a period of two months. After the reaction, each strip was dried and weighed. Sample designations, based on the type of catalyst and its wt% in solution, are given in the final column of the table.

Electron microscopy

A piece of each filled network, approximately 1 mm × 1 mm × 5 mm was mounted in an appropriate specimen holder, which was then placed into the cryostatic chamber (Sorvall FS 1000) of an ultramicrotome (Sorvall MT 6000). The entire slicing area was taken to and then maintained at -140°C , with a controller initiating the delivery of the precise amount of liquid nitrogen and heat necessary to maintain preset temperatures in the chamber. The liquid nitrogen filling system incorporates a

* Visiting scientist at IBM-San Jose, 1984–85 academic year.

Table 1. Conditions for network formation and silica precipitation.

End groups	$10^{-3} M^*$ (g mol ⁻¹)	Catalyst		Silica precipitation		Sample designation ^b
		Formula	Wt%	T (°C)	Reaction time (hours)	
Vinyl	13.0	C ₂ H ₅ NH ₂	2.0	50	0.5	EAM-2-1
Vinyl	13.0	C ₂ H ₅ NH ₂	2.0	50	1.0	EAM-2-2
Hydroxy	21.3	C ₂ H ₅ NH ₂	2.0	25	24.0	EAM-2-3
Hydroxy	8.0	CH ₃ COOH	5.0	25	1.0	HAC-5-1
Hydroxy	8.0	K ₂ HPO ₄	5.0	25	2.0	KPH-5-1
Hydroxy	8.0	C ₂ H ₅ NH ₂	50.0	25	0.17	EAM-50-1
Vinyl	7.4	C ₂ H ₅ NH ₂	2.0	25	1440.0	EAM-2-4

* Average molecular weight between crosslinks.

^b Cat-wt-%cat-number.

liquid gas separator designed to allow only liquid nitrogen into the chamber. Specimen slices having a thickness the order of 1000 Å were obtained using a diamond knife. They were collected on carbon-coated grids, and then examined in transmission with a Hitachi HS-7 electron microscope operating at 50 kV.

RESULTS AND DISCUSSION

The measured increases in weight of the sample strips were used to calculate values of the wt% filler introduced by the *in-situ* precipitation reaction. The results are given in the second column of Table 2.

The first two samples, EAM-2-1 and EAM-2-2, were prepared under conditions identical to those used in the previous study¹, except the temperature was 50°C instead of room temperature. Typical electron micrographs obtained for these two samples are shown in Figures 1 and 2, respectively. As in the previous case¹, the particles had a diameter of approximately 200 Å, were well defined, and were well dispersed (little aggregation). This is summarized in columns 5-6 of Table 2. Thus, moderate changes in temperature seem unimportant.

If very large amounts of silica are precipitated, aggregation becomes more pronounced, as should be expected. This is illustrated by sample EAM-2-3, which contains 81.5 wt% silica (~65 vol%). A typical micrograph obtained for it is shown in Figure 3.

The above three samples were obtained using ethylamine, a basic catalyst. The effects of changing to a highly acidic catalyst are illustrated by samples HAC-5-1 and KPH-5-1; they were prepared using solutions of acetic acid and a phosphate salt having pH's of 2.7 and 4.0, respectively. The results for the HAC sample, illustrated in

Figure 4, show the particles to be very poorly defined. This is consistent with results⁸⁻¹⁰ obtained for systems of interest in sol-gel-ceramics technology. It was there concluded that in the gelation process, acidic catalysts give structures that are less branched and less compact



Figure 1. Transmission electron micrograph of sample EAM-2-1 at a magnification of 60,600 \times . In this and the following Figures, the length of the bar corresponds to 1000 Å and details on the samples are given in Tables 1 and 2.

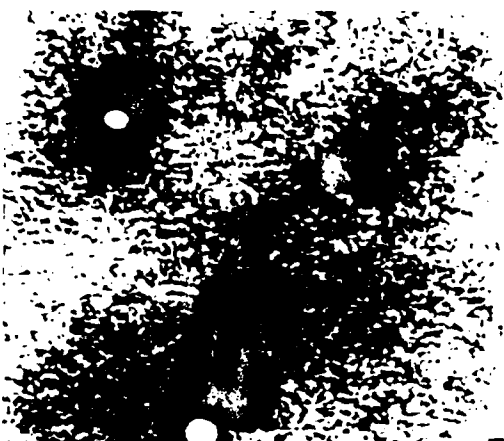


Figure 2. Micrograph of sample EAM-2-2 at 77,550 \times .

Table 2. Amounts and characteristics of silica precipitated.

Sample	wt% SiO ₂	Figure	Diameter ^a (Å)	Definition	Dispersion ^a
EAM-2-1	10.5	1	150-225	Good	Good
EAM-2-2	31.1	2	200-250	Good	Good
EAM-2-3	81.5	3	-	Fair	Poor
HAC-5-1	36.7	4	-	Poor	Fair
KPH-5-1	38.7	5	120-200	Good	Good
EAM-50-1	14.8	6	65-100	Good	Good
EAM-2-4	31.0	7	200	Excellent	Good

^a Lack of aggregation.

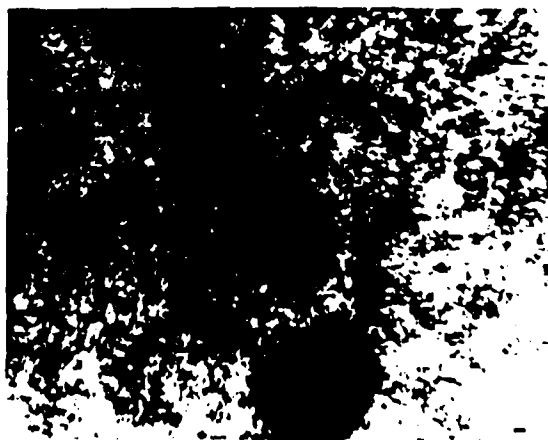


Figure 3 Micrograph of sample EAM-2-3 at 49830x

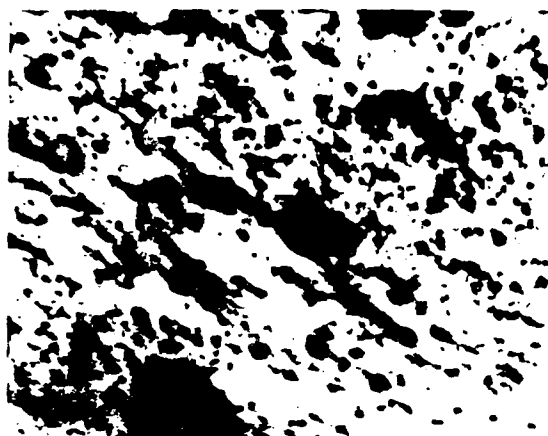


Figure 4 Micrograph of sample HAC-5-1 at 49830x



Figure 5 Micrograph of sample KPH-5-1 at 49830x

than those obtained from basic catalysts. As expected, the less acidic KPH catalyst does give better defined particles, as is illustrated in *Figure 5*.

The effect of using a very large amount of catalyst (50 wt%) is shown by sample EAM-50-1. The particles obtained are unusually small (65–100 Å), as shown in *Figure 6*.

The final sample, EAM-2-4, was permitted to remain in contact with its aqueous catalyst solution for two months. As is illustrated in *Figure 7*, this 'ageing' or 'digestion' process did seem to make the particles better defined, more uniform in size, and less aggregated. This suggests that some reorganization is occurring, at least in some steps in the hydrolysis reaction. Additional experiments would be required, however, to confirm this tentative but very provocative result.

ACKNOWLEDGEMENTS

It is a pleasure to acknowledge the financial support provided by the National Science Foundation through



Figure 6 Micrograph of sample EAM-50-1 at 77550x



Figure 7 Micrograph of sample EAM-2-4 at 77550x

Grant DMR 84-15082 (Polymers Program, Division of Materials Research) and by the Air Force of Scientific Research through Grant AFOSR 83-0027 (Chemical Structures Program, Division of Chemical Sciences). C.-Y.J. and M.-Y.T. also wish to thank the Dow Corning Corp. for the Research Fellowships they received.

REFERENCES

1. Mark, J. E. and Fan, S.-J. *Macromol. Chem., Rapid Commun.* 1982, 3, 683.
2. Jiang, C.-Y. and Mark, J. E. *Macromol. Chem.* 1984, 185, 2609.
3. Mark, J. E., Jiang, C.-Y. and Tang, M.-Y. *Macromolecules* 1984, 17, 2613.
4. Jiang, C.-Y. and Mark, J. E. *Colloid Polym. Sci.* 1984, 262, 754.
5. Ning, Y.-P., Tang, M.-Y., Jiang, C.-Y., Mark, J. E. and Rott, W. C. *J. Appl. Polym. Sci.* 1984, 29, 3209.
6. Liorente, M. A. and Mark, J. E. *Macromolecules* 1980, 13, 681.
7. Mark, J. E. and Sullivan, J. L. *J. Chem. Phys.* 1977, 66, 1000.
8. Schaefer, D. W. and Keeler, K. D. *Phys. Rev. Lett.* 1984, 53, 1383.
9. Brinker, C. J., Keeler, K. D., Schaefer, D. W., Assink, R. A., Kay, B. D. and Ashley, C. S. *J. Non-Cryst. Solids* 1984, 63, 45.
10. Schaefer, D. W. and Keeler, K. D. *Mater. Res. Soc. Symp. Proc.* 1984, 32, 1.

S C I E N C E O F
**CERAMIC CHEMICAL
PROCESSING**

EDITED BY

LARRY L. HENCH

*University of Florida
Gainesville, Florida*

DONALD R. ULRICH

*Air Force Office of Scientific Research
Washington, D. C.*

A WILEY-INTERSCIENCE PUBLICATION

JOHN WILEY & SONS

New York Chichester Brisbane Toronto Singapore

CONFORMATIONAL ANALYSIS OF SOME POLYSILANES, AND THE PRECIPITATION OF REINFORCING SILICA INTO ELASTOMERIC POLY(DIMETHYLSILOXANE) NETWORKS

J. F. MARK

Department of Chemistry,
University of Cincinnati
Cincinnati, Ohio

INTRODUCTION

The polysilanes $[-SiR_2-]$ are a new class of semi inorganic polymers with fascinating properties and considerable promise in a variety of applications. For example, some members of this series can be cast into transparent films, spun into fibers, and converted into silicon carbide at high temperatures.^{1,2} They can also be used as photoinitiators,³ resist in UV lithography,^{2,4} *p*-type semiconductors when properly doped,⁵ and as reinforcing media in ceramics when converted *in situ* into β - SiC fibers.⁶

Relatively little is known about the conformational characteristics of the polysilanes from either an experimental or theoretical point of view, although some work is in progress.⁶⁻⁹ For this reason, conformational energies were calculated for two of the simpler polysilanes. Information thus obtained can

be used to predict the regular conformations in which the polymers should crystallize,⁸ and the equilibrium flexibility of the chains in the undiluted amorphous state and in solution.⁸

The structurally related polysiloxanes $[-SiR_2O-]$ have long been known and extensively studied.⁸ The dimethyl polymer has been of particular interest because of its unusual flexibility. This property is exploited, for example, in the use of the crosslinked polymer as an elastomeric material⁹ in low-temperature applications. These elastomers, however, unlike their competitors such as natural rubber and butyl rubber, cannot undergo strain induced crystallization.^{10,11} They are therefore inherently weak and require reinforcement with a high surface area filler in practically all applications.⁹ Blending such fillers into (thickly viscous) polymers prior to crosslinking can be very difficult and filler agglomeration is almost impossible to avoid. For these reasons it could be highly advantageous to generate such filler *in situ*, for example, by the hydrolysis of silicates sufficiently nonpolar to dissolve in typical elastomers such as polydimethylsiloxane (PDMS). Such techniques have now been developed, and the results obtained should transcend the area of elastomer reinforcement, giving information useful as well in the area of sol-gel ceramics technology.¹²

CONFORMATIONAL ANALYSIS OF SOME POLYSILANES

Computational Details

The first polymer of interest was polysilane (PSI) itself, $[-SiH_2-]$, and the specific sequence investigated is shown in Fig. 47.1.⁷ The length l of the $Si \cdots Si$ skeletal bonds is 0.234 nm, which is considerably larger than the 0.153 nm length of the $C-C$ bonds in the hydrocarbon analogue, polyethylene (PE) $[-CH_2CH_2-]$.⁸ This should reduce repulsive interactions in polysilanes, but could be partially offset by the increased length of the $Si-H$ bond relative to the $C-H$ bond (0.148 versus 0.110 nm). Skeletal bond angles in PSI are approximately tetrahedral, as they are in PE.⁸ Rotational states are *trans* (T), *gauche*

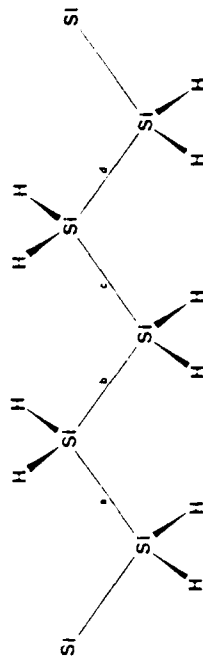


Figure 47.1. Skeletal structure of the polysilane chain $[-SiH_2-]$. Conformational energies are calculated as a function of the rotation angles about skeletal bonds a , b , and c .

positive (G^+), and *gauche* negative (G^-), and are expected to occur in the vicinity of the symmetric locations specified by the rotational angles $\phi = 0^\circ, 120^\circ$, and 240° , respectively. The second polymer was poly(dimethylsilylene) (PDMSI) [$-\text{Si}(\text{CH}_3)_2-$], shown in Fig. 47.2.⁷ The model for it was similar to that for PSL, but with the rotational angles of the methyl side groups representing additional variables.

Distances between all pairs of atoms were calculated in the usual manner,^{2,8} as a function of the skeletal and side chain rotational angles. Conformational energies were then calculated from these distances using empirical potential energy functions, and a torsional contribution corresponding to a barrier height of 0.4 kcal/mole (which is considerably smaller than that for PE, 2.8 kcal/mole).⁸ Entire contour maps of the energy against rotational angles were obtained, and then used to calculate configurational partition functions and to average the energies and rotational angles about the minima. In this way, configurational statistical weights were refined to include a preexponential or entropy factor. The statistical weights were then used in a matrix multiplication scheme to calculate values of the *characteristic ratio* $\langle r^2 \rangle_0/nl^2$, where $\langle r^2 \rangle_0$ is the chain dimension as unperturbed by excluded volume effects¹⁴ and n is the number of skeletal bonds. This ratio is much used as an inverse measure of equilibrium chain flexibility.⁸

Results for Polysilane

Polysilane was found to show a preference for pairs of *gauche* states of the same sign (G^+G^+) over the corresponding *trans* states (TT) by ca. 0.5 kcal/mole, in contrast to the analogous *n*-alkanes which prefer TT over G^+G^+ by ca. 1.0 kcal/mole.⁸ Even G^+G^+ states, commonly found to be prohibitively repulsive for most polymers, were preferred over the TT states by 0.4 kcal/mole.⁷ The predicted crystalline state conformation could thus be described as helical, of a pitch similar to that shown by polyoxymethylene [$-(\text{CH}_2\text{O})-$]. It is thus quite different from the PE preferred form, which is the planar, all *trans*, zig-zag

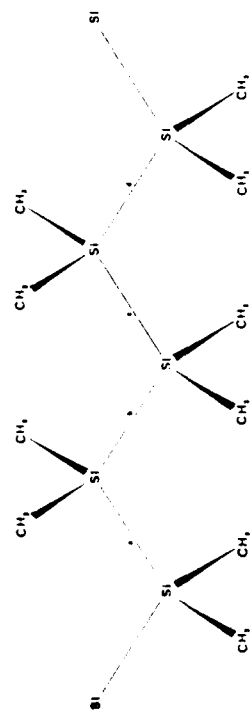


Figure 47.2 Sketch of the polydimethylsilylene chain.⁷

conformation. The same conclusion was reached in an earlier theoretical study of this chain⁶ which focused exclusively on discrete minima. As can be seen from Fig. 47.3, nearly all regions of configurational space were within 2 kcal/mole of the minima, indicating considerable chain flexibility. This was confirmed by the unusually low value, 4.0, calculated for the characteristic ratio. The value for PE is approximately 7.5.

Results for Poly(Dimethylsilylene)

Previous calculations⁶ on this polymer indicated the G^+G^+ conformation again preferred. The present results,⁷ however, indicate G^+G^+ and TTG^+ (or G^+TT) conformations to have essentially the same energies (0.08 versus 0.00 kcal/mole). If the energy difference is indeed this small, the conformation actually adopted by the chain upon crystallization would probably be determined by differences in chain packing energies.

Location of G^+ states at angles that minimize the energy would place them at 195° . This revision in the direction of the T state, and the diminished number

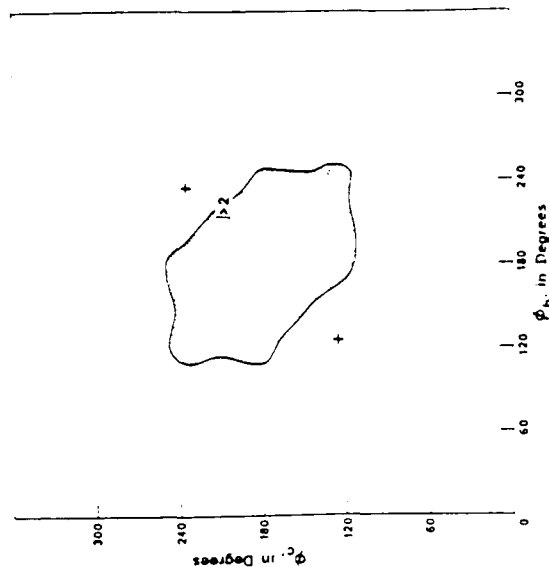


Figure 47.3 Conformational energy map for the polysilane segment giving the energy in kcal/mole relative to the conformational energy minima designated by $+$ on the map. The energy contours are shown as a function of the rotational angles ϕ_1 and ϕ_2 . The shaded regions correspond to energies greater than 2 kcal/mole above the minima.

of compact G^1 states should increase the characteristic ratio to the vicinity of 15. This would make the PDMSI chain considerably less flexible than both PSI and PI.

PRECIPITATION OF REINFORCING SILICA INTO ELASTOMERIC NETWORKS

Some Experimental Details

Silica may be prepared by the hydrolysis



of tetraethylorthosilicate (TEOS), in the presence of any of a variety of catalysts. There are three techniques by which silica thus precipitated can be used to reinforce an elastomeric material. First, an already cured network, for example, prepared from PDMS, may be swollen in TEOS and the TEOS hydrolyzed *in situ*.^{15, 20} Alternatively, hydroxyl-terminated PDMS may be mixed with TEOS, which then serves simultaneously to tetrafunctionally end link the PDMS into a network structure and to act as a source of SiO_2 upon hydrolysis.²¹⁻²³ Finally, TEOS mixed with vinyl terminated PDMS can be hydrolyzed to give a SiO_2 filled polymer capable of subsequent end linking by means of a multifunctional silane.²⁴

Precipitation Rates

The rates of the precipitation reaction were studied through plots of weight percent filler against time. Typical results for the $\text{C}_2\text{H}_5\text{NH}_2$ catalyzed system within an already cross linked PDMS elastomer are shown in Fig. 47.4.¹⁹ Although the rates increase with catalyst concentration,²⁰ as expected, they are seen to vary in a complex manner. One complication is the deswelling of the network due to migration of TEOS and the by product ethanol to the surrounding aqueous solution. The loss of TEOS should be smaller in the case of the more dilute $\text{C}_2\text{H}_5\text{NH}_2$ solution (since it is more hydrophilic), and this would explain the relatively simple monotonic form of the corresponding precipitation curves. In the case of the more concentrated $\text{C}_2\text{H}_5\text{NH}_2$ solutions the curves level off, because of the TEOS migration, and then turn downward, presumably because of loss of colloidal silica. At constant time, less filler is precipitated in the case of the networks having the larger value of the molecular weight between crosslinks, and this is probably due to larger losses of TEOS and silica from the larger "pores" in these networks in the highly swollen state.¹⁹

Mechanical Properties of the Filled Elastomers

The elastomeric properties of primary interest here are the nominal stress $f^* = f/l^*$ (where f is the equilibrium elastic force and l^* the undeformed

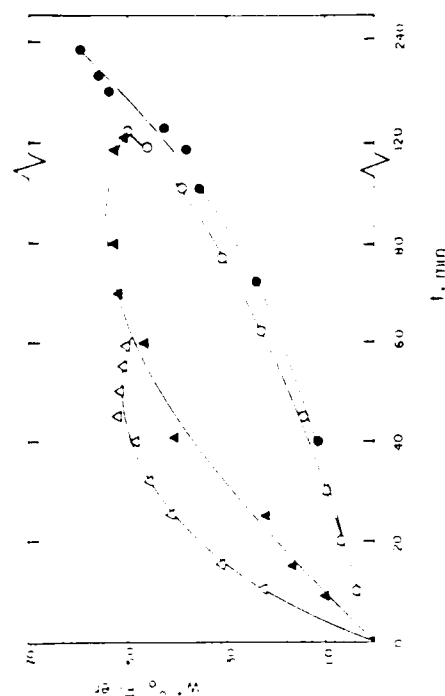


Figure 47.4 Weight percent filler precipitated as a function of time.¹⁹ The circles locate the results for 20 wt% ethylamine and the triangles the results for 25.0 wt% ethylamine. The open symbols are for networks having a molecular weight between crosslinks of 6.0×10^3 g/mole, and the filled symbols 21.3×10^3 g/mole.

cross sectional area), and the reduced stress or modulus $f^*/f^* \equiv f^*/(\pi \cdot \alpha^2)$ (where $\alpha = l/l^*$ is the elongation or relative length of the sample).

Typical stress-strain isotherms obtained on the *in situ* filled PDMS networks are given in Fig. 47.5. The data show²⁵ the dependence of the reduced stress on reciprocal elongation. The presence and efficacy of the filler are demonstrated by the large increases in modulus, with marked upturns at the higher elongations. Figure 47.6 shows the data of Fig. 47.5 plotted in such a way that the area under each stress-strain curve corresponds to the energy E_s of rupture, which is the standard measure of elastomer toughness. Increase in % filler decreases the maximum extensibility α , but increases the ultimate strength f^* . The latter effect predominates and E_s increases accordingly. In some cases, extremely large levels of reinforcement are obtained. Such networks behave nearly as thermosets, with some brittleness (small α), but with extraordinarily large values of the modulus $[f^*]^{1/2}$.

Characterization of the Filler Particles

Transmission electron microscopy,¹⁶ and light scattering and neutron scattering measurements²⁶ are being used to study the filler particles. As illustration, an electron micrograph for a PDMS elastomer in which TEOS has been hydrolyzed is shown in Fig. 47.7.¹⁶ The existence of filler particles in the network, originally hypothesized on the basis of mechanical properties,¹⁵ is clearly confirmed. The particles have average diameters of approximately 280 Å, which is in the range

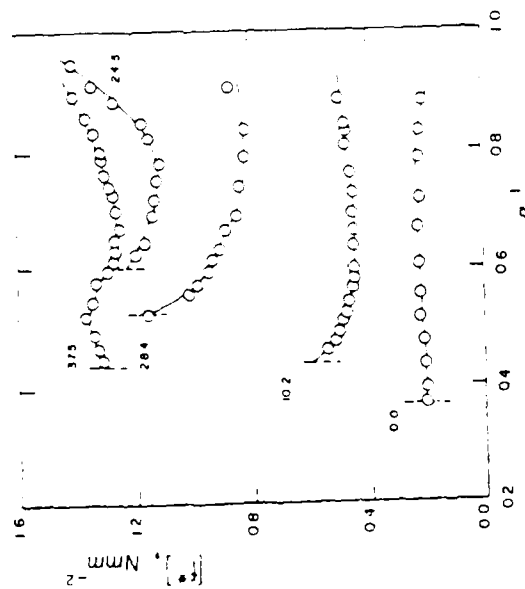


Figure 47.5 The reduced stress as a function of reciprocal elongation at 25°C for PDMS networks filled in 2.0 wt% $C_3H_7PH_2$ solution.¹⁹ Each curve is labeled with the wt% filler in the network including results for the unfilled elastomer.

of particle sizes of fillers typically introduced into polymers in the usual blending techniques. The distribution of sizes is relatively narrow, with most values of the diameter falling in the range 200–300 Å.¹⁶

Strikingly, particles aggregation invariably present in the usual types of filled elastomers is absent. These materials should be useful in characterizing effects of aggregation, and could be of practical importance as well.¹⁶

Other Novel Filling Techniques

In typical filled systems, anisotropy of mechanical properties can arise only if the filler particles or their agglomerates are asymmetric, since they are then oriented as a result of the flow of the uncrosslinked mix during processing operations. In fact, fibrous fillers are often used for the express purpose of introducing mechanical anisotropy. Recent studies, however, show that even when the particles are spherical, if they are magnetic and the filled elastomer is cured in a magnetic field, then highly anisotropic thermal²⁷ and mechanical²⁸ properties can be obtained.

The filler used in one study²⁸ was an extremely fine commercial magnetic powder (MCG 410 Magnaglo) in which the particles are very nearly spherical.

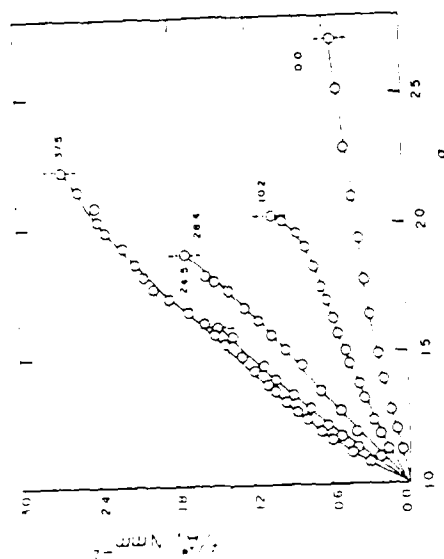


Figure 47.6 Reduced stress as a function of reciprocal elongation for the networks filled in the 50.0 wt% $C_3H_7PH_2$ solution.



Figure 47.7 Transmission electron micrograph (TEM) for an *in situ* filled PDMS network containing 33.4 wt% filler.¹⁸ The average particle diameter is 250 Å.

Chain packing in two aromatic heterocyclic polymers, one of which has a ladder structure

Kosmath Navak, James E. Mark*

Department of Chemistry and the Polymer Research Center, The University of Cincinnati, Cincinnati, OH 45221, USA

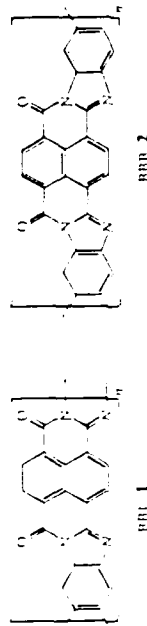
(Date of receipt: June 3, 1985)

SUMMARY

A semiempirical method was used to calculate the interaction energies in the ladder polymer poly(3,6-dioxo-1*H*-2,3,6,6a-tetrahydro-2,6a,11-triazaindeno[1,2-*b*]pyrene-2,8,9-triyl-1-ylidene-1-nitrilo) (BBL, 1) and the single-strand polymer poly(5,8-dioxo-4*b*,5,8,8a-tetrahydro-4*b*,8a,13,16-tetraazadiinden[1,2-*a*:1',2'-*d'*]pyrene-3,10-diyl) (BBB, 2), in order to elucidate their chain packing. The van der Waals contribution to the total intermolecular interaction energies was found to be more significant than the Coulombic one. The prediction of short-range interplanar spacings in the neighborhood of 3.3 Å along the *z* axis (chains above one another) and 8.8 Å along the *y* axis (chains alongside one another) is in good agreement with X-ray diffraction results.

Introduction

The heterocyclic ladder polymer poly(3,6-dioxo-1*H*-2,3,6,6a-tetrahydro-2,6a,11-triazaindeno[1,2-*b*]pyrene-2,8,9-triyl-1-ylidene-1-nitrilo) (BBL, 1)¹⁾ and the non-ladder polymer poly(5,8-dioxo-4*b*,5,8,8a-tetrahydro-4*b*,8a,13,16-tetraazadiinden[1,2-*a*:1',2'-*d'*]pyrene-3,10-diyl) (BBB, 2)²⁾ are of great interest because of their potential use as structural materials, their unique film-forming characteristics, and their



ability to form liquid crystalline solutions in strong acids. Recently these polymers were found to exhibit enhanced conductivity by 12 orders of magnitude when doped with suitable substances such as sulfuric acid and potassium naphthalide³⁾. These semi-crystalline polymers were found to have unique structures in the solid state, specifically fully conjugated and layered structures in two-dimensional arrays. X-ray diffraction studies and infrared analysis of both polymers⁴⁾ reveal compact interchain packing in solution as molecular aggregates, and in the bulk after being precipitated from solution. The present study attempts to elucidate the packing of these chains by means of calculations of intermolecular interactions.

Theory

The bond lengths and bond angles for the BBL (1) and BBB (2) repeat units were obtained from the crystal structures of polybenzimidazole (PBI) model compounds¹¹ and from naphthalene⁶. The Cartesian co ordinates and the atomic partial charge on each atom in the constitutional repeating units were determined by the geometry optimized (RHO)/2 (G) complete neglect of Differential Overlap method¹². In order to determine the optimal interchain packing distances between neighboring constitutional repeating units, calculations were made of the total intermolecular interaction energy E_c , which is the sum of the static or van der Waals energy E_{da} and the Coulombic energy E_c . Since both BBL (1) and BBB (2) are planar structures⁶, contributions from torsional potentials need not be included. The interactions between pairs of nonbonded atoms i and j separated by a distance r_{ij} were calculated from the Buckingham potential function^{8, 10},

$$E_{da} = \sum_{i < j} \{ A_{ij} \exp(-B_{ij}/r_{ij}) - C_{ij}/r_{ij}^6 \} \quad (1)$$

The attractive term coefficient C_{ij} was determined by applying the Slater Kirkwood equation in the slightly modified form¹⁰

$$C_{ij} = (3/2) e \left(\frac{h}{m^{1/2}} \right) \left(\frac{q_i q_j}{R_{ij}} \right)$$

where

$$R_{ij} = \left(\frac{q_i}{N_i} \right)^{1/2} + \left(\frac{q_j}{N_j} \right)^{1/2}$$

In these expressions, h is Planck's constant, where $h = h/(2\pi)$, m is the mass of an electron, e the electronic charge, q_i the atomic polarizability, and N_i the number of effective electrons surrounding the nucleus. The values of R for a like atom pair were taken from Scott and Scheraga¹¹ while values for an unlike pair were given by $R_{ij} = (R_i R_j)^{1/2}$. The values of A_{ij} were determined by minimizing Eq. (1) at $r_{min} = r_i + r_j$; r_i and r_j are the van der Waals radii of atoms i and j , respectively, and were obtained from the literature¹². In addition, different parameters were chosen for aliphatic and aromatic carbon atoms, with the latter being assigned an enhanced thickness in a direction perpendicular to the plane of the aromatic ring. The parameters used for the calculations are given in detail elsewhere^{9, 10}.

The Coulombic interaction energies were calculated from

$$E_c = \sum_{i < j} \frac{q_i q_j}{r_{ij}}$$

where q_i and q_j are, respectively, the partial charges on atom i and atom j , separated by a distance r_{ij} in a medium of bulk dielectric constant ϵ . The conversion factor ($K = 332.072$) was chosen to give E_c in units of kcal/mol. Four constitutional repeating units were chosen for the calculations in order to make the interaction energies (per repeating unit) as realistic as possible without making the calculations cumbersome. A Cartesian co ordinate system was chosen so that the x , y , and z axes lay along the length, width, and thickness, respectively, with the origin located at the center of mass of the constitutional repeating unit. The calculations were used to determine minimum energy arrangements of two parallel chains moved relative to one another along their axes.

Results and discussion

Interaction energies were calculated for a pair of constitutional repeating units of both BBL (1) and BBB (2) chains. For chains above one another the minimum intermolecular (non bonded) energy for BBL (1) was obtained at a displacement of $\Delta z =$


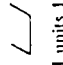
(chain packing in two aromatic heterocyclic polymers, one of which has a ladder structure 1549

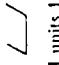
3.3 Å, $\Delta x = 3.3$ Å, and $\Delta y = 0.0$ Å. Similar calculations were carried out by considering chains side by side. The minimum interaction energy was obtained at the spacing $\Delta y = 8.8$ Å while the 2nd chain was displaced in the x direction by 5 Å.

The BBB polymer 2 was also examined to permit comparisons with BBL (1) and with experimental results. Correspondingly, the minimum energy displacements were $\Delta z = 3.3$ Å, $\Delta x = 3.0$ Å, and $\Delta y = 0.0$ Å for the chains above one another, and $\Delta y = 8.8$ Å, $\Delta x = 1.4$ Å, and $\Delta z = 0.0$ Å for the chains side-by-side. A summary of the results is given in Tab. 1. The results, specifically $\Delta z = 3.3$ Å and $\Delta y = 8.8$ Å are in good agreement with the results of X-ray diffraction studies^{2, 4}, which show the polymers to exhibit corresponding Bragg spacings in the neighborhood of 3.5 and 7.5 Å. These spacings in the z direction (i.e., 3.3 Å) are relatively small and are also close to the interplanar spacings of aromatic chains with planar or nearly planar structures⁶. For both BBL (1) and BBB (2) polymers, the shifting of the units out of register in the x direction was predicted for chains placed either above or alongside one another. Presumably, this reduces repulsive interactions between pairs of adjacent chains, and suggests the possibility of these chains forming nematic liquid-crystalline phases.

Tab. 1. Interchain spacings Δx , Δy , Δz , and energies (Coulombic E_c , van der Waals E_{da} , and total E) in minimum energy arrangement of polymers BBL (1) and BBB (2)

Polymer ^{a)}	Δx Å	Δy Å	Δz Å	E_c kcal/mol	E_{da} kcal/mol	E kcal/mol
1 a	3.3	0.0	3.3	0.9143	-38.2715	-37.3572
b	1.5	8.8	0.0	0.1789	4.1102	3.9313
2 a	3.0	0.0	3.3	0.8767	-45.9693	-45.0926
b	1.4	8.8	0.0	0.0377	-4.2650	-4.2273

^{a)} a: Chains above one another  at a spacing of Δz ; b: Chains alongside one another 

 at a spacing of Δy ; Δx is the displacement parallel to the chain axis

^{a)} In SI units 1 kcal = 4,184 kJ.

Model compounds of the ladder-type BBL polymer 1 resemble a layered and highly conjugated structure. On the other hand, the non ladder BBB (2) constitutional repeating units are linked together by single bonds about which they can exhibit rotational motions to some extent. The small spacings between constitutional repeating units in both BBL (1) and BBB (2) polymers support the view²⁾ that these chains could be aggregated to some extent, even in solutions of strong acids. As shown in Tab. 1, E_c is insignificant relative to the E_{da} , and also E_c is repulsive while E_{da} is attractive. Thus, the dielectric constant of the medium, on which E_c depends, has

little effect on the total intermolecular energy. This agrees with the similar predictions for benzobisoxazole and benzobisthiazole polymers¹⁰.

In some final calculations, both polymers were represented as having ellipsoidal sections with dimensions based on the calculated results given in Tab. I. Six ellipsoidal cylinders were closely packed around a central one. The densities for BBL (1) and BBB (2) polymers thus estimated¹⁰ were 1.56 and 1.37 g/cm³, respectively. The density of the BBB polymer 2 has not been reported, but the BBL polymer 1 has a density of 1.31 g/cm³ when cast as a film from solution. This suggests that the actual packing is simply less efficient than the perfect packing assumed in the calculations.

It is a pleasure to acknowledge the financial support provided by the *Air Force Office of Scientific Research (Chemical Structures Program, Division of Chemical Sciences)*, and several very helpful discussions with Dr. W. J. Welch of the University of Cincinnati.

- 1) I. E. Helminiak, R. C. Evers, *Preprints Polym. Mater. Sci. Eng.* **40**, 689 (1981).
- 2) I. E. Arnold, R. L. Van Deusen, *J. Appl. Polym. Sci.* **15**, 2035 (1971); I. E. Arnold, R. L. Van Deusen, *Macromolecules* **2**, 497 (1969).
- 3) G. Kim, *J. Polym. Sci., Polym. Lett. Ed.* **20**, 663 (1982).
- 4) G. C. Berry, T. G. Fox, *J. Macromol. Sci., Chem.* **3**, 1125 (1969).
- 5) M. Himmacher, W. W. Adams, A. V. Frattini, Report AFWAL-TR-82, March 1983.
- 6) "Tables of Interatomic Distances and Configuration in Molecules and Ions" edited by H. J. Bowen, L. F. Sutton, The Chemical Society, London 1958.
- 7) J. A. Pople, D. L. Beveridge, "Approximate Molecular Orbital Theory", McGraw-Hill, New York 1970.
- 8) P. J. Flory, "Statistical Mechanics of Chain Molecules", Wiley-Interscience, New York 1969.
- 9) W. J. Welch, D. Bhaumik, J. F. Mark, *Macromolecules* **14**, 947 (1981).
- 10) D. Bhaumik, W. J. Welch, H. H. Jaffe, J. F. Mark, *Macromolecules* **14**, 951 (1981).
- 11) R. A. Scott, H. A. Scheraga, *J. Chem. Phys.* **42**, 2209 (1965).
- 12) A. Bondi, *J. Phys. Chem.* **68**, 441 (1964).

BAND STRUCTURE ANALYSIS OF A BIS(OXALATO)PLATINATE COMPLEX

R. HAYAK, D. BLAUMIK and J. E. MARK

Department of Chemistry and the Polymer Research Center, The University of Cincinnati, Cincinnati, OH 45221 (U.S.A.)

(Received September 3, 1985; accepted January 9, 1986)

Abstract

The band structure of a bis(oxalato)platinate, $\text{Mg}_{0.82}\text{Pt}(\text{C}_2\text{O}_4)_2 \cdot 5 \cdot 3\text{H}_2\text{O}$ (MgDOP), has been analyzed by using extended Hückel calculations within the tight binding approximation. Results obtained on a sequence of three $\text{Pt}(\text{C}_2\text{O}_4)_2^{2-}$ groups indicate that the preferred conformation involves rotations of 60° between adjacent groups. The resulting staircase arrangement is in agreement with experiment. For partial oxidation states (from 0.1e to 0.6e) the total energy per unit cell was evaluated for different metal-metal distances $r_{\text{Pt-Pt}}$. Initial increase in degree of partial oxidation results in reduction of $r_{\text{Pt-Pt}}$ to ~2.8 Å, but with further increase $r_{\text{Pt-Pt}}$ increases again. A partial oxidation $x = 0.35e$ for Pt was calculated for $r_{\text{Pt-Pt}} = 2.815$ Å, the experimentally observed value.

Introduction

The partially oxidized quasi one dimensional cyano platinates [1-4], bis(oxalato)platinate complexes [5-7] and halocarbonylhydride compounds [8] have been much studied by X ray crystallography and neutron diffraction techniques because of their metallic conductivity along the columnar chain axis. Reis and Peterson [8] have reviewed the relationships between structural properties, metal-metal separation, ligand conformation and the non integral partial oxidation state of the metal atom in such complexes. These highly conducting inorganic compounds exhibit non stoichiometric molecular formulae and their (anisotropic) conductivities are reported to be high [9], suggesting the possibility of metallic behavior.

Evidence from crystallographic analysis [5-7] shows that the structures of $\text{K}_2\text{Pt}(\text{C}_2\text{O}_4)_2 \cdot 5 \cdot 3\text{H}_2\text{O}$ (KDOP) and $\text{Mg}_{0.82}\text{Pt}(\text{C}_2\text{O}_4)_2 \cdot 5 \cdot 3\text{H}_2\text{O}$ (MgDOP) complexes are similar. Both experimental findings [5] and intermolecular backbonding calculations [10] reveal that the oxalate ligands in the KDOP complex are staggered by 45° with respect to ligands directly above and below them along the chain axis. It has also been suggested [10]

that there might be only a small energy difference between the 15 and 60 conformations in this complex. In the case of MgDOP, X-ray diffraction results [7] indicate that the adjacent oxalate ligands are rotated 60° with respect to one other. However, in both cases an average inter-planar spacing of 2.815 Å has been observed.

The recent successes [11, 12] in using the extended Hückel method in studying similar metal complexes encouraged investigation of the structure of $\text{Pt}(\text{C}_2\text{O}_4)_2$, particularly with regard to the oxidation state of Pt.

Theory

In the extended Hückel method within the tight-binding approximation [13, 14], the n th crystal orbital $\psi_n(\mathbf{k})$ is defined as

$$\psi_n(\mathbf{k}) = \frac{1}{N^{1/2}} \sum_{\mathbf{r}} \exp(i\mathbf{k} \cdot \mathbf{r}) \psi_n(\mathbf{r}) \quad (1)$$

where N is the total number of cells explicitly used in computation, \mathbf{k} is the wave vector, \mathbf{r} is the total number of atomic orbitals in a cell and R_j is the one-dimensional position vector given by $R_j = ja$ (a being the translation vector of the crystal repeat unit). The factor C_{np} is the expansion coefficient of the linear combination and $\{X_p\}$ is the set of basis functions of Slater form. In the present calculation all the valence atomic orbitals of Pt, C and O atoms are included and the lattice sums are carried out to second nearest neighbors. The eigenvalues $E_n(\mathbf{k})$ are obtained from the eigenvalue equation

$$H(\mathbf{k})C_n(\mathbf{k}) - S(\mathbf{k})C_n(\mathbf{k})E_n(\mathbf{k}) \quad (2)$$

where $H(\mathbf{k})$ and $S(\mathbf{k})$ are the usual Hamiltonian and overlap matrices.

The set of all energy bands obtained from the secular eqn. (2) describes the band structures of the one-dimensional complex chain. Since the plot of $E_n(\mathbf{k})$ against \mathbf{k} would be symmetrical about the center of the first Brillouin zone, the calculations were carried out for only one half ($0 \leq \mathbf{k} \leq 0.5\mathbf{K}$, where $\mathbf{K} = 2\pi/a$ is the reciprocal lattice vector) of the energy band.

The geometric parameters such as bond lengths and bond angles were obtained from a single crystal X-ray study of MgDOP by Krogmann [7]. The Hückel parameters for Pt, C and O atoms were obtained from the literature [11, 12]. In order to determine the most stable conformation of the bis(oxalato)platinate, the total energy $\langle E \rangle$ per unit cell was calculated from the band structure as a function of the dihedral angle between adjacent oxalate moieties and the metal-metal separation. The equation employed was [11, 12]

$$\langle E \rangle = \frac{1}{K} \int_K E_n(\mathbf{k}) d\mathbf{k} \quad (3)$$

where $E_n(\mathbf{k})$ is the total energy at \mathbf{k} and, according to the extended Hückel method,

$$E_n(\mathbf{k}) = 2 \sum_{\text{occupied}} E_n(\mathbf{k}) \quad (4)$$

In order to determine the oxidation state of the Pt, the energy loss per unit cell was calculated for various degrees of partial oxidation ($x = 0.1, 0.2, 0.3, 0.4, 0.5, 0.6e$) of the upper most filled valence band of Pt. Using the integrated density of states $n(E)$ for the valence band, the Fermi level E_F or Fermi momentum K_F was obtained. Here $n(E)$ is defined as the number of electrons per unit cell when the energy levels are filled up to E . Spectrally,

$$n(E) = \frac{1}{V_b} \int_{E_b}^E g(E) dE \quad (5)$$

where E_b is the bottom of the valence band. The quantity $g(E)$, the density of states, is given by

$$g(E) = \frac{1}{\pi} \frac{d\mathbf{k}}{dE} \quad (6)$$

for one-dimensional systems.

Results and discussion

The first set of calculations was carried out for a pair of $\text{Pt}(\text{C}_2\text{O}_4)_2$ subunits, such as parts I and II of Fig. 1. Values of $\langle E \rangle$ were calculated as functions of the distance between Pt atoms and the dihedral angle ϕ_1 between the axes of the two ligands (with $\phi_1 = 0^\circ$ corresponding to the eclipsed arrangement). At fixed $r_{\text{Pt-O}}$ the reciprocal lattice vector \mathbf{K} is a constant and $\langle E \rangle$ is directly proportional to the area enclosed by the curve in a plot of $E_n(\mathbf{k})$ against \mathbf{k} [12]. The results for $r_{\text{Pt-O}} = 2.815 \text{ Å}$, the experimentally observed value [7], are shown in Fig. 2. They indicate that the lowest energy (preferred) conformation corresponds to $\phi_1 = 90^\circ$, which is in disagreement with the experimental value, 45° or 60° [5, 7].

In order to make the results more realistic, all three units shown in Fig. 1 were included in a subsequent calculation. The two dihedral angles ϕ_1 and ϕ_2 were set equal to one another, with counter clockwise rotations ranging from 0 to 90° . The distance $r_{\text{Pt-O}}$ was varied from 2.5 to 4.0 Å in increments of 0.1 Å . Figure 3 shows a typical plot of $E_n(\mathbf{k})$ versus \mathbf{k} , spectrally that obtained for $r_{\text{Pt-O}}$ set equal to 2.815 Å . The predicted preferred conformation now corresponds to $\phi_1 = \phi_2 = 60^\circ$, in excellent agreement with experiment [7]. The conformation $\phi_1 = \phi_2 = 15^\circ$ was found to be 1.9 kcal/mol higher in energy.

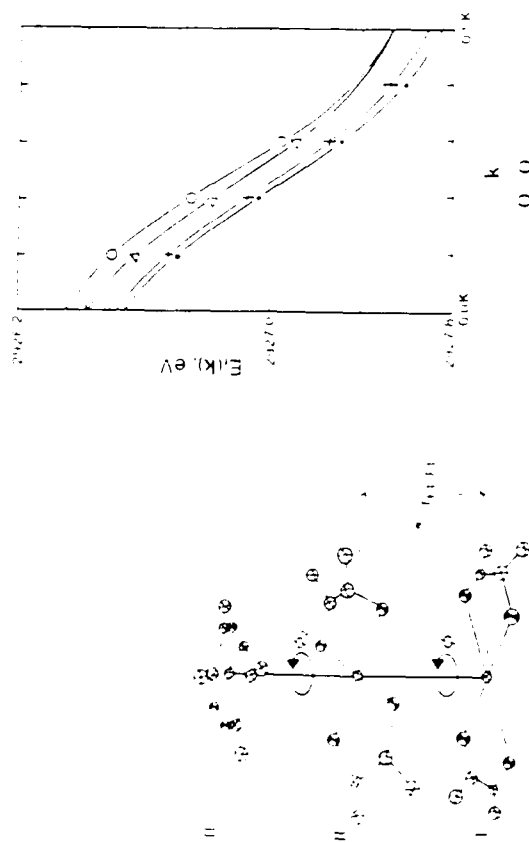


Fig. 1. Sketch of bis(oxalato) complex consisting of three $\text{Pt}(\text{OC}(\text{O})_2)_2$ repeat units. The partially filled circles represent the chelated oxygen atoms.

Fig. 2. Dependence of $E_1(k)$ on k for two $\text{Pt}(\text{C}_2\text{O}_4)_2$ units, at $r_{\text{Pt-Pt}} = 2.815 \text{ \AA}$, the experimentally observed separation [7]. The rotational angle ϕ_1 had the values 0° (\circ), 30° (Δ), 60° (\bullet), 75° (\times) and 90° (\odot).

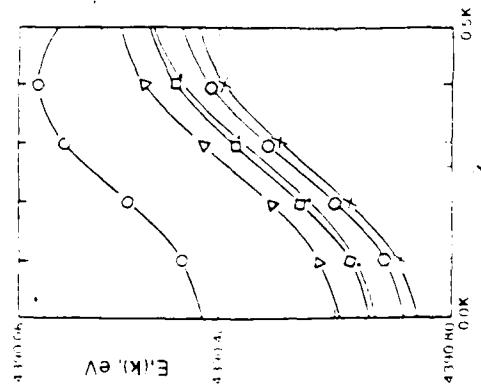


Fig. 3. Dependence of $E_1(k)$ on k for three units, at $r_{\text{Pt-Pt}} = 2.845 \text{ \AA}$. The rotational angles were 0° (\circ), 30° (Δ), 45° (\square), 60° (\bullet), 75° (\times) and 90° (\odot).

In order to predict the separation between metal atoms, $E_1(k)$ was calculated as a function of k and $r_{\text{Pt-Pt}}$ at the preferred angles $\phi_1 = \phi_2 = 60^\circ$. Typical results are shown in Fig. 4. Since k is not constant in these calculations, it was necessary to calculate $E_1(k)$ for each value of $r_{\text{Pt-Pt}}$ from eqn. (3), expressing $E_1(k)$ as a polynomial in k . The total energy per unit cell for the unoxidized $\text{Pt}(\text{C}_2\text{O}_4)_2$ chain was then determined for each value of $r_{\text{Pt-Pt}}$ in the range 2.5 to 4.0 \AA . The results, shown in Fig. 5, indicate that the energy decreases monotonically with increase in $r_{\text{Pt-Pt}}$. The absence of a bound state (minimum) is of course in disagreement with observation. It is presumably due to the fact that the calculations pertain to Pt with an oxidation state of +2, whereas the metallic character of the chain suggests additional partial oxidation of Pt^{+2} to $\text{Pt}^{+2.5x}$.

The above model was modified to take into account this partial oxidation of Pt. Electrons were removed from the highest occupied valence band (of d_{yz} character) in order to produce a partially filled valence band. The partial oxidations $x = 0.1, 0.2, 0.3, 0.4, 0.5$, and 0.6 in $\text{Pt}^{+2.5x}$ correspond to the removal of x electrons per metal atom or $3x$ electrons per unit cell. For various non integral oxidations, eqn. (3) was evaluated analytically with the corresponding values of E_1 , where $E_1(k)$ for the valence d_{yz} band was

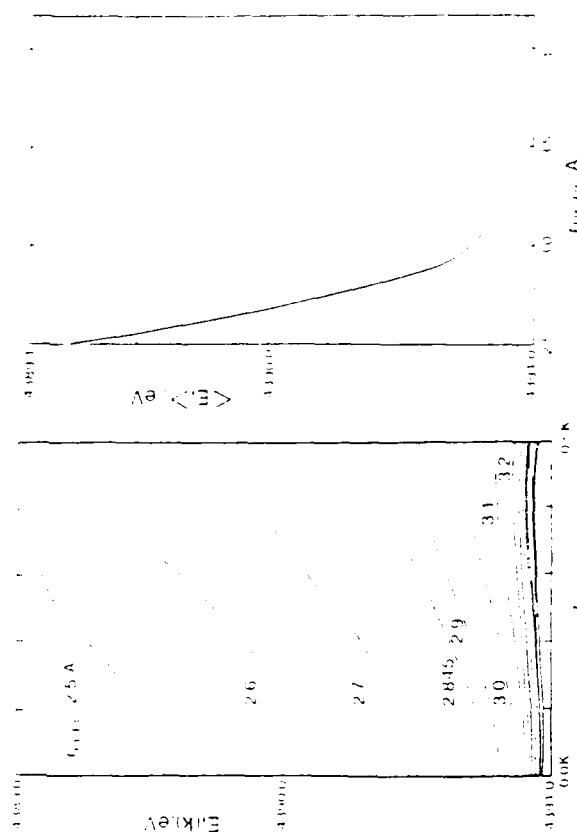


Fig. 4. Dependence of $E_1(k)$ on k at $\phi_1 = \phi_2 = 60^\circ$, for the specified values of the Pt-Pt separation. The near continuum of curves at the bottom of the figure corresponds to additional, monotonic decreases in $E_1(k)$ as $r_{\text{Pt-Pt}}$ increases from 3.3 to 4.0 \AA .

Fig. 5. The total energy per unit cell shown as a function of the Pt-Pt separation.

determined by a polynomial fit. In each case $n(E)$ was normalized so that it was equal to two electrons at the top of the d_{xy} band. The valence d_{xy} band and its integrated density of states are shown in Fig. 6 for $r_{Pt-Pt} = 2.845$ Å. The lines shown establish the correlation between the partial oxidation x and the Fermi momentum k_F . From the band structures, it was found that, up to partial oxidation of $x = 0.66$, electron removal occurred from the d_{xy} band. With the known values of Fermi momenta k_F , the energy loss per unit cell caused by electron removal was calculated. This permits estimation of the modified total energy per unit cell (E_t) for partially oxidized states at different values of r_{Pt-Pt} . These results are illustrated in Fig. 7, which shows that the partially oxidized states of $Pt(C_2O_4)_2^{2-}$ are bound. This also indicates that with initial increase in degree of partial oxidation, the equilibrium value of r_{Pt-Pt} decreases to a final value of ~ 2.8 Å, but with further increase r_{Pt-Pt} increases again. This minimum value of ~ 2.8 Å for r_{Pt-Pt} with the corresponding oxidation state of 2.35 for Pt is very similar to the experimental results of various complexes of $Pt(C_2O_4)_2^{2-}$ [15, 16] and also is in accord with theoretical predictions based on Pauling's empirical equations [17, 18] utilizing fractional bond orders and valences. The increase in the value of r_{Pt-Pt} for further increase in degree of partial oxidation is probably due to the repulsion between the adjacent positively charged Pt ions and more significantly due to the repulsions between the oxalate ligands for their typical structure and arrangement.

In conclusion, the band structure analysis presented here confirms the staircase conformation as well as the partial oxidation of Pt in its bis(oxalato) complex.

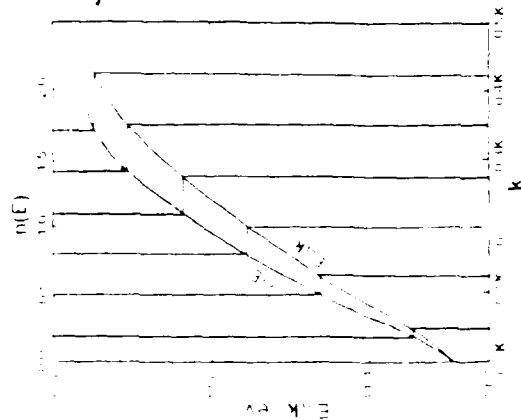


Fig. 6. The d_{xy} band and its integrated density of states at $r_{Pt-Pt} = 2.845$ Å. The lines show the correlation between x and the Fermi momentum k_F .

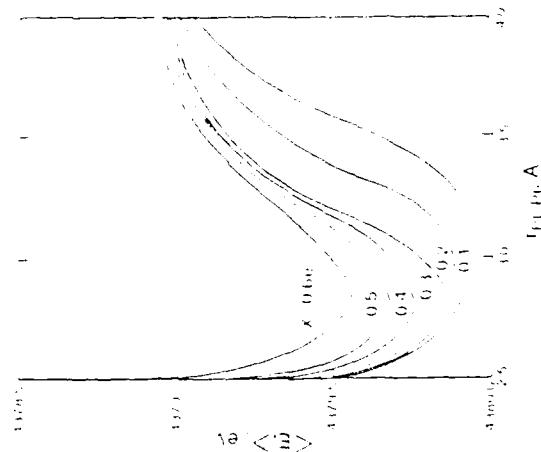


Fig. 7. Typical results showing the total energy per unit cell for the complex $Pt(C_2O_4)_2^{2-}$ with partially oxidized Pt^{2+} ions.

Acknowledgements

It is a pleasure to acknowledge financial support from the Air Force Office of Scientific Research (Chemical Structures Program, Division of Chemical Sciences).

References

1. J. M. Williams, M. Iwata, S. W. Peterson, K. A. Leshe and H. J. Copenhagen, *Phys. Rev. Lett.*, **34** (1975) 1653.
2. H. J. Deiseroth and H. Schullz, *Phys. Rev. Lett.*, **33** (1974) 963.
3. J. M. Williams, J. L. Peterson, H. M. Gerdes and S. W. Peterson, *Phys. Rev. Lett.*, **34** (1974) 1079.
4. C. Peters and C. F. Eagen, *Inorg. Chem.*, **15** (1976) 782.
5. A. H. Reis, Jr., S. W. Peterson and S. C. Liu, *J. Am. Chem. Soc.*, **98** (1976) 7839.
6. R. Mader and K. Krogmann, *Z. Anorg. Allg. Chem.*, **332** (1964) 247.
7. K. Krogmann, *Z. Anorg. Allg. Chem.*, **338** (1968) 97.
8. A. H. Reis, Jr. and S. W. Peterson, *Ann. N. Y. Acad. Sci.*, **313** (1978) 560.
9. F. N. LeCone, M. J. Almut and J. H. Perlstein, *Inorg. Nucl. Chem. Lett.*, **5** (1971) 173.
10. A. H. Reis, *Inorg. Nucl. Chem. Lett.*, **14** (1977) 231.
11. M. H. Whangbo and R. Hoffman, *J. Am. Chem. Soc.*, **100** (1978) 6093.

- 12 D. Bhaumik and J. E. Mark, *Synth. Met.*, **6** (1983) 299
- 13 J. Delhalle, in J. M. André and J. Ladik (eds.), *Electronic Structure of Polymers and Molecular Crystals*, Plenum Press, New York, 1974, p. 53
- 14 R. Hoffman, *J. Chem. Phys.*, **39** (1963) 1397
- 15 K. Krogmann, *Angew. Chem. Int. Ed. Engl.*, **8** (1969) 25
- 16 K. Krogmann and P. Dodel, *Chem. Ber.*, **99** (1966) 3402 and **99** (1966) 3408
- 17 L. Pauling, *The Nature of the Chemical Bond and the Structure of Molecules and Crystals*, Cornell University Press, Ithaca, NY, 1960, pp. 398-404.
- 18 L. Pauling, *J. Am. Chem. Soc.*, **69** (1947) 512

Odd-even variations in the melting points of some ethylene polyesters

D. Jhaumik*, J. E. Mark

Department of Chemistry and the Polymer Research Center, The University of Cincinnati, Cincinnati, Ohio 45221, USA

(Date of receipt: July 8, 1985)

SUMMARY

Molecular mechanics calculations on poly(ethylene adipate), poly(ethylene pimelate), and poly(ethylene suberate) indicate that the odd-even variation in the melting points of the polyesters $\{O(CH_2)_xOC(OCH_2)_yCO\}_n$ with the number y of methylene groups is due to differences in packing of the chains in the crystalline state.

Introduction

The interpretation of the melting point T_m of a polymer in terms of its enthalpy ΔH_m and entropy of fusion ΔS_m is obviously of interest with regard to the influence of structure on melting behavior^{1,2}. For example, a low melting point may be due to a low value of ΔH_m or to a high value of ΔS_m . It is therefore of considerable importance to study these two thermodynamic properties¹⁻⁹. Molecularly, these quantities are related to interchain interactions and chain flexibility, respectively, and both can be theoretically estimated^{10,11}.

The linear aliphatic polyesters $\{O(CH_2)_xOC(OCH_2)_yCO\}_n$ are interesting in this regard. They have characteristically low melting points which generally increase as the spacing between functional groups increases^{1,9}. This indicates that the entropy of fusion ΔS_m could significantly decrease with increasing $(x+y)$. From Tab. I, however, it is observed that at least for ethylene polyesters ($x=2$) the entropy change for either even or odd y is higher for the higher members; the increase in the melting point is therefore due to the higher rate of increase of the enthalpy of fusion. Further-

Tab. I. Melting points T_m and enthalpies and entropies of fusion^{a)} ΔH_m and ΔS_m of polyesters $\{O(CH_2)_2OC(OCH_2)_yCO\}_n$ with different y

Polymer	y	T_m K	$10^4 \Delta H_m$ kJ · mol ⁻¹	$10^4 \Delta S_m$ kJ · K ⁻¹ · mol ⁻¹
Poly(ethylene adipate)	4	338 ⁽⁷⁾ , 326 ⁽¹²⁾	2 100 ⁽⁷⁾ , 2 170 ⁽¹²⁾	6.2 ⁽⁷⁾ , 6.3 ⁽¹²⁾
Poly(ethylene pimelate)	5	309 ⁽¹²⁾ , 302 ⁽¹³⁾	2 708 ⁽¹²⁾	8.8 ⁽¹²⁾
Poly(ethylene suberate)	6	348.5 ⁽⁷⁾ , 336 ⁽¹²⁾	2 205 ⁽⁷⁾ , 2 186 ⁽¹²⁾	6.3 ⁽⁷⁾ , 6.5 ⁽¹²⁾
Poly(ethylene azelate)	7	320 ⁽¹²⁾ , 319 ⁽¹⁴⁾	3 363 ⁽¹²⁾	10.5 ⁽¹²⁾
Poly(ethylene sebacate)	8	356 ⁽⁷⁾ , 356 ⁽¹²⁾	2 284 ⁽⁷⁾	6.4 ⁽⁷⁾

a) Per mol of skeletal atoms.

0025-116X/86/0013-00

more, the melting points of these polyesters go through maxima and minima with increase in v , with even values giving the larger values of T_m .^{15,16} This odd-even effect is also observed for various other polymers.^{17,18} Since the entropy of fusion should not vary much in going from an even to an odd member, it is expected¹⁹ that this lowering of the melting points of odd-ethylene polyesters is due to differences in chain packing.

The goal of the present study is to employ the molecular mechanics method to study interchain interactions in poly(ethylene adipate) (PEA, $y = 4$), poly(ethylene pimelate) (PEP, $y = 5$), and poly(ethylene suberate) (PES, $y = 6$). The specific purpose is to investigate whether the interaction energy, related to the enthalpy of fusion, can at least qualitatively explain the variation of melting points with structure in these polymer chains.

Method of calculation

Potential energy functions. The total intermolecular interaction energy v is taken to be the sum

$$E = \sum_{i,j} V_{ij} \quad (1)$$

of the interaction energies between pairs of atoms i and j located on different chains and separated by the distance r_{ij} . Each separate contribution was calculated from the equation^{18,19}

$$V_{ij} = a_{ij} \exp(-b_{ij} r_{ij}) - c_{ij} \left(\frac{1}{r_{ij}^6} + k_{ij} q_i q_j / (r_{ij}^n) \right) \quad (2)$$

in which the first two terms (the "Buckingham potential function") represent the van der Waals or steric interactions, and the last term the Coulombic interactions. The parameters a_{ij} , b_{ij} , and c_{ij} in the Buckingham potential function differ of course for different atom pairs. The parameter c_{ij} in the attractive term was calculated from atomic polarizabilities²⁰ by application of the Slater-Kirkwood equation²⁰. The value of b_{ij} for a like atom pair was taken from Scott and Scheraga²¹, while the value for an unlike pair was given by the geometric mean $b_{ij} = (b_i b_j)^{1/2}$. The values of b and c thus obtained are essentially those used in a number of previous studies of conformational energies^{18,20}. The corresponding values of the parameter a were then determined by minimizing the first two terms of Eq. (2) at $r = R_{\text{min}} = R_0 + R_1$, where R_0 and R_1 are the van der Waals radii²⁰ of the interacting atoms. The resulting values of P_{min} , a , b , and c are given in Tab. 2. The Coulombic contributions were calculated from the last term of Eq. (2), in which $k = 1/380.5$ is a conversion factor giving energies in kcal/mol when q_i and q_j are in fractions of the electronic charge. The dielectric constant ϵ was taken to be 2.0, as it generally is in calculations of conformational energies.^{18,20} The partial charges q on the chain atoms were obtained using the quantum mechanical CNDO-2 (complete neglect of differential overlap) method²². For each polymer, the calculations were carried out on sequences having increasing numbers of repeat units, until constant values were obtained for the central unit in the sequence.

a) Systematic IUPAC nomenclature: $y = 4$, poly(oxoethyleneoxyadipoxy); $y = 5$, poly(oxoethyleneoxypimeloy); $y = 6$, poly(oxoethyleneoxysuberoy).

Tab. 2. Minimum van der Waals distances $r = R_{\text{min}}$ and parameters a , b , and c for the Buckingham potential functions (cf. Eq. (2))

Atom pair	R_{min} nm	a kJ mol ⁻¹	b nm ⁻¹	c kJ mol ⁻¹
H-H	0.24	29.41	45.4	189.1
C-C	0.34	2365.09	45.9	1518.8
C-O	0.34	3447.06	45.9	2412.8
O-O	0.40	519.01	45.9	908.8
C ^a -C ^b	0.30	881.34	45.9	173.9

^a Carbonyl carbon

^b Carbonyl oxygen

Structural geometry. The required structural information for the PEA and PES chains was obtained from the reported²³ crystal structure analysis data. It has been pointed out by Jones and Bunn²⁴ that the carbon-carbon chain in the $-\text{C}(\text{OCH}_2)_4\text{CO}-$ region of these polyesters is nearly parallel to the fiber axis. No structural information for PEP is available in the literature. In the present study, however, the geometry of PEP was assumed to be the same as that for PEA but with an added CH_2 group. The fiber repeat unit (of length 2.594 nm) of PEP contains two of its constitutional repeating units. For PEA and PES, however, the fiber length (1.172 nm for PEA, 1.428 nm for PES) are the same as their respective constitutional repeating unit lengths.

Calculations of intermolecular energies. As is known from previous studies^{18,19,25-30}, calculations of intermolecular interaction energies rapidly become impracticable as the number of atoms increases, particularly when this increase is due to an increase in the number of chains (since this increases both the number of interactions and the number of relative chain locations to be investigated). In addition, calculations of this type in their present state are really only semi-quantitative. The model¹⁸ employed here, however, (although necessarily rather simple) should nonetheless be very useful for elucidating the odd-even effect on the melting points of the above ethylene polyesters. The calculations were based on a pair of polyester chains, in their crystalline state configurations and maintained parallel to one another. The shorter chain in the pair was one fiber repeat unit long and the second chain was made considerably longer so as to minimize end effects; it was 4 periods long in all the present cases. The shorter chain was moved relative to the longer in increments of 0.05 nm in the three directions (x , y , z) of a Cartesian coordinate system (fixed on the longer chain, having x -axis along the axis of the chain, y -axis along the width, and z -axis along the thickness of the chain) and also rotated (ϕ) in increments of 10° about its axis. Intermolecular energies in kJ/mol were calculated as described above for each relative location and this was repeated for each polyester. To eliminate the effects of fiber repeat units of different lengths for different polyesters, the total interaction energies were normalized by dividing them by their number of skeletal atoms.

Results and discussion

The lowest values of the energy (maximum attractions) and the corresponding relative orientations for PEA, PEP, and PES chains in their crystalline state configurations are given in Tab. 3. Interchain attraction decreases in going from PEA to PEP and then again increases to PES. This clearly indicates that the origin of the zig

Tab. 3. Minimum values of the interaction energy F_{\min} and the corresponding relative orientations Δx along the axis, Δy along the width, and Δz along the thickness of the chain and also the rotation angle $\Delta\phi$ between two polyester chains

Polymer ^{a)}	F_{\min} ^{b)}	Δx nm	Δy nm	Δz nm	$\Delta\phi$
PFA	5.08	1.05	0.0	0.35	5°
PEP	5.02	0.35	0.1	0.35	15°
PFS	6.19	1.30	0.0	0.35	5°

^{a)} PFA: poly(ethylene adipate); PEP: poly(ethylene pimelate); PFS: poly(ethylene suberate).

^{b)} F_{\min} in kJ per mole of skeletal atoms.

zag nature of the melting point variation with number of backbone carbon atoms is due to the variation of the interchain interactions. It is also clear from Tab. 3 that this variation is due to the difference in chain packing. For the even polyesters PFA and PFS the packing is very similar, the difference between the shifts (Δx) along the axial direction being due to the difference in their repeat lengths (1,122 nm for PFA, 1,428 nm for PFS). The two PFA and PFS chains are packed one above the other, separated by 0.35 nm, with a relative shift of approximately 0.12 nm along the axis. This relative shift is approximately half the distance between next nearest neighboring methylene groups in these polyesters. From the calculated results it is also seen that the interaction energy in PFS is higher than in PFA, which explains the increase in melting point when going from poly(ethylene adipate) to poly(ethylene suberate) to poly(ethylene sebacate) (Tab. 1). The percentage increase in interchain interactions for PFA to PFS is roughly the same as the percentage increase in enthalpy of fusion (Tab. 1).

For the odd polyester, PEP, the relative shift Δx (0.35 nm) along the axis is different from that of the even polyesters. Also different is its packing arrangement (Tab. 3) when the chains are shifted alongside one other.

It would be extremely difficult to relate the interchain interactions and relative orientations calculated using this simplified model to the experimentally determined thermodynamic data¹²⁻¹⁶ and the crystal structures²⁰. However, the calculated results explain, at least qualitatively, the origin of the melting point variation in these polymers. It is also to be noted that, as was found in previous cases^{6,10}, only a small fraction (~3%) of the total interaction energies is due to the contributions from Coulombic interactions.

For the pairs of chains alongside one another, the spacing Δy (for $\Delta z = 0$) is predicted to be approximately 0.35 nm for all three polyesters. This, together with the above information, permits estimation of the densities of these polyesters in the crystalline state. The polymers were represented as having elliptical cross sections, with semi-major and semi-minor axes of 0.175 nm and 0.225 nm, respectively, and with six such ellipses closely packed around a central ellipse. The densities thus

estimated are given in Tab. 4. It is seen that although the calculated densities slightly over estimate their corresponding experimental values⁶, their variation from PFA to PFS is close to that observed.

Tab. 4. Calculated and experimentally determined densities of poly(ethylene adipate) (PFA), poly(ethylene pimelate) (PEP), and poly(ethylene suberate) (PFS) chains in the crystalline state

Polymer	$10^{-3} \times \text{density in kg/m}^3$	
	calc.	exptl.
PFA	1.508	1.364 ⁶⁾
PEP	1.477	1.278 ¹²⁾
PFS	1.442	1.244 ⁶⁾

It is a pleasure to acknowledge the financial support provided by the Air Force Office of Scientific Research through Grant AFOSR 83-0027 (Chemical Structures Program, Division of Chemical Sciences).

- ¹⁾ J. F. Flory, "Principles of Polymer Chemistry", Cornell University, Ithaca, N.Y., U.S.A. 1953.
- ²⁾ I. Mandelkern, "Crystallization of Polymers", McGraw-Hill, New York 1964.
- ³⁾ R. D. Evans, H. R. Mighetto, P. J. Flory, *J. Am. Chem. Soc.* **72**, 2018 (1950).
- ⁴⁾ I. Mandelkern, R. R. Garrett, P. J. Flory, *J. Am. Chem. Soc.* **74**, 3929 (1952).
- ⁵⁾ P. J. Flory, H. D. Reddon, F. H. Kefer, *J. Polym. Sci.* **28**, 151 (1958).
- ⁶⁾ S. Y. Hobbs, F. W. Billmeyer, Jr., *J. Polym. Sci., Part A 2*, **7**, 1119 (1969).
- ⁷⁾ S. Y. Hobbs, F. W. Billmeyer, Jr., *J. Polym. Sci., Part A 2*, **8**, 1387 (1970).
- ⁸⁾ S. Y. Hobbs, F. W. Billmeyer, Jr., *J. Polym. Sci., Part A 2*, **8**, 1395 (1970).
- ⁹⁾ M. Gilbert, F. J. Hybert, *Polymer* **15**, 407 (1974).
- ¹⁰⁾ D. Blaumark, J. F. Mark, *Macromolecules* **14**, 162 (1981).
- ¹¹⁾ A. E. Tonelli, *J. Chem. Phys.* **54**, 4637 (1971); A. E. Tonelli, *ibid.* **56**, 5533 (1972).
- ¹²⁾ K. Urbaniak, V. H. Karl, A. Allmeyer, *Fur. Polym. J.* **14**, 1045 (1978).
- ¹³⁾ V. V. Korshak, S. V. Vinogradova, E. S. Vlasova, *Bull. Acad. Sci. USSR, Div. Chem. Sci. (Engl. Transl.)* **3**, 8919 (1954).
- ¹⁴⁾ Y. Iwakura, Y. Tanaka, S. Uchida, *J. Appl. Polym. Sci.* **5**, 108 (1961).
- ¹⁵⁾ C. Ober, J. J. Jin, R. W. Lenz, *Polym. J.* **14**, 9 (1982).
- ¹⁶⁾ A. C. Griffin, T. R. Britt, *J. Am. Chem. Soc.* **103**, 4957 (1981).
- ¹⁷⁾ A. Rosiello, A. Sinigo, *Makromol. Chem.* **183**, 895 (1982).
- ¹⁸⁾ P. J. Flory, "Statistical Mechanics of Chain Molecules", Wiley Interscience, New York 1969.
- ¹⁹⁾ A. J. Hopfinger, "Conformational Properties of Macromolecules", Academic Press, New York 1973.
- ²⁰⁾ J. A. A. Kerkhof, "Chemical Constitution", Elsevier, New York 1958.
- ²¹⁾ K. S. Pitzer, *Adv. Chem. Phys.* **2**, 49 (1959).
- ²²⁾ R. A. Scott, H. A. Scheraga, *J. Chem. Phys.* **42**, 2209 (1965); R. A. Scott, H. A. Scheraga, *ibid.* **45**, 2091 (1966).
- ²³⁾ J. A. Momany, J. M. Cantow, R. F. McConnel, H. A. Scheraga, *J. Phys. Chem.* **70**, 1505 (1974).

- ⁹ A. Bondi, *J. Phys. Chem.*, **68**, 441 (1964)
- ¹⁰ J. A. Pople, D. L. Beveridge: "Approximate Molecular Orbital Theory", McGraw Hill, New York 1970
- ¹¹ A. Turner-Jones, C. W. Bunn, *Acta Crystallogr.*, **15**, 105 (1962)
- ¹² H. Tadokoro: "Structure of Crystalline Polymers", Wiley Interscience, New York 1979
- ¹³ D. F. Williams, *J. Chem. Phys.*, **47**, 4680 (1967)
- ¹⁴ R. L. McCullough, *J. Macromol. Sci., Phys.*, **9**, 97 (1974)
- ¹⁵ P. Dauber, A. J. Hagler, *Acc. Chem. Res.*, **13**, 105 (1980)
- ¹⁶ D. Bhaumik, W. J. Welsh, H. H. Jaffe, J. E. Mark, *Macromolecules*, **14**, 951 (1981)

Index

Volume 1 Number 6

September 1987

<i>Design automation techniques to play increasing role in materials science research</i>	1
<i>Battelle-Richland brings molecular approaches to polymer design</i>	1
<i>Welsh, Mark examine polymers as high-performance materials</i>	2
<i>Biosym consortium to improve force field calculation databases</i>	2
<i>High Sierra Group completes proposals for CD ROM standards</i>	3
<i>Pierce Nordquist to fund new materials ventures</i>	3
<i>Feature Supplement: Modeling in inorganic chemistry</i>	4
<i>DEC announces changes for MicroVAX II, VAXstations</i>	8
<i>STN International adds Japanese Partner</i>	9
<i>Meetings</i>	10
<i>Literature Review: Laboratory PC Users Group launches newsletter</i>	16
<i>Professional Opportunities</i>	17

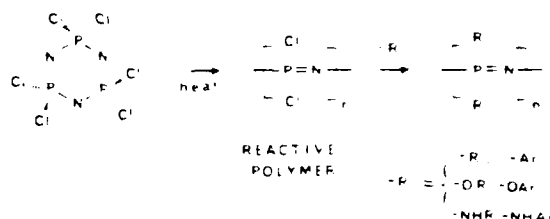
A Molecular Approach to the Design and Production of Inorganic Polymers

The term "inorganic polymers," implies an interest in looking beyond the second-row nonmetals of the periodic table (namely N, C, O) for polymer-chain elements which will provide new classes of materials to overcome limitations now posed by current so-called "organic polymers." Despite the enormous success of organic polymers in generating materials with new and desirable properties, some old materials problems still re-

main, and advanced technologies are now placing exotic and extreme demands upon polymer materials. Among the old problems are the needs for fire-retardant, non-toxic high molecular weight fluids, plastics and elastomers. The demand for elastomeric sealing materials (such as O-rings and gaskets), which remain flexible at very low temperatures while resisting thermal degradation at high temperatures, has not yet been met.

Continued on page 5

Figure 1:
Phosphazene
inorganic polymers
require substitution
of functional groups
on a reactive poly-
meric intermediate.



New Computational Tools Herald Promising Advances in Materials Design Research

In this issue **CDA News** examines programs available for computational studies in the general research area of materials sciences. It is not our intention to survey all the work ongoing in solid state studies, but rather to look at the practicality and utility of the computational tools available for commercial application. To this end, a brief look at the important problems being studied seems desirable.

Amorphous semiconductors have been the subject of numerous computational investigations in recent years. In particular, amorphous silicon has received attention because it is the simplest covalently bonded amorphous solid and serves as an important prototype for investigating the disordered solid state.

Continued on page 9

Statement of Editorial Policy

It is the express editorial policy of **Chemical Design Automation News** to publish objective information on matters of technical interest relating to the use of computer automation techniques in chemical and engineered materials research. In accordance with this policy, we welcome participation from all individuals and institutions involved in the field

This fall **CDA News** will publish a special feature which describes and assesses molecular modelling graphics systems. We invite you, our readers, to participate by submitting useful criteria you use to evaluate such software. We will incorporate your standards and suggestions in this study. Prompt responses should be sent to Barbara F. Graham, **Chemical Design Automation News**, P.O. Box 1597, Waltham, MA 02254.

CDA News is interested in publishing your experiences where research use of modelling tools are believed to represent the determining factor in the identification of structures exhibiting desired properties. Contact Barbara F. Graham.

Chemical Design Automation News

is published monthly.
ISSN 0886-6716.

Publisher: Luiz Aguiar
Editor: Barbara F. Graham
Chief Science Editor: Frank A. Momany
Production: James A. Woino
Address: P.O. Box 1597
Waltham, MA 02254
Subscription Rates: \$195 U.S.;
\$245 Canada, Mexico and Overseas;
\$45 Academicians.

Copyright 1986. No part of this publication may be reproduced in any form without the written permission of **CDA News**.

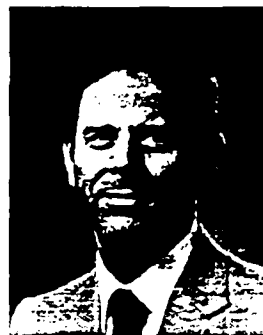
Theoretical Studies on Liquid-Crystalline Rodlike Polymers Used as High-Performance Materials

Synthetic polymers now pervade all industrialized societies, with new applications appearing on an almost daily basis (1). One example of the cases in which specially synthesized polymers have been particularly impressive in their replacement of non-synthetic or non-polymeric substances is in the area of "high performance" materials. Materials in this category are so designated because of their ability to main-

tain desirable properties over a wide range of temperatures, and frequently despite exposure to very hostile environments. Some specific examples of the superiority of man-made polymers are packaging films that are tougher than the cellulose-based materials they replace, and textile fibers such as Dacron, which are much more durable than most naturally occurring fibers. A

Continued on page 12

William J. Welsh, Ph.D. (left), Department of Chemistry, University of Missouri - St. Louis, and James E. Mark, Ph.D. (right), Department of Chemistry and Polymer Research Center, University of Cincinnati.



Biosym Establishes Industrial Consortium to Work on Next Generation of Man-Made Molecules

Biosym Technologies, Inc., of San Diego, CA, has announced the formation of a consortium of chemical, pharmaceutical and computer hardware and software companies to develop Potential Energy Functions. The consortium intends to derive more accurate force fields for use in computer programs which simulate and predict the properties of molecules. Such computer programs are applied to design pharmaceutical agents, agricultural chemicals, biomolecules, synthetic fibers and other molecules.

Joining Biosym in the effort are Abbott Laboratories, Cray Research, E. I. du Pont de Nemours, Merck, Sharpe & Dohme Research Laboratories, Monsanto, Rohm & Haas and the Upjohn Company. Each company will contribute financial and technical support to the three-year project.

A major limitation of many current computational methods has been the reliability of their underlying mathematical models. Optimal models have been developed for a particular class of compounds -- for example, to

Continued on page 11

Polymer Studies

Continued from page 2

more exotic example is the class of aromatic polyamides having high melting points and exhibiting strengths (on a weight basis) well above that of steel (1).

Research on liquid-crystalline polymeric materials has intensified in recent years with research and development activities proceeding at IBM, du Pont, Eastman Kodak, Celanese, Monsanto, Carnegie-Mellon University, the University of Massachusetts, Southern Mississippi University, the University of Missouri-St. Louis, the University of Cincinnati, SRI International, the University of Dayton Research Institute and Wright-Patterson Air Force Base. The focus is and will continue to be on fabricating ordered polymers into fibers, films and molded shapes that will open the door to a wide range of new products from bicycle wheels and sundry machine parts to automotive and aircraft components and electronic devices.

Particular interest has focused on a new type of *para*-catenated aromatic polymer being used in the preparation of high performance films and fibers of exceptional strength, thermal stability and environmental resistance, including inertness to essentially all common solvents. A polymer of this type, a poly(*p*-phenylene benzobisoxazole) (PBO), is illustrated in Fig. 1 (2). The isomer shown here is designated the *cis* form on the basis of the relative locations of the two oxygen atoms in the repeat unit. Other related poly-

mers of interest are the *trans*-PBO and the *cis* and *trans* forms of the corresponding poly(*p*-phenylene benzobisthiazole) (PBT), in which the two oxygen atoms are replaced by sulfur atoms.

These chains are extremely stiff, approaching the limit of a rigid-rod molecule. Because of their rigidity, they readily form liquid-crystalline phases (3-5), specifically nematic phases N in which the chains are aligned axially but are out of register in a random manner. The spinning of films from a liquid-crystalline dope of such a polymer has great advantages (1). The required flow of the system is facilitated, and the chains already have a great deal of the ordering they need in the crystalline fibrous state to exhibit the desired mechanical properties. Not surprisingly, PBO, PBT and related polymers are the focus of the US Air Force's "Ordered Polymers" Program (2,3,5) which has been established to develop high-performance materials for aerospace applications. Potential uses include not only as fibers and films, but also as reinforcing fibrous fillers in amorphous matrices to give "molecular composites" where they serve the same purpose as the macroscopic glass or graphite fibers widely used in multiphase polymer systems.

In this report we summarize some of our theoretical work on the structures, conformational energies, intermolecular interactions and electronic properties of PBO and PBT chains, including the protonated forms known to exist in strong acids. The emphasis is on how such studies provide a molecular understanding of the unusual properties and processing characteristics of this new class of materials.

Both empirical molecular mechanics (MM) and semiempirical CNDO/2 (Complete Neglect of Differential Overlap) molecular orbital methods (2,3) have been used for the (intramolecular) conformational energy calculations, while only the former has been used to date for the intermolecular interactions. Since model com-

pounds of *cis*-PBT have been shown (6) to assume a bowed configuration in the crystalline state, similar calculations (2) on this congener were more complicated and so are not presented here. Polarizabilities were calculated using three methods, specifically second-order perturbation theory combined with the formalism of CNDO/S CI (Configuration Interactions), an empirical scheme based on the additivity of atomic hybrid components, and the standard bond polarizability method (2). Electronic band structures, relevant to electrical conductivity, were calculated using the tight-binding scheme based on the Extended Huckel theory (2).

In spite of the rigidity of the PBO and PBT chains, some conformational flexibility should be permitted resulting from rotations ϕ about the single bond joining the *p*-phenylene to the heterocyclic moiety in each repeat unit (Fig. 1) (2,3). The preparation of high-strength materials consisting of rodlike polymers such as these requires a high degree of alignment of rods. Hence, the extent of intramolecular rotational flexibility and thus deviations from planarity are important in this regard, particularly in terms of chain-packing effects and the solubility characteristics of the polymers.

MM Calculations (2,3) indicated that the lowest energy conformation of *cis*- and *trans*-PBO should correspond to the coplanar conformations; this is in agreement with the planarity found for the corresponding model compounds in the crystalline state. *Trans*-PBT is predicted to be nonplanar ($\phi \approx 55^\circ$), largely due to the steric bulk of the S atom, compared with a value of 23.2° found experimentally for a model compound in the crystalline form (2). Inclusion of intermolecular interactions by minimizing the total intramolecular and intermolecular energy of a pair of *trans*-PBT sequences (2) shifts the predicted conformation to the range 0 to 25° , in much better agreement with experiment. The vibrational and electronic absorption spectra of

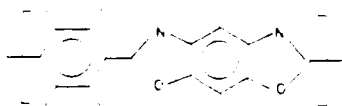


Figure 1: Repeat unit of the *cis*-PBO polymer.

Continued on page 13

Polymer Studies

Continued from page 12

model compounds in the crystalline state and in solution (7) are consistent with this interpretation.

CNDO-calculated conformational energy profiles for *cis*- and *trans*-PBO indicated preferred conformations corresponding to coplanarity; this result is thus in excellent agreement with the MM results and with experiment. The substantial barriers (near 2 kcal/mol) to rotation away from coplanarity imply that conjugation effects (favoring coplanarity) between the aromatic moieties dominate the steric repulsions (disfavoring coplanarity) (2).

Intermolecular energy calculations (2) can elucidate the nature of the chain packing and provide estimates of the corresponding densities, magnitudes of the total interaction energies, and the relative importance of van der Waals and Coulombic contributions. These "packing" calculations were based primarily on two parallel chains shifted relative to one another while the density estimates considered pairs of chains both above one another and alongside one another.

The calculations show that pairs of chains above one another are out of register by 3.0 Å in the case of the PBO polymers and by 1.5 Å in the case of the *trans*-PBT. X-ray crystallographic studies indicate axial shifts of approximately 4.5 Å in the case of model compounds for all three types of molecules (2). In the case of the vertical spacings, the theoretical results are in excellent agreement with an experimental value near ~ 3.5 Å for all three types of model compounds.

The interaction energies between chains were found to be rather large, with contributions from only a few repeat units adding up to values approaching typical bond dissociation energies. This suggests that in these polymers it is generally less costly in

terms of energy to break a bond along an individual chain than to separate two adjacent chains. The attractions are somewhat larger for the *trans*-PBT because S atoms give rise to larger van der Waals attractions than do O atoms. Coulombic contributions to the total interaction energy were found to be very small, suggesting that the dielectric constant of a potential solvent for these (unprotonated) polymers should be of no importance, and thus in agreement with experiment. (2).

Calculated densities were found to be in good agreement with the experimentally obtained densities of the model compounds (2), particularly in the way they vary with changes in the structure of the repeat unit. The results indicate that the higher density for the PBT polymer is due to the higher atomic weight of S relative to O, rather than to more efficient chain packing.

Because of their stiffness, the PBO and PBT chains are very nearly intractable, being insoluble in all but the strongest acids and very difficult to process into usable films and fibers. These materials may be made more tractable, however, by the insertion of a limited number of atoms or groups chosen so as to impart a controlled amount of additional flexibility to the chains. The insertion of even a small number of flexible molecular fragments or "swivels" into such chains will increase their flexibility and tractability by allowing mutual rotation of adjacent chain elements about the swivels' rotatable bonds. (Such swivels also have the advantage of facilitating the polymerization,

In swivels of the type Ph-X-Ph-X-Ph (Fig. 2), where Ph is phenylene and X is the single atom O, S, Se or Te, MM calculations (2,3) reveal that the sulfur swivel has the advantage both in equilibrium flexibility (more low-energy and thus accessible regions in configuration space) and in dynamic flexibility (lower barriers between energy minima). A number of somewhat more complicated swivels were also inves-

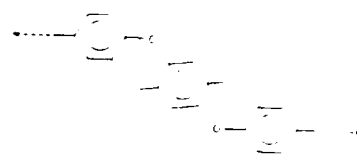


Figure 2: Example of a Ph-X-Ph-X-Ph swivel with $\lambda=0$

tigated, viz., $-\text{CO}-$, $-\text{SO}_2-$, $-\text{CH}_2-$, and $-\text{C}(\text{CF}_3)_2-$. On the basis of both thermal stability and conformational flexibility, the most promising swivels from this expanded group are $-\text{O}-$, $-\text{S}-$, $-\text{C}(\text{CF}_3)_2-$, and $-\text{CO}-$.

Wholly aromatic swivels, such as diphenylene and 2,2'-dipyridylene, should have the greatest thermal stability. They can maintain parallel continuation of the chain if bonded to *o*, either *ortho*, *ortho* (OO) or *meta*, *meta* (MM) (Fig. 3). CNDO/2 calculations (2) carried out on a number of the wholly aromatic swivels, viz., biphenyl, 2,2'-bipyridyl, 2-phenylpyridine, 2,2'-bipyrimidyl and 2-phenylpyrimidine, reveal that increase in the number of nitrogen substitutions generally decreases the energy of the coplanar conformation and increased the overall flexibility of the swivel.

Only very strong acids such as methane sulfonic acid and polyphosphoric

Continued on page 14



Figure 3: The wholly-aromatic diphenylene swivel.

Polymer Studies

Continued from page 13

acid are solvents for these materials. Protonation of the rodlike PBO and PBT chains and their model compounds in acidic media will have significant effects on their solubility, solution behavior, geometry and conformational characteristics. Freezing-point-depression measurements (2) on PBO and PBT model compounds have indicated that, depending on the acidity of the medium, the PBO model can exist as a di-protonated ion, presumably with one proton on each (highly basic) nitrogen atom, or as a tetra-protonated ion, presumably with the other two protons on the oxygen atoms. The PBT model compounds appear to prefer the di-protonated form owing to the lower basicity of sulfur atoms relative to oxygen atoms.

Intermolecular MM calculations (2) indicated that protonation of the chains should greatly decrease the intermolecular attractions, even at the very high dielectric constants characteristic of strong, undiluted acids. This conclusion is consistent with the fact that only extraordinarily strong acids are solvents for these types of polymers. Another effect of protonation is to enhance conjugation (favoring coplanarity) between the phenylene rings and the aromatic heterocyclic group (2,3). This increased stabilization of the coplanar forms appears to more than offset the repulsive effects of steric interferences. Changes in the UV-visible and Raman spectra (8) of these species upon protonation are consistent with this described increase in conjugation. Further, CNDO/2 calculations (2) predict the order of protonation within the *cis*-PBO model compound to be N, N, O, C which is consistent with the greater basicity of nitrogen relative to oxygen.

Computation of the polarizabilities of the PBO and PBT chains is of considerable importance in the interpretation of solution property studies such as flow birefringence measurements (9) which are carried out to obtain rheo-

logical time constants and orientation parameters relevant to the processing of these materials. The perturbation-CNDO method gave values of the average polarizability that were unrealistically small, but the atomic additivity and bond additivity schemes gave more realistic results, in good agreement with each other (2). The PBT chain is predicted to have a larger value of the average polarizability than the PBO chain, since the C-S bond is much more polarizable than the C-O one. The calculated results were used to estimate values of the anisotropic ratio δ directly applicable to the interpretation of flow birefringence data.

The same structural features that give the desired rigidity in PBO and PBT chains also give extensive charge delocalization and resonance stabilization. Such characteristics are common to polymeric materials exhibiting electrical conductivity. Electronic band structure calculations on *cis*-PBO, *trans*-PBO and *trans*-PBT chains in their coplanar conformations yielded band gaps in the axial direction of 1.72, 1.62 and 1.73 eV, respectively (2). Since *trans*-PBT is non-planar, calculations on it were also carried out as a function of its rotation angle. The band gap was found to increase markedly with increase in nonplanarity, as would be expected from the decrease in charge delocalization. No discernible dispersion of the energy bands perpendicular to the chains was indicated, suggesting that the neighboring chains are electronically non-interactive, as was found earlier for *trans*-polyacetylene and polyethylene (2). All of these values of the axial band gaps in PBO and PBT are very close to corresponding values of 1.4 to 1.8 eV reported for *trans*-polyacetylene (2), a much studied polymer with regard to electrical applications.

Acknowledgements:

It is a pleasure to acknowledge the financial support provided by the Air Force Office of Scientific Research (Grant 83-0027; Chemical Structures Program, Division of Chemical Sciences) and by the Plastics Institute of America.

By William J. Welsh, Ph.D.,
Department of Chemistry, University of Missouri-St. Louis,
St. Louis, MO 63121 and
James E. Mark, Ph.D., Department of Chemistry and Polymer Research Center, University of Cincinnati, Cincinnati, Ohio 45221-0172.

References

1. "Polymer Science and Engineering: Challenges, Needs and Opportunities," ed. by C. G. Overberger and R. Pariser, National Academy Press, National Research Council, Washington (1981).
2. W. J. Welsh, D. Bhaumik, H. H. Jaffe, and J. E. Mark, *Polym. Eng. Sci.*, **24**, 218 (1984), and references cited therein.
3. W. J. Welsh, "Conformational Characteristics of Some Liquid-Crystalline Aromatic Heterocyclic Polymers Useable as High-Performance Materials," in "Current Topics in Polymer Science - 1984," Vol. 2, *Polymer Physics*, Macmillan, New York (in press), and references cited therein.
4. G. C. Berry, in "Contemporary Topics in Polymer Sciences," Vol. 2, ed. by E. M. Pearce and J. R. Schaefgen, Plenum Press, New York (1977).
5. A number of relevant articles are in the December 1980 and March 1981 special issues of *Br. Polym. J.* and in the July/August 1981 special issue of *Macromolecules*.
6. M. W. Wellman, W. W. Adams, R. A. Wolff, D. R. Wit and A. V. Fratini, *Macromolecules*, **14**, 935 (1981).
7. G. M. Venkatesh, D. Y. Shen and S. C. Hsu, *J. Polym. Sci., Polym. Phys. Ed.*, **19**, 1475, (1981).
8. D. Y. Shen, et al., *J. Polym. Sci., Polym. Phys. Ed.*, **20**, 509 (1982).
9. S.-G. Chu, et al., *Macromolecules*, **14**, 939 (1981).

Conformational and electronic band structure analysis of a new type of high performance polybenzothiazole polymers

K. NAYAK

Department of Chemistry and Polymer Research Center, The University of Cincinnati
Cincinnati, Ohio 45221, USA

The energy-band structure and preferred (minimum energy) conformation of the recently synthesized polybenzothiazoles (PBT-AA and AB type), representing a new class of high-performance polymers, were determined by molecular orbital calculations. In the case of the AAPBT chain, the most stable conformation was obtained at ϕ_1 (rotation angle about the bond joining the two benzothiazole moieties) = 20° and ϕ_2 (rotation angle about the bond joining the benzothiazole group and the *p*-phenylene group) = 10° . In the case of the ABPBT chain, the corresponding minimum energy rotational angle (ϕ_1) was found to be 20° . These conformations agree fairly well with both theoretical and experimental observations. The calculated axial band gaps were 1.94 and 2.08 eV for the AAPBT and ABPBT polymers, respectively, and these values are close to the corresponding value for polyacetylene, considered a prototype electrically conducting polymer because of its novel electronic properties and manifold applications.

1. Introduction

There has been a growing interest to synthesize and characterize various types of aromatic heterocyclic polymers [1-3] because of their high thermal stability and resistance to most solvents. Their potential as high performance structural materials has been demonstrated in the fabrication of fibres, films and molecular composites of high mechanical strength and modulus [3-5]. Results of recent band structure calculations on similar polymers such as poly(*p*-phenylene benzobisoxazole) (PBO) and poly(*p*-phenylene benzobisthiazole) (PBT) [6] and the structurally related polymers AAPBO and ABPBO [7, 8] have shown their promise as semiconducting materials. In fact, their calculated band gaps were very close to that found for polyacetylene, a polymer extensively studied because of its unique electrical properties [9, 10].

Standard extended Hückel calculations have been found to reproduce band structures of hydrocarbon polymers [6, 7, 11-14] fairly well. It was therefore decided to investigate the electronic properties of a new type of PBT polymers by means of band structure analysis using the extended Hückel technique within the tight-binding approximation. The polymers of present interest are poly(*p*-benzothiazole-2,2'-diyl-1,4-phenylene) (AAPBT) and poly(2,5-benzothiazole-1,3'-diyl) (ABPBT) (Figs 1 and 2). In order to overcome some initial difficulties (such as nonalignment of a chemical repeat unit along a preferred direction and nonperiodicity), a specific periodic arrangement was chosen in which the second chemical unit was rotated 180° with respect to the first unit about the bond joining the two units. Similarly, in the case of ABPBT,

four chemical repeat units were chosen in which the second two units were rotated 180° with respect to the first two units about the bond joining the pair. Further support for selecting such an arrangement was furnished by explicit molecular orbital (MO) calculations of the extended Hückel type on model compounds of AAPBO and ABPBO polymers.

2. Theory

The present investigation employs the extended Hückel theory within the tight-binding approximation which has been discussed in detail elsewhere [6, 7, 11-14]. The extended Hückel method is also known as the Mulliken-Wolfsberg-Heimholtz technique [15], which employs an empirical Hamiltonian representing one-electron energy. The energy expectation values were evaluated using a linear combination of atomic orbitals (LCAO). Briefly, the set of all energy bands associated from the solution of the secular equation

$$H(k)C(k) = S(k)C(k)E(k) \quad (1)$$

describes the band structure of the one-dimensional polymer chain, where $H(k)$ is the Hamiltonian operator, $S(k)$ is the overlap matrix, and $C(k)$ is the expansion coefficient in LCAO. The Hamiltonian operator is modified according to this approximation as

$$H_i = KS(E_i + E_j)/2 \quad (2)$$

where K is a scaling parameter (usually 1.75) and E_i denotes the one-electron eigenvalues of the basis levels. Owing to symmetry considerations the energy bands are determined within the first Brillouin zone, $-0.5K \leq k \leq 0.5K$ (where $K = 2\pi/a$ is the

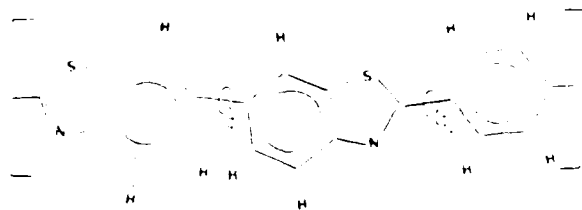


Figure 1. AAPBT with two chemical repeat units in which ϕ_1 and ϕ_2 are the rotation angles about the bond joining the two units.

reciprocal lattice vector and \mathbf{a} is the basis vector of the translational symmetry which is parallel to the chain axis. The preferred conformation was determined from calculating the total energy per unit cell, as given by

$$E = \frac{1}{K} \sum_{\mathbf{k}} E(\mathbf{k}) \quad (3)$$

where $E(\mathbf{k})$ is the total energy at the wave vector \mathbf{k} and according to the extended Hückel method,

$$E(\mathbf{k}) = 2 \sum_{\text{occupied}} E_i(\mathbf{k}) \quad (4)$$

The input values of the bond lengths and bond angles were obtained from the X-ray diffraction studies of PBT model compounds [16] and ABPBT itself [17]. The lattice sums were carried out only to first nearest neighbours because of the large size of the repeat unit. The extended Hückel parameters used for calculations were obtained from the literature [6, 12].

3. Results and discussion

A closed shell system has been adopted for the present calculations in which the repeat units of both AAPBT and ABPBT chains contain even numbers of valence electrons. Attempts have been made to determine the most stable conformation with respect to the rotations ϕ_1 and ϕ_2 by calculating the total energy of a unit cell as a function of \mathbf{k} for different values of the dihedral angles ($0^\circ \leq \phi_1 \leq 180^\circ$, $0^\circ \leq \phi_2 \leq 90^\circ$) using increments of 10° . The results for AAPBT chain are shown in Figs 3 and 4. Owing to the variations of the lattice vectors for each rotation, the reciprocal lattice vector \mathbf{k} is no longer a constant, the total energy per unit cell (E) was thus evaluated using a polynomial fit for $E(\mathbf{k})$ in Equation 3. From Fig. 3 it was observed that the minimum energy conformation was obtained for $\phi_1 = 20^\circ$ (or its supplement 160°) and $\phi_2 = 10^\circ$ with very small energy differences in the range of 0 to 20 and 160 to 180° . The value obtained for ϕ_1 , which is the rotation between the two biphenylthiazole

groups, is in good agreement with the corresponding conformation obtained for biphenyl [18]. The predicted value of 20° for ϕ_1 is also in excellent agreement with our previous studies [7] and the *ab initio* results of Almof [19]. The preferred orientation of the other twist angle ϕ_2 , which is the rotation of the lone phenylene ring with respect to the biphenylthiazole moiety, corresponds to $\phi_2 = 10^\circ$ and the bond exhibits considerable rotational flexibility in the range of $\phi_2 = 0^\circ$ to 20° . The corresponding preferred angle in case of AAPBO is 0° (planar conformation). The nonplanar conformation predicted in the case of AAPBT is probably due to the presence of the relatively large sulphur atoms in place of the oxygen atoms found in the AAPBO chain. For the biphenylthiazole moiety, in the planar form ($\phi_1 = 0^\circ$) the nonbonded distance between the closest orthohydrogens on adjacent phenyl rings is nearly 0.185 nm compared with the sum of van der Waals radii (0.24 nm). However, these repulsive interactions can be relieved by rotation to $\phi_1 = 20^\circ$ to 30° , at which the H-H distance would be about 0.21 nm. Such quasi-nonplanar structures could possibly result in interlocking the chains to form networks with improved chain packing.

Similar calculations were carried out for ABPBT, a typical plot of $E(\mathbf{k})$ against \mathbf{k} is shown in Fig. 6. The conformational energy ΔE as a function of rotational angle ϕ_1 is shown in Fig. 7. It indicates the minimum energy conformation at $\phi_1 = 20^\circ$ (160). The preferred conformation of $\phi_1 = 20^\circ$ (or its supplement 160°) is in good agreement with the results carried out on structurally similar model compounds of PBT [6]. It

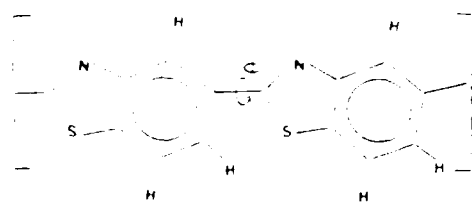


Figure 2. AAPBT with two chemical repeat units in which ϕ_1 is the rotation angle about the bond joining the two units.

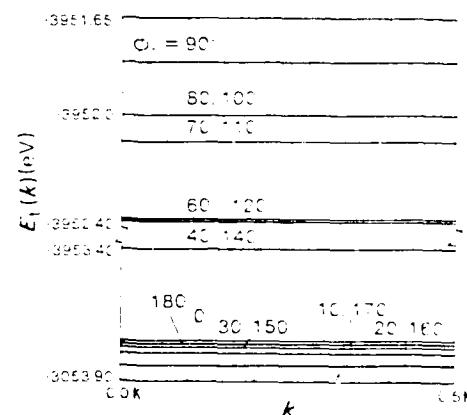


Figure 3. Dependence of $E(\mathbf{k})$ on \mathbf{k} and ϕ_1 and $\phi_2 = 10^\circ$ for AAPBT chain.

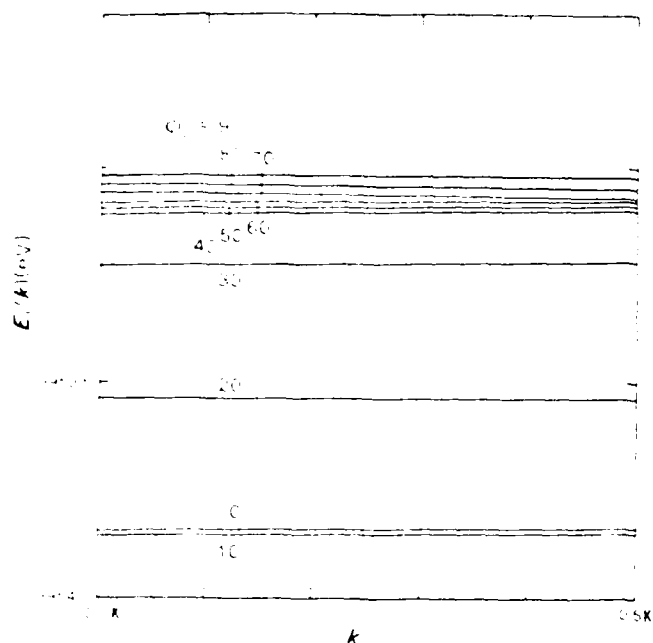


Figure 4. Energy band structure for AAPBT chain.

In this case the nonplanarity could be ascribed to the repulsive interactions between the sulphur atom and the adjacent ethylenic hydrogens on the neighbouring phenyl ring.

The axial band gaps (E_g) for the AAPBT and ABPBT chains in the preferred conformations were 4.4 and 2.9 eV, respectively. These values are comparable with that calculated previously for PBT (6) and also close to the experimentally observed values (4 to 5 eV) for polyacetylene (9–10), a polymer that started because of its promise as a conducting material upon doping with appropriate electron donors and electron acceptors. The present method could have been successfully employed to predict doped polyacetylene, upon doping with polyacetylene (11), polyvinylcarbazole (PBVC) and many other

polybenzimidazoles (PBT) (21) with acceptor dopants such as iodine or bromine. Thus, investigations are underway to examine these new class of polymers in the doped state. A portion of the electronic band structures for each polymer is shown in Figs 8 and 9, respectively. To further elucidate the electronic behaviour such as charge transport and electron mobility, the dispersion (bandwidth) of the highest occupied valence band of both polymers was measured. The flatness (dispersion) of the order of 0.1 eV of these bands as compared to bandwidth of polyacetylene (theoretical estimate of the orders of 0.54 eV) (9) might be due to the nonbonding character of the corresponding crystalline orbitals. Another possibility is the nonplanar conformations and the large size of the unit cells chosen for calculations which would

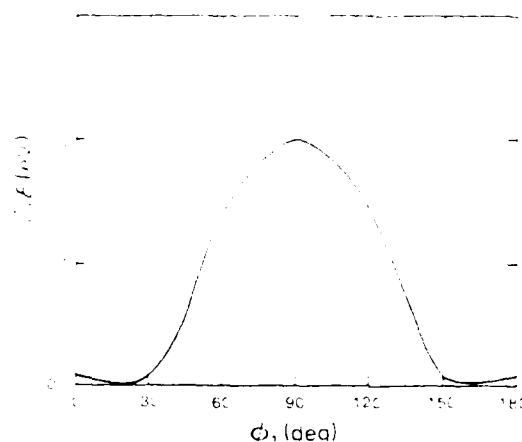


Figure 5. The conformational energy ΔE shown as a function of the relative angle ϕ for AAPBT, where ΔE is defined as the energy of a conformation relative to that of the preferred conformation.

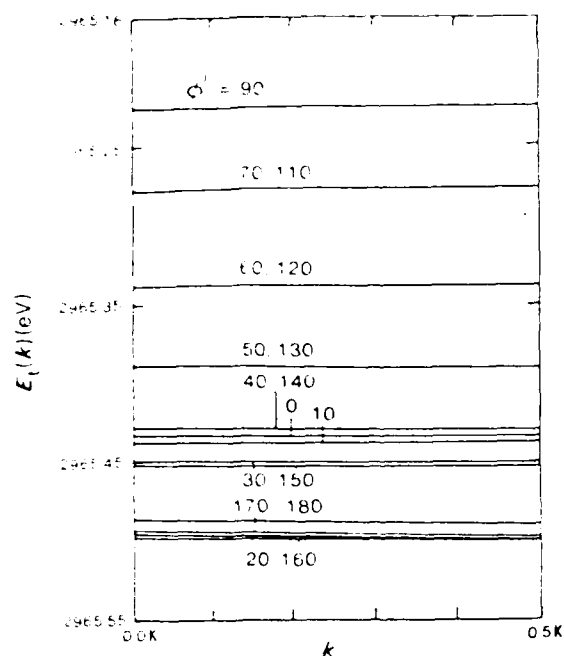


Figure 10. Energy band structure of AAPBT chain as a function of the rotational angle ϕ .

eliminate the opportunity for significant electron delocalization. Moreover, the bandgap was found to increase in the chains deviated from the coplanar conformation and was a maximum at the perpendicular conformation. This prediction is in agreement with the previous calculations on similar model compounds [1, 7]. The dependence of E_g on rotational angle ϕ for AAPBT is illustrated in Fig. 10. The ultraviolet-visible and Raman spectroscopic studies [5] have been made to examine the effect of protonation of a heterocyclic rigid-rod polymer polyvinylcarbazole, polycarbistiazole and its model compounds, belonging to the same class of polymers. Unfortunately, at present, there are no experimental results available for comparison with these theoretical findings of band gaps and bandwidths of these high performance polymers.

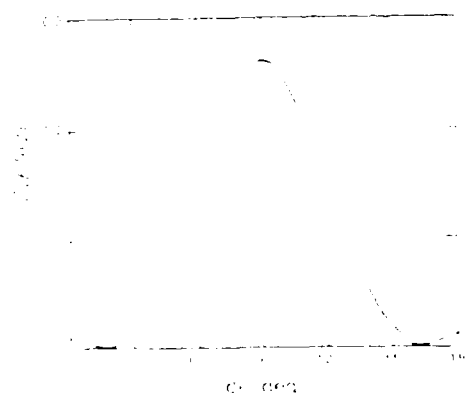


Figure 11. The conformational energy ΔE shows a variation of the rotational angle ϕ for AAPBT chain.

The results borne out by these calculations indicate the potential of these high performance polymers as semi-conducting materials.

Acknowledgements

It is a great pleasure to acknowledge financial support from the Air Force Office of Scientific Research (Chemical Structures Program, Division of Chemical Sciences) and Professor J. E. Mark of the University

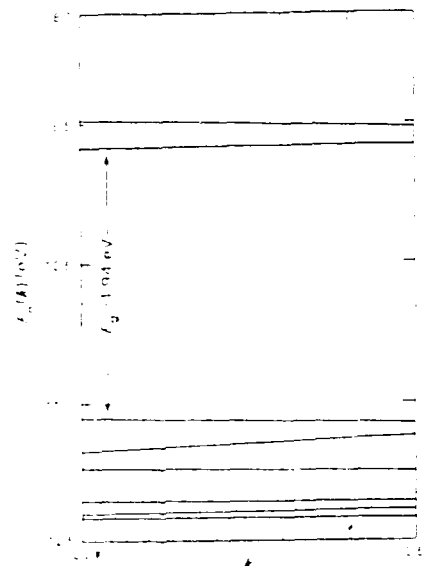


Figure 12. Energy band structure of the AAPBT chain as a function of conformational energy ϕ (in degrees) and $\phi = 20^\circ$ and $\phi = 90^\circ$.

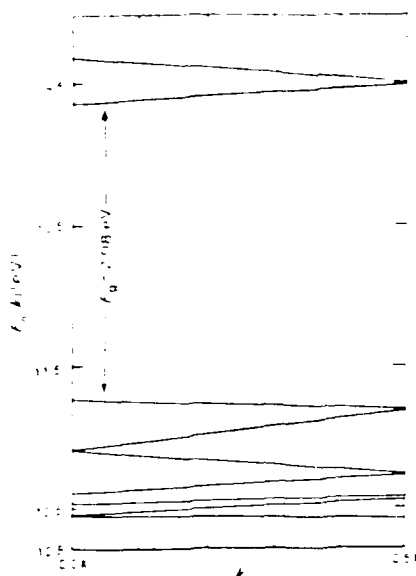


Figure 5. Electronic band structure of the AAPBI chain at the preferred conformation ($\alpha = 2$).

of Cincinnati for valuable advice and research fellowship. The author also expresses sincere thanks to Professor W. J. Welsh for his suggestions and reading the final draft.

References

1. *Macromolecules*, **14**, 1987 (1981).
2. T. E. HELMINTAK, *Frontiers*, **40**, *Polym. Chem. Ser.*, **Chem.**, **40**, 1979 (1975).
3. J. A. ODILL, A. KELLER, E. L. J. ATKINS, and M. J. MILES, *J. Mater. Sci.*, **16**, 1981 (1981).
4. K. SHIMAMURA, J. K. MINTER, and E. L. THOMAS, *J. Mater. Sci. Lett.*, **2**, 1983 (1983).
5. J. Y. SHEN, G. M. VENKATESH, J. J. BURKHILL, P. H. CHEN, and S. L. HSIEH, *J. Therm. Anal. Calor.*, **20**, 1982 (1982).
6. D. BHALMIK and J. E. MARK, *ibid.*, **21**, 1983 (1983).
7. K. NAYAK and J. E. MARK, *Macromol. Chem.*, **186**, 1985 (1985).
8. W. J. WELSH and J. E. MARK, *Polym. Eng. Sci.*, **25**, 1985 (1985).

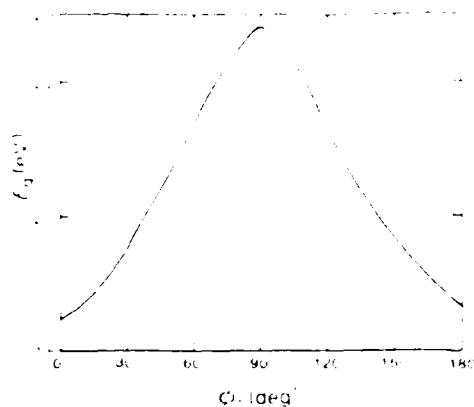


Figure 6. Dependence of the band gap E_g on the rotational angle α , $\alpha = 0$, for the AAPBI chain.

9. C. L. BRIDGES, K. E. CHANCE, E. D. BALGOMAN, and S. K. STEBBY, *J. Chem. Phys.*, **76**, 1982 (1982).
10. S. W. PARK, A. J. HELGEE, M. A. DREY, and A. G. MANDIARMI, *ibid.*, **74**, 1980 (1980).
11. K. HOFFMANN, *ibid.*, **39**, 1965 (1965).
12. M. H. WHANGBO and K. HOFFMANN, *J. Amer. Chem. Soc.*, **100**, 1978 (1978).
13. M. H. WHANGBO, K. HOFFMANN, and K. B. WOODWARD, *Proc. R. Soc.*, **423**, 1979 (1979).
14. A. IMAMURA, *J. Chem. Phys.*, **52**, 1970 (1970).
15. S. F. MCGLYNN, J. G. VANOLICKENBORN, M. KINOSHITA, and D. G. CARROLL, "Introduction to Applied Quantum Chemistry" (Holt, Rinehart, and Winston, New York, 1972), p. 67.
16. M. W. WELLMANN, W. W. ADAMS, K. A. WOLFE, K. A. DEDIS, D. K. WIFE, and A. V. FRATINI, *Macromolecules*, **14**, 1981 (1981).
17. A. V. FRATINI, E. M. CROSS, J. E. CURRIEN, and W. W. ADAMS, AEWI Report October (1984).
18. H. SUZUKI, *Bull. Chem. Soc. Jpn.*, **32**, 1959 (1959).
19. J. ALMLÖF, *Chem. Phys.*, **6**, 1974 (1974).
20. D. BHALMIK and J. E. MARK, *J. Therm. Anal. Calor.*, *Ed. in press*.
21. D. BHALMIK, private communication.

Received 17 June
and accepted 10 September 1985

Comparisons among some tetraalkoxysilanes in the hydrolytic precipitation of silica into elastomeric networks

G. S. Sauer,^{a,b} J. E. Mark*

Department of Chemistry and the Polymer Research Center, The University of Cincinnati, Cincinnati, Ohio 45221, USA

(Date of receipt: May 7, 1985)

SUMMARY

Four tetraalkoxysilanes, $\text{Si}(\text{OPh})_4$, were absorbed into networks of polydimethylsiloxane (PDMS), and then hydrolyzed, using a variety of catalysts, to give reinforcing silica particles. On the basis of the amount of silica precipitated and the extent of reinforcement, the (cleaving) order of effectiveness was found to be tetraethoxysilane, tetrapropoxysilane, tetrabutoxysilane, and tetramethoxysilane.

Introduction

A series of recent experimental investigations¹⁻¹² has focused on the hydrolysis of tetraethoxysilane (TEOS) [$\text{Si}(\text{OC}_2\text{H}_5)_4$] to give filler particles capable of reinforcing elastomeric networks. The reactions are typically carried out at room temperature within a TEOS swollen network of polydimethylsiloxane (PDMS), and yield essentially unagglomerated particles with diameters of 150–250 Å.⁹ The reinforcing effects of these fillers have been clearly demonstrated by measurements of stress-strain isotherms in elongation^{1-5,8,9}.

Since only TEOS has been used for this purpose to date, it should be very interesting to attempt the same *in situ* techniques using other tetraalkoxysilanes $\text{Si}(\text{OR})_4$ as well. The present study addresses this issue, using the hydrolysis of tetramethoxysilane (TMOs), tetraethoxysilane (TEOS), tetrapropoxysilane (TPOS), and tetrabutoxysilane (TROS). The amount of silica precipitated and the ultimate properties of the filled PDMS networks in elongation are used to evaluate the relative effectiveness of these four silanes.

Experimental part

Preparation of elastomers. Hydroxyl terminated PDMS having a number average molecular weight of 18000 g/mol was endlinked with tetraethoxysilane (TEOS) in the undiluted state, in the usual manner¹³⁻¹⁶. The resulting network sheets, which were approximately 1 mm thick, were extracted using tetrahydrofuran and methanol. Test strips cut from the sheets were approximately 4 mm wide and 150 mm long.

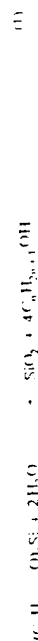
^{a)} Permanent address: Department of Chemical Engineering, Yonsei University, Daejeon 632, Korea

^{b)} Visiting Scientist at IPR, Sep. Dec., 1984–85 academic year

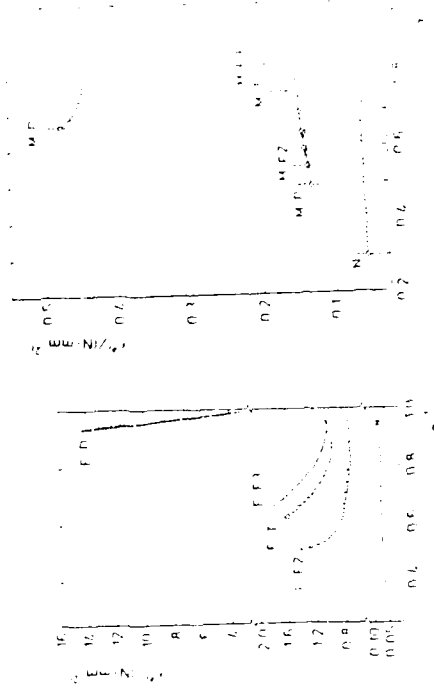
Stress-strain measurements. Uniaxial stress-strain data were obtained in the laboratory using a universal tester¹ on the specified samples at 25 °C. The nominal stress was given by $\sigma = F/A_0$, where F is the elastic force and A_0 the undeformed (cross-sectional area) of the sample. The nominal strain was given by $\epsilon = (L - L_0)/L_0$, where σ , F , A_0 is the elongation of the sample, L is the length of the sample, L_0 is the original length of the sample. All filled networks were thus studied, and several samples of each type.

Conclusion and discussion

All of the organofunctional silane compounds studied showed a significant increase in the rate of reaction.



They did vary considerably in their efficiency, however, as can be seen from the amounts of precipitated filler (given in the fourth column of Tab. I). Differences in the amount of filler precipitated are presumably due to different rates of hydrolysis, as well as to different amounts of silane present and some of the filler particles could



1993

Fig. 1. The reduced stress (σ^*) shown as a function of reciprocal elongation ϵ^{-1} for the PBTMS networks filled by the hydrogel of HOS at 25°C. A hysteresis is identified by the solid and dashed lines. The dotted-dashed lines locate the rupture point of the networks.

Fig. 7. The reduced stress (σ^*) shown as a function of reciprocal elongation α^{-1} for epoxy-amine networks filled by the hydrolysis of TMOS.

is in the

[illegible]

Table I. Precipitation reagents, amount of fiber precipitated, and ultimate properties of the fibered elastomers

Precipitated in reactive		Viscosity designation	Ultrasonic properties		
κ_{eff}	Catalyst		Wt % SiO_2 precipitated	ρ , mm s ⁻¹	σ_p , s ⁻¹
Phenol					
	H-105 ¹	DEAM ¹⁰	0.0	0.15	3.5
		DEAM ¹¹	10.1	2.88	1.1
		DEAM (2H ₂ O) ¹²	51.3	2.40	2.0
		DEAM (3H ₂ O) ¹³	51.3	1.60	2.3
H-105 ²	KH ₂ PO ₄ ¹⁴	18.9			
	DEAM ¹⁵	12.8	2.1	1.6	
	DEAM ¹⁶	9.3	0.50	1.5	
	DEAM (2H ₂ O) ¹⁷	5.1	0.20	1.8	
H-105 ³					
	H-105 ³	DEAM (4H ₂ O) ¹⁸	9.8	0.60	1.2
		KH ₂ PO ₄ ¹⁹	5.7	0.34	2.0
		DEAM ²⁰	5.0	0.12	1.3
		DEAM ²¹	33.9		
H-105 ⁴	DEAM (2H ₂ O) ²²	19.3	0.35	1.7	
	DEAM (4H ₂ O) ²³	18.7			
	KH ₂ PO ₄ ²⁴	23.2	1.0	1.8	
	DEAM ²⁵	49.1	0.26	1.6	
H-105 ⁵					
	H-105 ⁵	DEAM ²⁶	14.8		
		DEAM (2H ₂ O) ²⁷	15.0	0.18	1.8
		DEAM (4H ₂ O) ²⁸	13.7	0.21	2.3
		KH ₂ PO ₄ ²⁹	16.9	0.19	2.3
DEAM ³⁰	13.3	0.11	1.1		

Forming a new company

21. *Chrysomelidae* (continued)

...the ...

Environ Biol Fish (2016) 98:17–24
DOI 10.1007/s10641-015-0370-1

Abstract

of a procedure call of *sub* to *sub*.A, etc. and

Freezing rate of embryos to the antral follicle

2-Amino-2-bicyclohexylmethanol (100 g, 0.5 mol) was dissolved

Introduction

11. *Journal of the American Medical Association*, 1990; 263: 1025-1028.

Let's do this

therefore contain some only partially hydrolyzed silanes. In any case, the organofunctional silane compound which was most efficient in this regard was TEOS and the order of efficiency was TEOS \sim TPCOS \sim TBOS \sim IMOS.

The stress-strain isotherms obtained on the filled networks^{10, 20} were first represented as plots of the modulus against reciprocal elongation, as suggested by the Mooney-Rivlin equation^{17, 19}

$$[U^*] = 2C_1 + 2C_2 \alpha^{-1} \quad (2)$$

Typical isotherms, for networks chosen from the four kinds of organofunctional silane compounds, are shown in Fig. 1, 2, 3 and 4, respectively. The in situ filled networks are seen to have values of the modulus which are much higher than those of the corresponding unfilled network. Comparisons among the four figures show that

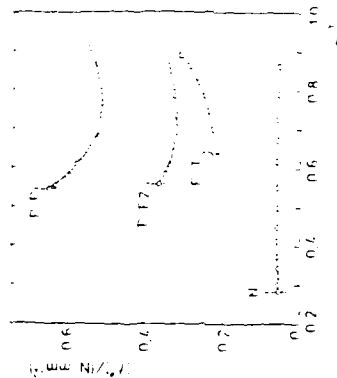


Fig. 1. The reduced stress $[U^*]$ shown as a function of reciprocal elongation α^{-1} for typical TEOS networks filled by the hydrolysis of TEOS.

the TEOS diethylamine system was the most efficient. Furthermore, the optimum in $[U^*]$ observed at higher elongations clearly demonstrate the desired reinforcing effects. The values of the ultimate properties, specifically the ultimate strength and maximum extensibility, are given for all the networks in the last two columns of Tab. 1. With regard to ultimate properties, the best networks resulted from the use of TEOS. They were followed by the TPCOS networks and these by the TBOS and IMOS networks. TBOS gave higher extensibilities α_f than the IMOS but lower values of the ultimate strength f_f .

Fig. 5 shows some representative data chosen from Figs. 1-4 plotted in such a way that the area under each stress-strain curve corresponds to the energy E_f of rupture²¹, which is a standard measure of elastomer toughness. The values of E_f for the curves shown range from 0.28 J mm⁻² (network N) to 0.82 J mm⁻² (network F F2). Thus, proper choice of silane and catalyst can easily give reinforcement amounting to a nearly three fold increase in toughness.

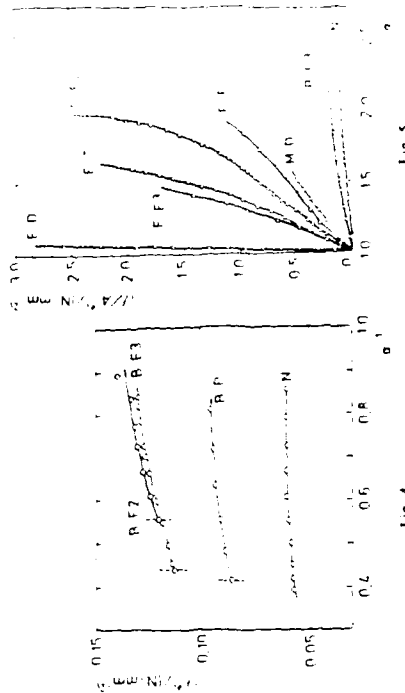


Fig. 4.

Fig. 4. The reduced stress $[U^*]$ shown as a function of reciprocal elongation α^{-1} for typical TBOS networks filled by the hydrolysis of TBOS.

Fig. 5. The nominal stress f shown as a function of elongation α for some networks for works. In this representation, the area under each curve corresponds to the energy E_f required for network rupture.

It is a pleasure to acknowledge the financial support provided by the National Science Foundation through Grant DMR 8415087 (Polymer Program, Division of Material Research) and by the Air Force Office of Scientific Research through Grant AFOSR 8310027 (Chemical Structures Program, Division of Chemical Sciences). G. S. S. also wishes to thank the Industrial Ministry of Korea for the Research Fellowship he received.

10. J. F. Mark, S. I. Pao, *Makromol. Chem., Rapid Commun.* **3**, 681 (1982).
11. C. Y. Jiang, J. F. Mark, *Makromol. Chem.* **185**, 2609 (1984).
12. M. Y. Tang, J. F. Mark, *Polym. Eng. Sci.* **25**, 29 (1984).
13. J. F. Mark, C. Y. Jiang, M. Y. Tang, *Macromolecules* **17**, 2613 (1984).
14. C. Y. Jiang, J. F. Mark, *Colloid Polym. Sci.* **262**, 758 (1984).
15. M. Y. Tang, A. L. Latham, J. F. Mark, *Colloid Polym. Sci.* **262**, 993 (1984).
16. Y. P. Ning, M. Y. Tang, C. Y. Jiang, J. F. Mark, and W. C. Roh, *J. Appl. Polym. Sci.* **29**, 3209 (1984).
17. Y. P. Ning, J. F. Mark, *J. Appl. Polym. Sci.* **30**, 3519 (1985).
18. J. F. Mark, Y. P. Ning, *Polym. Bull.* **12**, 413 (1983).
19. Y. P. Ning, Z. Righi, J. F. Mark, *Polym. Bull.* **13**, 155 (1985).
20. Y. P. Ning, J. F. Mark, *Polym. Eng. Sci.* **26**, 162 (1986).
21. J. F. Mark, *Rev. Polym. J.* **17**, 143 (1985).
22. J. F. Mark, J. J. Sullivan, *J. Chem. Phys.* **66**, 1006 (1977).

- (13) M. A. Lorente, A. L. Andrad, J. E. Mark, *J. Polym. Sci., Polym. Phys. Ed.* **19**, 621 (1981)
- (14) M. A. Lorente, A. L. Andrad, J. E. Mark, *J. Polym. Sci., Polym. Phys. Ed.* **18**, 2263 (1980)
- (15) J. E. Mark, *Adv. Polym. Sci.* **41**, 1 (1982)
- (16) J. E. Mark, P. J. Flory, *J. Appl. Phys.* **37**, 4635 (1966)
- (17) I. R. G. Irelor, "The Physics of Rubber Elasticity", Clarendon Press, Oxford 1975
- (18) J. E. Mark, *Rubber Chem. Technol.* **48**, 495 (1975)
- (19) Z. Righi, *Adv. Polym. Sci.* **36**, 21 (1980)
- (20) K. F. Polmanest, C. W. Leutz, *Rubber Chem. Technol.* **48**, 795 (1975)
- (21) B. B. Beonstia, *Polymer* **20**, 691 (1978)

Conformational Energies and Unperturbed Chain Dimensions of Polysilane and Poly(dimethylsilylene)

W. J. Welsh,* L. DeBolt, and J. E. Mark

Department of Chemistry and Polymer Research Center, University of Cincinnati, Cincinnati, Ohio 45221. Received April 1, 1986

ABSTRACT: Conformational energy calculations using molecular mechanics (MM) methods were carried out on segments of polysilane $[-SiH_2-]$ and poly(dimethylsilylene) $[-Si(CH_3)_2-]$, and the results were compared with the published full-relaxation calculations of Damewood and West. The three MM methods compared (designated NR for "no relaxation", PR for "partial relaxation", and FR for "full relaxation") differ in the extent to which they permit molecular relaxation (deformation) in order to achieve energy minimization. All three MM methods show polysilane to prefer G^*G^* states over the corresponding TT state by 0.5–0.7 kcal mol⁻¹, in contrast to the analogous *n*-alkanes, which prefer TT over G^*G^* by ca. 1.0 kcal mol⁻¹. Even G^*G^* states, commonly found to be prohibitively repulsive for the *n*-alkanes and most other polymers, were preferred over the TT states by 0.4 kcal mol⁻¹. Nearly all regions of configurational space were within 2 kcal mol⁻¹ of the minima, indicating considerable chain flexibility. For poly(dimethylsilylene) the three MM methods differ in terms of predicted conformational preferences. While the NR calculations predict preferences for TT and TG^{*} states over the corresponding G^*G^* states by ca. 4 kcal mol⁻¹, the FR calculations in contrast indicate preferences for G^*G^* states over TT and TG^{*} by ca. 0.9 kcal mol⁻¹, with the PR calculations yielding results intermediate between these two. Calculated values of the characteristic ratio C_{∞} for polysilane are rather low (4.02 at 25 °C) but increase with increasing temperature, indicating low chain extensibility and high flexibility with increased occurrence of the higher energy, chain-extending trans states over the preferred gauche states as temperature is increased. Values of C_{∞} for poly(dimethylsilylene) at 25 °C are 15.0, 13.2, and 12.5 based on the NR, PR, and FR results, respectively. These relatively large values reflect a more inflexible and extended chain. The close agreement in C_{∞} values yielded by the three MM methods for poly(dimethylsilylene), despite the differences in conformational preferences predicted by each, is a consequence of compensating factors.

Introduction

Polysilanes, having chain backbones consisting entirely of silicon atoms, represent a fascinating new class of polymeric materials with potential applications in such diverse areas as ceramics and semiconductors. Polysilane copolymers containing alternating phenylmethylsilyl and dimethylsilyl units, commonly known as "polysilastyrene", are soluble polymers that can be melted, molded, cast into films, or drawn into fibers. When exposed to ultraviolet light they undergo cross-linking, becoming rigid and insoluble, while heating above 800 °C converts the polymers to silicon carbide.¹ Experimental studies² indicate that polysilastyrene appears to become semiconducting upon addition of chemical dopants; thus this and possibly other polysilanes add to the growing list of conducting and semiconducting polymers.^{2–5} Investigations are also under way to measure some of the configuration-dependent properties of a series of substituted polysilanes.^{6,7} These results can be compared with those obtained by theoretical methods, based on the rotational isomeric state approximation using conformational energies computed from empirical potential energy functions,⁸ to provide information regarding the rotational flexibility and preferred conformations about individual backbone bonds. Damewood and West (DW), using full-relaxation (FR) empirical force-field techniques, have investigated the structure and conformational energies of molecular fragments of both polysilane $[H-(SiH_2)_2-H]$ and poly(dimethylsilylene) $[Me-(SiMe_2)_2-Me]$.⁹ The present study focuses on using the calculated structures and conformational energies of DW along with conformational energies calculated with two other, more simplified force fields, to compute the unperturbed chain dimensions $\langle r^2 \rangle_0$ of polysilane and poly(dimethylsilylene). Results are compared with those ob-

Table I
Structural Parameters for $[-SiH_2-]$ and $[-Si(CH_3)_2-]$ Used in the Present Calculations

	$[-SiH_2-]$	$[-Si(CH_3)_2-]$
bond lengths ^a		
Si-Si	2.34	2.35
Si-C		1.87
Si-H	1.48	
C-H		1.10
bond angles ^b		
Si-Si-Si	109.4	115.4
Si-Si-H	110.0	
Si-Si-C		105.5
Si-C-H		110.0

^a In angstroms. ^b In degrees.

tained by similar methods for some analogous hydrocarbon chains.

Methodology

Details of the methodology used by DW to calculate the structure and conformational energies of the two polymer chains are given in ref 9. Briefly, they employed the empirical force-field program known as MM2^{10,11} after deriving several Si-related parameters. DW adopted the option available in MM2 for complete relaxation of all internal degrees of freedom (viz., bond lengths, bond angles, and torsional angles) to achieve conformational-energy minimization. Hence, we refer to their technique as FR (for "full relaxation") to distinguish it from the two other force-field techniques to be described herein.

The two other techniques used to calculate conformational energies shall be referred to as NR for "no relaxation" and PR for "partial relaxation". They differ from the FR technique of DW basically in the degree to which they allow relaxation of the molecule's internal degrees of freedom in order to achieve energy minimization. The NR calculations employed a force field which includes both steric (nonbonded) and torsional terms and,

* Current address: Department of Chemistry, University of Missouri—St. Louis, St. Louis, MO 63121.

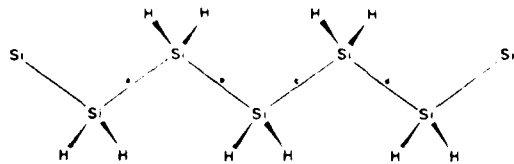


Figure 1. Illustration of the polysilane chain segment considered in the NR calculations.

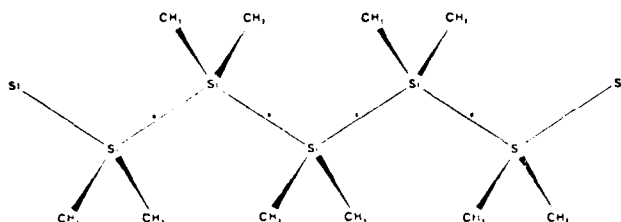


Figure 2. Illustration of the poly(dimethylsilylene) chain segment considered in the NR calculations.

for all conformations (i.e., torsional angles) considered, the energy was calculated without allowance for any molecular relaxation (deformation) as a means to achieve energy minimization. Hence, the molecule is modeled as being essentially stiff except for torsional rotations about the backbone bonds of the chain.

The PR force field differs from NR in that, for each conformation of poly(dimethylsilylene), the energy is minimized with respect to torsional rotations about the pendant Si-CH₃ bonds in the chain. In comparing the three force-field methods, we see a progression in the order NR, PR, FR of increased allowance for molecular deformation of the internal degrees of freedom so as to achieve energy minimization.

Conformational energies E calculated with the NR technique were obtained for the chain segments illustrated in Figures 1 and 2 as a function of the rotational angles ϕ_c and ϕ_s with bonds a and d held in the trans ($\phi = 0^\circ$) conformation. The PR calculations on poly(dimethylsilylene) considered the segment [Si(CH₃)₂]₅, so as to be compared directly with the FR calculations of DW.⁹ Each of the 10 methyl groups in this segment was permitted to rotate independent of one another about the Si-CH₃ bond.

Pertinent structural parameters used in the NR and PR calculations are summarized in Table I. The values chosen were taken from the FR calculations from DW⁹ as averages for the most stable (minimum energy) conformations. Thus the corresponding C-C (1.53 Å) and C-H (1.10 Å) bond lengths in the structurally analogous *n*-alkanes^{8,12} are substantially smaller, and the additional ~0.8-Å length of the Si-Si bond relative to the C-C bond would be expected to reduce considerably the severity of repulsive interactions in the polysilanes. At the same time, however, the additional length of 0.38 Å for the Si-H bond in polysilane over the C-H bond in the *n*-alkanes could act to offset this by rendering the pendant H atoms more proximate and hence the interactions more repulsive for certain conformations. Likewise, for some conformations CH₃...CH₃ interactions may be more repulsive in [-Si(CH₃)₂-] than in [-C(CH₃)₂-] owing to the greater length of the Si-CH₃ bond (1.87 Å) relative to the C-CH₃ bond (1.53 Å). The C-C-C and C-C-H bond angles in the *n*-alkanes are 112° and 109°^{8,12} respectively, and these are nearly identical with the corresponding angles used here for the polysilanes.

For the NR calculations, the nonbonded (NB) interac-

tions were described by the exp-6 potential energy function⁸

$$E_{NB} = A \exp(-Br) - C/r^6 \quad (1)$$

where r is the interatomic distance for a given interaction and A , B , and C are the nonbonded potential energy parameters, as given in Table II. The parameter C characterizing the attractions was calculated from atomic polarizabilities¹³ by application of the Slater-Kirkwood equation.¹⁴ Values of B for a like-atom pair were taken from Scott and Scheraga¹⁵ while values for an unlike pair were given by $B_{ij} = (B_{ii}B_{jj})^{1/2}$. The corresponding values of the parameter A were then determined by minimizing eq 1 at $r_{min} = r_1 + r_2$, where r_1 and r_2 are the "augmented"^{8,16} van der Waals radii, taken from crystal structure data.¹⁷

For the PR calculations, E_{NB} was expressed in terms of the familiar Lennard-Jones (LJ) 12-6 function

$$E_{NB} = A'/r^{12} - C/r^6 \quad (2)$$

with the attractive parameter C the same as above and the repulsive parameter A' , calculated in similar fashion as described for A above, given in Table II. These two equations, eq 1 and 2, yield virtually identical E_{NB} vs. r profiles for a given atom-atom interaction; however, use of the LJ 12-6 function obviates concern over the spurious maximum encountered in eq 1 for $r \ll r_{min}$.¹⁸

As a result of the larger size and greater polarizability of Si relative to C, the E_{NB} potential energy minimum for Si...Si is roughly 4 times as deep and located 0.50 Å more distant than that for the C...C interaction. Likewise, the E_{NB} minimum for the Si...H interaction is about twice as deep and 0.25 Å more distant than that for C...H.

In both the NR and PR calculations the torsional term was given by $E_{TOR} = (E_0/2)(1 - \cos 3\phi)$, with ϕ the rotational angle and E_0 the intrinsic torsional barrier height. The value of E_0 for the Si-Si bond was set at 1.2 kcal mol⁻¹, which is considerably smaller than the corresponding value (2.8 kcal mol⁻¹) used in most calculations for the C-C bond found in the *n*-alkanes.^{8,12,19} This feature will tend to flatten the potential energy surface of silanes relative to the analogous alkanes. In the PR calculations E_0 for the Si-CH₃ bond was taken as 0.40 kcal mol⁻¹. These E_0 values correspond closely to those used in the FR calculations of DW.⁹ Thus, the polysilanes and the *n*-alkanes differ markedly in terms of both their structure (i.e., bond lengths) and their energy parameters, and these differences manifest themselves in the potential energy surfaces calculated for the two types of chains.

While the PR methodology and more so the NR methodology represent simplifications relative to that employed by DW, they do offer several benefits in that (1) the computational speed and affordability of these calculations permit use of fine grids and (2) in scanning the full range of conformational space (rather than seeking energy minima only), these methods traverse the entire conformational terrain and quantify domain sizes and rotational barriers needed for an analysis of dynamic flexibility and configuration-dependent properties. Such methods are thus complementary to the computationally more rigorous full-relaxation methods such as that employed by DW, which are designed to locate energy minima (global or local) within conformational-energy space. The current literature contains numerous examples of configuration-dependent properties calculated for a variety of polymers on the basis of conformational energies derived from methodologies of the NR and PR type.^{8,12,19,20-24}

Conformational energy maps based on the NR and PR

Table IV
Relative Energies^a and Torsional Angles^b of Various Conformers of Polysilane As Calculated by the NR and FR^c Methods

	NR ^c		FR	
	(E) ^a	(ϕ) ^b	E ^a	ϕ ^b
TT	0.51	0.0	0.7	0.0
TG	0.21	125	0.4	121.4
GG	0.00	125	0.0	125.3
G ⁺ G ⁻	0.41	-120	0.4	-111.2

^a In kcal mol⁻¹, given relative to E = 0.0 kcal mol⁻¹ for the minimum-energy conformation. ^b In degrees, given relative to $\phi = (0^\circ, 0^\circ)$ for the all-trans, planar zigzag conformation. ^c Values of E and ϕ represent Boltzmann-weighted averages taken from the generated potential-energy maps.

terminated by the relative magnitudes of z , follows the more typical order TG > TT >> G⁺G⁻ >> G⁺G⁺. By comparison, in the analogous *n*-alkanes TT states are preferred over G⁺G⁻ states by ca. 1.0 kcal mol⁻¹, and G⁺G⁺ states are almost prohibitively high in energy.^{8,12} Given the preferences for successive gauche conformations and based on the assumption that intermolecular energies generally have only a small effect on conformation,⁸ the crystalline-state configuration of polysilane is predicted to be more likely helical rather than similar to the polyethylene [CH₂CH₂-] planar zigzag conformation. For polysilane nearly all regions of the conformational-energy space are within 2.0 kcal mol⁻¹ of the energy minima; this is in sharp contrast to the relatively high barriers (>6 kcal mol⁻¹) and large regions of prohibitively high energy found in the case of the *n*-alkanes.⁸

Values of the relative energies and associated conformations ϕ for polysilane, calculated by both the FR method of DW⁸ and the methods employed herein, are compared in Table IV. Agreement is satisfactory, as one would expect for such a structurally simple and conformationally flexible molecule as polysilane.

Poly(dimethylsilylene). The potential energy map for poly(dimethylsilylene) based on the PR calculations is given in Figure 4. Associated values of (E), z , and (ϕ_b , ϕ_c) are listed in Table V along with those derived from the NR calculations. A summary of the relative energies and their associated conformations for poly(dimethylsilylene) as calculated by the NR, PR, and FR methods is given in Table VI. In this case, substantial qualitative differences are noted among the results given by the three methods. Specifically, the most striking difference is that, whereas the GG state is found prohibitively high in energy by the NR calculation, it is the preferred state for the FR calculation. Since values of the bond lengths and backbone bond angles used in both methods are nearly identical, the discrepancy is largely attributable to torsional relaxation of the pendant Si-CH₃ groups afforded by the FR method. That the influence of torsional relaxation of pendant groups is dominant is corroborated by the results of the PR calculations, which, while allowing torsional relaxation only with respect to the Si-CH₃ bonds, show a marked reduction of the relative energy for the GG conformation, although not sufficient to render it the preferred conformation. Of course, other forms of structural relaxation (e.g., deformation of the Si-C-H and Si-Si-C bond angles, which the PR program as written does not include) would be expected to contribute but less so.

Notwithstanding this discrepancy, the three methods do yield some similarities in modeling the conformational characteristics of poly(dimethylsilylene). Specifically, all three find the G⁺G⁺ states prohibitively high in energy, and the relative conformational energy preferences of TT

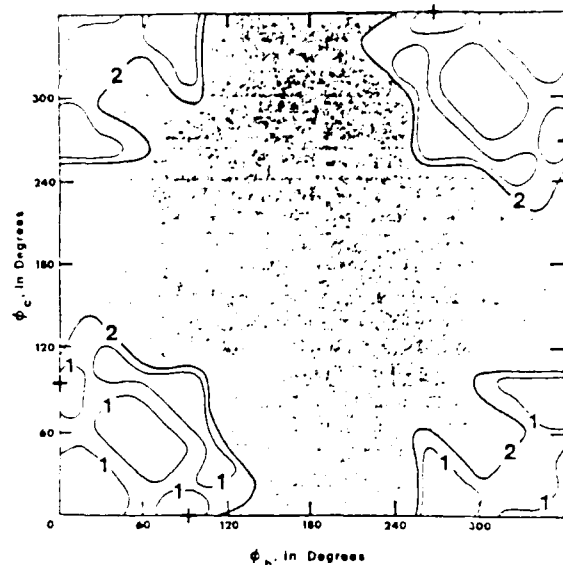


Figure 4. Conformational energy map for poly(dimethylsilylene) as determined by the PR calculations.

Table V
Pertinent Conformational Parameters for the Poly(dimethylsilylene) Chain Segment As Determined by the NR and PR Energy Calculations

	NR			PR		
	z , ^a	(E) ^a	(ϕ) ^c	z , ^a	(E) ^a	(ϕ) ^c
T(T)	1.00	-5.99	0	1.00	-16.7	0
T(G)	0.26	-6.04	125	0.82	-17.1	98
G(G)	~0.0	(~-2)	125	0.38	-17.0	89
G ⁺ (G ⁻)	~0.0	>>6	-115	~0.0		

^a Expressed relative to $z = 1.00$ for the TT state. ^b In kcal mol⁻¹, given as the Boltzmann-weighted averages derived from the conformational energy maps. ^c In degrees, in which 0° corresponds to the all-trans, planar zigzag conformation.

Table VI
Relative Energies^a and Associated Torsional Angles^b of Various Conformers of the Poly(dimethylsilylene) Segment As Calculated by the NR, PR, and FR^c Force-Field Methods

	NR ^c		PR ^c		FR	
	(E) ^a	(ϕ) ^b	(E) ^a	(ϕ) ^b	E ^a	ϕ ^b
T(T)	0.1	0.0	0.42	0	0.9	0.0
T(G)	0.0	125	0.00	98	0.8	120.3
G(G)	~4	125	0.08	89	0.0	125.3
G ⁺ (G ⁻)	>12	-115	d		38.4	-107.7

^a In kcal mol⁻¹, given relative to the energy of the minimum-energy conformation. ^b In degrees, given relative to $\phi = 0^\circ$, corresponding to the trans conformation. ^c Values (E) and (ϕ) correspond to Boltzmann-weighted averages derived from the respective potential energy maps. ^d Calculated energy was prohibitively high.

and TG states are in reasonable agreement. While corresponding values of ϕ given by the NR and FR methods are close, the PR calculations located gauche states quite smaller in magnitude (and thus correspondingly less compact) than conventional values (i.e., $\pm 120^\circ$).

Values of z obtained from both the NR and PR calculations indicate that the size of the domain associated with TT is larger than that for TG or GG. Figure 4 is noted for its large regions of prohibitively high energy, in contrast to that (Figure 3) for polysilane itself, for which nearly all regions are within 2 kcal mol⁻¹ of the energy minima. The difference is attributable to the steric bulk of the methyl groups in poly(dimethylsilylene) relative to that of the H atoms in polysilane.

Table VII
Values of the Statistical Weight Parameters Computed at
25 °C Derived from Results of the NR, PR, and FR
Conformational Energy Calculations

	polysilane			poly- (dimethylsilylene)		
	NR	PR	FR	NR	PR	FR
σ	1.6	...	1.6	0.27	0.82	1.2
ψ	1.5	...	2.0	0.00	0.56	3.8
ω	0.52	...	1.0	0.00	0.00	0.0

Chain Statistics. The structural information given in Table I and the dihedral angles listed in Tables IV and V for polysilane and poly(dimethylsilylene), respectively, were used in conjunction with eq 6 and 7 to calculate the characteristic ratio C_{∞} for the two chains. The statistical weight parameters σ , ψ , and ω computed at 25 °C for the two chains based on the NR, PR, and FR calculations are listed in Table VII. For polysilane, the corresponding C_{∞} values are 4.1 and 3.9 based on the NR and FR calculations, respectively. The nearly identical values reflect the similarity in conformational characteristics obtained by the two different force fields for this chain. The relatively small value of C_{∞} for polysilane is indicative of rather low chain extensibility, a feature consistent with the chain's overall conformational flexibility (i.e., no overwhelming preference for any one particular conformational state), its identifiable preferences for the more compact TG and G*G* states over the alternative and more chain-extending TT states, and, moreover, its allowance for G*G* states, whose occurrence typically leads to reversals in chain direction. For comparison, values of C_{∞} at 25 °C for two other flexible polymers, polyethylene and poly(dimethylsiloxane), are 6.7²² and 6.4²⁶ respectively.

Values of C_{∞} at 25 °C for poly(dimethylsilylene) were 15.0, 13.2, and 12.5 based on the NR, PR, and FR calculations, respectively. Given the differences in conformational preferences predicted by the three force-field methods, the closeness in the values is surprising. Specifically, the value $C_{\infty} = 12.5$ obtained based on the FR calculations is only slightly smaller than the corresponding value of 15.0 based on the NR results, yet the FR results indicated clear preferences for GG states over the alternative TT and TG states where, in contrast, the NR results yielded precisely the opposite preferences (i.e., TT and TG states over GG). These substantial quantitative and qualitative differences are obviously not strongly reflected when comparing the corresponding C_{∞} values.

An explanation for the closeness of C_{∞} values in this case and the consequent lack of sensitivity to the MM method used can be found in a detailed analysis of the sequences of states allowable based on the conformational preferences elucidated by the MM calculations. In point, the helix associated with ...G*G*G*G*G*... sequences, predicted by the FR calculations as having a high probability of occurrence, is more compact than either that associated with the ...TTTTT... or ...TG*TG*T... sequences predicted by the NR calculations. However, this is compensated somewhat by the fact that the NR calculations also indicate high probability for sequences such as ...TG*TG*T... and ...TG*TTG*T..., whose inclusion of nearby gauche states of opposite sign will tend to divert chain direction and thus foreshorten the dimensions of the chain. The FR calculations predict relatively low probability of occurrence of such sequences and, in general, of any sequences corresponding to reversal or redirection of chain propagation. Thus in different but nearly compensatory ways the NR and FR calculations allow for sequences of states more compact than the fully extended

all-trans configuration. In fact, if the poly(dimethylsilylene) chain adopted an all-trans conformation, then as $n \rightarrow \infty$ the calculated value of C_{∞} would approach ∞ rather than the values (12.5–15.0) obtained here.

As would be expected from the intermediate nature of its calculated conformational energies, the PR method yielded $C_{\infty} = 13.2$, nearly midway between the values obtained from using the NR C_{∞} and FR calculations. The value of C_{∞} obtained from the PR results would have been somewhat closer to that (12.5) obtained from the FR results except that the locations (i.e., 90–100°) of the gauche states obtained in the PR calculations are more extended than those found in the NR and FR calculations (120–125°).

The NR results yield C_{∞} values of 3.85, 4.02, 4.15, and 4.25 at 0, 25, 50, and 75 °C, respectively, for polysilane and 15.0 at all four temperatures for poly(dimethylsilylene). That the values for polysilane increase slightly as the temperature increases reflects the greater accessibility of the higher energy and chain-extending trans states. Values of C_{∞} for poly(dimethylsilylene) are negligibly affected in this temperature range, as would be expected given the virtual exclusion of all states except TT and TG indicated by the NR calculations.

Acknowledgment. We acknowledge the financial support provided the Air Force Office of Scientific Research through Grant AFOSR 83-0027 (Chemical Structures Program, Division of Chemical Sciences) to J.E.M. We also acknowledge the encouragement and suggestions derived from discussions with Prof. James R. Damewood, Department of Chemistry, University of Delaware, and Prof. Robert West, Department of Chemistry, University of Wisconsin—Madison.

Registry No. Polysilane, 32028-95-8; poly(dimethylsilylene), 28883-63-8.

References and Notes

- West, R.; David, L. D.; Djurovich, P. I.; Stearley, K. L.; Srinivasan, K. S. V.; Yu, H. *J. Am. Chem. Soc.* 1981, 103, 7352.
- Trefonas, P., III; Djurovich, P. I.; Zhang, X.-H.; West, R.; Miller, R. D.; Hofer, D. *J. Polym. Sci.* 1983, 21, 819.
- Trefonas, P., III; West, R.; Miller, R. D.; Hofer, D. *J. Polym. Sci.* 1983, 21, 823.
- West, R. *J. Organomet. Chem.* 1986, 300(1–2), 327.
- Chiang, C. K.; Drey, M. A.; Gau, S. C.; Heeger, A. J.; MacDiarmid, A. G.; Park, Y. W.; Shirakawa, H. *J. Am. Chem. Soc.* 1978, 100, 1013.
- Chiang, C. K.; Park, Y. W.; Heeger, A. J.; Shirakawa, H.; Louis, E. J.; MacDiarmid, A. G. *J. Chem. Phys.* 1978, 69, 5098.
- Ivory, D. M.; Miller, G. G.; Sowa, J. M.; Shacklette, L. W.; Chance, R. R.; Baughman, R. H. *J. Chem. Phys.* 1979, 71, 1506.
- Rabolt, J. F.; Clarke, T. C.; Kanazawa, K. K.; Reynolds, J. R.; Street, G. B. *J. Chem. Soc., Chem. Commun.* 1980, 347.
- Kanazawa, K. K.; Diaz, A. F.; Geiss, R. H.; Gill, W. D.; Kwak, J. F.; Logan, J. A.; Rabolt, J. F.; Street, G. B. *J. Chem. Soc., Chem. Commun.* 1979, 854.
- Bnaumik, D.; Mark, J. E. *Polym. Prepr., (Am. Chem. Soc., Div. Polym. Chem.)* 1982, 23, 105.
- Welsh, W. J.; Beshah, K.; Ackerman, J. L.; Mark, J. E.; David, L. D.; West, R. *Polym. Prepr., (Am. Chem. Soc., Div. Polym. Chem.)* 1983, 24, 131.
- Flory, P. J. *Statistical Mechanics of Chain Molecules*; Interscience: New York, 1969.
- Damewood, J. R., Jr.; West, R. *Macromolecules* 1985, 18, 159.
- Allinger, N. L., et al. *QCPE* 1981, 13, 395.
- Hummel, J. P.; Stackhouse, J.; Mislow, K. *Tetrahedron* 1977, 33, 1925.
- Tribbie, M. T.; Allinger, N. L. *ibid.* 1972, 28, 2147.
- Abe, A.; Jernigan, R. L.; Flory, P. J. *J. Am. Chem. Soc.* 1965, 87, 631.
- Ketelaar, J. A. A. *Chemical Constitution*; Elsevier: New York, 1958.
- Pitzer, K. S. *Adv. Chem. Phys.* 1959, 2, 59.
- Scott, R. A.; Scheraga, H. A. *J. Chem. Phys.* 1965, 42, 2209; 1966, 45, 2091.

- (17) Allinger, N. L.; Miller, M. A.; Catledge, F. A.; Hirsch, J. A. *J. Am. Chem. Soc.* 1967, 89, 4345.
- (18) Bondi, A. *J. Phys. Chem.* 1964, 68, 441.
- (19) Hirschfelder, J. O.; Curtiss, C. F.; Bird, R. B. *Molecular Theory of Gases and Liquids*; Wiley: New York, 1954.
- (20) Welsh, W. J.; Mark, J. E.; Riande, E. *Polym. J. (Tokyo)* 1980, 12, 467.
- (21) Jorgensen, W. L. *J. Am. Chem. Soc.* 1981, 103, 677; *J. Phys. Chem.* 1983, 87, 5304.
- (22) Sundararajan, P. R. *Macromolecules* 1978, 11, 256.
- (23) Suter, U. W. *J. Am. Chem. Soc.* 1979, 101, 6481.
- (24) Suter, U. W.; Flory, P. J. *Macromolecules* 1975, 8, 765.
- (25) Abe, A. *J. Am. Chem. Soc.* 1984, 106, 14.
- (26) Sundararajan, P. R.; Flory, P. J. *J. Am. Chem. Soc.* 1974, 96, 5025.
- (27) Crescenzi, V.; Flory, P. J. *J. Am. Chem. Soc.* 1964, 86, 141.

Translational Diffusion of Linear and 3-Arm-Star Polystyrenes in Semidilute Solutions of Linear Poly(vinyl methyl ether)

T. P. Lodge* and L. M. Wheeler

Department of Chemistry, University of Minnesota, Minneapolis, Minnesota 55455.

Received April 29, 1986

ABSTRACT: The technique of dynamic light scattering from isorefractive ternary solutions has been used to investigate the translational diffusion behavior of linear and 3-arm-star polymers in linear polymer matrices. Diffusion coefficients have been obtained for four polystyrene (PS) samples present in trace amounts in solutions of poly(vinyl methyl ether) (PVME) in *o*-fluorotoluene over the range 0.001–0.1 g/mL in PVME concentration. The high molecular weight of the PVME sample, 1.3×10^6 , guarantees that these concentrations extend well into the entangled regime. For PS with molecular weights around 4×10^5 , a 3-arm star diffuses slightly more rapidly than its linear counterpart. However, when the PS molecular weight exceeds 1×10^6 , a 3-arm star diffuses much less rapidly than its linear counterpart at the higher matrix concentrations. These data are interpreted as evidence for the importance of topology in determining diffusion rates for polymers in concentrated solutions. While this observation is consistent with the reptation mechanism, it is also apparent that reptation cannot dominate the diffusion process until the diffusing molecules are thoroughly entangled with the matrix.

Elucidation of the mechanisms by which polymer molecules in entangled solutions and melts diffuse, relax stress, or renew their conformations is an aim with great practical and theoretical importance. Over the past decade, a large number of experimental and theoretical studies have been undertaken to examine the validity and range of applicability of the reptation concept; the subject has recently been reviewed.¹ For polymer melts, diffusion coefficients measured by a wide variety of techniques are consistent with the M^{-1} power law, which can be considered the signature of reptation. However, the experimentally well-established $M^{-1/4}$ power law for shear viscosity is not in agreement with the reptation prediction. It is not yet clear whether this discrepancy can be explained by modifications to the basic reptation hypothesis, which was originally proposed for linear chains in fixed obstacles,² or whether fundamentally different molecular-level processes need to be invoked. In polymer solutions above the coil overlap concentration, the situation is even less clear. Reptation-based predictions for the molecular weight, concentration, and solvent quality dependence of the translational diffusion coefficient have all been compared with experimental results, with distinctly differing degrees of agreement.^{1,3}

The solution situation may be more complicated than that of the melt due to several factors including the enhanced mobility of the molecules surrounding a test polymer, the role of solvent quality, and the concentration dependence of the monomeric friction coefficient. Among the possible contributing mechanisms that have been suggested, in addition to reptation, are (1) constraint release, or tube renewal, in which a test chain moves laterally into a vacancy created by the departure of a neighboring chain;^{4–6} (2) the "noodle effect", in which a diffusing chain drags other entangling chains for finite distances;⁷ (3)

Stokes-Einstein diffusion, in which the test chain moving as a hydrodynamic sphere experiences only the bulk solution viscosity;^{4,8} and (4) diffusion through a field of obstacles that generate hydrodynamic screening.^{9–13} To design experiments to distinguish among these possibilities, given that they are not mutually exclusive, is challenging. One promising approach is to compare the diffusion coefficients of model branched polymers with those of linear molecules under identical conditions.

In the framework of reptation, the presence of long-chain branches should severely impede translational diffusion;¹⁴ studies of 3-arm-star diffusion in the melt support this picture.^{15–17} However, apparently no similar studies in solution have been reported. The pioneering diffusion studies of von Meerwall et al.^{18,19} on dilute solutions of 3-arm-star polystyrenes, polyisoprenes, and polybutadienes did extend into the semidilute regime in some cases, but not for sufficiently high molecular weights to expect entanglement. These NMR measurements were performed on binary solutions, i.e., identical test and matrix polymers, and thus represent a different physical situation from that examined here. Nevertheless, these authors' conclusion that 3-arm-star and linear polymer diffusion behaviors are qualitatively indistinguishable is interesting in light of the results presented below. The importance of pursuing diffusion measurements in entangled solutions is underscored by considering that, unlike reptation, none of the four mechanisms listed above explicitly considers the topology of the diffusing polymer. As a result, linear and 3-arm-star polymers with either equal numbers of entanglements per molecule (cases 1 and 2) or equivalent hydrodynamic radii (cases 3 and 4) should diffuse at comparable rates. To test this hypothesis, diffusion data are presented for two 3-arm and two linear polystyrenes (PS) in semidilute solutions of linear poly(vinyl methyl ether)

Ethylamine and Ammonia as Catalysts in the In-Situ Precipitation of Silica in Silicone Networks*

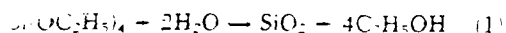
Y. P. NING and J. E. MARK

Department of Chemistry and the Polymer Research Center
The University of Cincinnati,
Cincinnati, Ohio 45221

Both ethylamine and ammonia in aqueous solutions catalyze the hydrolysis of tetraethylorthosilicate to precipitate silica filler within poly(dimethylsiloxane) elastomers. The rate of filler precipitation can vary in a complex manner, possibly due to loss of colloidal silica and, in the case of the ethylamine solutions, deswelling of the networks. Increase in catalyst concentration increases the precipitation rate, and increase in amount of filler precipitated dramatically increases the modulus and ultimate strength of the networks, thus demonstrating the desired reinforcing effects.

INTRODUCTION

Silica filler may be precipitated into an already cross-linked elastomer by the hydrolysis



of tetraethylorthosilicate (TEOS) present as diluent in the network structure (1-6). The concept of such an "in-situ" precipitation is novel, and of practical importance since hard mineral fillers, however introduced, can give considerable reinforcement to an elastomer (7-11). A variety of substances have been found (2) to act as catalyst for this hydrolysis, but very little has been done to characterize the rate of the reaction.

The present study concerns the use of aqueous solutions of ethylamine and ammonia as catalysts for this in-situ precipitation reaction. They were chosen in part because of their volatility, which makes them easy to remove from the filled polymer network. Of primary interest is the effect of the hydrolysis conditions on the amount of silica precipitated and the elastomeric properties of the resulting filled elastomers.

EXPERIMENTAL DETAILS

The networks investigated were prepared from two samples of hydroxyl-terminated poly(dimethylsiloxane) (PDMS) $[\text{Si}(\text{CH}_3)_2\text{O}]_n$ having number-average molecular weights of 5.0 and $21.5 \times 10^3 \text{ g mol}^{-1}$, respectively. The samples were generously provided by the Dow Corning Corporation of Midland, MI. They were tetrafunctionally end-linked using $\text{Si}(\text{OC}_2\text{H}_5)_4$ with stannous-2-ethylhexanoate as catalyst, in the usual manner (12, 13). The resulting networks were extracted with tetra-

hydrofuran and then toluene for several days to remove soluble material (found to be present to the extent of a few percent).

Two series of samples were cut from the extracted and dried network sheets. The first consisted of a large number of relatively small pieces to be used to obtain the amount of filler precipitated as a function of hydrolysis time. The second consisted of a smaller number of larger pieces, in the form of strips suitable for stress-strain measurements in elongation. The dependence of the wt percent filler on time and catalyst concentration can be expected to differ somewhat for the two series since the TEOS hydrolysis and its loss to the surrounding solution would depend on the ratio of sample surface area to volume, and thus on sample size and shape.

One strip cut from each network sheet was set aside as a reference material (0 wt percent filler). The other network strips were swelled with TEOS to the maximum extent attainable, which corresponded to a volume fraction of polymer of approximately 0.3 and 0.2, respectively. The swollen strips were then placed into aqueous solutions of either ethylamine or ammonia, at a series of concentrations. The hydrolysis of the TEOS was permitted to occur at room temperature for various periods of time, and values of the wt percent filler incorporated were obtained from the weights of the dried strips.

The strips cut from the networks were used in elongation experiments to obtain the stress-strain isotherms at 25°C (12-15). The elastomeric properties of primary interest were the nominal stress $\bar{f} \equiv f/A^*$ (where f is the equilibrium elastic force and A^* the undeformed cross-sectional area), and the reduced stress or modulus, $(15-18) [\bar{f}^r] \equiv \bar{f}/(\alpha - \alpha^{-2})$ (where $\alpha = L/L_0$ is the elongation or relative

*Presented in part at a meeting of the Rubber Division of the American Chemical Society, Los Angeles, 1983.

len of the strips. All stress-strain measurements were carried out to the rupture points of the samples, and were generally repeated in part to test for reproducibility.

RESULTS AND DISCUSSION

The rates of the precipitation reaction were studied through plots of weight percent filler against time. Typical results for the $C_2H_5NH_2$ -catalyzed system are shown in Fig. 1. Although the rates increase with catalyst concentration (6), as expected, they are seen to vary in a complex manner. One complication is the deswelling of the network due to movement of TEOS and the byproduct ethanol to the surrounding aqueous solution. The loss of TEOS should be smaller in the case of the more dilute $C_2H_5NH_2$ solution (since it is more hydrophilic), and this would explain the relatively simple monotonic form of the corresponding precipitation curves. In the case of the more concentrated $C_2H_5NH_2$ solutions the curves level off, because of the TEOS migration, and then turn downward, presumably because of loss of colloidal silica. At constant time, less filler is precipitated in the

case of the networks having the larger value of the molecular weight between crosslinks, and this is probably due to larger losses of TEOS and silica from the large "pores" in these networks in the highly swollen state.

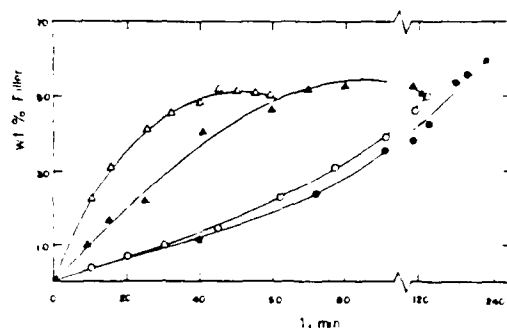


Fig. 1. Weight percent filler precipitated shown as a function of time for several illustrative systems. The circles locate the results for 2.0 wt percent ethylamine and the triangles the results for 25.0 wt percent; the open symbols are for networks having a molecular weight between crosslinks of 6.0×10^3 g mol $^{-1}$, and the filled symbols 21.3×10^3 g mol $^{-1}$.

Table 1. Reaction Conditions, Amount of Filler Precipitated, and Ultimate Properties of the Filled Elastomers

Reaction Conditions				Ultimate Properties			
$10^{-3} M_{c,0}$ g mol $^{-1}$	Catalyst	Wt % Catalyst	Time, min	Wt % Filler	$\alpha,^\circ$	$f_r,^\circ$ N mm $^{-2}$	$10^3 E_r,^\circ$ J mm $^{-2}$
8.0	$C_2H_5NH_2$	2.0	0	0.0	2.72	0.539	0.547
			25	10.2	2.16	1.05	0.478
			50	24.5	1.60	1.44	0.497
			60	25.4	1.80	1.69	0.800
			90	37.5	2.23	2.65	1.86
		25.0	25	20.4	2.00	1.36	0.711
			37	25.6	2.33	2.34	1.64
			45	34.3	1.92	2.22	1.29
		35.0	5	5.2	1.92	0.650	0.465
			13	13.4	2.07	1.05	0.697
			20	20.1	1.87	1.32	0.698
			60	23.0	1.59	1.67	0.731
		50.0	5	7.6	2.07	1.00	0.563
			11	22.2	1.39	1.55	0.523
			20	17.1	1.45	0.866	0.309
			42	15.4	1.66	1.65	0.578
21.3	$C_2H_5NH_2$	2.0	0	0.0	2.61	0.257	0.297
			75	23.9	2.51	1.25	0.998
			110	37.9	2.29	1.47	1.07
			150	44.7	1.74	1.46	0.670
8.0	NH_3	5.0	0	0.0	1.64	0.491	0.266
			65	10.0	1.99	0.603	0.462
			85	16.0	2.07	1.21	0.693
			130	26.8	1.73	1.31	0.618
			140	37.2	1.86	2.06	0.842
		10.0	23	10.1	1.87	0.663	0.309
			32	16.4	1.82	0.747	0.375
			42	27.9	1.86	1.25	0.547
			81	37.7	1.65	1.70	0.669
		15.0	115	36.2	1.30	2.21	0.516
			19	16.4	1.56	0.705	0.240
			27	27.7	1.73	0.836	0.320
			62	37.3	1.66	1.65	0.643
		30.0	67	36.2	1.45	1.91	0.540
			27	8.6	1.73	0.636	0.291
			30	15.6	1.82	0.671	0.347
			38	20.0	2.27	1.39	1.47

$^\circ$ Number-average molecular weight between crosslinks of PDMS network.

$^\circ$ Expressed at rupture.

$^\circ$ Ultimate strength, as represented by broken stress at rupture.

$^\circ$ Energy required for rupture.

The rate curves for the NH_3 -catalyzed systems are very similar to those for the diure $\text{C}_2\text{H}_5\text{NH}_2$ solution, so that the wt percent filler tends to increase monotonically with time. This may be due to NH_3 having less affinity for the TEOS, which would decrease the amount of network deswelling.

Information on the amounts of filler precipitated into the actual strips used in the stress-strain measurements is given in the first five columns of Table I. Typical stress-strain isotherms obtained as described above are presented in Figs. 2 and 3. The data are shown in the usual way (16-18), as the dependence of the reduced stress on reciprocal elongation. It is interesting to note that increase in wt percent filler does not always increase the reduced stress $[f^*]$. This must be due to differences in the nature of the filler particles, in particular their average size, size distribution, or degree of agglomeration [characteristics which can be studied by transmission electron microscopy (5)]. Also, as is frequently observed (7-11), some of the isotherms for the more heavily filled networks did not exhibit complete reversibility. In any case, the presence and efficacy of the filler are demonstrated by the marked increases in modulus, with some upturns at the higher elongations.

The data of Figs. 2 and 3 can also be represented in plots of f^* against α , in which case the area under each stress-strain curve corresponds to the energy E_r of rupture (13), which is the standard measure of elastomer toughness. Its values, along with values of the maximum extensibility α_r and ultimate strength f_r^* are given in the last three columns of Table I. Although the results show some scatter, as is generally the case (15), some trends are apparent. Thus, increase in wt percent filler decreases α_r but increases f_r^* . The latter effect predominates and E_r increases accordingly. In some cases, extremely large levels of reinforcement are obtained, as is illustrated in Fig. 4. Such networks behave nearly as thermosets, with some brittleness (small α_r), but with extraordinarily large values of the modulus E_r .

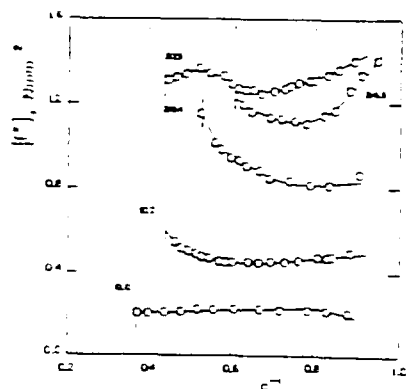


Fig. 2 The reduced stress shown as a function of reciprocal elongation, at 25°C, for the PDMS networks having $M_c = 8,000$ and filled in the 2.0 wt percent $\text{C}_2\text{H}_5\text{NH}_2$ solution. Each curve is sampled with the wt percent filler present in the network and the results for the unfilled elastomer are included.

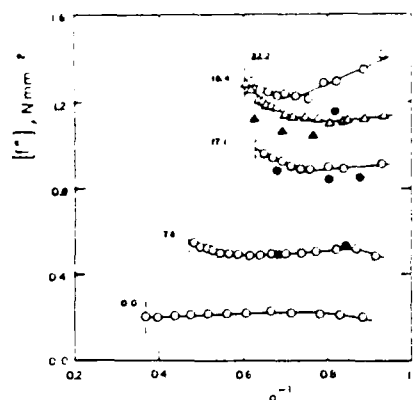


Fig. 3 The reduced stress shown as a function of reciprocal elongation for the networks having $M_c = 8,000$ and filled in the 50.0 wt percent $\text{C}_2\text{H}_5\text{NH}_2$ solution. Filled symbols are for results obtained out of sequence to test for reversibility.

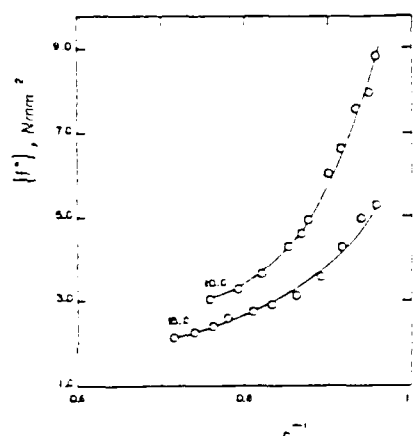


Fig. 4 The reduced stress shown as a function of reciprocal elongation for networks prepared in a 10.0 wt percent NH_3 solution (35.3 wt percent filler), and in a 15.0 wt percent NH_3 solution (37.2 wt percent filler).

Correlation of results such as these with information on the particles obtained from scattering experiments are in progress.

ACKNOWLEDGMENTS

It is a pleasure to acknowledge the financial support provided by the National Science Foundation through Grant DMR 79-15903-03 (Polymers Program, Division of Materials Research) and by the Air Force Office of Scientific Research through Grant AFOSR 85-0027 (Chemical Structures Program, Division of Chemical Sciences).

REFERENCES

1. J. E. Mark and S.-J. Fan, *Makromol. Chem., Rapid Comm.*, **3**, 681 (1982).
2. C.-Y. Jiang and J. E. Mark, *Makromol. Chem.*, **185**, 2609 (1984).
3. M.-Y. Tang and J. E. Mark, *Polym. Eng. Sci.*, **24**, 218 (1984).
4. M.-Y. Tang, A. Lenton, and J. E. Mark, *Colloid Polym. Sci.*, **262**, 890 (1984).
5. Y.-P. Ning, M.-Y. Tang, C.-Y. Jiang, J. E. Mark, and W. C.

6. J. E. Mark and Y. F. Ng, *Polym. Bulletin*, **12**, 43 (1981).
7. W. J. Koros et al., "Rubber Technology," Ed. by M. Morton, Van Nostrand Reinhold, New York, 1975.
8. M. F. Wagner, *Rubber Chem. Technol.*, **49**, 703 (1976).
9. E. L. Warrick, O. K. Pierce, K. E. Folmanteer, and J. C. Saure, *Rubber Chem. Technol.*, **52**, 437 (1979).
10. B. B. Boonstra, *Polymer*, **20**, 691 (1979).
11. Z. Krigb, *Adv. Polym. Sci.*, **36**, 21 (1980).
12. J. E. Mark and J. L. Sullivan, *J. Chem. Phys.*, **66**, 1006 (1977).
13. M. A. Laurent, A. L. Andrad, and J. E. Mark, *J. Polym. Sci., Polym. Phys. Ed.*, **19**, 621 (1981).
14. M. A. Laurent, A. L. Andrad, and J. E. Mark, *J. Polym. Sci., Polym. Phys. Ed.*, **18**, 2263 (1980).
15. J. E. Mark, *Adv. Polym. Sci.*, **44**, 1 (1982).
16. J. E. Mark and P. J. Flory, *J. Appl. Phys.*, **37**, 4635 (1966).
17. L. R. G. Treloar, "The Physics of Rubber Elasticity," Clarendon Press, Oxford (1975).
18. J. E. Mark, *Rubber Chem. Technol.*, **48**, 495 (1975).

Precipitation of iron oxide filler particles into an elastomer

S. Liu and J. E. Mark*

Department of Chemistry and the Polymer Research Center, University of Cincinnati,
Cincinnati, OH 45221, USA

Summary

Samples of peroxide-cured butyl rubber were impregnated with anhydrous FeCl_3 , which was then hydrolyzed in a magnetic field to give ferric hydroxide particles. The filler thus formed in situ was found to give good reinforcement of the elastomer. A relatively small but significant anisotropy was found for both the elongation modulus and the equilibrium degree of swelling.

Introduction

There has now been a number of studies in which filler particles are precipitated into a polymer to produce a reinforced elastomeric material (1-8). One of the advantages of this novel technique is the control it gives over the degree of agglomeration of the filler. The particles obtained thus far have been of a ceramic nature, for example silica (1,4,5,7) and titania (5,8) produced by the in-situ hydrolysis of silicates and titanates.

Another novel approach to reinforcing elastomers involves the use of magnetic particles which are dispersed into a polymer prior to its being cross-linked in a magnetic field (9,10). In this case, it is possible to manipulate the particles with the field, thus producing anisotropic reinforcement even from spherical particles.

The present investigation combines these two techniques. The in-situ hydrolysis of ferric chloride (11-15) is used to precipitate ferric hydroxide particles into a cross-linked polyisobutylene (PIB) elastomer. It is anticipated that at least some of the particles formed will have sufficient response to a magnetic field to give anisotropy as discernible from stress-strain and swelling equilibrium measurements.

Experimental Details

The PIB sample employed was a "butyl rubber" copolymer (16) containing 2 mol % unsaturated repeat units to permit cross-linking. It had a number average molecular weight of 4.56×10^5 g/mol, and it was generously provided by Dr. E. N. Kresge of the Exxon Chemical Company.

* To whom all correspondence should be sent.

Aqueous ferric chloride (FeCl_3) was dissolved in volume to give a series of solutions having nominal molarities in the range 0.2 - 0.8. Insolubles were removed by filtration. Each extracted PIB sample was asswelled with one of these solutions for 4 hrs. Values of the volume fraction of polymer in these swollen samples ranged from 0.111 to 0.161. The samples were evaporated to dryness and placed into vials containing aqueous solutions of hydrochloric acid at the molarities given in the second column of Table I. Each vial was mounted between the poles of a

Aqueous ferric chloride (FeCl_3) was dissolved in volume to give a series of solutions having nominal molarities in the range 0.2 - 0.8. Insolubles were removed by filtration. Each extracted PIB sample was asswelled with one of these solutions for 4 hrs. Values of the volume fraction of polymer in these swollen samples ranged from 0.111 to 0.161. The samples were evaporated to dryness and placed into vials containing aqueous solutions of hydrochloric acid at the molarities given in the second column of Table I. Each vial was mounted between the poles of a

Preparation of Samples, Elongation Moduli, and Swelling Results

Preparation of Samples					Swelling Equilibrium ^c v_2^d	$1/l_1$
Exp.	HCl Conc., (Molarity)	Wt % Filler	Axial Orientation ^a	$\{\epsilon\}^b$ (cm^{-2})		
1	-	0.00	-	0.165	-	-
	-	9.21%	-	0.170	-	-
2	0.01	8.97	-	0.344	0.450	1.21
	0.01	8.97	-	0.345	0.454	1.20
3	0.1	8.98	-	0.403	0.435	1.24
	0.1	8.98	-	0.400	0.433	1.26
4	1	1.55	//	0.198	0.222	1.53
	1	1.55	\perp	0.198	0.223	1.56
5	1	3.02	//	0.262	0.301	1.66
	1	3.02	\perp	0.262	0.311	1.38
6	1	5.07	//	0.306	0.286	1.65
	1	5.07	\perp	0.269	0.296	1.66
7	1	10.0	//	0.463	0.322	1.33
	1	10.0	\perp	0.463	0.397	1.21

 λ = ratio of elongation of polymer in the swollen network, relative to magnetic lines of force, $\lambda = 0.7$, \bar{c} in benzene at room temperature.

Two sets of strips ($-1 \times 4 \times 30 \text{ mm}^3$) were cut with their long axes parallel (*H*) to what had been the magnetic lines of force, and two other sets were cut perpendicular (\perp). For purposes of comparison, two reference strips were cut from a sheet of unfilled polymer, and from a sheet of polymer filled with unhydrolyzed FeCl₃, respectively. Two pairs of additional reference strips were obtained by cutting strips in arbitrary but mutually perpendicular directions from two sheets prepared in the absence of a magnetic field. The reference strips are described in the first four columns and the first six rows of Table I, and the test strips filled in the presence of the field in the corresponding columns of the last eight rows.

Results and Discussion

Values of the equilibrium value f of the elastic force, the undeformed cross-sectional area A_0 , and the elongation or relative length were used to calculate the reduced stress or modulus:

(1)

The resulting values are shown as a function of reciprocal elongation in Figure 1, and the specific values at a reciprocal elongation $\alpha^{-1} = 0.7$ are given in column five of the Table.

The first pair of experiments demonstrates that unhydrolyzed FeCl₃ dissolved in the network causes very little change in modulus. Both of the next two pairs of isotherms confirm the expectation that precipitating the filler in the absence of a magnetic field should give a nearly mechanically isotropic system. Comparison of the results for pair two (with three, and pair five with six, indicates that decrease in pH (increase in HCl molarity) has essentially no effect on the wt % filler precipitated, but does cause an increase in modulus. This may be due to the fact that low pH gives particles that are more rodlike in shape (12). In any case, experiments two through seven clearly demonstrate a strong reinforcing effect, with its magnitude increasing with increase in filler content. Also, as is shown in column five of the Table and in the figure, the modulus is higher in the direction that was parallel to the

AD-A190 700

HIGH-PERFORMANCE POLYMERIC MATERIALS(U) CINCINNATI UNIV 3/3
OH DEPT OF CHEMISTRY J E MARK 07 DEC 87
AFOSR-TR-87-2011 AFOSR-83-0027

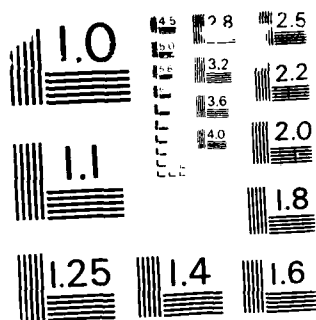
UNCLASSIFIED

F/G 7/6

NL



END
DATE
FILMED
58
21



MICROCOPY RESOLUTION TEST CHART
NATIONAL BUREAU OF STANDARDS - 1963

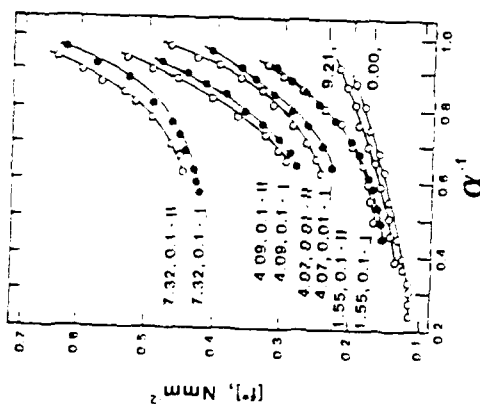


Figure 1. Representative stress-strain isotherms for the F1R networks in elongation at 25°C. The labels give the v_2 filler precipitated into the elastomer, the molarity of the acid used in the FeCl_3 hydrolysis, and the orientation of the long axis of the sample relative to the lines of force of the magnetic field, if present. See Table I.

magnetic lines of force and the difference increases with increase in v_2 filler. Some particle orientation was obviously obtained by means of the magnetic field and the conditions that maximize this effect are presently being sought.

The swelling equilibrium results are first described in terms of the volume fraction v_2 of polymer present in the network (with the volume of the filler being ignored in the present comparisons). Its values are given in column six of the Table. In general, increase in v_2 filler is seen to increase v_2 , as expected. Also, some anisotropy is observed in the swelling, as demonstrated by the values of v_2 and by the increases in the length of the strips reported in the final column of the Table. In particular, the increases in length are smaller (less swelling) in the perpendicular direction and the differences generally increase with increase in v_2 filler. In this case the decreased swelling direction corresponds to lower modulus, in agreement with some earlier results (9), but the opposite correlation has also been observed (10).

The observed anisotropy, and its control by means of a magnetic field, could be of practical as well as fundamental importance.

Acknowledgements

It is a pleasure to acknowledge the financial support provided by the Army Research Office through Grant DAMR-86-K-0032 (Materials Science Division) and by the Air Force Office of Scientific Research through Grant AFOSR 83-0027 (Chemical Structures Program, Division of Chemical Sciences).

References

1. J. E. Mark, *Brit. Polym. J.*, **17**, 144 (1985), and relevant papers cited therein.
2. Y.-P. Ning and J. E. Mark, *J. Appl. Polym. Sci.*, **30**, 3519 (1985).
3. J. E. Mark and G. S. Sur, *Polym. Bulletin*, **14**, 325 (1985).
4. J. E. Mark, Y.-P. Ning, C.-Y. Jiang, M.-Y. Tang, and W. C. Roth, *Polymer*, **26**, 2069 (1985).
5. G. S. Sur and J. E. Mark, *Eur. Polym. J.*, **21**, 1051 (1985).
6. Y.-P. Ning and J. E. Mark, *Polym. Eng. Sci.*, **26**, 167 (1986).
7. G. S. Sur and J. E. Mark, *Makromol. Chemie*, **187**, 2861 (1986).
8. S.-B. Wang and J. E. Mark, *Polym. Bulletin*, **17**, 271 (1987).
9. Z. Righi and J. E. Mark, *J. Polym. Sci., Polym. Phys. Ed.*, **23**, 1767 (1985).
10. G. B. Sohoni and J. E. Mark, *J. Appl. Polym. Sci.*, **33**, 3009 (1987).
11. E. Matijevic, *Prog. Colloid Polym. Sci.*, **61**, 74 (1976).
12. E. Matijevic, *J. Colloid Interface Sci.*, **63**, 509 (1978).
13. S. Kratochvil, E. Matijevic, and M. Ozaki, *Colloid Polym. Sci.*, **262**, 804 (1984).
14. E. Matijevic, *Ann. Rev. Mater. Sci.*, **15**, 483 (1985).
15. E. Matijevic, *Colloid Polym. Sci.*, **265**, 155 (1987).
16. C. C. Sun and J. E. Mark, *J. Polym. Sci., Polym. Phys. Ed.*, **25**, 909 (1987).
17. C. H. Griffiths, M. F. O'Horo, and T. W. Smith, *J. Appl. Phys.*, **50**, 7108 (1979).
18. H. Remy, "Treatise on Inorganic Chemistry", Vol. 2, Elsevier, New York, 1956.
19. J. E. Mark and J. L. Sullivan, *J. Chem. Phys.*, **66**, 1006 (1977).
20. M. A. Llorente, A. L. Andraday, and J. E. Mark, *J. Polym. Sci., Polym. Phys. Ed.*, **18**, 2263 (1980).

Accepted May 20, 1987 K

California Group Develops Accurate Free Energy Differences from Perturbation Theory

A powerful computational method for the calculation of free energies has recently created a surge of interest throughout the world among researchers engaged in computer simulation of molecular systems. The technique, known as the perturbation method, is based on the principles of statistical mechanics, a discipline which seeks to explain the macroscopic properties of matter from its nature at the molecular level. Like the alchemists' dream, the perturbation method involves transmutation of the elements. During the course of the computer simulation, one molecule is "mutated" to another. When applied

to the amino acids of a protein, this simulates the effects of site-specific mutagenesis.

The perturbation method has created excitement in the molecular simulation community because of its ability to simply and accurately calculate the difference in free energy between two molecular systems that may differ in charge, bonding and even atomic makeup. The method is robust and gives values in good accord with experiment. The ability to calculate free energies allows making realistic predictions of such properties as the binding of drugs to macromolecular

receptors, the effects of site-specific mutation on enzyme catalysis, the relative solubility of small molecules in water or other solvents and the effects of solvent on reaction energies.

The predominant techniques of computational chemistry, quantum mechanics, molecular mechanics and molecular dynamics, only allow calculations of internal energies, or in some cases enthalpies. While these quantities have predictive ability in favorable cases, these methods normally do not consider the effect of entropy. Further, to ascertain the

Continued on page 7

Index

Seibel investigates free energy perturbation theory	1
What's ahead in computer graphics for 1987	1
New Products	2
People	2
Polygen introduces ChemNote	3
Welsh explores electrical conductivity in polymers	4
Meetings	10
Professional Opportunities	14

The Next Step for Molecular Modelling: Interactive Graphics Supercomputing

A new generation of **graphics supercomputer** systems with the power of more than 20 VAX 11/780's in a desksize package will be available within one year. The power of these systems will have a dramatic impact on the fields of molecular modelling and computational chemistry. The potential productivity improvements go far beyond a mere speed-up of computations. They will deliver truly **interactive supercomputing** to the individual researcher.

A typical molecular modelling installation today consists of a

superminicomputer with one or more attached graphics terminals. Additional compute cycles may be available in the form of an array processor or a corporate mainframe.

A configuration such as this has two very serious limitations. First, the computational performance is inadequate; typical molecular energy calculations take hours. Second, the graphics terminal is a view-only device that has little or no interaction with the computational part of the task.

Continued on page 13

MDL, Chemical Design, Beckman Offer New Products

Molecular Design Ltd., San Leandro, CA, has announced the immediate availability for chemists of volumes 8-10 of the Journal of Synthetic Methods (JSM) in graphical computer-readable form, tailored for use with REACCS, MDL's reaction indexing software. JSM, which is published by Derwent Publications Ltd., London, covers novel reactions and new synthetic methods, new compound classes and functional groups and extended applications of known reactions. For additional information,

contact Marie Comez at MDL, 2132 Farallon Drive, San Leandro, CA 94577 (425-895-1313).



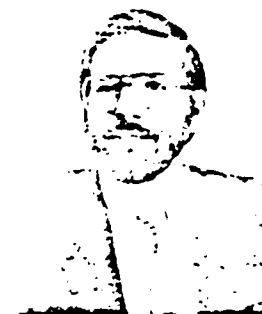
Chemical Design, Ltd., Oxford, England, is now offering a range of "intelligent" customized raster graphics terminals tailored for use with its Chem-X molecular modelling software. The new machines are based on the 6000 series displays produced by Sigmex, a European computer graphics manufacturer. The 3D custom firmware in Chemical Design's S6264L and S6234L terminals is used by the ChemMovie module of Chem-X to perform calculations locally. This allows 3D transformation of chemical structures in real time. Depth-cueing and shading options are also included. Up to 256 different colors may be displayed simultaneously, selected from a palette of more than 16 million.

The terminals can be purchased independently or as part of a MicroGRAF molecular modelling workstation, integrating graphics display, MicroVAX II computer subsystem and Chem-X software. For more information contact Dr. John Dunn, Chemical Design Inc., Box 120, 200 Route 17, Mahwah, NJ 07430 (201-529-3323) in the U.S.; readers outside the U.S. may contact Helen Gasking, Chemical Design, Ltd., Unit 12, 7 West Way, Oxford, OX2 0JB ENGLAND (865-251-483).



Beckman Instruments, Inc., Fullerton, CA, has announced a new laboratory information management system which operates on large IBM main-frame computers under the VMS operating system. The new product will allow large bioindustrial companies

Dennis H. Smith has recently joined Molecular Design Limited, San Leandro, CA, as Vice President, Product Development. Smith was formerly director, Biotechnology Research and Development and principal investigator of the BIONET National Computer Resource of



Dennis H. Smith, Ph.D.,
Molecular Design Limited

IntelliGenetics, Mountain View, CA. Prior to that he was Group Leader, Director, Research Applications Development at Lederle Laboratories, Pearl River, NY.

Smith holds a B.S. in chemistry from the Massachusetts Institute of Technology and a Ph.D. in chemistry from the University of California, Berkeley. He spent 15 years doing research at Berkeley, the University of Bristol and Stanford, where he was a senior research associate and key contributor to the Dendral Project, an early artificial intelligence program.

to integrate laboratory information with other corporate databases and systems. The user can choose from IBM, DEC VAX and HP1000A Series to suit the total computing environment of a particular installation. For additional information contact Beckman Instruments, Inc., 2500 Harbor Boulevard, Fullerton, CA 92734-3100 (714-871-4848).

Statement of Editorial Policy

It is the express editorial policy of *Chemical Design Automation News* to publish objective information on matters of technical interest relating to the use of computer automation techniques in chemical and engineered materials research. In accordance with this policy, we welcome participation from all individuals and institutions involved in the field.

Chemical Design Automation News

is published monthly.
ISSN 0886-6716.

Publisher: Luiza Aguiar
Editor: Barbara F. Granam
Chief Science Editor: Frank A. Momany
Production: James A. Wojno

Address: 200 Fifth Avenue
Warrham, MA 02254
(617) 890-2888

Subscription Rates: \$195 U.S.;
\$245 Canada, Mexico and Overseas.
\$45 Academicians.

Copyright 1987. No part of this publication may be reproduced in any form without the written permission of CDA News.

Polygen Sketching Tool to Aid Chemists in Depicting Molecules

Editors Note: This begins the first in a series of articles we will be publishing on PC-based chemical design products. We invite readers to submit articles on this subject to CDA News.

The ChemNote Sketching Tool is a molecular sketch, display and coordinate-generating tool that runs on IBM PC/AT-compatible microcomputers. The program allows the chemist to sketch a two-dimensional molecule, do a quick conversion into three dimensions, and display and manipulate the 3D molecule interactively. To our knowledge, this is the first commercially-available program written for the microcomputer environment that combines all these abilities. The ChemNote Sketching Tool will be formally released 9 March at the Pittsburgh Conference, Booth #11035, in Atlantic City, NJ. Pre-release copies are currently available from Polygen Corporation, Waltham, MA.

The ChemNote Sketching Tool is not intended to replace true molecular modelling programs based on more powerful hardware. Rather, it is intended to serve as a "quick-look"

tool, helping the chemist decide which structures should be submitted to a modelling program for a more extensive modelling run. Once a molecule is built in ChemNote, the 3D coordinates of the atoms, as well as atom and bond types, can easily be extracted for use as a starting point in a modelling run. Currently, Polygen also offers a utility that converts a ChemNote molecule file into a CHARMM input file (Chemistry at Harvard Molecular Mechanics, a molecular mechanics program also available from Polygen) and also provides a convenient front end to CHARMM. Polygen will release a number of additional file conversion utilities to popular mainframe and microcomputer-based modelling programs such as MM2, MOPAC, GAUSSIAN80 and CNDO2, etc., later this year.

ChemNote utilizes a mouse to provide the chemist with a user-friendly interface to the software. Pull-down menus and graphical icons eliminate the need for complex keyboard commands. A help line, always visible at the bottom of the screen, alerts the user to errors and warnings and supplies general instructions.

The Two-Dimensional Construction Mode of ChemNote allows the chemist to sketch a new molecule or fragment from the information in any file directory, display it on the screen and edit the structure as required. Single, double, triple, resonant and hydrogen bonds may be used to build the molecule, as can any atom from the periodic table. A set of prefabricated ring structures can also be employed. The mouse is used to build objects on the screen and to facilitate positioning during editing. ChemNote highlights atoms or bonds whenever the cursor contacts them. All these functions allow rapid construction and editing of structures.

In addition to the sketching capabilities, the 2D construction mode allows one to assign chemical properties, such as partial atomic charges, chirality, isotope number, free radical position, cis/trans bonds and ring conformation to atoms and bonds as appropriate. This mode is more than just a pretty-picture drawer; it is the first step in generating a three-dimensional structure.

Continued on page 14

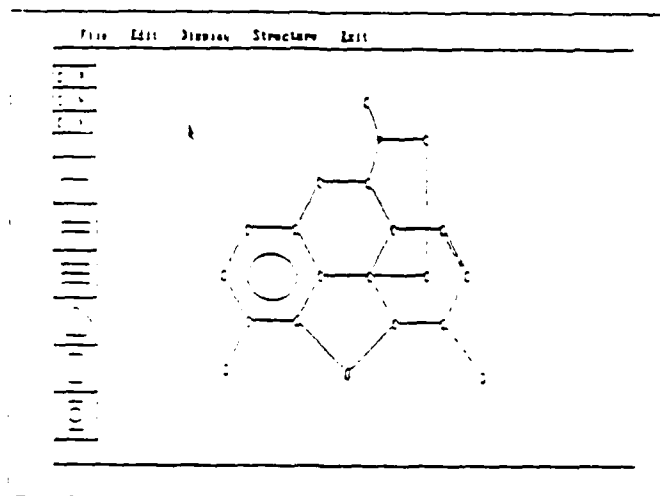


Figure 1. Two-dimensional diagram of morphine constructed in ChemNote.

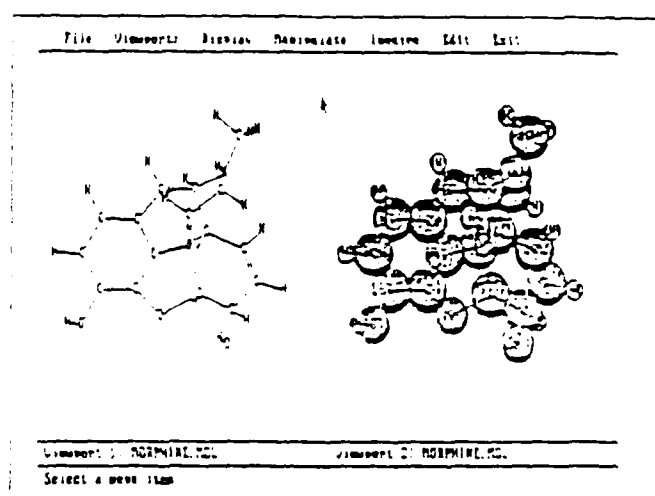


Figure 2. Three-dimensional vector and spacefilling displays of morphine in ChemNote.

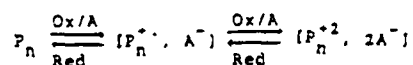
Theoretical Studies of Electrical Conductivity in Polymers

Highly conducting organic polymers comprise a promising and rapidly expanding new research area. Indeed, the interest generated in the conducting and semiconducting properties of organic polymers stems from their potential wide applications in antistatic equipment, electromagnetic shielding, switchable contact bridges, rectifying devices and photovoltaic cells, and rechargeable battery cells and electro-optical devices, to name just a few.¹ Nevertheless, many fundamental aspects of the physical and chemical mechanisms underlying the remarkable electronic properties of these polymers are not well understood. Much more theoretical work is therefore needed to establish a sound basis for interpreting and even predicting the electronic properties of these materials from their structure.

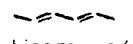
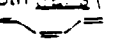
Interest in conducting polymers intensified in the last decade with the discovery that the electrical conductivity of certain polymers can be controlled over a wide range, from insulating to metallic, by the appropriate treatment with chemical oxidants and reductants ("dopants"). The breakthrough came in 1971 when Shirakawa found that acetylene can be polymerized to produce a freestanding film with promising mechanical properties,² and when, somewhat later, MacDiarmid and Hager showed that polyacetylene becomes conductive by exposing it to oxidizing agents such as iodine or arsenic pentafluoride.³ Since these findings, a plethora of fundamental investigations have arisen from the ranks of chemists, physicists, materials scientists and theoreticians, both in academia and industry, with the common goal of producing a new generation of materials endowed with the physical properties of plastics and the electrical conductivity of metals.

It is now generally accepted that conductivity arises from the oxidation

or reduction of a suitable neutral precursor polymer with the concomitant generation of a salt in which electrical charge residing along the polymer backbone is counterbalanced by gegenions.⁴ For example, in the reaction between a penodic segment of a polymer chain P_n and an oxidizing agent A , a cation radical of P_n is formed in the first redox reaction and a di-cation by the second electron transfer



In the language of solid-state physicists, the ion-radical is called either a soliton if the charge and spin are mobile without the necessity to cross an energy barrier while traversing the chain, or a polaron if it is linked to an elastic bond distortion and thus cannot move without picking up energy. The di-cation P_n^{2+} is referred to as a bipolaron by analogy.

The prototype of conducting polymers is polyacetylene $[-CH=CH]_n$, the simplest and certainly to date the most thoroughly studied material in this area. Pure polyacetylene, which exists in both *trans* () and *cis* () isomeric forms, is an insulator like all other pure polymers. It is made conductive by adding iodine, bromine or other oxidizing and reducing agents, with the conductivity rising sharply with dopant concentration. Several other polymers also become conductive upon doping, for example the polyphenylenes,



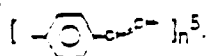
the polypyrroles,



the polyniobiphenes



and the polyparaphenylene vinylenes



They all have one salient feature in common: they possess conjugated double bonds, i.e., extended sequences of alternating single and double bonds. Hence, it is reasonable to assume that these conjugated or aromatic sequences provide a continuous overlapping set of molecular orbitals which is necessary if not sufficient for electrical conductivity.

While the list of conducting and semiconducting polymers is continually expanding, most experts believe that conductive polymers are five to ten years away from leaving the laboratory for the commercial market. The difficulty lies in the fact that these doped polymers are highly unstable and quite difficult to process into useable forms. To render a polymer conducting, dopants must diffuse through the polymer in concentrations much higher than that used to convert silicon into a semiconductor. This causes large-scale distortion of the polymer's backbone, rendering it more susceptible to degrading agents such as oxygen. As a result, the polymer eventually loses its conductivity and converts into a brittle non-processable material. Hence the search continues for polymers that possess high conductivity yet remain stable and processable.

The approach taken by the author and coworkers has been to calculate the so-called band structures of various candidate polymer chains using quantum mechanical procedures based on the Extended Hückel Theory (EHT)⁵ and, more recently, the Valence Effective Hamiltonian (VEH) Theory.⁷ These calculated band structures are akin to those commonly illustrated in discussions of the "band theory of metals" included in many introductory chemistry courses. (See Figure 1). One of the

Continued on page 5

Electrical Conductivity

Continued from page 4

calculations is the so-called band gap (E_g) which is the difference in energy between the highest electron-filled band (i.e., valence band) and the lowest unoccupied band (i.e., conduction band). In insulators the energy gap (Figure 1) is sufficiently large so as to virtually preclude excitation of electrons from the valence band to the conduction band; in metals the valence and conduction bands overlap, thus affording electrons in the valence band free movement through the conduction band. In a semiconductor, the energy gap is small enough that some electrons make the transition simply by acquiring extra thermal energy (hence the conductivity of semiconductors increases with temperature).

As an example, we have carried out band structure calculations on several halogen-substituted polyacetylenes such as $[-CX=CX]_n$ and $[-CH=CX]_n$ with $X=F$ or Cl .⁸ Our interest in these systems is based on experiments suggesting that substitution of halogen atoms for some or all of the H atoms in polyacetylene imparts improved stability and, possibly, solubility.⁹ Encouragingly, our calculated band gaps for both the fluorinated and chlorinated analogues were comparable to those similarly calculated for polyacetylene itself. However, enthusiasm must be tempered in that these calculations portray the chains as perfect conjugated arrays (i.e., no defects) and oriented with the backbone atoms lying in the same plane so as to maximize the orbital overlap (and hence minimize the band gap). These models may therefore be unrealistic and, in fact, subsequent conformational energy calculations on some of the chlorinated analogues indicate that the steric bulk of the chlorine atoms forces these chains out of a planar array with subsequent and sharp increases in the band gap. Similarly, experiments have indicated that random substitution of $Si(CH_3)_3$

Figure 1. Simplified illustration of the band structure of a solid

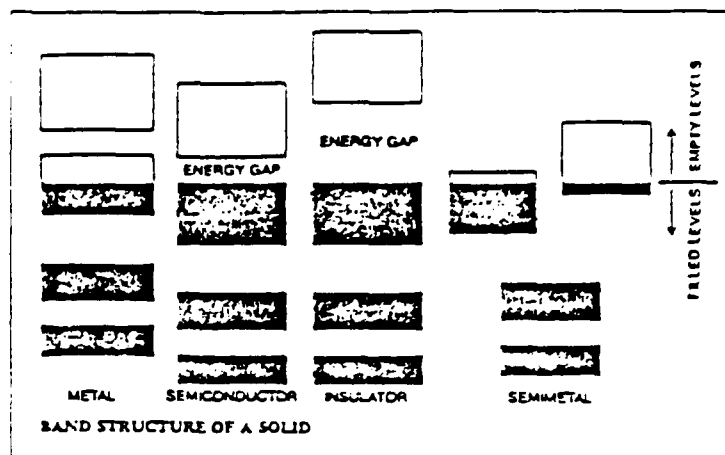
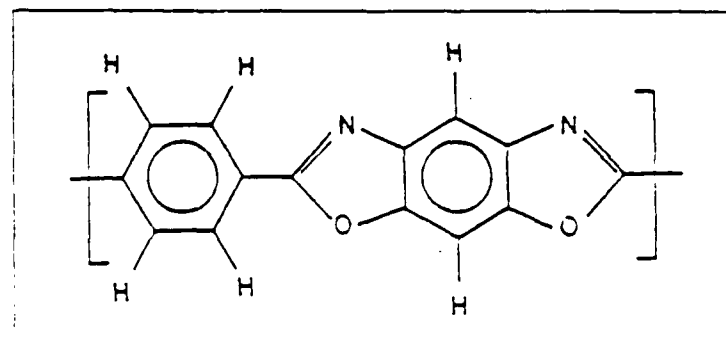


Figure 2. The *as*-PBO repeat unit



groups along the polyacetylene chain improve solubility and tractability.⁹ Unfortunately, these calculations show that such substitutions have the effect of increasing the band gap and, as in the chlorine case, distorting the conjugated chain array from its preferred planar orientation.

Our interest in the polyacetylenes has extended to the analogous polyynes, including $[-C\equiv C]_n$ and $[-C\equiv C-X]_n$ with $X=S$, Se or SiH_2 .¹⁰ While the calculated band gap for $[-C\equiv C]_n$ was comparable to that found for polyacetylene, in all cases the "X" substitutions caused a more than doubling of the band gap. It is evident that such substitutions along the polymer backbone disrupt the chain conjugation and consequent orbital overlap. (They also produce "kinks" in the otherwise rodlike $[-C\equiv C]_n$ chain).

These studies also include polymers with aromatic backbones. Much of our focus has been on a group of paracat-

enated aromatic heterocyclic polymers whose films and fibers are noted for their exceptional strength, thermal stability and environmental resistance.¹¹ As such, these materials are the focus of the U.S. Air Force's "Ordered Polymer" program, the aim of which is to exploit these high-performance features for aerospace applications.

A polymer of this type, poly(*p*-phenylene benzobisoxazole) (PBO), is illustrated in Figure 2. Other analogues are abbreviated PBT and ABPBI in which the O atoms are replaced by S and NH, respectively. The same extended aromaticity and rodlike structure that give rise to the exceptional physical properties of these polymers should also be conducive to electrical conductivity. Band structure calculations on PBO (See Figure 3) and PBT yield band gaps in the same range as that found for polyacetylene, thus encouraging further

Continued on page 6

Electrical Conductivity

Continued from page 5

acetylene, thus encouraging further theoretical and experimental studies of these and related chains. Indeed, recent band structure calculations on AAPBO and ABPBO chains (See Figure 4), two structurally-related but more flexible analogs of PBO, have yielded band gaps of 1.86 eV and 2.31 eV, respectively, compared with 1.4 - 1.8 eV for our benchmark polyacetylene.¹²

Electrically conducting polymers are a new and exciting class of materials with a wide range of potential applications. While stability remains a serious problem for current polymers exhibiting conductivity, it is hoped that the theoretical studies undertaken by the author and coworkers and by other research groups will uncover polymer types exhibiting controllable electrical conductivity yet high stability so that these applications can be realized.

Acknowledgements:

The author gratefully acknowledges the support provided by the Air Force

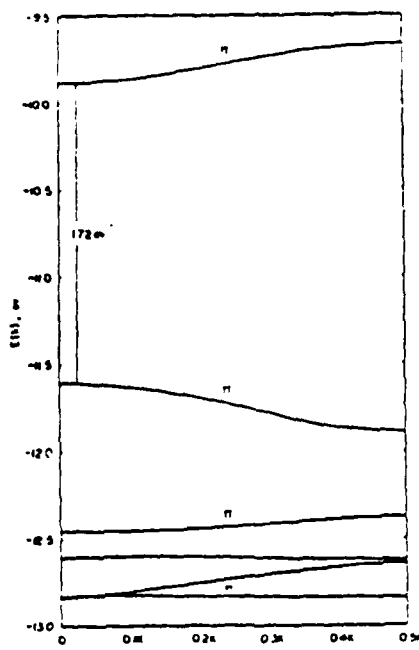


Figure 3. Portion of a calculated band structure of *cis*-PBO in the coplanar conformation with a band gap of 1.72 eV indicated

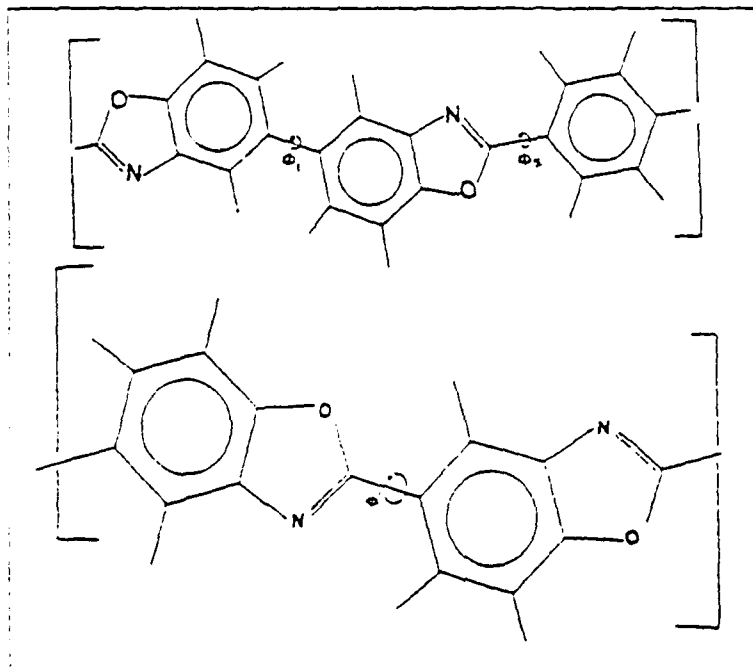
Office of Scientific Research (Grant AFOSR 83-0027) and the the Plastics Institute of America

By William J. Welsh, Ph.D.,
Department of Chemistry,
University of Missouri-
St. Louis, St. Louis, MO 63121

References

1. Munstedt, H. (1985) in *Electronic Properties of Polymers and Related Materials* (Kuzmany, H. and Roth, S., eds.) 8-17, Springer-Verlag, New York.
2. Shirakawa, H. and Ikeda, S. (1971) *Polymer Journal* 2, 231.
3. Heeger, A. J., MacDiarmid, A. G., et al. (1977) *Physical Review Letters* 39, 1089.
4. Wegner, G. (1986) *Makromolekulare Chemie Macromolecular Symposium* 1, 151.
5. Roth, S. (1985) in *Electronic Properties of Polymers and Related Materials*, (Kuzmany, H. and Roth, S., eds.) 2-7, Springer-Verlag, New York.
6. Whangbo, M.-H. and Hoffmann, R. (1979) *Journal of the American Chemical Society*, 100, 6093; Whangbo, M.-H., Hoffmann, R. and Woodward, R. B. (1979) *Proceedings of the Royal Society of London Series A*, 366, 23.
7. André, J. M., Burke, L. A., Delhalle, J., Nicolis, G. and Durand, Ph. (1984) *International Journal of Quantum Chemistry Symposium*, 13, 283.
8. Metzger, K. C. and Welsh, W. J. (1984) *Polymer Preprints*, 25 (1), 195, Division of Polymer Chemistry, American Chemical Society; *ibid.*, 25 (2), 268.
9. Ziegler, S. Sandia National Laboratories, private communications.
10. Metzger, K. C. and Welsh, W. J. (1984) *Polymer Preprints*, 25 (2), 270, Division of Polymer Chemistry, American Chemical Society.
11. Welsh, W. J., Bhaumik, D., Jarfe, H. H. and Mark, J. E. (1984) *Polymer and Engineering Science*, 24 (3), 218, and pertinent references cited therein.

Figure 4.
The AAPBO
and ABPBO
repeat units



Appendix

The thermodynamic relation between C_p and C_v is

$$C_p - C_v = TVK\beta^2$$

where V is the specific volume, K is the bulk modulus and β the volume coefficient of thermal expansion. Taking $V = 0.71 \times 10^{-6} \text{ m}^3 \text{ g}^{-1}$, $K = 5000 \text{ MPa}$ and $\beta = -7 \times 10^6 \text{ K}^{-1}$ as reasonable values¹¹ for CO(HBA/HNA) at 100 K yields $C_p - C_v \approx 10^{-5}$.

Acknowledgements

The authors thank Professor I. M. Ward, FRS, for his interest in the work and for obtaining copolyester samples, which originated from the Celanese Research Corporation, Summit, New Jersey, USA. We also thank Professor J. S. Dugdale and Dr P. G. Hall for helpful discussions and A. A. M. Croxon for help in technical

matters. We thank the Science and Engineering Research Council for continuing financial support.

References

- 1 Crispin, A. J. and Greig, D. *Polymer* 1986, 27 (Commun.), 264
- 2 Dainton, F. S., Evans, D. M., Hoare, F. E. and Melia, T. P. *Polymer* 1962, 3, 277
- 3 Tucker, J. E. and Reese, W. J. *Chem. Phys.* 1967, 46(4), 1388
- 4 Reese, W. and Tucker, J. E. *J. Chem. Phys.* 1965, 43(1), 105
- 5 Wunderlich, B. *J. Chem. Phys.* 1962, 37(6), 1203
- 6 Greig, D. (Developments in Oriented Polymers) (Ed. I. M. Ward), Applied Science Publishers, 1982
- 7 Ziman, J. M. 'Electrons and Phonons', 1960, Clarendon Press, Oxford
- 8 Blackwell, J., Biswas, A., Gutierrez, G. A. and Chivers, R. A. *Faraday Discuss. Chem. Soc.* 1985, 79(6), 2
- 9 Chivers, R. A. and Blackwell, J. *Polymer* 1985, 26, 997
- 10 Biundell, D. J. *Polymer* 1982, 23, 359
- 11 Troughton, M. J. and Ward, I. M. personal communication
- 12 Keese, W. J. *Appl. Phys.* 1966, 37(11), 3959

Reinforcement of a non-crystallizable elastomer by the precipitation *in situ* of silica

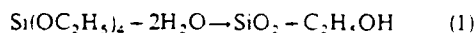
S. J. Clarson and J. E. Mark

Department of Chemistry and the Polymer Research Center, The University of Cincinnati, Cincinnati, Ohio 45221, USA

(Received 14 May 1987)

Introduction

In many of their commercial applications siloxane polymers $[-\text{SiRR}'\text{O}-]$ are filled with silica (SiO_2) in order to improve their mechanical properties¹⁻⁵. A series of recent investigations have shown the feasibility of precipitating silica into poly(dimethylsiloxane) (PDMS) polymers or elastomers by the catalysed hydrolysis of an alkoxysilane or silicate³⁻²¹. In the case where the PDMS is swollen by using tetraethylorthosilicate (TEOS), the reaction is simply



The filler particles generated *in situ* have been shown to be unagglomerated and to have diameters of 150–250 Å^{4,16}. This technique has also been successfully extended to incorporate silica into polyisobutylene (PIB) elastomers²².

The commercially important poly(methylphenylsiloxane) (PMPS) elastomers are also relatively weak materials in the unfilled state^{23,24} and require reinforcement in most of their applications^{1,2}. Furthermore, their atactic nature^{24,25} eliminates the possibility of strain-induced crystallization, which leads to improved properties of a variety of elastomers at high elongations²⁶⁻²⁸, and, when it can occur, is facilitated by the presence of filler^{29,30}. It is the purpose of this communication to report the reinforcement of non-crystallizable, stereochemically well-characterized PMPS elastomers resulting from the precipitation *in situ* of silica.

Experimental

The linear PMPS used in this investigation was prepared by an anionic ring-opening polymerization of cyclic tetramer $(\text{PhMeSiO})_4$ by using potassium hydroxide as the catalyst and has been described in detail elsewhere^{25,31,32}. The linear PMPS, $\text{Me}_3\text{SiO}(\text{PhMeSiO})_n\text{SiMe}_3$ had a weight-average molar mass, M_w , of $186\,000 \text{ g mol}^{-1}$ and a heterogeneity index, M_w/M_n , of 2.0, as determined by low-angle laser light scattering and gel permeation chromatography, respectively^{31,32}. The ^1H n.m.r. spectrum of the polymer was determined in deuterated chloroform solution by using a 300 MHz spectrometer. The α -methyl protons were used to obtain the stereochemical structure of the polymer^{24,25,33,34}, and gave the fraction of meso, f_m , and racemic, f_r , diads to be 0.53 and 0.47, respectively, and hence the linear PMPS was found to be stereochemically atactic.

Two elastomers were prepared from the PMPS as described below. The linear polymer was dissolved in toluene (50% w/w) and benzoyl peroxide was added as a crosslinking agent. The solution was then thoroughly mixed before being transferred to a Teflon (Du Pont registered trademark) lined glass mould. The toluene was evaporated from the mixture at reduced pressure and the polymer was degassed at 323 K. The sample was then crosslinked at 393 K for 1 h under a dry nitrogen atmosphere at reduced pressure (10 mm Hg), and finally postcured at 373 K for six hours.

Each of the elastomers were then extracted for five days by using toluene to remove any soluble material that they contained. After deswelling by using methanol as the non-solvent, the elastomers were dried to constant weight and the volume fraction, v_{2c} , of polymer incorporated into the network was determined in each case. The sample having the lower value of the approximate high-deformation modulus, $2C_1$, was chosen to study the filler reinforcement due to its higher extensibility (larger elongation, α_r , at rupture). These preliminary results are summarized in Table 1.

The silica was precipitated *in situ* into the PMPS elastomer by the procedure described below. The elastomer was divided into test strips that were immersed in TEOS (Fischer) for time intervals in the range 5 min to 24 h and the amount of TEOS incorporated in each case was measured. The strips were then placed in an aqueous solution of 2% (by weight) of the catalyst ethylamine (Kodak), and the hydrolysis of the silane was permitted to proceed for 24 h at 298 K. The samples were then dried to constant weight in a vacuum oven before determining the weight of filler introduced in each case.

Portions of the unfilled elastomers and those filled *in situ* were then used in the uniaxial elongation experiments made to obtain the stress-strain isotherms at 298 K^{26, 28}. The nominal stress was given by $f^* = f/A^*$, where f is the elastic force and A^* is the undeformed cross-sectional area, and the reduced stress or modulus by

$$[f^*] = f^*/(2 - \alpha^{-2}) \quad (2)$$

where $\alpha = L/L_0$ is the elongation or length of the sample, L_0 relative to its initial (unextended) length, L_0 . All measurements were made to the rupture points of the samples.

Table 1 Characteristics of the unfilled polyimethyphenylsiloxane elastomers

Network	Peroxide (wt %)	v_{2c}^a	$2C_1^b$ (N mm ⁻²)	$2C_2^b$ (N mm ⁻²)	$(2C_2/2C_1)^b$	α_r^c
1	1.67	0.86	0.0174	0.0133	0.7644	2.22
2	3.89	0.73	0.0466	0.0253	0.7915	2.06

^a Gel fraction.

^b Mooney-Rivlin elasticity constants (see equation (3)).

^c Elongation at rupture.

Table 2 Results of filler precipitations and stress-strain measurements

Precipitation results		Strain-strain results				
v_{2c}^a	SiO ₂ content (wt %)	$2C_1$ (N mm ⁻²)	$2C_2$ (N mm ⁻²)	α_r	$(f/A^*)^b$ (N mm ⁻²)	$10^4 E_r^c$ (J mm ⁻³)
1.00	0.0	0.0174	0.0133	2.22	0.0435	0.0034
0.51	7.0	0.0310	0.0357	2.14	0.1151	0.0074
0.37	9.7	0.0231	0.0554	1.92	0.1279	0.0062
0.26	13.0	0.0447	0.0519	1.56	0.1125	0.0036
0.13 ^d	38.8	0.4970	0.0166	1.43	0.4527	0.0069

^a Volume fraction of polymer in the TEOS-swollen network.

^b Nominal stress at rupture.

^c Energy required for rupture.

^d Equilibrium swelling at 298 K.

Results and Discussion

The amounts of filler incorporated into the PMPS network are shown in the second column of Table 2. The sample swollen to its equilibrium state with TEOS clearly corresponds to the maximum amount of filler that it was possible to incorporate by this technique, which, for this particular network, was 38.8% (by weight) of silica.

The stress-strain isotherms obtained at 298 K for the unfilled PMPS networks and those filled *in situ* are shown in terms of $[f^*]$ and α^{-1} in Figure 1. The linear parts of the isotherms were represented by the Mooney-Rivlin equation^{27, 28}

$$[f^*] = 2C_1 + 2C_2\alpha^{-1} \quad (3)$$

and the values for the constants $2C_1$ and $2C_2$ are given in columns 3 and 4, respectively, of Table 2. The former represents an approximation of the high-deformation modulus, and $2C_2$ and $2C_2/2C_1$ measure the extent to which the non-affineness of the deformation increases with elongation³⁵. Also of interest are the elongation, α_r , at rupture and the nominal stress, $(f^*A^*)_r$, at rupture, and these values are presented in columns 5 and 6 of Table 2. Figure 2 shows the elasticity data of the unfilled PMPS networks and those filled *in situ* plotted in such a way that the area under each curve corresponds to the energy, E_r , of rupture³⁶, which is the standard measure of elastomer roughness. These values are given in the last column of Table 2.

As can be clearly seen in Figure 1, the modulus or reduced stress of the PMPS elastomers increases as a

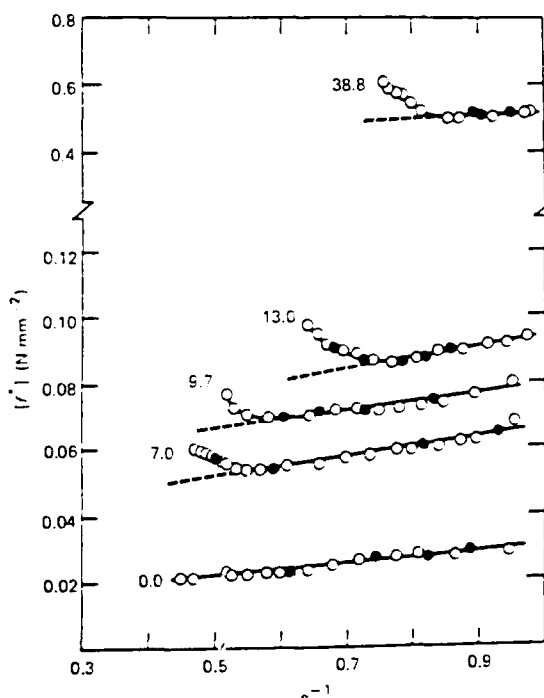


Figure 1 The reduced stress shown as a function of reciprocal elongation for the polyimethyphenylsiloxane networks at 298 K. Each curve is labelled with the weight percentage of filler present in the elastomer. Open circles locate results obtained from using a series of increasing values of α , and filled circles the results obtained out of sequence to test for reversibility. The broken lines help to locate the elongations at which the reduced stress shows an upturn. The data terminate at the rupture points.

function of the amount of silica precipitated *in situ* into the networks. Such increases are comparable with those observed in the correspondingly filled PDMS networks^{3,21}. It is also noted, however, that an increase in the filler content reduces the extensibility of the PMPS elastomers, as represented by α_r , as shown in Table 2.

The experimental data in Figure 1 also reveals an upturn in the modulus at the highest elongations for all the PMPS elastomers filled *in situ*. No upturn was observed for either of the two unfilled PMPS networks described in this study. Similar upturns have been reported previously for PDMS elastomers, filled by analogous methods^{8,13-15,20}. It has also been reported that the crystallization rate of PDMS is increased by the presence of silica²⁹. This has been attributed to the partial preorientation of the adsorbed polymer (roughly 2–3 nm in thickness) or the crystallization nuclei being affected by the presence of the silica³⁰. It should be noted, however, that the effects of strain-induced crystallization do not manifest themselves for unfilled PDMS elastomers³⁷⁻⁴⁰ at room temperature, due to both the high local mobility of the PDMS chains⁴¹⁻⁴³ and the relatively low elongations, α_r , at rupture for such materials³⁷⁻⁴⁰. Since the PMPS elastomers, which are atactic and hence amorphous polymers, also shown the upturns in modulus at high elongations when filled *in situ* with silica, this effect obviously does not occur exclusively as a result of strain-induced crystallization. One source of the additional reinforcement at high elongation is the adsorption of polymer chains onto more than one filler particle⁴⁴, by interactions between surface hydroxyl groups on the silica particles and the siloxane polymer backbone. It is hoped that calorimetric studies and electron micrographs of polymers filled *in situ* in both the unstretched and stretched states will provide further information on such complicated, but nevertheless technologically important, effects.

Further studies of elastomeric materials filled by the precipitation *in situ* of hydrophilic and hydrophobic silica particles and also titanium dioxide particles^{17,45} are in progress.

Acknowledgements

It is a pleasure to acknowledge the financial support provided by the Air Force Office of Scientific Research through Grant AFOSR 83-0027 (Chemical Structures Program, Division of Chemical Sciences) and the Army Research Office through Grant DAAL03-86-K-0032 (Materials Science Division).

References

- Noll, W. 'The Chemistry and Technology of Silicones', Academic Press, New York, 1968.
- Warrick, E. L., Pierce, O. R., Polmanteer, K. E. and Saam, J. C. *Rubber Chem. Technol.* 1979, 52, 437.
- Mark, J. E. and Fan, S.-J. *Makromol. Chem., Rapid. Comm.* 1982, 3, 681.
- Ning, Y.-P., Tang, M.-Y., Jiang, C.-Y., Mark, J. E. and Roth, W. C. *J. Appl. Polym. Sci.* 1984, 29, 3209.
- Jiang, C.-Y. and Mark, J. E. *Colloid Polym. Sci.* 1984, 262, 758.
- Ning, Y.-P. and Mark, J. E. *Polym. Bull.* 1984, 12, 407.
- Mark, J. E. and Ning, Y.-P. *Polym. Bull.* 1984, 12, 413.
- Mark, J. E., Jiang, C.-Y. and Tang, M.-Y. *Macromolecules* 1984, 17, 2613.
- Jiang, C.-Y. and Mark, J. E. *Makromol. Chemie* 1984, 185, 2609.
- Tang, M.-Y., Letton, A. and Mark, J. E. *Colloid Polym. Sci.* 1984, 262, 990.
- Tang, M.-Y. and Mark, J. E. *Polym. Eng. Sci.* 1985, 25, 29.
- Ning, Y.-P., Rigbi, Z. and Mark, J. E. *Polym. Bull.* 1985, 13, 155.
- Mark, J. E. *Brit. Polym. J.* 1985, 17, 144.
- Ning, Y.-P. and Mark, J. E. *J. Appl. Polym. Sci.* 1985, 30, 3519.
- Mark, J. E. and Sur, G. S. *Polym. Bull.* 1985, 14, 325.
- Mark, J. E., Ning, Y.-P., Ning, Jiang, C.-Y., Tang, M.-Y. and Roth, W. C. *Polymer* 1985, 26, 2069.
- Sur, G. S. and Mark, J. E. *Eur. Polym. J.* 1986, 26, 167.
- Ning, Y.-P. and Mark, J. E. *Polym. Eng. Sci.* 1986, 26, 167.
- Mark, J. E. in 'Science of Ceramic Chemical Processing' (Eds. L. L. Hench and D. R. Ulrich), Wiley, New York, 1986.
- Sur, G. S. and Mark, J. E. *Makromol. Chemie* 1986, 187, 2861.
- Mark, J. E. in 'Proceedings of the Third International Conference on Ultrastructure Processing' (Eds. J. D. Mackenzie and D. R. Ulrich), Wiley, New York, 1986.
- Sun, C.-C. and Mark, J. E. *J. Polym. Sci., Polym. Phys. Edn.*, in press.
- de Candia, F. and Turturro, A. *J. Macromol. Sci. Chem.* 1972, A6(7), 1417.
- Llorente, M. A., de Pierola, I. F. and Saiz, E. *Macromolecules* 1985, 18, 2663.
- Clarson, S. J., Dodgson, K. and Semiven, J. A. *Polymer*, in press.
- Flory, P. J. 'Principles of Polymer Chemistry', Cornell University Press, Ithaca, 1953.
- Treloar, L. R. G. 'The Physics of Rubber Elasticity', Clarendon Press, Oxford, 1975.
- Mark, J. E. *J. Chem. Educ.* 1981, 58, 898.
- Sazykina, O. N. and Zakordonets, S. M. *Kolloidn. Zh.* 1976, 38, 1016.
- Warrick, E. L., Pierce, O. R., Polmanteer, K. E. and Saam, J. C. *Rubber Chem. Technol.* 1979, 52, 437.
- Clarson, S. J. and Semiven, J. A. *Polymer* 1986, 27, 1633.
- Clarson, S. J., Dodgson, K. and Semiven, J. A. *Polymer* 1987, 28, 189.

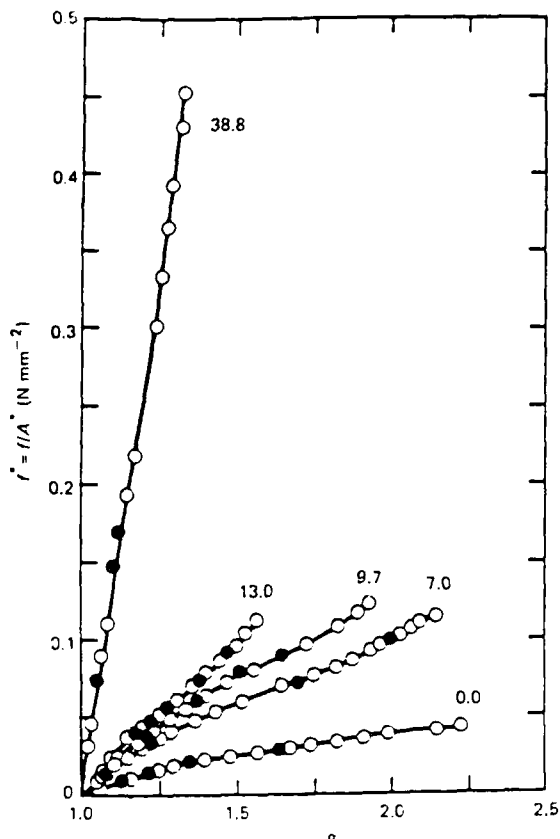


Figure 2 The stress-strain isotherms represented as the dependence of the nominal stress on elongation, thus permitting identification of the area under each curve with the energy of rupture. See legend to Figure 1.

33. Bovey, F. A. 'High Resolution NMR of Macromolecules', Academic Press, New York, 1972.
34. Bovey, F. A. 'Chain Structure and Conformation of Macromolecules', Academic Press, New York, 1982.
35. Flory, P. J. *Brit. Polym. J.* 1985, **17**, 96.
36. Llorente, M. A., Andrad, A. L. and Mark, J. E. *J. Polym. Sci., Polym. Phys. Edn.* 1981, **19**, 621.
37. Mark, J. E. and Flory, P. J. *J. Appl. Phys.* 1966, **37**, 4635.
38. Johnson, R. M. and Mark, J. E. *Macromolecules* 1972, **5**, 41.
39. Mark, J. E. and Sullivan, J. J. *Chem. Phys.* 1977, **66**, 1006.
40. Mark, J. E. *Adv. Polym. Sci.* 1982, **44**, 1.
41. Rahalkar, R. R., Lamb, J., Harrison, G., Barlow, A. J., Hawthorne, W., Semlyen, J. A., North, A. M. and Pethrick, R. A. *Faraday Symp. Chem. Soc.* 1983, **18**, 103.
42. Clarson, S. J., Dodgson, K. and Semlyen, J. A. *Polymer* 1985, **26**, 930.
43. Phan-Van Cang, C., Bokobza, L., Monnerie, L., Clarson, S. J., Semlyen, J. A., Vandendriessche, J. and De Schryver, F. *Polymer* in press.
44. Polmanteer, K. E. and Woods, C. M. *Colloq. Int. C.N.R.S.* 1975, **231**, 253.
45. Polmanteer, K. E. and Helmer, J. D. *Rubber Chem. Technol.* 1965, **38**, 123.
46. Vondracek, P. and Schatz, M. *J. Appl. Polym. Sci.* 1977, **21**, 3211.
47. Wang, S.-B. and Mark, J. E. *Polym. Bull.*, in press.

High molecular weight polyethylene: An n.m.r. approach to partial crystallinity and swelling properties of thermoreversible gels

J. P. Cohen-Addad and G. Feio*

Laboratoire de Spectrométrie Physique associé au CNRS, Université Scientifique, Technologique et Médicale de Grenoble, B.P. 87-38402 St Martin d'Heres, Cedex, France

A. Peguy

Centre d'Etudes et de Recherches sur les Macromolécules Végétales, Université Scientifique, Technologique et Médicale de Grenoble, B.P. 68-38402 St Martin d'Heres Cedex, France
(Received 1E March 1987, revised 9 June 1987)

N.m.r. was used to investigate crystalline properties of swollen polyethylene gels obtained by quenching semidilute solutions of high molecular weight chains. The two concentrations used were 0.9% and 0.4% (w/w). The entanglement concentration determined from initial solutions was shown to control concentrations and sizes of crystallites in swollen gels, at room temperature. Also, the slow elimination of solvent was shown to induce a high-crystallinity state in the dried gel; whereas, dried gels molten for a short time and then quenched at room temperature exhibit smaller extent of crystallinity and less thermodynamically stable crystallites.

(Keywords: polyethylene; thermoreversible gel; swelling; crystallinity; n.m.r.)

Introduction

This work deals with n.m.r. investigations concerning thermoreversible high molecular weight polyethylene gels, obtained by quenching semidilute solutions. These physical gels are known to originate fibres and films that exhibit ultra-high moduli¹⁻⁴. Searching for high drawability, it has been shown that under well defined conditions of polymer concentration, chain molecular weight and gelation temperature, the draw ratio of polyethylene gels may be as high as $\lambda_{max} = 300$, leading to a Young modulus and a tensile strength equal to 202 and 6.2 GPa, respectively⁵. In these systems, interlinkages of chains are mainly mediated by crystallites and the high drawability is usually assumed to result from the low concentration of trapped entanglements, determined by the semidilute solution originating the network structure^{2,6}. More precisely, it is currently considered that the dried gels, observed at room temperature, are determined from a two-component structure.

The first one is associated with partly crystallized clusters that control coupling junctions of chains. The second component corresponds to a crystallization process occurring between interlinkage domains. Resulting crystallites have been clearly identified with those obtained from dilute solutions of polyethylene⁷. The high drawability observed at about 373 K is assumed to reflect first the disappearance of crystallites located

between coupling junctions; then, these are supposed to dissociate, leading to chain sliding, until irreversible knots are formed and a break of the polymer sample occurs.

The present n.m.r. approach is aimed at attempting to physically discriminate between the two crystallized components participating in PE gel structures. Crystallites represent a solid state; therefore, protons embedded in these domains must exhibit a solid-state spin-system response. This n.m.r. observation was supposed to be contrasted to that of chain segments joining crystallites, by originating a chain unfolding effect. Considering swollen PE gels, at room temperature, protons attached to chain segments connecting crystallized domains were expected to behave like spin-systems pertaining to semidilute solutions. N.m.r. has already been extensively used to study partial crystallization processes and swelling effects in gels⁸⁻¹¹.

Experimental

Material. Measurements were made on a currently used linear polyethylene sample (Hercules 1900 UHMW/90189); its molecular weight and intrinsic viscosity were equal to 6×10^6 and $30 \text{ cm}^3 \text{ g}^{-1}$, respectively. Gels were prepared in decalin; 2,6-di-*t*-butyl-*p*-cresol was added to solutions to prevent PE samples from oxidation (0.1% w/w). Dried gels were subsequently swollen by using deuterated toluene (99.7% D; C.E.N., Saclay, France).

* On leave from: Centro de Física da Materia Condensada, Av. Prof. Gama Pinto, 2-1699 Lisbon, Portugal.

4.1 CONFORMATIONAL CHARACTERISTICS OF SOME LIQUID CRYSTALLINE AROMATIC HETEROCYCLIC POLYMERS USABLE AS HIGH-PERFORMANCE MATERIALS

by William J. Welsh

Department of Chemistry
University of Missouri - St. Louis
St. Louis, Missouri 63121
U.S.A.

Reprinted from
"Current Topics in Polymer Science, Volume I"
edited by R. M. Ottenbrite, L. A. Utracki and S. Inoue
© Copyright by Hanser Publishers,
Munich Vienna New York 1987

ABSTRACT

This review focuses on a new type of para catenated aromatic polymer being used in the preparation of high performance films and fibers of exceptional strength, thermal stability, and environmental resistance, including inertness to essentially all common solvents. Polymers of this type include the *cis*- and *trans* poly(p-phenylene benzobisoxazole) (PBO), the *cis*- and *trans* forms of the corresponding poly(p-phenylene benzobisthiazole) (PBT), and the structurally similar poly(5,5'-bibenzoxazole-2,2'-diyl 4,4'-phenylene) (AABPO) and poly(2,5-benzoxazole) (ABPO) and their sulfur-containing analogues. Because of their rigidity, these polymers become highly oriented in solution and some display liquid crystalline behavior. The purpose of this paper is to summarize the authors' theoretical work on the structures, conformational energies and intermolecular interactions for these chains, including, in some cases, the so-called articulated structures and the protonated forms known to exist in strong acids. The emphasis is on how such studies provide a molecular understanding of the unusual properties and processing characteristics of this new class of materials.

INTRODUCTION

Synthetic polymers now pervade all industrialized societies, with new applications appearing on an almost daily basis.¹ One example of a case in which specially synthesized polymeric substances have been particularly impressive in their replacement of non-synthetic or non-polymeric substances is the area of "high-performance" materials. Materials in this category are so designated because of their ability to maintain desirable properties over a wide range of temperatures despite exposure to some very hostile environments. Some specific examples of the superiority of man-made polymers are packaging films far tougher than the cellulose-based materials they replace, and textile fibers such as Dacron[®], which are much more durable than most naturally occurring fibers. A more exotic example is the class of aromatic polyamides having high melting points and exhibiting strengths (on a weight basis) well above that of steel.¹

The present review focuses on a new type of para catenated aromatic polymer being used in the preparation of high performance films and fibers of exceptional tensile strength and modulus, thermal stability, environmental resistance (including inertness to essentially all common solvents), and low specific gravity compared to glass, carbon and steel. A polymer of this type, a poly(p-phenylene benzobisoxazole) (PBO), is illustrated in Figure 1. The isomer shown here is designated the *cis* form on the basis of the relative locations of the two oxygen atoms in the repeat unit. Other related polymers of interest are the *trans* PBO and the *cis* and *trans* forms of the corresponding poly(p-phenylene benzobisthiazole) (PBT), in which the two oxygen atoms are replaced by sulfur atoms.²⁻¹¹

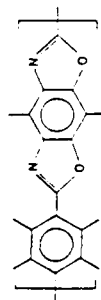


Figure 1 Illustration of the *cis* PBO repeat unit

As can be seen from the sketch, these chains are extremely stiff, approaching the limit of a rigid rod molecule. Because of their rigidity, they readily form liquid crystalline phases, specifically nematic phases in which the chains are aligned axially but are out of register in a random manner.^{2,3,11} Spinning films from a liquid crystalline dope of such a polymer has

great advantages.¹² The required flow of the system is facilitated, and the chains already have a great deal of the ordering they need in the crystalline fibrous state to exhibit the desired mechanical properties. Not surprisingly, PBO and PBT chains are the focus of the U.S. Air Force's "Ordered Polymers" Program, which has been established to develop low-weight high performance materials for aerospace applications.⁷ They are being used not only as fibers and films, but also as reinforcing fibrous fillers in amorphous matrices to give "molecular composites", where they serve the same purpose as the macroscopic glass or graphite fibers widely used in multi-phase polymer systems.^{7,10,11} The intended payoff is that these materials will replace many metal components in aircraft and space vehicles, especially where light weight is crucial.

The strength, heat resistance, and environmental stability of these liquid crystalline polymers stems from their highly ordered chemical structure.^{1,2} The polymers consist of long rod-like molecules that, under specific conditions of temperature and concentration in a solution or melt, arrange themselves in groups (known as domains) of anisotropic liquid crystalline phases.^{2,17} While the polymer molecules within each domain are parallel, the domains themselves are usually not. However, during processing, the individual domains are brought into alignment, creating a far more compact and orderly arrangement than is found in ordinary plastics.

While most ordinary plastics are processed through a melt phase, this technique is not possible with PBO and PBT, which undergo decomposition before they reach their melting point. Instead, PBO and PBT must be dissolved in strong acids, such as methane sulfonic acid or chlorosulfonic acid, before they can be spun into fibers.^{2,8} These acids present disposal problems and are hazardous, expensive, and hard on equipment.

Alternatively, one would prefer to process these polymers through the melt phase or from a solution using aprotic solvents. Researchers are investigating ways of reducing the polymers' rigidity, and hence, decreasing the melting point and/or increasing the solubility in aprotic solvents, by slightly altering their molecular structures.³ One method of interest is to insert molecular "swivels" or spacers containing flexible chemical moieties, such as $-O-CH_2-$, $-S-$, $-CH_2-$, and $-Ar-$ (where "Ar" refers to various aromatic ring systems), into the otherwise rigid polymer chain (Figures 2 and 3).^{10,11} The resulting polymers are referred to as "articulated" PBO and PBT. These articulated PBOs and PBTs are expected to retain the liquid crystalline forming properties of the parent molecules yet exhibit differences from them in terms of solubility, thermal characteristics, and morphology. Certainly, the conformational characteristics of these molecular swivels are of the utmost importance in this regard and have been the focus of several theoretical studies.^{10,11}

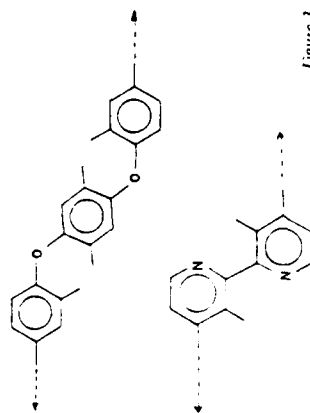


Figure 2 Two adjacent oxygen para phenylene swivels

Figure 3 A 2,2'-diphenylene swivel

While these molecular alterations provide many benefits, they also tend to diminish the polymer's strength and thermo oxidative stability.^{2,17} Still, the correct combination of rods

of liquid crystalline phases and the subsequent preparation of high-strength materials consisting of rod-like polymers such as these are facilitated by high degree of alignment of the rods. The extent of intramolecular rotational flexibility and thus deviations from planarity are important in this regard, particularly in terms of chain packing effects and the solubility characteristics of the polymers.

The MM calculations¹⁷ on the segment shown indicated that the lowest energy conformation of *cis*- and *trans*-PBO should correspond to $\phi = 0^\circ$; this is in agreement with the planarity found for the corresponding model compound in the crystalline state.¹⁸ Significant nonplanarity is predicted for *trans*-PBI with ϕ estimated to be approximately 55° .²² The nonplanarity predicted for the PBI, but not for the PBO polymers, is due to the fact that the S atom has a much larger van der Waals radius than the O atom (1.85 versus 1.40 Å).¹⁷ This increases the severity of steric interferences involving the *ortho*-hydrogens in the phenylene ring, which can be alleviated by rotation ϕ out of the coplanar form. The pertinent experimental value of ϕ , obtained from a crystalline *trans*-PBI model compound, is 23.2° .¹⁶

The lack of quantitative agreement between theoretical and experimental results is less significant than the numerical differences in ϕ might suggest. First, the calculated energy changes only gradually with ϕ near the energy minimum; specifically, the entire range $\phi = 25^\circ$ to 90° gives energies within 1.00 kcal mol⁻¹ of the minimum value, and this indicates considerable uncertainty in locating the preferred value of ϕ .²² Second, the discrepancy between theory and experiment could be due to intermolecular forces, which strongly favor a more nearly planar conformation to provide more efficient chain packing.²⁴ The effect of including intermolecular interactions by minimizing the total (intramolecular and intermolecular) energy of a pair of *trans*-PBI sequences²⁷ does shift the predicted conformation from 55° to 25° , in much better agreement with the experiment.¹⁶ The vibrational and electronic absorption spectra of model compounds in the crystalline state and in solution²⁸ are consistent with this interpretation. The situation is thus very similar to that of biphenyl, for which the dihedral angle is 42° in the vapor phase, 23° in the melt, and 0° in the crystalline state.²⁹

Another problem with the intramolecular MM calculations is that the torsional barrier chosen in these calculations may underestimate the true barrier to rotation. Specifically, in the rigid-rod polymer, the coplanar conformation may be favored by long-range conjugation effects which are absent in benzaldehyde, the model compound used for the estimate of the barrier. Some evidence in support of this possibility exists in that the length of the bridging bond in the polymers of interest is smaller than the lengths of corresponding bonds in analogous low-molecular-weight species, which suggests some partial double-bond character in these C—C bonds.²⁷

The possible ramifications of the limitations of MM calculations as applied to these systems suggested recourse to C/NDO/2 calculations, the results of which are summarized in Figure 7. In the case of *cis*- and *trans*-PBO, very similar conformational energy profiles were obtained. In both cases, the preferred conformation corresponds to $\phi = 0^\circ$ (coplanarity); this result thus is in excellent agreement with the MM results²² and with experiment.¹⁶ The substantial barriers to rotation away from coplanarity imply that conjugation effects between the aromatic moieties (favoring coplanarity) dominate the steric repulsions (disfavoring coplanarity) between the *ortho*-hydrogen atoms on the phenylene group and nearby atoms within the heterocyclic group.

The C/NDO/2 conformational energy profile of the *trans*-PBI model compound is quite different. The preferred angle is $\phi = 20^\circ$, in good agreement with experiment;¹⁶ however, the energy barrier to coplanarity is only about 0.5 kcal mol⁻¹. Beyond $\phi = 20^\circ$, the barrier rises sharply and monotonically, yielding a maximum barrier of 6 kcal mol⁻¹ at $\phi = 90^\circ$. The barrier to rotation is relatively large and should be considered an upper estimate because geometry optimization was not available for sulfur-containing molecules such

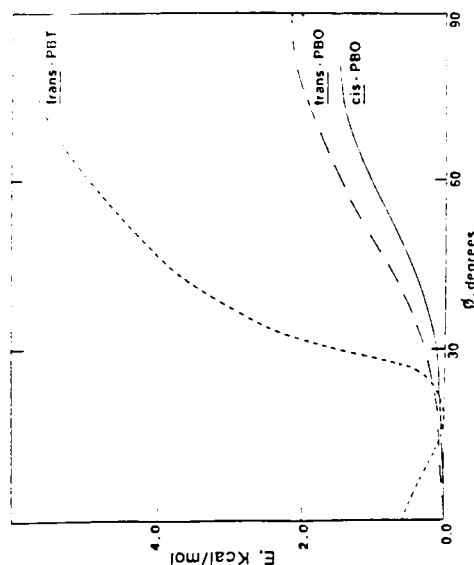


Figure 7. Dependence of the C/NDO/2 calculated conformational energy E on the torsional angle ϕ for the *cis*-PBO, *trans*-PBO, and *trans*-PBI model compounds.

as PBI. The *cis*-PBI chain is also predicted to be significantly nonplanar, but the experimental results¹⁶ indicate a deviation of only 2.8 to 5.8 degrees from planarity. However, molecules of this type are much more complicated than the three others in that they have considerable "bowing" within the repeat unit, a subject¹ dealt with separately in a later section of this review.

In the case of the two PBO polymers, geometry optimization gave bond lengths and bond angles in excellent overall agreement with those observed for the model compounds in the crystalline state.¹⁸

2. Chain Packing and Intermolecular Interactions

The specific goals of these calculations²⁷ were the elucidation of the nature of the chain packing and the estimation of the corresponding densities, magnitudes of the total interaction energies, and the relative importance of van der Waals and Coulombic contributions.

Because of the complexity of these systems, the calculations were of necessity very approximate, being based on only a pair of chains of a given type oriented in either their planar or nonplanar conformations. The first chain was one repeat-unit long, with the second being assigned a series of lengths in an attempt to make the interaction energies (per repeat unit) as realistic as possible without making the calculations unwieldy. In the initial series of calculations, the chains were first placed in parallel arrangements, one above the other, and then one chain was rotated about its axes. The rotations invariably increased the energy, and such arrangements were therefore not considered further. Thus, the calculations to determine minimum-energy arrangements were based primarily on two parallel chains shifted relative to one another. In the case of the density estimates, there are two specific sets of calculations which are relevant, one for a pair of chains above one another, and the other for a pair of chains along side of one another.

The results²⁷ show that, for pairs of chains above one another, the chains are out of register by 3.0 Å in the case of the two PBO polymers (which would place a phenylene group of

the upper chain over the bond bridging the two ring systems of the repeat unit of the lower chain) and by 1.5 Å in the case of the trans-PBT. These are rather approximate results, in part because of the large number of energy minima occurring as the chains are slid by one another. The latter displacement was predicted to be smaller than the former because of the large size of a sulfur atom relative to oxygen and the much more irregular cross section of the nonplanar PBT molecule. Nevertheless, these results are in at least qualitative agreement with the results of x-ray structural studies.¹⁶ The experimental values of these axial shifts were found to be approximately 4.5 Å in the case of model compounds for all three types of molecules.^{15,16} The agreement between theoretical and experimental values could, of course, be considerably better for the polymeric chains, which have not yet been studied experimentally in this regard. In the case of the vertical spacings, the theoretical results are in excellent agreement with the experimental value of 3.5 Å for all three types of model compounds.^{15,16} For the pairs of chains along side one another, the spacing is predicted to be approximately 6.1 Å. Although there are no experimental values of this quantity available for comparison, it is important for density estimates which are discussed below.

The interaction energies were found to be rather large,²¹ with contributions from only a few repeat units adding up to values approaching typical bond dissociation energies. This suggests that the failure mechanism in such materials in the solid state might generally be bond breakage rather than chain slippage. The interchain attractions are somewhat larger for trans-PBT than for cis- or trans-PBO because S atoms give rise to larger van der Waals attractions than do O atoms, a consequence of their much larger polarizability. The Coulombic contributions to the total interaction energy were found to be very small, which suggests that the dielectric constant of a potential solvent for these (unprotonated) polymers should be of no importance, and thus in agreement with experiment.¹⁹

The above information also permits estimation of the densities of PBO and PBT polymers in the crystalline state.²¹ The two polymers were represented as cylinders having elliptical cross sections with six such ellipses closely packed around a central ellipse. The densities thus estimated were found to be in good agreement with the experimentally obtained densities of the model compounds,^{15,16} particularly in the way they vary with the changes in the structure of the repeat unit. The results indicate that the higher density for the PBT polymer is due to the higher atomic weight of S relative to O, rather than to more efficient chain packing.²

3. "Bowing" in the Cis PBT Chains

Model compounds of the cis-PBT polymer chain, as illustrated in Figure 8,¹ have been shown to assume a slightly "bowed" configuration in the crystalline state.¹⁶ The bowing is a result of the planar thiazole rings being inclined in the same direction from the best plane through the atoms of the fused benzene ring by an average of 2.6°. The bowing corresponds to an average inclination of 4.2° between the bonds connecting the end phenylene to the benzobisthiazole and the best plane through the benzobisthiazole group. If present in polymeric cis-PBT, this bowing would be expected to interfere with alignment of chains and, hence, have a deleterious effect on desirable properties.

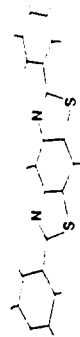


Figure 8. The cis-PBT model compound with bowing illustrated in two dimensions.

Of primary interest here was gaining a rough estimate of the strain energy responsible for inducing this molecule to bow out of the planar conformation, as exists in the trans-PBT and cis- and trans-PBO model compounds. To this purpose, the CINDO/2 total energy of the cis-PBT model was calculated¹ and compared with that of a fictitious planar cis-PBT

model molecule. The planar cis-PBT was assigned essentially the same structural parameters (i.e., bond angles and bond lengths) as the actual "bowed" molecule since values of the latter bond angles and bond lengths in trans-PBT and cis-PBT model compounds have served to be nearly identical in the crystalline state.¹⁶ Thus, the planar cis-PBT form studied here for comparison is analogous to trans-PBT, apart from the fact that the planar cis form apparently experiences considerable strain.

The results¹ yielded an enormous energy difference per model molecule (>1000 kcal/mol)¹ in favor of the "bowed" form. These numbers should be regarded as highly approximate upper limits since geometry optimization could not be implemented and CINDO/2 energies involving second-row atoms like sulfur are typically less reliable. Nevertheless, these results do indicate that rather large energy decreases are realized as a result of bowing. Apparently, after bowing, the molecule's bond angles and bond lengths "relax" to values experimentally indistinguishable from those of trans-PBT.

4. Chains Containing Molecular Swivels

Because of their stiffness, the PBO and PBT chains are very nearly intractable, being insoluble in all but the strongest acids (even when pendant groups are attached to the chains) and very difficult to process into usable films and fibers.² These materials may be made more tractable, however, by the insertion of a limited number of atoms or groups chosen so as to impart a controlled amount of additional flexibility to the chains. The insertion of even a small number of flexible molecular fragments or "swivels" into such chains will increase their flexibility and tractability by allowing mutual rotation of adjacent chain elements about the swivel's rotatable bonds. (Such swivels also have the advantage of facilitating the polymerization.) It is obviously of considerable importance to investigate the effect of the structure, number and spacing of such swivels along the chain. For example, two closely spaced swivels, as illustrated in Figure 2, would decrease the rigidity of the chains but still permit occurrences of nearly parallel conformations conducive to formation of the desired molecular alignment or organization.^{10,11}

In swivels of the type Ph-X-Ph (Fig. 2), where Ph is phenylene and X is the single atom O, S, Se, or Te, the pairs of rotatable angles should be mutually independent to a good approximation, and the problem, therefore, treated in terms of two single swivels. The energy maps obtained for these swivels from MM calculations¹⁰ reveal that the sulfur swivel has the advantage both in terms of equilibrium flexibility (more low-energy, and thus more accessible regions in configurational space) and of dynamic flexibility (lower barriers

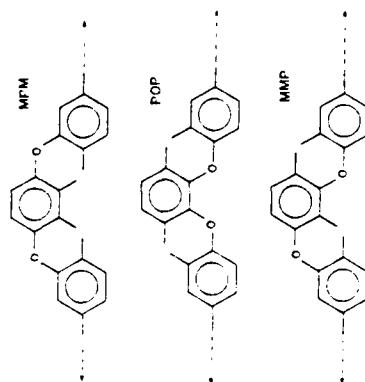


Figure 9. The three combinations of isomers of the "double oxygen swivel" which permit nearly colinear continuation of the chain.

between energy minima). Also, the Ph-S-Ph swivel has a larger fraction of its conformational energy map that is energetically accessible. In the case of the double swivels containing two flexibilizing atoms or groups, as in Figure 2b, it is of course important to consider which combination of isomeric linkages (o, m, p) has conformations which give nearly coplanar continuation of the chain, or at least parallel continuation. The oxygen double swivels have three isomers (mmp, pmp, and mmp) (Fig. 9) that provide coplanarity and seven that permit parallel continuation. The sulfur double swivels have no isomers giving coplanarity and, again, seven giving parallelism.¹⁰ The presence or absence of coplanar isomers is related to the values of the various bond angles within the segment. Specifically, the similarity between the bond angles (120°) within the aromatic ring and the C(O) bond angle (123°) in the oxygen swivel increases the number of nearly coplanar arrangements. This fortunate circumstance does not occur in the case of the sulfur swivels for which the C(S) bond angle is 109°.

A number of somewhat more complicated swivels were also investigated, viz., $-\text{C}(\text{O})-\text{SO}_2-\text{O}-\text{CH}_2-\text{O}-\text{C}(\text{O})-$ and $-\text{C}(\text{O})-\text{SO}_2-\text{O}-\text{CH}_2-\text{O}-\text{C}(\text{O})-$ and conformational flexibility¹⁰; it seems that the most promising swivels from this expanded group are $-\text{O}-\text{S}-\text{O}-\text{C}(\text{O})-$ and $-\text{C}(\text{O})-$.

As is evident from Figures 2 and 9, H atoms attached to aromatic carbons which are a part of the swivel linkage can force the swivel out of the desired coplanar conformation. A simple way to reduce these offending H...H repulsions would be to eliminate the responsible atoms altogether. As an example, one or both of the phenylenes in the swivel could be replaced by a pyridylene (Pyr) group in which the nitrogen in the ring replaces the offending CH group, as shown in Figure 10. It is found that when even only one of the phenylenes is thus replaced, as in Pyr-O-Ph or Pyr-S-Ph, the repulsions in the coplanar arrangement are greatly reduced and, in general, the flexibility of the swivel increases. As expected, replacement of both of the Ph groups increases both effects.

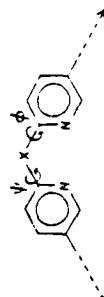


Figure 10 Illustration of an $\text{R}_1-\text{X}-\text{R}_2$ swivel having $\text{R}_1=\text{R}_2=\text{Pyr}$ (a pyridylene group).

Wholly aromatic swivels, such as diphenylene and 2,2'-dipyridylene (Fig. 3), should have the greatest thermal stability. They can maintain parallel continuation if bonded either o,o or m,m (Fig. 11); although the p,p isomer provides coplanarity, it does not, of course, give the "link" needed for additional flexibility. Replacement of one or both of the phenylenes by the 2-pyridylene group would be expected to relieve much of the inter ring congestion, as already described, and MM calculations give results in agreement with this expectation.¹⁰

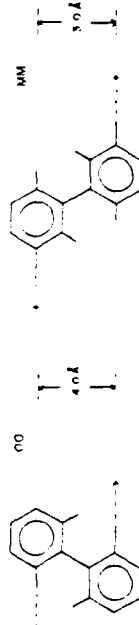


Figure 11 The ortho,ortho (o,o) and meta,meta (m,m) diphenylene swivels.

Geometry-optimized CNDO/2 calculations were also carried out on a number of the wholly aromatic swivels, viz., biphenyl, 2,2'-bipyridyl, 2-phenyl pyridine, 2,2'-bipyrimidyl and 2-phenylpyrimidyl.¹⁰ In agreement with the MM calculations and with intuition, increase in the nitrogen substitutions generally decreases the energy of the coplanar conformation and increases the overall flexibility of the swivel.¹¹

B. Effects of Protonation

1. The PBO and PBI Chains

As already noted, only very strong acids, such as methane sulfonic acid, chlorosulfonic acid, and polyphosphoric acid are solvents for these materials.^{20,21} Protonation of the red like PBO and PBI chains and their model compounds in acidic media will have significant effects on their solubility, solution behavior, geometry, and conformational characteristics. Recent interest has therefore focused on the extent, nature, and effect of protonation of the polymers in order to gain insights into their solubility behavior and solution properties.

Freezing point-depression measurements²² on PBO and PBI model compounds have indicated that, depending on the acidity of the medium, the PBO model compound can exist as a diprotonated ion, presumably with one proton on each (highly basic) nitrogen atom, or as a tetraprotonated ion, presumably with the other two protons on the oxygen atoms. The PBI model compounds appear to have a greater preference for the diprotonated form owing to the lower basicity of sulfur atoms relative to oxygen atoms. The CNDO/2 method was used to obtain charge distributions for such protonated PBO and PBI chains, and MM calculations were then carried out to estimate the magnitudes of the inter chain Coulombic repulsions.²³ It is difficult to relate such results quantitatively to the polymer solvent dissolution process which is, of course, controlled by changes in free energy. They are nonetheless of considerable interest in that they indicate that protonation of the chains should greatly decrease the intermolecular attractions, even at the very high dielectric constants characteristic of strong, undiluted acids. This conclusion is highly consistent with the fact that only extraordinarily strong acids are solvents for these types of polymers.^{20,21}

Geometry-optimized CNDO/2 calculations were also carried out to characterize the effects of protonation on the conformations of the PBO chain, and the results are shown in Fig. 12²⁴ for all three forms, i.e., the unprotonated chain and the diprotonated and tetraprotonated ions of the cis-PBO model compound, the preferred conformation corresponding

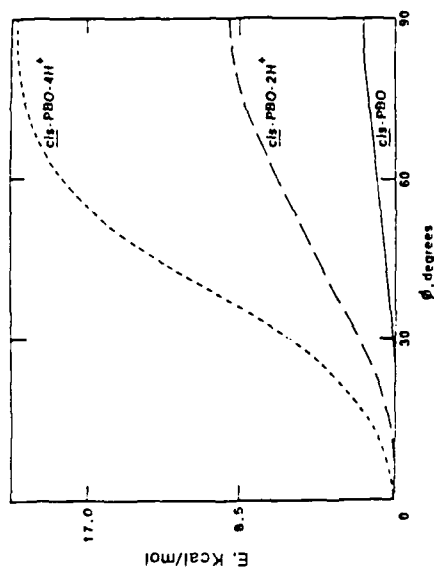


Figure 12 Dependence of the CNDO/2 calculated conformational energy E on the torsional angle ϕ for the unprotonated form and the diprotonated and tetraprotonated ions of the cis-PBO model compound.

to rotation angle $\phi = 0^\circ$, the coplanar form. As ϕ increases, the energy barrier increases monotonically; the maximum barrier is located at $\phi = 90^\circ$ with an energy E of ~ 2.0 , 9.0 and 20.0 kcal mol $^{-1}$ above that of the coplanar form for the unprotonated form, the diprotonated ion, and the tetraprotonated ion, respectively. In other words, the barrier to rotation away from the coplanar form increases as a result of increased protonation. These conclusions are somewhat surprising in that steric arguments would suggest that repulsions between the ortho hydrogens on the phenyl rings and the acidic protons on the benzoxazole ring should render the coplanar conformations less preferred than other orientations, and certainly less preferred than the coplanar form for the unprotonated case. However, inspection of the geometry optimized structures of the three species in the coplanar form shows that the rotatable bond decreases in length with increased protonation. Specifically, the bond lengths are 1.45, 1.42, and 1.38 Å for the unprotonated form and the diprotonated and tetraprotonated ions, respectively. Such contractions are typically indicative of strengthening of a bond, in this case the result of enhanced conjugation (favoring coplanarity) between the phenylene rings and the aromatic heterocyclic group. This increased stabilization of the coplanar forms appears to more than offset the repulsive effects of steric interferences.

These conclusions are corroborated by construction of resonance structures (Figure 13) which indicate significant contributions from resonance forms wherein the rotatable bond assumes a double bond in the case of protonated forms.²⁴ Additional evidence for the significant contributions of these resonance structures upon protonation is noted in the slight shortening (and thus strengthening) of phenylene C—C bonds more nearly parallel to the C=C rotatable bond. Finally, changes in the UV-visible and Raman spectra of PBO upon protonation are consistent with this described increase in conjugation.

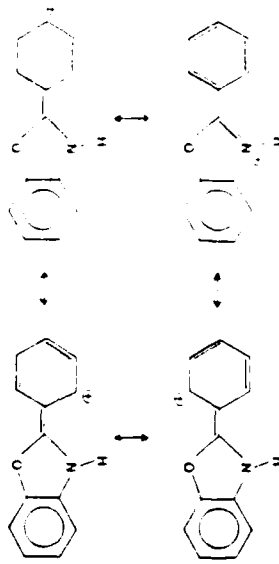


Figure 13. Selected resonance forms of the protonated PBO model compound showing increased double bond character of the rotatable bond.

Additional geometry optimized (CNDO/2 calculations²⁵) were carried out to predict the order of protonation within the *cis*-PBO model compound. The results indicate that protonation occurs in the order N, N, O, O, which is consistent with the greater basicity of nitrogen relative to oxygen. Thus, repulsive Coulombic effects between the acidic protons have only a negligible influence on the precise sequence of protonation. That N is preferred over O as the second site of protonation is a consequence of the protons having a smaller partial charge in this case, which offsets their closer proximity.²⁵

2. Molecular switches

It is likely and indeed desirable, in order to promote solubility, that the nitrogen-containing switches will be protonated in the strong acidic medium in which the PBO and PBz chains are soluble. (CNDO/2 calculations,¹¹ for example, showed that mono- and di-protonation of 2,2'-bipyridyl (Fig. 14) had large effects on its conformational characteristics. While the

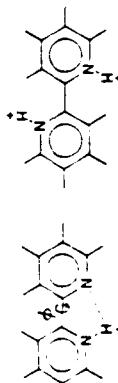


Figure 14. Illustration of mono-protonated and diprotonated forms of 2,2'-bipyridyl shown in their conformationally most stable "cis" and "trans" forms, respectively.

parent molecule and the diprotonated species both prefer the *trans* over the *cis* coplanar conformation, just the opposite is true for the mono-protonated case. Hence, the particular coplanar conformation preferred by a particular species will be a function of the acidity of the medium, with *trans* preferred in neutral media (unprotonated form) followed by a preference for *cis* (mono-protonated form) and then back to *trans* (diprotonated form) with increasing acidity. The results suggest the presence of hydrogen bonding for the mono-protonated bipyridyl in the *cis* coplanar conformation, as evidenced by the strong preference for this conformation and by the bending of the exo ring angles about the swivel atom in order to shorten the interatomic distances to reasonable values for the N...H $^+$ —N hydrogen bond. The species 2,2'-bipyridyl H $^+$ (Fig. 15) and 2,2'-bipyrimidyl 2H $^+$ were also studied in this manner, each in two initial configurations, one with an O...H bond pointing to each N atom, and the other with an O...H bond normal to the swivel bond. For each species, the former configuration is the preferred one.¹¹

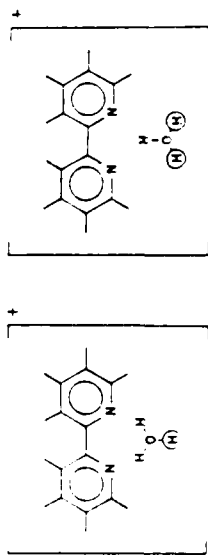


Figure 15. Illustration of the two initial configurations of the 2,2'-bipyridyl H $^+$ complex studied.

C. The AAPBO and ABPBO Polymers

1. Conformational Energies

Chains such as AAPBO and ABPBO should possess at least some flexibility perpendicular to the axial direction as a result of rotations (indicated by ϕ , ϕ_1 , and ϕ_2 in the Figures 4 and 5) about the single bonds joining the aromatic moieties. Geometry optimized (CNDO/2 calculations^{11,26}) were carried out on AAPBO and ABPBO chain segments to obtain conformational energies with respect to the rotations indicated in the sketches.²⁶ Of particular

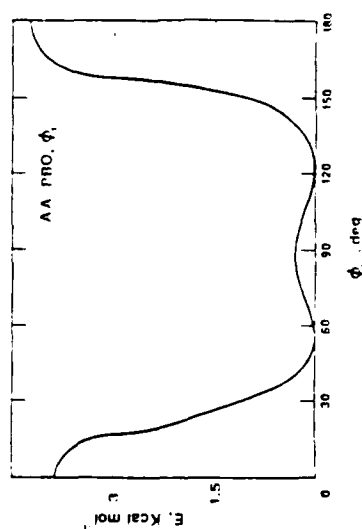


Figure 16. Dependence of the (NDO) 2 calculated conformational energy E on the torsional angle ϕ_1 in AAPBO.

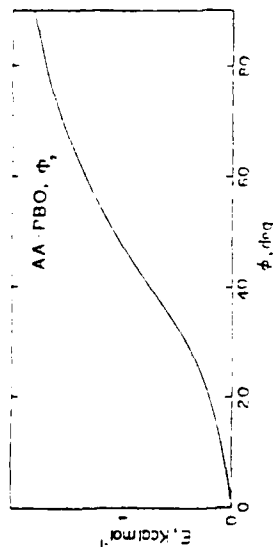


Figure 17. Dependence of the (NDO) 2 calculated conformational energy E on the torsional angle ϕ_2 in AAPBO.

interest was determining the preferred conformations and assessing the extent of rotational flexibility about these bonds. The results can be compared with those obtained in similar studies of the PBO polymers.¹¹

Conformational energies E as a function of ϕ_1 and ϕ_2 in AAPBO are plotted in Figures 16 and 17, respectively. A broad energy minimum was found in the region $60^\circ < \phi_1 < 120^\circ$ (within the 0–180° conformational energy space). On either side of this minimum, the energy rises sharply and continuously, giving two similar energy maxima of $E = 3.6$ kcal mol⁻¹ at 0° and 180° . Thus the conformational energy profile obtained is nearly identical to that calculated for biphenyl in a similar analysis.¹¹ This is reasonable since the two species are structurally similar in the vicinity of the rotatable bond. The high repulsive energy associated with the coplanar conformations can be ascribed primarily to steric repulsions between *ortho*-hydrogens on adjacent ring systems. Specifically, at $\phi_1 = 0^\circ$ and 180° , these *ortho*-H interaction distances are 1.8–1.9 Å, which are considerably smaller than the sum (2.6 Å) of their van der Waals radii.¹⁷ The preference for non coplanar conformations calculated¹¹ for these moieties is consistent with the experimental findings for biphenyl in the gaseous state ($\phi = 42^\circ$)¹⁸ and in the liquid state ($\phi = 23^\circ$).¹⁴

The structural geometry of AAPBO in the vicinity of ϕ_2 is nearly identical to that found in PBO model compounds, and the results of calculations on both^{14,28} indicate a preference

for the coplanar conformations with a maximum of $E = 1.8$ kcal mol⁻¹ at $\phi_2 = 90^\circ$. The results also agree with the coplanar conformations observed by x-ray crystallographic analysis of PBO model compounds in the crystalline state.¹¹

Values of E vs. ϕ' in ABPBO are plotted in Fig. 18.²⁸ Conformational energy minima were found at $\phi' = 0^\circ$ and 180° (the coplanar forms) with a maximum energy of 1.6 kcal mol⁻¹ located at $\phi' = 90^\circ$ (the perpendicular form). It should be noted that the absence of exact symmetry in energy profile about $\phi' = 90^\circ$, most conspicuous in Fig. 18, is a consequence of the absence of complete conformational symmetry for these species about $\phi = 90^\circ$, as inspection of Figs. 4 and 5 will confirm. Again, these results are in agreement with those obtained from both theoretical¹⁴ and x-ray crystallographic¹¹ studies of the structurally analogous PBO polymer model compounds. They are also consistent with the coplanarity or near coplanarity observed for the ABPBO polymers in the crystalline state.²⁷

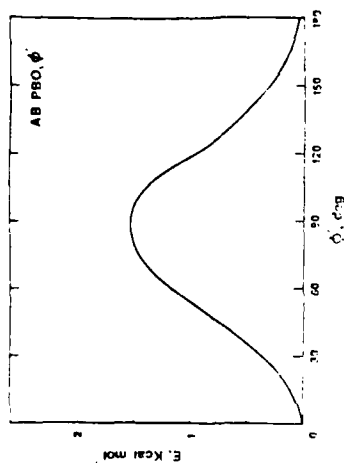


Figure 18. Dependence of the (NDO) 2 calculated conformational energy E on the torsional angle ϕ' in ABPBO.

2. Calculated Structures

Both the preference for coplanar conformations and the shortness of the C—C rotatable bond (1.45–1.47 Å) in these species relative to that (1.53 Å) for a typical C—C single bond suggest a considerable degree of conjugation between adjacent ring systems in these chains.^{27,28} The variation of selected bond lengths and atomic partial charges with ϕ for ABPBO corroborates this conclusion. Specifically, with rotation away from the coplanar conformation ($\phi' = 0^\circ$) the lengths of bonds C12–C14 and C15–C16 (see Fig. 5) increase, while those of bonds N11–C12 and C12–O13 decrease. These changes are exactly as would be predicted based on the reasonable assumption that conjugation between adjacent ring systems should be a maximum near $\phi' = 0^\circ$ and a minimum near $\phi' = 90^\circ$. This loss in conjugation, concomitant with rotation away from coplanarity, is further evidenced by noting the changes in the atomic partial charges with ϕ' , these being the result of shifts in electron density from C12 and C14 (i.e., from the rotatable bond) to N11 and other nearby atoms within the rings.

In summary, the present results show AAPBO to prefer a non coplanar conformation while ABPBO prefers a coplanar one.²⁸ Thus, the conformational profiles of AAPBO and ABPBO are qualitatively different, and these differences are consistent with the liquid crystalline behavior observed for solutions of ABPBO but not for those of AAPBO.^{28,29}

Conclusions and Future Work

Although until very recently DuPont's Kevlar is the only liquid crystal forming polymer to have reached the marketplace, research on these materials has intensified in recent years. Research and development activities are proceeding at such locations as IBM, DuPont, Eastman Kodak, Celanese, Monsanto, ICI (England), Bayer (West Germany), the University of Missouri - St. Louis, Stanford University, Carnegie Mellon University, the University of Massachusetts, the University of Southern Mississippi, the University of Cincinnati, SRI International, University of Dayton Research Institute, and Wright Patterson Air Force Base. The focus is and will continue to be on fabricating liquid crystalline polymers into fibers, films and molded shapes that will open the door to a wide range of new products, ranging from bicycle wheels and sundry machine parts to automotive and aircraft components and electronic devices.⁴⁷

The research carried out by the author and his coworkers has focused on using theoretical methods to gain an understanding of the exceptional physical properties, solution behavior, and processing characteristics of a class of rod like and stiff chain polymers, some of which form highly oriented, liquid crystalline phases. This review has attempted to interpret these properties in terms of calculated structural geometries and conformational and interchain energies.

The interest in our laboratory in high performance liquid crystalline polymers has stimulated research in several related areas. Given the aromatic nature of the PBO and PBI chain backbones, extensive calculations of the electronic band structures of these molecules have been carried out as a means of predicting the extent of electrical conductivity in these systems.^{41,44} These "band structure" calculations have been extended to other, more flexible, polymers in order to afford comparisons for the purpose of developing structure property relationships.^{45,46} Polarizabilities have also been calculated for PBO and PBI⁴⁷ and for related systems.⁴⁸ Also, a number of molecules possessing structural features in common with PBO and PBI have been studied in our laboratory using similar NIM and molecular orbital procedures in order to derive conformational and configurational information. These include the polysulfides,⁴⁹⁻⁵¹ 2 (4-morpholinobenzothiazole),⁵² poly(organophosphazenes),⁵³ polysilanes,⁵⁴ polysulfones,⁵⁵ thyroid hormones,⁵⁶ and some anticancer drugs.^{57,58}

Acknowledgement

It is a pleasure to acknowledge the financial support provided by the Air Force Office of Scientific Research (Grant 81-0027; Chemical Structure Program, Division of Chemical Sciences). The author also wishes to acknowledge coworkers Drs. D. Bhaumik and J. E. Mark whose work is included in this review.

References

1. "Polymer Science and Engineering: Challenges, Needs and Opportunities", ed. by C. G. Overberger and R. Pariser, National Academy Press, National Research Council, Washington (1981).
2. J. E. Helminiak, *Prepr. Am. Chem. Soc. Div. Org. Coatings Plast. Chem.*, **40**, 475 (1979); a number of articles on PBO and PBI polymers are in the July, August, 1981, issue of *Macromolecules*.
3. W. J. Welch and J. E. Mark, *J. Mat. Sci.*, **18**, 1119 (1983).
4. W. J. Welch, D. Bhaumik, H. H. Jaffe, and J. E. Mark, *Polym. Eng. Sci.*, **24**, 218 (1983).
5. G. M. Venkatesh, D. Y. Shen, and S. L. Hsu, *J. Polym. Sci. Polym. Phys. Ed.*, **19**, 1475 (1981).

6. D. Y. Shen, G. M. Venkatesh, D. J. Burchell, P. H. C. Shu, and S. L. Hsu, *J. Polym. Sci. Polym. Phys. Ed.*, **20**, 509 (1982).
7. W. T. Hwang, D. R. Wiff, C. L. Benner and T. E. Helminiak, *J. Macromol. Sci. Phys.*, **B22**(2), 231 (1983).
8. J. R. Minter, K. Shimamura, and F. L. Thomas, *J. Mat. Sci.*, **16**, 3303 (1981); J. A. Odell, A. Keller, E. D. I. Atkins, and M. J. Miles, *ibid.*, **1309**.
9. D. Y. Shen and S. L. Hsu, *Polym. J.*, **23**, 969 (1982).
10. W. J. Welch, D. Bhaumik, and J. E. Mark, *J. Macromol. Sci. Phys.*, **B20**, 59 (1981).
11. W. J. Welch, H. H. Jaffe, J. E. Mark, and N. Kondo, *Die Makromol. Chem.*, **181**, 801 (1982).
12. P. J. Flory, *Proc. Royal. Soc. Part A*, **234**, 60, 73 (1956).
13. M. Warner and P. J. Flory, *J. Chem. Phys.*, **73**, 6327 (1980), and pertinent references cited therein.
14. J. E. Helminiak and G. C. Berry, *Prepr. Am. Chem. Soc. Div. Polym. Chem.*, **18**, 152 (1977).
15. G. C. Berry, in "Contemporary Topics in Polymer Science", Vol. 2, E. M. Pearce and J. R. Schaefer, Eds., Plenum Press, New York (1977); D. C. Trevoresk in "Polymer Liquid Crystals", A. Keller, W. R. Krigbaum and R. R. Meyer, Eds., Academic Press, New York (1982).
16. C. P. Wong, H. Ohnuma, and G. C. Berry, *J. Polym. Sci. Polym. Symp.*, **65**, 173 (1978), and other papers in the same issue.
17. A number of relevant articles are in the Dec. 1980 and March 1981 special issues of *Brit. Polym. J.*
18. G. Hussman, J. E. Helminiak, and W. W. Adams, *Prepr. Am. Chem. Soc. Div. Org. Coatings Plast. Chem.*, **40**, 797 (1979).
19. M. Wellman, G. Hussman, A. K. Kulshreshtha, and T. E. Helminiak, *Prepr. Am. Chem. Soc. Div. Org. Coatings Plast. Chem.*, **41**, 183 (1980).
20. G. C. Berry, P. Metzger Coits, and S. G. Chu, *Brit. Polym. J.*, **13**, 47 (1981).
21. C. Arnold, Jr., *Macromol. Rev.*, **14**, 265 (1979).
22. W. J. Welch, D. Bhaumik and J. E. Mark, *Macromolecules*, **14**, 947 (1981).
23. D. Bhaumik, W. J. Welch, H. H. Jaffe, and J. E. Mark, *Macromolecules*, **14**, 951 (1981).
24. W. J. Welch and J. E. Mark, *Polym. Eng. Sci.*, **23**, 140 (1983).
25. W. J. Welch and J. E. Mark, *Polym. Bull.*, **8**, 21 (1982).
26. J. F. Wolfe, SRI International, private communications.
27. A. V. Tratini, E. M. Cross, J. F. O'Brien, and W. W. Adams, *J. Macromol. Sci. Phys.*, **B24**, 159 (1985, 86).
28. W. J. Welch and J. E. Mark, *Polym. Eng. Sci.*, **25**, 965 (1985); *ibid.*, *Prepr. Am. Chem. Soc. Div. Polym. Chem.*, **24**, 318 (1983).
29. E. I. Thomas, private communications.
30. P. J. Flory, "Statistical Mechanics of Chain Molecules", Academic Press, New York (1968).
31. A. J. Hopfinger, "Conformational Properties of Macromolecules", Academic Press, New York (1971).
32. J. A. Pople and D. L. Beveridge, "Approximate Molecular Orbital Theory", McGraw-Hill, New York (1970).
33. H. H. Jaffe, CNDO/S and CNDO/2 (FORTRAN IV), Quantum Chemistry Program Exchange, *QCPE*, 175 (1977).
34. H. Kondo, H. H. Jaffe, H. Y. Lee, and W. J. Welch, *J. Comp. Chem.*, **5**, 84 (1984).
35. M. W. Wellman, W. W. Adams, D. R. Wiff, and A. V. Tratini, Air Force Technical Report AFML-TR-79-4184, Part I, private communications.
36. M. W. Wellman, W. W. Adams, R. A. Wolff, D. R. Wiff, and A. V. Tratini, *Macromolecules*, **14**, 935 (1981).
37. A. Bondi, *J. Phys. Chem.*, **68**, 441 (1964).
38. J. C. Holste, C. J. Glover, D. T. Magnuson, K. C. B. Dangayach, T. A. Powell, D. W. Chung and D. R. Person, Air Force Technical Report AFML-TR-79-4107.
39. G. C. Berry, Y. Einaga, R. Funakawa, and C. C. Lee, Air Force Technical Report AFWAL-TR-81-4092.
40. A. Almenningen and O. Bastiansen, *Sk. K. Nor. Vidensk. Selsk. No. 4* (1958).
41. H. Suzuki, *Bull. Chem. Soc. Jpn.*, **32**, 1340 (1959).
42. The May, 1982, issue of *Phys. Today* features a series of pertinent articles on liquid crystals, including one by F. T. Samulski entitled "Polymeric Liquid Crystals".
43. D. Bhaumik and J. E. Mark, *J. Polym. Sci. Phys. Ed.*, **21**, 1111 (1983).
44. D. Bhaumik and J. E. Mark, *J. Polym. Sci. Phys. Ed.*, **21**, 2543 (1983).
45. K. C. Metzger and W. J. Welch, *Prepr. Am. Chem. Soc. Div. Polym. Chem.*, **25**, 184, 268, 270 (1984).

46. D. Bhaumik, and J. E. Mark, *Synthetic Metals*, 6, 299 (1983).
47. D. Bhaumik, H. H. Jaffe and J. E. Mark, *Macromolecules*, 14, 1125 (1981).
48. D. Bhaumik, H. H. Jaffe and J. E. Mark, *J. Mol. Structure. THEOCHEM*, 87, 81 (1982).
49. E. Riande, J. Guzman, W. J. Welsh and J. E. Mark, *Makromol. Chem.*, 183, 2555 (1982).
50. W. J. Welsh, J. E. Mark, E. Riande, and J. Guzman, *Makromol. Chem.*, 183, 2565 (1982).
51. W. J. Welsh, J. E. Mark, E. Riande, and J. Guzman, *Makromol. Chem.*, 183, 2573 (1982).
52. D. Bhaumik and J. E. Mark, unpublished results.
53. W. J. Welsh and M. A. Harrigan, "Physical Properties of High-Performance Poly(Organophosphazenes)", 12th Biennial Polymer Symposium, Maui, Hawaii, December, 1984.
54. R. West, J. Damewood, L. Debolt, W. J. Welsh and J. E. Mark, "Conformational Energies and Unperturbed Dimensions of Various Polysilanes and Poly(Organophosphazenes)", National Meeting of the Amer. Chem. Soc., Miami Beach, April, 1985.
55. W. J. Welsh, J. Ackerman and J. E. Mark, *Prepr. Am. Chem. Soc. Div. Polym. Chem.*, 24, 131 (1983).
56. A. Letton, J. R. Fried and W. J. Welsh, *Macromolecules* (in press).
57. V. Cody and W. J. Welsh, "Theoretical Studies on Some Thyroid Hormones and Analogues", National Meeting of the Amer. Chem. Soc., St. Louis, April, 1984.
58. W. J. Welsh, V. Cody, J. E. Mark and S. F. Zakrzewski, *Cancer Biochem. Biophys.*, 7, 111 (1983).
59. W. J. Welsh, J. E. Mark, V. Cody, and S. F. Zakrzewski, in "Chemistry and Biology of Pteridines", J. A. Blair, Ed., Walter de Gruyter and Co., Berlin, 463 (1983).
60. V. Cody, W. J. Welsh, S. Opitz and S. F. Zakrzewski, in "QSAR in Design of Bioactive Compounds, Proceedings of the 1st Telesymposium on Medicinal Chemistry", J. R. Prous Publishers, Barcelona (1984).

Polymer-modified silica glasses

I. Control of sample hardness

J.E. Mark and C.-C. Sun

Department of Chemistry and the Polymer Research Center, University of Cincinnati,
Cincinnati, OH 45221, USA

Summary

The functionality of divinyl-terminated poly(dimethylsiloxane) (PDMS) was greatly increased by a substitution reaction to give PDMS with triethoxysilyl chain ends. Samples having number-average molecular weights of 720 and $17.6 \times 10^3 \text{ g mol}^{-1}$, and mixtures thereof, were added to tetraethoxysilane (TEOS) or a related silane. The functionalized PDMS-silane mixtures were hydrolyzed in the usual sol-gel technique to give polymer-modified silica glasses. The hardness of the glasses was measured, and then related to the molecular weight of the PDMS, its molecular weight distribution, the composition of the PDMS-silane mixtures, and the nature of the silane.

Introduction

The catalyzed hydrolyses of alkoxysilanes such as the symmetric molecule $\text{Si}(\text{OR})_4$ and alkylalkoxysilanes and arylalkoxysilanes such as $\text{R}'\text{Si}(\text{OR})_3$ have become of great interest to both ceramists and polymer chemists. In the ceramics area, for example, tetraethoxysilane (TEOS) has been hydrolyzed to a gel which can be dried and then fired into a porous silica (SiO_2) ceramic or glass (1). In the polymer area, TEOS can be used for the in-situ precipitation of reinforcing SiO_2 particles in elastomers (2,3), with substituted tri- or dialkoxysilanes used in an attempt to introduce some deformability in the filler particles (4). Also, in applications that combine both areas, Schmidt (5) has used mixtures of silanes and Wilkes and coworkers (6) have used mixtures of silanes and dihydroxy-terminated poly(dimethylsiloxane) (PDMS) [$\text{Si}(\text{CH}_3)_2\text{O}$] to obtain organically-modified glasses, some of which can be very interesting hybrids of polymers and glasses. One obvious goal in this polymer-ceramic area is the preparation of ceramic-type materials having decreased brittleness. In a sense this is related to attempts (7) to improve the impact resistance of (short-chain) thermosets by bonding much longer chains within the network structure.

The present investigation extends some of this work. It employs PDMS heavily functionalized with ethoxy groups (8) to maximize its bonding to silica-type phases generated by the hydrolyses of some of the silanes mentioned above. The high functionality should also suppress simple chain extension and the occurrence of dangling chains. Of particular interest in this first part of the project is control of the

hardness of the polymer modified chains through changes in the nature of the polymer and the silane, and their proportions in the mixtures being hydrolyzed.

Some Experimental Details

The starting polymers were two samples of vinyl terminated PMMA having number average molecular weights of 492 and 17,640 g/mol, respectively. The nonfunctional vinyl ends were converted (B) into trifunctional trichlorosilyl groups (BTTT) by treating the samples with a small excess of trichlorosilane, using chlorophosphoric acid as catalyst, in sealed flasks at 100°C for one day. Removal of unreacted trichlorosilane under reduced pressure gave the desired products as colorless viscous liquids. A small portion of each was characterized by standard chemical titration. The reduced values of B were 120 and 17.6 g/mol, respectively.

The silanes employed were trimethylchlorosilane, trimethylmethoxysilane, with η -butyl phenyl, methyl, and vinyl, respectively. In addition, some samples of hydrolyzed BTTT, designated H100, were prepared by treating BTTT with the appropriate amount of distilled water, in isopropanol and tetrahydrofuran (THF), using acetic acid as catalyst. The reaction was conducted under agitation at 60°C for ten hours. The resulting solution was washed with distilled water, dried over MgSO_4 , and the desired product recovered by removal of the solvent by evaporation.

The vinyl chain BTTT was hydrolyzed in the pure state and also in a series of limited mixtures with the four chain PMMA. Compositions are described in the first three columns of Table I, and the suitably averaged values of η are given in column six. The nature of the silane employed and the relative amount, are given in columns seven and eight. A stoichiometric amount of distilled water, and isopropanol and THF were used as the hydrolysis medium hydrochloric acid in a molar ratio 30/1/silane. 0.005 was used as catalyst (B). The BTTT and silane were simultaneously added to this solution and then held at 100°C, with agitation, for 70 min. The resulting solutions were poured into 1000 ml glass dishes, covered, and allowed to react for 48 hrs. at room temperature (B). The samples were then measured and permitted to further react and to dry, for a period of at least 47 hrs. Columns nine of the table give values of the modulus ratio B/T of alkyl groups to silicon atoms in the resulting polymer modified chains.

The hardness measurements were carried out using a Barcol 100 Hardness Tester, which has been designed to measure the indentation hardness of plastics and similar materials. It works on a principle similar to that of the American Society for Testing and Materials (ASTM). As in customary, the hardness of each sample was expressed as a relative "B value", with 17 being typical for a *polymer polymer*.

Results and Discussion

The samples formed as described above formed homogeneous, but very hard transparent films and had no obvious flaws or cracks. The "B hardness

TABLE I
Characteristics of the Components and the Resulting Classes

Exp	Chains ^a	Wt % Short	Wt % Long	Total Wt %	Polymer ^a	Chains ^b	Mol % Short	M _n ^c	g mol ⁻¹	Wt %	Wt %	HTOS ^d	R/SI	Values	Polymer-Modified Classes
1	52.0	0.0	52.0	52.0	100.0	720	48.0	48.0	0.0	0.0	0.0	1.00	45	1.00	45
2	46.2	5.8	52.0	52.0	99.5	804	48.0	48.0	0.0	0.0	0.0	1.05	50	1.10	50
3	41.8	10.2	52.0	52.0	99.0	889	48.0	48.0	0.0	0.0	0.0	1.10	50	1.16	50
4	36.4	15.6	52.0	52.0	98.0	1057	48.0	48.0	0.0	0.0	0.0	1.16	25	1.16	25
5	22.7	29.3	52.0	52.0	95.0	1550	48.0	48.0	0.0	0.0	0.0	1.31	20	1.31	20
6	17.8	2.2	20.0	20.0	99.5	804	80.0	80.0	0.0	0.0	0.0	0.52	18	0.52	18
7	53.5	6.5	60.0	60.0	99.5	804	40.0	40.0	0.0	0.0	0.0	1.15	2	1.15	2
8	71.8	8.2	80.0	80.0	99.5	804	20.0	20.0	0.0	0.0	0.0	1.36	50	1.36	50
9	40.1	9.9	50.0	50.0	99.0	889	50.0	50.0	0.0	0.0	0.0	1.00	60	0.92	60
10	52.0	0.0	52.0	52.0	100.0	720	48.0	48.0	0.0	0.0	0.0	1.29	11	1.29	11
11	75.0	0.0	75.0	75.0	100.0	720	0.0	0.0	0.0	0.0	0.0	20.0	40	20.0	40
12	80.0	0.0	80.0	80.0	100.0	720	0.0	0.0	0.0	0.0	0.0	20.0	40	20.0	40
13	17.8	2.2	20.0	20.0	99.5	804	80.0	80.0	0.0	0.0	0.0	0.46	57	0.46	57
14	46.6	5.4	50.0	50.0	99.5	804	50.0	50.0	0.0	0.0	0.0	0.97	40	0.97	40
15	53.7	6.3	60.0	60.0	99.5	804	0.0	0.0	0.0	0.0	0.0	1.09	4	1.09	4
16	71.8	8.2	80.0	80.0	99.5	804	0.0	0.0	0.0	0.0	0.0	1.33	4	1.33	4

^a Relative to total weight of polymer-silane mixture. ^b Relative to total number of moles of polymer. ^c Barcol. ^d Too large to measure.

values they exhibited are given in the third column of the table.

The first five experiments, carried out with H100, were used to determine the effect of the molecular weight of the PPHG on sample hardness. The hardness values obtained are given in the first five rows of the table and are shown in Figure 3 as a function of η_{sp} at a constant 52

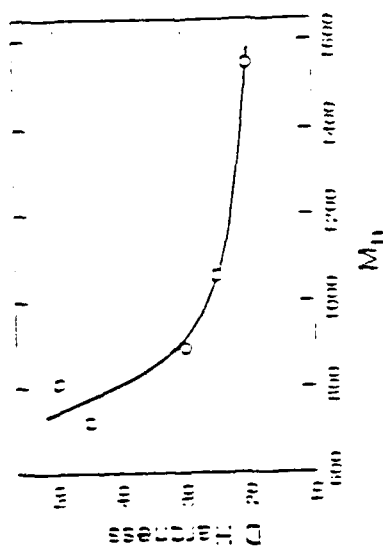


Fig. 3. The effect of PPHG molecular weight on sample hardness.

wt % PPHG. As can be seen, increase in η_{sp} causes a significant decrease in hardness. Part of the decrease in hardness could be due to an increased tendency for phase separation as the molecular weight of the PPHG increases (6). Unlike the case of elastomers at high elongations (7), the bimodal distribution of PPHG seems independent. It could possibly be explained, however, in conjunction with the amount of PPHG dispersed in the phase plane (low η_{sp}) and the amount forming a separate elastomeric phase (high η_{sp}) (6).

Experiment 6, through 8, establish the extent of the decrease in hardness on the total wt % PPHG in the blend, when H100 is used as the filler. The hardness obtained in experiment 9 relative to that in experiment 3 indicates that H100 phase separates approximately as hard as those obtained from H100. Experiment 10, through 12, also carried out using H100, confirm the decrease in hardness with increase in total wt % PPHG established in experiments 2 and 6. The combined sets of results are shown in Figure 2.

Figure 1 shows the dependence of the hardness on the polymer content of the phase, as represented by the ratio R/Si. Samples having a hardness in the range 30-65 seemed to be the toughest, and this in turn to be achieved at values of R/Si of approximately 0.9 to 1.0.

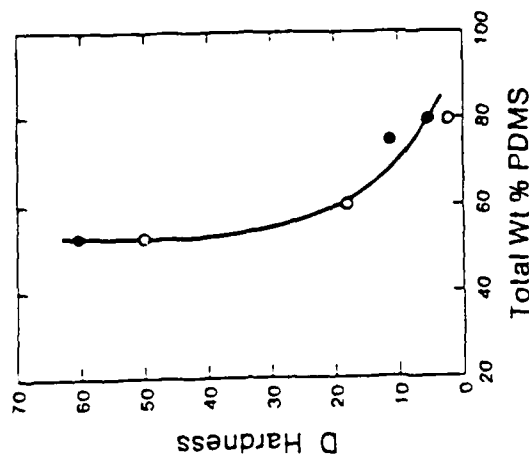


Fig. 2. The effect of total wt % PDMS on sample hardness, as obtained from experiments 2, 7, 8 (○) and 10-12 (●).

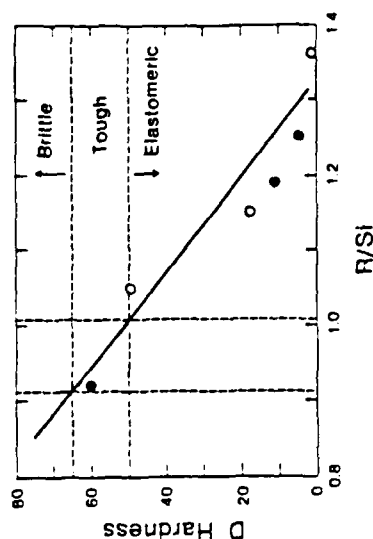


Fig. 3. The dependence of the hardness on the molar ratio of alkyl groups to silicon atoms in the glass; see legend to figure 2.

Experiments 13-16, carried out using a bimodal PDMS distribution, confirm the decrease in hardness with increase in total wt % PDMS shown by the unimodal distributions used in experiments 10-12.

In a final series of experiments, hydrolyses were conducted on three pure samples of $\text{R}'\text{Si}(\text{OEt})_3$, with R' being equal to phenyl, methyl, and vinyl, respectively. The first gave a brittle glass, whereas the second and third were tougher, with hardness values of 65 and 55, respectively. This clearly demonstrates the importance of the nature of the R group in the trialkoxysilanes being hydrolyzed.

Future work will correlate these results with the values of other important properties such as impact resistance, ultimate strength, and maximum extensibility.

Acknowledgment

It is a pleasure to acknowledge the financial support provided by the Air Force Office of Scientific Research under Grant 83-0027 (Chemical Structures Program, Division of Chemical Sciences), and the National Science Foundation under Grant DMR 84-15082 (Polymers Program, Division of Materials Research).

References

1. L. I. Hench and D. R. Ulrich, Eds., "Science of Ceramic Chemical Processing", Wiley, New York, 1986.
2. J. E. Mark, *Brit. Polym. J.*, **17**, 144 (1985).
3. S. J. Clarson and J. E. Mark, *Polym. Comm.*, **28**, 000 (1987).
4. J. E. Mark and G. S. Sur, *Polym. Bulletin*, **14**, 325 (1985).
5. H. Schmidt, *Mat. Res. Soc. Symp. Proc.*, Vol. 32, p. 327, Elsevier, New York, 1984.
6. H.-H. Huang, B. Orler, and G. L. Wilkes, *Polym. Bulletin*, **14**, 557 (1985).
7. H.-Y. Tang, A. Letton, and J. E. Mark, *Colloid Polym. Sci.*, **262**, 990 (1984).
8. G. S. Sur and J. E. Mark, *Eur. Polym. J.*, **21**, 1051 (1985).

Accepted June 29, 1987 K

A C S S Y M P O S I U M S E R I E S 346

Polymers for High Technology

Electronics and Photonics

Murrae J. Bowden, EDITOR
Bell Communications Research

S. Richard Turner, EDITOR
Eastman Kodak Company

Developed from a symposium sponsored by
the Division of Polymeric Materials: Science and Engineering
at the 192nd Meeting
of the American Chemical Society,
Anaheim, California,
September 7-12, 1986



American Chemical Society, Washington, DC 1987

Band-Structure Calculations on Polymeric Chains

William J. Welsh

Department of Chemistry, University of Missouri—St. Louis, St. Louis, MO 63121

Electronic band structures were calculated for several polymeric chains structurally analogous to polyacetylene ($-\text{CH}=\text{CH}-$) and carbyne ($-\text{C}\equiv\text{C}-$). The present calculations use the Extended Hückel molecular orbital theory within the tight binding approximation, and values of the calculated band gaps E_g and band widths W were used to assess the potential applicability of these materials as electrical semiconductors. Substitution of F or Cl atoms for H atoms in polyacetylene tended to decrease both the E_g and W values (relative to that for polyacetylene). Rotation about the backbone bonds in the chains away from the planar conformations led to sharp increases in E_g and decreases in W . Substitution of $-\text{SiH}_3$ or $-\text{Si}(\text{CH}_3)_3$ groups for H in polyacetylene invariably led to an increase in E_g and a decrease in W , as was generally the case for insertion of 'y' (where $Y = \text{O}, \text{S}, \text{NH}, \text{CH}_2, \text{SiH}_2$) in carbyne to give $[-\text{C}\equiv\text{C}-Y-\text{C}\equiv\text{C}-]$. The degree of bondlength alternation appears to play a major role in determining the electrical conductivity of a conjugated polymer, with values of E_g decreasing (favoring conductivity) as bond-length alternation decreases.

Polyacetylene, $[-\text{CH}=\text{CH}-]$, the simplest organic polymer with a fully conjugated backbone, has generated considerable interest due to its unusual electronic properties. Specifically, through selective doping of the polymer its electrical conductivity can be made to vary many orders of magnitude, from insulator to semiconductor (1-3). The structure of the polymer chain appears to be one of the key determinants for the electronic properties of polymer/dopant systems (1-3). Recent structural evidence and theoretical calculations (1-3) suggest a planar backbone structure for cis and trans forms of $[-\text{CH}=\text{CH}-]$. However, many aspects of the structure and the configurational characteristics of $[-\text{CH}=\text{CH}-]$ are not well-defined due to its intractability, its instability to oxidation, and its insolubility in most solvents. Many other polymeric systems have thus been proposed or actually investigated with regard to their potential as conductors or semi-conductors (1-3), among these the halogen-substituted polyacetylenes (4). For example, Zeigler has recently synthesized the perfluoropolyacetylene $[-\text{CF}=\text{CF}-]$ (4).

It appears that electrical conductivity is particularly

sensitive to the degree of conjugation and planarity along the chain backbone (1-3,5,6). In the case of substituted polyacetylenes in particular, it is crucial for effective conductivity that the substituent's steric bulk not cause appreciable deviations from planarity in an attempt to reduce steric conflicts. With regard to the halogen-substituted polyacetylenes, the fluorine atom is just small enough ($r_{\text{vdw}} = 1.30 \text{ \AA}$) to render the F...F interactions attractive even for the planar chain in which case the four-bond F...F interatomic distance is closest (2.60 \AA). However, with substitution of chlorine ($r_{\text{vdw}} = 1.80 \text{ \AA}$) steric conflicts between pendant chlorine atoms will render the planar conformation highly repulsive, and this effect would become more severe in the case of Br and I substitution.

In this study, quantum mechanical methods were used to calculate the electronic band gaps E_g and band widths W of the $[-\text{CF}=\text{CF}-]$ chain and compared with those similarly calculated for $[-\text{Cl}=\text{CH}-]$ itself. Other halogen-substituted polyacetylenes considered are the chains $[-\text{CF}=\text{Cl}-]$ and $[-\text{CF}=\text{CF}-\text{Cl}-\text{CH}-]$ and their chlorinated analogs. Calculations were carried out as a function of rotation about the single bonds along the chain backbone in order to assess the dependence of conductivity on chain planarity. Likewise, the sensitivity of the calculated band gaps to small changes in structure (i.e., bond angles, bond lengths) has been investigated.

Depending on the size of the substituents and their sequence, the extent of steric interference between the 1- and 3-substituents (Figure 1) and between the 2- and 4-substituents in the planar trans conformation may vary considerably. In the planar cis conformation, the critical interactions in terms of possible steric conflicts are between the 2...3 and 1...4 substituents, where the latter interaction becomes particularly significant due to the decreased interatomic separation. For a given halogen-atom substituent X, steric interferences will generally increase in the order $[-\text{CH}=\text{CH}-\text{CX}-]$, $[-\text{CH}=\text{CX}-]$, $[-\text{CX}-\text{CX}-]$. Comparison of the size of the substituent atoms ($r_{\text{vdw}} = 1.20 \text{ \AA}$), $r_{\text{vdw}} = 1.30 \text{ \AA}$) and $\text{Cl}(r_{\text{vdw}} = 1.80 \text{ \AA})$ suggests that steric effects will be much more significant in the chlorinated derivatives.

Another structurally analogous group of substituted polyacetylenes are of the type $[-\text{CH}=\text{CX}_1-\text{CH}=\text{CX}_2-\text{CH}-]$ with X_1 and X_2 chosen from among H, Cl, SiH₃ and Si(CH₃)₃. The choice of Si(CH₃)₃ as a substituent has been suggested (4) as a means to improve the solubility and hence the processibility of the otherwise intractable polyacetylene.

Other conjugated polymeric systems have been suggested as possible electrical conductors (1-3,6,7), including $[-\text{C}\equiv\text{C}-\text{X}-\text{C}\equiv\text{C}-]$ where X may be a group IV, V or VI element. Undoped organosilicon polymers have been shown to possess resistivities that classify them as organic semiconductors. Consequently, band structure calculations on chains of the type $[-\text{C}\equiv\text{C}-\text{X}-\text{C}\equiv\text{C}-]$ are included here for the case $\text{X} = \text{O}, \text{S}, \text{NH}, \text{CH}_2$ and SiH₂. For comparison, calculations have also been carried out on carbyne $[-\text{C}\equiv\text{C}-]$ to assess the effect of the 'y' atom or group on the otherwise fully conjugated system.

Theory

For any molecule, including polymers, the LCAO approximation and Bloch's theorem can be used to describe the delocalized crystal-line orbitals $\psi(k)$ as a periodic combination of functions centered at the atomic nuclei. For a one-dimensional system in which N_1-1 cells (repeat units) interact with the reference cell and for a basis set of length ω describing the wave function within a given cell, the n th crystal orbital $\psi_n(k)$ is defined as (8-11)

$$\psi_n(k) = \sum_{\mu} C_{n\mu}(k) \phi_{\mu}(k) \quad (1)$$

where $\{\phi_{\mu}\}$ is the set of Bloch basis functions

$$\phi_{\mu}(k) = \frac{1}{N_1^{1/2}} \sum_{j=1}^{(N_1-1)/2} \exp(ik \cdot R_j) X_{\mu}(\tau - R_j) \quad (2)$$

the quantity k is the wave vector. The position vector R_j , in the one-dimensional case, is given by

$$R_j = j_1 a_1 \quad (3)$$

where a_1 is the basic vector of the crystal. The crystal orbitals are, therefore,

$$\psi_n(k) = \frac{1}{N_1^{1/2}} \sum_{j=1}^{(N_1-1)/2} \sum_{\mu=1}^{\omega} \exp(ik \cdot R_j) C_{n\mu}(k) X_{\mu}(\tau - R_j) \quad (4)$$

where $C_{n\mu}(k)$ is the expansion coefficient of the linear combination. The basis functions X_{μ} are exponential functions of the Slater form. The present one-dimensional calculations included all the valence atomic orbitals of the H, C, N, and F atoms but for all other atoms only s and p orbitals could be considered.

Using the extended Hückel approximation, we obtain the corresponding eigenvalues $E_n(k)$ and coefficients $C_{n\mu}(k)$ from the eigenvalue equation

$$H(k)C_n(k) = S(k)C_n(k)E_n(k) \quad (5)$$

where $H(k)$ and $S(k)$, are respectively, the Hamiltonian and overlap matrices between Bloch orbitals defined as

$$H_{\mu\nu}(k) = \langle \phi_{\mu}(k) | H_{\text{eff}} | \phi_{\nu}(k) \rangle \quad (6)$$

and

$$S_{\mu\nu}(k) = \langle \phi_{\mu}(k) | \phi_{\nu}(k) \rangle \quad (7)$$

The distribution of the $E(k)$ values for a given n with respect to k (usually within the first Brillouin zone $(-0.5\pi \leq k \leq 0.5\pi)$, where $K = 2\pi/a_1$) is the n th energy band. In the present calculations, lattice sums were extended to include second nearest neighbors. The set of all energy bands describes the band structures of the polymers. From the calculated band structures, values of the band gap E_g and the band width W were used to predict the potential for electrical conductivity in a given polymer chain. To determine the most probable conformation in some cases, values of the total energy per unit cell $\langle E \rangle$ were calculated from their band structures as a function of the dihedral angle ϕ . The equation employed was (10, 12)

$$\langle E \rangle = \frac{1}{K} \int_{-K/2}^{K/2} E_n(k) dk \quad (8)$$

where $E_n(k)$ is the total energy at k and, according to the Extended Hückel method,

$$E_n(k) = 2 \frac{\sum_{\text{occupied}} E_n(k)}{n} \quad (9)$$

Structural Parameters

Pertinent values of the structural parameters (i.e., bond lengths and bond angles) used in the present calculations are given in Table I.

Table I. Structural Parameters Used in Calculations for Polyacetylene and Its Halogenated and Silylated Analogue

	(-Cl-Cl-)	Fluoro	Chloro	Silyl
Bond Lengths (Å)				
C-C	1.342	1.352	1.349	1.342
C-C	1.436	1.400	1.483	1.436
C-X ^a	1.121	1.336	1.715	1.870
Bond Angles (Degrees)				
C-C-C	127.0	128.6	123.4	127.0
C-C-X ^a	118.0	117.3	122.0	118.0

^a X-H, F, Cl, Si, respectively.

The above values were selected, in the case of polyacetylene, from averages taken from available experimental and theoretical structural data. For the halogenated chains, appropriate values were selected from the results of both ab initio and CNDO/2 molecular orbital calculations and from structural data available on small-molecule analogues. Due to the unavailability of structural data for the silylated analogues, values were taken from those used for polyacetylene (except, of course, for those bonds and angles associated with an 'x' atom) so as to deduce the effect of the substitution alone without inclusion of concomitant structural modifications along the polymer backbone resulting from such substitutions.

For the calculations on carbyne (-C≡C) and the (-C≡C-X-C≡C) chains, values of the bond lengths for the C≡C bond (1.116 Å) and C-C bond (1.339 Å) were taken from results of ab initio studies on carbyne (13). Associated values for the Y-C bond lengths and C-Y-C bond angles were collected from experimental structural data for small molecular analogs (14) or, in their absence, assigned standard values.

Results And Discussion

Calculated values of the band gaps E_g and band widths BW for (-CH=CH) and some halogenated analogues, all in the trans ($\phi = 0^\circ$) conformation, are presented in Table II.

Table II. Values of the Band Gap E_g and Band Width BW for the Chains in the Planar trans Conformation

Chain	E_g^a	BW ^a
(-CH=CH)	1.2	6.9
(-CF=CF)	0.72	6.9
(-CH=CF)	1.0	6.9
(-CH=CH-CF=CF)	0.67	6.3
(-CCl=CCl)	0.24	6.2
(-CH=CCl)	0.25	6.1
(-CH=CH-CCl=CCl)	0.67	5.7

^a In units of electron-volts.

Based on these results, it appears that substitution of F or Cl for H has an appreciable effect on the band structure of the chain. The band gap for (-CH=CF) is somewhat higher than expected in comparison with (-CF=CF) and (-CH=CH-CF=CF). However, such variation is expected given the great sensitivity of the calculated E_g values to small changes in structural geometry (6). Substitution of Cl for H has a pronounced effect on the value of E_g . Specifically, the E_g values for (-CCl=CCl) and (-CH=CCl) are significantly lower than that calculated for (-CH=CH). However, due to the large size of the Cl atom relative to H and F, steric conflicts will effectively

preclude the chains from attaining the planar conformations at which these band gaps were calculated. The E_g value of (-CH=CH-CCl=CCl) is conspicuously higher than that of (-CH=CCl) and of (-CCl=CCl); whether the unusually high E_g values obtained for (-CH=CF) and (-CH=CH-CCl=CCl) are artifactual or the result of the structural differences among the chains is currently under examination.

It would appear that the chlorinated analogues have the greatest potential as possible conducting polymers. However, due to the large size of the Cl atom ($r_{\text{Cl}} = 1.80$ Å), severe repulsions would be encountered in the planar trans conformation. The relative magnitude of the steric interferences would decrease for the series (-CCl=CCl) > (-CH=CCl) > (-CH=CH-CCl=CCl) in which highly repulsive Cl...Cl interactions are replaced by the sterically more favorable H...H and H...Cl interactions. However, even for the latter cases the H...Cl interatomic distances (2.50 Å) in the trans conformation are not nearly large enough to accommodate the steric bulk of the Cl atom. As a result, large deviations from chain planarity are expected for all of the chlorinated derivatives.

In the case of the fluorine derivatives, the F atom is just small enough ($r_{\text{F}} = 1.30$ Å) to render F...F interactions attractive in the trans conformation where the 1...3 and 2...4 substituent interatomic distances (Figure 1) are at their closest (2.60 Å). The presence of attractive F...F interactions in the trans conformation is analogous to the attractive H...H interactions in (-CH=CH), which has been shown through structural and theoretical investigations to exist in the planar conformation in the crystalline state (1-3).

Of course, steric repulsions occurring in the planar conformations may be reduced by rotations ϕ about the C-C single bonds along the backbone. Calculated values of E_g and BW as a function of ϕ are presented in Tables III and IV. For each polymer, the value of E_g is a minimum for the planar conformations ($\phi = 0^\circ$ and $\phi = 180^\circ$) and a maximum where the planes of the chain segments on either side of the rotated bond are mutually perpendicular ($\phi = 90^\circ$). This behavior is as expected since the degree of π overlap along the chain backbone is also a maximum for the planar conformations and a minimum for the perpendicular ones. The band width BW, which is related to the delocalization of the π system along the chain backbone and to the charge carrier mobility in the band (1-3), will be larger the greater degree of π overlap. This prediction agrees with the values of BW obtained here, which are a maximum for the planar conformations of each polymer.

The preferred conformations for these chains can be predicted from the calculated band structures by computing the total unit cell energy $\langle E \rangle$, using Eq. 8, for selected values of ϕ , with the preferred conformation (i.e., value of ϕ) given as that associated with minimum $\langle E \rangle$. Using this method, the preferred conformations are $\phi = 0^\circ$ (i.e., trans) for both (-CH=CH) and all of the fluorinated analogues, $\phi = 90^\circ$ for (-CCl=CCl), and $\phi = 120^\circ$ for both (-CH=CCl) and (-CH=CH-CCl=CCl). The values of E_g for each of these chains in their calculated preferred conformation are given in Table V. Inspection reveals that among the halogenated polyacetylenes, the fluorinated ones offer the greatest potential as semiconductors, and that the large values of E_g obtained for the chlorinated derivatives in their preferred, non-planar, conformations render them less attractive.

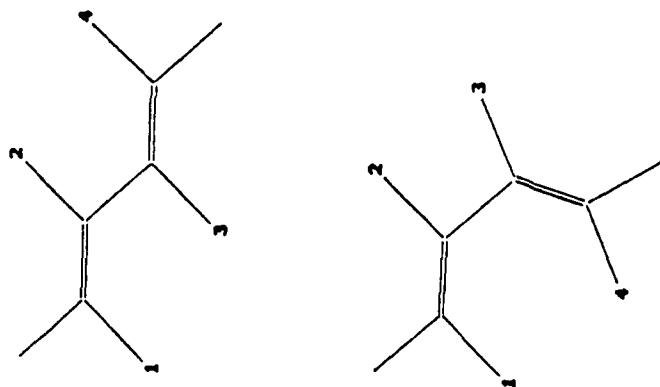


Figure 1. The trans isomeric form of polyacetylene shown in its planar trans and cis conformations, with pertinent substituents numbered.

Table III. Values of E^a and BW^a for $(-CH-CH)$ and Some Fluorinated Analogues as a Function of Rotational Angle ϕ

ϕ	$(-CH-CH)$		$(-CF-CF)$		$(-CH-CF)$		$(-CH-CH-CF-CF)$	
	E_g	BW	E_g	BW	E_g	BW	E_g	BW
0°	1.2	6.9	0.7	6.9	1.0	6.9	0.7	6.3
30°	1.6	5.3	1.6	5.3	1.8	5.4	1.3	5.1
60°	3.5	3.7	3.4	3.8	3.6	4.8	3.2	4.4
90°	4.3	3.5	4.2	3.5	4.2	4.6	3.9	3.1
120°	2.7	4.7	2.5	4.6	2.6	4.7	2.4	4.3
150°	1.2	6.1	1.1	6.0	1.4	6.2	1.1	5.4
180°	1.1	6.8	0.6	6.8	1.0	6.9	0.6	6.2

^a In units of electron-volts

Table IV. Values of E^a and BW^a for Some Chlorinated Analogues of $(-CH-CH)$ as a Function of Rotational Angle ϕ

ϕ	$(-CCl-CCl)$		$(-CH-CCl)$		$(-CH-CH-CCl-CCl)$	
	E_g	BW	E_g	BW	E_g	BW
0°	0.3	6.2	0.3	6.1	0.9	5.7
30°	1.8	5.0	1.9	5.2	1.6	4.8
60°	3.4	3.8	3.5	3.8	3.2	3.5
90°	4.2	3.7	4.1	3.7	3.9	3.3
120°	2.8	4.5	2.6	4.6	2.5	4.1
150°	2.3	5.5	1.5	5.6	1.3	5.0
180°	1.7	6.6	1.2	6.3	0.9	5.7

^a In units of electron-volts

Table V. Values of the Band Gap E_g^a for Each Polymer Chains at its calculated preferred value of ϕ as determined by Equation 8

Chain	Preferred Value of ϕ	E_g
(-Cl-Cl)	0°	1.2
(-CF-CF)	0°	0.7
(-Cl-CF)	0°	1.0
(-Cl-CH-CF-CF)	0°	1.0
(-CCl-CCl)	90°	4.2
(-Cl-CCl)	120°	2.6
(-Cl-Cl-CCl-CCl)	120°	2.5

^aIn units of electron-volts.

The value of the rotational angle ϕ will have a direct influence on the extent of steric interactions between substituent atoms (Figure 1). Specifically, as ϕ increases from 0° (trans) to 180° (cis), the interatomic distances 1...3 and 2...4 will increase while 1...4 and 2...3 will decrease. Of these, the 1...4 interaction in the cis conformation is particularly critical since here contacts are encountered with the potential for severe steric conflicts. In fact, for (-CCl-CCl) the cis conformation is essentially precluded since the 1...4 interactions are exclusively Cl...Cl. In (-Cl-CCl) and (-Cl-Cl-CCl-CCl), the Cl...Cl interactions are replaced by H...Cl which reduce the steric conflicts encountered in the planar conformations, but only slightly so.

The experimentally determined value of E_g for (-Cl-Cl) is 1.4-1.8 eV (14). Inasmuch as these experimental values fall closer to that given by these calculations for $\phi = 0^\circ$ and 180° ($E_g = 1.2$ eV) than for $\phi = 90^\circ$ ($E_g = 4.3$ eV), the present results suggest a high degree of planarity along the backbone.

The results listed in Table V, illustrate to what degree the band structure of polyacetylene (corresponding to $X_1 = X_2 = H$ in the Table VI) is affected by periodic substitution of the pendant H atoms along the chain. While substituting a pendant H by a Cl, appears to have a negligible effect on the values of E_g and BW, substitution instead by SiH_3 or $Si(CH_3)_3$ increases E_g and decreases BW (suggesting poorer conductivity). A trend appears to exist for increased E_g values (and decreased BW values) with an increase in the steric bulk of the substituent X. Since in these immediate calculations all chains were considered in their trans planar zig-zag conformation, it would not seem that the steric bulk of the substituent would have a major effect on the calculated band structures.

Table VI. Calculated Values of the Band Gap E_g^a and Bandwidth^a BW for Segments of Polymer Chains with Repeat Unit (-Cl-CH-Cl-CH-Cl-CH-Cl-)

X1	X2	E_g^a	BW ^a
H	H	1.2	3.8
H	CH ₃	1.1	3.4
CH ₃	CH ₃	1.4	3.6
H	SiH ₃	1.4	2.2
SiH ₃	SiH ₃	1.8	2.4
Si(CH ₃) ₃	Si(CH ₃) ₃	2.4	1.5

^aIn units of electron-volts

The results in Table VII depict how the band structure of carbyne [-C≡C] (corresponding to $Y = H$ in Table VII) is affected by periodic inclusion of selected atoms or groups which, by introducing a kink into the otherwise rectilinear chain of carbyne, would provide greater conformational versatility and therefore possibly improve processability. The chains were considered in their trans planar zig-zag conformation. It is seen that any of the modifications to carbyne indicated in Table VII produces an increased E_g value and a decreased BW value. That electrical conductivity would be adversely affected is reasonable given the disruption of the conjugated system caused by such modifications. As yet, no clear relationship is apparent between the specific molecular nature of Y and the effect of its inclusion on E_g and BW; the relatively minor effect for the case $Y = CH_2$ is noteworthy and under continued study.

It may be surprising that, compared with (-Cl-CH), (-C≡C) yields a considerably larger E_g value and smaller BW value. Recent

Table VII. Calculated Values of the Band Gap E_g^a and Bandwidth BW^a for Segments of Polymers Having Repeat Unit [-C≡C-Y-C≡C-]

Y	E_g^a	BW ^a
H	1.5	2.3
CH	2.8	1.9
S	3.2	0.2
NH	3.4	0.8
CH ₂	1.7	1.8
SiH ₂	2.1	1.8

^aIn units of electron-volts

studies suggest an explanation based on bond-length alternation (1-1,6). Specifically, in calculations on $(-\text{CH}=\text{CH})$ the alternating single and double bonds were assigned lengths of 1.435 Å and 1.342 Å, respectively. Correspondingly, the lengths given for the single and triple bonds in $(-\text{C}\equiv\text{C})$ are 1.339 Å and 1.116 Å, respectively. Hence, the disparity in lengths between the two types of bonds is much smaller in $(-\text{CH}=\text{CH})$ [0.094 Å] than in $(-\text{C}\equiv\text{C})$ [0.223 Å]. Our studies, on model systems, such as $(-\text{C}=\text{C})$ having complete uniformity in bond lengths, indicate a correlation between bond-length uniformity along the backbone and favorable values of E_g and BW (15). Of course, bond-length uniformity and conjugation within these chains are essentially equivalent concepts, hence these results again point to a correlation between conjugation along the chain backbone and conductivity.

The choice of structural parameters (i.e., bond lengths and bond angles) in these types of calculations will certainly influence the values of E_g and BW obtained, hence it was of interest to assess the sensitivity of our calculated E_g and BW values to changes in structural geometry. Our reference polymer trans $(-\text{CH}=\text{CH})$ and its perfluorinated analogue trans $(-\text{CF}=\text{CF})$ were used for this purpose. The most spectacular effect was obtained by simultaneously increasing the lengths of the C-C bonds and decreasing those of the C-C bonds. For $(-\text{CF}=\text{CF})$ in the trans conformation, such a modification of only 0.02 Å reduced the value of E_g from 0.72 eV to 0.40 eV. This result is reasonable since such a modification is tantamount to increasing the extent of conjugation along the chain, and this should translate to a lower E_g value. In the other direction, decreasing the C-C bond lengths and increasing the C-C bond lengths by 0.02 Å resulted in an increase in E_g from 0.72 eV to 1.04 eV.

In contrast, calculated E_g values were largely insensitive to small ($\pm 2.0^\circ$) changes in backbone bond angles. These results confirm that conductivity is directly and strongly dependent on the degree of conjugation along the chain backbone, and that structural modifications that give rise to a decrease in bond-length alternation should provide a means for developing improved electrically conducting polymeric materials.

acknowledgments

The author wishes to acknowledge the support provided for this research by the Plastics Institute of America and by the Air Force Office of Scientific Research (Grant AFOSR 83-0027, Chemical Structures Program, Division of Chemical Sciences).

Literature Cited

3. Roth, S. In Electronic Properties of Polymers and Related Compounds, Kuzmany, H.; Mehring, H.; Roth, S., Eds.; Springer-Verlag, 1985.
4. Zeigler, J., Sandia National Laboratories, Albuquerque, private communications.
5. Wheland, R. C. J. Am. Chem. Soc. 1976, **98**, 3926.
6. Brédas, J. L.; Silbey, R.; Boudreaux, D. S.; Chance, R. R. J. Am. Chem. Soc. 1983, **105**, 6555.
7. Gourley, K. D.; Lillya, C. P.; Reynolds, J. R.; Chien, J. C. W. Macromolecules 1984, **17**, 1025.
8. Andrie, J.-M. In The Electronic Structure of Polymers and Molecular Crystals, Andrie, J.-M.; Ladik, J., Eds.; Plenum: New York, 1974.
9. Hoffmann, R. J. Chem. Phys. 1963, **39**, 1397.
10. Whangbo, M.-H.; Hoffmann, R. J. Am. Chem. Soc. 1978, **100**, 6093.
11. Whangbo, M.-H.; Hoffmann, R.; Woodward, R. B. Proc. R. Soc. London Ser. A 1979, **A366**, 23.
12. Imamura, A. J. Chem. Phys. 1970, **52**, 3168.
13. Teramae, A.; Yamabe, T. Theoret. Chim. Acta 1983, **64**, 1.
14. Brédas, J. L.; Chance, R. R.; Baughman, R. H. J. Chem. Phys. 1982, **76**, 3673.

RECEIVED February 13, 1987

Baughman, R. H.; Brédas, J. L.; Chance, R. C.; Elsenbaumer, R.; Schacklette, L. W. Chem. Rev. 1982, **82**, 209, and references cited therein.

Hegner, G. Makromol. Chem., Macromol. Symp. 1986, **1**, 151, and references cited therein.

IN-SITU GENERATION OF CERAMIC PARTICLES FOR THE REINFORCEMENT OF ELASTOMERIC MATRICES

J. E. MARK

Department of Chemistry and the Polymer Research Center
The University of Cincinnati
Cincinnati, Ohio

1. INTRODUCTION

The chemical reactions used in the sol-gel technology^{1,2} for preparing ceramics are illustrated by the hydrolysis of an alkoxysilane:



The process first gives a swollen gel, which is then dried, fired, and densified into the final, monolithic piece of silica. There have now been a number of additional studies using essentially the same reactions, but in a very different context.³⁻²² Specifically, the hydrolysis reactions are carried out within a polymeric matrix, with the silica generated in the form of very small, well-dispersed particles. When the matrix is an elastomer, these particles provide the same highly desirable reinforcing effects obtained by the usual blending of a filler (such as carbon black) into polymers (such as natural rubber) prior to their being cross-linked or cured into tough elastomers of commercial importance.^{23,24}

Although the focus of these studies has been on the elastomer reinforcement that the particles provide, the emphasis can easily be switched to the particles themselves. Thus, the elastomeric matrix can be viewed as acting in the same way as the frozen low-molecular-weight matrices, which are much used to immobilize and stabilize molecular fragments in order to permit their spectroscopic characterization.²⁵ It is hoped that characterization of the dispersed ceramic particles—for example, by scattering experiments²⁶—would provide information on the intermediate and final products obtained from reactions such as that given in Eq. (1). It could thus provide information which would complement that obtained from the possibly more complicated monolithic ceramic objects of primary interest in the sol-gel technology.^{1,2}

2. VARIOUS CURING-FILLING SEQUENCES

2.1. Filler Precipitation After Curing

In this technique the polymer is first cured or vulcanized into a network structure using any of the well-known cross-linking techniques such as high-energy irradiation,²⁷ thermolysis of peroxides,²⁸ nonselective reaction with sulfur or metal oxides,²⁹ or selective reaction of functional groups on the polymer with

a multifunctional small molecule.²⁰⁻²² The network is then swelled with the silane or related molecule to be hydrolyzed and is subsequently exposed to water at room temperature, in the presence of a catalyst, for a few hours. The swollen sample can be either placed directly into an excess of water containing the catalyst^{17,18,20,22} or merely exposed to the vapors from the catalyst-water solution.⁵ Drying the sample then gives an elastomer that is filled (and thus reinforced) with the ceramic particles resulting from the hydrolysis reaction.

Although a phase-transfer catalyst can be used in such a reaction,¹ it was found to be unnecessary at least for relatively small specimens. Large samples could of course have a nonuniform distribution of particles, a possibility being investigated by solid-state ²⁹Si nuclear magnetic resonance spectroscopy.¹¹

Different alkoxysilanes can swell an elastomeric network to different extents and can hydrolyze at different rates. Tetraethoxysilane (TEOS) seemed to be the best for the present purpose, as judged by the amount of silica precipitated and the extent of reinforcement obtained.²⁰ Using the same criteria, basic catalysts seemed more effective than acidic ones.⁹ Some preliminary studies on the effects of catalyst concentration⁷ in particular and the hydrolysis kinetics¹⁸ in general have been carried out. It was found that the rate of particle precipitation can vary in a complex manner, possibly due to the loss of colloidal silica and partial deswelling of the networks when placed into contact with the catalyst solution.¹⁸

Most of the studies to date have been carried out on polydimethylsiloxane (PDMS) because of the great extent to which its networks swell in TEOS. The same technique has, however, been shown to give good reinforcement of polyisobutylene elastomers.²¹ Titanates have been used in place of silanes, with the resulting titania particles also giving significant improvements in elastomeric properties.²²

2.2. Filler Precipitation During Curing

It is also possible to mix hydroxyl-terminated chains (such as those of PDMS) with excess TEOS, which then serves simultaneously to tetrafunctionally end-link the PDMS into a network structure and to act as the source of silica upon hydrolysis. This simultaneous curing and filling technique has been successfully used for PDMS elastomers having a unimodal distribution of chain lengths⁸ as well as for PDMS elastomers¹¹ and thermosets¹⁰ having bimodal distributions.

The roles may also be reversed, by putting triethoxysilyl groups at the ends of PDMS chains,¹⁷ as illustrated in Fig. 1. Reactive groups at the surface of the *in-situ*-generated silica or titania particles then react with the chain ends to simultaneously cure and reinforce the elastomeric material.

2.3. Filler Precipitation Before Curing

In the above techniques, removal of the unreacted TEOS and the ROH by-product causes a significant decrease in volume, which could be disadvantageous in some applications. This problem can be overcome by precipitating the particles into a polymer that is inert under the hydrolysis conditions—for example, vinyl-terminated PDMS.¹⁴ The resulting polymer-filler suspension, after removal of the other materials, is quite stable. It can be subsequently cross-linked—for example, by silane reaction with the vinyl groups—with only the usual, very small change in volume.

3. MODIFIED FILLER PARTICLES

3.1. Surface Modification

If an *in-situ*-filled elastomer is extracted with a good solvent, its modulus and ultimate strength are frequently significantly increased.⁶ The effect is probably

due to hydrolytic formation of additional reactive groups on the particle surface or to removal of absorbed small molecules, thus increasing the number of sites for particle-polymer bonding.

3.2. Induced Deformability

In some applications, it may be advantageous for the filler particles to have some deformability. It may be possible to induce such deformability by using a molecule that is only partially hydrolyzable—for example, a triethoxysilane $R'Si(OR)_3$, where R' could be methyl,¹¹ ethyl,¹² vinyl,¹³ or phenyl.¹⁴

From MKS, Jonard, "Organic R/Si(OR)₃ Compounds."

4. TYPICAL IMPROVEMENTS IN ELASTOMERIC PROPERTIES

4.1. Mooney-Rivlin Representation/

5/

One of the two standard ways of representing elastomeric data in elongation is by plotting the modulus $[f^*] \equiv f^*/(\alpha - \alpha^{-2})$ against α^{-1} , where f^* is the nominal stress and $\alpha = L/L_0$ is the relative length or elongation. Typical results are shown in Fig. 2.⁶ Generating the filler particles *in-situ* greatly increases the elastomer modulus; also, as mentioned in Section 3.1, extraction with a solvent gives further significant improvements.

4.2. Stress-elongation Isotherms

5/

Another typical representation shows the nominal stress as a function of elongation, as illustrated for titania-filled PDMS in Fig. 3.²² The advantage of this type of plot is that the area under the curves corresponds to values of the energy required for rupture, a standard measure of toughness.

4.3. Ultimate Properties

Generation of filler particles generally increases the ultimate strength ($[f^*]$ or f^* at rupture) but frequently decreases the maximum extensibility (α at rupture). The former effect usually predominates, with a corresponding increase in the energy of rupture.

5. CHARACTERIZATION OF PARTICLES

5.1. Densities

Comparisons between the values of wt % filler obtained from density measurements and the values obtained directly from weight increases can give very useful information on the filler particles. For example, the fact that the former estimate is smaller than the latter in the case of silica-filled PDMS elastomers⁶ indicates that there are probably either voids or unreacted organic groups in the filler particles.

5.2. Electron Microscopy

The transmission electron micrograph¹⁸ shown in Fig. 4 reveals (1) that the particles in this silica-filled PDMS network have an average diameter of approxi-

mately 80 Å, a very desirable size for reinforcement.^{21,22} (2) that there is a relatively narrow size distribution, (3) that a very small amount of the agglomeration, which is usually a problem, consists of filler-blended elastomers,^{21,24} and (4) that there are well-defined surfaces. The good definition generally occurs when the catalyst is a base, as is the ethylamine used for this sample. Use of an acidic catalyst, on the other hand, gives poorly defined, "fuzzy" particles, as illustrated in Fig. 5.¹⁶ This lack of definition is consistent with results²⁵ in the sol-gel ceramics area, where it was concluded that acidic catalysts give structures that are less branched and less compact than those obtained from basic catalysts.

5.3. Small-Angle X-Ray and Neutron Scattering

Some typical small-angle X-ray scattering results are shown in fig. 6.²⁶ The radii of gyration thus obtained can be correlated, for example, with electron microscopy results and with various elastomeric properties. Also, the shapes of the curves can give information on the distribution of particle sizes, and the terminal slopes can indicate whether the particles are well defined (slope of -4) or poorly defined (-3). Similar experiments being carried out using neutron scattering should also prove to be very useful in characterizing ceramic particles of this type.

ACKNOWLEDGMENTS

It is a pleasure to acknowledge the financial support provided by the Air Force Office of Scientific Research through Grant No. AFOSR 83-0027 (Chemical Structures Program, Division of Chemical Sciences), the Army Research Office through Grant No. DAALO3-86-K-0032 (Materials Science Division), and the National Science Foundation through Grant No. DMR 84-15082 (Polymers Program, Division of Materials Research).

REFERENCES

1. L. L. Hench and D. R. Ulrich, Eds., *Ultrastructure Processing of Ceramics, Glasses, and Composites*, John Wiley & Sons, New York (1984).
2. L. L. Hench and D. R. Ulrich, Eds., *Science of Ceramics, Chemical Processing*, John Wiley & Sons, New York (1986).
3. J. E. Mark and S.-J. Pan, Reinforcement of Polydimethylsiloxane Networks by *In-Situ* Precipitation of Silica: A New Method for Preparing Filled Elastomers, *Makromol. Chem., Rapid Commun.*, **3**, 681 (1982).
4. Y.-P. Ning, M.-Y. Tang, C.-Y. Jiang, J. E. Mark, and W. C. Roth, Particle Sizes of Reinforcing Silica Precipitated Into Elastomeric Networks, *J. Appl. Polym. Sci.*, **29**, 3209 (1984).
5. C.-Y. Jiang and J. E. Mark, The Effect of Relative Humidity on the Hydrolytic Precipitation of Silica Into an Elastomeric Network, *Colloid Polym. Sci.*, **262**, 758 (1984).
6. Y.-P. Ning and J. E. Mark, Treatment of Filler-Reinforced Silicone Elastomers to Maximize Increases in Ultimate Strength, *Polym. Bull.*, **12**, 407 (1984).
7. J. E. Mark and Y.-P. Ning, Effects of Ethylamine Catalyst Concentration in the Precipitation of Reinforcing Silica Filler in an Elastomeric Network, *Polym. Bull.*, **12**, 413 (1984).
8. J. E. Mark, C.-Y. Jiang, and M.-Y. Tang, Simultaneous Curing and Filling of Elastomers, *Macromolecules*, **17**, 2613 (1984).
9. C.-Y. Jiang and J. E. Mark, The Effects of Various Catalysts in the *In-Situ* Precipitation of Reinforcing Silica in Polydimethylsiloxane Networks, *Makromol. Chem.*, **185**, 2609 (1984).
10. M.-Y. Tang, A. Letton, and J. E. Mark, Impact Resistance of Unfilled and Filled bimodal Thermosets of Polydimethylsiloxane, *Colloid Polym. Sci.*, **262**, 990 (1984).
11. M.-Y. Tang and J. E. Mark, Elastomeric Properties of Bimodal Networks Prepared by a Simultaneous Curing-Filling Technique, *Polym. Eng. Sci.*, **25**, 29 (1985).
12. Y.-P. Ning, Z. Riebi, and J. E. Mark, Hydrolysis of Several Ethyltriethoxysilanes to Yield Deformable Filler Particles, *Polym. Bull.*, **13**, 155 (1985).
13. J. E. Mark, Bimodal Networks and Networks Reinforced by the *In-Situ* Precipitation of Silica, *Br. Polym. J.*, **17**, 144 (1985).
14. Y.-P. Ning and J. E. Mark, Precipitation of Reinforcing Filler Into Polydimethylsiloxane Prior to its End Linking into Elastomeric Networks, *J. Appl. Polym. Sci.*, **30**, 3519 (1985).
15. J. E. Mark and G. S. Sur, Reinforcing Effects from Silica-Tyrene Fillers Containing Hydrocarbon Groups, *Polym. Bull.*, **14**, 325 (1985).
16. J. E. Mark, Y.-P. Ning, C.-Y. Jiang, M.-Y. Tang, and W. C. Roth, Electron Microscopy of Elastomers Containing *In-Situ* Precipitated Silica, *Polymer*, **26**, 2069 (1985).
17. G. S. Sur and J. E. Mark, Elastomeric Networks Cross-Linked by Silica or Titania Fillers, *Eur. Polym. J.*, **21**, 1051 (1985).
18. Y.-P. Ning and J. E. Mark, Ethylamine and Ammonia as Catalysts in the *In-Situ* Precipitation of Silica in Silicone Networks, *Polym. Eng. Sci.*, **26**, 167 (1986).
19. J. E. Mark, Conformational Analysis of Some Polysilanes and the Precipitation of Reinforcing Silica into Elastomeric Networks, in: L. L. Hench and D. R. Ulrich, Eds., *Science of Ceramic Chemical Processing*, John Wiley & Sons, New York (1986).
20. G. S. Sur and J. E. Mark, Comparisons Among Some Tetra-Alkoxy silanes in the Hydrolytic Precipitation of Silica into Elastomeric Networks, *Makromol. Chem.*, **19**, 0000 (1986).
21. C.-C. Sun and J. E. Mark, *In-Situ* Generation of Reinforcement in Polyisobutylene Networks, *J. Polym. Sci., Polym. Phys. Ed.*, **24**, 000 (1986).
22. S.-B. Wang and J. E. Mark, *In-Situ* Precipitation of Reinforcing Titania Fillers, manuscript in preparation.
23. B. B. Boonstra, Role of Particulate Fillers in Elastomer Reinforcement: A Review, *Polymer*, **20**, 691 (1979).
24. Z. Riebi, Reinforcement of Rubber Carbon Black, *Adv. Polym. Sci.*, **36**, 21 (1980).
25. S. Craddock and A. Hinchliffe, *Matrix Isolation*, Cambridge University Press, New York (1975).
26. D. W. Schaefer and J. E. Mark, unpublished results.
27. A. Chapiro, *Radiation Chemistry of Polymeric Systems*, Wiley-Interscience, New York (1962).
28. A. Y. Coran, Vulcanization, in: *Science and Technology of Rubber*, F. R. Eirich, Ed., Academic Press, New York (1978).
29. J. P. Gueslet and J. E. Mark, Molecular Interpretation of the Modulus of Elastomeric Polymer Networks, *Adv. Polym. Sci.*, **65**, 135 (1984).
30. J. E. Mark, Molecular Aspects of Rubberlike Elasticity, *Acc. Chem. Res.*, **18**, 202 (1985).
31. J. L. Ackerman and J. E. Mark, unpublished results.
32. D. W. Schaefer and J. D. Keeler, Fractal Geometry of Silica Condensation Polymers, *Phys.*

Figure 1. Sketch of process for cross-linking (end-linking) triethoxysilyl-terminated PDMS chains by means of reactive surface groups on silica or titania filler particles.¹¹

c/

Figure 2. The modulus shown as a function of reciprocal elongation for unfilled and filled PDMS networks at 25°C.¹² The numbers correspond to the wt % filler in the network, and the letter T specifies treatment (extraction) with tetrahydrofuran. Filled symbols are for results obtained out of sequence to test for reversibility, and the vertical dashed lines located the rupture points.

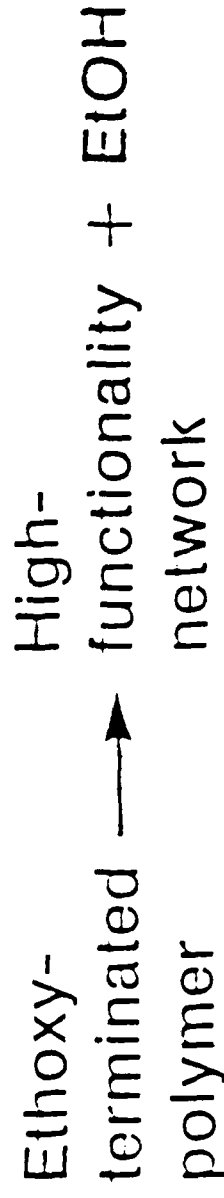
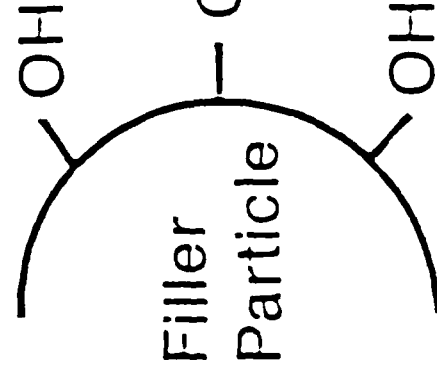
Figure 3. The nominal stress shown as a function of elongation for PDMS networks at 25°C.¹² Each curve is labeled with the wt % titania present in the network.

Figure 4. Electron micrograph of a PDMS network containing well-defined silica particles obtained in an ethylamine/base-catalyzed hydrolysis of TEOS.¹³ The length of the bar in this figure corresponds to 1000 Å.

Figure 5. Electron micrograph of a PDMS network containing "fuzzy" silica particles obtained in an acetic-acid-catalyzed hydrolysis of TEOS.¹³ The length of the bar in this figure corresponds to 1000 Å.

Figure 6. Small-angle X-ray scattering (SAXS) intensity shown as a function of the scattering vector for PDMS networks containing 17.3 and 8.4 wt % silica.¹⁴ The labels give the values for the radius of gyration R_g and the terminal slope.

Cross Linking with Silica or Titania



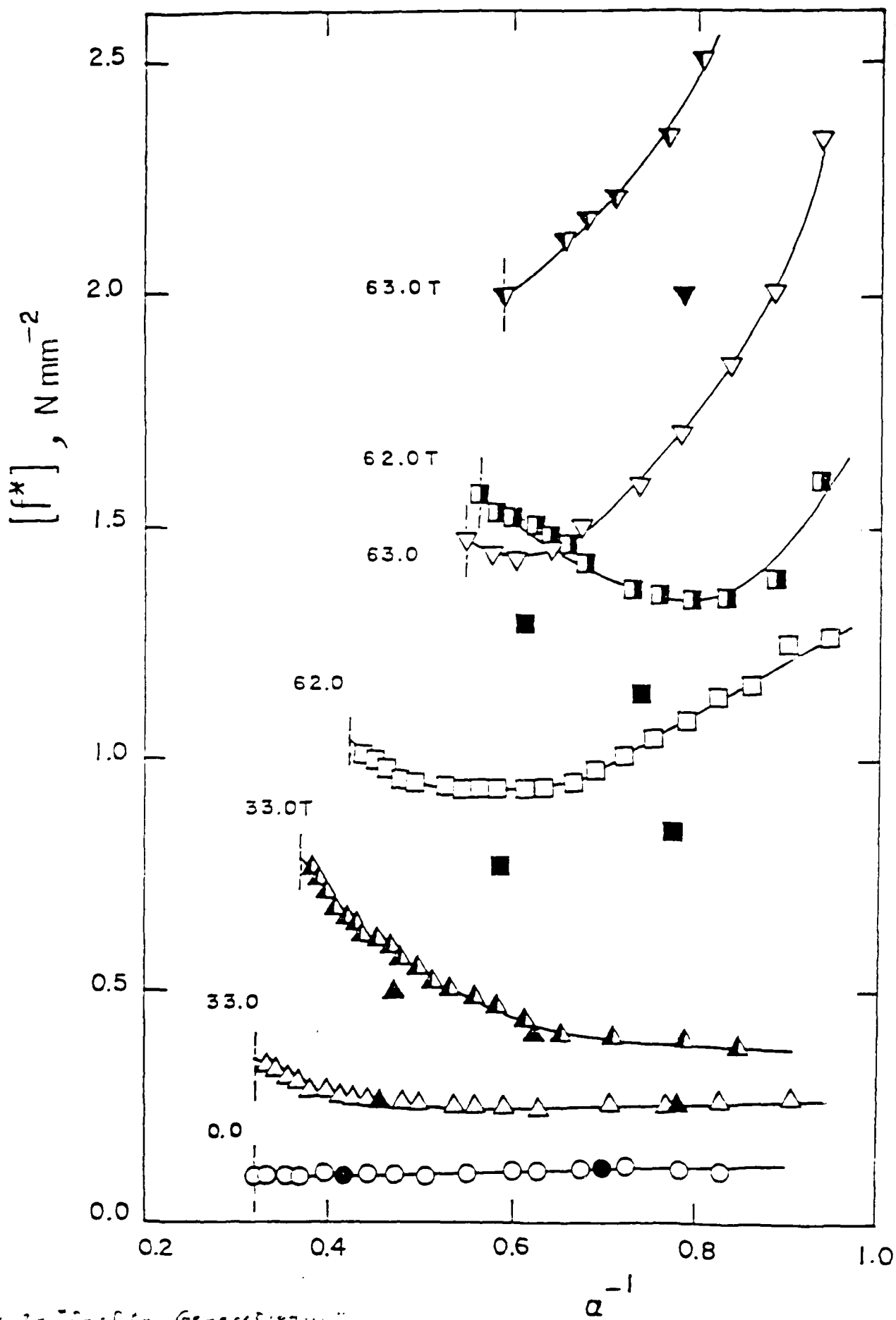


Fig. 2- "S-S" Generation...

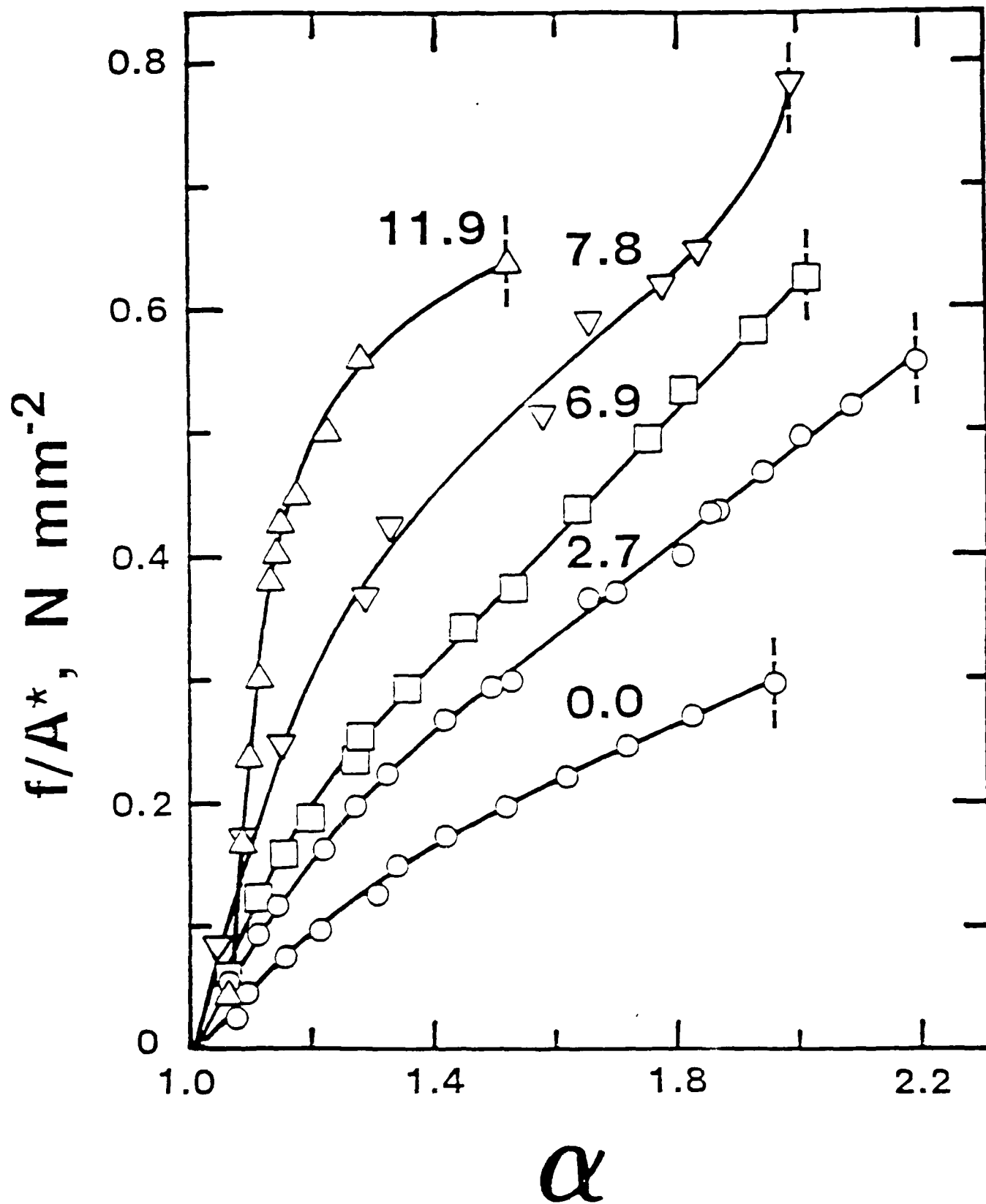


Fig. 3- In-Situ Generation ...
1/2 mm

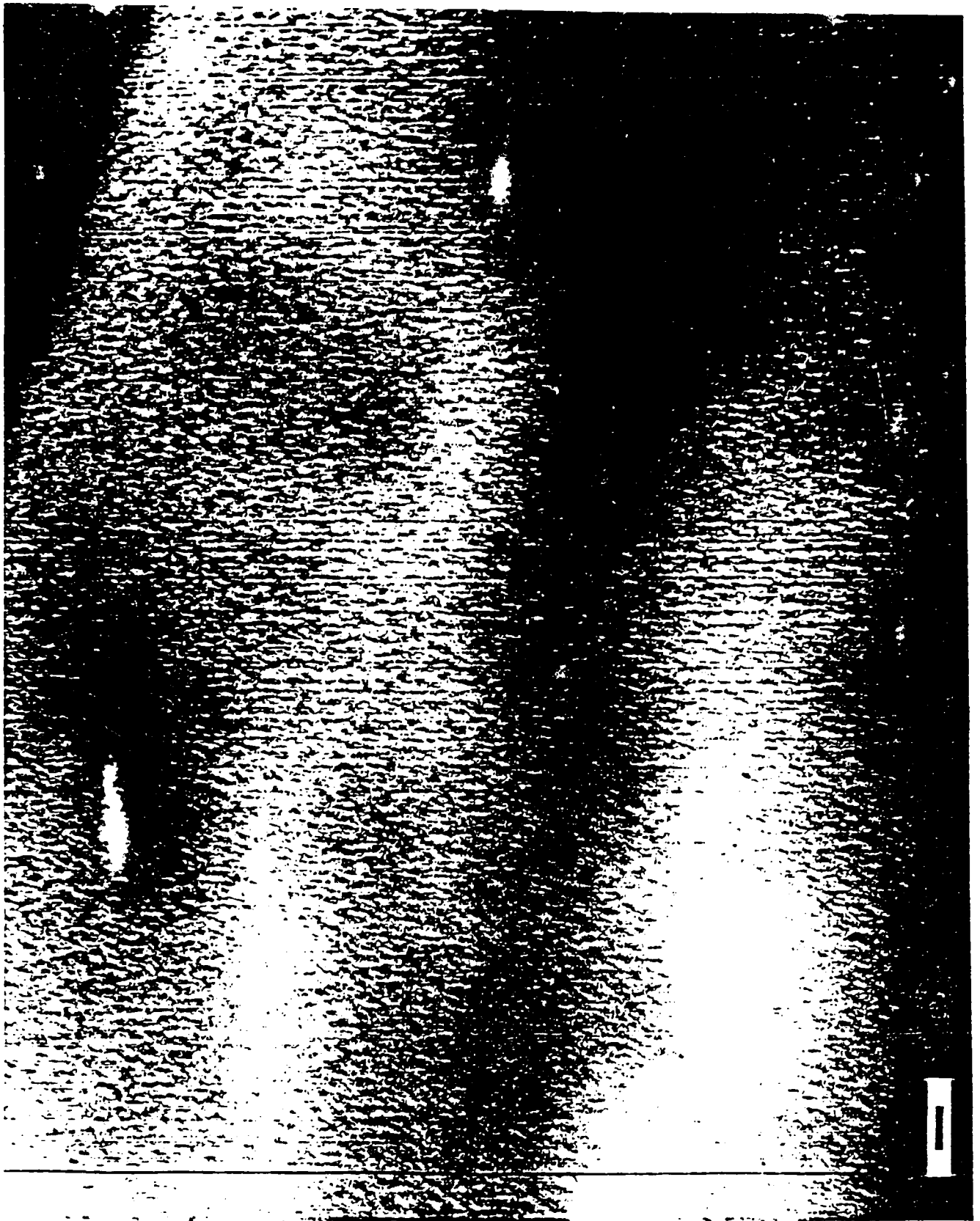


Fig. 11 - In-Situ Generation - J. E. M. 1954



Fig. 5 - "I. S. C. Generation"

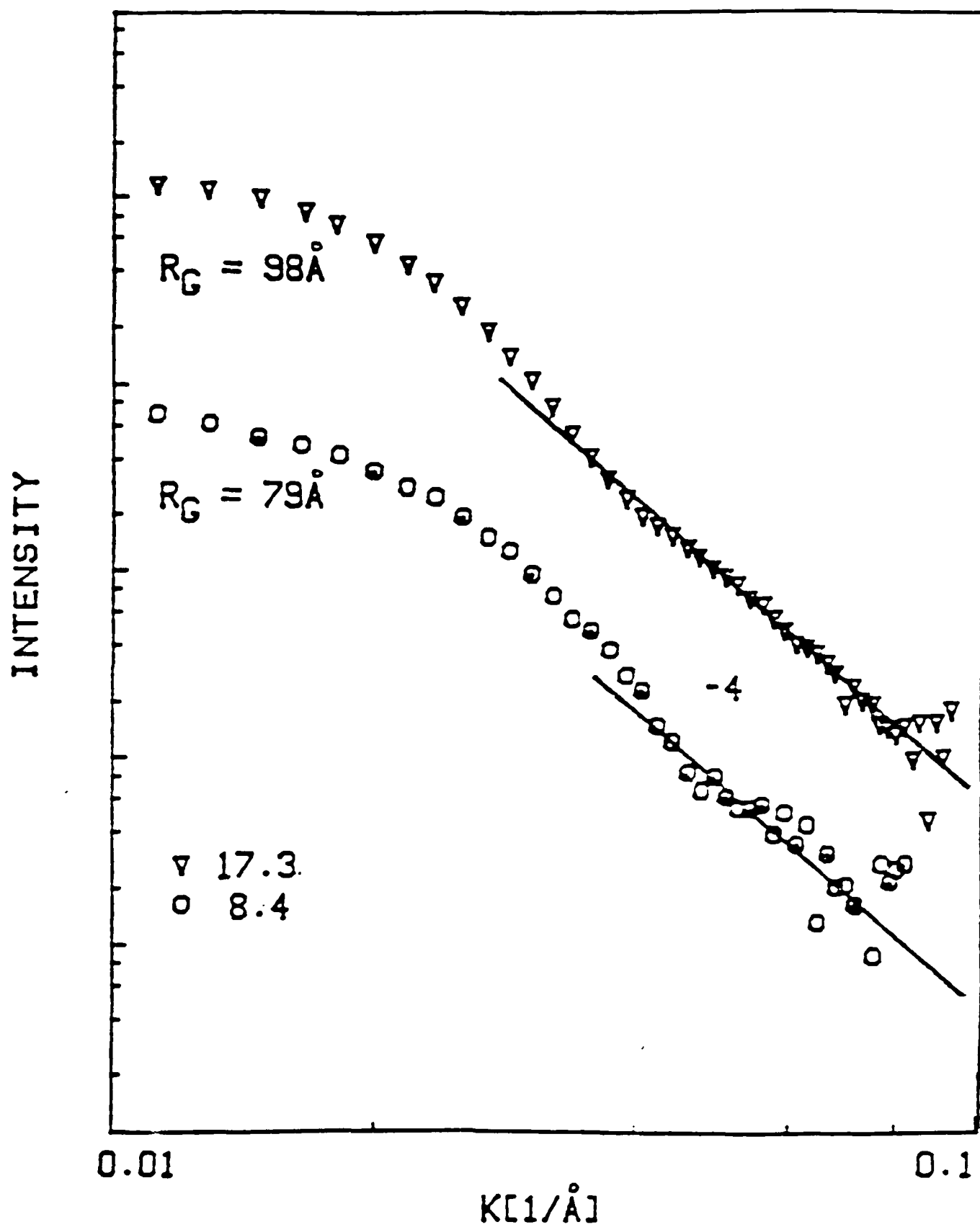


Fig. 6 - In-Situ Generation ...
 5/8/82

AM1 AND MNDO/2 MOLECULAR ORBITAL CONFORMATIONAL
ENERGY CALCULATIONS ON MODEL COMPOUNDS OF
SIMPLE POLYSILANES AND POLYGERMANES

William D. Johnson and William J. Welsh

Department of Chemistry, University of Missouri-St. Louis
St. Louis, Missouri 63121, U.S.A.

MNDO/2 and AM1 molecular orbital calculations have been carried out on a series of structurally related polysilane and polygermane model compounds. Conformational energies have been computed as a function of rotation ϕ about a bond along the chain backbone. For each conformation, geometry optimized values of the bond angles and bond lengths were obtained. For polysilane $[-SiH_2]$ the results indicate nearly equal preferences for both trans and gauche states and a high degree of rotational flexibility. For poly(permethylsilane) $[-Si(CH_3)_2]$ the results show a broad minimum surrounding trans with slightly shallower and steeper minima at the gauche states. Overall this chain is less flexible and exhibits greater preferences for specific conformational states (i.e., trans and gauche). For poly(permethylgermane) $[-Ge(CH_3)_2]$ the results indicate a broad minimum located at trans with steeper and slightly shallower minima near the gauche states. Compared with poly(permethylsilane), poly(permethylgermane) exhibits qualitatively a very similar profile except that the barriers are substantially lower. The authors wish to acknowledge the financial support provided by the Plastics Institute of America and the Air Force Office of Scientific Research (AFOSR).

INTRODUCTION

SOLUBLE POLY(DI-N-ALKYLSILANES) OF HIGH MOLECULAR WEIGHT CONSTITUTE A NEW AND FASCINATING CLASS OF POLYMERS WITH POTENTIAL APPLICATIONS AS SELF-DEVELOPING DEEP-UV RESISTS, SILICON CARBIDE CERAMIC PRECURSORS, AND PHOTOCONDUCTORS FOR PHOTOCOPYING APPLICATIONS. AMONG THEIR MORE UNUSUAL PROPERTIES IS A THERMOCHROMIC UV TRANSITION OCCURRING BOTH IN THE SOLID STATE AND IN SOLUTION. INTERESTINGLY, IT HAS BEEN FOUND THAT POLYSILANE DERIVATIVES SUBSTITUTED WITH LONG-CHAIN ALKYL SUBSTITUENTS [e.g. POLY(DI-N-HEXYLSILANE)] SHOW A REMARKABLE RED SHIFT TO 370-380 nm. MORE RECENT STUDIES ON POLYGERMANE ANALOGUES BY R.D.MILLER, et al., SUGGEST A SIMILAR BEHAVIOR IN THIS CASE. THIS PHENOMENON HAS BEEN ATTRIBUTED BY SOME TO THE OCCURRENCE OF TRANS-GAUCHE CONFORMATIONAL TRANSITIONS ALONG THE CHAIN BACKBONE.

IN THE PRESENT STUDY, WE REVEAL THE RESULTS OF CONFORMATIONAL ENERGY CALCULATIONS CARRIED OUT ON SEVERAL SIMPLE POLYSILANE AND POLYGERMANE MODEL COMPOUNDS. ENERGIES WERE CALCULATED AS A FUNCTION OF ROTATION ABOUT A CHAIN BACKBONE BOND TO OBTAIN A CONFORMATIONAL ENERGY PROFILE E vs. ϕ . THE RESULTS ARE INTERPRETED IN TERMS OF THE PREFERRED CONFORMATIONS, ROTATIONAL ENERGY BARRIERS, AND OVERALL ROTATIONAL FLEXIBILITY OF EACH POLYMER. RESULTS OF SIMILAR CALCULATIONS CARRIED OUT ON HYDROCARBONS ANALOGUES ARE ALSO PRESENTED FOR COMPARISON

METHODOLOGY

THE AMPAC (M.J.S. DEWAR, et al., QCPE 506) SUITE OF SEMI EMPIRICAL MOLECULAR ORBITAL PROGRAMS WAS USED FOR THE PRESENT STUDY. MNDO PARAMETERS FOR Ge WERE OBTAINED FROM M.J.S. DEWAR, et al., ORGANOMETALLICS 6, 186 (1987) AND ADDED TO THE PROGRAM. FOR EACH POLYMER SEGMENT, CALCULATIONS WERE CARRIED OUT USING BOTH THE AM1 AND MNDO/2 HAMILTONIANS CONTAINED IN AMPAC. THIS WAS DONE TO TEST THE SENSITIVITY OF THE RESULTS TO THE METHODOLOGY CHOSEN. FULL GEOMETRY OPTIMIZATION WAS IMPLEMENTED FOR ALL CALCULATIONS.

RELATIVE CONFORMATIONAL ENERGIES E (IN KCAL/MOLE) WERE DETERMINED FOR EACH POLYMER SEGMENT BY TAKING DIFFERENCES IN CALCULATED MOLECULAR ENERGIES PROVIDED BY AMPAC WITH THE LOWEST ENERGY ARBITRARILY NORMALIZED TO 0.00 KCAL/MOLE.

MOLECULAR ENERGIES WERE GENERALLY CALCULATED FOR ϕ VARIED FROM 0-180° IN INCREMENTS OF 15-30°. THE REGIONS $\phi=0^\circ$ -180° AND 180°-360° ARE RENDERED EQUIVALENT BY THE ROTATIONAL SYMMETRY OF THESE CHAINS.

RESULTS

THE RESULTS OF THE CONFORMATIONAL ENERGY CALCULATIONS ARE PRESENTED AS PLOTS OF E (KCAL/MOLE) vs. ϕ (DEGREES). REPRESENTATIVE VALUES OF THE GEOMETRY-OPTIMIZED STRUCTURAL PARAMETERS (i.e., BOND LENGTHS, BOND ANGLES) ARE PRESENTED IN TABLES. THE CIS AND TRANS CONFORMATIONS WERE TAKEN AS $\phi=0^\circ$ AND $\phi=180^\circ$, RESPECTIVELY.

POLYSILANE

THE MNDO/2 RESULTS INDICATE A GLOBAL MINIMUM LOCATED NEAR $\phi = \pm 60^\circ$ (GAUCHE) WITH A LOCAL MINIMUM LOCATED NEAR $\phi = 180^\circ$ (TRANS) ONLY ABOUT 0.05 KCAL/MOLE ABOVE GAUCHE. THE MAXIMUM BARRIERS TO ROTATION ARE LOCATED NEAR $\phi = \pm 120^\circ$ (ECLIPSED) AND $\phi = 0^\circ$ (CIS) WITH BARRIERS IN THE RANGE OF $E = 0.30 - 0.35$ KCAL/MOLE. HENCE THE CHAIN IS PREDICTED TO BE HIGHLY FLEXIBLE WITH MINIMAL BARRIERS TO ROTATION AND TO PREFER THE TRANS AND GAUCHE STATES NEARLY EQUALLY.

THE AM1 RESULTS ARE QUALITATIVELY IN AGREEMENT. HOWEVER, AM1 SHOWS A BARRIER PEAK OF $E = 0.32$ KCAL/MOLE AT $\phi = 180^\circ$ (TRANS) AND YIELDS SUBSTANTIALLY LOWER BARRIERS TO THE CIS ($\phi = 0^\circ$) CONFORMATION. ALSO, AM1 SHIFTS THE GAUCHE MINIMUM TO $\phi = 30^\circ$.

THE MNDO/2 RESULTS AGREE CLOSELY WITH EARLIER MM2 FORCE-FIELD CALCULATIONS (W.J. WELSH, et al., MACROMOLECULES 19, 2978 (1986); R.J. DAMEWOOD AND R. WEST, MACROMOLECULES 18, 159 (1985)).

POLY(PERMETHYLSILANE)

THE MNDO/2 RESULTS INDICATE A GLOBAL MINIMUM ENERGY REGION TRAVERSING THE TRANS ($\phi = 180^\circ$) CONFORMATION WITH SOMEWHAT SHALLOWER AND STEEPER MINIMA NEAR THE GAUCHE ($\phi = \pm 60^\circ$) STATES. THE MAXIMUM BARRIER TO FREE ROTATION IS LOCATED AT CIS WITH $E = 22$ KCAL/MOLE; LOCAL BARRIERS SOME 2.7 KCAL/MOLE ABOVE THE MINIMUM ENERGY ARE LOCATED AT THE ECLIPSED ($\phi = \pm 120^\circ$) CONFORMATIONS. THE AM1 RESULTS ARE IN QUALITATIVE AGREEMENT WITH MNDO/2 BUT INDICATE SUBSTANTIALLY LOWER BARRIERS (1.0 KCAL/MOLE) TO FREE ROTATION.

AGAIN, THESE RESULTS ARE CONSISTENT WITH THE MM2 RESULTS OF WELSH, et al. AND OF DAMEWOOD AND WEST.

POLY(PERMETHYLGERMANE)

THE MNDO/2 RESULTS INDICATE A BROAD GLOBAL MINIMUM LOCATED NEAR TRANS WITH STEEPER AND SLIGHTLY SHALLOWER MINIMA LOCATED NEAR GAUCHE ($\phi = \pm 60^\circ$). THE PROFILE APPEARS REMARKABLY SIMILAR TO THAT OBTAINED FOR POLY(PERMETHYLSILANE) EXCEPT THAT THE BARRIERS ARE UNIFORMLY LOWER. THIS IS REASONABLE SINCE THE Ge-Ge BONDS ARE LONGER THAN THE Si-Si BY ABOUT 0.4 Å, AND THIS ADDITIONAL LENGTH SHOULD REDUCE STERIC CONGESTION.

THE AM1 RESULTS AGAIN SHOW QUALITATIVELY SIMILAR BEHAVIOR EXCEPT THAT THE BARRIERS TO ROTATION ARE SUBSTANTIALLY LOWER.

POLYMETHYLENE

BOTH MNDO/2 AND AM1 RESULTS INDICATE A PREFERENCE FOR TRANS ($\phi = 180^\circ$) WITH LOCAL GAUCHE MINIMA ABOUT 1.0 KCAL/MOLE ABOVE TRANS. THE MAXIMUM BARRIERS LOCATED AT CIS IS ABOUT 3.8 KCAL/MOLE ABOVE THE MINIMUM. IN GENERAL THE RESULTS SHOW BOTH POLYSILANES AND POLYGERMANES TO BE MORE FLEXIBLE THAN THE CORRESPONDING HYDROCARBON CHAIN.

SUMMARY AND CONCLUSIONS

1. MNDO/2 AND AM1 MOLECULAR ORBITAL CALCULATIONS HAVE BEEN CARRIED OUT ON A SERIES OF STRUCTURALLY RELATED POLYSILANE AND POLYGERMANE MODEL COMPOUNDS. CONFORMATIONAL ENERGIES HAVE BEEN COMPUTED AS A FUNCTION OF ROTATION ϕ ABOUT A BOND ALONG THE CHAIN BACKBONE. FOR EACH CONFORMATION, GEOMETRY OPTIMIZED VALUES OF THE BOND ANGLES AND BOND LENGTHS WERE OBTAINED.

2. FOR POLYSILANE $[\text{SiH}_2]$ THE MNDO/2 RESULTS INDICATE NEARLY EQUAL PREFERENCES FOR BOTH TRANS AND GAUCHE STATES AND A HIGH DEGREE OF ROTATIONAL FLEXIBILITY. THE MAXIMUM BARRIERS TO FREE ROTATION ARE SMALL AT ABOUT 0.35 KCAL/MOLE, HENCE THE CHAIN IS PREDICTED TO HAVE HIGH ROTATIONAL FLEXIBILITY. THE AM1 RESULTS ARE QUALITATIVELY IN AGREEMENT EXCEPT FOR A BARRIER (0.3 KCAL/MOLE) RATHER THAN A MINIMUM AT TRANS, AND THE BARRIERS TO CIS ARE SUBSTANTIALLY LOWER.

3. FOR POLY(PERMETHYLSILANE) $[\text{Si}(\text{CH}_3)_2]$ THE MNDO/2 RESULTS SHOW A BROAD MINIMUM SURROUNDING TRANS WITH SLIGHTLY SHALLOWER AND STEEPER MINIMA AT THE GAUCHE STATES. THE MAXIMUM BARRIER TO ROTATION LOCATED AT CIS, IS HIGH AT ABOUT 22 KCAL/MOLE. OTHER BARRIERS OF ABOUT 2.7 KCAL/MOLE ARE LOCATED AT THE ECLIPSED ($\phi = \pm 120^\circ$) STATES. HENCE, OVERALL THIS CHAIN IS LESS FLEXIBLE AND EXHIBITS GREATER PREFERENCES FOR SPECIFIC CONFORMATIONAL STATES (i.e. TRANS AND GAUCHE). THE AM1 RESULTS ARE AGAIN IN QUALITATIVE AGREEMENT EXCEPT FOR SUBSTANTIALLY LOWER ROTATIONAL FLEXIBILITY.

4. FOR POLY(PERMETHYLGERMANE) $[\text{Ge}(\text{CH}_3)_2]$ THE MNDO/2 RESULTS INDICATE A BROAD MINIMUM LOCATED AT TRANS WITH STEEPER AND SLIGHTLY SHALLOWER MINIMA NEAR THE GAUCHE STATES. COMPARED WITH POLY(PERMETHYLSILANE), POLY(PERMETHYLGERMANE) EXHIBITS QUALITATIVELY VERY SIMILAR PROFILE EXCEPT THAT THE BARRIERS ARE SUBSTANTIALLY LOWER. THIS IS REASONABLE SINCE THE LONGER Ge-Ge BONDS COMPARED TO THE ANALOGOUS Si-Si BONDS SHOULD REDUCE STERIC CONFLICTS FOR CONFORMATIONS. AGAIN, AM1 IS QUALITATIVELY CONSISTENT WITH MNDO/2 EXCEPT FOR EXHIBITING LOWER BARRIERS.

ACKNOWLEDGMENT

THE AUTHORS WISH TO ACKNOWLEDGE THE FINANCIAL SUPPORT PROVIDED BY THE PLASTICS INSTITUTE OF AMERICA AND THE AIR FORCE OF SCIENTIFIC RESEARCH (AFOSR)

WM. D. JOHNSON and W. J. WELSH,
DEPARTMENT OF CHEMISTRY, UNIVERSITY OF MISSOURI ST. LOUIS
ST. LOUIS MO. 63121

DIPOLE MOMENTS OF SOME POLY(DIMETHYLSILOXANE) LINEAR CHAINS AND CYCLICS

E. RIANDE* and J. E. MARK†

*Instituto de Plástico Y Caucho, Madrid-6, Spain and †Department of Chemistry and the Polymer Research Center, The University of Cincinnati, Cincinnati, OH 45221, U.S.A.

(Received 26 April 1983)

Abstract—Dielectric constant measurements were carried out on poly(dimethylsiloxane) (PDMS) linear chains $\text{CH}_3\text{--}[\text{Si}(\text{CH}_3)_2\text{O}]_x\text{--Si}(\text{CH}_3)_3$ and cyclics $[\text{Si}(\text{CH}_3)_2\text{O}]_x$ for $x \approx 10, 15$ and 70 , in cyclohexane and in benzene at 30°C . Mean-square dipole moments $\langle \mu^2 \rangle$ were calculated from these data, using the method of Debye. The values thus obtained for the linear chains are consistent with results previously reported for short, linear PDMS chains in the undiluted state. Discernible differences among the values in the two solvents and undiluted state are manifestations of the "specific solvent effect" known to be important in longer linear chains the networks of PDMS. The cyclics were found to have dipole moments very similar to those of the corresponding linear chains. The cyclics also showed a specific solvent effect, in the same direction as shown by the linear molecules.

INTRODUCTION

The chain molecules which have been most extensively studied with regard to conformation-dependent properties are those of poly(dimethylsiloxane) (PDMS). Experimental investigations have focused on their random-coil dimensions [1], dipole moments [2-4], network thermoelasticity [1, 5], stress-optical coefficients [6, 7], and ring-chain cyclization constants [8, 9]. Theoretical studies carried out to interpret, and even predict, such properties are based on the well-known rotational isomeric state theory [1], and have been notably successful in this regard. Unusual features of these chain molecules which make them attractive to both experimentalists and theorists are their tractability and high-temperature stability [10, 11], semi-inorganic nature [12], marked polarity [1, 2-4], unusual equation of state parameters [13], abnormal entropies of dilution and excess volumes [14], extraordinary flexibility and permeability [10, 11, 15], and (because of unequal skeletal bond angles) a low-energy conformation that approximates a closed polygon [1, 2]. Another interesting feature is the existence of cyclics $[\text{Si}(\text{CH}_3)_2\text{O}]_x$ covering a wide range in degree of polymerization x [8, 9, 16], as well as the unusual linear chains $\text{CH}_3\text{--}[\text{Si}(\text{CH}_3)_2\text{O}]_x\text{--Si}(\text{CH}_3)_3$.

The present investigation is concerned with the determination of experimental values of the mean-square dipole moment $\langle \mu^2 \rangle$ of PDMS linear chains

and cyclics having $x \approx 10, 15$ and 70 . The required dielectric constant measurements are carried out in solution, in both cyclohexane and benzene. Comparisons with previous results [2, 3] obtained on short, linear PDMS chains in the undiluted state are used to document the dependence of $\langle \mu^2 \rangle$ on solvent medium. Also of interest are possible differences in $\langle \mu^2 \rangle$ between linear chains and cyclics having essentially the same degree of polymerization [16].

EXPERIMENTAL

Three PDMS linear polymers (L1, L2, L3) and three cyclics (C1, C2, C3) were generously provided by Professor J. A. Semlyen. The (number-average) number n of Si—O and O—Si skeletal bonds and polydispersity indices are given in the second and third columns of Table 1.

At least four solutions of each of the samples were prepared in both cyclohexane and benzene, with the weight fraction w of polymer ranging from 0.0035 to 0.036. Specific volumes v of the solutions were then determined by dilatometry, indices of refraction \bar{n} by differential refractometry, and dielectric constants ϵ with the usual capacitance bridge and a miniature three-terminal cell [17]. All measurements pertain to 30°C .

RESULTS AND DISCUSSION

Values of the concentration dependence of the quantities of interest were expressed as $d\epsilon/dw$, $d\Delta\epsilon/dw$, and $d\Delta\bar{n}/dw$, where $\Delta\epsilon = (\epsilon - \epsilon_0)$ is the

Table 1. Experimental data and results for the PDMS linear chains and cyclics in cyclohexane at 30°C .

Polymer	n	M_w/M_n	$-d\epsilon/dw$	$d\Delta\epsilon/dw$	$-d\Delta\bar{n}/dw$	$\langle \mu^2 \rangle / \text{nm}^2$
L1	20.1	1.01	0.215	0.433	0.016	0.178
L2	31.6	1.01	0.255	0.473	0.006	0.190
L3	141.1	1.07	0.250	0.502	0.004	0.213
C1	19.7	1.13	0.220	0.542	-0.002	0.182
C2	29.6	1.05	0.252	0.524	0.006	0.209
C3	139.2	1.06	0.260	0.491	0.008	0.203

FILMED
58